The Pennsylvania State University

The Graduate School

College of the Liberal Arts

PROCONSUL HESELONI FEET FROM RUSINGA ISLAND, KENYA

A Thesis in

Anthropology

by

Holly M. Dunsworth

Submitted in Partial Fulfillment
of the Requirements
for the Degree of
Doctor of Philosophy

December 2006

The thesis of Holly M. Dunsworth was reviewed and approved* by the following:

Alan Walker
Evan Pugh Professor of Biological Anthropology and Biology
Thesis Adviser
Chair of Committee

Joan T. Richtsmeier
Professor of Biological Anthropology

George R. Milner
Professor of Professor of Archaeological Anthropology

John H. Challis
Associate Professor of Kinesiology

Nina G. Jablonski
Professor of Biological Anthropology
Head of the Anthropology Department

*Signatures are on file in the Graduate School.

ABSTRACT

In the mid 1980s, teams from Johns Hopkins University and the National Museums of Kenya colleted a minimum of ten *Proconsul heseloni* individuals from the Kaswanga Primate Site (KPS), Rusinga Island, Kenya. Five of them have nearly complete right and/or left feet. The preservation and anatomy of the KPS tarsals and metatarsals are described and analyzed here.

Bivariate and multivariate analyses of the linear proportions of the feet and hindlimbs of the individuals illuminate arboreal characteristics in the *Proconsul* foot. Because the KPS individuals died at different stages of development, their foot and hindlimb proportions through ontogeny are investigated. Comparative cross-sectional ontogenetic samples include 222 *Pan troglodytes*, 65 *Gorilla gorilla gorilla*, and 115 *Macaca mulatta* and adult samples include 15 *Pan paniscus*, 24 *Colobus* (*angolensis, guereza, and badius*), 10 *Nasalis proboscis*, and 12 *Hylobates lar*.

Proconsul aligned with *Colobu*s and *Nasalis* in overall proportions and with apes in certain metatarsal proportions. Dissimilarities to macaques and similarities to apes in growth patterns suggest *Proconsul* was not born with large feet like macaques and other non-hominoid primates. Thus, *Proconsul* may have shared life history traits with *Pan* and *Gorilla* like increased altriciality in infant locomotor and positional behaviors.

In order to investigate strength properties of the metatarsals, the midshafts of a total of 29 *Proconsul* metatarsals from six individuals were scanned with high-resolution microCT. Biplanar radiography and the latex cast method were used to obtain cross-sectional properties of the metatarsals from an extant cross-sectional ontogenetic sample of 52 *Macaca mulatta* (260 metatarsals) and 74 *Pan troglodytes* (370 metatarsals). Regression plots showed much closer similarity between *Proconsul* and *Macaca* than *Proconsul* and *Pan* in overall strength properties and cross-sectional shapes when normalized for metatarsal length and for body size. However, the first metatarsal of *Proconsul* showed greater resistance to bending and torsional forces for its length than *Macaca*, which is more like *Pan.*

Overall results support previous interpretations on partial and incomplete *Proconsul* pedal fossils, and on other parts of the postcranial skeleton, that *Proconsul* was a generalized arboreal quadruped that grasped tree branches with a long, strong hallux.

TABLE OF CONTENTS

LIST OF TABLES

LIST OF FIGURES

ACKNOWLEDGMENTS

My utmost gratitude goes to my advisor Alan Walker. Much of graduate school for me was about catching the ideas that are freely popping out of his brain, slapping myself on the forehead wishing I had thought of them, and then cultivating them into projects of my own. The other part was training my own brain to think that creatively, and no matter how far into left field I wandered, Alan was always delightfully supportive. He lives by the assumption that any imaginable question can be answered and I hope that even the tiniest bit of that rubbed off on me. The hardest part of finishing this thesis was coping with the looming inevitability that I would be leaving Alan's lab when it was all over.

My second-most gratitude goes to my committee for their sharp advice, encouragement, patience (especially for reading Chapter 3), and collegial support: Joan Richtsmeier, John Challis, and George Milner. Timothy Ryan deserves a great deal of appreciation for writing the computer program I used for my cross-sectional geometry analysis and for the many tutorials on imaging software. Masato Nakatsukasa very nobly saved my dissertation by scanning the *Proconsul* metatarsals. The experts Matthew O'Neil and Christopher Ruff graciously tutored me in cross-sectional geometry methods. Corey Sparks, Zachary Whitley and C.R. Rao provided much needed statistical advice. I could not have survived without Pablo Rivera's computer virus extermination and hard drive resuscitation. I also thank the on-line librarians at Paterno and Pattee Libraries.

The L.S.B. Leakey Foundation generously funded this research. For their additional financial support, I would also like to thank the Hill Foundation and the Baker Fund of the Department of Anthropology at Penn State, the Research and Graduate Studies Office of the College of Liberal Arts at Penn State, an award from the Penn State Graduate School Alumni Association, and some very generous patrons of paleoanthropology.

Thanks to Mark Teaford, Kamoya Kimeu, Blasto Onyango, Carol Ward, Chris Beard, David Begun, Alan Walker, and their colleagues for enduring the painstaking process of identifying and gluing thousands of miniscule fragments of bone to piece together the individuals from the Kaswanga Primate Site. Without their efforts, we could not realize the astonishing scope of this collection, nor would I have been capable of completing this dissertation.

Thanks to all of the people I worked with in the institutions I visited, all of the people I stayed with, and those colleagues I crossed globetrotting paths with and shared ideas with along the way: Jean Spence (AMNH); Paula Jenkins, Daphne Hills, Alfred Rosenberger (The Natural History Museum); Malcolm Harman and the Teale Family (The Powell-Cotton Museum); Marcel Zefferer and Frau M. Müller (University of Zurich); Wim Wendelen, Wim van Neer, and Willem van Hoef, and Carla Marteens (The Royal Museum of Central Africa, Tervuren and the Gasthuisberg Hospital in Leuven, Belgium); The Government of Kenya, Edward Opiyo at the Ministry of Science, Education and Technology, Dr. Farrah -The Director General, Dr. Emma Mbua – Head of Paleontology, Samuel Ngui Muteti, Mary Muungu, Katie Binetti, Joe Ferraro, Leslea ("big sis") Hlusko (The National Museums of Kenya); Terry Kensler, Myriam S. Viñales Mendes, Carlos Reyes Rivera and John G. H. Cant (The University of Puerto Rico

Medical School); Carol Ward (University of Missouri, Columbia, MO); Judith Chupasko, Corwin Sullivan, Leon Claessens, Herman Pontzer, Susanne Cote (Harvard Museum of Comparative Zoology and X-ray Lab). Big thanks to Kyoto University for putting a posh camera stand in room A10 at the National Museums of Kenya. Lyman Jellema at the CMNH deserves special thanks for all his help and advice about measuring equipment. Thanks also to the kind ladies of the Penn State Anthropology department - Diane Snyder, Nancy Fogelman, Kim Miller and Wendy Fultz - for their support.

I've had some tremendous teachers and supervisors during this journey: Mr. Boggs, Mrs. Weisenbarger, Mr. Sidlik, Mr. Harris, Mr. Baumer, Jeffrey Kurland, Lee Newsom, Jim Wood, Claire Milner, Dean Snow, Ken Weiss, and Susan Antón. Thanks so much to all of you.

Pat Shipman has been an enormously supportive friend and source of strength throughout graduate school. I truly believe that sharing an office with Mary Silcox made me smarter by association. Gail Krovitz made me a faster swimmer and was a daily reminder why I got into this business. William Harcourt-Smith is a wonderful co-conspirator in foot-ology. Many thanks to Christopher Campisano for his technological wizardry. If it weren't for the many outings with my Kristina Aldridge, Sharon DeWitte, Brenda Frazier, Craig Goralski, and Cheryl Hill this experience would not have been anywhere near as fun. A big warm thanks goes to Kevin Stacey for providing the inspirational soundtrack for the project.

And finally, Dad, if you had never helped me get that brick-powered egg-transporting vehicle with a dowel-rod chasse and tuna can wheels to roll across the back porch, I would have given up on science a long time ago. And, Mom, if you hadn't bestowed unto me your gene for collecting carcasses and storing them in desk drawers and freezers, I would be disgusted by dead things like all normal people. With tremendous appreciation, love and admiration, this dissertation is dedicated to you both.

Chapter 1

INTRODUCTION

Over twenty years ago, expeditions from the Johns Hopkins University and the National Museums of Kenya collected a cache of *Proconsul* fossils, comprising a minimum of ten individuals, from the newly discovered Kaswanga Primate Site on Rusinga Island, Kenya. Since then researchers have analyzed the specimens, one anatomical region at a time. The feet are analyzed here. Six individuals had preserved tarsals and metatarsals and five of them had preserved nearly complete right and/or left sides. Because they are in direct contact with the substrate, feet are good indicators of locomotion and positional behavior. The foot bones can be used to better reconstruct the locomotion of the fossil ape *Proconsul* for an improved understanding of its role in catarrhine evolution.

Specific Aims of the Dissertation

1. The preservation and comparative anatomy of *Proconsul heseloni* metatarsals and tarsals from the Kaswanga Primate Site, Rusinga Island, Kenya will be described.

2. The foot and hindlimb proportions of *Proconsul heseloni* will be compared to extant catarrhines.

3. The mechanical properties (cross-sectional geometry) of the metatarsals of *Proconsul heseloni* will be analyzed using high-resolution microcomputed tomography (microCT).

Each of these analytical angles will provide insights into the foot use of *Proconsul heseloni* and when combined will comprise the most thorough assessment of the extinct species' foot morphology, both external and internal, to date. This will have implications for the interpretation of *Proconsul* functional morphology and for its phylogenetic position within the catarrhines.

This study also represents the first time the metatarsals of a fossil primate (including fossil humans) have been analyzed using cross-sectional geometry methods. This method of determining bones' biomechanical properties offers the opportunity to gain a much deeper understanding of bone adaptation and function, and thus behavior, in *Proconsul*.

As the Kaswanga specimens died at different developmental ages, the hindlimb proportions and the cross-sectional properties of the metatarsals of immature *Proconsuls* can be compared to ontogenetic series of modern catarrhines (Old World monkeys and apes). The results offer insights into the evolution of growth and development and life history traits in extant catarrhines.

***Proconsul*: State of the Taxon, 2006**

Proconsul fossils have been studied for nearly 70 years. In 1927, farmer and former medical officer H. L. Gordon discovered the first fossil remains of *Proconsul* at a limestone quarry in Koru, Western Kenya. A.T. Hopwood of the British Museum subsequently named them *Proconsul* (Hopwood, 1933). Since then, discoveries in Western Kenya and Eastern Uganda have made *Proconsul* the best-known Miocene primate genus (Walker & Shipman, 2005).

The four species of *Proconsul* range from 20-17 Ma and are mainly distinguished by body size and locality (Walker & Shipman, 2005). *Proconsul africanus* from Koru and Songhor in Western Kenya and *P. heseloni* from Rusinga Island are the smallest *Proconsul* species with adult body masses estimated between 9 and 15 kg (Rafferty et al., 1995; Ruff, 2003a; Walker et al., 1993). *Proconsul nyanzae*, from Rusinga and Mfangano Islands, is larger with males about 36 kg and females about 27 kg (Rafferty et al., 1995; Ruff, 2003a). *Proconsul major*, known only from a few remains from Koru and Songhor, as well as Napak, Uganda, is the largest with a body size comparable to that of a female gorilla weighing between 60-90 kg (Harrison, 1982; Rafferty et al., 1995; Ruff, 1989, 2003a; Ruff et al., 1989; Walker et al., 1993). Senut and her colleagues later assigned this largest *Proconsul* species to the new genus *Ugandapithecus* (Senut et al., 2000), but few have adopted this recommendation, and recently MacLatchy and Rossie contended that there is little reason to separate *P. major* generically from the other *Proconsul* species (MacLatchy & Rossie, 2005).

All *Proconsul* species have dental morphology consistent with a frugivorous diet (Kay and Ungar, 1997; Ungar and Kay, 1995) and all are sexually dimorphic in body size and canine size (Walker, 1997). Although *P. heseloni* and *P. nyanzae* may have different facial morphology (Rae, 1997), so far there are few known inter-specific differences in *Proconsul*'s postcranial functional morphology (Langdon, 1986; Rose, 1994; Walker & Pickford, 1983; Ward, 1998). One exception may be the posteriorly, rather than proximally, extended olecranon process in *P. nyanzae* as compared to *P. heseloni*, suggesting more of an emphasis on terrestrial locomotion in the much larger *P. nyanzae* (Fleagle, 1999).

Although there is more fossil evidence for the *Proconsul* genus than for any other Miocene primate, its morphological affinities and phylogenetic position are debated. The root of the argument lies in the generalized postcranial morphology of *Proconsul*. Despite the consensus that *Proconsul* was an arboreal quadruped, there is an argument over its phylogenetic position and which living primate is its best analog. There are three major phylogenetic hypotheses (Figure 1.1): *Proconsul* is either a basal catarrhine (Harrison, 1982; Harrison, 1987; Harrison, 1993; Harrison, 2002), a stem hominoid (Andrews, 1985; Andrews and Martin, 1987; Harrison, 1993; Szalay and Delson, 1979; Walker, 1997), or the sister group to great apes and humans (Rae, 1993; Rae, 1997; Walker and Teaford, 1989).

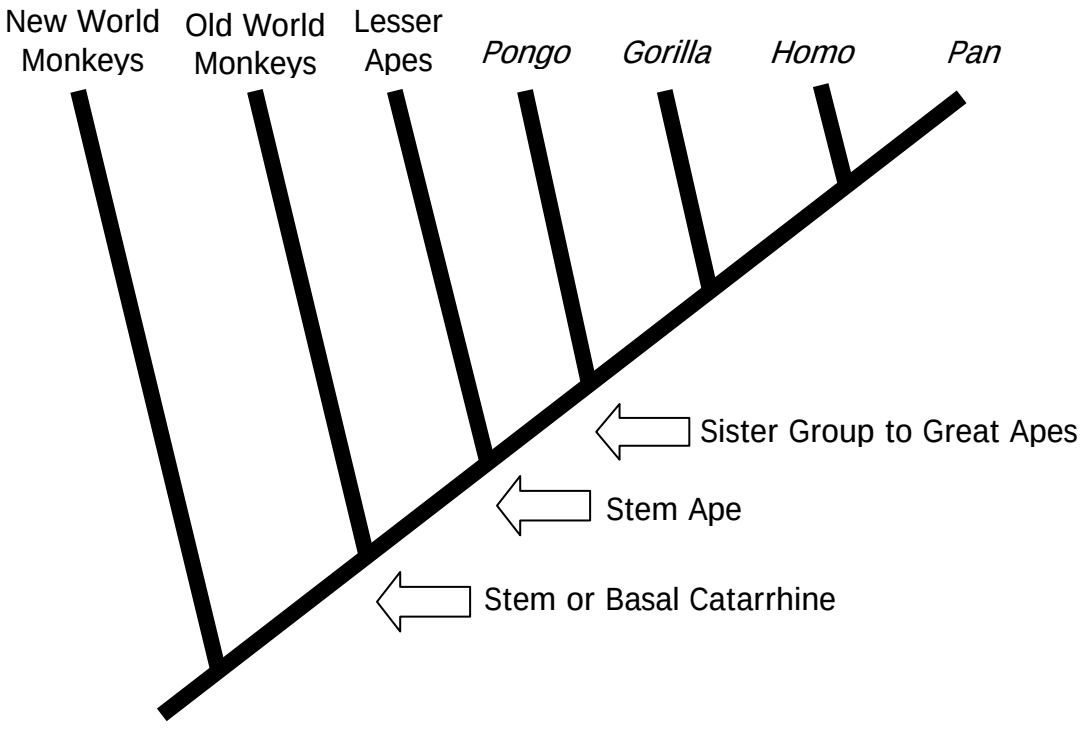

Figure 1.1. Three hypotheses for *Proconsul* evolution.

There is no doubt that *Proconsul* is a full-fledged catarrhine; it is even more like extant catarrhines than preceding Oligocene propliopithecids in tooth, cranial, and skeletal morphology (Rae, 1997; Seiffert & Simons, 2001). But exactly where *Proconsul* should be placed in catarrhine evolution is debated.

Harrison (2002) argues that the overall postcranium of *Proconsul* indicates the locomotion of the genus was most similar to those of arboreal non-hominoid primates, specifically colobines and larger platyrrhines. For instance, he points out that the intermembral index of *Proconsul*, between 85 and 90, differs from any living hominoid and is within the range of arboreal quadrupedal monkeys. Non-human hominoid indices range between 116-147 (Fleagle, 1999). *Proconsul* also has a long, flexible monkey-like vertebral column, and a narrow rib cage. The presence of these traits caused Harrison to consider *Proconsul* a non-hominoid basal catarrhine (Harrison, 2002).

On the other hand, despite its non-specialized locomotor behavior, *Proconsul* lacks all of the derived skeletal features of living cercopithecoid monkeys and has some synapomorphies with extant hominoids (Walker, 1997). These hominoid-like features include a lack of tail (Nakatsukasa et al., 2004; Ward, 1991), a more rounded humeral head, an ape-like distal humerus (Rose, 1988) and ulna (Richmond et al., 1998), anatomy of the carpal joints (Beard et al., 1993), the robustness of the fibula, some details of the pollex, and the morphology of the tarsals and hallux (Langdon, 1986; Lewis, 1989; Strasser, 1993). Furthermore, *Proconsul* lacks ischial callosities which great apes and humans also lack (Ward et al., 1993), and which are derived in Old World monkeys; however, this is a primitive trait.

Proconsul also has a frontal sinus (Walker & Pickford, 1983), a feature that has been traditionally accepted as hallmark anatomy in great apes and humans. However, Rossie and colleagues described the presence of an ethmoid sinus, which is developmentally linked to the frontal sinus, in the skull of *Aegyptopithecus*. Its presence in the Oligocene stem catarrhine led them to argue the trait as primitive and uninformative about *Proconsul*'s relationship with later hominoids (Rossie et al., 2002).

Although many of *Proconsul's* hominoid traits are under investigation, its hominoid-like characteristics suggest that *Proconsul* is situated at the base of the hominoid branch. This hypothesis has gathered momentum now that we have abandoned the classic assumption that hominoids experienced a monkey-like evolutionary stage before becoming the apes we see today (see McHenry & Corruccini, 1983).

It is probable that many hominoid characteristics are actually primitive for catarrhines. Along this line, some researchers have posited that the great ape body plan is actually the primitive hominoid condition, as opposed to that seen by the specialized brachiators *Hylobates* (Pilbeam & Young, 2004; Young & MacLatchy, 2004). The original modern ape adaptation is probably that of a basic orthograde body moving about by vertical climbing (Fleagle, 1976; Sarmiento, 1988). If this hypothesis is correct, we should find this morphology in the earliest fossil hominoids. Gebo (1997) and MacLatchy and colleagues (2000) maintain just that, but they argue that there are certain characteristics in *Morotopithecus bishopi* from Uganda - a fossil that predates *Proconsul* - that are associated with the great ape condition. These features are not present in *Proconsul* (Rose, 1993) and furthermore *Proconsul* lacks many of the features seen in the brains of great apes (Falk, 1983).

The 20 million-year-old *Morotopithecus bishopi* of Uganda is known from facial and dental remains, lumbar vertebrae, two partial femora and a possible glenoid fossa of the scapula (Gebo et al., 1997, but see Pickford et al., 1999 who claim it is not a hominoid). This rather large hominoid, with an estimated size of 40-60 kg, is interpreted to have been a cautious climber. That is, its discoverers argue it is an arboreal primate that employed climbing, brachiating, quadrupedalism and arm-hanging postures within its locomotor repertoire (Gebo et al., 1997). Gebo and colleagues advocate that certain derived great ape and ateline features present in the shaft and distal portion of the *Morotopithecus* femur are not present in *Proconsul,* cercopithecines, or hylobatids. So far these interpretations have not convinced the paleoanthropological community that *Morotopithecus* is the stem great ape, especially since the dating is contentious and the identification of some of the specimens has not been solidly verified. Until better evidence is provided, *Proconsul* cannot be excluded from the lineage leading to great apes.

Molecular clocks offer an alternative method for testing the *Proconsul* hypotheses, especially while there is still a need to fill in the gaps in the fossil record leading up to and immediately following *Proconsul*. Depending upon the calibration used, molecular clock results support all three hypotheses for *Proconsul* evolution. The date of the first appearance of the genus in the fossil record, about 20 million years ago, lies within the 95% confidence interval of the estimated split between cercopithecoids and hominoids, circa 23 Ma (Stauffer et al., 2001). This date falls outside the range of that for the great ape split unless one follows recent work by Steiper and colleagues (2004). They used a method that does not calibrate with a root fossil; instead, they

calibrated from the "canopy" with the fossil evidence for the split of hominins from chimpanzees (7-6 Ma) and the split of macaques from baboons (7-5 Ma). They estimated cercopithecoid-hominoid split to be about 34.5-29.2 Ma (Steiper et al., 2004) which extends over a sparse stretch of the primate fossil record. According to this estimate, *Proconsul* fits comfortably along either the cercopithecoid or the hominoid lineage.

***Proconsul* from the Kaswanga Primate Site**

Fossils on Rusinga Island were first reported in 1927 by geologist E.J. Wayland, sparking expeditions by L.S.B. Leakey and D.G. MacInnes in the early 1930s. Once Leakey found a *Proconsul nyanzae* mandible in 1942, the island garnered even more paleontological attention and became a popular early Miocene laboratory during the 1950s, 60s and 70s (Andrews, 1981).

In the mid 1980s Alan Walker, then at the Johns Hopkins University, noticed some *Proconsul* bones collected by Louis Leakey and colleagues from Rusinga Island (housed in the museum in Nairobi) had been misidentified as other animals. This inspired a joint team from the Johns Hopkins University and the National Museums of Kenya to go to Rusinga Island to re-examine sites there. The expeditions were successful; not only did they recover more overlooked *Proconsul* bones (at site R114 where the type skeleton of *P. heseloni*, KNM-RU 2036, is from) but they also solved the mystery of site R114 ("Whitworth's Pothole") by deducing it was actually a fossilized tree that had once been a hollow animal den. And to top it all off, while working on the tree, the team discovered a new site on the Kaswanga peninsula. The site came to be called the Kaswanga Primate Site (KPS) because of the wealth of *Proconsul* bones collected from the surface and *in*

situ (Walker & Teaford, 1988). In all, a minimum of ten individuals of varying developmental ages were collected from the KPS.

The functional anatomy of *Proconsul* is relatively well known because nearly every skeletal element is represented in the record. And now thanks to the KPS, we have new teeth (Beynon et al., 1998), carpals (Beard et al., 1993), patellae (Ward et al., 1995), vertebrae (Ward et al., 1993), hand and foot phalanges (Begun et al., 1994), femora (Rafferty et al., 1995) and many other unpublished remains including several well-preserved feet. The new remains also allowed for better understanding of sexual dimorphism, body size and proportions (Rafferty et al., 1995; Ruff et al., 1989; Teaford et al., 1993; Walker, 1997; Walker et al., 1993). Based on observations of the metaphyseal margins and surfaces of the KPS femora, tibiae and ulnae, Duren (2001) concurred with many earlier interpretations that although it is evident that *Proconsul* was an arboreal quadruped, it is probable that the manner in which *Proconsul* moved in the trees, "may have been a unique form of above-branch quadrupedalism yet to be identified".

The new KPS finds provided the first opportunity to look at *Proconsul* life history. Beynon and colleagues looked at the life history of the Kaswanga *Proconsul* fossils by comparing dental development and microstructure (Beynon et al., 1998). The first molar crown assigned to KPS Individual IV shows 15 months of growth, making the individual 14 months old at the time of death (Beynon et al., 1998). According to the rate of root enamel deposition, the researchers were able to calculate the timing of permanent molar eruption for *P. heseloni*. Weaning, or the eruption of the first molar, occurred at 24-26 months, the crown of M2 was formed at 27 months, the crown of M3 was formed

at 43.5 months, and adulthood, or the completion of both crown and root of M3, occurred at 78 months or 6.5 years (Beynon et al., 1998). This pattern is consistent with the pattern of permanent molar eruption in rhesus macaques (Kenney, 1975). During this study Beynon and colleagues also identified microanatomical features of *Proconsul* enamel and dentine that resemble those in hominoids, with some that are unique to *Proconsul*. *Proconsul* tooth microstructure shares only one similarity with New and Old World monkeys: the cross striation repeat interval of 5 or 6 days between regular striae of Retzius (Beynon et al, 1998).

Primate Foot Notes: A brief survey of evolutionary research

Until the collection of non-human primate fossils gathered momentum, studies of foot evolution, ontogeny and functional morphology were relegated to those of humans with few comparisons with other taxa, usually great apes.

In one of the earliest works to compare human and non-human primate feet, Volkov noted the differences between feet of humans, apes, monkeys, prosimians, and species across all mammalian orders (Volkov, 1903, 1904). At the end of a treatise filled with numerous tables of metric data, he concluded that the feet of prosimians are probably much like those of ancient mammals and look like intermediates between primitive mammals and monkeys. Prosimian foot morphology, he concluded, is the result of a primitive arboreal adaptation which is why prosimian feet share similarities with those of some rodents. Volkov's goal was to describe the anatomy of the human foot, and as was unfortunately common at the time, he stressed the climbing characteristics that feet of "inferior races" share with apes. Furthermore, he observed that there are

anatomical traits particular to ethnic groups that are intermediate between the flat feet of apes and the proper, arched feet of humans like Europeans. A hundred years later, we have learned that the variation in modern human foot morphology is not due to degrees of evolutionary distance from apes or even to varying modes of bipedalism. It can be influenced by activity over an individual's lifetime and whether or not an individual regularly wears shoes (Barnicot & Hardy, 1955; Musiba et al., 1997; Trinkaus, 2005). An early description of this phenomenon is offered by Morton who wrote about his observations on the feet of a male champion sprinter. The athlete had 20% longer metatarsals than average as well as other "modifications throughout the foot structure, which conformed specifically with the mechanical requirements of that specialized usage" (p. 19, 1924).

Volkov's study was followed by many early studies on the function and evolution of the foot as a whole (Elftman & Manter, 1935; Gregory, 1920; Keith, 1923, 1929; Morton, 1922, 1924a;1924b, 1926, 1927; Schultz, 1926, 1930; Straus, 1927, 1949; Weidenreich, 1923).

It is no surprise that much of the pioneering work in comparative human anatomy and osteology focused on the human foot. As a functional unit, it is probably the most distinct from apes out of all the parts of the human postcranial skeleton because of its derived adaptations for bipedalism. The evolution of this unique morphology continues to perplex scientists today, and as Dudley J. Morton wrote in 1922, "It seems to the writer that the apparent impossibility of deriving the human, highly specialized terrestrial foot from a type similar to the modern and known arboreal foot of the anthropoid apes, has been largely responsible for the diversity of opinion among scientists as to the origin of

the human race" (p. 306, 1922). Without the aid of a fossil record, Morton speculated about the evolution of the primate foot. At the time, the common ancestor of apes and humans was thought to have evolved in the early Miocene, nonetheless he hypothesized that the foot of the common stock of apes and humans, "would have been of a generalized gorilloid type, intermediate between the modern chimpanzee and gorilla types, and with some macaque features" (p. 334, 1922). This prediction, as the subsequent pages and chapters will attest, has carried through to modern research since there is still a dearth of pedal remains from the crucial period of ape and human evolution between 18-5 Ma. Morton also emphasized the differences between "carrying the weight" between the hallux and the second digit like apes and carrying it over the third digit like monkeys (Morton, 1922, 1924).

With few exceptions (Gregory, 1920; Morton, 1924a; Schultz, 1926; Straus, 1927), these early works very rarely looked at the foot through ontogeny. When they did, they focused on fetal growth as compared to adults. Operating under a modified version of the then-prevalent Recapitulation Theory (like Volkov, 1904), Straus examined human fetal feet in search of evolutionary information. Based on his analysis of fetuses, he concluded that the feet of humans and other anthropoids are alike in the early stages of development but grow divergently into distinct adult forms (Straus, 1927). The only growth study reported in the paper, however, was on humans. The studies on monkey and ape fetuses were alluded to only. However Straus did list some observations about human fetal feet through ontogeny that can be compared to other primates and through postnatal stages of ontogeny: 1) the foot becomes relatively narrower, 2) The foot becomes shorter

relative to the hindlimb, 3) the leverage of the foot becomes greater, so that the power arm grows more rapidly than the load arm (Straus, 1927).

Probably the most useful study of the comparative anatomy of the primate foot is Schultz's 1963 analysis of the varying proportions of primate feet (Schultz, 1963a;1963b). He was the first to quantify the units of the foot, emphasizing the importance of interpreting the bones of the feet in concert instead of in isolation.

The evolution of the primate foot has been studied in detail thanks to the numerous discoveries of pedal fossils, especially in the latter half of the 20th century. Much is also known about the preservation of different parts of the skeleton from taphonomic studies of carnivore cave assemblages, both modern and fossil. Bones of the feet and hands are often preserved because they are small, abundant, and if eaten by a carnivore they are more likely to be preserved in scat than other consumed parts (Carlson & Pickering, 2003). Small foot and hand bones are often swallowed whole and even partially articulated (see references in (Carlson & Pickering, 2003)). Furthermore, ingested primate digits are often protected from digestive corrosion because they are covered in skin, ligaments and nails (Pickering, 2001). Foot bones are not only preserved in closed cave sites but also at closed sites like the in-filled trees and burrows on Rusinga Island, and this is, at least for *Proconsul*, probably due to a cheetah-like carnivore's distaste for feet (in (Walker, 2006)). Fortunately such a well-preserved body part as the foot is highly diagnostic for the Order Primates because of the revealing morphology.

All primates, aside from the modifications seen in orangutans, African apes and humans, have a semi-plantigrade grasping foot (Gebo, 1993). Furthermore, all living nonhuman primates have a grasping hallux which is apparent in fossil adapids and

omomyids and therefore evolved at least by the earliest Eocene (Dagosto, 1983; Dagosto, 1988; Decker and Szalay, 1974; Gebo, 1988; Gebo et al., 1991; Gregory, 1920; Simpson, 1940). This pedal adaptation has been allocated a major role in the evolutionary success of the Order (Cartmill, 1972; Cartmill, 1974; Gregory, 1920; Martin, 1968; Sussman, 1991; Szalay, 1977), making fossil foot remains diagnostic for reconstructing the origin of Primates in the Paleocene (Dagosto, 1988; Gebo, 1993).

It is also possible to reconstruct phylogenetic history within the Order Primates based on feet. The record of primate pedal remains spans the entire history of the Order (Gebo, 1993), and the modifications on the basic primate foot bauplan, and their implications for locomotor evolution, can be tracked through time.

Even before primates, from the very beginning of the mammalian fossil record, foot morphology is used to decipher lineages and track evolution. For example, specific adaptations in the foot (specifically on the astragalus (talus), navicular, and phalanges) for climbing and tree-dwelling in *Sinodelphys szalayi,* a skeleton from the Yixian Formation, China dated to about 125 Ma, indicate its close relationship with metatherians (including extant marsupials) rather than eutherians (including extant placentals) (Luo et al., 2003). Based on the diversity of mammalian foot morphology seen in the early Cretaceous, Luo and colleagues speculate that the arboreal and scansorial adaptations in the foot and the rest of the skeleton may have permitted the diversification of the earliest metatherians and eutherians as compared to their terrestrial ancestors.

Foot bones of some of the putative earliest primates, plesiadapiforms from the late Paleocene, exhibit traits associated with a grasping hallux. Bloch and Boyer (2002) have used evidence from a partial plesiadapiform skeleton, dated to about 55.5 Ma from the

Clarks Fork Basin, Wyoming, to argue the link between *Carpolestes* and the grasping Euprimates. They also use their findings to argue that arboreal, pedal grasping adaptations for terminal branch feeding are primitive for primates, contending with the alternative hypotheses that the Order Primates was founded by specialized leapers or visually directed predators. Their argument is based on the feet and ankles of *C. simpsoni*; the morphology of the entocuneiform (medial cuneiform), hallucal metatarsal, and hallucal distal phalanx are all consistent with a divergent and opposable hallux capable of a strong degree of abduction-adduction, which was well-adapted for strong grasping of small-diameter supports (Bloch & Boyer, 2002). Furthermore, their cladistic analysis, which spans the entire available postcranial skeleton, showed that *Carpolestes* and Euprimates (sample consisting of Eocene omomyids and adapids) evolved the specialized grasping foot from a common ancestor. Their most parsimonious explanation is that the primate adaptations for leaping and forward facing eyes must have evolved from a *Carpolestes*-like ancestor (Bloch & Boyer, 2002). The euprimates Bloch and Boyer examined in their analysis have been on record for many years. Tali of Paleocene and Eocene primates, like adapids with lemur-like tarsals and omomyids with tarsier and haplorhine-like tarsals, have been crucial to the reconstruction of early primate evolution (Decker et al., 1974; Gebo et al., 2001; Szalay, 1977; Szalay & Delson, 1979).

The oldest known postcranial anthropoid fossils are from the middle Eocene genus, *Eosimias* (Gebo et al., 2000). The tarsal and hallucal morphology of preceding omomyids is considered sufficient to link them evolutionarily to anthropoids (Szalay & Dagosto, 1988). *Eosimias* tali and calcanei share morphology with both prosimians and anthropoids. Joint morphology suggest the *Eosimias* foot was less stable in the inverted

position for grasping vertical supports, and was therefore probably involved in more horizontal locomotor behaviors than prosimians, like modern anthropoids. The primitive prosimian-like features portray its leaping ancestry. Gebo and colleagues (2000) used the tarsal morphology to support the hypothesis that the anthropoid lineage split early in the Cenozoic without relation to adapids.

Tali of the late Eocene anthropoid *Catopithecus* from the Egyptian Fayum shares apomorphic features with *Aegyptopithecus* and Miocene-Recent catarrhines (Seiffert & Simons, 2001). Combined with other dental and skeletal evidence, the ankle morphology of *Catopithecus* supports its position as a stem catarrhine.

Postcranial remains of the Oligocene catarrhines *Aegyptopithecus* and *Propliopithecus*, suggest that they were generalized arboreal quadrupeds lacking adaptations for terrestrial, arm-swinging, or suspensory locomotion.

Like early catarrhines, stem hominoids have also been characterized as arboreal quadrupeds, but there are some major differences between the Oligocene and Miocene taxa. One major difference in the foot is at the talar trochlea; *Aegyptopithecus* has parallel-sided trochlea while Early Miocene large hominoids like *Afropithecus* have trochlea that taper posteriorly (Leakey & Walker, 1997). In most postcranial features, *Afropithecus* resembles *Proconsul* (Leakey et al., 1988).

In 2004, Ishida and colleagues (2004) reported on a new *Nacholapithecus kerioi* skeleton from northern Kenya, dated to about 15 Ma. In many ways this skeleton is similar to modern apes and is interpreted to have adaptations for forelimb dominated arboreal activities. The *N. kerioi* talus is not as wedged as *Proconsul* but has a more prominent lateral trochlear rim. Like *Proconsul* the groove for the *M. flexor hallucis*

longus is deep indicating the foot was capable of strong grasping. Compared to *Proconsul nyanzae, N. kerioi* has very long pedal digits, mostly due to the phalanges (Nakatsukasa et al., 2003) and the long fifth metatarsal. The long pedal rays indicate to the authors that *Nacholapithecus* locomotion was specialized for forelimb-dominated arboreal positional behaviors, presumably because if it were more terrestrial and quadrupedal, one would expect the pedal digits to be shorter. They write that the same interpretation can be made for *Proconsul* yet suggest that *Nacholapithecus* is adapted for a substantially greater component of orthrograde behaviors than *Proconsul*. That is to say *Nacholapithecus* locomotor behavior emphasized vertical climbing, hoisting and bridging, similar to that reconstructed for the orangutan ancestor *Sivapithecus* (Madar et al., 2002).

The foot of the ancestor to great apes should have a talus that tapers posteriorly and a long hallux. Unfortunately, there are no pedal elements of the purported great ape *Morotopithecus* available to test whether or not it had ape-like feet. *Kenyapithecus* - a portion of which is called *Equatorius* by Ward et al., (Ward et al., 1999) - was probably a more forelimb-dominated ape with a propensity for terrestrial positional behaviors (McCrossin & Benefit, 1997; McCrossin et al., 1998; Sherwood et al., 2002), so it is expected the foot morphology would resemble that of chimpanzees or gorillas. So far the only described *Kenyapithecus* (*Equatorius*) pedal material is a robust hallucal metatarsal and a medial cuneiform with flat, restricted joint morphology suggesting to Ward and Duren (2002) that the hallux was habitually adducted. However, they do not discuss whether the hallux was more or less adducted than in living apes.

The *Proconsul* Foot

Le Gros Clark and Leakey (1951) were the first to report on *Proconsul* pedal elements. They gave a meticulous anatomical description of two tali and a calcaneus that articulates with one of them (C.M.H. 145 (talus) articulating with 146 (calcaneus) now known as KNM-SO 389/390 and C.M.H. 147 (talus) now called KNM-SO 392. They were cautious not to assume these bones belonged to *Proconsul*, but were clearly convinced they did. They indicated the limitations on any sweeping functional implications of the foot since they were working only with the two tarsals. However, they did make some broad observations.

The anterior portion, the relatively long talar neck and the morphology of the front of the calcaneus, does not show the "shortening that is characteristic of the modern large apes" (p. 91). Drawing on Morton (1924) they related this morphology to an extreme arboreal specialization which was not then believed to have been present in early ancestors of the Hominidae. Instead, the *Proconsul* tarsals resembled quadrupedal cercopithecoids who have this morphology to provide "an effective leverage from the heads of the metatarsal bones in movements of leaping and running" (p. 91).

Le Gros Clark and Leakey (1951) also pointed out that the particular orientation of the calcaneus under the talus, the angle and plane of the sustentaculum, and the manner of articulation between the sustentaculum and the talar head, all "show that the foot was held in a more everted plantigrade position similar to that of the cercopithecoid foot, and strongly suggests quadrupedal functions whether on the ground or among the branches of trees" (p. 91). But they pointed out that these hominoids were probably too

big to spend much time in the trees, which we now know is not necessarily true based on recent observations of great apes (Pontzer and Wrangham, 2004).

Furthermore, Le Gros Clark and Leakey added that the strong ligamentous attachment sites to the talus and calcaneus and the deep excavation of the cuboid facet show that, like cercopithecoids, the *Proconsul* foot was "designed for bearing strains and stresses associated with rapid running movements, rather than for the greater mobility required for specialized arboreal habits" (p. 92). Overall, the joints are stronger and more rigid, especially in full dorsi-flexion when the ankle is locked, and this, they said, "would permit resting in a relaxed squatting position, with the ankle fully dorsi-flexed, and it would also make possible sudden and rapid leaping movements from this position of rest" (p. 92).

As was understandable for the time, Le Gros Clark and Leakey (1951) used the opportunity to address the evolution of bipedalism. "The posterior position of the basal tubercle of the calcaneum [sic] and the backward extension of the main facet for the talus appear to indicate that if *Proconsul* occasionally raised itself on its hinder extremities like the modern Pongidae, it was able to throw its weight back more towards the heel, and thus to balance itself in the erect posture more effectively" (P. 92). The authors are careful not to imply that *Proconsul* is necessarily an ancestor of the Hominidae, but they still thought it probable that the human foot may have been "more readily derived" from a foot like *Proconsul* than from a foot like any of the living great apes.

In 1951, while doing a geological survey of Gumba Peninsula of southwest Rusinga Island, Whitworth discovered bones in a vertical pipe of fine green tuff, which he called an "in-filled pothole". He speculated, based on the large accumulation of

mammalian fossils inside, that animals may have been trapped there when they went for a drink. Of course, it is now known that the pothole at site R114 was a fossilized, in-filled tree trunk (Walker, 2006). Regardless of the geologic interpretation at the time, Whitworth discovered the first and only partial skeleton of *Proconsul.* Originally this skeleton (KNM-RU 2036) was referred to as the "Gumba specimen" and it was placed in *P. africanus,* but now it is placed in the similar species *P. heseloni.*

Napier and Davis (1959) described the skeleton which included some pedal remains. At this initial stage there was a medial cuneiform, first metatarsal with phalanges, one sesamoid bone and fragments of other metatarsals, phalanges, with some epiphyses. Later Walker and Pickford (1983) found additional components of the skeleton, including foot bones. The authors included only an anatomical description of the pedal remains, with scant functional interpretations. They did note, however, that the foot was adapted for arboreality citing evidence from the widely divergent hallux, short medial cuneiform, medio-laterally compressed metatarsals, and flat, non-expanded middle phalanges (Napier & Davis, 1959).

Inspired by Straus' research in 1927, Lisowski (1967) was one of the first to apply the accumulating knowledge of human foot evolution towards the analysis of Miocene-Pleistocene fossils including hominids. In his comparisons he found that *Proconsul* used its foot more like monkeys and apes than humans. However, he claimed the same for the *Homo habilis* foot which is widely considered to have bipedal adaptations (Day & Napier, 1964). Many years later it was discovered that what Lisowski had labeled "*Proconsul*" fossils were really those of *Theropithecus* (relatively recent fossil baboons) (Alan Walker, pers. comm.), which would explain the strong similarities to monkeys.

Day and Wood (1969) analyzed the controversial tali from Songhor and Rusinga and concluded that their ape-like morphology warranted their placement as fossil hominoids. Four years later Wood reassessed his evidence by adding Old World monkeys to the comparison (the previous study used only humans and apes) (Wood, 1973). He reported that the Rusinga tali are more similar to the quadrupeds *Papio* and *Cercopithecus* than they are to *Gorilla*, *Pan*, *Colobus* or *Pongo* (Wood, 1973). However, the Songhor talus (KNM-SO 389) did not cluster with any extant group so he suggested it to be a separate species from Rusinga, a finding that other researchers, with more evidence, would later corroborate.

Preuschoft, one of the pioneers in applying biomechanical principles to the interpretation of fossil anatomy, wrote about the available *Proconsul* foot bones at the time (which included at least seven tali and at least four calcanei of *P. nyanzae* and *P. africanus*, as well as the hallucal complex from the *P. heseloni* skeleton KNM-RU 2036) (Preuschoft, 1973). The middle phalanx of RU 2036 shows adaptations for maximal forces in flexion rather than extension of the interphalangeal joints, which is a feature of all primates that is more marked in arboreal ones than terrestrial ones. He notes that the morphology of the RU 2036 hallux is rather ordinary for primates who walk quadrupedally with an abducted hallux and also adduct it for grasping during climbing (Preuschoft, 1973). Since the joint surface on the head is broad on the dorsal side but narrow on the plantar side, the hallux is built to withstand the greatest stresses in extension rather than in strong flexion (Preuschoft, 1973). At this time, with the fossils available, Preuschoft makes it explicit that no solid conclusions about posture and locomotion can be determined from the feet.

An expert on mammalian hand and foot anatomy, Lewis contributed to the dialogue on primate and *Proconsul* foot evolution, first with a study of the hallucal joint at the medial cuneiform (Lewis, 1972), then with a series of studies on the joints (Lewis, 1980) and later with a book (Lewis, 1989). As was the goal of many of his predecessors and successors, Lewis's aim was to reconstruct the evolution of the bipedal human foot. Because hominid fossils were the focus, quite often his comparative sample for interpreting *Proconsul* was comprised only of great apes and humans. Lewis illuminated some important features of the *Proconsul* tali and calcanei. For instance, the cuboid surface of the smaller *Proconsul* calcanei most closely resembles *Pan* in the degree of excavation. However, he suggests that the larger ones belonging to *P. major* resemble larger apes like *Pongo* and *Gorilla*. In general he concludes that *Proconsul* tali and calcanei show arboreal adaptations. They are primitive when compared to extant knuckle-walkers *Pan* and *Gorilla,* but possess the appropriate morphology to be excellent candidates for the ancestor of great apes.

In the early 1980s, Walker and Pickford (1983) realized that there were *Proconsul* bones still in blocks of matrix from site R114 in storage at the National Museums of Kenya. They reported on newly found components of the *P. heseloni* skeleton KNM-RU 2036 from preparation of these rocks as well as on newly discovered *P. nyanzae* remains from locality R1-3 on Rusinga. Both finds included numerous foot bones. Napier and Davis (1959) had already described the medial cuneiform, first metatarsal, some phalanges, and other fragments of the right foot of RU 2036, but Walker and Pickford were able to add a nearly complete calcaneus, talus, and most of the navicular. In addition, much of the left foot was found together in a block of matrix which included

most of the calcaneus, the talus, the navicular, and all three cuneiforms, nearly complete first, second and third metatarsals, fragments of the fourth and fifth metatarsals, and several parts of phalanges including the proximal phalanx of the hallux.

The new *P. nyanzae* foot (KNM-RU 5872) included all the tarsals, midtarsals and metatarsals in varying degrees of preservation, with some of the phalanges as well. At this time, they were able to document the observable size difference between *P. nyanzae* and *P. heseloni* (then *africanus*) postcrania, yet they did not discover any proportional or morphological differences between the species (Walker and Pickford, 1983). Later Conroy and Rose found *P. major* showed no differences either (Conroy & Rose, 1983). Regarding foot morphology, Walker and Pickford (1983) observed a pattern of hominoid-like features consistent with that of a generalized arboreal quadruped. They emphasized the indicators on the fibula and hallux for a strong *M. flexor hallucis longus* for strong grasping and climbing capabilities, like in *Pan.* Their observations contradicted the consensus at the time, based on interpretations of the forelimb, that *Proconsul* was most like New and Old World monkeys. These new foot and hindlimb remains reported by Walker and Pickford (1983) illuminated for the first time the provocative mosaic of features in the *Proconsul* skeleton. They characterized this condition as a "gradient of features along the limb such that features that are more hominoid-like are found more proximally. In the hindlimb the gradient is reversed, with more hominoid-like features more distally" (p. 350).

Right on the heels of Walker and Pickford, in an in-depth study aimed specifically at feet, Conroy and Rose (1983) also concluded that the *Proconsul* foot was an "all-purpose tool for use during a wide range of general arboreal activities". Although it is a

mosaic of anthropoid pedal characteristics, they argued that the *Proconsul* foot is a gracile version of an African ape foot, while sharing many tarsal and digital joint similarities with generalized arboreal New and Old World monkeys. Other features of the proportions, the calcaneocuboid joint and the hallux, suggest the foot was used for a range of climbing and suspensory activities like those employed by some cebids and some great apes (Conroy& Rose, 1983). So in general, the *Proconsul* foot lacks specializations, particularly for partial terrestriality seen in the feet of some monkeys and apes, which is consistent with the mosaic and generalized nature of the rest of the *Proconsul* postcranium.

In a survey of most known Miocene hominoid foot fossils at the time as well as some fossil cercopithecoids, Langdon (1986) analyzed the functional morphology of the *Proconsul* foot. Based on comparative anatomy, he concluded that the *Proconsul* foot has adaptations for both monkey-like pronograde quadrupedalism and ape-like grasping and climbing. He noted that this reconstructed behavior is similar to that of atelines, yet the bones of the *Proconsul* foot do not share many specific traits with atelines.

After Langdon's work, the Kaswanga Primate Site was discovered, providing morphologists with even more *Proconsul* material, particularly pedal remains. Strasser (1993) worked on the proportions of the nearly complete foot skeleton of *P. heseloni* (KNM-RU 2036) from Rusinga as well as the KPS feet, as compared to colobines, cercopithecines, and apes. (She did not include New World monkeys - perhaps for phylogenetic or sampling reasons.) In a paper that was presented at a conference but never published, Strasser concluded that *Proconsul* is similar to colobines and apes in different respects. It is colobine-like in the relative length of its tarsus, the ratio of power

arm to load arms, and the relative lengths of its metatarsals and phalanges (Strasser, 1993). For its body mass, *P. heseloni* is most similar to colobines in the lengths of the third metatarsal, third proximal phalanx relative to foot length, in the ratios for the third proximal phalanx to the third metatarsals, and the relative length of the first metatarsal to the third metatarsal. Strasser found that the *P. heseloni* hallucal proximal phalanx is ape-like (hylobatid-like in particular) in proportions, having longer hallucal components than similarly-sized cercopithecids.

Bacon analyzed the ankle (distal tibia) of *Proconsul* and suggested that the orientation of the tibial internal malleolus indicates climbing activities close to that of many small-sized platyrrhines and cercopithecoids (Bacon, 1994). However, he also found, in the same analysis, that the rotational component of the knee is intermediate between monkeys and great apes. He concluded that the movements of the *Proconsul* talocrural and knee joint were consistent with load-bearing and grasping functions, but did not show any of the specialized features of climbing that are seen in some New World monkeys, *Pan,* and *Gorilla*.

Rose re-entered the *Proconsul* discussion in 1994 (Rose, 1994). Because by this point nearly the entire skeleton of *Proconsul* was known, researchers were able to make much wider comparisons to other fossil and extant taxa as well as make much more specific interpretations of the morphology (although, aside from Strasser's abstract, the KPS feet were not included in any analyses and, as they remained unpublished, they garnered little attention until now). Rose stressed traits of the feet that indicated above branch quadrupedal locomotion rather than suspension, like the absence of the plantar process on the heel of the calcaneus which is the site of origin of part of the short digital

flexor, indicating the lack of adaptation for independent toe grasping while the foot is plantarflexed in suspensory activities (Sarmiento, 1983 in Rose, 1994). Rose also stressed the cebid-like traits in the *Proconsul* foot: a long and narrow tarsal region with relatively long metatarsals. The talocrural, subtalar, and transverse tarsal joints all indicate mobility associated with quadrupedal locomotion and with conforming the foot to the surface, but their morphologies fall short of allowing the kind of movement associated with suspensory activities (Rose, 1994). Like Walker and Teaford (1989), he agreed that *Proconsul* was a predominantly arboreal quadrupedal primate that moved deliberately with a plantigrade foot. Although there are many differences between *Proconsul* and modern orangutans, Rose referred to Cant's (1987 in Rose, 1994) observations of orangutans and his suggestion that *Proconsul* may have moved by horizontal quadrupedal clambering with the trunk held vertically. Rose offered his thoughts on what the postcranial mosaic of *Proconsul*: "One has to imagine for *Proconsul* a style of quadrupedalism somewhere among those of a pygmy chimpanzee utilizing palmigrade hand placement, and atelid not using its prehensile tail, and an arboreal cercopithecid, in an animal with the proportions and degree of limb elongation of the latter" (p. 407). However, now that it is clear *Proconsul* did not have a tail (Nakatsukasa et al., 2004; Ward & Walker, 1991), one would expect more suspensory adaptations to be evident in the skeleton, especially in the feet, than are present.

Later, Ward (1998) concurred that *Proconsul* feet were most likely used in climbing and grasping and postulated they were not used nearly as extensively in suspensory or bridging activities. She also helped describe a partial skeleton of *P. nyanzae* that included a right talus and calcaneus (KNM-MW 13142 C and B) (Ward et

al., 1993). She observed, as did her predecessors with other *Proconsul* fossils, a powerful grasping hallux, evident by the large grooves on the talus and calcaneus for the flexor hallucis muscle and a large fibula where the hallucal muscles originate. The talocrural joint is generalized, or relatively unspecialized, but the "fairly deep trochlear groove, together with cup-shaped medial malleolar facet and deep pits for the attachment of the deltoid and talofibular ligaments, suggest that mediolateral stability during flexion and extension at this joint was of greater importance in *Proconsul* than in modern African apes" (p. 108). Ward and colleagues suggested that the talocrural joint of *P. nyanzae* is primitive for catarrhines and indicates arboreality. They came to a similar conclusion for the mobile subtarsal and midtarsal joints of the specimen, which all together point to a pattern of generalized arboreality lacking morphological specializations seen in either cercopithecoid or hominoid feet (Ward et al., 1993).

Begun and colleagues (1994) identified 224 separate manual and pedal phalanges in the KPS *Proconsul* collection. The authors observed that the pattern of differences between *Proconsul* manual and pedal phalanges is monkey-like rather than ape-like, but that the manual and pedal grasping features (i.e. generally wide and shallow articular surfaces) were well-developed compared to those of extant generalized arboreal quadrupeds (Begun et al., 1994). They also noted that the KPS pedal phalanges are quite stout and slightly curved. This morphology caused them to conclude that *P. heseloni* was a cautious, slow-moving but powerful arboreal quadruped capable of powerful grasping of horizontal and vertical supports. Later, after *Nacholapithecus* hallucal phalanges were discovered, Nakatsukasa et al. (2002) compared them to other East African fossil

hominoids as well as extant anthropoids. They found, in accordance with Begun et al. (1994), that *Proconsul* has an especially long hallucal proximal phalanx.

Clearly, the *Proconsul* foot has enjoyed much attention over the past 50 years and one may wonder if there is anything left to be said about it. But never before has there been such a collection of fossil primate foot bones (prior to the middle Pleistocene record of fossil baboons and humans), ranging in ages from infant to adult, with some discovered articulated and preserved in their entirety, as the one analyzed in the following pages. Furthermore, no one has analyzed the cross-sectional properties of the metatarsals of any fossil primate before, and such a study should give much deeper insight as to the function of the *Proconsul* foot.

With the exceptions of *Nacholapithecus* from about 15 Ma, *Kenyapithecus* (*Equatorius*) from 14 Ma, and *Afropithecus* from 18-17 Ma there are very few hominoid pedal remains to compare with *Proconsul* in the East African fossil hominoid record. Outside of Africa, the only known pedal remains of mid to late Miocene hominoids are both rare (*Dryopithecus* (Begun, 2002)) and unusual (*Oreopithecus* (Szalay & Langdon, 1986)).

The 13-12.5 million year old partial skeleton of the hominoid *Pierolapithecus catalaunicus* from a site near Barcelona, Spain has some preserved tarsals and fragmentary metatarsals, as shown in the photograph of the specimen; however, they are not discussed in the only publication to date (Moyà-Solà et al., 2004). It will be very interesting to learn about the foot anatomy since the rest of the *Pierolapithecus* postcranium is a mosaic made-up of mostly great ape components: the craniofacial

characteristics link it to living apes; the ribs and lumbar vertebrae indicate it had a broad thorax and a short, rigid lower back; the wrist bones are built for mobility like modern brachiators. However, the short hand phalanges, with palmigrade characteristics, are monkey-like and not similar at all to the hooked phalanges of extant apes.

Until additional fossils are found from the middle-late Miocene of East Africa, *Proconsul* will continue to serve as the foundation for studies of the evolution of the hominoid foot including the transition to bipedalism.

Chapter 2

BACKGROUND

Even though the *Proconsul* skeleton is a mosaic of morphological features and that it is likely that its particular form of quadrupedal progression was unlike any extant anthropoid (Rose, 1994), the comparative method is still a powerful approach and it is employed in the analysis here. In order to apply the functional morphology of the feet of living taxa towards interpreting *Proconsul* pedal fossils to reconstruct positional behavior, it is important to appreciate the varieties and similarities in positional behavior of the extant catarrhine subjects used in the study.

Catarrhine Positional Behavior: A review of the extant comparative sample

How each species locomotes and uses its feet and lower limbs in postures will be reflected in its foot morphology. Here the positional behaviors are reviewed for the primates used in this study and a summary is located in Table 2.1. The ceboids and baboons were used only in the comparative anatomy portion of Chapter 3 because specimens were available at the National Museums of Kenya. All the rest of the taxa discussed here were used in the quantitative analysis of proportions. Only macaques (*Macaca mulatta*), chimpanzees (*Pan troglodytes*), and gorillas (*Gorilla gorilla gorilla*) were used in the ontogenetic component of proportions analysis - a consequence of available samples. Only *M. mulatta* and *P. troglodytes* were included in the cross-sectional geometry analysis - a consequence of available imaging equipment.

Table 2.1. Body masses, locomotor categories and foot positions of taxa in the comparative collection, grouped at the genus level. Body masses are averaged by female (F) and male (M). Locomotor substrates are designated arboreal (A) and terrestrial (T), and it is important to note that most, if not all, primates prefer to sleep in the trees when possible.[1]Fleagle (1999). [2]Rowe (1996). [3]Gebo (1993).

Superfamily	Species	Common name	Body Mass[1] (kg)		Locomotor Substrate[1,2]		Foot Position[3]
			F	M	Travel	Feed	
Ceboidea	*Ateles paniscus*	black spider monkey	8.44	9.11	A	A	semi-plantigrade
	Alouatta seniculus	howler monkey	5.21	6.69	A	A	semi-plantigrade
Cercopithecoidea	*Colobus guereza, C. angolensis**	black and white colobus	9.2	13.5	A	A	semi-plantigrade
	*Colobus badius**	red colobus	8.2	8.36	A	A	semi-plantigrade
	Macaca mulatta	rhesus macaque	5.37	7.71	T	A/T	semi-plantigrade
	Papio anubis	olive baboon	13.3	25.1	T	A/T	semi-plantigrade
	Nasalis larvatus	proboscis monkey	9.82	20.4	A	A	semi-plantigrade
Hominoidea	*Hylobates lar*	white-handed gibbon	5.9	5.349	A	A	semi-plantigrade
	Gorilla g. gorilla	western lowland gorilla	71.5	170.4	T	T/A	plantigrade
	Pan t. troglodytes	common chimpanzee	45.8	59.7	T	A	plantigrade
	Pan t. schweinfurthii	common chimpanzee	33.7	42.7	T	A	plantigrade
	Pan paniscus	bonobo	33.2	45	T	A	plantigrade

Ceboids

The atelines *Ateles* and *Alouatta* are almost exclusively arboreal (Rose, 1996). They are considered below-branch suspensory primates with long prehensile tails that aid in suspension and feeding. Their limb and trunk morphology is similar to apes (Fleagle, 1999). Spider monkeys, *Ateles*, are known to leap, tail-arm brachiate, and pronograde climb through their high canopy habitat of the rainforests of Central and northern South America, but quadrupedalism and suspensory behaviors are their normal

modes of travel (Cant, 1986). Howlers sit on or suspend beneath branches in the lower portion of central South American forests. On the move, they combine quadrupedalism with climbing and bridging (Cant, 1986). They tend to range just below 100 (or equal) in terms of intermembral index so their hindlimbs are hardly longer than their forelimbs. *Ateles*, on the other hand, ranges slightly above 100 (Fleagle, 1999). The increase in forelimb length in *Ateles* is correlated to increase in versatility of forelimb use (Rose, 1996).

Cercopithecoids

Cercopithecoids are generally larger than Ceboids and contain groups that display varying locomotor modes including arboreal, suspensory, and terrestrial. The terrestrial cercopithecoids include rhesus macaques and baboons. Macaques are almost totally quadrupedal walking and running creatures. They engage in very little leaping and only very rarely hang suspensorily from their hindlimbs during feeding (Fleagle, 1999). *Macaca mulatta*, the rhesus monkey, is considered terrestrial in comparison to other cercopithecoids and con-generics like the more arboreal *M. fascicularis.* Rhesus monkeys feed arboreally and are native to the range between Afghanistan- India and Thailand-southern China (Rowe, 1996). Baboons, native to sub-Saharan and South Africa, are some of the most terrestrial cercopithecoids, spending most of their time on the ground, but climbing trees to sleep or avoid predators (Fleagle, 1999; Rowe, 1996). These terrestrial cercopithecoids have slightly longer hindlimbs than forelimbs. The non-hallucal metatarsals of cercopithecines project with similar distances so that ground

reaction forces can be better diffused and share more equally across the metatarsal heads (Strasser, 1992).

Colobines have a reduced second digit to better oppose the hallux while grasping branches (Strasser, 1992). All colobine monkeys are arboreal quadrupeds, living in the main canopy levels of forests. They are more arboreal than cercopithecines (e.g. *Macaca mulatta*), occasionally employ suspensory maneuvers, and are also better leapers. Monkeys of the *Colobus* genus are specialized leaf-eaters in sub-Saharan Africa. *Nasalis larvatus*, or the proboscis monkey from the mangrove swamps of Borneo, is the most sexually dimorphic of all colobines, with males being almost twice the size of females (Fleagle, 1999). *Nasalis* is known for its frequent suspensory behavior. Proboscis monkeys are adept climbers, leapers and even swimmers (Fleagle, 1999).

According to Gebo (1993), "all of the highly arboreal recent Old World monkeys are secondarily arboreal" and this must have occurred very recently in time because few arboreal adaptations are obvious in the foot. Colobines display some rare modifications for increased arboreality in their elongated fourth digit, increased size of the flexor digitorum longus muscle, and elongated posterior calcaneal facet (Gebo, 1993; Strasser, 1988). Old world monkeys must have begun arboreal, then experienced a terrestrial phase during which they lost their long toes and much of the mobility in the foot joints, and then re-entered the arboreal niche very recently (Gebo, 1993). Fossil evidence supports this explanation with ancestral Old World monkey *Victoriapithecus* - dated to 16-15 Ma from Maboko Island, Kenya - showing terrestrial adaptations in digitigrade hands and feet, including a reduction in the ability to abduct the hallux (Harrison, 1989).

Hominoids

Hylobates lar, white handed gibbons from Indonesia and south Asia, are the most suspensory of all primates. They are also the least sexually dimorphic of the hominoids (Fleagle, 1999). They move through the trees almost exclusively by two-armed brachiation and by quadrumanous climbing in between brachiating bouts. When on the ground, they walk bipedally, but it is rare. Gibbons have very high intermembral indices, with very long arms and hands, and very short legs and feet.

The African great apes, existing mostly in regions of west and central Africa, are the most terrestrial of the hominoids. Those employed for this study are *Gorilla gorilla gorilla* (the western lowland gorilla), *Pan paniscus* (bonobo), and *Pan troglodytes.* When walking quadrupedally, they all walk on the knuckles, or non-hallucal middle phalanges, of their forelimb both on the ground and on horizontal tree-branches. These apes have longer arms than legs, landing just above equal on the intermembral index.

With the largest body size, gorillas are the most terrestrial. Gorillas often feed on vegetation on the ground, as opposed to exploiting food sources in the trees like the smaller-bodied chimpanzees and bonobos. In large part due to body size, gorillas nest on the ground, as opposed to chimpanzees and bonobos who build sleeping nests in trees. When moving about arboreally, gorillas, bonobos and chimpanzees use both quadrupedal and suspensory locomotor behaviors. Although slow deliberation characterizes the majority of gorilla climbing bouts, the large apes are capable of very fast high-energy arm-swinging, like the displays or fleeing behaviors of chimpanzees and bonobos. The frequency of arboreal behaviors, especially for gorillas, depends upon the size of the trees that accommodate them. When chimpanzees or gorillas climb tree trunks, they usually

keep their feet under them as opposed to up on the side (Tuttle, 1986). Large, non-compliant vertical supports like tree trunks demand large-bodied apes have a robust divergent hallux for strong grip (Hunt, 2004).

Much more of the African ape foot anatomy has been studied than the other non-human primates, because of its aid in interpreting the evidence for the evolution of the human foot and bipedalism. African apes and humans are the only primates with plantigrade feet, with which they strike the ground with the lateral heel. All other primates walk with a raised heel in a semi-plantigrade posture when moving quadrupedally (e.g. Gebo, 1992, 1993; Meldrum, 1991; Morton, 1924a; 1924b; Susman, 1983; Tuttle, 1970; Weidenreich, 1923). This adaptation is probably related to terrestriality (Gebo, 1993) and is possibly an accommodation for increased body size and larger ground reaction forces in the foot. Chimpanzees will often curl their toes under when walking (Goodall, 1965; Langdon, 1986), which may cause a difference in plantar pressure distribution, especially at the metatarsal heads.

Chimpanzees use their feet in a variety of ways aside from its obvious weight-bearing and locomotor role (both on the ground and in the trees). As a grasping organ, feet are used to bend, break and hold branches while feeding and while building nests (Goodall, 1962). The chimpanzee foot is adapted primarily for powerful grasping with some accommodations for terrestrial activities (Tuttle, 1970). Overall the foot is long and narrow with a short mid-tarsal region. The hallux is long, abducted and strong, and opposes long curved lateral toes.

Bonobos use their feet in very similar ways during similar behaviors to those of common chimpanzees. However, they are considered by many to more arboreal (Doran,

1993) and have even been observed to hang solely by their feet (Patterson, 1979). They are also said to walk with a more inverted foot, so that more of the lateral portion of the foot is in contact with the ground than in common chimpanzees (Patterson, 1979). However, bonobos are poorly habituated and the scant amount of observational data on terrestrial postures may not correlate to real ecology, especially since their diets include a significant amount of terrestrial vegetation (Doran, 1993; Malenky et al., 2004). Because of its implications for foot use, it is worth noting the difference between bonobos and chimpanzees in substrate choice. When moving through the trees, chimpanzees favor trunks, while bonobos use boughs and branches more frequently (Doran, 1993). Data on the structural properties of the tree species and how they may differ between habitats, however, has not been reported.

Gorilla feet display more terrestrial adaptations which may just be an artifact of the larger body size, which in cyclical fashion correlates with more terrestriality. Grasping abilities exist in the gorilla foot, but are compromised so that gorillas use their feet less frequently for grasping tools than do chimpanzees and bonobos (Tuttle, 1970). Feet are hardly used for feeding or food acquisition. Shorter, less curved toes relative to chimpanzees and bonobos make it comparatively difficult for gorillas to grasp. In fact, the lateral digits are often webbed up to the first inter-phalangeal joint, making these toes even shorter functionally (Fleagle, 1999). The gorilla hallux, although still long and capable of opposition, is short and less abducted. There are subtle differences between the feet of the two subspecies of gorilla. Mountain gorillas have further projecting and more adducted halluxes than western lowland ones (Schultz, 1930). Habitats for mountain and lowland gorillas are distinct enough to warrant such morphological

differences, because the montane habitats of mountain gorillas offer fewer climbable trees compared to the rainforests that lowland gorillas inhabit (Hunt, 2004; Remis, 1995). Overall the gorilla foot is broad and the heel is large for weight-bearing like in humans, which, combined with the less abducted hallux, is why many researchers have compared early hominid foot fossils to gorillas. However, despite our current understanding of molecular genetics placing chimpanzees as our closest relatives, it is important to point out that gorillas probably evolved "human-like" feet in response to mechanical and behavioral changes associated with an enlarged body size, whereas relatively small-bodied hominids evolved human-like feet to walk bipedally and attained large body size later. Both experienced an increase in the ground reaction force through the hindlimb: one by walking upright and one by gaining body size.

Significance of Ontogenetic Studies

Growth series in the primate fossil record are uncommon and are mostly represented by cranial and dental remains of fossil hominids. Postcranial growth series are even rarer and no growth studies have been performed on the fossil primate foot.

Unusual opportunities to glimpse life history traits of fossil species are significant for evolutionary studies because changes in phenotype occur through changes in growth and developmental processes (Gould, 1977) beginning with the first cell division. Ontogenetic data can also provide information on sociality and life history. For instance, the pattern and scheduling of tooth eruption indicates how long a primate suckles before it can eat an adult diet, which in turn is correlated to the length of the mother-dependent juvenile period, which in turn is correlated with the period of learning, which in turn is

correlated to intelligence. Attainment of sexual maturity and patterns of sexual selection in primates can be tracked through canine eruption (Cheverud, 1981; Leigh et al., 2005). Also, relative rates of hominoid body size growth may correlate to behavioral and ecological demands or risks such as feeding and mate competition (Leigh & Shea, 1995, 1996).

In a similar fashion, perhaps behavioral stages can be determined from the functional morphology of the growing postcranial skeleton. During the time it takes an animal to develop adult limb proportions, it can experience locomotor patterns that differ from how it will behave as an adult. It is possible that immature postcranial proportions and morphology may be adapted for particular age-specific locomotion and positional behaviors.

In order to distinguish between Old World monkeys and apes in the fossil record, Kelley (1997) suggested we define their life history profiles more precisely. In order to understand why phenotypic changes have occurred, it is imperative we study the patterns of growth and development where these phenotypic shifts take place. Beynon and colleagues began this endeavor with the Kaswanga *Proconsul* fossils by comparing dental development and microstructure (Beynon et al., 1998). In the present study, the foot and hindlimb proportions and metatarsal mechanics are studied through ontogeny.

All primates experience ontogenetic changes in locomotor behavior because primates are relatively altricial at birth; they are not precocial like a horse's foal that is capable of walking like an adult minutes after birth (Portmann, 1990). Humans are the best-known example of this phenomenon, spending the first several months relatively

incapable of self-propulsion, the next few crawling and then, around one year of age, adopting bipedalism.

A very practical goal of ontogenetic studies of primate bones is to search for and evaluate the kinds of information we can glean from immature primate fossils. Many important specimens in the primate fossil record, especially along the hominid lineage, are immature (e.g. KNM-ER 15000, the Nariokotome *Homo erectus* juvenile). Ontogenetic studies help determine the kinds of inferences about the phylogeny or behavior of extinct primates that we can realistically make based on juvenile fossils. Much of these interpretations are based on whether ontogenetic data indicate the fossils grew similarly or differently from extant taxa. A frequent result of ontogenetic analysis of fossils is that the extinct species grew up in a unique way that is similar to not one, but a variety of comparative taxa, for a variety of reasons.

Besides providing behavioral and phylogenetic information, ontogenetic studies can also reveal possible developmental constraints on morphological change (Alberch, 1990). They have the potential to distinguish between traits that are discretely contributing to an adaptive complex, from those that participate in the complex simply because of linked developmental pathways (Lovejoy et al., 1999). In other words, ontogenetic data can elucidate which features are biologically independent and which are biologically linked, which is particularly important for features comprising functional complexes like the foot.

Until the migration, proliferation, and genetic controls of all the cells in various primate embryos are mapped, the best we can do through osteology and paleontology is to track the changes that occur in the skeleton along the way to adulthood. One

complication of this approach may be that if bone prioritizes growth over locomotor adaptations in immature individuals, some or all behavioral signatures particular to an age-specific behavioral repertoire may be impossible to detect in an immature skeleton. This, of course, assumes that age-specific behavior will be reflected in the immature skeleton in the first place.

All of these issues present challenges for interpreting evolutionary and behavioral evidence from a fossil with a unique suite of traits that may have behaved unlike anything known today. The comparative method, combining data from behavior, bones, and genes, will continue to provide solutions to these problems. In the present study, the feet and hindlimbs of six *Proconsul* individuals ranging in age from infant to adult are compared to cross-sectional growth series of three taxa: rhesus macaques (*Macaca mulatta*), chimpanzees (*Pan troglodytes*) and western lowland gorillas (*Gorilla g. gorilla*).

Rhesus Macaque Growth and Locomotor Ontogeny

Much is known about the life history and growth and aging of rhesus macaques (e.g. Cheverud, 1981; DeRousseau, 1985a; DeRousseau, 1985b; Gavan, 1967; Smith, 1994). Wells and Turnquist (2001) observed the ontogeny of locomotion in the free-ranging colony of rhesus macaques at Cayo Santiago. They linked early postnatal changes in locomotion to their prior study on the development of the musculoskeletal system (Turnquist and Wells, 1994). By the time juveniles reach 18 months their locomotion is fully adult-like.

The ontogeny of limb mass distribution in baboons (*Papio cynocephalus*) was later studied by Raichlen (2004). Although he found that baboons experience a

faster transition from dependent to independent locomotion during development than macaques, his results are useful in terms of macaque foot and hindlimb ontogeny. Since functional demands placed on the limbs during ontogeny impact strongly the development of limb mass distribution patterns (Raichlen, 2004), they most likely also affect the robusticity of the long bones, including the metatarsals.

Chimpanzee and Gorilla Growth and Locomotor Ontogeny

Like macaques, chimpanzees and gorillas have been studied intensively and much is known about their life history and growth. Ages of life history stages are well-documented for weaning (Pusey, 1983), locomotor independence (Doran 1997), menarche (Goodall, 1986; Pusey, 1990), first birth (Goodall, 1986; Nishida et al., 1990), male growth completion (Goodall, 1986; Pusey, 1990), female growth completion (Leigh & Shea, 1995), and interbirth interval (Goodall, 1986; Nishida et al., 1990). The two subspecies of gorillas differ in habitat and locomotor profiles. Much more is known about mountain gorilla (*G. g. beringei*) ecology and behavior because the lowland subspecies (*G. g. gorilla*) is poorly habituated to human observers (Hunt, 2004).

Growth in body size, skeletal development and ossification, and timing and patterns of tooth eruption have also been well-documented for chimpanzees and gorillas (Kuykendall, 1996; Kuykendall and Conroy, 1996; Leigh and Shea, 1995; Leigh and Shea, 1996; Schultz, 1926; Schultz, 1960; Smith, 1994; Taylor, 1997; Winkler, 1996).

Chimpanzee infants cling to their mother's bellies by their hands and feet (Goodall, 1965), however gorilla infant feet may not be capable of grasping as mothers must support clinging infants (Fossey, 1983). Goodall observed juvenile chimpanzees to

be much more adept arborealists than adults (Goodall, 1965), perhaps because the habitat at Gombe National Park is relatively open woodland. In general, juveniles and females are more suspensory than adult males, which is at least partially, if not mostly, due to the larger body size of males.

Like macaques, little is known about how morphological changes during chimpanzee and gorilla ontogeny correlate with behavioral changes and furthermore, how they influence one another developmentally. Doran has tracked the ontogeny of locomotor behavior and substrate use in chimpanzees and gorillas (Doran, 1992; Doran, 1997). She found that chimpanzees reach locomotor independence after age five and mountain gorillas after age 2.5 with roughly adult-like locomotion achieved by age 4 (Doran, 1997). Gorilla juveniles achieve near complete use of knuckle-walking (99.7% of the time in quadrupedal locomotion) between ages 2-5 years. Chimpanzees use the behavior less often and by age 2 70% of their quadrupedal activity is knuckle-walking (Doran, 1997).

Inouye (1992, 1994) tracked the changing morphology of the metacarpals in chimpanzees and gorillas to assess the process by which they adopt knuckle-walking behavior. She determined that during ontogeny, chimpanzees use their fifth digit consistently less often than the other ones when knuckle-walking. Gorillas, she found, use all digits (2-5) in knuckle-walking throughout ontogeny. Body size may drive the early adoption of knuckle-walking in gorillas, but differences in ontogeny of locomotion may also be influenced by chimpanzee use of a wider variety of substrates as juveniles.

These modern models will be used to identify and interpret characteristics of the anatomy, proportions and cross-sectional properties of *Proconsul* foot bones in order to better reconstruct its locomotion and positional behavior. Knowledge about how ontogeny of locomotion in extant primates will be useful for linking patterns of growth and development in the foot and to life history traits in the modern sample and in *Proconsul*.

Chapter 3

TARSALS AND METATARSALS OF *PROCONSUL HESELONI* FROM THE KASWANGA PRIMATE SITE, RUSINGA ISLAND, KENYA

The fossils described here were collected in 1984 and 1985 at the Kaswanga Primate Site (KPS) on Rusinga Island in Lake Victoria, Kenya, by joint field expeditions from the National Museums of Kenya and the Johns Hopkins University (Walker and Teaford, 1988).

The Kaswanga Primate Site (KPS)

The KPS was discovered by Bwana Peter Nzube while the teams were excavating "Whitworth's Pot-hole", which turned out to be hollowed-out and in-filled tree trunk, at nearby site R114 (Walker & Pickford, 1983). The KPS is located at 34°09' East, 0°24' South near Kaswanga on the northern set of exposures at Kaswanga Point and is about 110 meters ESE of the Kenya Government meteorological station (Fig. 3.1). The exposures are part of locality R5 which was identified by Le Gros Clark & Leakey (1951) as a "Red Band in upper part of Kathwanga Series" at Luanga. Since then Andrews & Van Couvering (Andrews & Van Couvering, 1975) and Pickford (1986) have collected there.

The fossils from the KPS, found both on the surface and *in situ*, come from the Fossil Bed Member of the lower Hiwegi Formation, which at Kaswanga Point dates to the later Early Miocene at 17.8 Ma (Drake et al., 1988). This most recent study of the Rusinga geochronology suggests that the KPS is roughly 2 Ma younger than the *Proconsul*-producing deposits at Songhor and Koru. The fossils at Kaswanga come from

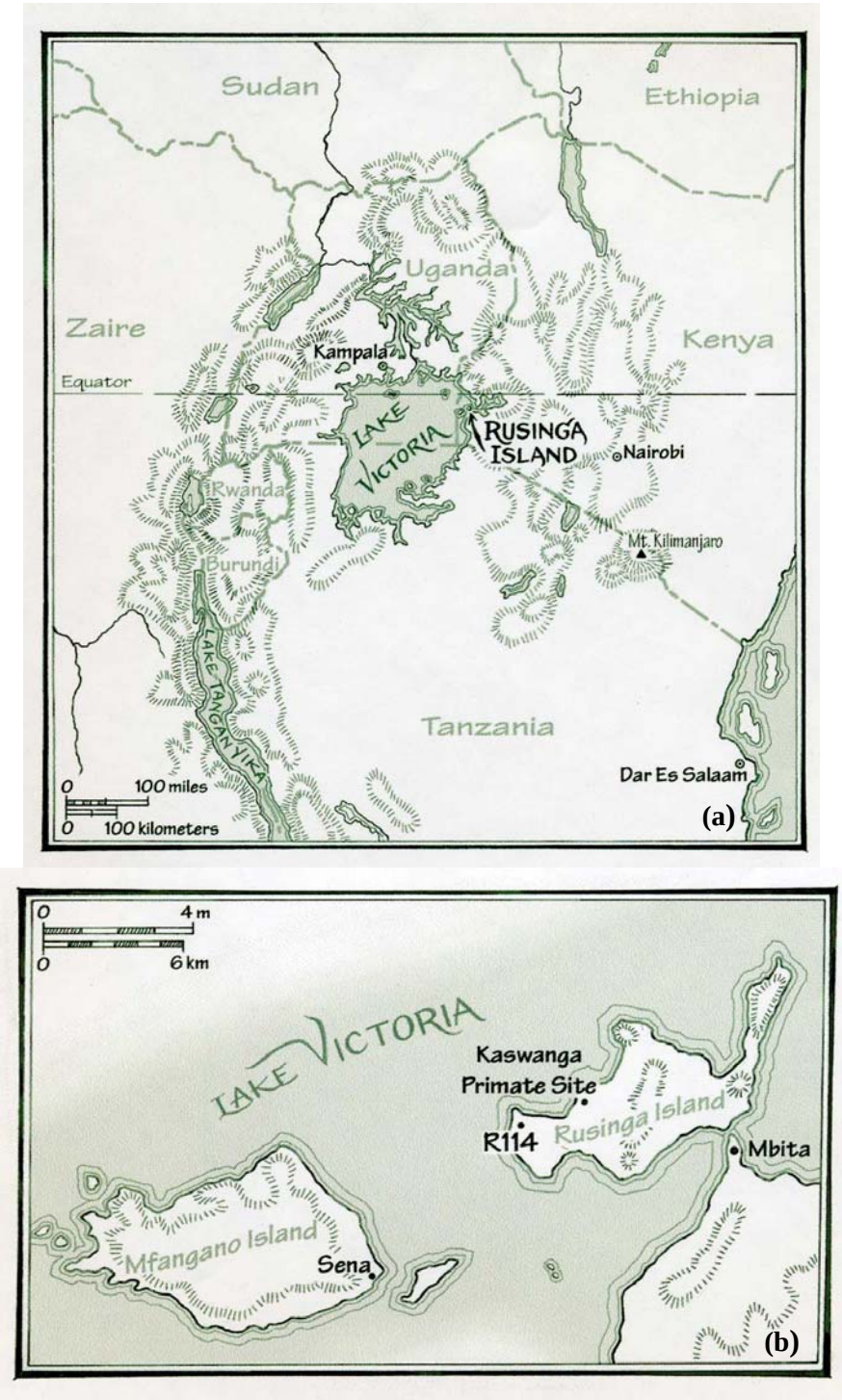

Figure 3.1. Map of Lake Victoria region in East Africa (a) and a closer view (b) of the Kenyan waters of eastern Lake Victoria containing Mfangano and Rusinga Islands, showing locations of site R114 and the Kaswanga Primate Site (KPS). m = miles. From Walker & Shipman (2005).

an infilling of Fossil Bed Member silts into a steep but shallow channel or burrow cut into the Grit Member of the Hiwegi Formation (Van Couvering & Miller, 1969) making a disconformity between the two units (Walker & Teaford, 1988). There is no proof to support the interpretation that the feature was a burrow. The in-filled matrix with bones is less compacted but identical to the surrounding rock and the features were filled with low-energy sedimentary fine-grained tuffaceous silts and clays containing *Proconsul* and other small mammal remains (Walker, 2006). Leaves and fruits were restricted to the tops of the feature (Walker, 2006). The channels were probably filled in one brief slumping episode, and as a result some of the *Proconsul* body parts were found in articulation (Walker, 2006). The bones excavated from the deepest parts of the feature, although numerous, were all disarticulated with epiphyses also separated, so there is no reason to assume anything other than post-mortem association between the individuals (Walker, 2006). Further information on the excavation as well as the site plan can be found in Walker (Walker, 2006).

Some of the KPS *Proconsul* fossils were excavated *in situ* and their three-dimensional positions plotted (e.g. KPS III and IV feet). However, the KPS paleosols are full of clays which shrink and swell in dry and wet conditions causing many of the fossils to break apart into tiny pieces. In order to collect many of the bone fragments, sediment was washed through mosquito netting in Lake Victoria. After the painstaking process of identifying and gluing the tiny broken bits together, the collectors were able to determine that a minimum of ten *Proconsul* individuals were represented: two subadult males with all epiphyses unfused and M3s only as germs; three adult females; two subadult females, one with epiphyses fused by epiphyseal line showing and the other not as well developed;

one juvenile with M1s erupted and M2s and M3s still only as germs; one infant with dm1 erupted and dm2 still only as a germ. For a complete list of the bones and teeth from the KPS see Walker (2006). The individuals were sorted by several methods. First, some parts of the skeletons were still articulated *in situ* (III and IV), and pieces recovered through screening and washing were glued directly to them. Other bones were sorted by size, color, manganese staining patterns, ossification stage or age, congruency of articulation or interstitial facets, similar distortions, and mirror-imaging (Walker, 2006). The specimens were marked with one small dot each of water-soluble colored paint according to the individual to which they belong.

Taphonomy

The KPS Individuals are mostly represented by isolated teeth, fore-and hind-limbs, more pelves than shoulder girdles, and hands and feet that are often articulated, but with very few vertebrae and ribs. Walker (2006) determined that this pattern of postcranial preservation is consistent with the remains left by cheetahs that were fed baboon carcasses (Brain, 1981). There were no cheetahs yet at this time in the Miocene, so we can imagine a small-jawed, cheetah-like carnivore, or a medium-sized hyaenodontid creodont was responsible for the *Proconsul* bones. The lack of appreciable mammalian fossils occurring at this site aside from two small lagomorph partial skeletons suggests this carnivore specialized in hunting *Proconsul* (Walker, 2006).

Age, Sex and Grouping of the Individuals

Individual I is considered a male because of its size; it is even larger than Individual III which is fully mature. The immature states of many of the epiphyses

indicate that it is a subadult. Based on the stages of ossification of the navicular, calcaneus, and metatarsals, this individual is roughly similar in development to a 2-4 year old rhesus macaque and a 6-7 year old chimpanzee.

The feet of Individual III were discovered articulated *in situ*, so their preservation is exceptional. Because it is an adult, all the epiphyses are fully ossified and fused including the metatarsal heads.

The teeth assigned to Individual IV (particularly its upper first molar crown) show that it died before weaning at about 14 months, which is before eruption of M1 at 24-26 months (Beynon et al., 1998). The foot bones were found associated *in situ*. The anterior end of the calcaneus is concave with a cuboid facet, not convex and bulbous like in baby apes. The *Proconsul* infant also has sharper, more delineated facets on the talus and calcaneus than *Pan troglodytes* of the same dental age. However, at a similar dental age, *Macaca mulatta* has similar joint development and other similarities to the infant *Proconsul* as well: the calcaneal tuber is fusing, the navicular is formed, but the posterior protuberances on the talus are not. The joint surfaces are better developed than chimpanzees of the same dental age.

The tarsals of Individual VI are similar to those from IV and are therefore, along with indicators from associated limbs and teeth, assumed to belong to an infant.

Overall size and lack of epiphyseal fusion indicate Individual VII is immature. However, there are no teeth in association with or assigned to the postcranial remains to aid in aging. Foot bones were grouped based on size and development. There are also some metapodial heads and some indeterminate metatarsal fragments with this individual.

No teeth are associated with Individual VIII, but it is definitely a subadult. The heel has just fused, and if aged like a chimpanzee, based on the calcaneus, it would be older than 7 and probably at least 9. In that case it would have all its permanent teeth but the third molars and canines would still be descending.

Descriptions of KPS Tarsals and Metatarsals

The following descriptions are restricted to the preservation and morphology of the tarsals and metatarsals. The phalanges have already been described (Begun et al., 1994). Researchers should be forewarned that some of the foam cut-outs at the National Museums of Kenya in Nairobi that hold the fossils tend to group left bones with right feet and vice versa. Because they are small bones of the feet, researchers also tend to redistribute the bones into the incorrect places in the foam.

In many cases, distortion was assessed by comparing the KPS bones with non-distorted ones belonging to the type *P. heseloni* skeleton KNM-RU 2036. All measurements are in millimeters unless otherwise indicated. To simplify the descriptive passages, some measurements for the metatarsals are condensed together in Table 3.1 and those for the intermediate and lateral cuneiforms are condensed in Table 3.2. Appendix A provides an explanation of the abbreviations used for the measurements throughout. A summary of overall morphological trends is discussed separately following the descriptions.

Table 3.1. Lengths in millimeters of metatarsals (MT1-MT5) of the KPS Individuals. MT4L is not available for any of the specimens. Measurement abbreviations are listed in Appendix A.

Specimen	MT1L	MT1D	MT2L	MT2D	MT3L	MT3D	MT4D	MT5L	MT5D
KPS I (right)	43.1	39.7		50.2		51.2	52.2		42.2
KPS I (left)	42.9	38.9		48.5		53	53.4		
KPS III (right)	43.5		54.2		58.4		53.6		53.3
KPS III (left)	46.2		56.9		59.5		57.7		
KPS IV (right)		25.4							
KPS IV (left)	28	24.7	36.5	32.5		32.4	33	33.1	30.5
KPS VII (right)									
KPS VII (left)		29.3					45.8		
KPS VIII (right)	43	39.1		52.7		51.8	49		
KPS VIII (left)	43.1	39.6		52.7		48.6	54.5		

Table 3.2. Measurements in millimeters of intermediate (ICun) and lateral (LCun) cuneiforms of the KPS Individuals. Measurements for KPS I (ICun and LCun only) were taken on casts.

Specimen	ICun1	ICun2	ICun3	ICun4	LCun1	LCun2	LCun3	LCun4
KPS I (right)	9.3	6.8	7.8	8.3	11.0	11.3	8.7	7.1
KPS I (left)					12.1	11.3	9.7	6.6
KPS III (right)	8.1	7.4	7.5	7.0	10.3	11.0	9.4	7.3
KPS III (left)	8.1	7.4	7.4	6.5	10.7	11.0	9.1	7.2
KPS IV (right)	5.0	4.9	5.4	4.9				
KPS IV (left)					7.8	7.9	5.8	5.0
KPS VII (right)	6.8	5.2	5.6	3.9	8.1	10.6	6.5	5.1
KPS VII (left)					9.4	10.3	7.0	6.3
KPS VIII (right)	9.2	7.3	7.3	7.6	11.2	11.8	9.6	7.0
KPS VIII (left)	9.3	7.7	7.0	7.1	11.3	11.1	8.1	6.2

Individual I: Subadult Male (Violent Pink; Figure 3.2)

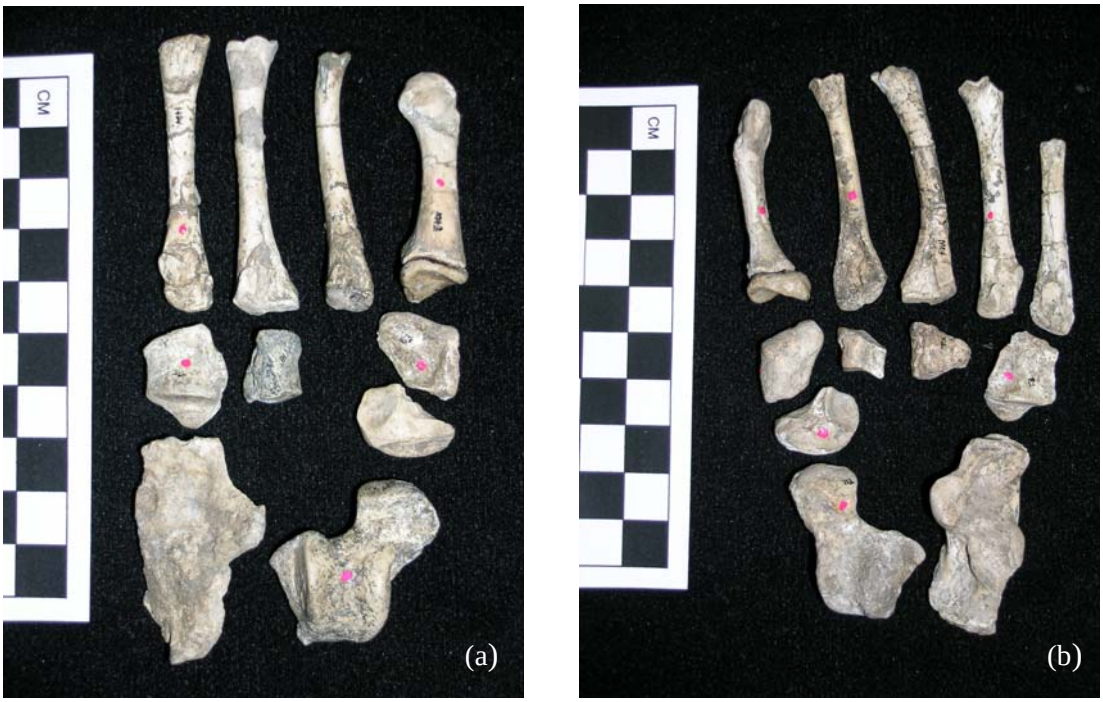

Figure 3.2. Left (a) and right (b) tarsals and metatarsals of KPS Individual I. Photographs are not scaled to one another, but scale of each is in centimeters.

Right Calcaneus - T13 This fossil is complete and compressed in the dorsoplantar plane. The length is 41.2 and the greatest width across from the sustentaculum tali is 23.1. Just plantar to the peroneal tubercle, running from the heel to level with the anterior-most part of the posterior talar facet, the surface is crushed about 2-3 deep on the plantar/lateral side of the posterior body. A bit of surface bone is chipped away at the posterior lateral margin of the posterior facet as well as at the distal corner of the anterior facet and on the dorsal surface proximal to the cuboid facet.

The cuboid facet is compressed dorsoplantarly, but still holds its crescent shape with the opening facing medioplantarly. The dorsal margin is thicker than the plantar one. The pit for the attachment of the cuboid ligament is evident. The mediolateral length is 14 and the dorsoplantar length is 9.7. The dorsal surface just proximal to the cuboid joint is

concave both mediolaterally and proximodistally, with the deepest area located just at the base of the posterior facet.

The anterior talar facet is very thin and barely visible along the medial border of the distal sustentaculum tali. It connects to the much larger, oval-shaped middle facet, however the distal margin of the middle facet is still well-delineated. It is 10.7 long and 7.9 wide (mediolaterally) at its greatest and faces slightly distally.

The posterior facet has a crack running proximodistally on the lateral half, which does not disturb its morphology. The facet is tear-drop shaped with the apex located proximally, delineated by a raised border. The most distal margin has no raised border and connects nearly perpendicular to the body here. The distance from proximal to distal margin is 17 and the greatest breadth is 11.8.

The dorsal half of the posterior body is characterized by a sharp crest running from the posterior talar facet to the heel a distance of 9.1 from the posterior-most margin of the posterior facet to the heel. Looking at the crest superiorly, the pit for the lateral calcanal-fibular ligament can be seen on the concave lateral side, while the medial side has a convex superior portion but becomes concave plantarly. The rough epiphyseal surface shows that the tuber is unfused. The greatest height at the tuber calcanei is 18.4 and the greatest breadth is 9.7. The dorsoplantar axis of the tuber is rotated about 40 degrees laterally relative to the long axis of the bone.

The peroneal tubercle is present but merges with the damage adjacent to it on the plantar side. It appears to extend into a keel that separates the dorsal portion from the plantar portion of the anterior body.

The groove for the *flexor hallucis longus* is prominent but obviously compressed to appear smaller than in life. The ridge under the sustentaculum tali runs from the very end of the bone to just beneath the posterior edge of the posterior facet. The ridge itself is shelf-like in that it is flat on the side for the tendon and rounded underneath as it joins with the body. The corresponding edge of the groove on the plantar side of the sustentaculum tali is marked by a nearly invisible indentation. The greatest breadth of the groove between the ridge and the indentation is about 4.9. The underside of the sustentaculum tali is concave. Measured from this side it is 13.8 long proximodistally and protrudes 6.4 from the ridge below. The anterior tubercle is present as a cylindrical mass oriented proximodistally.

Left Calcaneus – T12 This fossil has been strongly compressed dorsoplantarly. Furthermore, the entire dorsal part of the posterior body is sheared off down to the level of the sustentaculum tali. Thus the specimen is nearly two-dimensional. All articular surfaces are gone. The length is 42.3 and the greatest breadth is 25.1.

The cuboid facet is lost but the width of the region can be measured at 15.6. The groove for the *M. flexor hallucis longus* is visible but the ridge that runs 17.8 long is abraded and its mate on the underside of the sustentaculum tali is imperceptible. The sustentaculum tali measures 14.3 proximodistally and protrudes about 9 from the groove's ridge below. Despite the damage, the dorsal surface of the sustentaculum tali is oriented distally like its antimere.

The small bit of tuber that is visible at the dorsal edge is not fused. The anterior or plantar tubercle is barely visible. There is a slight depressed fracture on the lateral plantar

side that is similar in size and location to the damage seen in the antimere. Basically aside from several millimeters of surface on the plantar side and the distal dorsal region, the entire specimen is severely abraded.

Right Talus – T11 This talus is complete and has been compressed dorsoplantarly. The trochlear ridges are leaning medially with the highest being the medial one. (Without deformation one expects the crests to be nearly even in height and leaning neither medially nor laterally.) The surfaces of the plantar portion of the head as well as most of the anterior calcaneal facet have been lost. The medial edge of the head has been roughly abraded. Most of the surface bone of the trochlea is abraded. The medial tubercle is absent.

The maximum length (Ward et al., 1993) is 30.7 and the total, diagonal length from the tip of the head to the proximolateral corner of the trochlea is 36.6. The length of the trochlea is 18.6 from proximal to distal and the breadth of the ridges at their highest is about 9. At a glance, the trochlear ridges appear parallel because of the deformation, but with a closer look it is evident that they taper proximally. The groove for the *M. flexor hallucis longus* is present but not discrete due to the loss of the medial tubercle.

The lateral malleolar facet is like a rounded rectangle, the only sharp corner being the most lateral point that juts out. The entire dorsal half of the surface is abraded. The remaining lateral surface is concave. The proximodistal length is 18.1, the height is about 16. It is difficult to measure the protrusion because of the deformation of the trochlea. Just proximal to the facet is a very shallow pit for the talofibular ligament.

Most of the medial malleolar facet has been lost but the attachment site for the deltoid ligament is visible.

The talar neck is 10.8 at its narrowest point. Despite the missing parts of the articular surface of the head, the width and height are 14.3 and 11.6 respectively. The navicular articular surface is dorsally oriented to compensate for the raised heel posture and hence downward orientation of the articulated calcaneus and talus. The attachment for the talonavicular ligament is difficult to see entirely due to abraded bone and some unremoved matrix, but it extends from the dorsal part of the anterior trochlear "saddle" region up to the navicular facet for about 10.3. It is also hard to assess the depth of the sulcus tali because of the deformation and the loss of the medial edge that connects to the lost medial tubercle. What is present has a sharp and crescent shaped proximal lip. Only a strip of the lateral anterior calcaneal facet is left which is slightly convex and measures 11.3 long and 4.1 at its widest mediolaterally. The posterior facet is 4.9 across the sulcus tali from the anterior facet. It is mostly present minus a bit chipped away at the medial border. The surface of the facet is abraded and is only smooth at the distal end. It is concave and 17.5 long in the proximodistal direction. The distal region of the facet spills over onto the anterior surface near the trochlea since it abuts against the deep dorsal surface of the calcaneus in eversion.

Left Talus – T10 This talus is complete but deformed. The square length is 30.7 and the diagonal length is 36.7. It has been compressed dorsoplantarly without visible affect on the trochlea. The medial side of the head is pinched dorsoplantarly into a sharp crest that extends along the entire medial side, becoming the lip on the sulcus tali and extending

around to the most proximal, or posterior, part of the talus. This pinching event appears to have drawn out the anterior facet medially, thus widening the sulcus tali. The head is 16.8 wide and 9 high. The narrowest width of the neck is 12.8 and is low around the proximal margin of the medial malleolar facet.

As in the antimere, the anterior calcaneal facet is abraded. Its medial distal half is gone, along with part of the navicular articulation on the head. The proximal lateral surface is intact. Five across the sulcus tali the posterior calcaneal facet is concave, rectangular, about 17.7 long and abraded on the proximal half.

The attachment site for the talonavicular ligament is not filled with matrix as in the antimere so one can see that it is fairly deep, at least 3, with a length of 10.5 and a width of 4.9.

The trochlea is 19.8 long, 16.8 at its widest and 12.7 from ridge to ridge at the most superior point. The ridges only slightly taper proximally. The lateral ridge protrudes more distally while the medial ridge protrudes more proximally. The rounded distal end of the medial ridge merges to form a rounded ridge with the distal margin of the medial malleolar facet. This facet is deformed medially because of the pinched crest. Proximally, the pit for the deltoid ligament attachment is present despite appearing compressed.

The lateral malleolar facet is damaged on the plantar/lateral edge. The compression event created a fault line running proximodistally and pushed the lateral portion of the facet upward so that there is no longer a smooth slope down from the ridge; there is a sharp shelf instead. The facet appears to take up the entire lateral side of the

talus because of the abrasion on the proximal end. The groove for the *M. flexor hallucis longus* is present.

Right Navicular – T5 It is complete and only slightly damaged. The greatest mediolateral length is 18.5. The proximal-distal width at the midpoint is 6. There is a crack running mediolaterally along the articular surface for the medial cuneiform. Just plantar to the facet for the intermediate cuneiform there is a linear pit bordered by the prominent lip on the planter edge of the facet for the lateral cuneiform. The talar facet is preserved nicely, keeping in mind that the medial side is not fully developed. It is shaped like a tear-drop with a squared-off apex. It is encircled by a discrete margin except for directly proximal to the lateral cuneiform facet where it becomes the facet for the cuboid and slopes away to join the medial lip of the lateral cuneiform facet. The plantar joint of these two surfaces forms a peak. The facet for the lateral cuneiform is bordered on the plantar and dorsal sides by a raised lip. It is rhomboidal. The medial edge measures 6, the lateral is 7.8, the dorsal is 8, and the plantar is 6.7.

Left Navicular – T6 This navicular is complete and also not fully developed medially. Furthermore, the medial end is slightly pinched dorsoplantarly in the same plane as the talar head with which it articulates. Both the preserved cuneiforms articulate properly with this bone despite the deformation. The length is 18.9. The thickness of the middle is 7.4, lateral is 5.4 and medial is 5.8. The dorsal surface between the proximal and distal facets is a large linear pit. The facet for the lateral cuneiform is large and square with the dorsal side rounded. The dorsal edge, measuring 8.3, is also flush with the surrounding

bone while the other margins are delineated by a raised lip. The plantar edge, measuring 6.6, joins with the small facet for cuboid which joins the large talar head facet. The medial and lateral edges measure 6.3 and 5.6 respectively. The talar facet is shaped like a tear drop with clear margins all around except where it joins with the small cuboid facet. It is 16.4 long.

Right Medial Cuneiform – T15 It is complete and totally undistorted. A small bit of the medial plantar edge of the navicular facet has been abraded away. The length at the middle is 12.7. The width of the distal end is 14.8 and the proximal end is 10.5. The superior margin of the hallucal facet is not bordered by a lip; it is flush with the surrounding bone. The hallucal facet is not as s-shaped as the other KPS. It also lacks the plantar distal tubercles, just below the margin of the metatarsal facet, that are present in adults. The length and width of the navicular facet are 10.5 by 7.2. The length and depth of the facet for the second metatarsal are 5.1 by 7.8.

Left Medial cuneiform – T9 This bone is flattened mediolaterally resulting in a small navicular facet that is 8.7 long and 4.4 wide. It is 12.8 long at the middle. The plantar side is completely, unnaturally flat and has been abraded. The facets are visibly deformed although mostly complete. The distal and proximal widths are15.9 and 9.9 respectively.

Right Intermediate Cuneiform – T7 Like the neighboring right medial cuneiform, this is a complete and undistorted bone. The edges, delineating the articular facets, are sharp.

The pock mark on the dorsal surface may be excavation or preparation-induced trauma. It articulates well with the right navicular and the right medial cuneiform.

The non-articular surface is roughly a square shape with the medioproximal corner jutting away at less than a ninety degree angle from this quadrilateral. The anteromedial facet is present and well defined. The posteromedial facet is somewhat abraded but still visible as an arc along the side of the proximal facet. The lateral facet is not well-defined but a smooth surface for the lateral cuneiform is present. The distal facet is generally flat with slight elevation towards an apex where the plantar corner of the distomedial facet meets its margin, making a raised corner. The proximal facet is concave and triangular.

Right Lateral Cuneiform - T1 The plantar ridge or projection is damaged leaving only half of the concave distal and convex proximal facets intact on the body. The tip of the plantar tubercle is broken. This region is much deeper than it antimere. In general, it looks like this bone has been abraded on all edges although remnants of the lateral facets are visible.

Left lateral cuneiform – T16 The left one is more complete and far less damaged than the right. Both distal and proximal facets are complete; the distal one being triangular and concave and the proximal being square and convex. The distal edge of the plantar ridge is missing although the bulk of the tubercle is perfectly intact. The lateral facets are present. The posterior one is a rounded square and takes up half the length of the lateral side up until that side juts slightly laterally. This element articulates well with the left navicular.

Right Cuboid – T3 This cuboid is complete but almost two-dimensional in the mediolateral plane because of dorsal-plantar compression. The only exception to the flatness is the dorsal edge of the calcaneal facet which retained much of its integrity, helping it articulate with the right calcaneus. The main features of the bone are still visible, however. The medial and lateral lengths are 13.4 and 11.2. The distal and proximal widths are 10.8 and 15.1. The thickness or depth of the medial side of the distal end is 5.4. The overall length is 19.9.

Left Cuboid – T4 Like its antimere, this one is compressed dorsoplantarly, but not as severely. The overall length is 19.4. Its medial and lateral lengths are 15.1 and 10. The distal and proximal widths are 13.3 and 14.5. The thickness at the medial side of the distal end is 8.3. The proximal projection for articulation with the pit on the calcaneus is strong.

Right MT1 - MT14 Although complete, the diaphysis and head are compressed dorsoplantarly. The cortical bone has collapsed into the medullary cavity down the dorsal side making a gutter. The epiphysis is present, but it is unfused and totally undeformed, but it still fits onto the shaft well. The tuberosity is forming on the epiphysis, more so than in Individual VII. There are two breaks across the shaft.

Left MT1 - MT2 The epiphysis is present, unfused and undeformed or damaged aside from a small bit missing on the lateral-plantar edge. The shaft is complete but

flattened dorsoplantarly with one major fracture through the middle. Two large pieces are missing: one on the proximal plantar side and one on the dorsal part of the head where it has been compressed.

Right MT2 - MT12 It is complete apart from missing its head which had not fused with the shaft. Some surface bone on the medial side of the distal shaft is gone. The proximal end is compressed mediolaterally but facets are still present. Some of the cortical bone of the shaft is missing on the medial side above the dorsal facet for the medial cuneiform. The facet for the medial cuneiform is absent. There are two fractures across the shaft.

Left MT2 - MT8 This bone is complete and relatively undeformed. There are breaks at one and two thirds across the shaft. The epiphyseal surface is present but the head is unfused and absent. All facets are present and complete. Some bone has been lost distal to the medial facets. The shaft is curved medially at the distal shaft towards the absent head. The head, if present, would be oriented to face slightly laterally.

Right MT3 - MT4 This bone shows very little deformity. It is lacking the unfused head and only the plantar part of the epiphyseal surface remains. There are four fractures through the shaft. All facets are complete and present.

Left MT3 - MT7 It is slightly compressed mediolaterally at the proximal end. The shaft is not compressed. There is a fracture through the midshaft. The mediolaterally

compressed epiphyseal surface is visible but the head is neither fused nor present. On the lateral side of the distal end, there is a missing piece of bone. All facets are complete.

Right MT4 - MT6 The head is unfused and missing. There is no deformation, although there are three fractures through the shaft. The plantar and dorsal surface bone of the distal shaft is damaged and chipped away. All facets are complete and present.

Left MT4 - MT1 The proximal end is compressed mediolaterally. All facets are present and complete. The head is also compressed and as a result the surface bone at the distal shaft is damaged. But most of the diaphysis resisted the force and is still oval in section. There are three major fractures through the shaft. The epiphyseal surface is complete, albeit flattened. The head is neither present nor fused.

Right MT5 - MT3 The shaft is broken twice, at about one third and two thirds of the shaft. The proximal end is flattened mediolaterally. There is a clear facet for the fourth metatarsal that articulates well with it. The epiphyseal surface is gone, so the diaphysis is not complete, and the epiphysis is not fused or present.

Individual III: Adult Female (Purple; Figure 3.3)

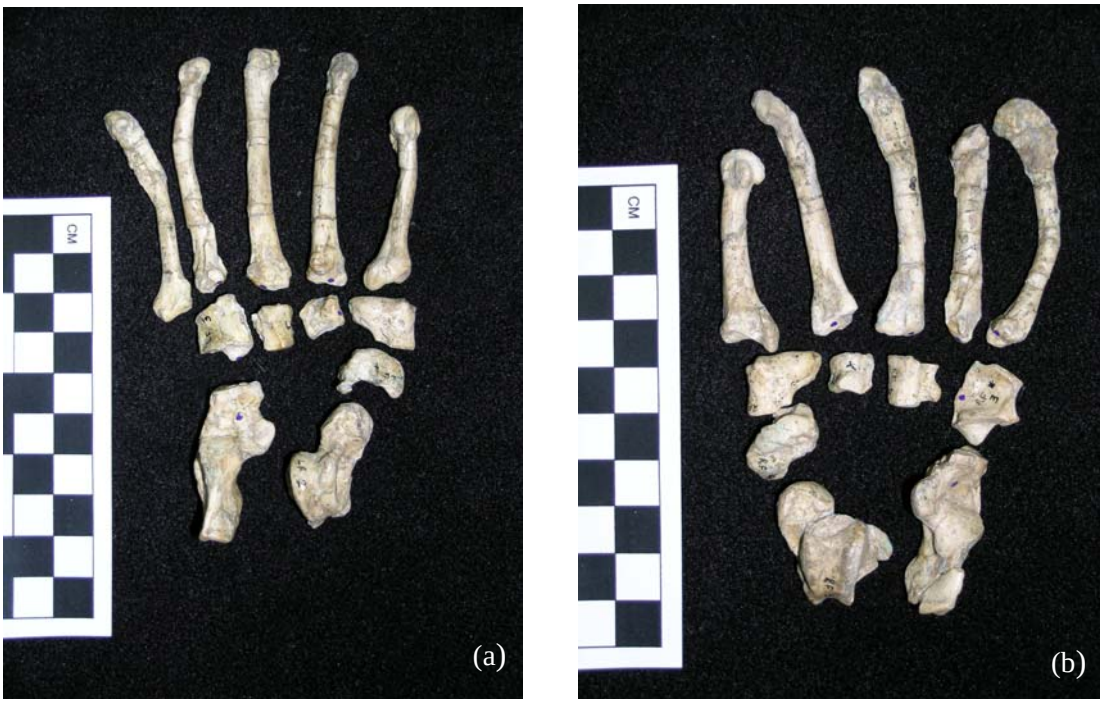

Figure 3.3. Left (a) and right (b) tarsals and metatarsals of KPS Individual III. Photographs are not scaled to one another, but scale of each is in centimeters.

Right Calcaneus -RF1 This calcaneus is basically complete and shows no signs of deformity, but has small pieces of bone missing in places. About 2.5 from both the medial and lateral tips of the cuboid facet are broken away. The top half of the posterior portion broke right at the indentation in the heel that marks the edge of the Achilles tendon attachment. This piece was glued on and is 9.7 high at the heel, 8.2 long across the dorsal crest and 11.6 in total length. Because of this damage, the medial and lateral edges of the tuber are jagged and abraded. The width of this joint is 13.4 and the height is 8.3.

Inside the crescent-shaped cuboid facet the pit for the attachment of the cuboid ligament is deep, about 3.5. It is oriented superiorly, about 17 degrees from

perpendicular. The dorsal surface just proximal to the cuboid facet is cup-shaped, that is it is concave in all directions with the deepest part just distal to the root of the posterior facet.

Most of the anterior talar facet was lost with the medial tip of the cuboid facet, but the part that is visible appears to be connected to the middle facet by a very narrow bridge. The middle facet is bean-shaped and is 7.5 long by 4.9 wide.

The posterior facet, which characteristically sweeps around the posterior body facing first distally then medially, is 3.5 from the sustentacular facet. The distal facing portion is mostly flat but the rest is unevenly convex as it bends around medially until the most proximal edge faces proximally. All the margins are discrete raised edges except the distal one which rises out of the dorsal concavity. It is 12.6 along its length and 10 at its widest perpendicular to the sagittal axis. The superior or dorsal margin has been lost, probably due to the same incident that caused the large break just proximal to it.

The dorsal surface proximal to posterior joint has formed a sharp crest. Because of the large piece missing on the lateral side just plantar to the crest it is impossible to see the nature of the surface, but the medial side slopes away with concavity first and then convexity as one moves plantarly from the crest.

The total height of the tuber is 16.8 and the width is 8.7. The bottom of the tuber surface is a rounded square. Total height was taken from this edge to the top despite the fact that it is not quite perpendicular to the bone's long axis. Because of the loss of bone, it is difficult to quantify the torsion of the heel relative to the anterior portion. The medial tubercle bulges slightly with a small ridge on its medial side.

The peroneal tubercle is present and appears to protrude more than it should due to a compressed peri-mortem fracture just superior to it. There is also a bit of similar damage on its plantar side, all of which looks to be carnivore induced. The anterior tubercle is rugose but only slightly raised. Adjacent to this region is a prominent ridge delineating one side of the groove for the *M. flexor hallucis longus*. This ridge is 19 long starting at the pit for the cuboid ligament and ending where it fades away plantar to the posterior facet. The underside of the sustentaculum tali has a lip marking the superior edge of the groove and if one looks down the long axis, half of a cylindrical tube is visible. At its widest, the groove for the *M. flexor hallucis longus* is 6.2 from rim to rim. The sustentaculum tali protrudes 7.3 from the ridge beneath and is 10.9 long proximodistally.

Left Calcaneus - LF1 This is complete and undistorted, with very little damage. There is a carnivore tooth mark plantar to the peroneal tubercle which is about 4.8 wide by 6.5 long. The depressed fracture is oriented as if the tooth moved anteriorly as it crunched against the bone. The sustentaculum tali has been glued back on after breaking off but only a very small bit of bone between the middle and posterior facets was lost in the event.

The cuboid facet is complete aside from abrasion on the dorsal edge. The depression leading to the pit for the ligament has some residual matrix covering it. The facet is 12.9 wide and 11 high (dorsoplantarly). The dorsal surface just proximal to the joint is bumpy and is excavated down to the root of the posterior facet. Some of the anterior facet has been abraded but the thin connection to the middle facet is visible and

is 3.2 at the waist. The middle facet is oval with a subtle point on the proximal side. It is 7.3 long by 5.5 wide and it is oriented superiorly about 12 degrees from perpendicular. There is a gap of about 3.2 between the middle and posterior facets. The posterior facet wraps around the posterior half of the bone facing first anteriorly, then medially, and finally posteriorly at the most proximal end. Medial edge is elevated from the bone and the superior edge forms a sharp crest. The anterior and posterior margins are flush with the bone surface. It is 12.5 long and 10.1 wide (measured perpendicular to the long axes).

The crest on the superior and lateral margins of the posterior facet is sharp and continues as a salient ridge that extends posteriorly from the facet to the tuber. This distance from facet to the superior apex of the tuber is 9.7. The bone on either side of the crest is concave. The distance from the apex to the bottom of the articular surface is 16.5 and the total height of the tuber calcanei is 19.9. The width is 8.5. The superior apex of the heel is oriented. The surface of the heel is depressed relative to the margins, but only in the first two parts. The third, bottom part is convex. The bottom is not squared like the antimere but appears more pointed with the apex on the medial side. The medial tubercle is present but smaller than on the antimere so that it does not form a discrete bulge. The posterior end is rotated about 25 degrees laterally relative to the long axis.

The peroneal tubercle is present and it sits in line with the lateral keel of the bone toward the cuboid facet. The anterior tubercle is visible and small. Just adjacent to it, the bottom ridge for the groove for the *M. flexor hallucis longus* is prominent. It measures about 16. The groove is 6.5 across from the lip on the underside of the sustentaculum tali to the longer dorsal ridge. As in the antimere, the bone inside the groove is concave and forms half of a tube if one looks down the long axis of the bone.

Right Talus - RF2 This talus is complete and articulates well with the right calcaneus. The bone on the distal end of the trochlea is deformed from compression by the tibia *in situ.* The trauma is localized, however, because neither the head nor the trochlea appear deformed.

The square length is 27.3 and the diagonal length is 28.8. The length of the trochlea is 19.7. the width outside the main tibial facet is 13.2 and the distance between the crests at the fulcrum is 8. The ridges taper posteriorly and the lateral one, which is abraded on the superior edge, projects furthest distally and superiorly. The groove for the *M. flexor hallucis longus* is 1.8 deep. The medial tubercle is bulbous and rounded in all directions but the medial side which is nearly flat. It is much larger than the lateral tubercle.

The tip of the lateral malleolar facet was broken and is glued on. The facet is triangular but missing the distal, superior and proximal margins due to abrasion of the lateral ridge. It is 13.3 long, 14 high (straight line), and projects about 6.7 from the lateral ridge. Just posterior to it is a pit for the posterior talofibular ligament measuring 5.8 long by 3.3 high that is nestled between the posterior edge of the lateral ridge and the posterior edge of the lateral malleolar facet.

The medial malleolar facet is crater-like and prominent on the dorsal side of the neck. It is flat on the distal end making it appear triangular. The facet is 8.2 long and 5.5 wide (to the base of the medial ridge). It is surrounded by lipped walls that slope away from the “crater”, the distal of which abuts the medial portion of the navicular facet on

the talar head. The facet is continuous with the articular surface along the medial side of the medial trochlear ridge.

Posterior to the medial malleolar facet there is a small pit for the cervical ligament. Posterior to that, the articular strip on the medial side of the medial ridge becomes concave (as opposed to convex anteriorly) and rounds off 3.1 from the end of the medial tubercle.

The narrowest width of the neck is 11.9. The head is 12.5 wide and 11.1 high. The navicular and anterior calcaneal facet complex is fractured on the surface and some bone has been chipped away. The medial/plantar corner of the articular surface of the head is missing from the "roof" above the pit for the talonavicular ligament. This pit is bordered by dorsal and plantar pillars. 10.8 by 8 wide of the anterior calcaneal facet is intact, rectangular in shape, and slightly convex. The sulcus tali is deeply excavated.

The posterior calcaneal facet is 3 from the closest border of the anterior facet. It measures 14.6 long and 7 at its waist. Its lateral border has a rounded posteriorly pointing apex and its medial border is squarer than, and does not overlap with, the medial tubercle.

Left Talus - LF2 It is has been compressed from the medial side onto the lateral side causing the trochlear ridges to be much closer together than they should be and squeezing the ends of the posterior calcaneal facet together. The tip of lateral malleolar facet (5 long) is gone but it is otherwise complete.

The square length is 26.7 with a 32.2 diagonal length. The length of the trochlea is 19.5, its width is 10.8 and from ridge to ridge it measures about 8 with the deformation. The trochlea tapers posteriorly, that is even with the deformation it is obvious that it is a

wedge shape. The lateral ridge projects further distally and superiorly than the medial one. The groove for the *M. flexor hallucis longus* tendon is evident and it extends around to the plantar side. The medial tubercle is bulbous and flattened medio-laterally because of the distortion. Although the lateral side of the trochlea also extends posteriorly, it is not a tubercle as much as it is just the edge of the posterior calcaneal facet on the plantar side.

The medial malleolar facet is 15.6 long. The height and protrusion cannot be measured because of the missing lateral tip. Aside from some damage to the superior and lateral surfaces, the facet is smooth and concave for the most part. The pit for the talofibular ligament is located posterior to this facet and plantar to the most posterior tip of the articular surface on the lateral side of the lateral ridge. It measures 5.6 long by 4.5 high and is rectangular in shape.

The medial malleolar facet slopes convexly down from the medial ridge into a concave oval shaped crater that faces medially and posteriorly. There is a small pit located medial to the center with radiating fractures. The posterior edge is rounded unlike the lipping of the other edges and abuts the pit for the deltoid ligament. This pit runs posterior-superiorly with the facet margin and measures 4.4 high by 2.2 wide. The surface posterior to the pit is flat and oriented medial-superiorly. It has no diagnostic topography aside from its clear delineation from the medial tubercle.

The narrowest measure of the neck is 9.9 taken where there was a repaired break clean through the neck. The head measures 13 in the mediolateral plane. It is 9.8 high. The navicular facet joins the anterior calcaneal facet making a unit. The anterior calcaneal facet is rectangular shaped with nearly parallel sides that slightly taper

posteriorly. It is 5.4 wide at this end. The pit for the talonavicular ligament is large and prominent. It is shaped like a parallelogram and measures 8.4 long by 5 wide. It is totally encased by rounded margins including a dorsal pillar along the talar neck originating between the trochlear ridges.

The sulcus tali is 3.6 across the closest borders of the anterior and posterior calcaneal facets. It is not as deeply excavated as the antimere due to the compression. While missing the anterior lateral corner, the posterior facet is 13.2 long. It is roughly rectangular in shape and anteroposteriorly concave with a narrow middle (8.3) and a protruding posterior lateral corner that flares to face a bit laterally.

Right Navicular - RF4 Except for a 4 mm^3 piece missing on the plantar side including a bit of the talar facet, this is complete. The facet for the lateral cuneiform is cracked and there is one major break through the middle of the bone that has been repaired. The total length is 17.9 and the length of the talar head facet is 12.2. The thickness at the lateral end is 3.8, at the middle is 7.9, and at the medial end is 10.6.

Left Navicular - LF4 The lateral portion is mangled; the facet for the lateral cuneiform is gone and thus the medial part of the talar facet is gone with it. The other facets are present and undistorted. The total length is 19.2. The middle thickness is 8 and the medial thickness is 10.1.

Right Medial Cuneiform - RF5 This is a beautifully complete specimen. Only a very small piece medial to the apical margin of the navicular facet is chipped away. The

length at the middle is 11.1. The distal and proximal widths are 16.5 and 9.7 respectively. The navicular facet is 9.3 long and 7 wide. The two lateral facets look as though they are joined but it is difficult to tell due to some damage. The facet for the second metatarsal is 5.6 long and 8.7 deep. There are two tiny tubercles on either side of the keel splitting up the superior facet. Also, the plantar tubercle adjacent to the end of the hallucal facet is prominent.

Left Medial Cuneiform - LF5 This is an equally undistorted and complete specimen to its mirror-image antimere. Only a small portion of the medial side of the apex margin of the navicular facet is chipped away. The length at the middle is 10.8. The distal and proximal widths are 16.6 and 10. The dimensions of the navicular facet are 8.8 long by 6.7 wide. The facet for the second metatarsal is 5.1 long and 8.4 deep.

Right Intermediate Cuneiform - RF7 This is a complete and undistorted specimen. There is only a small bit chipped off the medial margin of the proximal facet.

Left Intermediate Cuneiform - LF7 This is complete and undistorted aside from the loss of much of the major and minor facets for the medial cuneiform to abrasion. The distal facet has been crushed causing a portion of the lateral side to be lost. The proximal facet has also been fractured. As in the antimere, the dorsal surface appears flatter than KPS I.

Right Lateral Cuneiform - RF6 It is complete with no distortion. There is also a small bit of abrasion on the tubercle. The bridge of bone to the tubercle is extremely thin.

The two facets on both the lateral and medial sides are intact. The dorsal surface appears to be waisted midway up the surface on either side where the two facets are separated by small grooves. The distal facet on the medial side is rounded proximally. The proximal facet on this side is rectangular and 4.4 long. It is 4.2 deep and tapers distally. The distal facet on the lateral side is also round and the proximal one is larger and more oval.

Left Lateral Cuneiform - LF6 This is also undistorted but its plantar ridge is broken off just behind the proximal facet, taking the plantar peninsula of the distal facet with it. The proximal facet is intact and is roughly a flat square. The edges of the medial facets are abraded. The lateral ones are much better preserved. The distal one is round and the proximal one is larger and shaped like half an oval, the flat part bordering the lateral side of the proximal facet measuring 5.

Right Cuboid - RF3 This cuboid is complete but flattened dorsoplantarly and there are some fracture lines on the facets. The overall length is 17.8 and the medial and lateral lengths are 14.7 and 9.2 respectively. The distal and proximal widths are 12.2 and 14.7. There is a large calcaneal process that is longest plantarly and nearly medial-most on the proximal facet. All the smaller facets are present. The medial side of the distal facet is 7.7 deep.

Left Cuboid - LF3 There is a crack like a strike-slip fault running proximal-distally right through the middle of the fossil separating the lateral half from the medial half that has been pushed distally past it. As a result the calcaneal process does not jut out as far as

it should. The proximodorsal edge is lifted up and out from being pushed over the edge of the cuboid facet *in situ.* The mediodistal corner is gone together together with some of the plantar edge of the distal facet. There is a hole excavated on the plantar side where the proximal end of the first metatarsal was crushed against the cuboid *in situ.* The overall length is 15.9. The medial and lateral lengths are 13.7 and 9.7. The distal and proximal widths are 12.1 and 13.6.

Right MT1 This specimen is complete save for some bone missing on the lower lateral shaft and abrasion on the head. There is one major fracture running through the midshaft. The proximal facet does not extend over all of the tuberosity; this is probably not natural since the antimere has a facet extended onto the tuberosity. The proximal facet is oval and squashed to appear very concave.

Left MT1 It is complete but it is compressed dorsoplantarly and the dorsal cortical bone is collapsed into the medullary cavity creating a gutter along the shaft. The total length is longer than in the right side since it is flattened at the proximal end and the tuberosity juts out further.

Right MT2 The proximal end is unharmed, but the head is tattered, flattened and bent dorsally. The distal half of the shaft is compressed dorsoplantarly like the head. Three major fractures run across the shaft. The proximal facet is triangular.

Left MT2 The proximal end is undistorted. The shaft is also unharmed aside from the several fractures riddling it. The proximal facet is triangular. The head has been badly crushed.

Right MT3 Again, the proximal end is well preserved but the lateral side of the diaphysis is crushed and flattened against the still rounded medial side. The head is flattened mediolaterally. The proximal facet is t-shaped but the plantar portion is compressed and leaning medially.

Left MT3 Again, the proximal end is undistorted. The plantar portion leans laterally. The shaft is unharmed aside from several fractures. There is a crater on the mediodistal end where the proximal end of the second proximal phalanx was pushed up against it *in situ*.

Right MT4 The plantar part of the proximal end is sheared-off due to its vulnerable position *in situ.* The head is bent dorsally, perpendicular to the shaft which is flattened dorsoplantarly.

Left MT4 The head and the distal third of the shaft are leaning slightly laterally and there are three major fractures through the shaft. The facet for the cuboid was crushed against the edge of the cuboid *in situ* so it is not complete. Lateral and medial facets are present.

Right MT5 The shaft is fractured and bent in the middle so that the distal end is pointing plantarly. The head is completely compressed medio-laterally. Despite its mangled appearance the proximal end preserved much of its morphology.

Left MT5 The proximal end is well-preserved but the head is bent laterally and compressed dorsoplantarly. Three major fractures run through the shaft. There is also a crater on the dorsal distal end of the shaft from being pushed against the head of the first metatarsal *in situ*.

Individual IV: Infant (Blue; Fig. 3.4)

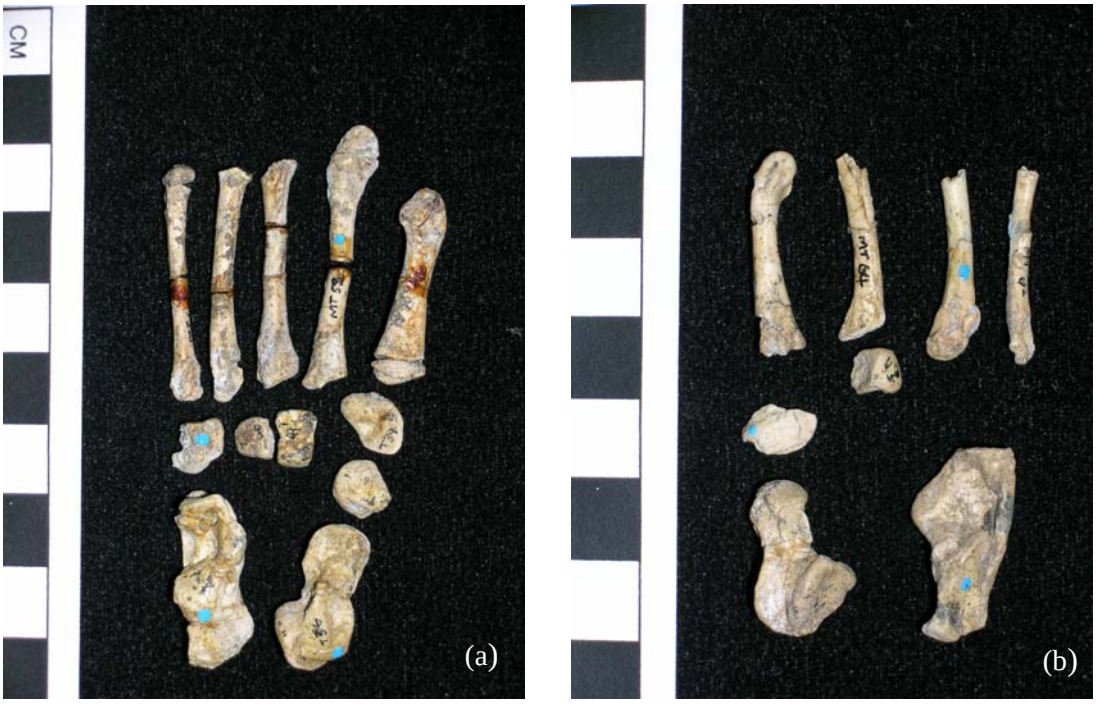

Figure 3.4. Left (a) and right (b) tarsals and metatarsals of KPS Individual IV. Photographs are not scaled to one another, but scale of each is in centimeters.

Right Calcaneus - T42 This is complete and nearly a mirror-image of the left one except that it is slightly crushed dorsoplantarly. The dorsal tip of the cuboid facet has been chipped away. The heel epiphysis is neither present nor fused and 4 long of the superior half of the tuber had been broken off and was glued *in situ*. The total length is 25.3 and the greatest breadth is 12.4.

The cuboid facet is 7.5 wide by 3.5 tall. The lateral corner protrudes furthest distally even though its tip has been lost. The surface of the facet is flat, not convex or bulbous as expected in the very young, and faces distally. Inside the indentation sits the pit for the cuboid ligament. The lateral edge juts out the furthest distally.

The dorsal surface proximal to the cuboid joint, the basin, has a large indentation at the root of the posterior facet as well as a smaller pit between it and the anterior portion of the sustantacular facet for the attachment of the talar neck ligament.

The sustentacular facets are one unit connected by a thin neck. The unit is 10.5 long and 1.4 at the waist of the neck. The anterior portion is no larger than this connecting neck and the middle portion is oval measuring 7.1 long by 4.4 wide.

About 2 away is the posterior facet. The surface bone is lost down the entire long axis of it. The most proximal part faces only hints at facing posteriorly. The medial edge is raised and the superior border forms a sharp crest that is thinnest just proximal to the facet and widens as it approaches the apex of the heel. Lateral to this crest, the bone is basically flat. On the medial side, the bone is convex for 3 until the pit for the attachment of the deltoid ligament which measures 3.3 long by 1.4 high.

The heel is 8.7 in total height. The upper surface is oriented to face slightly laterally. Some of the billowing of the epiphyseal surface is evident. The medial plantar corner slopes forward to join the plantar surface at a gentler angle than the square-ish lateral corner. Torsion of the heel is difficult to measure without the epiphysis. The surface is convex and faces distally.

The very edge of the peroneal tubercle is abraded but does not diminish the already diminutive state of the tubercle which is difficult to distinguish from the lateral keel. In this case the lateral keel resembles a gunwale; dorsal edge is flattened resembling a shelf posteriorly, but raised above the dorsal surface anteriorly as if it would hold it afloat. This could possibly have been caused by slight mediolateral compression.

The anterior tubercle is present and cylindrical similar to the right calcaneus of Individual I but not as raised and discrete from the surrounding bone.

The ridge and lip outlining the groove for the *M. flexor hallucis longus* are not sharply delineated as in adults but still present. The ridge runs for 10.4 and the groove is 4.7 wide. The sustentaculum tali projects 5.3 medially over the ridge and is 9.4 long.

Left Calcaneus - T35 As mentioned above, this calcaneus is a near mirror-image of its antimere. There was a break clean through the posterior portion, roughly 7 of the total length, just proximal to the posterior facet. The total length of the calcaneus is 24.9 and the greatest breadth is 11.1. The only major damage is to the lateral/dorsal edge of the cuboid facet where a piece about 3.2 wide and 5.2 high is broken away. The width of the entire facet cannot be measured accurately but the height is 6.5 and the pit for the ligament is visible. The excavated bone at the root of the posterior facet has a lip on the lateral side and is triangular in shape. Distal to it lies what looks to be an incipient second pit. The sustentacular facets are present. The anterior portion is extremely small, and indistinguishable from the connection to the larger middle facet. The length of this until is 8.3. The middle facet is shaped like a kidney bean and measures 4.6 long by 3.7 wide. There is no obvious gap between the middle and posterior facets. The posterior facet is complete aside from a bit of the proximal superior edge being lost possibly in the event that caused the large break. The medial margin is raised from the lower bone and there is a clean line on the superolateral margin. Like in the antimere, the proximal portion does not quite face posteriorly as in adults. The keel running along the superior edge is very sharp and curves laterally to the apex of the heel. The bone on the lateral

side is flat, with a very small pit and the surface gradually protrudes toward the rounded lower lateral side as one looks down. There is an indentation on the medial side halfway down the face that is consistent with that seen in adults but looks exaggerated in this tiny individual.

The heel is 10.8 high. Exactly like the asymmetry seen in Individual III, the heel is not at all the same shape of its antimere. The right side was squared-off on the bottom while this left one comes to a point at the medial side of the base. The surface is billowy and young. The medial side of the uppermost part faces medially, otherwise the surface is convex and faces distally.

Again, the peroneal tubercle is a mere roughening along the lateral keel just lateral to the posterior facet. And again, the keel has a sharp edge along the border with the dorsal surface. The anterior tubercle is present but appears to have usurped the distal portion of the plantar ridge because the ridge bends laterally here to join it. The plantar ridge measures 11.3 and ends just proximal to the sustentaculum tali. There is a very thin lip on the underside of the sustentaculum tali and the distance between it and the ridge is 3.7.

Right Talus - T43 This talus is complete but slightly compressed mediolaterally. It is 18.5 long measured squarely and 19.6 long diagonally. There was a clean break across the narrowest part of the neck which was glued together *in situe*. The broken lateral edge of the dorsal side of the neck was also glued together *in situ*. Much of the trochlear surface between the ridges is abraded.

The lateral trochlear ridge projects the furthest distally. The ridges are 5.4 apart at the most superior part of the crests. The medial tubercle is very small, round and flat mediolaterally. The adjacent groove for the tendon for the *M. flexor hallucis longus* is present and shallow. The lateral malleolar facet is complete and appears to take up the entire lateral side. But this is an illusion because the pit for the talofibular joint, although shallow and difficult to see, is palpable. The lateral malleolar facet is 8.5 long and 8.8 high and protrudes 2.5 from the lateral ridge. The protrusion does not appear to have been affected by the compression, but it is difficult to say for sure since the antimere is missing most of the lateral corner of this facet.

The medial malleolar facet is very small but has a distal border that is lipped, distinguishing it from the bone of the neck and head. The distance from this margin to the tip of the medial tubercle is 14. There is a very small pit posterior to the facet, about 1.8 in diameter and filled with matrix, that is for the deltoid ligament

The narrowest neck measure is 5.7. The head measures 7.3 wide by 7.5 high. The navicular facet on the head is abraded and some of it has been lost on the medial side. This facet joins with the nearly flat anterior facet that descends the plantar side of the neck with a rectangular outline until it ends at the shallow sulcus tali. The pit for the talonavicular joint is relatively large and deep for the size of the bone, similar to that seen in young apes. It is oval shaped and measures 5.1 long by 3.4 wide.

The posterior facet is narrower than it should be due to the deformation. There are no obvious edges to the facet, to the length is estimated to be 8.3 and the width 3.1.

Left Talus - T36 This talus is complete but has undergone shear deformation running towards the neck across the trochlea and similarly oriented, and, probably related, dorsoplantar compression at the neck and head. The neck broke at its narrowest but has been repaired. The square length is 19 and the diagonal is 21.2. Although deformed the trochlear ridges taper posteriorly and the lateral ridge rises higher than the medial one. However, since the medial ridge has been pulled out along the talar neck with the deformation, it appears longer than the lateral one. The groove for the tendon of the *M. flexor hallucis longus* is barely visible. The medial tubercle is also very small and hard to see. The lateral malleolar facet and the adjacent posterior calcaneal facet are shrunken due to plastic deformation. The lateral malleolar facet measures 8.3 by 7 and, although smaller, it held its triangular shape. It has been flattened and does not project laterally from the trochlea. The posterior calcaneal facet is barely rectangular as it should be, measuring 6.5 by 5.4 but is unnaturally flat.

The medial malleolar facet is small, round and shallow and delimited by a raised distal lip. The pit for the deltoid ligament sits posteriorly to it and measures 3.1 by 2.1.

The narrowest part of the neck measures 6.8. The head measures 8.7 wide by 5.4 high. There is a pinched rim encircling it in the medial plane, mostly on the lateral side, due to compression. The medial side of the navicular facet joins the anterior calcaneal facet which is facing much too medially and is much too convex. The pit for the talonavicular ligament is deep but partially filled with an unidentified piece of bone. The sulcus tali is bordered by an unnaturally sharp and thin medial lip.

Right Navicular - T62 This navicular is mostly complete but not fully formed. The dorsolateral corner is broken away where the facet for the lateral cuneiform would be. The only remaining part of this facet is a hint of concavity on the lateral side. The cuneiform facets are indistinguishable and the entire distal surface is smooth. It is 9.4 long (mediolaterally) and 3 wide proximodistally at the midpoint. There is a 5 long linear pit running along the plantar edge which may be exaggerated due to compression. The facet for the talar head is eye-shaped with points on the medial and lateral ends measuring 8 across. The entire bone is flat because it has not yet fused its medial tuberosity.

Left Navicular - T37 This one is much rounder than its antimere but asymmetry is to be expected since the bones are still forming. It also may be due to mediolaterally deformation since the talar head facet is bent a bit proximally in that plane, evident by a slight crease running dorsoplantarly along the fact. No cuneiform facets are distinct but there is a generic smooth rounded convex surface on the distal side that dips down with slight concavity to where the lateral cuneiform articulates. The very medial part of the distal facet is broken away taking that corner of the talar head facet with it. It is 8.4 across, shorter than it should be due to the missing medial tip, and 3.3 wide at the midpoint.

Left Medial Cuneiform - T39 The dorsal and plantar edges are sharp suggesting this specimen has been compressed mediolaterally. The dorsal part of the superior facet

is visible and the hallucal facet is complete. The length at the middle is 8.2. The distal and proximal widths are 7.8 and 5.1.

Right Intermediate Cuneiform - C48 This was originally thought to be a carpal, thus the "C" designation. Because it is young it is bulbous with rounded edges. There is some bone chipped off the length of the plantar edge so getting a good measurement of depth is not possible.

Left Intermediate Cuneiform - T40 This is just the dorsal surface with the small remaining portions of the distal, proximal and lateral facets enabling its identification.

Left Lateral Cuneiform - T41 Only the dorsal surface and the proximal facet are intact in this specimen. All else has broken away. However small, it is evident that the distal facet is concave and the proximal convex. The proximal facet is 3.3 deep. Waisting is evident on the lateral midpoint of the dorsal surface already at this young age.

Right Cuboid - T38 This is just the distal facet. It is underdeveloped with no obvious articular surface boundaries. The distal width is 5.6 and the depth of the medial side of this facet is 5 (assuming it is from the right side). This was originally labeled as a left cuboid, but it is quite possibly a right one. However, it is difficult to determine with certainty and there is no antimere.

Right MT1 - MT61 The proximal end is broken away showing a tiny bit of the epiphyseal surface on the dorsal side. Although there are two fractures through the shaft it is in good condition. The head is compressed dorsoplantarly.

Left MT1 - MT56 The epiphysis is glued on and has a small young protuberance associated with an incipient tuberosity on the shaft. Aside from the epiphysis, the shaft is compressed dorsoplantarly. There is one major break through the midshaft.

Left MT2 - MT58 The young head is present, but compressed medio-laterally along with the distal shaft. The shaft has two main breaks. The proximal facet is damaged dorsally, and the medial side at this end has lost some bone.

Right MT3 - MT64 It is not clear which metatarsal this is, due to the absence of distinctive morphology. The diameter of the shaft suggests it belongs as a second or third. Although at first glance it appears proximal because the dorsal side of the end is not rounded, it is probable that this is the shaft and mediolaterally compressed distal end of the second or third metatarsal.

Left MT3 - MT57 This is complete minus the head. There are two main breaks through the shaft which is otherwise in good shape. The proximal end has been crushed a bit but the large facet is complete. Because it is young, it does not have the medial and lateral components of the t-shape that adults have.

Right MT4 - MT63 The proximal end has been damaged so that it is not complete. The shaft is in good form but end before the epiphyseal surface. There is one major break through it.

Left MT4 - MT59 All but the head is present although the proximal end has been mangled. There is one major break through the midshaft.

Right MT5 (MT62) Two thirds from the proximal end is present. The shaft is still round, but the proximal end has been crushed.

Left MT5 (MT60) This is the complete metatarsal with the head glued on top. The proximal end has been slightly crushed and there is a break through the midshaft.

Individual VI: Infant (Yellow; Figure 3.5)

Figure 3.5. Calcaneus (a,b) and talus fragment (c) of Individual VI. Photographs are not scaled to one another, but scale of each is in centimeters.

Right Calcaneus (T64) The total length is 18.6. It was broken in half anterior to the posterior facet and is repaired. It is complete aside from the missing dorsal half of the calcaneal tuberosity, which is unfused. It is also missing the proximal half of the sustentaculum tali and adjacent posterior facet margin. It has been mediolaterally compressed overall. The posterior length is 10.7 and the anterior length is 15. The length of the posterior facet is 6.5 and the width is 4. The width and depth of the cuboid facet are 4.2 by 4.6. The width of the heel is 2.9. The medial surface of the posterior part is smooth until the visible groove for the *M. flexor hallucis longus*. It measures 2 across. A very small anterior tuberosity is present. There is a very thin but deep groove between the lateral border and the anterior body due to the compression.

Right Talus (MH15) The head is broken off at the middle of the neck. The total length is 9.9. it is 5.3 wide at the center and 3.5 from ridge to ridge of the trochlea. The trochlear ridges are well preserved. There is no visible medial malleolar facet yet and it is hard to tell how developed the lateral malleolar facet was since it is missing the plantar part. The

medial crest rides up the neck but the lateral ridge is still longer overall. Only a portion of the posterior calcaneal facet is visible, otherwise the entire plantar surface is abraded. The groove for the tendon of the *M. flexor hallucis longus* is not visible.

Individual VII: Juvenile Female (Maasai Red; Figure 3.6)

Figure 3.6. Left (a) and right (b) tarsals and metatarsals of KPS Individual VII. Photographs are not scaled to one another, but scale of each is in centimeters.

Right Calcaneus (T18) This is only the anterior two-thirds of the right calcaneus and is 27.3 long. The posterior portion behind the posterior talar facet is gone, most likely due to carnivores. There is also fractured and flaked-away surface bone just under the peroneal tubercle.

The cuboid facet is flat with a distinct dorsal border and a very shallow indentation for the cuboid. The pit for the cuboid ligament is extremely small and sits dorsal to a 3 puncture mark. The lateral and plantar parts of the cuboid facet have been abraded away, leaving only the dorsal portion.

The dorsal surface just proximal to the joint lacks the bumpy characteristics of the others because it has been smoothed and abraded. It is concave and deepest at the root of

the posterior facet. The pillar or thickening just medial to the lateral keel that abuts the cuboid facet margin is gone.

A thin band, part of the connecting bridge (8.5 by 2.6), is all that remains of the sustentaculum tali articular surfaces. Although it is obvious that the anterior facet was extremely small to begin with and was probably not distinct from the band connecting it to the middle facet. On this bone however, the middle facet has been broken and abraded leaving nothing to measure. Most of the posterior facet is intact but the posterior edge was lost with the tuber calcanei and the superior edge is abraded.

The peroneal tubercle is present and is part of the lateral keel that separates dorsal from plantar portions of the bone. There is a rough patch of bone where the anterior tubercle should be which may be a sign it is beginning to develop. The medioplantar ridge for the groove for the *M. flexor hallucis longus* is prominent but only extends as far as the underside of the posterior edge of the sustentaculum tali. Its length is 12.5. Although the sustentaculum tali is broken, the lip for the groove on the underside is visible so the width of the groove can be measured at 5.

Left Calcaneus (T17) This calcaneus is broken at the common spot, just proximally to the posterior talar facet and although it was cast with the tuber intact, the tuber is missing from the specimen in the musem. Without the tuber it is 26.2 long. The cast of the full specimen with the tuber measures 31.71 long. It appears to have been compressed mediolaterally in comparison to its antimere but that is an illusion brought on by the missing medial side anterior to the sustentaculum tali.

The intact cuboid joint shows that it is more L-shaped than crescent-shaped as in adults and it has a very shallow indentation for the cuboid. The pit for the cuboid ligament is not obvious, probably because it is very small and there is manganese staining where it should be. It is 6.6 and 8.4 high.

The dorsal surface posterior to the joint has a strong pillar or thickening on the lateral side of the joint margin and is excavated towards the root of the posterior facet. The anterior facet and its bridge to the middle facet have broken off. The sustentaculum tali was glued together right at its junction with the body of the calcaneus. This bit is missing in some casts. The oval-shaped middle facet is 8.9 long. Because the margins are blurred from damage it is difficult to obtain the proper dimensions, but it is obvious that it is oriented slightly anteriorly.

Due to the break, there is no clear cut border between the middle and posterior facets. The superior margin is chipped away but a good measurement of the length can still be obtained at 13. The medial margin is raised above the surrounding bone.

The peroneal tubercle is gone but the lateral keel that it contributes to is intact all the way to its end at the cuboid facet. Again, as in the antimere, there is a rugosity where the anterior tubercle was forming. The ridge on the plantar side of the groove for the *M. flexor hallucis longus* is about 12 long. Measuring from this ridge to the lip on the underside of the sustentaculum tali, the groove is 6.2 wide. The sustentaculum tali is 11 long.

Right Talus Fragment (T26) This is a fragment comprised of the lateral distal corner of the right talus. It preserved three surfaces: lateral, anterior and plantar. The distal curve of

the lateral malleolar facet including the lateral apex, although damaged is concave and round. The distal portion of the posterior calcaneal facet is flat most distally but quickly becomes concave on its medial end (facing mediodistally) the articular surface spills over the lip as seen in KNM-MW 13142. The non-articular surface that faces anteriorly, is wedged between the two facets. The fragment is 13.8 wide and 8.5 long (proximodistally).

Right Talus Head (T63) This is the dorsoplantarly compressed head of the right talus minus the neck. It is 11.2 wide and 5.6 thick. The plantar half of the navicular facet is abraded and just the beginning, or the distal portion, of the anterior calcaneal facet is apparent.

Right Navicular (T31) It is compressed dorsoplantarly. The distal facets are now on the dorsal side and the lateral cuneiform facet is on the plantar side of this artificial topography. The talar head facet is visible because it is still concave but it is highly compressed. The total mediolateral length is 13.5.

Left Navicular (T30) This navicular is undeformed but is not yet fully developed. Its length is 11.7. The length of the talar head facet is about 9.9. The lateral side is 4.6 thick and the middle is 1.7 thick. Some of the bone on the medial-most edge has been abraded away and here it is 2.8 thick. The lateral cuneiform facet is not distinct from the neighboring facet for the intermediate cuneiform although it does eventually become concave as it tapers off plantarly. The length of this plantar side of the facet is 3.8. The

cuboid facet is not visible although there is a small area where it may be in its incipience. The medial side of the facet for the talar head is slightly crushed but overall the facet is oval shaped. The dorsal non-articular surface is rugose and characterized by a long linear pit like in KPS I.

Left Medial Cuneiform (T34) This bone is lacking all the sharp margins on the facets for probably two reasons; First it appears to have been plastically deformed and abraded, and second, it is still young. It is cracked along the distal-most ridge of the hallucal facet. The length at the middle is 9.4. the distal and proximal widths are 10.3 and 7.

Left Intermediate Cuneiform (T32 or 52) This is complete but abraded on the plantar edge as well as the medial and lateral sides. The medial and lateral facets are not clearly delineated but they are present.

Right Lateral Cuneiform (T33) This specimen has immaturity as well as deformity to blame for its poor condition. The plantar spine of the bone has been pushed laterally relative to the dorsal surface and has been compressed to a very sharp ridge. Medial and lateral facets do not have distinct outlines but their locations are evident. The distal facet is deformed but concave and the proximal is convex but also slightly deformed from the square shape it should hold.

Left Lateral Cuneiform (T43/44) This one is in worse condition than the antimere. The edges of the dorsal surface look like melted wax. The length had to be taken between

the two edges measuring 10.4. The surface in between the edges is compressed and fractured. The plantar spine is heavily abraded. The distal facet is cracked and incomplete. The proximal facet is also cracked and incomplete. Neither the medial nor the lateral facets are visible. Although it is obvious that there is a waist halfway up the lateral side of the dorsal edge as in adults.

Left Cuboid (T21) This specimen is complete but damaged. It has been flattened dorsoplantarly and also abraded so that none of the articular surfaces are smooth. The distal width is 7 and the proximal is 11.2. The overall length is 14.3.

Right MT1 (MT52) This is just the distal third of the bone. It is crushed with a large indentation just posterior to the head on the dorsal side. The ridge on its head and on the antimere is more like a hump than the sharper adult form.

Left MT1 (MT27) This is complete except for missing the epiphysis. It is crushed down into the medullary cavity from the dorsal side. The surface bone chipped away on the medial side of the proximal half.

Right MT2 (MT28) Just the proximal third is preserved. It is crushed along the medullary cavity. The medial facet has been pushed onto the dorsal side. But both lateral facets are visible and undeformed.

Left MT2 (MT30) This is most of the shaft with the proximal end but it is missing the epiphyseal surface. A piece of bone is missing from the proximal medial side on the lower shaft and the whole shaft is crushed along the medial side into the medullary cavity.

Right MT3 (no number) This is the proximal half of the bone with some cortical bone cracked away. It is undistorted but the facets are indistinct.

Left MT3 (MT41) Again, this is just the proximal half of the bone. There is a piece missing just above the proximal facet on the medial side of the shaft. The plantar tip is missing from the proximal facet.

Right MT4 (MT24) Just the proximal half is preserved. The large medial facet is mostly broken away. No distortion is evident.

Left MT4 (MT29) Almost the entire bone is preserved except for the epiphysis. The dorsal side of the proximal end is crushed but all the facets are complete.

Right MT5 (no number) Just the proximal half is preserved. The medial portion of the proximal facet is broken away.

MT5 (MT65) This is just a shaft that is smaller than the others and tapers up towards the head which is absent. The shaft is small, round and unharmed. It is possible that this is

the distal portion of the right fragment. Together they measure 45 long, and some cracks and lines seem to match up.

Metapodial Heads There are several metatarsal heads associated with this individual unfortunately none articulate with the metatarsals because of damage and deformation.

Individual VIII: Subadult Female (Light Green; Figure 3.7)

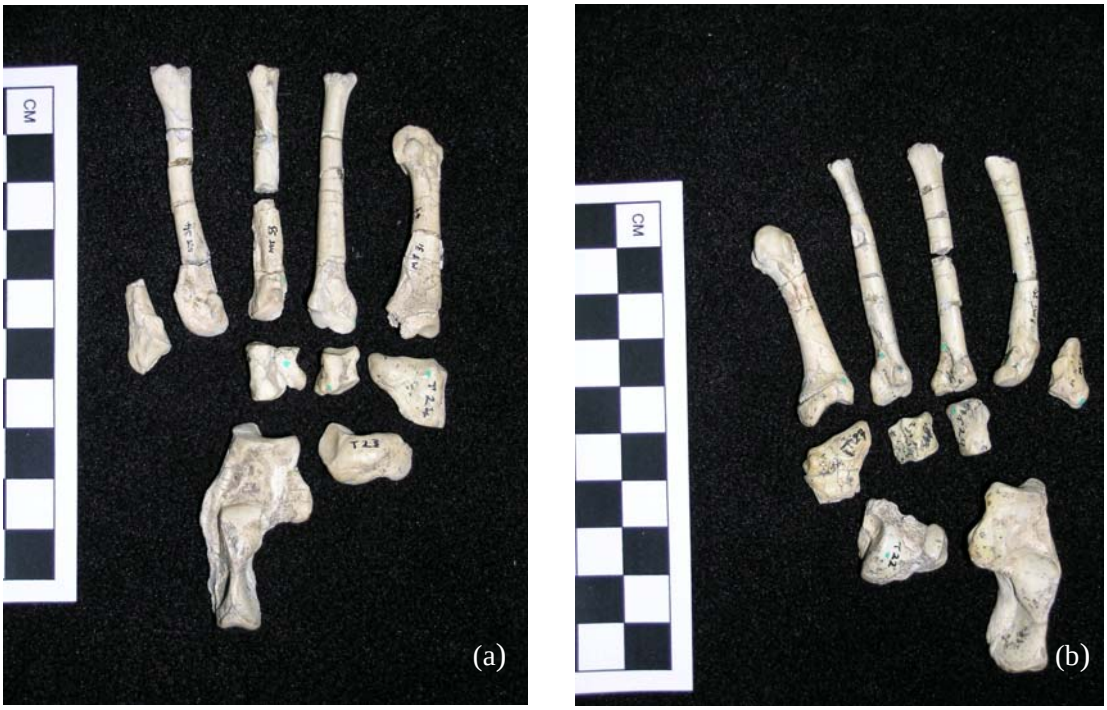

Figure 3.7. Left (a) and right (b) tarsals and metatarsals of KPS Individual VII. Photographs are not scaled to one another, but scale of each is in centimeters.

Right Calcaneus (T20) This is a nearly complete, only slightly deformed, right calcaneus. It was broken straight across, proximal to the sustentaculum tali and just anterior to the posterior facet. It is 40 long and 21.2 across at the widest (medial edge of sustentaculum tali to lateral keel).

A small bit of the rim around the cuboid facet is gone on the dorsolateral side and the plantar corner has been abraded off. The joint is oriented about 20 degrees superiorly from perpendicular. It is 12.7 wide and 7.1 high and crescent-shaped. The dorsal perimeter is much thinner than the lateral and plantar portions. The margins are flat until they dip down towards a pit medial to the center. The medial corner recedes down into

the pit the steepest while the rest of the facet has a more gradual slope to the indentation. More than the others, looking down from the superior aspect, the cuboid rim is convex, the medial and lateral tips jutting out distally. The lateral tip extends the furthest and contributes to the length of the calcaneus.

The dorsal surface proximal to the cuboid facet is rugose with the main indentation located at the root of the posterior facet where the lateral-most part of the posterior facet on the talus fits. There is also a pit between this large depression and the anterior facet for the attachment of the talar neck ligament.

This specimen has the best preserved sustentacular facets. The anterior and the middle are connected by a thin bridge which is 2.5 at its waist. The entire facet complex is 15.6 long. The majority of the anterior facet is oval and faces superiorly, with a slight convexity as it descends from the cuboid joint margin. A smaller portion of the anterior facet folds over the medial edge and faces medially. The middle facet is larger and teardrop-shaped with the apex approaching the waist of the connecting bridge. It is 4.2 from the posterior facet.

The only damage to the posterior facet is a 6.6 by 4.2 erosion on the dorsal part at its most proximal edge. The distal and proximal margins are flush with the surface, but the lateral margin has a tiny lip and the medial one is raised. The superior portion formed a ridge that widens as it continues to the apex of the heel. The bone on the lateral side slopes away very convexly and then becomes a pit. The bone on the medial side slopes away very flatly facing medially until it hits the protruding rounded portion that runs parallel to the superior crest and to the long axis of the bone and which participates in the formation of the plantar body.

The heel is recently fused. An epiphyseal line is still visible around most of the circumference but there is no gap. The linear indentation marking the bottom of the attachment for the Achilles tendon, looks as if it were made by pushing a thumbnail into putty because of the slight superior convexity. It runs parallel to the mediolateral axis and is 8.9 down from the heel's apex. The apex of the heel faces more superiorly than the rest below it that faces posteriorly. The medial and lateral edges protrude further than the bone in the middle. The second portion is 12.9 from the apex and the entire heel is 13.8 tall. The width is 9.6. The apex is toward the lateral side with the medial side rounding up and over to meet it. The shape of the heel is rectangular and it is squared at the bottom due to deformation. The medial tuberosity is very small. The angle of torsion is about 10 degrees laterally.

The peroneal tubercle is well-developed and is part of a ridge that runs from the lateral pit on the proximal end to team up with the keel on the lateral side of the dorsal surface that separates dorsal from plantar portions of the body. There is an oval-shaped region of damage to the surface that is about 14 long and is just plantar to the peroneal tubercle, with a distinct tooth mark towards the distal part. The anterior tubercle is visible.

The plantar ridge for the groove for the *M. flexor hallucis longus* is thick and prominent. There is a 4.5 long piece missing from the middle and it is 18.9 long if one includes the distally tapering portion. The underside of the sustentaculum tali is smooth with a sharp lip for the groove for which the width is measured at 5.8 from ridge to lip. The sustentaculum tali protrudes 7.9 from the plantar ridge and is 12 long.

Left Calcaneus (T19) This calcaneus is complete with a recently fused heel as in the antimere. The posterior portion just proximal to the posterior facet and all the way down to the equivalent location on the plantar side was broken off and repaired. It is 40 long and 21.8 at its widest.

The cuboid facet is complete with barely visible abrasion on the medial tip. It is crescent-shaped and because it is round at the lateral side and curves up and around counterclockwise to a point on the medial side. The joint surface is oriented about 18 degrees superiorly from perpendicular. The larger lateral side is flat and the thin medial side dips at a slope down to the central indentation, instead of dropping off like a cliff on the lateral side. The pit for the cuboid ligament is visible and is located at the midpoint of an imaginary line between the two tips of the facet. It is 13.3 wide and 10.4 high.

The dorsal surface proximal to the cuboid surface is concave and rugose with two major landmarks: the large excavated depression at the root of the posterior facet and the smaller pit just distal to it. The two sunken surfaces are separated by a tiny lip that surrounds the larger one. The smaller distal pit is located a little more laterally in this specimen than in the antimere. On the distal lateral margin there is a pillar or buttress branching off from the lateral keel leading to the cuboid facet edge.

Because the sustentaculum tali was found broken (and reattached), the sustentacular facets are not as smooth and delineated as in the antimere. The anterior portion is indistinguishable from the surrounding bone and the middle facet is riddled with cracks. The medial edge of the middle facet is the only one visible. The posterior region of the middle facet has lost some bone to the break a making the separation between it and the posterior facet impossible to measure accurately.

The posterior facet is abraded and cracked on the most distal, medial surface and has also lost about 4 thick on its superior edge. It is wrapped around in the same manner as its antimere with the proximal portion facing posteriorly and becoming flush with the surrounding bone. The only raised edge is on the medial side where some bone has chipped away.

The sharp crest originating at the posterior facet continues to, and widens as it approaches, the apex of the heel. It slopes off convexly to the medial side and then after that, the bone is flat and faces medially. The bones slopes away convexly on the lateral side and shortly hits an oval pit for the calcaneofibular ligament that is 77 long and 4.6 high.

The width of the heel is 8.9. It is 9 down to the line at the Achilles attachment, 12.1 down to the bottom of the articular surface and a total of 13.9 high. Like its partner, the very bottom is squared-off and flat against the plantar side from deformation. The apex is toward the lateral side. The angle of torsion is negligible. The medial edge protrudes further posteriorly than the lateral one but both protrude more than the bone in the middle.

The peroneal tubercle is stuck on the lateral part of the keel separating dorsal from plantar on that side. It is distinguishable from the rest of the keel by its bumpiness. There is a line that almost looks like a crack separating the bone rising to the anterior tubercle and the plantar ridge for the groove for the *M. flexor hallucis longus*. This ridge is 15.2 long and measuring from its edge to the damaged but visible lip on the underside of the sustentaculum tali, the groove is 6.8 across. The sustentaculum tali projects 7.8 medially past the ridge and is 11.2 long.

Right Talus (T22) This is a fragment of the body of a right talus that articulates with the right calcaneus. The head and neck are gone along with the proximolateral corner. The bone surface is chipped across the distal margin of the trochlea between the ridges and across the distal medial ridge. The posterior part is broken off diagonally from 8.3 down (proximally) the lateral margin across to near the proximal end of the medial ridge. It is evident that the lateral ridge rides superior to the medial one and that it also projects most distally. The width of the trochlea present is 13.2. Most of the lateral malleolar facet is present, minus the posterior tapering tail. The height and protrusion can be measured at 11.3 and 2.9 respectively. The medial malleolar facet is present but missing all but 3.2 of the medial margin. The pit for the deltoid ligament is small but distinct measuring 2.8 long by 1.5 high. The posterior portion of the posterior calcaneal facet is gone leaving 10.9 long of the anterior portion. Only a thin strip of the anterior facet is left but it is evident that the posterior margin lies almost flush with the bone with only a small ridge.

Left Navicular (T23) This bone is complete with a tiny bit abraded off the distal medial edge, just medial to the articular surface. Its length is 19. The center of the talar facet has been crushed and has a rough surface but the entire facet is intact and is the shape of a pyriform in outline. It is concave and 13.5 long. The medial, middle and lateral thicknesses are 8.9, 4.6 and 7.4 respectively. The lateral cuneiform facet is shaped like a square with a rounded superomedial border, measuring 7 long, which is flush with the adjacent facet for the intermediate cuneiform. The rest of the lateral cuneiform facet has rounded, raised margins and the plantar edge abuts the wedge-shaped cuboid facet which

is largest in this individual above all the others. The dorsal non-articular surface has a triangular shaped pit proximal to the medial cuneiform facet.

Right Medial Cuneiform (T27) This bone is mostly complete. The navicular facet has been lost and there is considerable abrasion to the lateral-proximal and plantar sides. There is a fracture running superior-inferiorly along the middle of the medial side. Otherwise the superior and hallucal facets are well-preserved. The length at the middle is 12.7 and the distal width is 16.7. The facet for the second metatarsal is 4.5 long and 9.2 deep.

Left Medial Cuneiform (T24) This specimen is perfectly complete and undistorted aside from a small bit of abrasion on the very edge of the join between the inferior and navicular facets. The plantar tubercle is prominent and oriented laterally. The length at the middle is 12.7. The distal and proximal widths are 16.1 and 8.7. The navicular facet measures 8.7 long by 5.6 wide. The facet for the second metatarsal is 4.7 long and 9.1 deep.

Right Intermediate Cuneiform (T28) This is a perfectly preserved specimen similar in morphology to the intermediate cuneiforms of KPS I and III.

Left Intermediate Cuneiform (T25) Aside from a tiny pock mark on the middle of the superior border of the distal facet, this bone is perfectly complete and mirrors its partner on the right side morphologically.

Right Lateral Cuneiform (T29) The plantar spine is broken away taking with it the plantar apex of the distal facet, but it is otherwise complete. The distal medial tip is also broken away. The waist is exaggerated because the distal lateral corner juts very far out laterally. Of all four side facets, the distal lateral one is the only concave one.

Left Lateral Cuneiform (T23) This is complete with a repaired break through the thin bridge of bone to the plantar spine. The lateral distal corner, along with the side facet, is broken away and there is a small bit of abrasion on the proximal dorsal margin. The tubercle is small and round.

Right Cuboid Fragment (T61) Just the distal facet has been preserved. It is concave with the steepest edge leading to the medial facet for the lateral cuneiform. Using the bit of the plantar and dorsal surfaces that remain, it is evident that the distal facet is oriented slightly plantarly as seen in the others individuals. The distal facet width is 11.2 and the depth of the medial edge is 8.5.

Right MT1 (MT36) This is a complete bone. It is ossified but the epiphyseal line is still visible. It is a bit crushed on the dorsal proximal surface of the shaft due to compression of the shaft and head. There are three breaks through the shaft. The ridge in the center of the head that separates the sesamoids is oriented towards the medial side. The proximal facet gets wider as it goes dorsally. It is very concave due to compression.

Left MT1 (MT31/43) The entire bone is flattened mediolaterally. The tuberosity is gone taking part of the facet with it. There are three breaks through shaft. The flattening is much more severe proximal to the break at midshaft; the bone distal to this break is only partially flattened showing that the bone was broken before deformation was complete. There is a visible epiphyseal line as in the antimere. It is the same length as the right side despite it missing the tuberosity because of the deformation. There is a prominent crest in the center of the head.

Right MT2 (MT37) It is complete and mostly undeformed, but missing the epiphysis. There is a small (less than 2 mm^3) piece missing from distal third of shaft and there are four breaks through the shaft. Because the distal end is slightly deformed it is hard to tell how much torsion exists. The proximal facet is T-shaped and oriented medially.

Left MT2 (MT32) This one is complete and undeformed but missing the epiphysis. There are four breaks through the shaft. The distal end is twisted laterally about 15 degrees relative to the proximal end. Two puncture marks on the lateral side of proximal end could be carnivore tooth marks. The facet for the third metatarsal is large. The shaft is straight.

Right MT3 (MT38) This is a complete proximal end and shaft that is missing its epiphysis. There are four breaks in the shaft. The plantar corner of the proximal end is broken off and glued back in place. All the proximal facets are visible. The medial facet flares out from the shaft.

Left MT3 (MT33) Like the antimere, the plantar side of the proximal end is broken away, but otherwise it is complete. There are three breaks through the shaft and the midshaft is missing some bone. The proximal end is oriented medially with the dorsal margin slanting distomedially. The proximal facet is convex. The proximal shaft it is crushed, a portion of the middle shaft is missing, and the distal segment, although not crushed, is fractured. Both dorsal facets, lateral and medial, are visible. The lateral one for the fourth metatarsal is concave.

Right MT4 (MT39) The distal end is broken away just below the epiphyseal surface. There are two shaft breaks and the dorsal surface of the proximal end is abraded.

Left MT4 (MT34) It is complete, relatively undeformed and missing the epiphysis. There are four breaks through the shaft. The shaft is narrow like its antimere. It is compressed at the proximal end. The head is leaning slightly medially. The most proximal point is lateral on the proximal facet.

-

Right MT5 (MT40) This is only the proximal end. It is broken just as it tapers up into the shaft but all the facets are complete.

Left MT5 (MT35) It looks like a near mirror image of its antimere except it is broken just a bit higher up on the shaft and the lateral protuberance is larger. The facets are exactly the same size.

Comparative Anatomy

There are clear adaptations for a strong, grasping hallux like arboreal monkeys and apes. The grooves on the calcaneus and talus for the *M. flexor hallucis longus* are pronounced in *P. heseloni*. This confirms, as previous anatomists have noted on other specimens (Ward et al., 1993), that the *M. flexor hallucis longus* is relatively large in *Proconsul,* indicating strong grasping during climbing.

Like hylobatids and Old World monkeys, the *Proconsul* calcaneal tuber does not have a prominent plantar process. Sarmiento showed the plantar process to be the origin for the superficial head of the *M. flexor digitorm brevis* and argued that its presence in great ape and humans their common ancestor was probably a slow climber (Sarmiento, 1983). Its presence in great apes and atelines and howler monkeys correlates also to the musculature involved in foot suspension. Sarmiento (1983) argued that the absence of the heel process in hylobatids (which resembles other catarrhines) is a retention of the primitive hominoid condition which is illustrated well in *Proconsul.*

The cuboid facet on the calcaneus is c-shaped and open on the medioplantar side. The conical pit is deep and is located off-center, toward the open portion. Lewis (1980, 1989) compared this region to the great apes and saw similarities with *Pan.* There are also similarities with *Colobus* – another arboreal species that requires screw-like movement at the calcaneocuboid joint for eversion and inversion. The lateral side is much thicker and juts out more distally than the medial side in most specimens and the facet is angled superiorly like raised-heel walkers.

Other evidence of raised-heel, semi-plantigrade locomotion lies at the calcaneal tuber; the most proximally projecting point on the heel in *Proconsul* is higher (like

monkeys) than in plantigrade chimpanzees. The tuber is narrow for its height and for the length of the bone, which is consistent with Langdon's (1986) observations and proves it is not an artifact of deformation. The height of the tuber is affected by the inferior tubercle which gives the plantar axis a slightly arched appearance. It is not as pronounced in *Proconsul* as in *Pan* and is more like *Papio.* This arch swings medially as it approaches the tubercle like *Papio* and *Pan,* unlike the straight axis of *Colobus*.

The peroneal tubercle is small compared to *Colobus, Pan,* and *Papio*. But the lateral keeling of *Proconsul* is more prominent than in any of these three genera, with *Colobus* resembling it the most. There is a lateral pillar on dorsal anterior part, medial to the peroneal keel, and leading to the cuboid facet in *Proconsul*. In *Pan* and in the juvenile Individual IV it is only a tubercle, but in *Papio* it is large and buttress-like. It is not present in *Colobus*.

There is considerable inversion movement at the subtalar joint (Rose, 1983). There is a small pit where the interosseus talocalcaneal ligament attaches on the dorsal anterior surface that is also present in *Papio,* but is not visible in *Pan* or *Colobus*. The relatively conspicuous attachment site may indicate the ligament was strong for providing stability during inversion and for tolerating very little of it. This surface is deep just as it is on the *P. nyanzae* KNM-MW 13142 which may be an adaptation for ankle eversion (Langdon, 1986; Lewis, 1980, 1989; Walker & Pickford, 1983; Ward et al., 1993).

The talocrual joint is a complex one in higher primates (Barnett & Napier, 1952). *Proconsul's* relatively deep talar trochlea with moderate wedging of the articular surface (that is, narrower proximally and wider distally), and the relatively steep-sided facets for the fibular and tibial maleoli, indicate that during the later stages of the stance phase,

when the foot is transitioning from dorsiflexion to extension, abduction occurred but very little inversion was permitted (Rose, 1983). Wedging of the talus is significant because the wider the distal portion of the talar trochlea the better the tibia gets locked during dorsiflexion and this tight fit leads to immobility, or stability, at the ankle joint. This stability is necessary for a powerful push off. The opposite is true for plantarflexion where the tibia articulates with the proximal talar trochlea which, when wedged, is not as wide. This results in talocrural mobility for reaching out to grasp the branch to begin the next stance phase. Anatomy of the KPS individuals is consistent with Rose's 1983 observations that the *Proconsul* ankle had "good stability in dorsiflexion, when the trochlea and the malleolar-talar 'subjoint' are both fully engaged" (p. 413), which is consistent with a slow-moving arboreal quadruped.

The overall talocrural joint morphology is also consistent with the observations made by Ward and colleagues (1993) on the *P. nyanzae* talus, KNM-MW 13142C. "The presence of a fairly deep trochlear groove, together with [the] cup-shaped medial malleolar facet and deep pits for the attachment of the deltoid and talofibular ligaments, suggest that mediolateral stability during flexion and extension at this joint was of greater importance in *Proconsul* than in modern African apes" (p. 107-8). Ward and colleagues concluded this morphology was primitive for catarrhines and is consistent with an arboreal primate.

The attachment site for the talofibular ligament is *Colobus*-like in shape and size. It is less similar to the shallow indentation in *Pan* and much different than *Papio* with its long, linear and deep pit. The medial side, however, is just the opposite. The medial malleolar facet is much more pronounced than in *Colobus*. It is similar in shape to *Papio*,

but not *Pan.* The pit for the deltoid ligament is deeper and more prominent than in *Colobus*, but it is not as deep or as linear as *Papio*. It is most like *Pan*. The pit for the talonavicular ligament is like *Colobus* and *Ateles* but deeper than both which may correlate to its overall size being larger than those monkeys. It has a dorsal pillar which *Pan* and *Papio* do not have but is present in *P. nyanze* (KNM-MW 13142). In the infant, the pit for the talonavicular joint is relatively large and deep for the size of the bone and is similar to that seen in young apes.

The anterior calcaneal facet is slightly convex like *Colobus* and not as flat as *Pan* or *Papio*. The posterior edge is more like *Pan* than *Colobus* and very different from *Papio*. The resulting shape of the sulcus tali is *Pan*-like and also a bit *Colobus*-like.

The tuberosity on the navicular is more robust than in *Colobus* making it look less hook-like. It is actually more like the shorter and stouter tuberosity of *Papio* and nothing like *Pan*. However, the shapes of the facets are *Pan*-like. The talar facet shows the talus head and the navicular had extensive contact and the cuboid facet shows that extensive contact with the cuboid took place. The navicular of the subadult male KPS I is stout in comparison to the adult female KPS III which has nearly the same dimensions.

The distal and proximal ends of the medial cuneiform are much closer to parallel in chimps than in *Colobus, Macaca,* and *Papio*. These ends in *Proconsul* appear to be near parallel as well, even moreso than *Pan*. The hallucal facet in KPS I is not as s-shaped as the other KPS Individuals. The other KPS Individuals and KNM-RU 2036 are s-shaped like *Pan*; *Papio* and *Colobus* are straight in comparison. KPS I also lacks the plantar-distal tubercles seen in the adults and KNM-RU 2036. The distal facet is less medially oriented than in *Papio* and *Colobus* which have the entire facet on the distal

medial side. It is more like *Pan* in its orientation and shape implying similar adaptations for abduction.

The intermediate cuneiform appears to be twisted in all the KPS *Proconsuls*, especially Individual I. The proximal facet is rotated counterclockwise relative to the distal facet. Thus, the distomedial and the proximolateral corners are the furthest to project superiorly. The navicular facet is triangular with the longest side laterally. There are two medial facets and one lateral. The distal and proximal facets resemble *Pan* more than *Papio*. This element is much smaller in *Colobus* which makes comparisons difficult.

Lateral cuneiforms of *Proconsul* do not have the same proximal medial corner as chimps and gorillas. In *Pan* and *Gorilla*, the point floats dorsally on the rounded proximal facet. In *Proconsul* the point is located at the actual corner of the facet, even in *P. nyanzae* which is large and more bulbous at this end. The proximal half is very square, like *Ateles*, but not exactly like *Pan* or *Colobus*, and most distinct from *Papio*. The distal half is wider, which seems common, and there is usually a bit of waisting in the middle, which is only apparent in *Papio*. The proximal facet is oriented medially relative to the distal facet like *Papio* and *Pan*, but not *Colobus* or *Ateles* which are much squarer. The tubercle is not at all like the bumpy one in *Pan*; it is more like *Papio* and *Colobus*. The distal facet is shaped like *Papio*, but the proximal facet is shaped like none of the comparative taxa. It is flat and square with nice sharp edges.

The metatarsal facet on the cuboid is angled plantarly like *Colobus* and *Papio*, unlike *Pan*. There is a very strong beak-like calcaneal process akin to that on chimpanzee cuboids; *Alouatta* have only a small bump and baboons have a flat facet. This beak fits well into the deep distal calcaneus when the forefoot supinates about the

hindfoot which completes inversion at the subtalar joint (Rose, 1983). The distal and proximal joint surfaces of the cuboid are more parallel than *Alouatta* and *Ateles* where the distal end is slanted laterally. The distal facet is flat, with no lateral facing portion for the fifth metatarsal.

The proximal joint surfaces on the metatarsals are narrow like monkeys and more like the width of the shaft than wider as in apes – a trend that must be heavily influenced by body size. The middle crest on the head of the hallucal metatarsal is more asymmetrical than *Colobus, Papio,* and *Pan*. It is nearly flat on the medial side and rounded over on the lateral. Just like monkeys and apes it is oriented towards the second metatarsal (or laterally). The hallucal-cuneiform joint indicates the hallux faced laterally and plantarly (Rose, 1983). The dorsal edge of the proximal facet on the second metatarsal is oriented more medially like monkeys, unlike the more strictly proximal orientation of *Pan*. Also, the facet is triangular, not t-shaped, which is more like *Colobus* than *Papio, Alouatta,* or *Pan*. The proximal facet on the third metatarsal is t-shaped with the long axis veering laterally like *Ateles*. And like the second metatarsal, the dorsal edge of the cuneiform facet is oriented medially like monkeys, not like *Pan* which faces more proximally. There is a monkey-like plantar medial facet on the fourth metatarsal, not seen in *Pan*. The medial and lateral sides of the fourth proximal facet are parallel like monkeys and do not taper plantarly like *Pan*. The fourth metatarsal is longer than or equal in length to the second metatarsal, which is a monkey, not an ape, condition. The fifth metatarsal has no significant lateral tuberosity and its side has no distinct sesamoid facet like *Papio.* The cuboid surface is oriented superiorly unlike *Pan* setting the metatarsal in a

dorsiflexed position. The dorsal facet on the fifth metatarsal for the fourth metatarsal has a plantar lip that is noticeably raised from the surrounding bone like in *Papio*.

The anatomy of the KPS pedal remains is consistent with previous descriptions and analyses made by researchers on previously collected *Proconsul* tarsals and metatarsals (Langdon, 1986; Lewis, 1980, 1989; Napier & Davis, 1959; Preuschoft, 1973; Rose, 1983; Walker & Pickford, 1983; Ward et al., 1993). These prior observations were based on incomplete feet and sometimes fragmentary bones, yet my observations of the KPS collection (which contains numerous representatives of all the elements of the foot), show that the earlier findings still hold: The *Proconsul* foot is a mosaic of monkey- and ape-like anatomy and, furthermore, individual bones themselves have both monkey- and ape-like features.

Chapter 4

FOOT AND HINDLIMB PROPORTIONS OF *PROCONSUL HESELONI*

Foot proportions differ among catarrhines and these differences, although constrained by phylogenetic history, align with differences in locomotion and substrate use (Schultz, 1963a; Langdon, 1986; Manley-Buser, 1991; Strasser, 1992; 1994; Gebo 1993; Wunderlich 1999; and others).

Schultz was one of the first to realize the importance of studying the foot as a whole, as opposed to describing the morphology of each individual bone. He and others since then have emphasized the difference in mechanical and anatomical proportions in anthropoid feet (Figure 4.1).

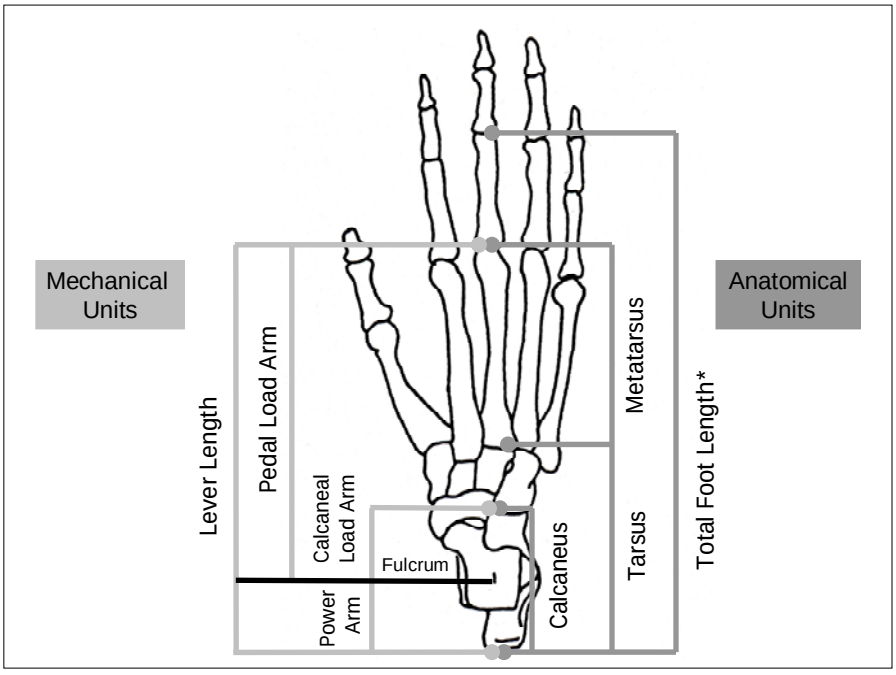

Figure 4.1. Mechanical and anatomical units of the primate foot. (*) Total foot length does not include the middle and distal phalanges because they are often missing from skeletal collections or impossible to identify when the foot skeleton is incomplete (Strasser, 1992).

Mechanical units of the foot are modeled as a lever. The power arm is the length of the posterior portion of the calcaneus and the pedal load arm is the lever-arm of body weight. The power arm determines the force and the speed at which the load arm can be plantar-flexed about the fulcrum which lies at the center of the crural joint between the talus and the tibia. This is equivalent in linear distance to the center of the posterior facet of the calcaneus (Strasser, 1992), which is the measure used in this study.

The flat posterior portion of the calcaneal tuber (heel) is the attachment site and the lever arm for the *triceps surae*. A shorter calcaneal tuber allows faster rotation under the talus and tibia, while a longer one lengthens the moment and results in slower rotation (Schultz, 1963; Langdon, 1986). Although a longer calcaneal tuber sacrifices quickness, it provides stability and strength and is found in larger bodied primates (Schultz, 1963). This is not, however, a mammal-wide trend (Maynard-Smith and Savage, 1956).

Another way to conceptualize foot mechanics is to imagine the fulcrum at the non-hallucal metatarsal heads during plantigrade walking or leaping, with the tarsus and metatarsus acting as a second-class lever for the *triceps surae* and the load acting at the talocrural joint (Strasser, 1992).

However, for arboreal monkeys and apes that grasp branches between the hallux and the lateral digits, the fulcrum probably lies at a joint or joints near the web of flesh between the hallux and the lateral digits (Jolly, 1965 Ph.D. thesis, in Strasser, 1992). With the fulcrum position changed, the lever would also have to change. For now, however, it is still best to compare the standard lever (from heel to third metatarsal)

across catarrhines while workers continue to gather more data on foot postures and pressures (Meldrum, 1991, Wunderlich, 1999). Differences among mechanical units of the feet between arboreal and terrestrial species need to be considered carefully.

Among cercopithecoids, the power arm has a positively allometric relationship with body mass but the pedal load arm has a negative one, allowing larger animals to maintain the mechanical equivalence of smaller ones (Strasser, 1992). By reducing the load arm and increasing the power arm, the required muscle force is reduced for larger animals to push-off with their feet. Furthermore, shortening the load arm reduces the compressive and bending forces in the foot for larger animals (Strasser, 1992). Colobines have shorter power arms and longer load arms presumably for leaping during arboreality, as compared to generalized, and often more terrestrial quadrupeds like cercopithecines. This is the predicted pattern for all leaping animals: to have a "high gear" ratio that contributes to increasing take-off velocity (Hildebrand, 1988).

Anatomical units group whole bones of the foot together (Figure 4.1). They often combine different mechanical segments and are thus more useful for comparing metatarsals and phalanges than for analyzing the tarsals. For instance, the tarsus combines the power arm of the triceps surae and a part of its load arm. Also, foot length combines the power arm and load arm of the *triceps surae* plus phalangeal length which comprises the load arm for the digitial flexor muscles.

Arboreal primates have longer pedal phalanges and metatarsals for grasping during climbing than terrestrial ones which have shorter metatarsals and especially shorter phalanges. The reduction of phalangeal length in cercopithecids is associated with the decreased importance of grasping in locomotion and an early phase of digitigrade

locomotion (Strasser, 1992). Reduced phalanges relative to foot proportions is also indicative of greater terrestriality in gorillas and dedicated terrestriality in humans (Schultz, 1963). However, the long calcaneus in gorillas is more closely associated with body size and is not necessarily indicative of terrestriality (Manley-Buser, 1991). Although increased body sizes usually leads to both a reduction of arboreality in apes and an increase in terrestriality so there may not need to be a distinction here. Gorillas have large body sizes, they are more terrestrial and they have a long calcaneus that is typical of both terrestrial primates and large bodied primates. Within gorillas, lowland gorillas (*G. g. gorilla*) are much more arboreal because the habitat for mountain gorillas (*G. g. beringei*) has fewer trees (Hunt, 2004; Remis, 1995).

Proportions of the *Proconsul* foot have only received brief attention. In a 1993 abstract, Strasser reported results from a preliminary analysis of the KPS foot proportions which were never published as a paper (Strasser, 1993). She compared the proportions of the adult KPS III to colobines, cercopithecines and hominoids. She found that in the relative length of the tarsus, compared to foot length, *Proconsul* is most similar to colobines. The ratio of the *P. heseloni* power to load arms in the foot are also colobine-like. For its body mass, *P. heseloni* is most similar to colobines and arboreal cercopithecines in the lengths of the third metatarsal, third proximal phalanx relative to foot length, and the relative length of the first metatarsal to the third metatarsal. Strasser found that the *P. heseloni* hallucal proximal phalanx is ape-like (hylobatid-like in particular), having longer hallucal components than similarly-sized cercopithecids.

The relationship between body size and foot proportions has been studied among species and through ontogeny in primates (Schultz, 1963; Strasser, 1992, 1994; Manley-

Buser, 1991). Geometric similarity or isometry is usually the null hypothesis tested in such studies; that is, shape is equivalent no matter the size (Gould 1966). For feet, as for the rest of the skeleton, linear metric changes during growth were accompanied in life by areal and volumetric changes. These changes do not occur at the same rates since area is a squared metric and volume is a cubed one. As an animal increases its body mass during growth (volume) its muscles and bones must compensate at a proportionally greater rate to maintain functional equivalence. This trend often leads to allometric scaling that differs from isometry and is one that is frequently observed in primate post-cranial studies (e.g. Jungers, 1985; Manley-Buser, 1991).

Foot proportions change through ontogeny. That is, units of the foot do not behave isometrically with respect to one another as individuals mature. A major influence in this pattern is the increase of body size (ontogenetic scaling). But another potentially influencing factor may be the need to maintain functional equivalence (biomechanical scaling). When changes in scale are not ontogenetic or biomechanical they may represent novel adaptive changes in the group (Gould, 1977). And this is what is happening during the ontogeny of the human foot (Manley-Buser, 1991). For instance the calcaneal tuber becomes much more robust compared to other hominoids in order to withstand the high impact force of heel strike (Manley-Buser, 1991). Changes in foot use and locomotion during development are also potentially influencing changes in foot proportions during ontogeny. Primates that spend their early years clinging to their mother may show different foot proportions early in life because they are not yet walking around like adults. These types of changes may not be apparent by simply regressing linear metrics against body size of sample means lumped together by dental age (Manley-Buser, 1991).

Proportional changes (ratios or indices of linear metrics) of across species grouped by dental stages, and ideally, of individuals against real or estimated chronological ages may reveal patterns of growth that align with ontogenetic changes in locomotion.

Specific Aims

Here the foot and hindlimb proportions of various catarrhines are analyzed and compared to those of six *Proconsul* individuals. Both ontogenetic as well as strictly adult comparisons are made in order to better reconstruct the function of the *Proconsul* foot as well as interpret patterns of growth. The first goal of the analysis is to detect and track ontogenetic changes in foot proportions (Ho = There are no changes in hindlimb proportions through ontogeny). Foot proportions of the ontogenetic sample of *Gorilla gorilla*, *Macaca mulatta* and *Pan troglodytes* will be analyzed by age and body size and compared to *Proconsul*. If changes in hindlimb proportions are detected, their correlation to known ontogenetic shifts in locomotor behavior will be discussed.

The second goal is to choose an extant model for *Proconsul* foot morphology. Previous workers have already shown that there are differences between catarrhine species in foot proportions. Therefore, the test of this hypothesis will only be repeated briefly, but it is important to do so in order to show that the comparative taxa are useful for building a diagnostic multivariate model to classify *Proconsul.*

Materials and Methods

Sample

Data were collected from a sample of 462 catarrhine skeletons and compared to *Proconsul*. Only those individuals with at least one complete femur were included in the study since femoral head breadth is used to estimate body mass and femur length is compared to foot proportions. Of the extant sample, 217 are adults and the sample sizes by species are listed in Table 4.1. Individuals with third molars in occlusion are considered adults. Orangutans (*Pongo pygmaeus*) were not sampled because of their unique, highly inverted foot positioning when walking terrestrially (Tuttle, 1970).

Bones of the hands and feet can be problematic for study in skeletal collections. Often these elements are left inside the skins, are left articulated with mummified muscles, ligaments and tendons, or are re-articulated with wires. In the latter two cases,

Table 4.1. Adult specimens and their locations. CPRC = Caribbean Primate Research Center, University of Puerto Rico Medical School, San Juan; HTB = Hamann-Todd Collection, Cleveland Museum of Natural History; MCZ = Museum of Comparative Zoology, Harvard University; PCM = Powell-Cotton Museum, Birchington, Kent; RCMA = Royal Museum of Central Africa, Tervuren, Belgium; Zurich = University of Zurich, Switzerland.

Species	**Institution**	**Female**	**Male**	**Total**
Colobus angolensis *Colobus guereza* *Colobus badius*	PCM, RCMA	12	12	24
Gorilla g. gorilla	HTB, PCM, RMCA	6	12	18
Hylobates lar lar *Hylobates lar mulleri*	MCZ	6	6	12
Macaca mulatta	CPRC	15	14	29
Nasalis larvatus	MCZ	4	6	10
Pan paniscus	RMCA	9	6	15
Pan t. troglodytes *Pan t. schweinfurthii*	HTB, PCM, RCMA, Zurich	74	35	109

the individual may still be listed in the catalog (if there is such detail) as possessing the hands and feet, but they are unusable. So anticipated sample sizes for studies that focus on manual and pedal elements are always higher than can actually be obtained.

Standard linear measures (Langdon, 1986; Manley-Buser, 1991; Schultz, 1963; Strasser, 1992) were taken from the tarsals, metatarsals and proximal phalanges (Figure 4.2) using Mitutoyo calipers to the nearest 0.1 mm. Measurements, indices (proportional ratios of foot measures), abbreviations, and their definitions are listed in Appendix A.

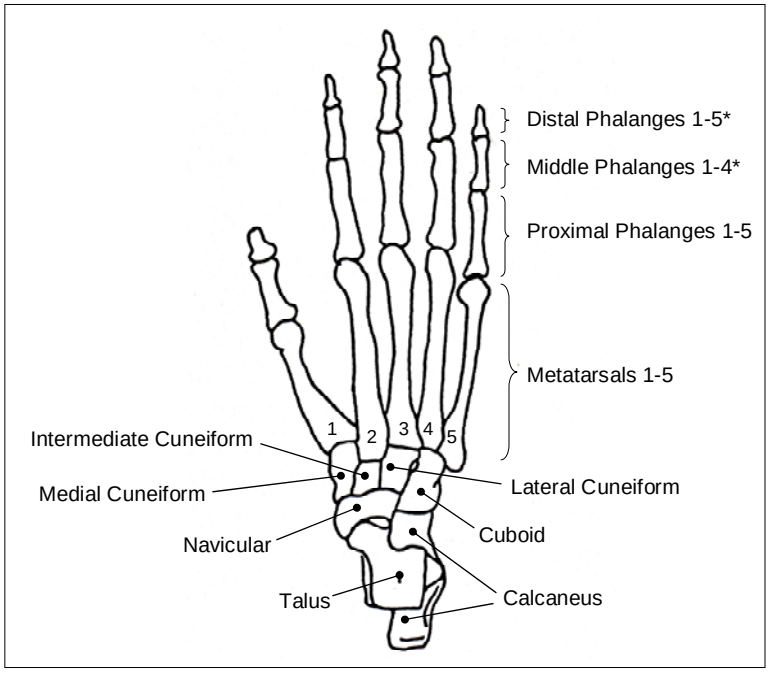

Figure 4.2. Bones of the primate foot. (*) Middle and distal phalanges are not analyzed in this study.

Ontogenetic data were collected from a cross-sectional sample of macaques and chimpanzees (Table 4.2). Growing bones, particularly of very young individuals, can be problematic when collecting metric data. Immature tarsals with only partly calcified

cartilaginous anlagen can appear amorphous until they take their adult shape, so identifying metric landmarks on such bones can be difficult. This is particularly the case with the navicular, cuboid, and cuneiforms. The majority of the measurements taken for the analysis were obtainable from individuals across the developmental spectrum.

The fossil sample (Table 4.3) consists of six *P. heseloni* KPS Individuals III and the left foot from the partial juvenile skeleton, KNM-RU 2036, which is the type specimen of *P. heseloni* (Walker et al., 1993).

	1	**2**	**3**	**4**	**5**	**Total**
Gorilla g. gorilla	8	17	11	11	18	65
Macaca mulatta	12	16	27	31	29	115
Pan troglodytes	16	47	35	15	109	222

Table 4.2. Sample size breakdown by age group for each taxon in the ontogenetic sample.

Table 4.3. *Proconsul heseloni* individuals in the sample. (*) Sex determined by lower canine shape (Kelley, 1995).

Specimen	**Age and Sex**	**Reason**	**Age Group**
KPS Individual I	subadult male	Some fusion, size	4
KPS Individual III	adult female	Fully fused	5
KPS Individual IV	infant	M1 crown	1
KPS Individual VII	juvenile female	Little fusion, size	3
KPS Individual VIII	subadult female	Some fusion, size	4
KNM-RU 2036	subadult female*	Canines present, third molars erupting, size	4

Macaques and chimpanzees are good comparative taxa for the ontogenetic analysis for several reasons. They have different locomotor repertoires within quadrupedalism and both species have been proposed as models for *Proconsul* functional morphology (Li et al., 2002). Macaques are classic terrestrial and arboreal quadrupedal cercopithecoids. Chimpanzees, by comparison, climb and brachiate in the trees and

knuckle-walk terrestrially and arboreally. The two species represent a good contrast between a hindlimb driven, mostly terrestrial quadrupedal monkey and a more forelimb-reliant quadrupedal ape. *Proconsul heseloni* shares similarities with macaques in body size and proportions (Walker & Pickford, 1983; Ruff et al., 1989) and with chimpanzees in hallucal morphology and proportions (Strasser, 1993). Since they are located on separate evolutionary branches, macaques and chimpanzees represent distinct phylogenetic categories as well, which is important considering *Proconsul*'s temporal proximity to the split between Old World monkeys and apes. Most importantly in this case, however, is that relatively large and well-curated skeletal collections exist for macaques and chimpanzees of all ages. *Gorilla gorilla* individuals were included in the ontogenetic sample in order to track effects of large body size on foot proportions.

The sample of rhesus macaques was derived entirely from the skeletal collection at The Caribbean Primate Research Center, located at the University of Puerto Rico. This collection was ideal for this study because it contains a large number of complete well-curated rhesus macaque skeletons of all developmental stages. The skeletons are derived from a colony of free-ranging monkeys reared in a uniform environment that are extremely well-documented from long term observation (Rawlins and Kessler, 1986).

Age Estimation

Macaques at the CPRC all have documented ages at death, but dental eruption stages were noted according to Kenney (1975) and Cheverud (1981). Dental ages of chimpanzees and gorillas were determined using the eruption schedules in Dean and Wood (1981). In order to compare the extant samples to the fossils, macaque and

chimpanzee specimens were placed into age groups according to dental eruption stages (Table 4.4). *Proconsul* individuals were then placed into age groups according to associated dental remains, to the state of epiphyseal fusion, and to general size (Table 4.3).

Table 4.4. Developmental age groups constructed according to dental eruption stages according to years after birth. *Macaca mulatta* and *Pan troglodytes* show similar order of eruption timing (Cheverud, 1981). Locomotor information based on observational data: Macaques achieve adult locomotor patterns by 18 months (Wells and Turnquist, 2001), gorillas by 4 years and chimpanzees by 5 years (Doran, 1997).

Macaca **Age in years**	***Pan, Gorilla*** **Age in years**	**Tooth Stage**	**Age Group**	**Locomotion**
<1	<3	Only deciduous teeth visible	1	Immature
1-<2.5	3-<6	M1 erupting	2	Transitional
2.5-<4.5	6-<8	Stage 2 complete and M2 erupting	3	Adult
4.5- <7	8- <11	Stage 3 complete and M3 erupting	4	Adult
>7	>11	All teeth in occlusion	5	Adult

Body Size Estimation

Body mass standardization is necessary for interpreting functional analyses of postcrania between individuals and taxa (Jungers, 1985). It is also important to account for body size in ontogenetic studies in order to tease out the effects of the inevitable trend of a growing body size and mass from any other changes occurring in the skeleton.

Body weights at death were not recorded for the macaques that died on Cayo Santiago because they decompose quickly in the tropical environment. Likewise, body weights are unknown for most of the chimpanzees in the sample, and for the strictly adult groups as well.

Body masses were calculated using femoral head breadth (FHB) according to the following equations (Ruff, 2003a) and are reported in Table 4.5 along with estimations of *Proconsul* body masses (Rafferty et al., 1995).

***Pan* and *Gorilla*:** **ln Body Mass = ln FHB * 3.019 - 6.668**

***Hylobates*:** **ln Body Mass = ln FHB * 3.024 - 6.718**

***Macaca*:** **ln Body Mass = ln FHB * 2.389 - 4.541**

***Colobus* and *Nasalis*:** **ln Body Mass = ln FHB * 2.424 - 4.684**

Table 4.5. Body mass estimates and descriptive statistics made using equations in Ruff (2003a) of the adults in the extant comparative sample with the estimates for *Proconsul* made by Rafferty et al. (1995).

Estimated Body Mass (kg)						
	N	Mean	SE Mean	StDev	Minimum	Maximum
Colobus	**24**	**8.098**	**0.242**	**1.187**	**5.868**	**10.602**
Female	12	7.72	0.333	1.153	5.868	9.832
Male	12	8.476	0.33	1.143	6.662	10.602
Gorilla	**18**	**146.8**	**13**	**55.2**	**75.3**	**222.6**
Female	6	76.528	0.381	0.934	75.325	77.19
Male	12	181.87	7.47	25.88	156.87	222.59
Hylobates	**12**	**5.629**	**0.259**	**0.896**	**4.207**	**6.703**
Female	6	5.629	0.406	0.994	4.207	6.703
Male	6	5.629	0.36	0.883	4.224	6.552
Macaca	**29**	**8.118**	**0.328**	**1.764**	**5.549**	**11.859**
Female	15	6.671	0.188	0.73	5.549	7.931
Male	14	9.668	0.284	1.061	8.292	11.859
Nasalis	**10**	**13.62**	**1.19**	**3.77**	**9.02**	**20.52**
Female	4	10.661	0.179	0.358	10.158	10.956
Male	6	15.59	1.52	3.72	9.02	20.52
P. paniscus	**15**	**40.71**	**1.67**	**6.47**	**30.3**	**55.67**
Female	9	39.85	2.03	6.08	30.3	50.07
Male	6	41.99	3.02	7.39	35.55	55.67
P. troglodytes	**104**	**48.753**	**0.979**	**9.988**	**31.721**	**81.579**
Female	72	46.44	1.01	8.53	31.72	70.14
Male	32	53.96	1.97	11.15	31.82	81.58
Estimated Body Mass (kg) for *Proconsul*						
KPS I			Male	13.6		
KPS III			Female	10.9		
KPS 2036			Female	9.8		

For most of the analysis femoral head breadth (FHB) serves as a surrogate for body mass according to methods used by previous workers (Manley-Buser, 1991; Strasser, 1992) (Figure 4.3). FHB provides a body size variable for the ontogenetic sample since equations using bones of the hindlimb are not yet available for estimating immature body masses in catarrhines; it is not yet known how the relationship between long bone dimensions and body mass behaves throughout ontogeny. However, parameters to make such estimations may soon be available. Recent work by Raichlen shows that baboons (*Papio cynocephalus*) have a near isometric relationship between hindlimb length and body weight during their first year which includes the transition to locomotor independency (Raichlen, 2004).

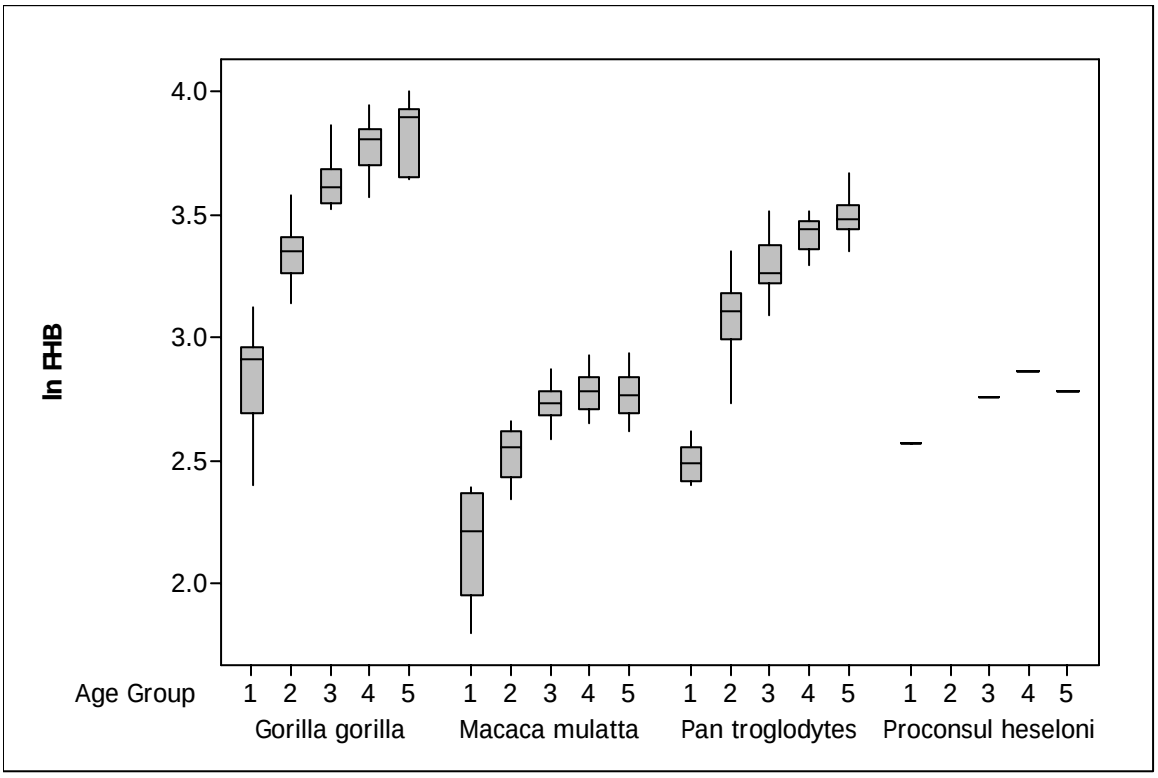

Figure 4.3. Femoral head breadth (natural log-transformed) for the ontogenetic sample.

Since femoral head breadth is used to estimate body mass, and since it was measured in all the immature individuals, and was available for four of the six *Proconsuls* (KPS I, III, IV, VII), it will be used as a surrogate for body size. Calcaneus length correlates well with the femoral head breadth across the sample (Table B.1, Appendix B; Calc1 vs FHB, R = 0.96) and it is the only such variable shared by all *Proconsuls*, however it is not used as a general size variable because the calcaneus length, particularly posterior length, is variably affected by function and body size and it is already an element of many of the important mechanical and anatomical units being compared.

The *Proconsul* data contains entries for left and right feet, with one foot often preserving different measurable parts from the other. Since it is reasonable to expect that the right and left foot are of similar size, the data from the right and left feet were collapsed into a composite for each *Proconsul* individual. In the case of contradictory measures due to deformation of a bone on one side, the measure from the best preserved side was kept and that from the deformed bone was discarded. Once composite *Proconsul* feet were constructed, a list of measures that all *Proconsuls* share could be tallied since the multivariate statistical methods do not tolerate missing values.

Statistical Methods

The goal of this study is to interpret *Proconsul* morphology, not to analyze the overall allometry and ontogeny of the catarrhine foot. In order to understand *Proconsul* foot proportions it was necessary to collect data from a comparative sample, but since rigorous analyses of the pedal differences between the species have been performed by

previous workers, they are not repeated here. Scaling patterns and proportions within the foot and hindlimb are investigated insofar as to determine that the data were collected well and that they are useful for building a discriminant model with which to predict affiliation of *Proconsul*. All statistical analyses were carried out using the statistical software Minitab® version 14.

There are two aims of the statistical analysis:

1. To test whether or not foot proportions change during ontogeny using bivariate analysis.

One-way analyses of variance (ANOVAs) and least-squares regressions are used to test if measures and proportions of the foot are correlated to one another and to body size through development within species in the ontogenetic sample. All data were natural log-transformed prior to analysis as is standard in order to maintain linearity of functions, to make visualization easier, and to prevent larger primates from disproportionately affecting results (Sokal and Rohlf, 1995). Indices were first multiplied by 100 according to standard (Strasser, 1992).

Tukey's tests were applied to all pairwise comparisons between age groups within each species for means of each index of foot measures. Patterns of growth and development of *Gorilla gorilla*, *Macaca mulatta*, and *Pan troglodytes* feet are inspected by analyzing changes in relative foot proportions. The relative proportions of the foot were compared at different developmental stages using ANOVA of natural log-transformed data. Individuals were correlated by dental age for interspecific comparisons (Table 4.4). Box-plots show means, interquartile ranges and outliers. *Proconsul* is

included for visual inspection. Scatterplots of these proportions by real (*Macaca*) and estimated chronological age (*Gorilla* and *Pan)* show a more continuous look at changes through growth than the integer-based age groups in the box-plots. There is only one age estimate for the KPS collection and that is for KPS IV at 1.2 years old (Beynon et al., 1998) and it is plotted in graphs where the data for the individual were preserved. Slopes of regression lines can be compared to the general trends in the box-plots.

In regression analyses, a high R-squared indicates the model fits the data well and a significant p-value indicates there is a strong relationship between the two variables. Slopes were determined for a subset of metrics (focused on here because they are shared by the parts preserved in *Proconsul*) and for the indices for each species in the ontogenetic sample against age and femoral head breadth (FHB). Positive correlations indicate positive allometry for the ratios, lack of a significant correlation may indicate isometry (Mosimann and James, 1979). If the numerator has a more positive allometric relationship with body size than does the denominator, the index will have a positive correlation with body size. And if the numerator has a more negative allometric relationship with body size than does the denominator, the index will have a negative correlation with body size. If the two measures in the index have the same allometric relationship with body size, then the index will have no correlation with body size (Strasser, 1992). Significance level is set at $P < 0.05$ throughout. Statistical analyses were complemented with visual inspection of box-plots and scatterplots.

Proconsul, with its small sample size, cannot be run through these tests but its position on scatterplots and box-plots can be visually assessed.

Adult apes beyond age 10 are not included in the analyses using chronological age since their ages were not estimated as precisely as younger ones; all individuals with full third molar occlusion were labeled 11 years old and if included would unnaturally skew the results. However, the older macaque individuals do have known ages at death and are included.

Proconsul has not been likened to gorillas in foot or hindlimb morphology, however they are included in the comparative ontogenetic analysis for some very important reasons. They are one of the few species to be strongly represented across ages in museum skeletal collections. More importantly, since they are closely related to chimpanzees but grow to be much larger, they serve to model the effect of large growth in body size on the changes in foot proportions during ontogeny.

The second aim of the statistical analysis is:

2. To use the results of aim 1 to discern which extant species is the best model for *Proconsul* using multivariate analysis.

First a cursory look at adult proportions is made using ANOVA and regression. Taxa are grouped by genus except for *Pan.* Bonobos (*Pan paniscus*) are kept separate from common chimpanzees (*Pan troglodytes*) to compare the two closely related species. Regressions by group against FHB are performed on the subset of metrics as mentioned above. The focus, however, is on comparisons of indices of the foot and do not take body size into account. Further comparisons could be done by regressing these indices against FHB, however, a more comprehensible multivariate method will be used instead, that

will separate out the groups by foot morphology and will use that to align *Proconsul* with modern groups.

Principal components analysis (PCA) and linear discriminant analysis (LDA) are used to build a model that can discriminate between foot morphology of extant groups which is used to classify the morphology of the *Proconsul* individuals.

Linear Discriminant Analysis (LDA) is a popular statistical approach to classification (Balakrishnamma & Ganapathiraju, 2003). It is similar to linear regression but instead of computing the line that produces the least squares error, it computes a line (in the case of two variates) or a hyperplane (in the case of multivariate) that separates classes while minimizing the between and within class variation.

The error rate is computed by counting the total number of misclassified observations produced by the linear split. This error rate is usually too optimistic because the data being classified are the same data that were used to build the model.

A more reasonable estimate of classification error rate is provided by the cross-validation error rate which is estimated by leaving an observation from the data set out when computing the linear discriminant function. Then that observation is classified. This procedure is repeated until each observation has been excluded.

Here several LDA classifiers for family (apes and monkeys) and genus (*Colobus, Gorilla, Hylobates, Macaca, Nasalis, Pan*) were built for different combinations of traits.

The data are sparse for many of the *Proconsul* individuals; that is, most have missing pedal elements so some variables are unknown. LDA removes all observations that contain at least a single missing value. So traits that were most often shared by *Proconsuls* were emphasized, although some trials explored the use of interesting traits

that did exclude some *Proconsuls*. No composite measures (e.g. foot length) were used in the model because they are perfectly correlated with the variables used to compute them.

Metrics for the multivariate analysis were divided by the geometric mean which is defined as the nth root of the product of all variables (for each individual), where n is the number of variables. The geometric mean condenses the overall size of an individual as shown in the measurements into one quantity or dimension and is highly correlated with volume of the structure being measured (Jungers et al., 1995; Mosimman, 1970). The geometric mean is calculated for each individual, and then each linear measure is divided by it to get a new dataset of size-adjusted variables. The geometric mean is commonly used by physical anthropologists to remove body size from the dataset (Aiello et al., 1999; Lockwood et al., 1996).

Once the variables were size-adjusted they were run through a principal components analysis (PCA). Components with Eigen values greater than 1.0 are conventionally considered significant and these were run through the LDA. Then they were fed back into the model for classification. In anatomical analyses, PC1 is almost always representative of body size.

The linear discriminant function gives the equation by which samples are classified. The classification is made as follows:

$$\mathbf{Group(x_1,x_2) = c + ax_1 + bx_2}$$

For example, "family" is classified as follows:

$$\mathbf{Group_{ape}\,(PC1,PC2) = A + B*PC1 + C*PC2}$$

$$\mathbf{Group_{monkey}\,(PC1,PC2) = D + E*PC1 + F*PC2}$$

Where,

PC1 & PC2 = Principal components 1 & 2

A, B, C & **D,E,F** = Computed constants (A,D) and variables (B,C,E,F) in the linear discriminant functions

The observation is classified into $Group_{monkey}$ if after its principal components scores are entered into the discriminant function $Group_{monkey} > Group_{Ape}$ and vice versa.

The decision boundary (line) is calculated by setting the two functions equal to each other and then solving for one of the variables:

$$\mathbf{PC2 = (E - B)/(C - F) * PC1 + (D - A)/(C - F)}$$

Scatterplots of PC1 and PC2 for each trial of the LDA show the decision boundary. Only the first two principal components are plotted even when more were used in the LDA because they account for most of the variation and are therefore the best visual representations of the discriminant function results.

Multicolinearity is an issue with multivariate analyses. It arises when predictor variables are highly correlated with each other. The presence of multicolinearity implies that the predictor variables contain a high degree of redundant information. Minitab will automatically remove variates that are highly correlated. Table B.1 shows that most of the metrics of the bones of the foot are strongly correlated.

To reduce multicolinearity principal components were computed first, then used in the linear discriminant analyses (LDA). Principal components construct a new

orthogonal basis for the data with the most information contained in the first component, the remaining in the second, and so on.

The maximum number of variables that is safely tolerated in LDA is about fifteen. Normally variables are run through a stepwise procedure to choose which ones best discriminate between groups prior to loading them into the LDA. However, there are only a limited number of variables that all *Proconsuls* share, due to preservation issues, and these, along with anatomical information, were used to inform model construction in five separate trials.

Bivariate Results: Ontogenetic Sample

Pearson's correlation coefficients were calculated between natural log-transformed metrics (which produces the same results when performed on the raw data) for the pooled-age sample of all extant taxa. Pearson's R is a measure of the amount of linear association between the variables of interest. All but three of the significant correlations are significant at $p = 0.000$. The few that are not significant involve immature measures and they are the only ones to have negative R. The navicular is one of the last bones to ossify, so measures of NAV3 and NAV4 were not reported for many immature individuals and thus, the low sample size probably affected its insignificant correlation with MT1D. Cub2 does not correlate with femur diaphysis (FemurLD) because of its variability and its low availability in immature individuals. Estimated body masses using the femoral head breadth (FHB) are only reported for adults and did not significantly correlate with any of the metatarsal diaphyseal lengths or the fibular diaphysis (FibLD) because most adults do not have these values reported. All significant

correlations are positive indicating that as one variable increases the other increases. When just adults are analyzed all are significantly correlated and all but one have p = 0.000. Overall, there are very strong pairwise correlations between all measures of the feet across this sample of catarrhines.

Regression statistics for indices against age are presented in Tables B.2-B.4, Appendix B. However, because the two ape species' ages are estimated, the "true" continuous nature of the growth curve is compromised, as most individuals' ages are reported as an integer. The macaque ages are much more precise and include partial years, so the function and its regression statistics are based on more precise data.

Regressions found not to be significant for indices versus age and FHB are considered to indicate isometry between the two variables in the index. *Gorilla* and *Pan* show far more instances of isometry across the age groups than *Macaca*. Many of the indices are also significantly correlated with femoral head breadth which means that they are experiencing allometric shape change associated with body size increase which is to be expected (Tables B.2-B.4).

Further regression statistics for a subset of the linear metrics that are shared by all the *Proconsul* individuals are reported in Tables B.2 - B.4. That is, all KPS individuals and KNM-RU 2036 have these parts preserved for measurement. They are the same traits used in the multivariate analysis.

Summaries of results for each index are discussed below.

Figures 4.4 - 4.48 and Tables 4.6 - 4.20 contain results for proportional changes in the foot through ontogeny. See Appendix A for explanations of the indices used. For each index a box-plot, an ANOVA table and two scatterplots illustrate proportional data and are defined as follows:

Figures 4.4, 4.7, 4.10, 4.13, 4.16, 4.19, 4.22. 4.25, 4.28, 4.31, 4.34, 4.37, 4.40, 4.43, 4,46. Box-plots of natural log-transformed index showing medians, interquartile ranges and outliers (starred) of each age group (1-5) within each species. *Proconsul* is graphed for comparison.

Tables 4.6 - 4.19. Results of ANOVA of variables (labeled) between the age groups within each species. Pairwise comparisons between age groups of Tukey 95% confidence intervals are marked "x" when means are significantly different.

Figures 4.5, 4.8, 4.11, 4.14, 4.17, 4.20, 4.23, 4.26, 4.29, 4.32, 4.35, 4.38, 4.41, 4.44, 4.47. Scatter-plots of index (labeled) against actual or estimated chronological age by species with regression line. Statistics are reported in Tables B.2, B.3, B.4, Appendix B).

Figures 4.6, 4.9, 4.12, 4.15, 4.18, 4.21, 4.24, 4.27, 4.30, 4.33, 4.36, 4.39, .42, 4.45, 4.48. Scaling of foot proportions with body size. Scatterplots and taxon-specific regression lines for natural log-transformed indices (labeled) against femoral head breadth (FHB) for individuals in the ontogenetic sample. Statistics are reported in Tables B.2, B.3, B.4, Appendix B.

Tibia/Femur (Figures 4.4- 4.6, Table 4.6)- This ratio is commonly called the crural index and out of the modern taxa here *Macaca* has the highest. The two apes are relatively stable across age groups but *Macaca* is showing a clear increase in femur length relative to tibia length through development. *Gorilla* and *Pan* achieve adult proportions by age group 2. *Gorilla* tibia growth exceeds femur growth slightly with age. *Proconsul* plots above everything with the highest crural index and it is showing an increase in tibia growth through time and a slow down of femur growth most similar to *Gorilla* out of the three modern taxa. KPS IV (infant) plots near *Pan.* The infant groups closer to *Pan* infants, but the two oldest *Proconsuls* cluster near the *Macaca* adults.

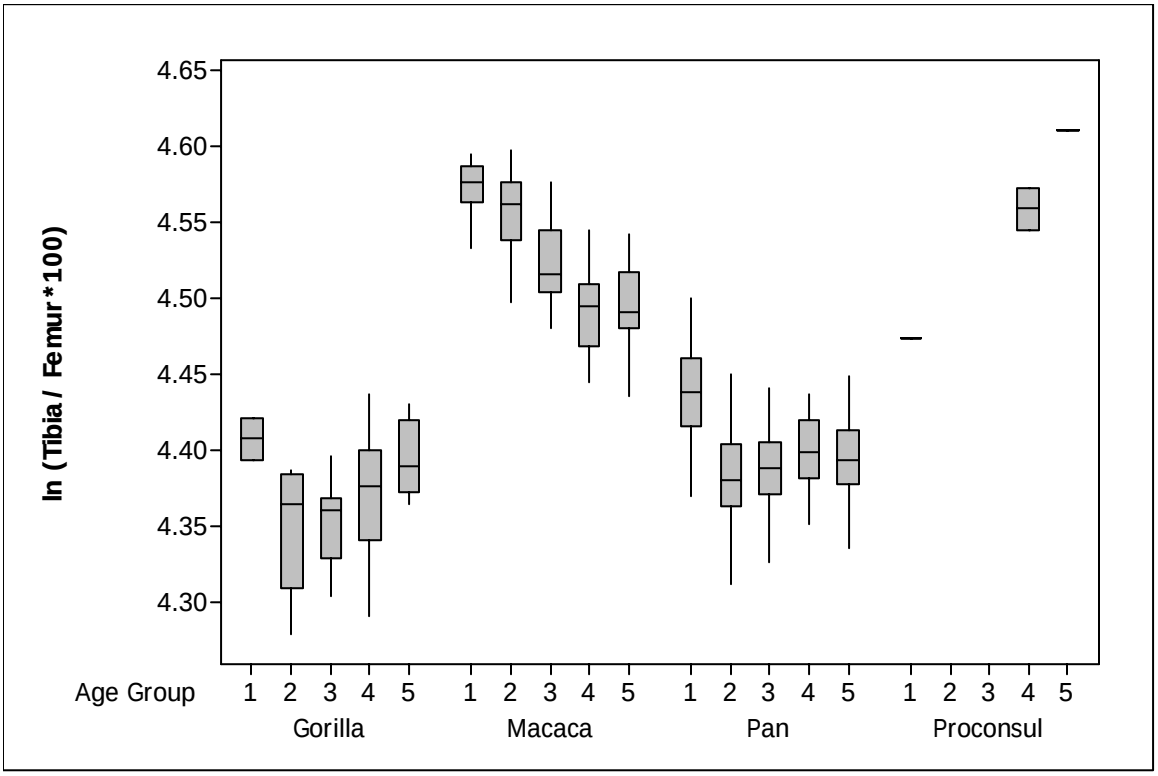

Figure 4.4. Tibia/ Femur by age group.

Table 4.6. ANOVA for Tibia/Femur by age group

Gorilla gorilla						*Macaca mulatta*						*Pan troglodytes*					
N		**1**	**2**	**3**	**4**	**n**		**1**	**2**	**3**	**4**	**n**		**1**	**2**	**3**	**4**
2	**1**					12	**1**					14	**1**				
7	**2**					16	**2**					36	**2**	**x**			
10	**3**					27	**3**	**x**	**x**			34	**3**	**x**			
11	**4**					30	**4**	**x**	**x**	**x**		34	**4**				
18	**5**		**x**	**x**		28	**5**	**x**	**x**	**x**		14	**5**	**x**			
F = 4.92, P = 0.002						F = 41.97, P = 0.00						F = 9.41, P = 0.00					
R-Sq = 31.38%						R-Sq = 60.85%						R-Sq = 15.84%					

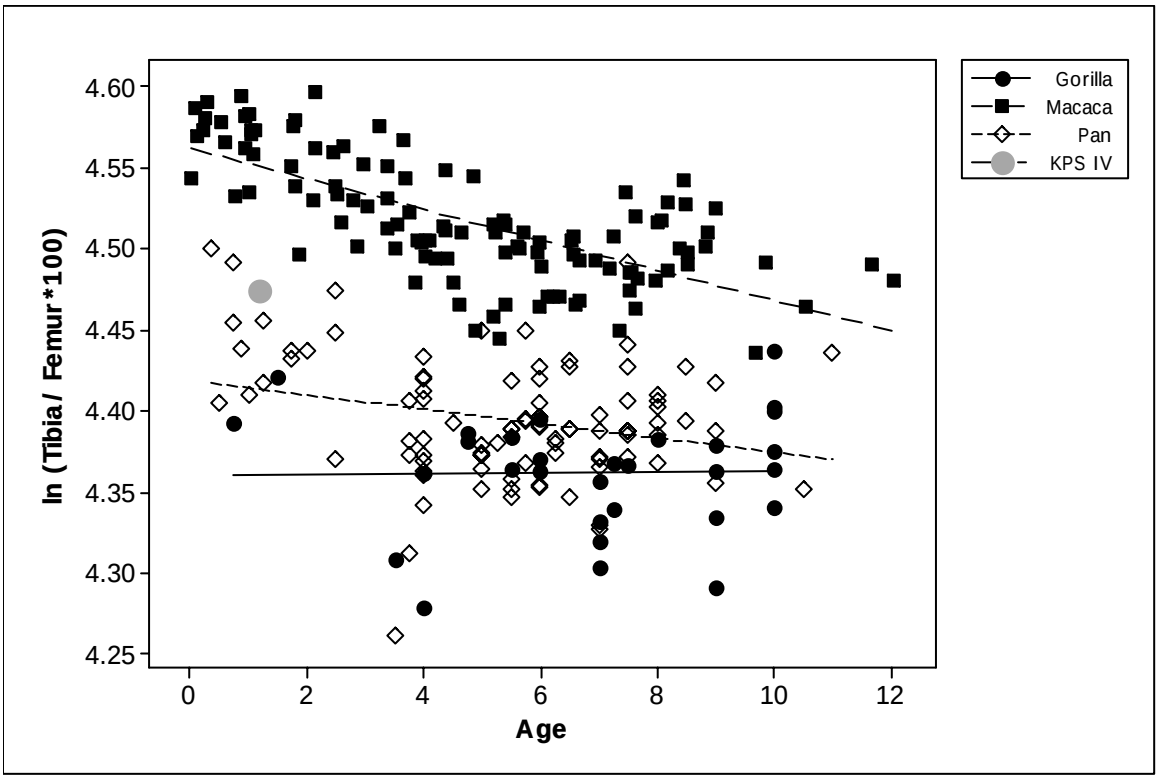

Figure 4.5. Tibia/ Femur by age.

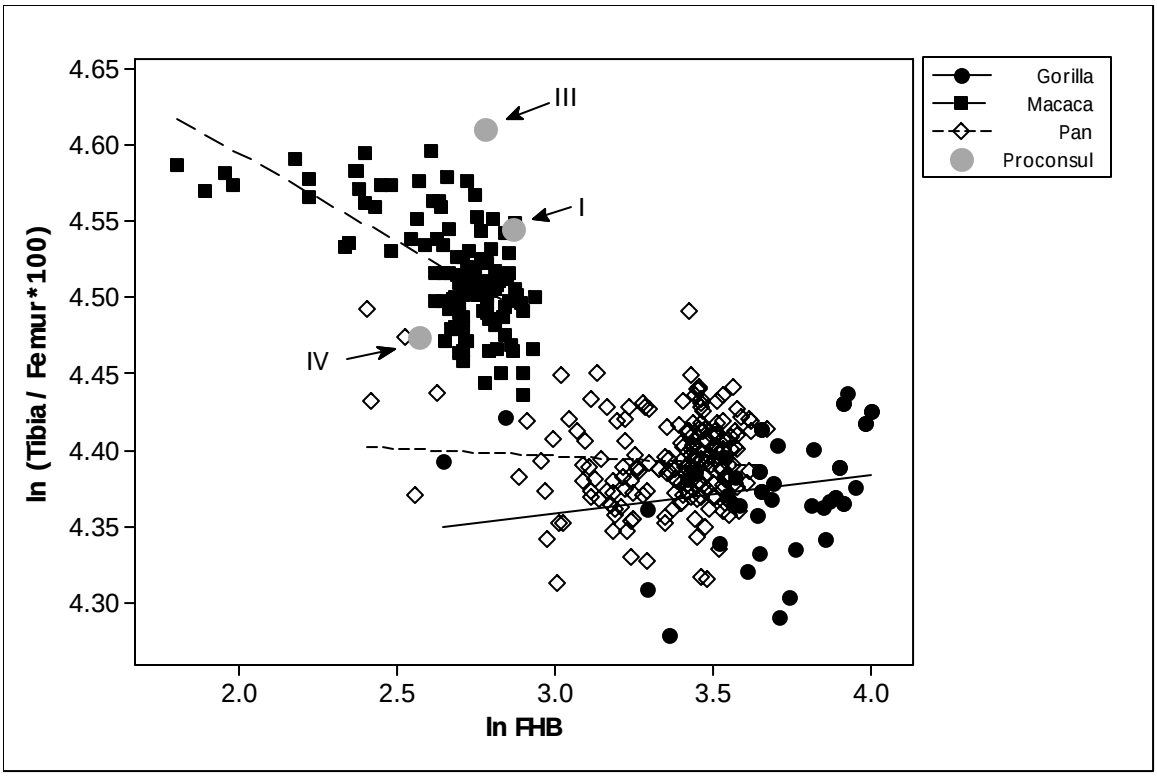

Figure 4.6. Tibia/ Femur by FHB.

Tarsus/ Foot (Figures 4.7- 4.9, Table 4.7) - There is a dramatic decrease in *Macaca* compared to the relatively stable proportions across the ages in the apes. The composite measures of tarsus and foot length both share the components of calcaneus length and cuboid length. Foot length is essentially the tarsus plus the third digit. So this figure is indicating an increase in growth of the third digit compared to the tarsus through development.

Indices for *Proconsul* are low, meaning that the third metatarsal and proximal phalanx are relatively longer like adult *Macaca* and *Pan*. This trend is present at both available age groups, 1 and 5. *Pan* is similarly static across the age groups. In the plot versus FHB, the infant and the adult cluster with *Macaca* adults.

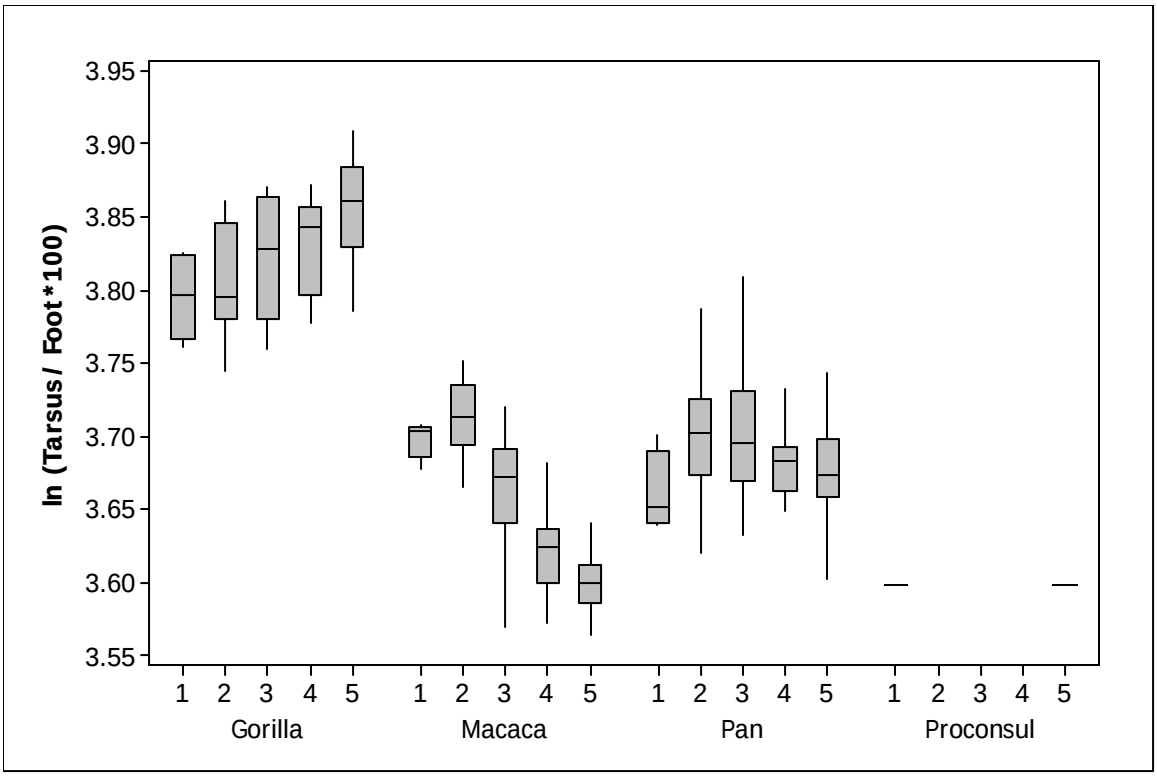

Figure 4.7. Tarsus/ Foot by age group.

Table 4.7. ANOVA for Tarsus/ Foot by age group.

Gorilla gorilla						*Macaca mulatta*						*Pan troglodytes*					
N		**1**	**2**	**3**	**4**	**n**		**1**	**2**	**3**	**4**	**n**		**1**	**2**	**3**	**4**
6	**1**					5	**1**					4	**1**				
14	**2**					15	**2**					44	**2**				
8	**3**					27	**3**		**x**			32	**3**				
10	**4**					30	**4**	**x**	**x**	**x**		12	**4**				
16	**5**	**x**	**x**			29	**5**	**x**	**x**	**x**		107	**5**		**x**	**x**	
F = 5.19, P = 0.001						F = 53.89, P = 0.00						F = 5.85, P = 0.00					
R-Sq = 29.76%						R-Sq = 68.09%						R-Sq = 10.76%					

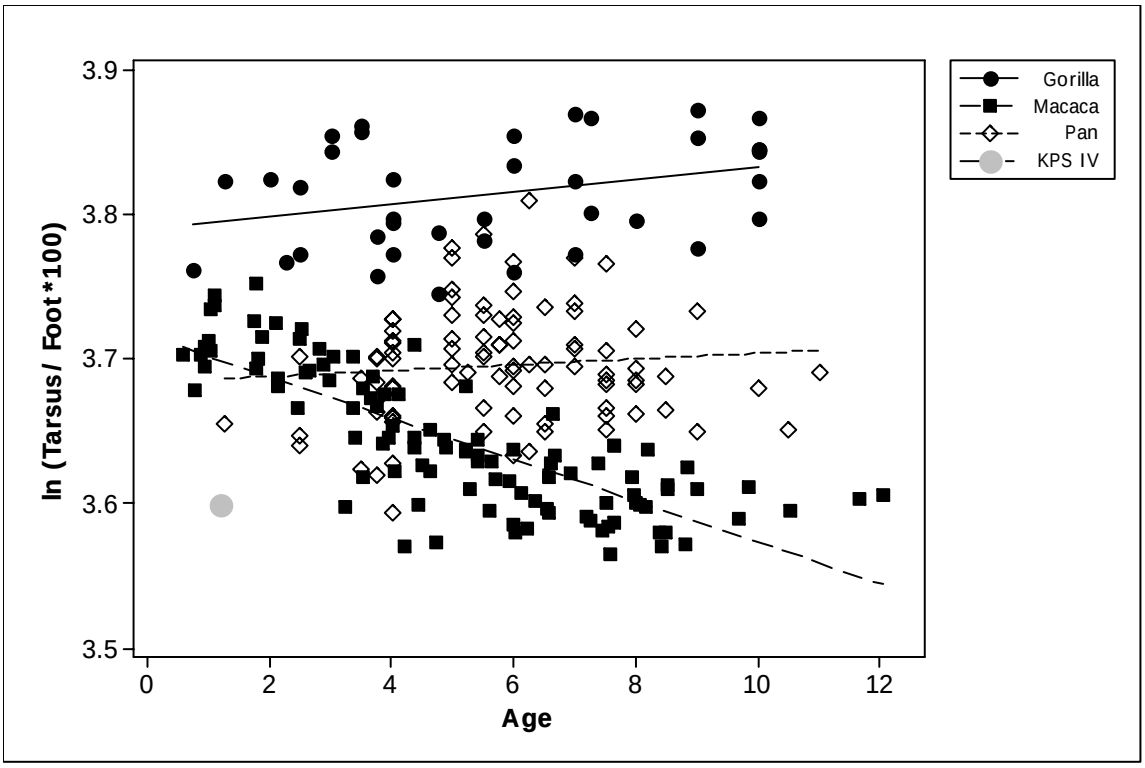

Figure 4.8. Tarsus/ Foot by age.

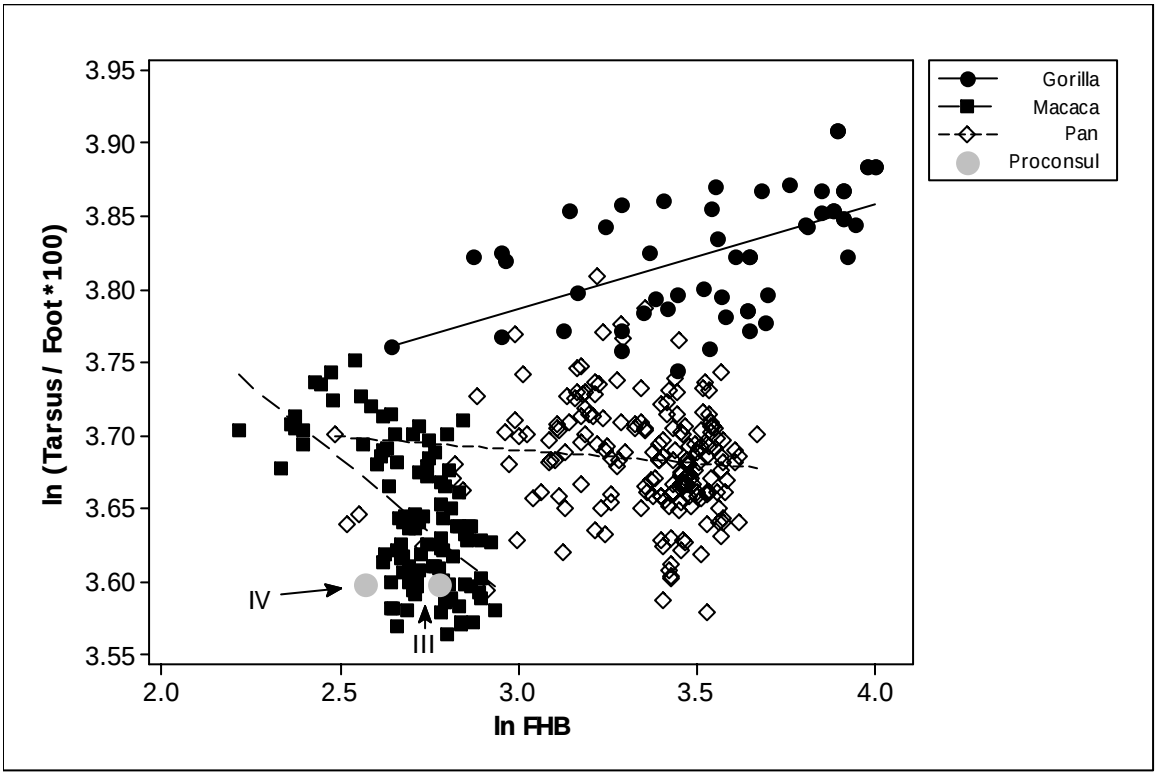

Figure 4.9. Tarsus/ Foot by FHB.

MT3/ Foot (Figures 4.10- 4.12, Table 4.8) - *Macaca* has the longest MT3 compared to the length of its foot. It also has the steepest increase in the third metatarsal relative to foot length through development. Pan and Gorilla are static. KPS IV plots near *Macaca* and *Pan* at the same age. Against age and FHB, the infant plots near the beginning of the *Pan* growth curve but the adult resembles the adult *Macaca*.

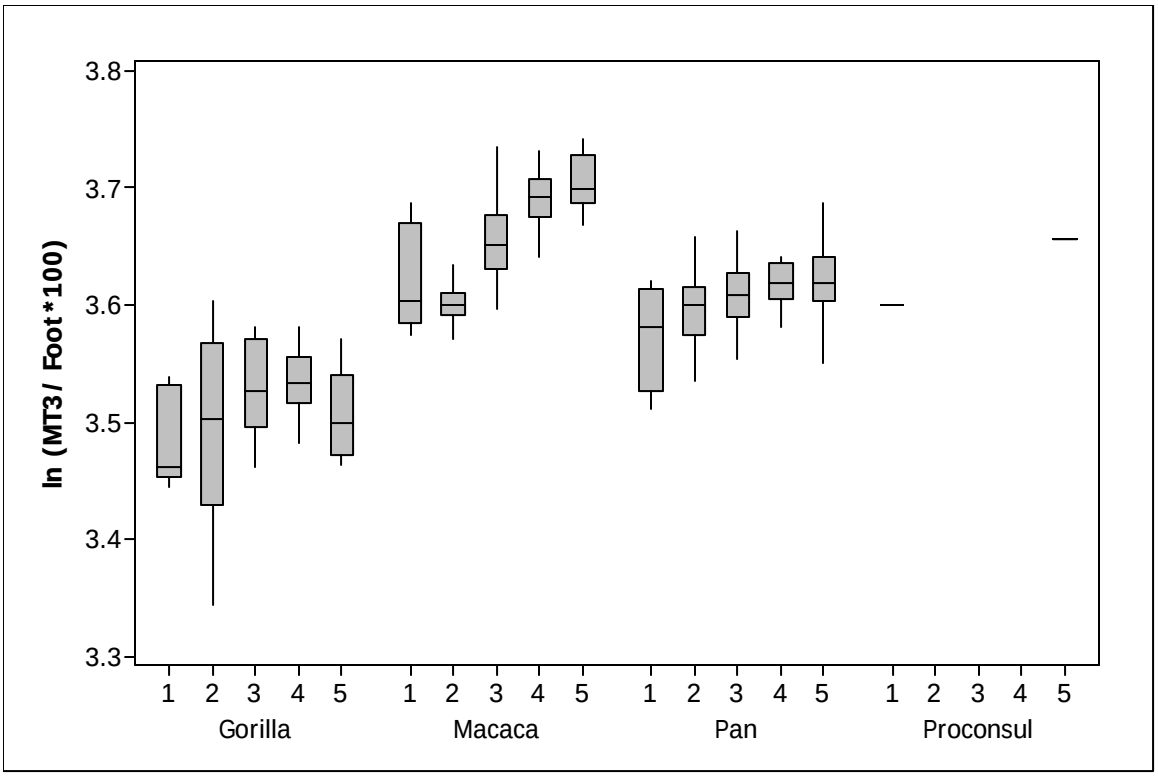

Figure 4.10. MT3/ Foot by age group.

Table 4.8. ANOVA for MT3/ Foot by age group.

Gorilla gorilla						*Macaca mulatta*						*Pan troglodytes*					
n		**1**	**2**	**3**	**4**	**n**		**1**	**2**	**3**	**4**	**n**		**1**	**2**	**3**	**4**
6	**1**					7	**1**					4	**1**				
17	**2**					15	**2**					44	**2**				
8	**3**					27	**3**	**x**	**x**			32	**3**				
10	**4**					30	**4**	**x**	**x**	**x**		12	**4**				
16	**5**					29	**5**	**x**	**x**	**x**		107	**5**		**x**	**x**	
F = 1.54, P = 0.205						F = 42.822, P = 0.00						F = 6.15, P = 0.00					
R-Sq = 10.58%						R-Sq = 62.45%						R-Sq = 11.25%					

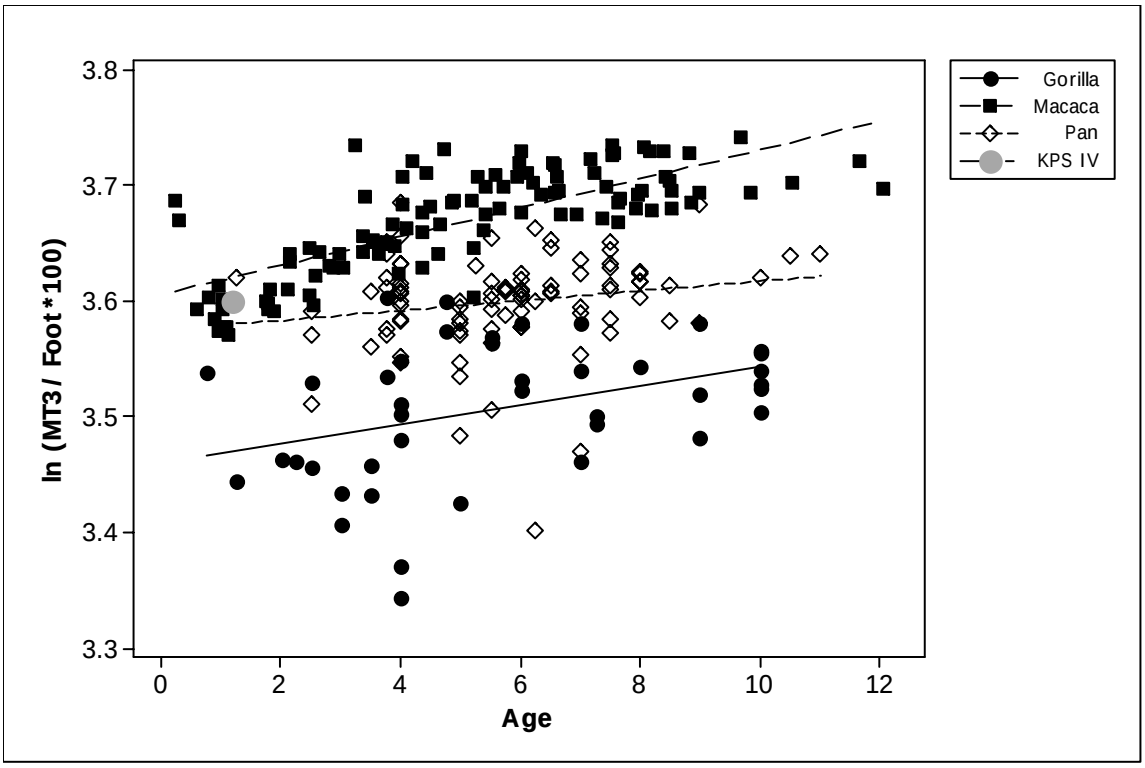

Figure 4.11. MT3/ Foot by age.

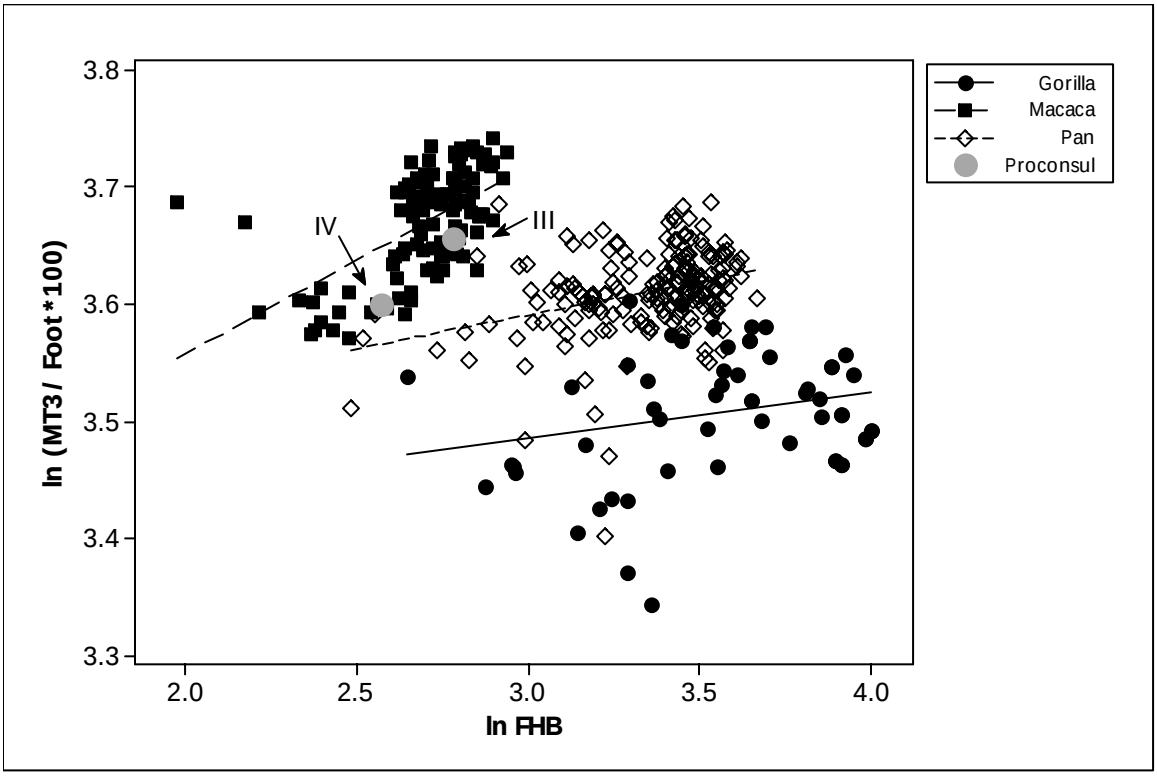

Figure 4.12. MT3/ Foot by FHB.

MT3/ Calcaneus (Figures 4.13- 15, Table 4.9) - *Macaca* has the relatively longest MT3. KPS IV plots above all three taxa of comparable age, indicating the MT3 is particularly long. KPS VII (age group 3) shows an exaggerated index compared to the other *Proconsuls,* up at the upper extreme of adult macaques. All cluster with *Macaca* however, the infant KPS IV and KPS VII (age group 3) plot higher than macaques of similar ages further down the curve.

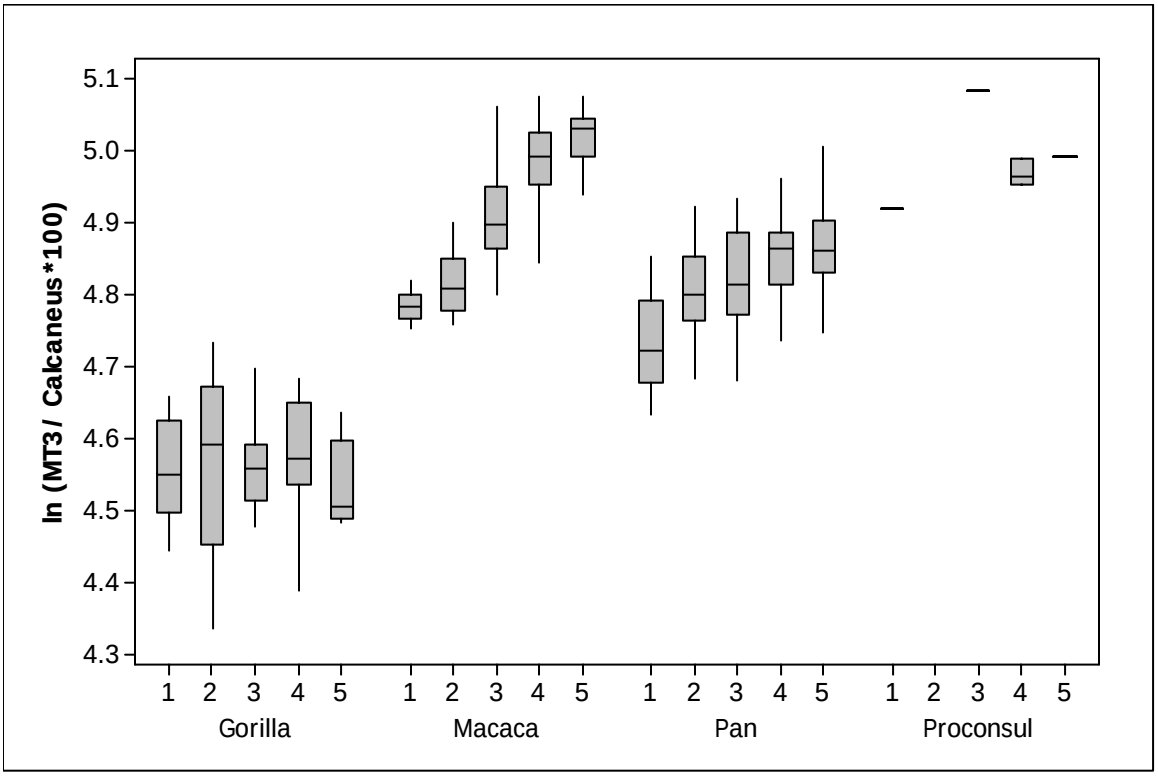

Figure 4.13. MT3/ Calcaneus by age group.

Table 4.9. ANOVA for MT3/ Calcaneus by age group.

Gorilla gorilla						*Macaca mulatta*						*Pan troglodytes*					
n		**1**	**2**	**3**	**4**	**n**		**1**	**2**	**3**	**4**	**n**		**1**	**2**	**3**	**4**
8	**1**					11	**1**					16	**1**				
17	**2**					16	**2**					47	**2**	**x**			
11	**3**					26	**3**	**x**	**x**			35	**3**	**x**			
11	**4**					31	**4**	**x**	**x**	**x**		15	**4**	**x**			
18	**5**					29	**5**	**x**	**x**	**x**		109	**5**	**x**	**x**	**x**	
F = 0.30, P = 0.880						F = 81.17, P = 0.00						F = 17.30, P = 0.00					
R-Sq = 1.93%						R-Sq = 75.04%						R-Sq = 24.18%					

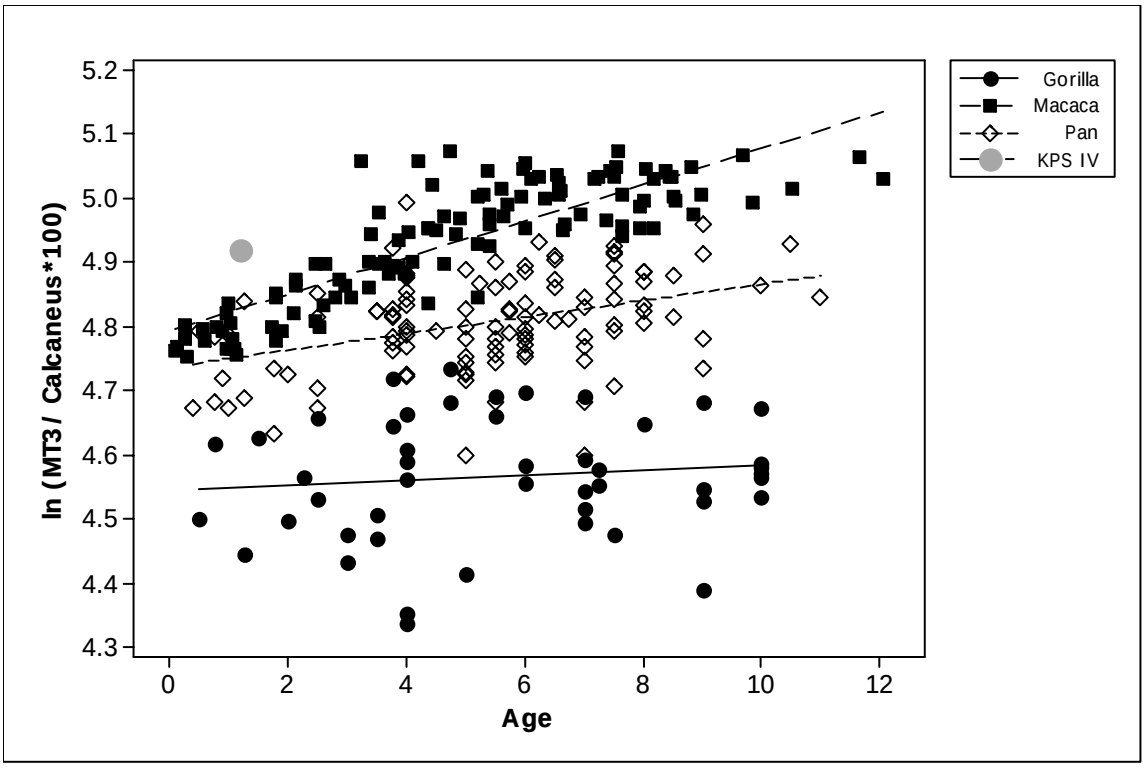

Figure 4.14. MT3/ Calcaneus by age.

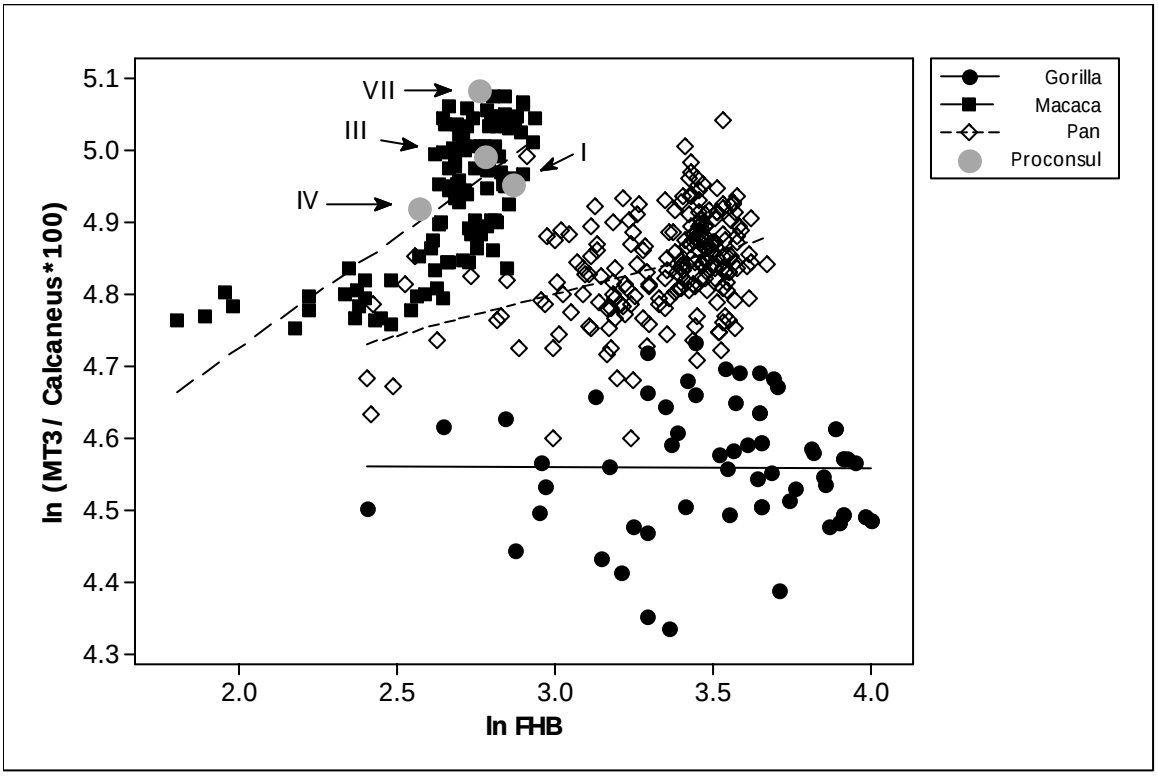

Figure 4.15. MT3/ Calcaneus by FHB.

PH3/ Foot (Figures 4.16-18, Table 4.10) – Foot length outgrows PH3 length in Gorillas much more drastically than the other two taxa that are static in comparison (minus those in age group 1). Although only ages 1 and 5 are available, *Proconsul* seems to be showing the *Pan* proportions. As has been the pattern, the infant *Proconsul* plots among *Pan* infants, but the adult plots near *Macaca adults* of comparable body size.

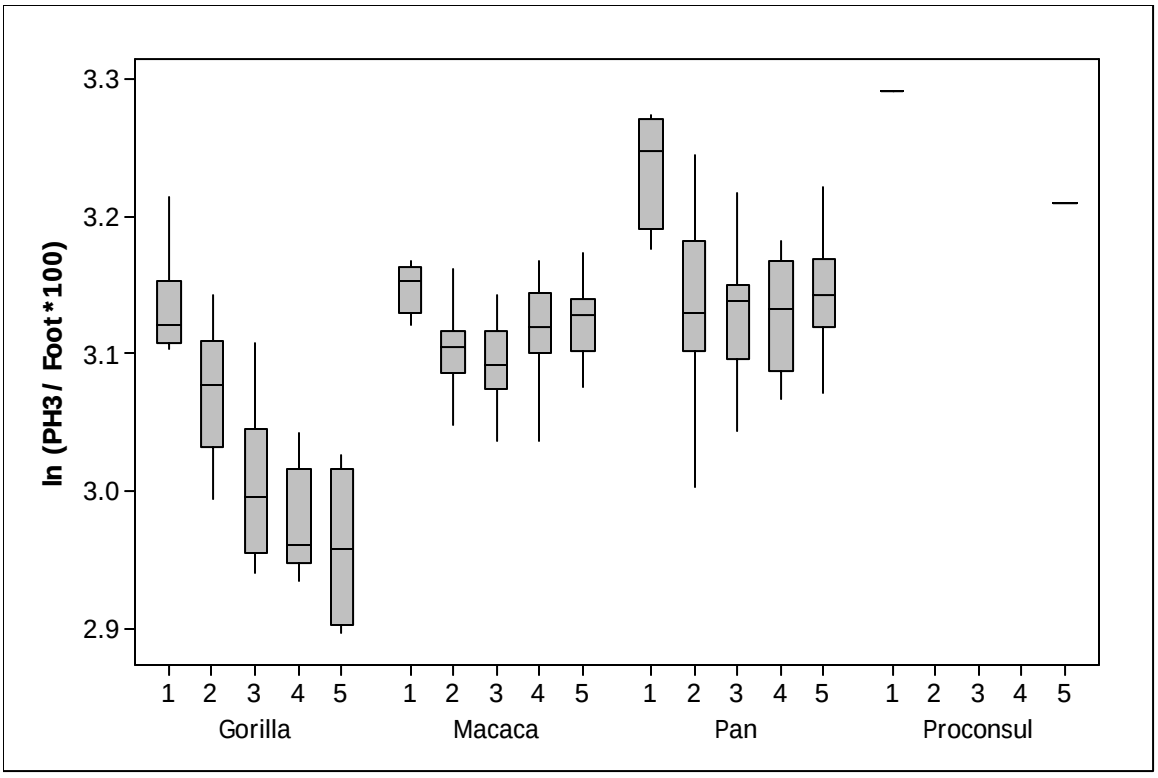

Figure 4.16. PH3/ Foot by age group.

Table 4.10. ANOVA for PH3/ Foot by age group.

Gorilla gorilla						*Macaca mulatta*						*Pan troglodytes*					
n		**1**	**2**	**3**	**4**	**n**		**1**	**2**	**3**	**4**	**n**		**1**	**2**	**3**	**4**
6	**1**					5	**1**					4	**1**				
17	**2**	**x**				15	**2**					44	**2**	**x**			
8	**3**	**x**	**x**			27	**3**	**x**				32	**3**	**x**			
10	**4**	**x**	**x**			30	**4**					12	**4**	**x**			
16	**5**	**x**	**x**			29	**5**			**x**		107	**5**	**x**			
F = 21.88, P = 0.00						F = 4.14, P = 0.004						F = 6.23, P = 0.00					
R-Sq = 62.73%						R-Sq = 14.088%						R-Sq = 11.38%					

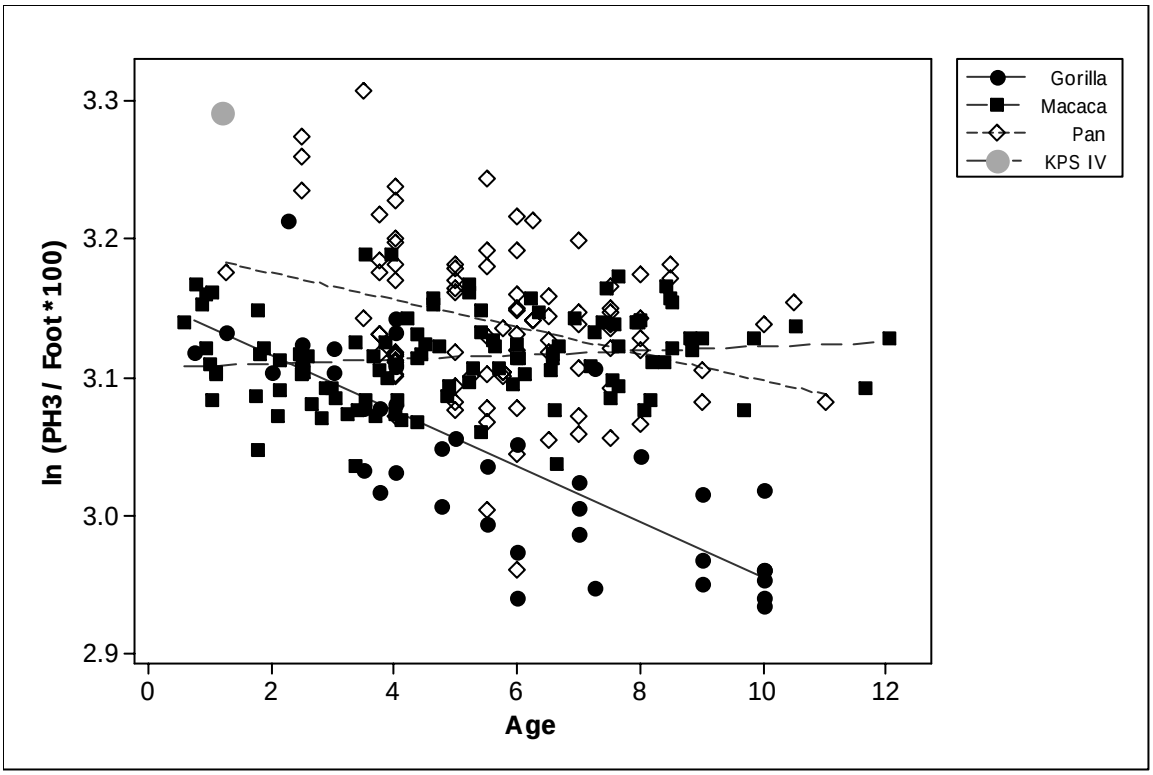

Figure 4.17. PH3/ Foot by age.

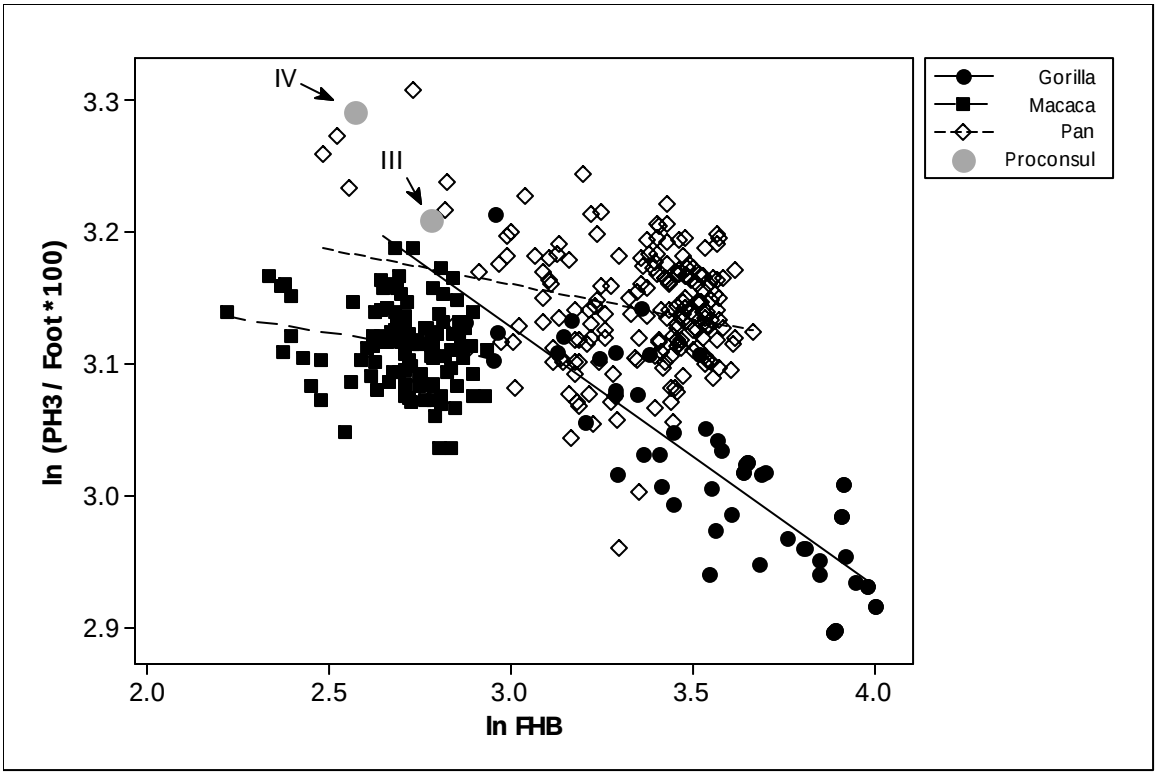

Figure 4.18. PH3/ Foot by FHB.

PH3/ Calcaneus (Figures 4.19 – 4.21, Table 4.11) – The three modern taxa each show distinctive trends. The calcaneus of *Gorilla* is growing steadily faster than the PH3. *Macaca* shows the opposite with the PH3 outgrowing the calcaneus and achieving the relatively longest one. *Pan* appears to reach adult proportions during age group 2 with much more similar proportions to the monkey than to the other, more closely related, ape. *Proconsul* plots above all three taxa, illustrating the long length of the third proximal phalanx in relation to the calcaneus. The same pattern for index against FHB is evident as in that for PH1/ Foot.

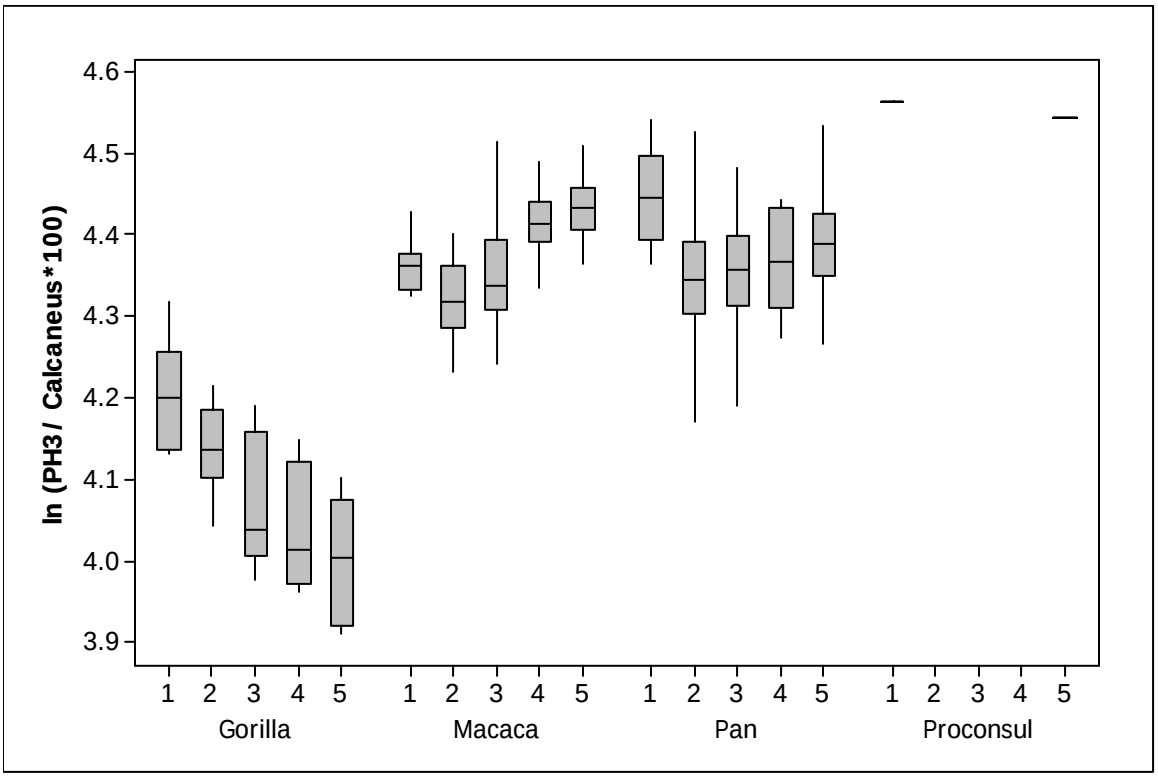

Figure 4.19. PH3/ Calcaneus by age group.

Table 4.11. ANOVA for PH3/ Calcaneus by age group.

Gorilla gorilla						*Macaca mulatta*						*Pan troglodytes*					
n		**1**	**2**	**3**	**4**	**n**		**1**	**2**	**3**	**4**	**n**		**1**	**2**	**3**	**4**
6	**1**					8	**1**					15	**1**				
17	**2**					16	**2**					45	**2**	**x**			
8	**3**	**x**				27	**3**					32	**3**	**x**			
10	**4**	**x**	**x**			30	**4**		**x**	**x**		12	**4**	**x**			
16	**5**	**x**	**x**			29	**5**	**x**	**x**	**x**		107	**5**	**x**	**x**	**x**	
F = 14.88, P = 0.00						F = 20.32, P = 0.00						F = 8.92, P = 0.00					
R-Sq = 53.37%						R-Sq = 43.64%						R-Sq = 14.76%					

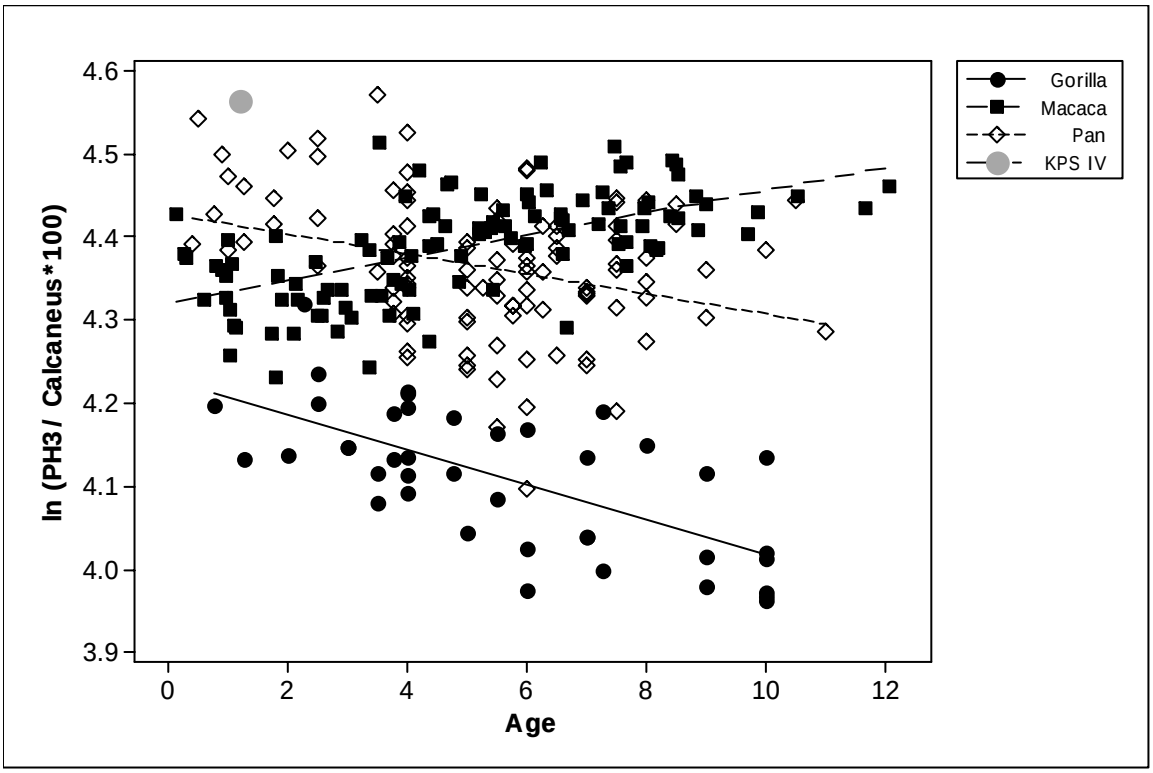

Figure 4.20. PH3/ Calcaneus by age.

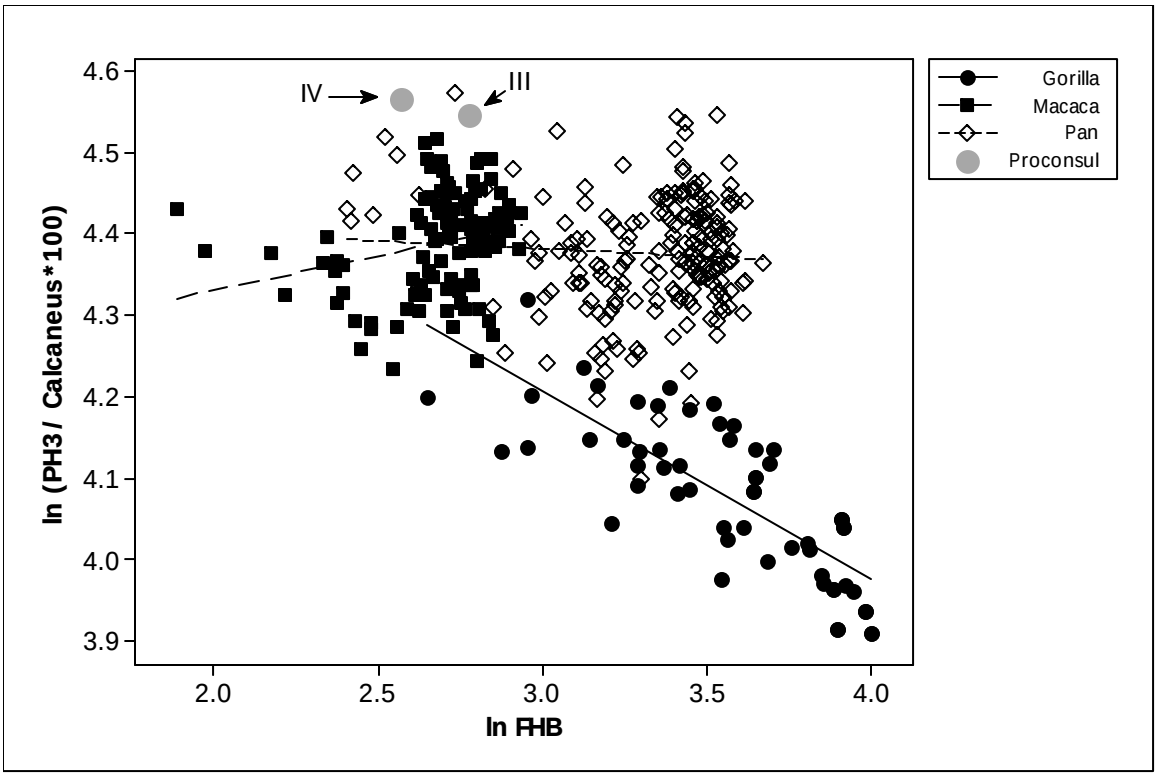

Figure 4.21. PH3/ Calcaneus by FHB.

Power Arm/ Calcaneal Load Arm (Figures 4.22 -4.24, Table 4.12) - All the taxa increase in this ratio in a very similar manner throughout development. That is to say that the posterior portion of the calcaneus outgrows the anterior portion in all three taxa. These results are illustrating the strong necessity for these taxa to maintain biomechanical equivalence of the power and calcaneal load arms during growth in body size. KPS IV plots right on the *Pan* line, but KPS VII (age group 3) is again landing high above the rest of the individuals. Overall, however, the pattern is *Pan*-like. The infant plots with young *Pan* and the adults plot with adult *Macaca,* except KPS VII is much higher than expected for its age.

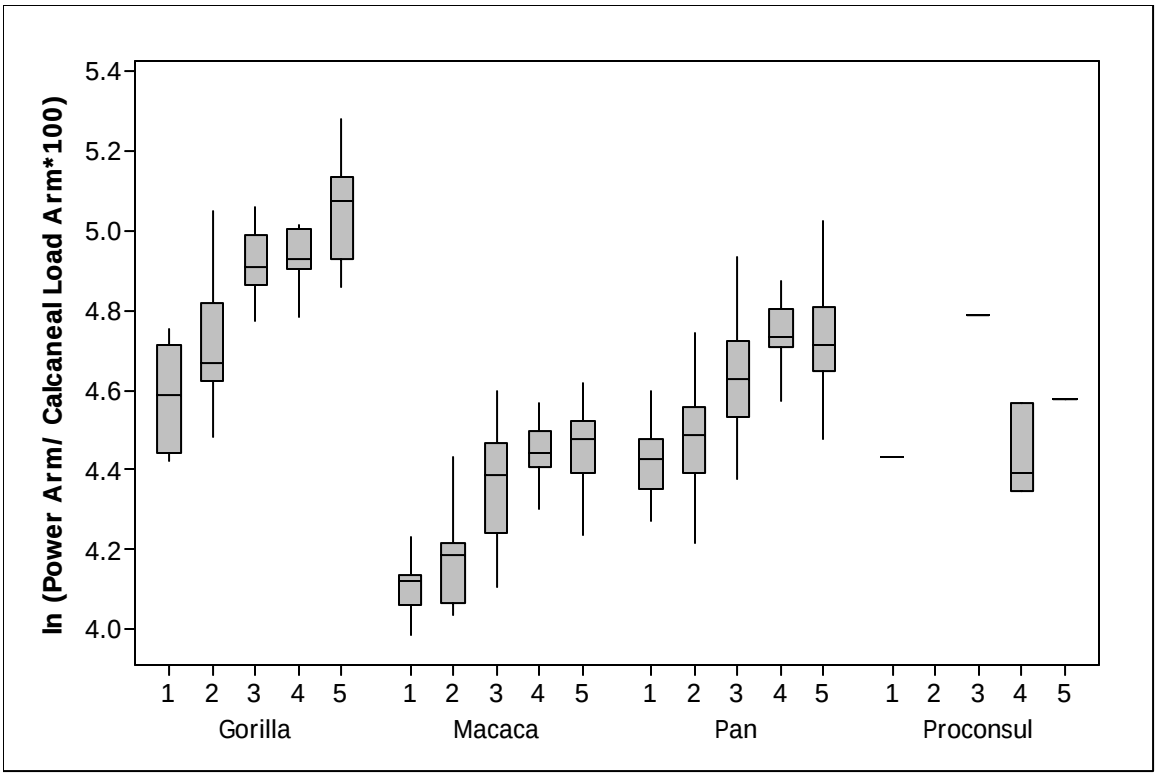

Figure 4.22. Power Arm/ Calcaneal Load Arm by age group.

Table 4.12. ANOVA for Power Arm/ Calcaneal Load Arm by age group

Gorilla gorilla						*Macaca mulatta*						*Pan troglodytes*					
n		**1**	**2**	**3**	**4**	**n**		**1**	**2**	**3**	**4**	**n**		**1**	**2**	**3**	**4**
8	**1**					12	**1**					16	**1**				
17	**2**					16	**2**					45	**2**				
11	**3**	**x**	**x**			27	**3**	**x**				35	**3**	**x**	**x**		
11	**4**	**x**	**x**			31	**4**	**x**	**x**	**x**		15	**4**	**x**	**x**	**x**	
18	**5**	**x**	**x**			29	**5**	**x**	**x**	**x**		108	**5**	**x**	**x**	**x**	
F = 23.61, P = 0.00						F = 43.75, P = 0.00						F = 50.22, P = 0.00					
R-Sq = 61.15%						R-Sq = 61.40%						R-Sq = 48.42%					

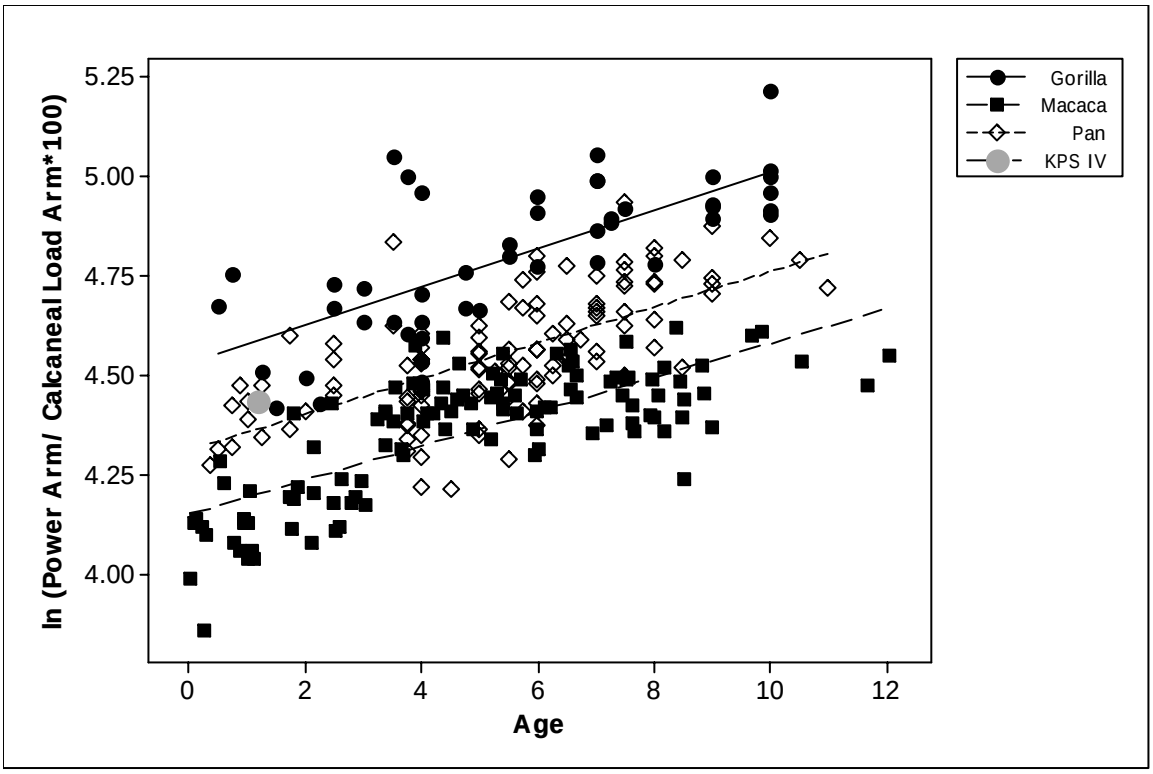

Figure 4.23. Power Arm/ Calcaneal Load Arm by age.

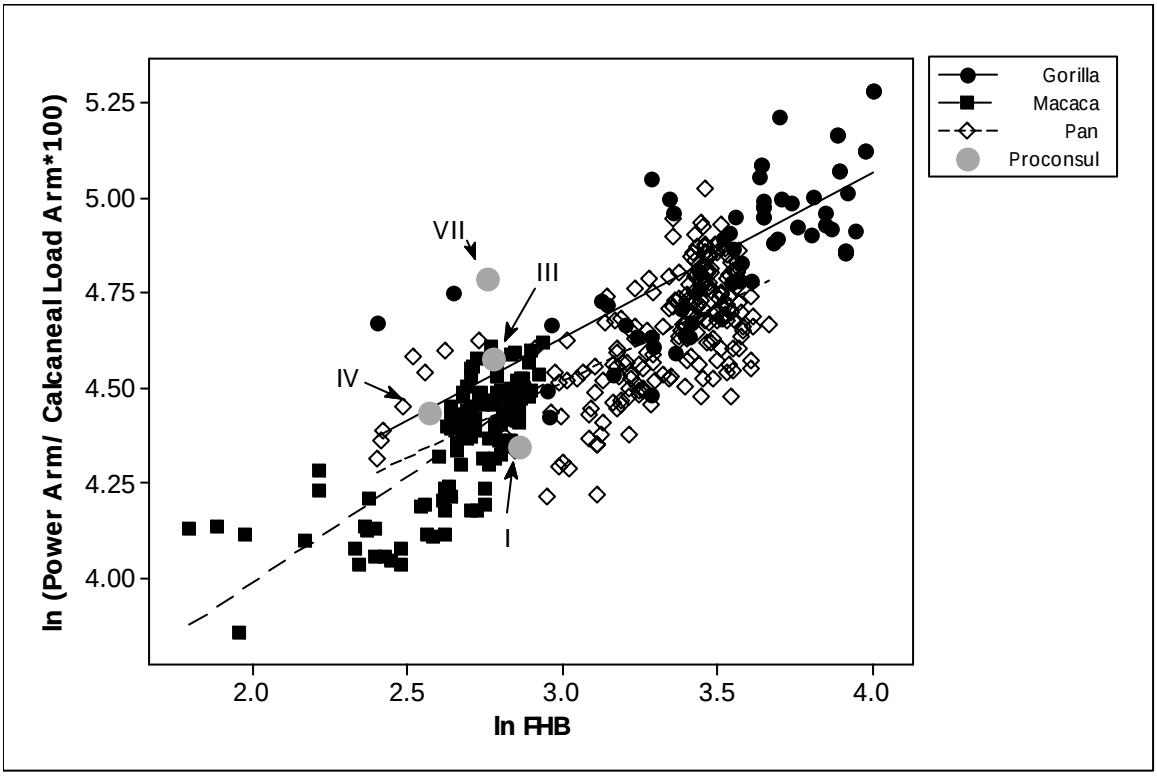

Figure 4.24. Power Arm/ Calcaneal Load Arm by FHB.

Power Arm/ Pedal Load Arm (Figures 4.35- 4.27, Table 4.13) – *Macaca* is showing the slowest amount of pedal load arm increase during growth out of the three modern taxa. *Gorilla* has a much larger power arm than the other taxa. At age group 1, *Proconsul* is up near *Macaca* and *Pan* but the rest of the age groups fall below, which is most likely a consequence of small body size. All the *Proconsuls* are clustered very close together around *Macaca*. KPS IV is also plotting near the beginning of the *Pan* curve.

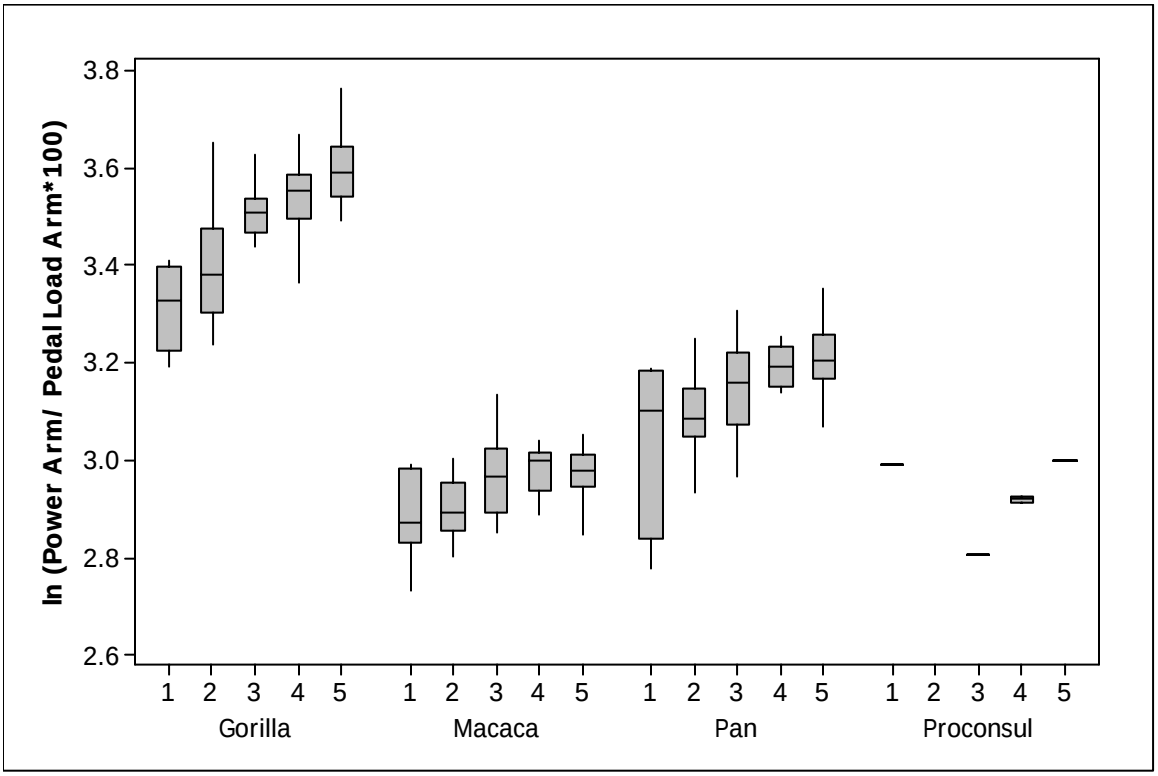

Figure 4.25. Power Arm/ Pedal Load Arm by age group.

Table 4.13. ANOVA for Power Arm/ Pedal Load Arm by age group.

Gorilla gorilla						*Macaca mulatta*						*Pan troglodytes*					
n		**1**	**2**	**3**	**4**	**n**		**1**	**2**	**3**	**4**	**n**		**1**	**2**	**3**	**4**
7	**1**					7	**1**					4	**1**				
17	**2**					15	**2**					43	**2**				
11	**3**	**x**	**x**			27	**3**	**x**				34	**3**		**x**		
11	**4**	**x**	**x**			31	**4**	**x**	**x**			13	**4**		**x**		
18	**5**	**x**	**x**			29	**5**	**x**	**x**			108	**5**	**x**	**x**	**x**	
F = 18.39, P = 0.00						F = 9.78, P = 0.00						F = 18.58, P = 0.00					
R-Sq = 55.50%						R-Sq = 27.33%						R-Sq = 27.40%					

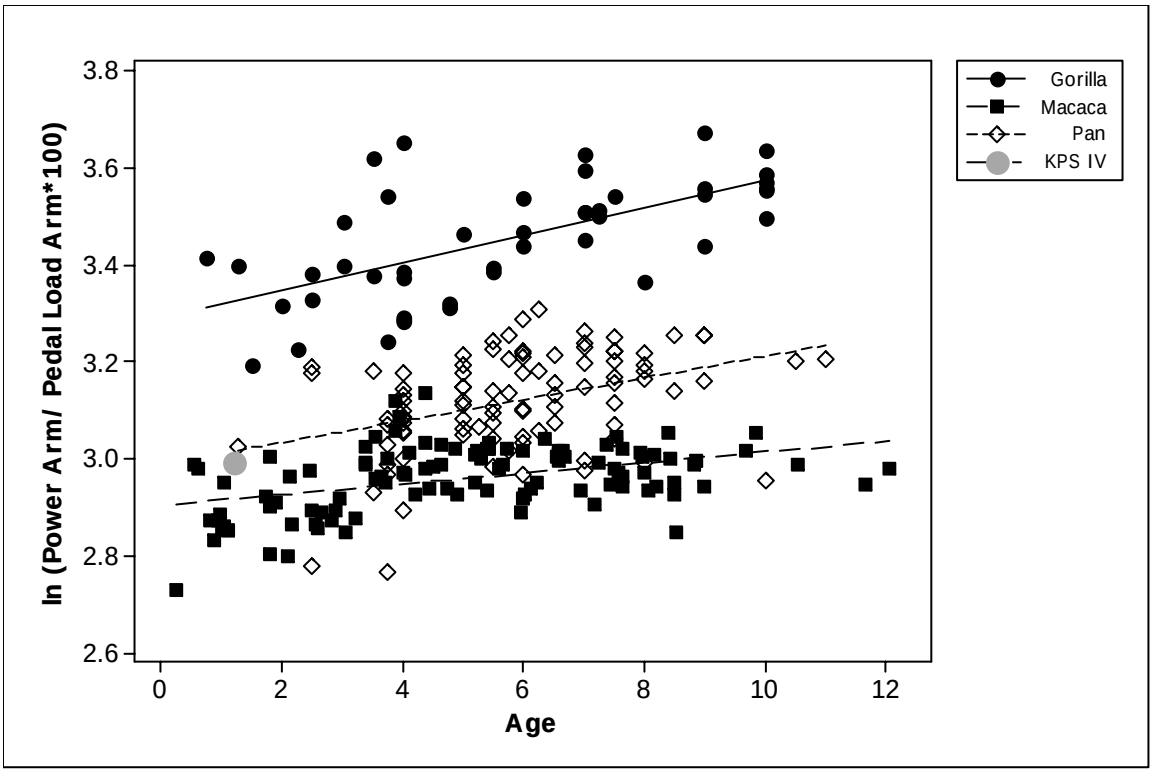

Figure 4.26. Power Arm/ Pedal Load Arm by age.

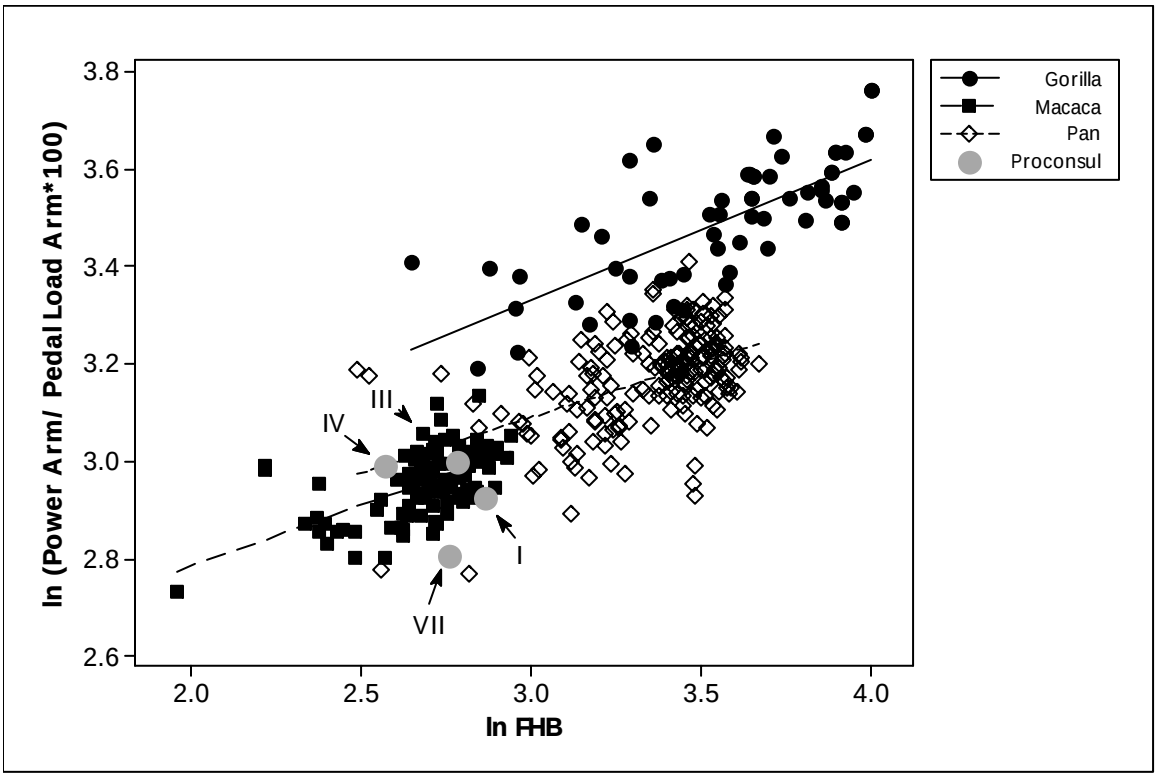

Figure 4.27. Power Arm/ Pedal Load Arm by FHB.

Foot/ Femur (Figures 4.28-4.30, Table 4.14) – As with Tibia/ Femur, *Macaca* shows a drastic change through ontogeny while the apes remain relatively the same throughout development. The exception being that first age group in *Pan* that has shown differences in other indices from the rest of the age groups. The *Macaca* femur outgrows the foot during ontogeny. That is to say, *Macaca* is born with a large foot, while the apes are born with the relatively same-sized foot as their parents. Moreover, *Macaca* adults have relatively longer feet than the two apes. *Proconsul* is showing the opposite trend of *Macaca*, but without ranges with these small *Proconsul* samples it is possible that the real trend is obscured. The infant *Proconsul* plots with similar-aged *Gorilla* and *Pan* and falls in the range of adult *Macaca*. The infant plots with young *Pan* against FHB but the adult plots with maturing *Macaca*.

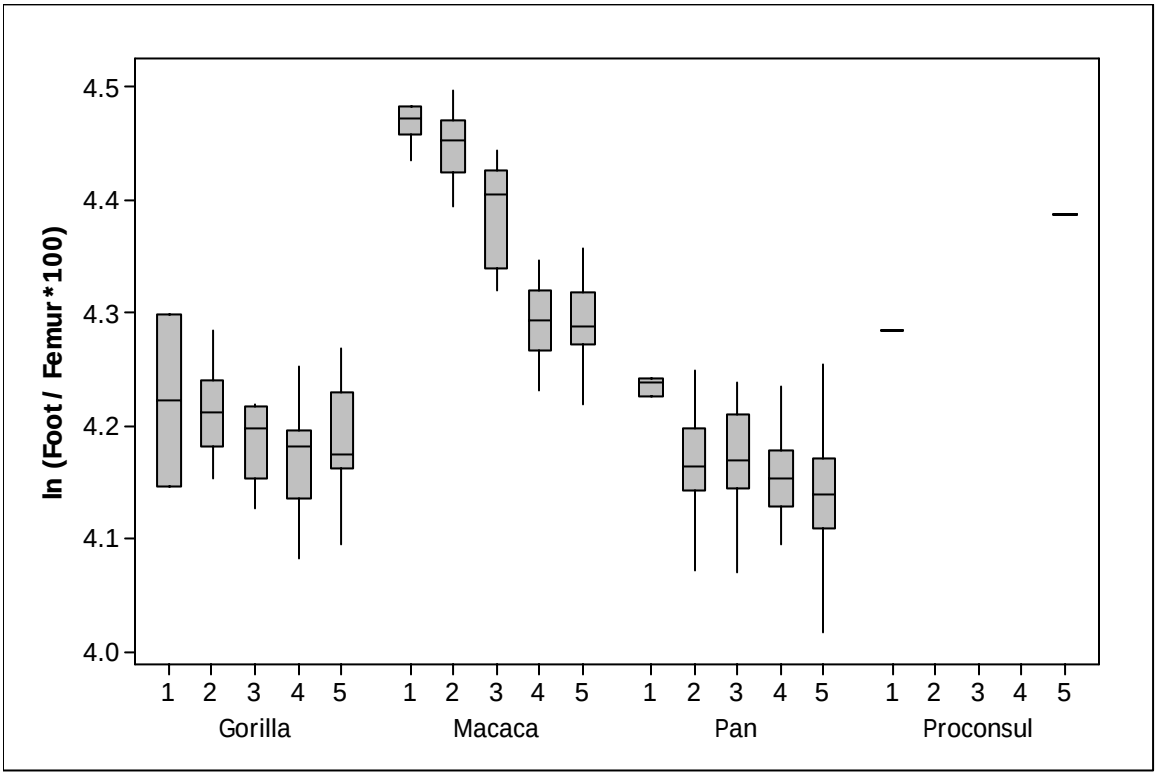

Figure 4.28. Foot/ Femur by age group.

Table 4.14. ANOVA for Foot/ Femur by age group.

Gorilla gorilla						*Macaca mulatta*						*Pan troglodytes*					
n		**1**	**2**	**3**	**4**	**n**		**1**	**2**	**3**	**4**	**n**		**1**	**2**	**3**	**4**
2	**1**					7	**1**					3	**1**				
10	**2**					15	**2**					37	**2**	**x**			
7	**3**					22	**3**	**x**				31	**3**				
10	**4**					27	**4**	**x**	**x**	**x**		12	**4**	**x**			
16	**5**					29	**5**	**x**	**x**	**x**		107	**5**	**x**	**x**	**x**	
F = 1.28, P = 0.295						F = 98.53, P = 0.00						F = 8.96, P = 0.00					
R-Sq = 11.32%						R-Sq = 80.58%						R-Sq = 16.23%					

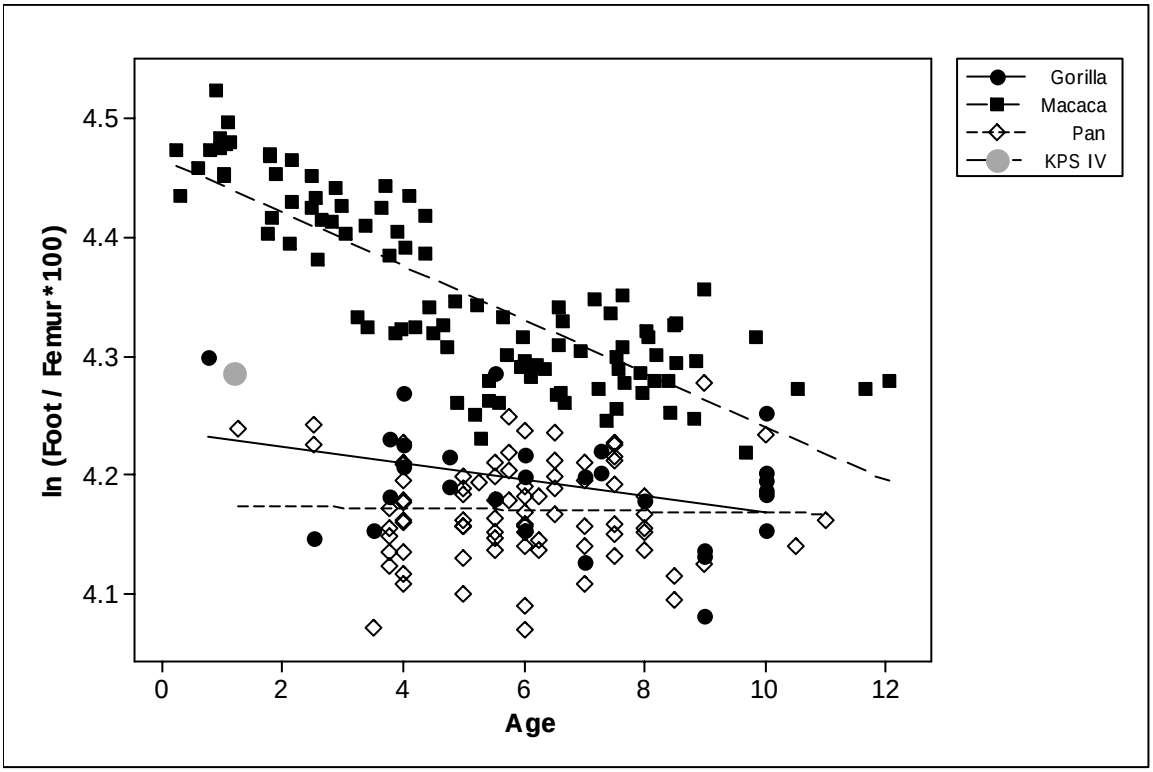

Figure 4.29. Foot/ Femur by age.

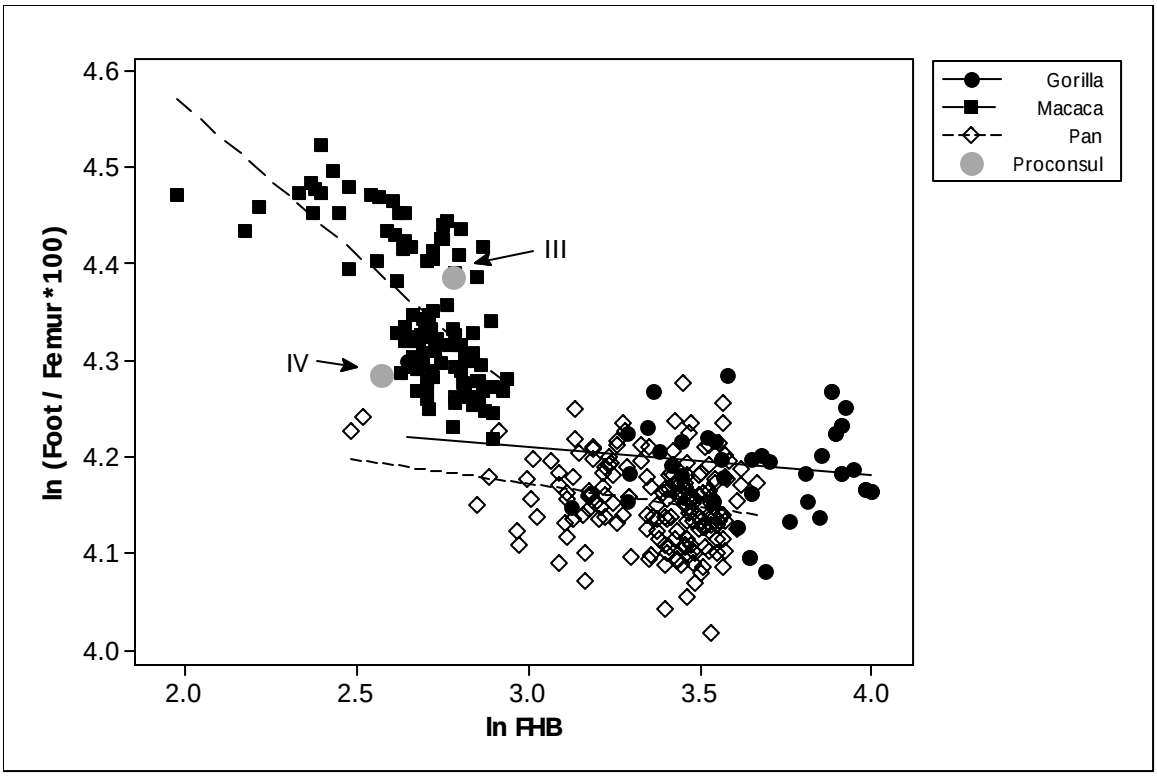

Figure 4.30. Foot/ Femur by FHB.

MT1/ Foot (Figures 4.31 – 4.33, Table 4.15) – Both apes show the same proportions throughout development but the MT1 in *Macaca* outgrows foot length. However, *Macaca* ends up with proportions very similar to *Gorilla* while *Pan* has a longer MT1. The infant *Proconsul* plots with young *Gorillas* and the adult exceeds the upper cluster of *Macaca* adults, falling out with young *Pan.*

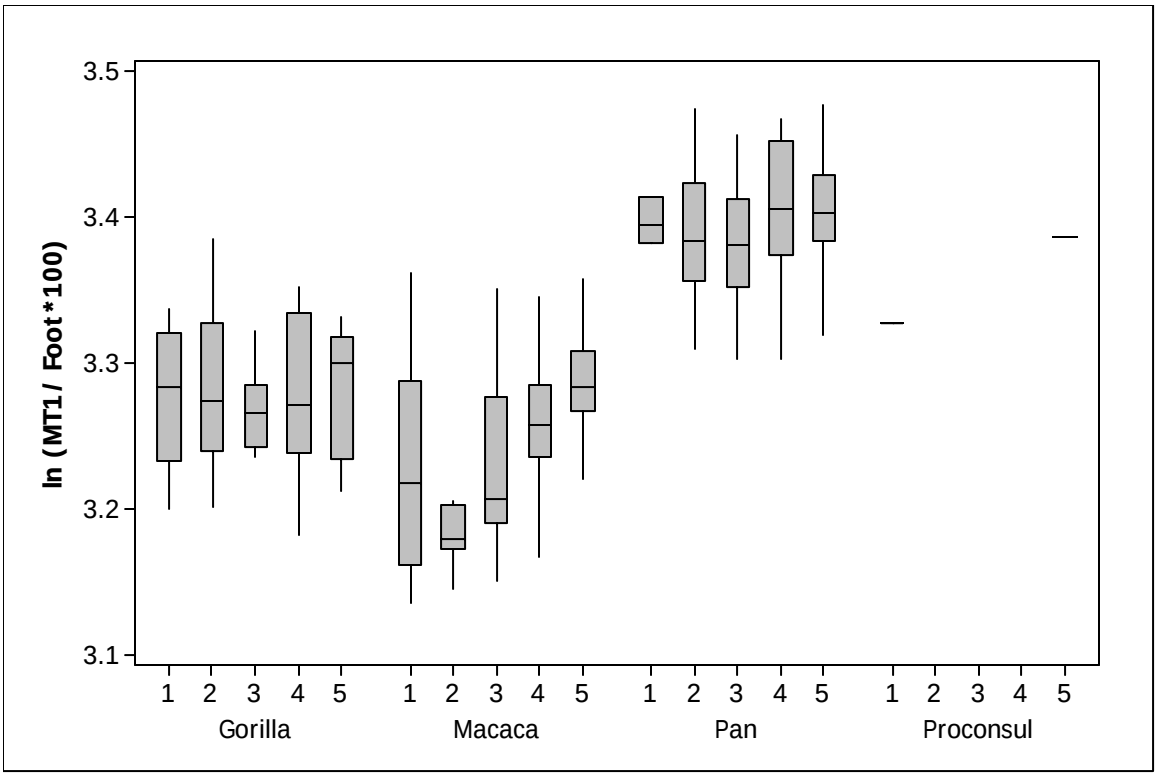

Figure 4.31. MT1/ Foot by age group.

Table 4.15. ANOVA for MT1/ Foot by age group.

Gorilla gorilla						*Macaca mulatta*						*Pan troglodytes*					
n		**1**	**2**	**3**	**4**	**n**		**1**	**2**	**3**	**4**	**n**		**1**	**2**	**3**	**4**
6	**1**					7	**1**					3	**1**				
17	**2**					15	**2**					43	**2**				
8	**3**					26	**3**		**x**			32	**3**				
10	**4**					28	**4**		**x**			12	**4**				
16	**5**					29	**5**	**x**	**x**	**x**		106	**5**				
F = 0.15, P = 0.961						F = 13.70, P = 0.00						F = 2.40, P = 0.052					
R-Sq = 1.16%						R-Sq = 35.40%						R-Sq = 4.78%					

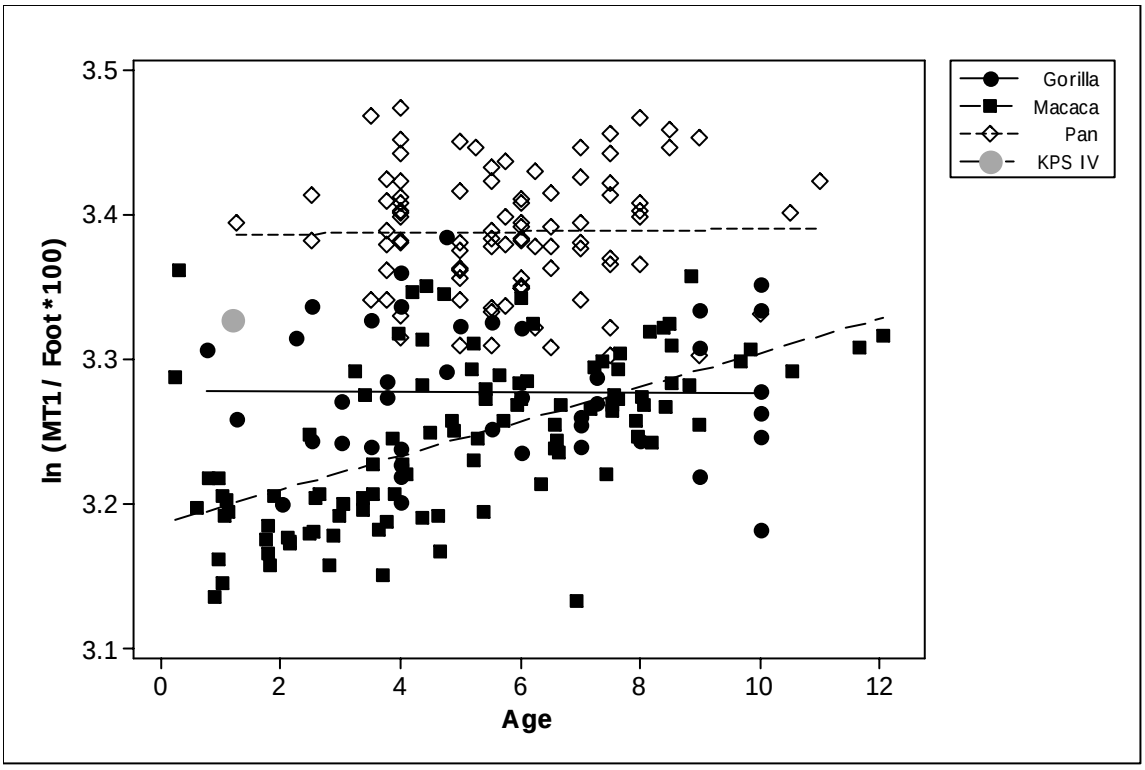

Figure 4.32. MT1/ Foot by age.

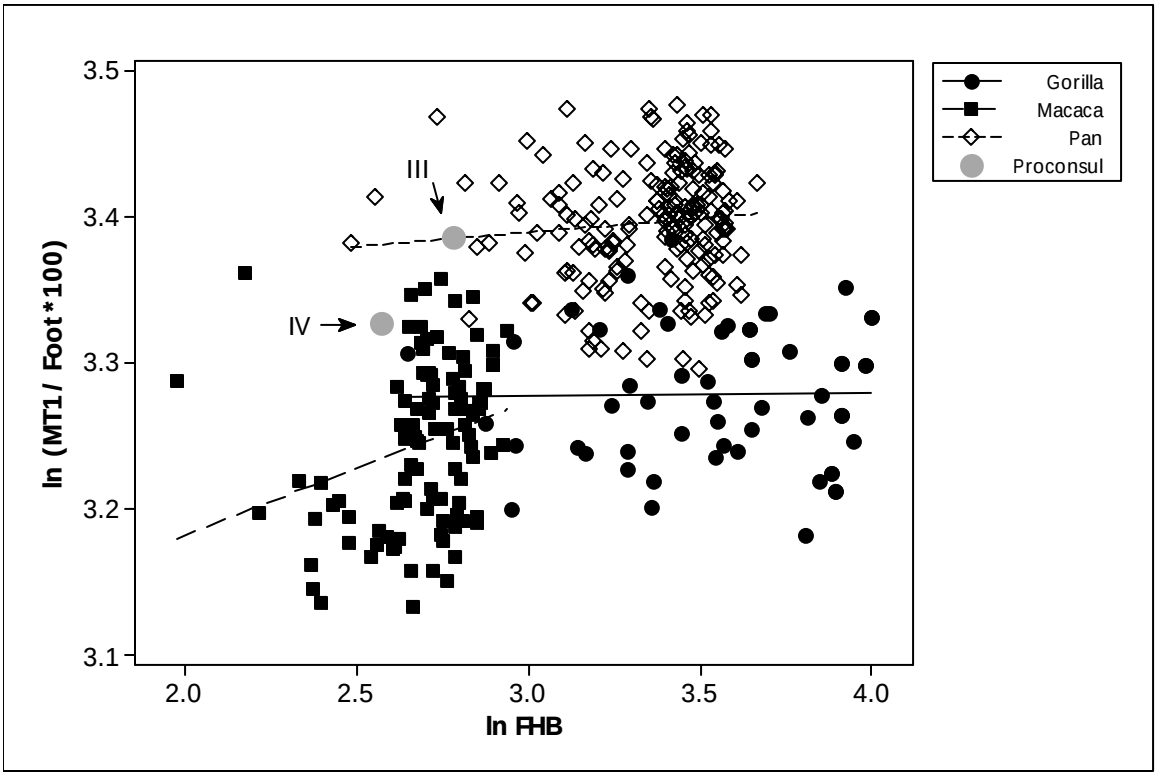

Figure 4.33. MT1/ Foot by FHB.

MT1/ Calcaneus (Figures 4.34 – 4.36, Table 4.16) – *Gorilla* and *Pan* are basically static through growth in this index, having the same sized MT1 relative to calcaneus length (which is highly correlated to body size) throughout development. *Pan* has the relatively longest MT1. *Macaca*, on the other hand, again shows more of an increase in MT1. The infant *Proconsul* is showing similar proportions to the adult (III) and here more *Proconsul*s fill in the rest of the growth trajectory. All three *Proconsuls* but the infant are tracking with the *Macaca* group against FHB, albeit a little higher than expected for the age of KPS VII. This clustering is close to immature *Pan* proportions. The infant is much higher than expected for the rest of *Proconsul* and is closer to *Pan* of similar ages.

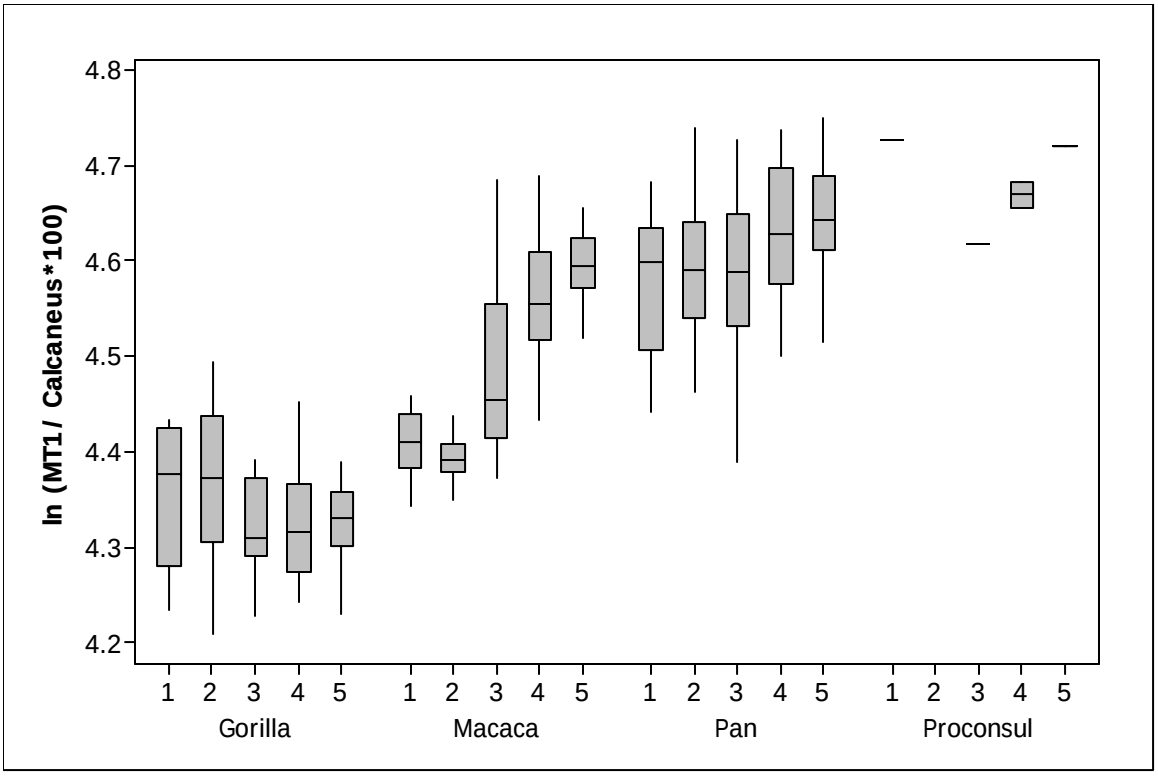

Figure 4.34. MT1/ Calcaneus by age group.

Table 4.16. ANOVA for MT1/ Calcaneus by age group.

Gorilla gorilla						*Macaca mulatta*						*Pan troglodytes*					
n		**1**	**2**	**3**	**4**	**n**		**1**	**2**	**3**	**4**	**n**		**1**	**2**	**3**	**4**
8	**1**					11	**1**					16	**1**				
16	**2**					16	**2**					47	**2**				
11	**3**					26	**3**	**x**				35	**3**				
11	**4**					31	**4**	**x**	**x**	**x**		15	**4**				
18	**5**					29	**5**	**x**	**x**	**x**		109	**5**	**x**	**x**	**x**	
F =1.31, P = 0.276						F = 40.82, P = 0.00						F =10.28, P = 0.00					
R-Sq = 8.18%						R-Sq = 60.19%						R-Sq = 15.93%					

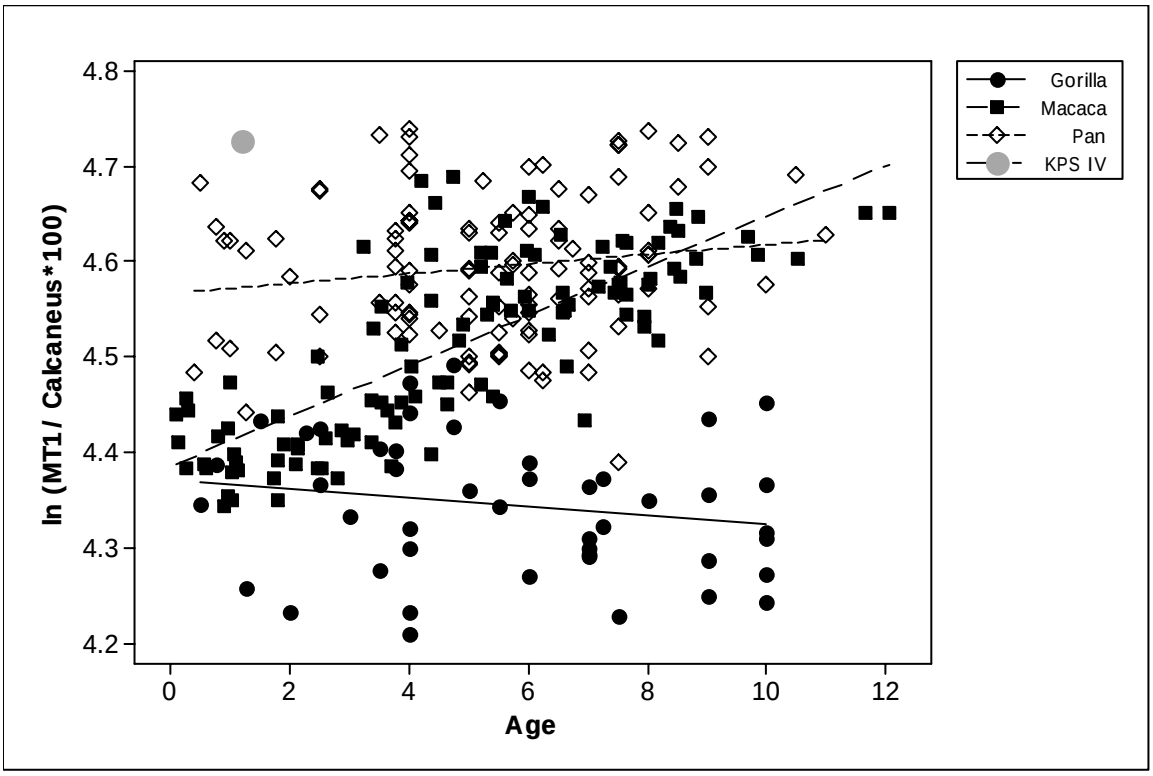

Figure 4.35. MT1/ Calcaneus by age.

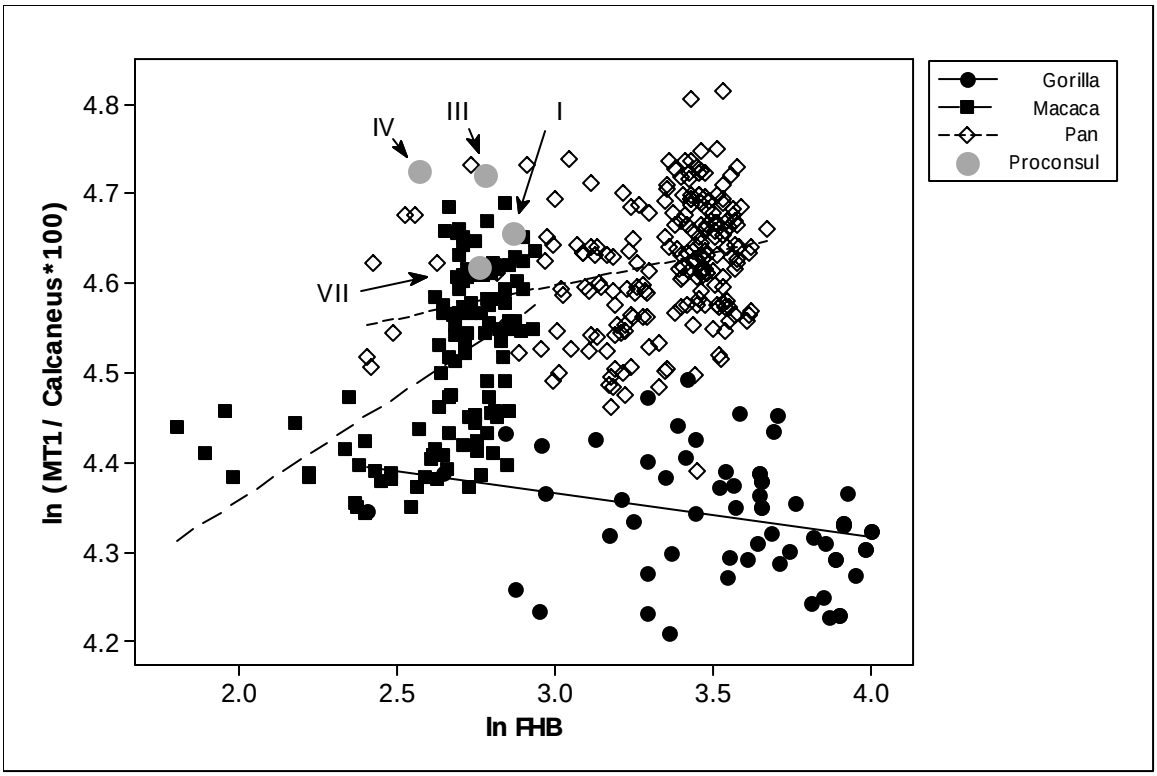

Figure 4.36. MT1/ Calcaneus by FHB.

PH1/ Foot (Figure 4.37 - 4.39, Table 4.17) – This is one of the few indices that is basically the same across all age groups in all the modern taxa. *Pan* has the relatively longest PH1. The only *Proconsul* with the available measures is the adult KPS III. It resembles *Pan* in its long first proximal phalanx relative to foot length. Like many of the FHB plots, the adult (III) falls just above *Macaca* with immature *Pan* of comparable body size.

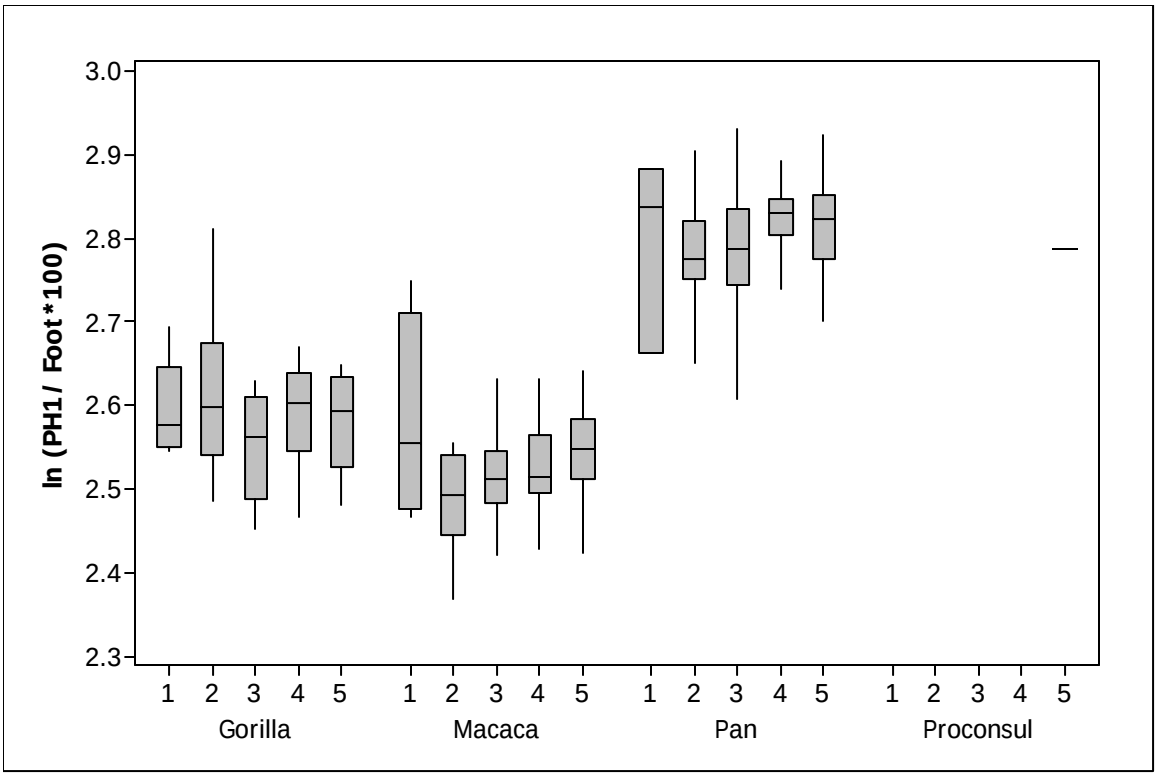

Figure 4.37. PH1/ Foot by age group.

Table 4.17. ANOVA for PH1/ Foot by age group.

Gorilla gorilla						*Macaca mulatta*						*Pan troglodytes*					
n		**1**	**2**	**3**	**4**	**n**		**1**	**2**	**3**	**4**	**n**		**1**	**2**	**3**	**4**
6	**1**					7	**1**					3	**1**				
16	**2**					15	**2**	**x**				44	**2**				
8	**3**					27	**3**					31	**3**				
10	**4**					30	**4**					12	**4**				
16	**5**					28	**5**		**x**			105	**5**		**x**		
F = 0.95, P = 0.446						F = 3.46, P = 0.11						F = 2.78, P = 0.028					
R-Sq = 6.9%						R-Sq = 11.94%						R-Sq = 5.53%					

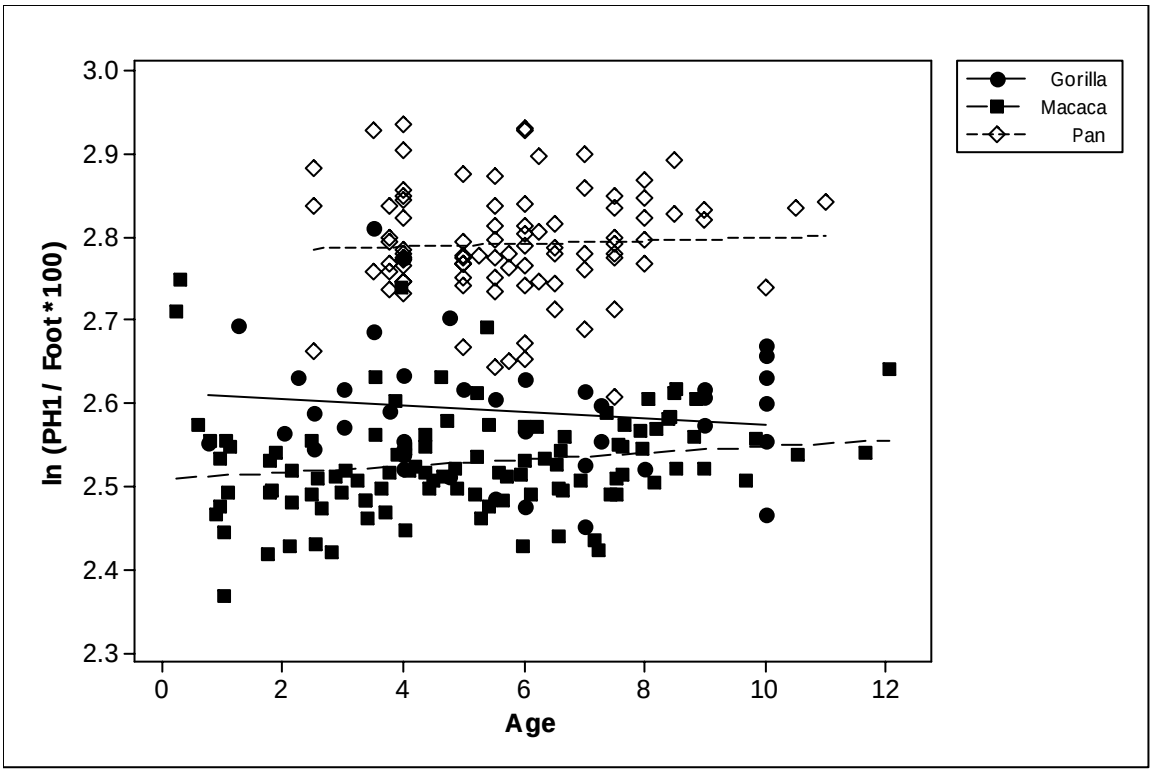

Figure 4.38. PH1/ Foot by age.

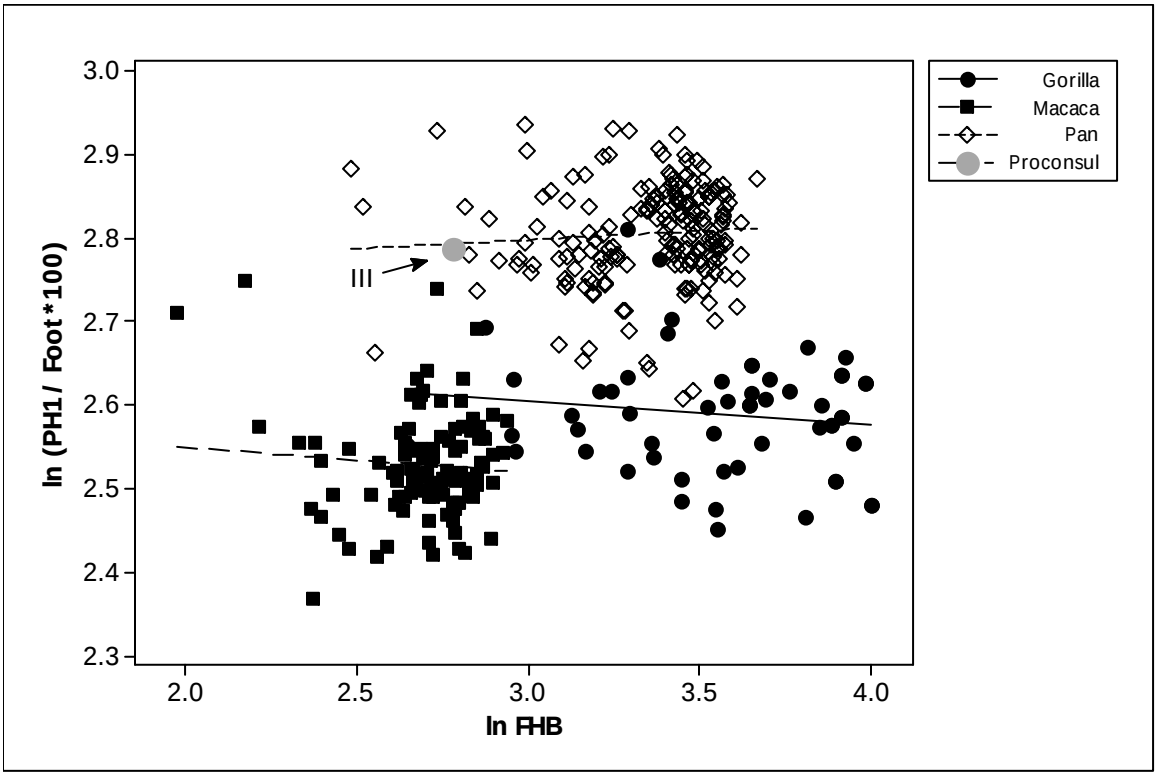

Figure 4.39. PH1/ Foot by FHB.

PH1/ Calcaneus (Figures 4.40 – 4.42, Table 4.18) – The two apes, again, do not change in this index throughout growth and development, but the PH1 of *Macaca* outgrows the calcaneus. This index, although similar to PH1/Foot, allows the addition of the age group 4 *Proconsuls* (RU 2036, KPS I). *Proconsul* has a *Pan*-like first proximal phalanx relative to calcaneus length (which is a large component of foot length). The two *Proconsuls* straddle the *Pan* line but the subadult male (I) falls comfortably with the *Macaca* adults and the adult (III) exceeds the highest of the *Macaca* indices.

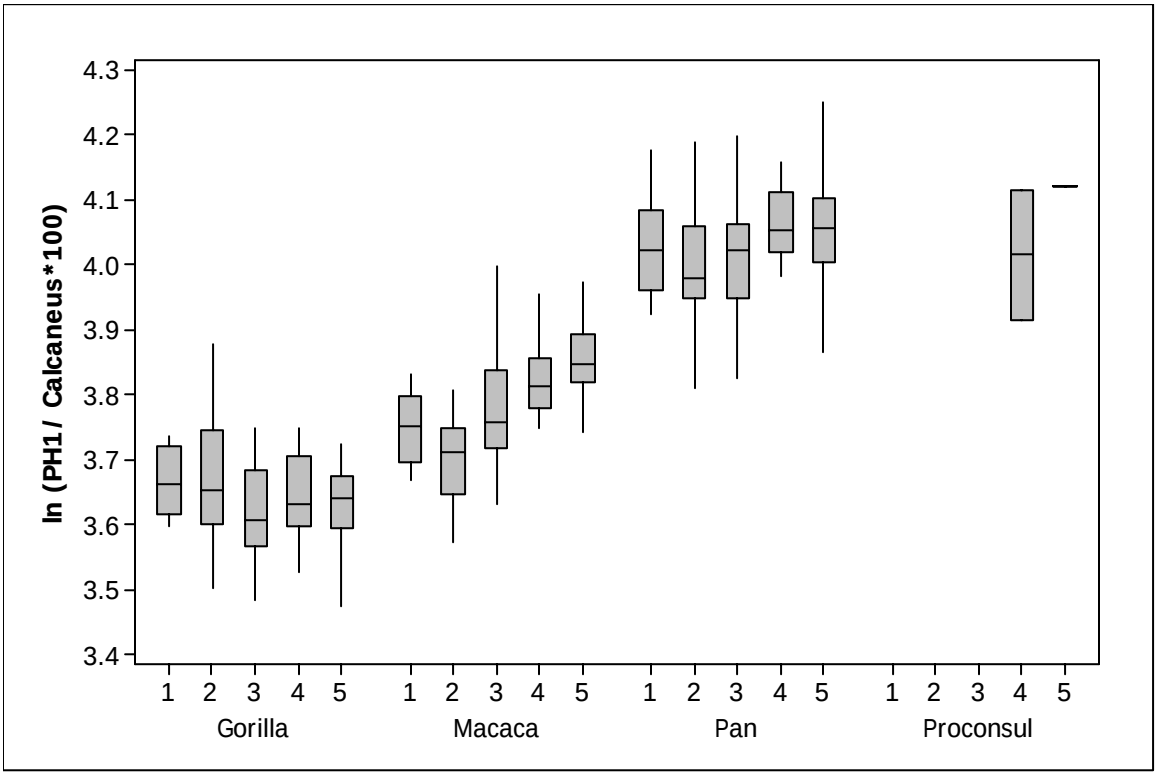

Figure 4.40. PH1/ Calcaneus by age group.

Table 4.18. ANOVA for PH1/ Calcaneus by age group.

Gorilla gorilla						*Macaca mulatta*						*Pan troglodytes*					
n		**1**	**2**	**3**	**4**	**n**		**1**	**2**	**3**	**4**	**n**		**1**	**2**	**3**	**4**
6	**1**					9	**1**					14	**1**				
16	**2**					16	**2**					46	**2**				
11	**3**					27	**3**		**x**			33	**3**				
11	**4**					31	**4**	**x**	**x**	**x**		12	**4**				
18	**5**					28	**5**	**x**	**x**	**x**		107	5		**x**	**x**	
F = 41.08, P = 0.374						F = 17.64, P = 0.00						F = 6.532, P = 0.00					
R-Sq = 7.06%						R-Sq = 39.96%						R-Sq = 11.21%					

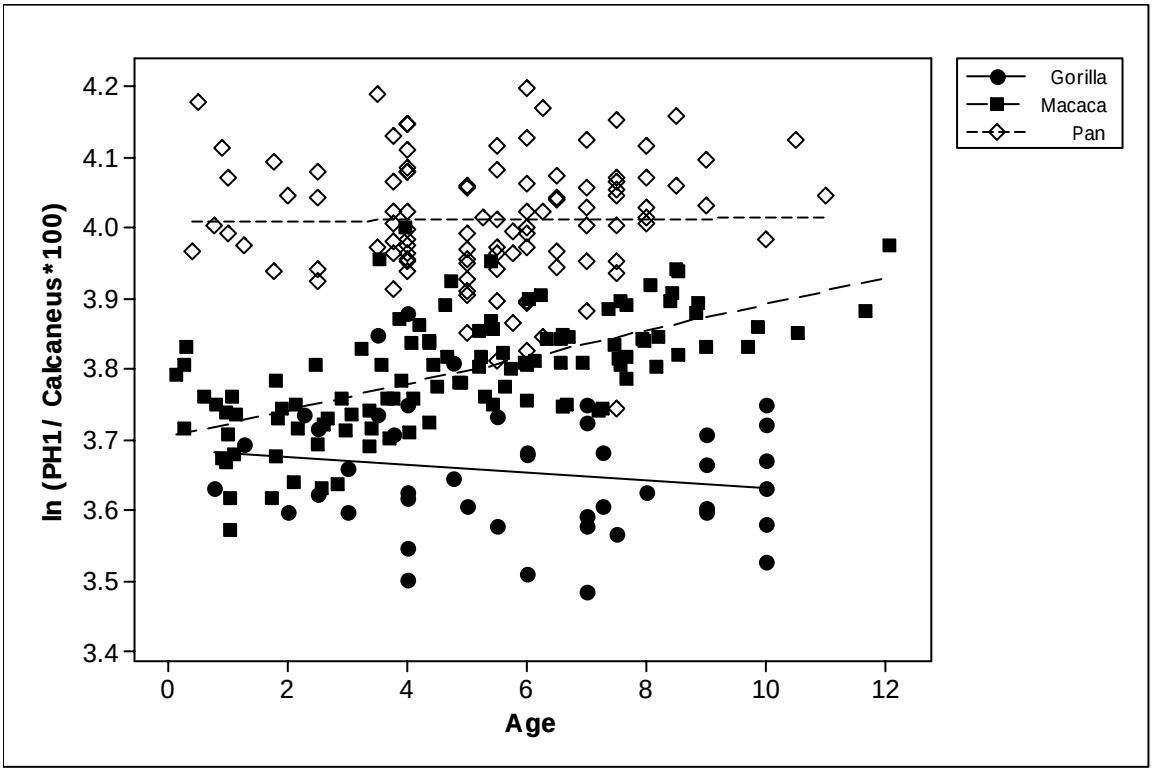

Figure 4.41. PH1/ Calcaneus by age.

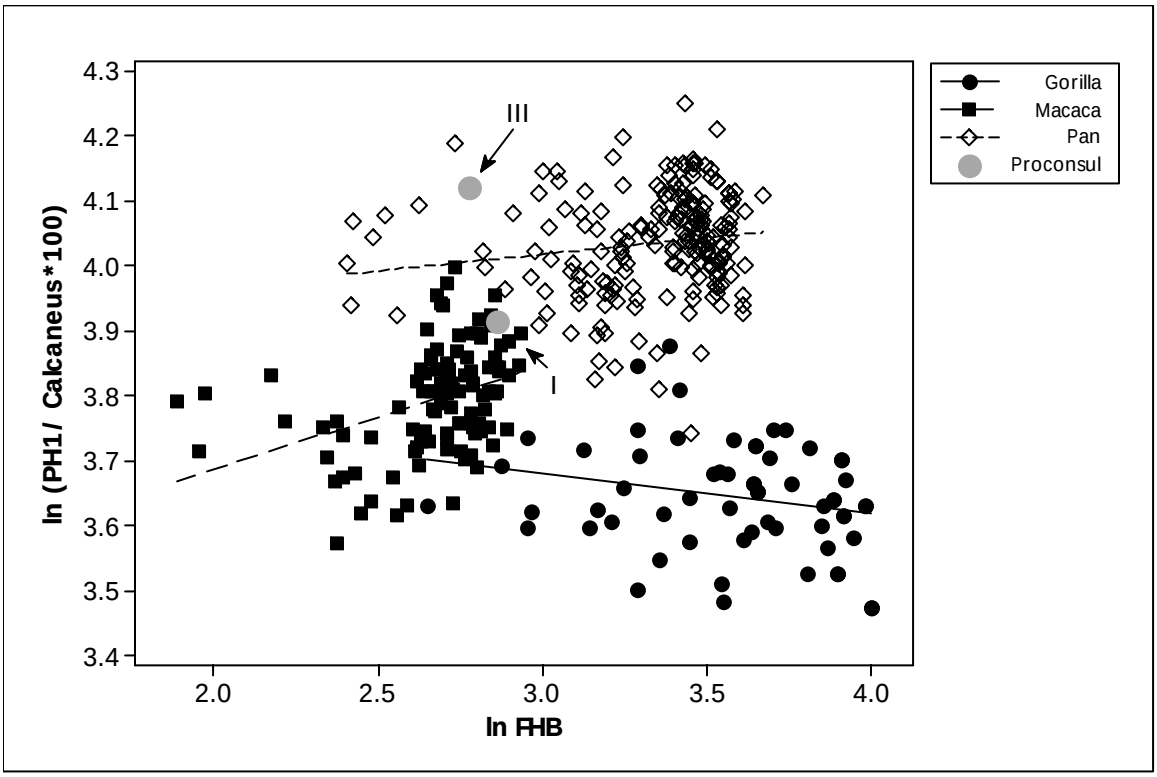

Figure 4.42. PH1/ Calcaneus by FHB.

PH1/ PH3 (Figures 4.43 – 4.45, Table 4.19) – *Macaca* does not show changes through development in this index, but the two apes do. PH1 outgrows PH3 in *Gorilla* and *Pan* and both have longer PH1 relative to PH3 than *Macaca.* Only the adult KPS III has the available measures for this index and it falls within range of all three taxa.

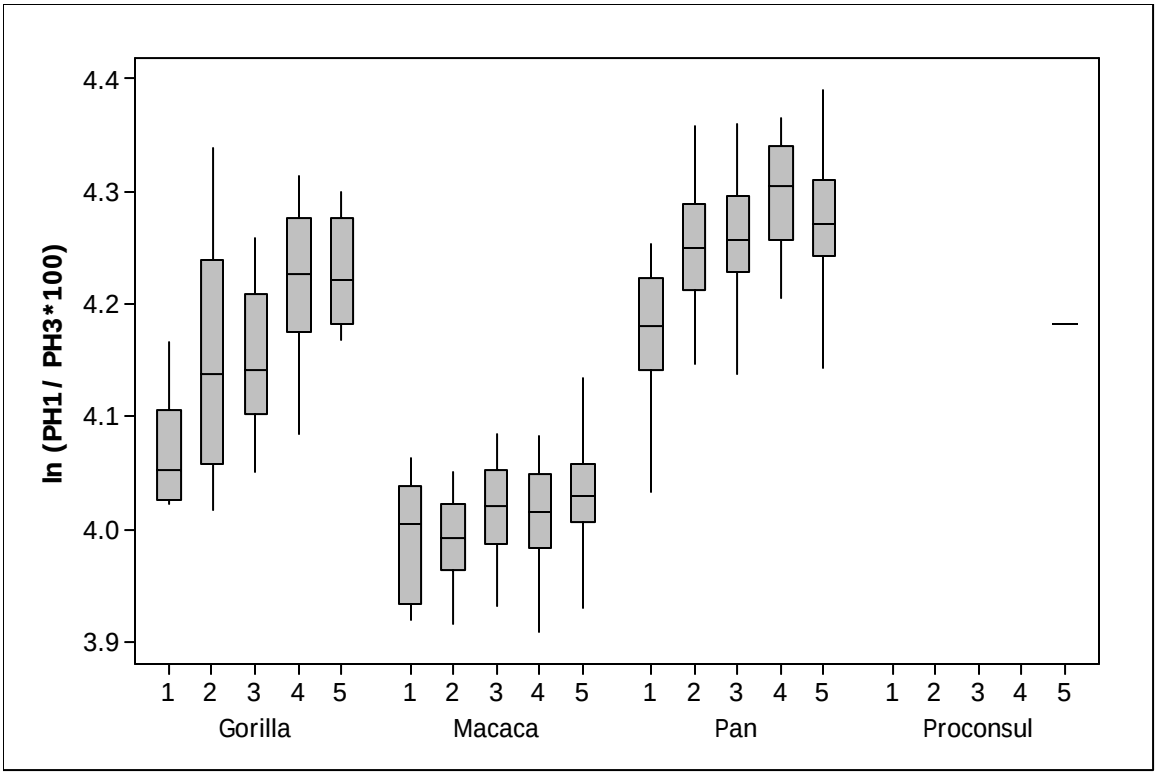

Figure 4.43. PH1/ PH3 by age group.

Table 4.19. ANOVA for PH1/ PH3 by age group.

Gorilla gorilla						*Macaca mulatta*						*Pan troglodytes*					
n		**1**	**2**	**3**	**4**	**n**		**1**	**2**	**3**	**4**	**n**		**1**	**2**	**3**	**4**
6	**1**					8	**1**					14	**1**				
16	**2**					16	**2**					45	**2**	**x**			
8	**3**					27	**3**					30	**3**	**x**			
10	**4**	**x**				30	**4**					12	**4**	**x**	**x**		
16	**5**	**x**	**x**			28	**5**					105	**5**				
F = 6.62,. P = 0.00						F = 2.40, P = 0.55						F = 9.182, P = 0.00					
R-Sq = 34.16%						R-Sq = 8.44%						R-Sq = 15.45%					

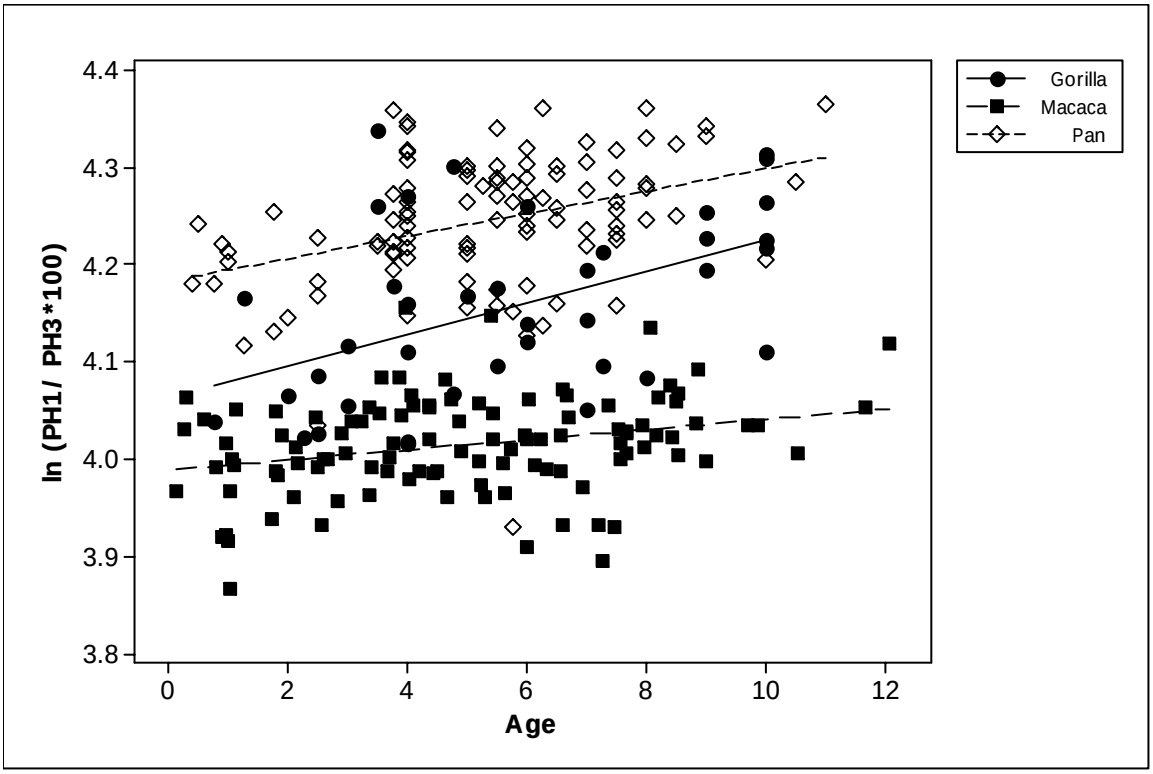

Figure 4.44. PH1/ PH3 by age.

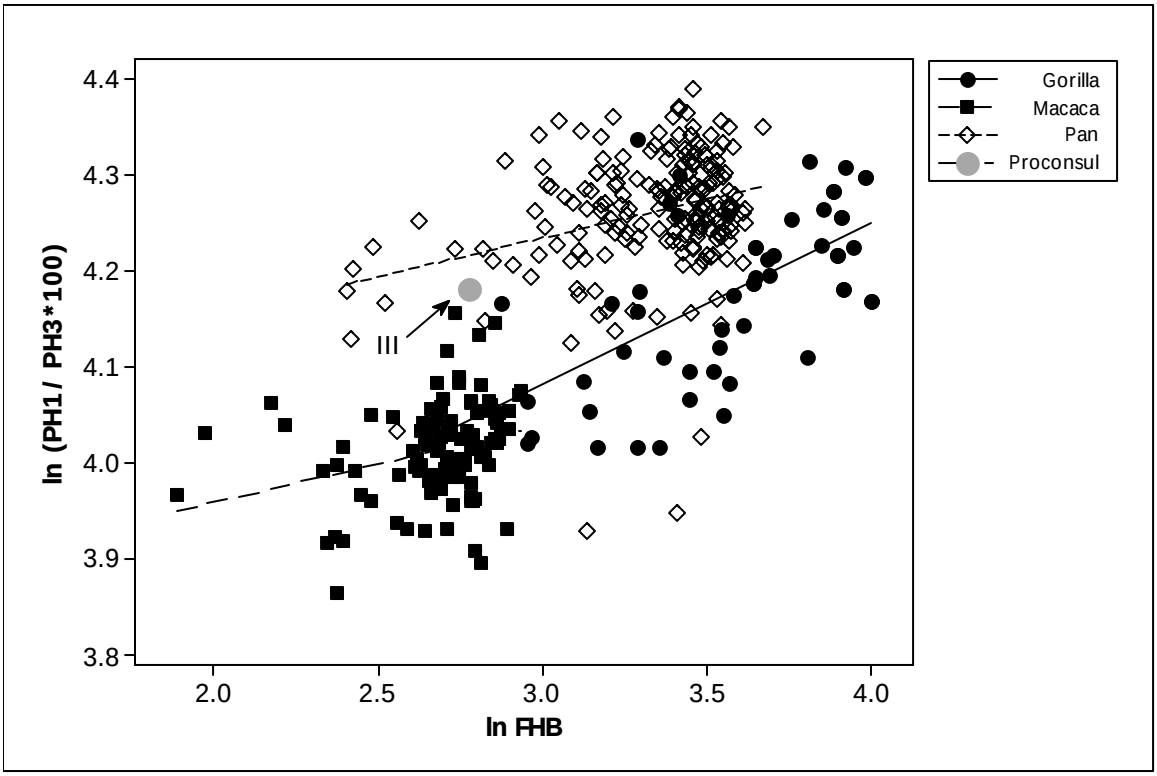

Figure 4.45. PH1/ PH3 by FHB.

MT1/ MT3 (Figures 4.46 – 4.48, Table 4.20) – All three modern taxa show basically the same proportions throughout development. The apes have a longer MT1 relative to MT3 than *Macaca.* KPS VII (age group 3) falls low with *Macaca* but the older *Proconsuls* fall in between the monkeys and the apes. The infant has the highest index and falls dead on the *Gorilla* and *Pan* lines at that age. Against FHB, KPS IV, I and III follow the ape trend fairly well albeit, at younger ages than expected. However, the juvenile VII plots with *Macaca.*

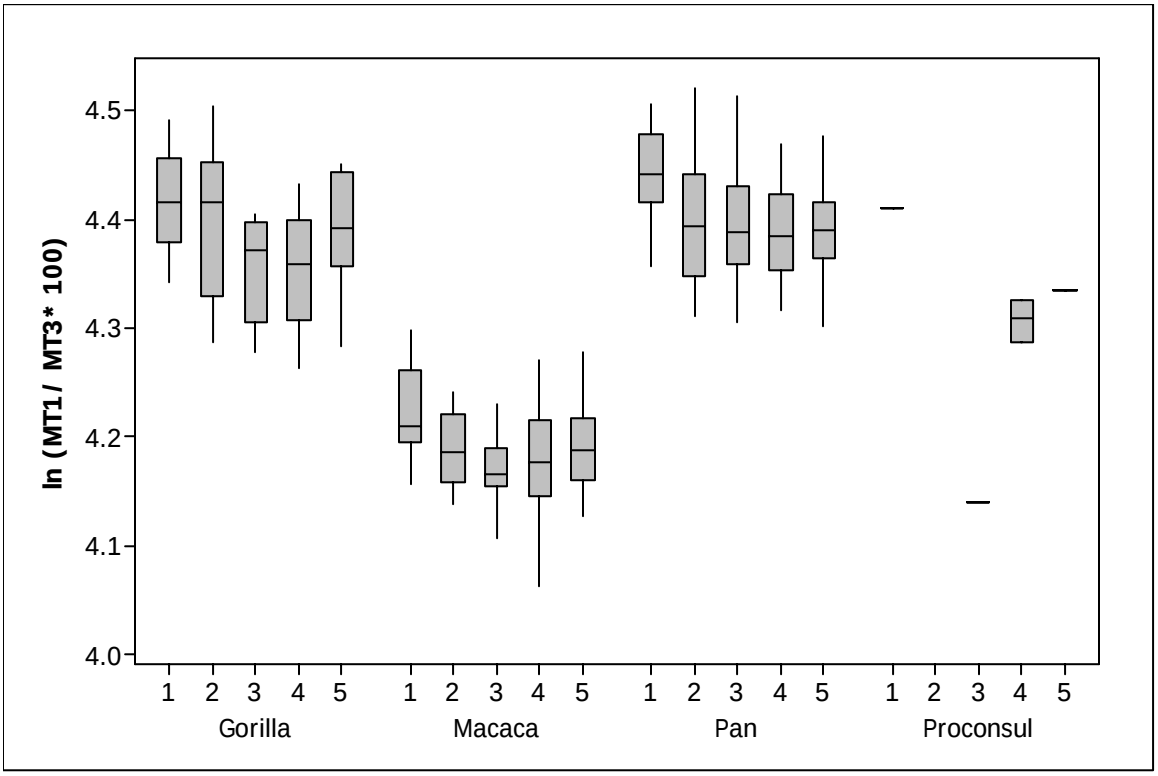

Figure 4.46. MT1/ MT3 by age group.

Table 4.20. ANOVA for MT1/ MT3 by age group.

Gorilla gorilla						*Macaca mulatta*						*Pan troglodytes*					
n		**1**	**2**	**3**	**4**	**n**		**1**	**2**	**3**	**4**	**n**		**1**	**2**	**3**	**4**
8	**1**					11	**1**					15	**1**				
17	**2**					16	**2**					46	**2**	**x**			
11	**3**					26	**3**	**x**				35	**3**	**x**			
11	**4**					31	**4**	**x**				15	**4**	**x**			
18	**5**					29	**5**					109	**5**	**x**			
F = 2.40, P = 0.059						F = 3.14, P = 0.018						F = 4.34, P = 0.002					
R-Sq = 13.82%						R-Sq = 10.40%						R-Sq = 7.48%					

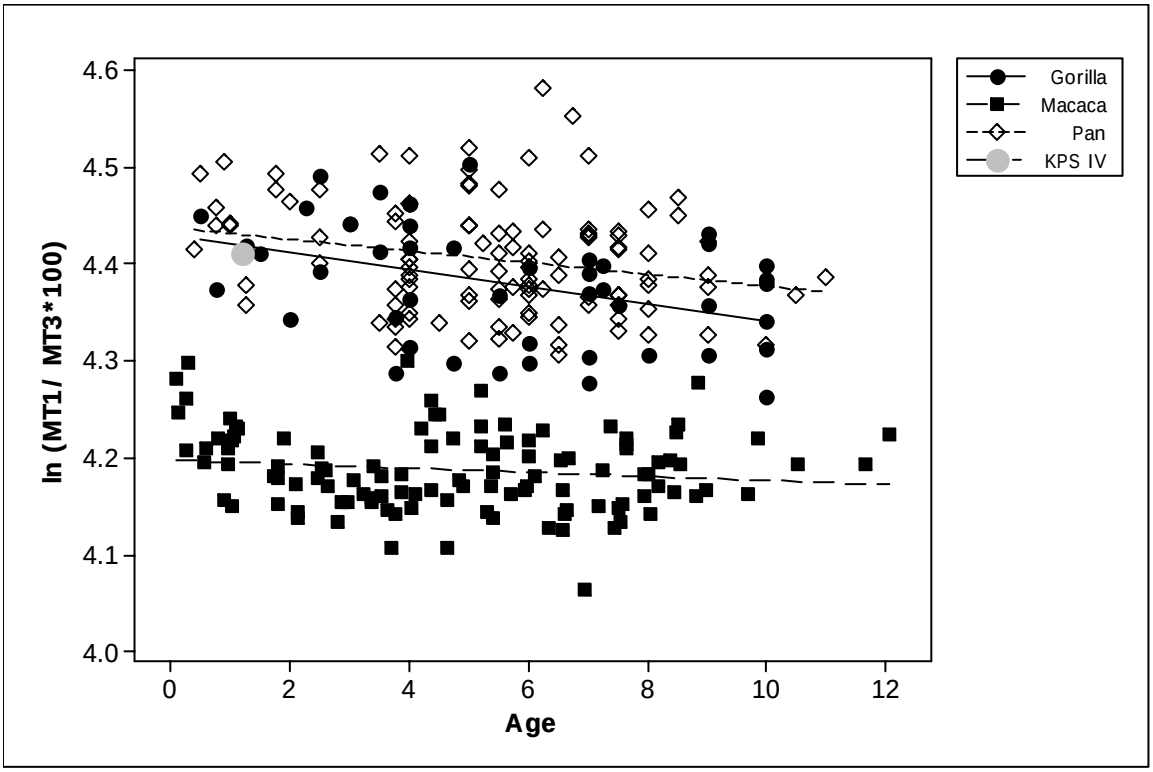

Figure 4.47. MT1/ MT3 by age.

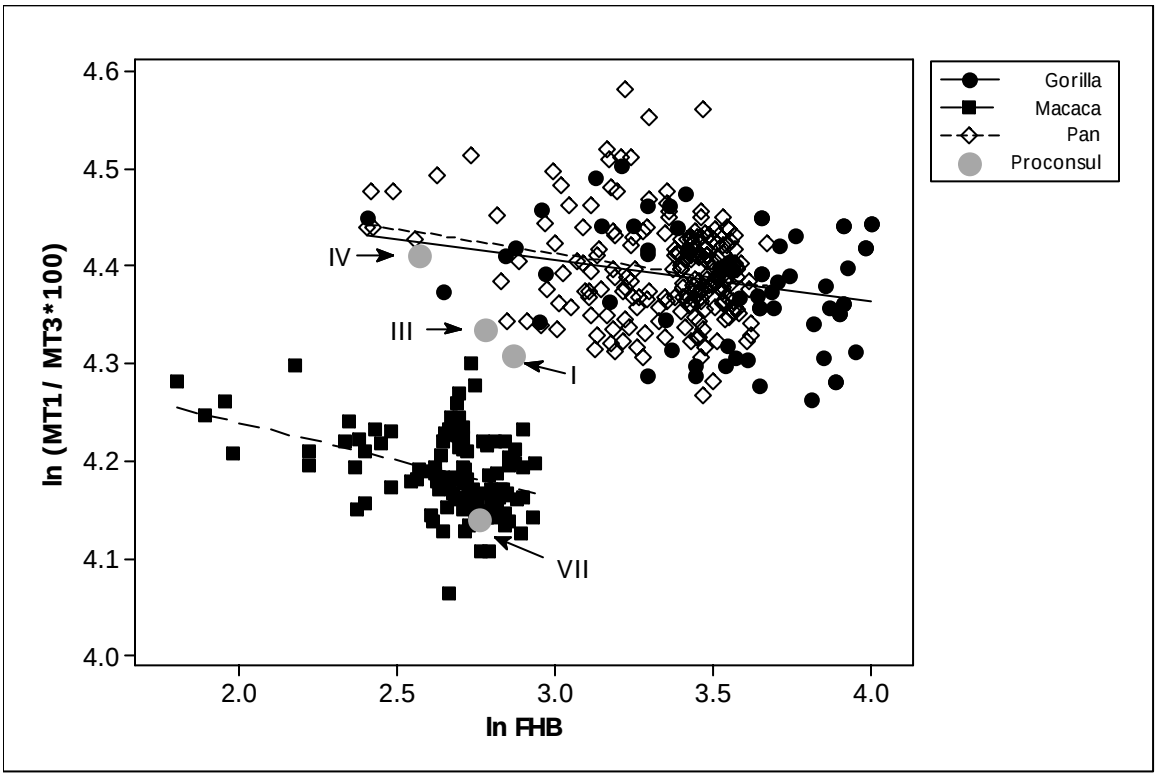

Figure 4.48. MT1/ MT3 by FHB.

Bivariate Results: Adult Sample

Comparisons among just the adults in the comparative sample show that, except for *Hylobates* and *P. paniscus*, measurements and indices within groups correlate strongly with FHB (Tables B.5-B.12, Appendix B). ANOVA distinguished between many of the species in mean proportions. *Nasalis* is absent from indices involving PH3 because those bones were unidentifiable for those individuals.

Figures 4.49 – 4.63. Comparisons of foot proportions among adult taxa. Indices specific to each graph and table are labeled.

(A) Box-plots of natural log-transformed index showing means, interquartile ranges and outliers (starred) for each group. KPS III is plotted for comparison.

(B) Results of ANOVA between the groups. Pairwise comparisons between Tukey 95% confidence intervals are left blank when significantly different ($P < 0.05$) and are marked "=" when means are not significantly different.

A

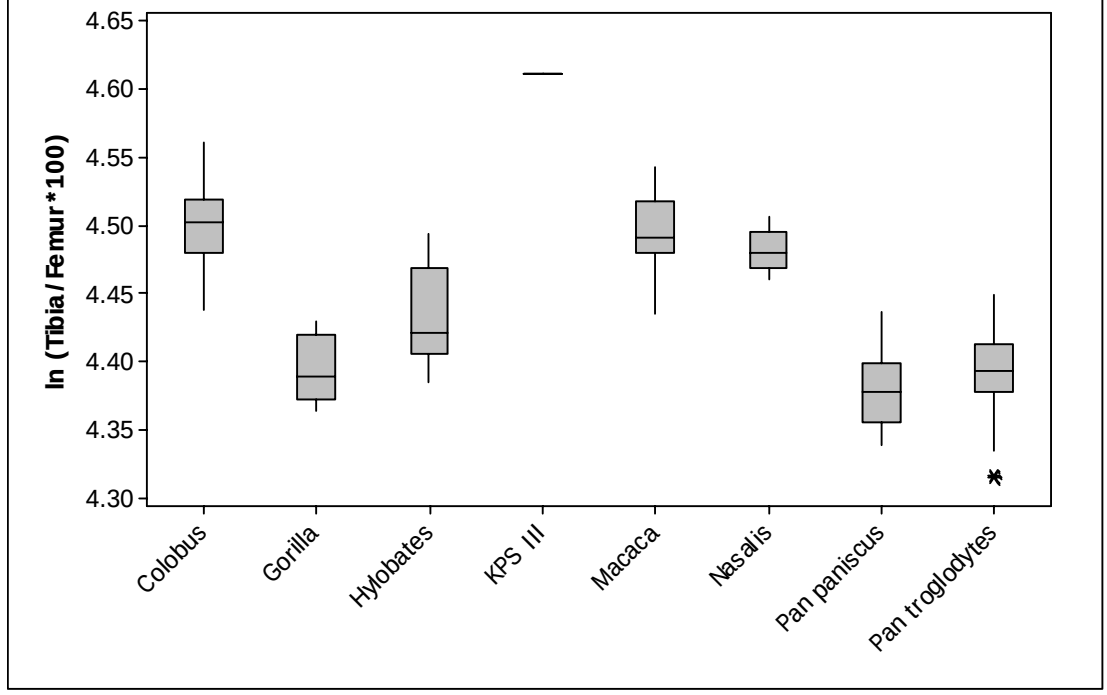

B

n		*Colobus*	*Gorilla*	*Hylobates*	*Macaca*	*Nasalis*	*P. pansicus*
24	*Colobus*						
18	*Gorilla*						
12	*Hylobates*						
28	*Macaca*	=		=			
10	*Nasalis*	=		=	=		
15	*P. pansicus*		=				
107	*P. troglodytes*		=				=
R-Sq = 75.45%, F = 106.02, P = 0.00							

Figure 4.49. Adult Tibia/ Femur box-plots and ANOVA.

Tibia/Femur (Figure 4.49)– This index groups the great apes apart from *Hylobates* and the monkeys. KPS III has the highest index of all.

A

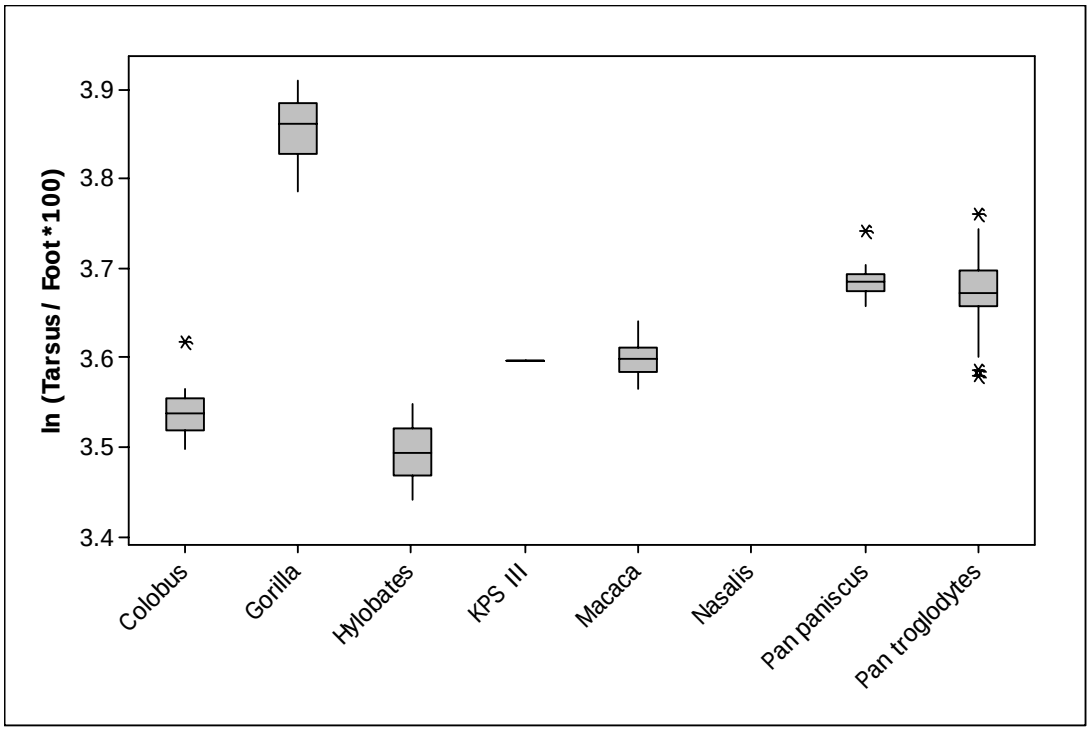

B

n		*Colobus*	*Gorilla*	*Hylobates*	*Macaca*	*Nasalis*	*P. pansicus*
14	*Colobus*						
16	*Gorilla*						
12	*Hylobates*						
29	*Macaca*						
x	*Nasalis*						
13	*P. pansicus*						
107	*P. troglodytes*						=
R-Sq = 87.52%, = 259.53, P = 0.00							

Figure 4.50. Adult Tarsus/ Foot box-plots and ANOVA.

Tarsus/ Femur (Figure 4.50) – the only groups that are equal are the two *Pan* species. *Proconsul* closely resembles *Macaca.*

A

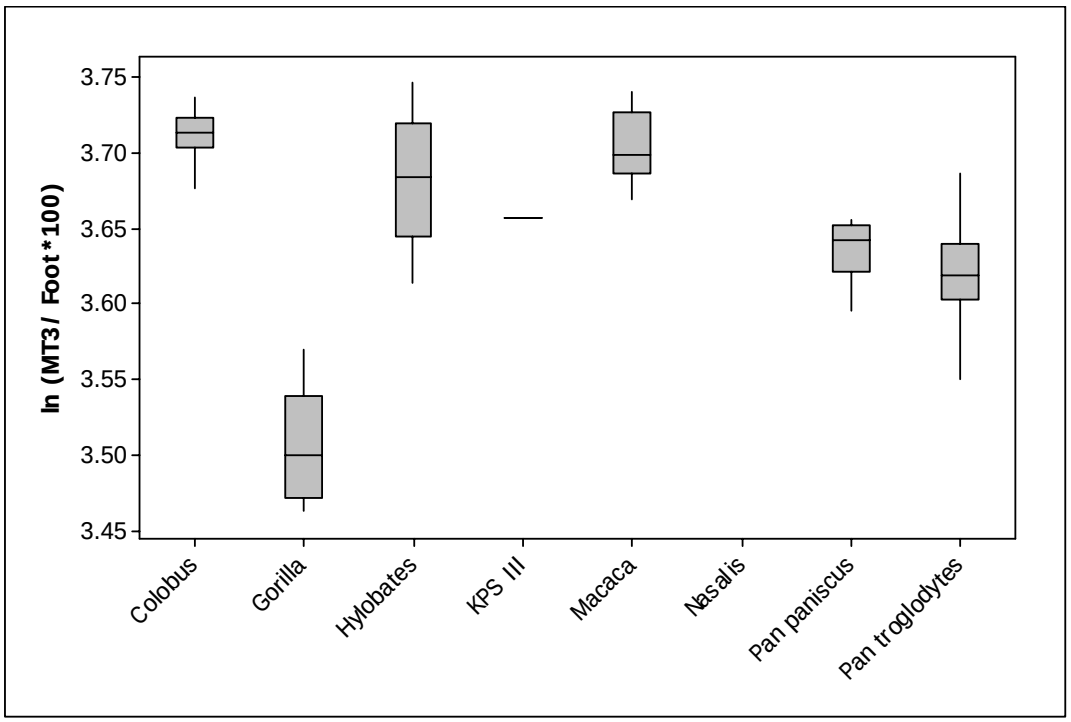

B

n		*Colobus*	*Gorilla*	*Hylobates*	*Macaca*	*Nasalis*	*P. pansicus*
14	*Colobus*						
16	*Gorilla*						
12	*Hylobates*						
29	*Macaca*	=		=			
x	*Nasalis*						
13	*P. pansicus*						
107	*P. troglodytes*						=
R-Sq = 79.93%, F = 147.32, P = 0.00							

Figure 4.51. Adult MT3/ Foot box-plots and ANOVA.

MT3/ Foot (Figure 4.51) – The *Pan* species group together and so do the monkeys with *Hylobates* to the exclusion of gorillas. *Proconsul* is within or close to the range of all species but gorillas.

A

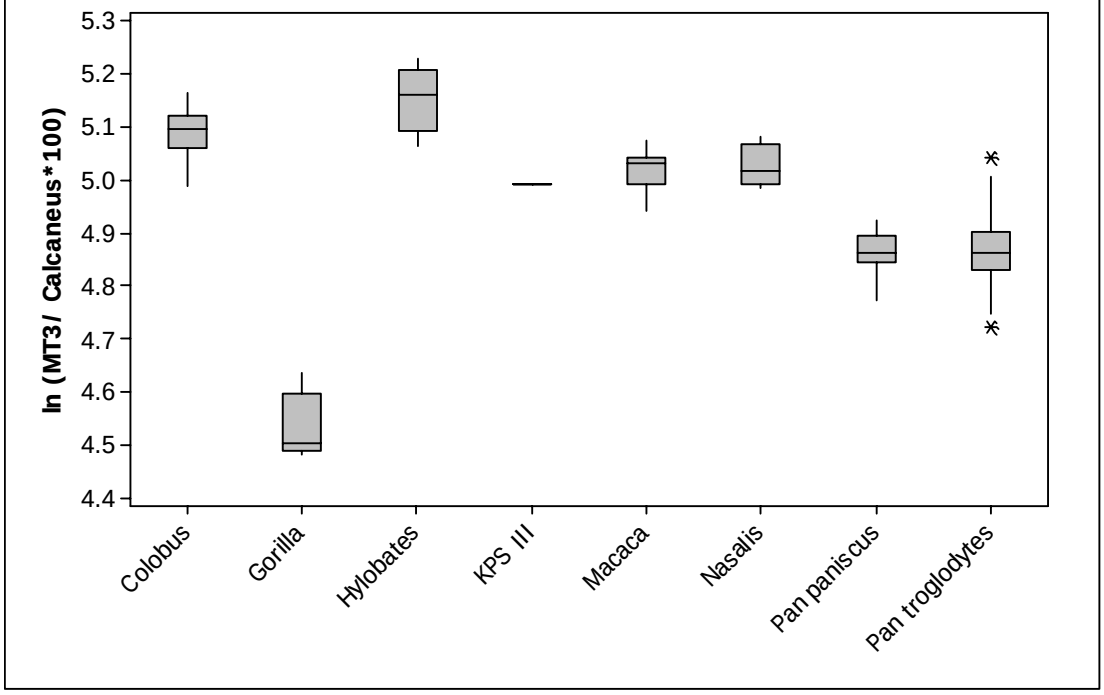

B

n		*Colobus*	*Gorilla*	*Hylobates*	*Macaca*	*Nasalis*	*P. pansicus*
24	*Colobus*						
18	*Gorilla*						
12	*Hylobates*	=					
29	*Macaca*						
10	*Nasalis*				=		
15	*P. pansicus*						
109	*P. troglodytes*						=
R-Sq = 89.05%, F = 284.51, P = 0.00							

Figure 4.52. Adult MT3/ Calcaneus box-plots and ANOVA

MT3/ Calcaneus (Figure 4.52) – This is a similar pattern to the previous one except it is clearer that *Proconsul* resembles *Colobus*, *Macaca* and *Nasalis*.

A

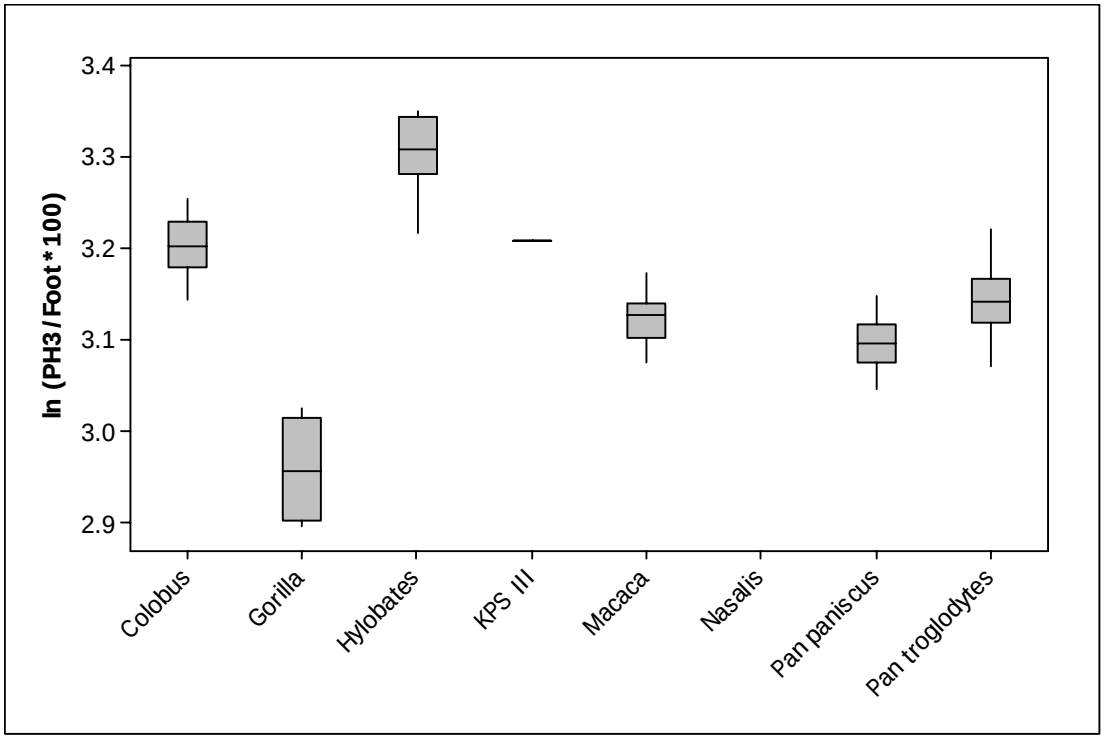

B

n		*Colobus*	*Gorilla*	*Hylobates*	*Macaca*	*Nasalis*	*P. pansicus*
14	*Colobus*						
16	*Gorilla*						
12	*Hylobates*						
29	*Macaca*						
x	*Nasalis*						
13	*P. pansicus*				=		
107	*P. troglodytes*						
R-Sq = 81.23%, F = 160.14, P = 0.00							

Figure 4.53. Adult PH3/ Foot box-plots and ANOVA.

PH3/ Foot (Figure 4.53) – Only macaques and bonobos show similar patterns.

Proconsul has a higher index more like *Colobus, Hylobates or P. troglodytes.*

A

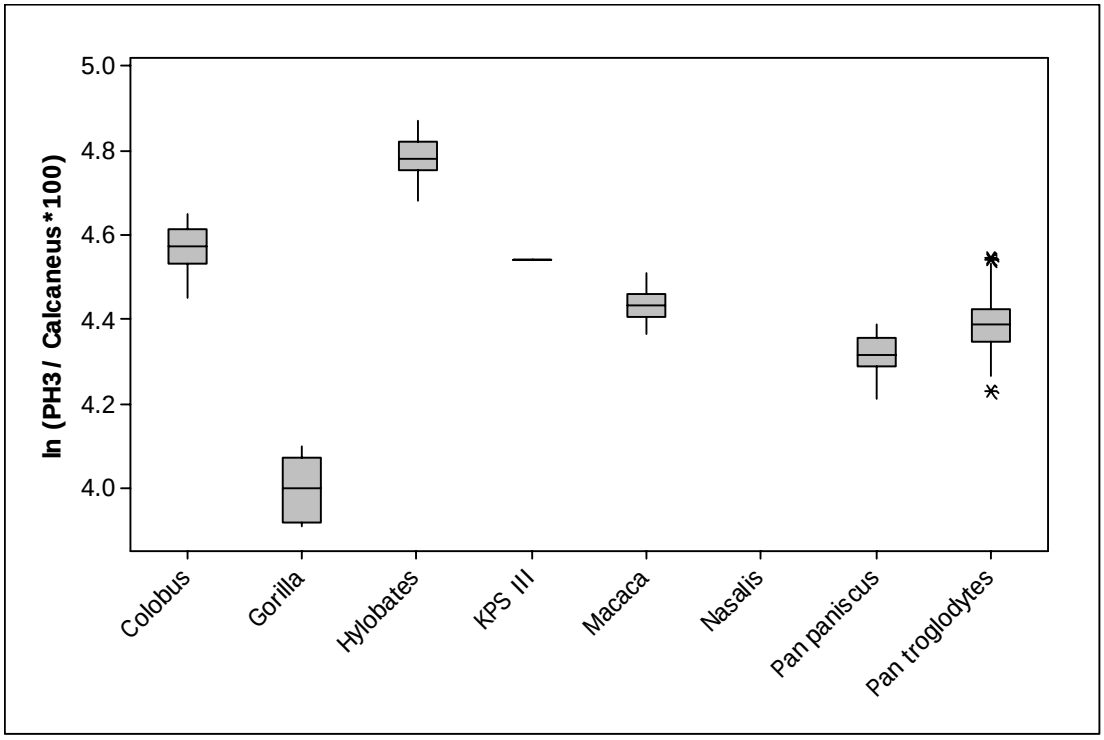

B

n		*Colobus*	*Gorilla*	*Hylobates*	*Macaca*	*Nasalis*	*P. pansicus*
14	*Colobus*						
16	*Gorilla*						
12	*Hylobates*						
29	*Macaca*						
x	*Nasalis*						
13	*P. pansicus*						
107	*P. troglodytes*						
R-Sq = 89.02%, F = 299.98, P = 0.00							

Figure 4.54. Adult PH3/ Calcaneus box-plots and ANOVA.

PH3/ Calcaneus (Figure 4.54) – All groups are significantly different. KPS III overlaps with *Colobus* and *P. troglodytes.*

A

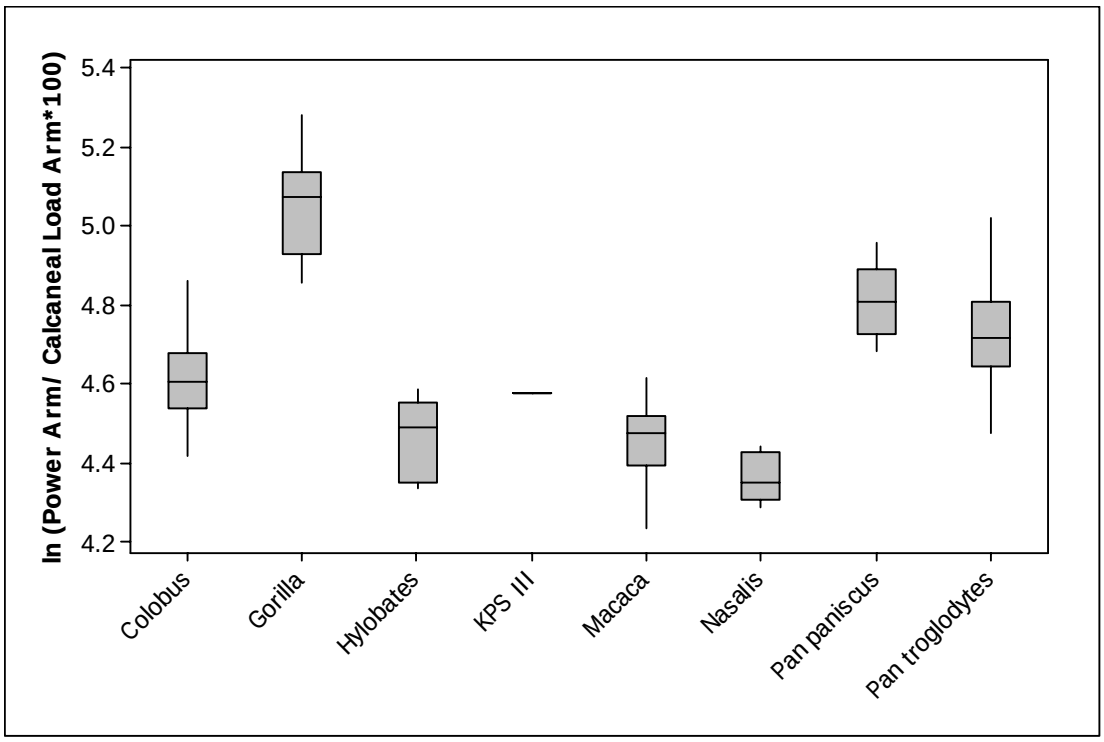

B

n		*Colobus*	*Gorilla*	*Hylobates*	*Macaca*	*Nasalis*	*P. pansicus*
24	*Colobus*						
18	*Gorilla*						
12	*Hylobates*						
29	*Macaca*			=			
10	*Nasalis*			=	=		
13	*P. pansicus*						
108	*P. troglodytes*						=
R-Sq = 70.80%, F = 84.47, P = 0.00							

Figure 4.55. Adult Power Arm/ Calcaneal Load Arm box-plots and ANOVA.

Power Arm/ Calcaneal Load Arm (Figure 4.55) - *Colobus* and *Gorilla* are isolated, *Hylobates, Macaca* and *Nasalis* group together and so do the two *Pan* species. *Proconsul* falls among *Colobus, Hylobates, Macaca,* and *P. troglodytes*.

A

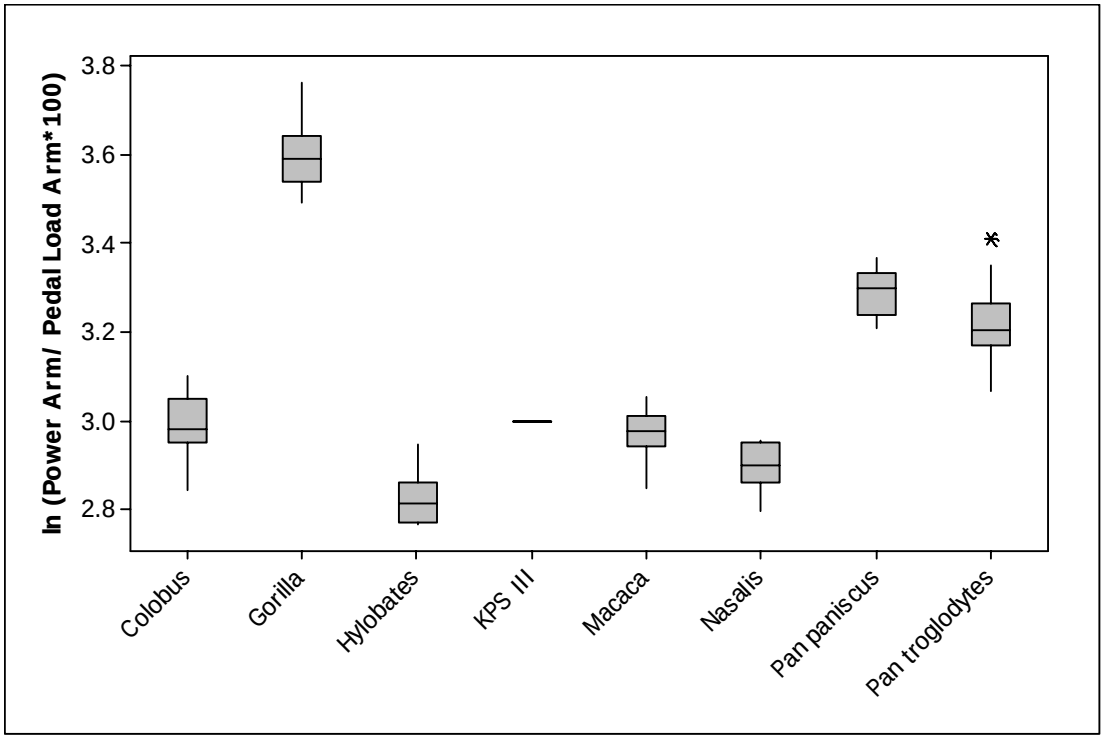

B

n		*Colobus*	*Gorilla*	*Hylobates*	*Macaca*	*Nasalis*	*P. pansicus*
24	*Colobus*						
18	*Gorilla*						
12	*Hylobates*						
29	*Macaca*	=					
10	*Nasalis*			=			
13	*P. pansicus*						
108	*P. troglodytes*						
R-Sq = 89.99%, F = 313.14, P = 0.00							

Figure 4.56. Adult Power Arm/ Pedal Load Arm box-plots and ANOVA.

Power Arm/ Pedal Load Arm (Figure 4.56) – The great apes are isolated and *Proconsul* falls among the gibbons and monkeys.

A

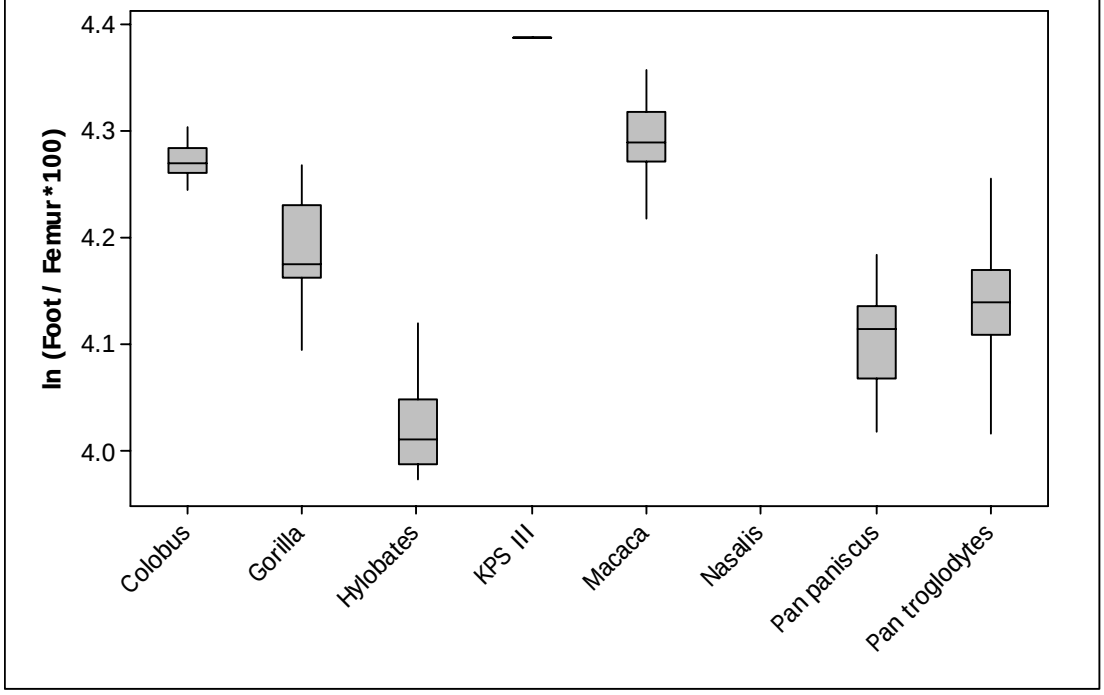

B

n		*Colobus*	*Gorilla*	*Hylobates*	*Macaca*	*Nasalis*	*P. pansicus*
14	*Colobus*						
16	*Gorilla*						
12	*Hylobates*						
29	*Macaca*	=					
x	*Nasalis*						
13	*P. pansicus*						
107	*P. troglodytes*		=				=
R-Sq = 76.66%, F = 121.55, P = 0.00							

Figure 4.57. Adult Foot/ Femur box-plots and ANOVA.

Foot/ Femur (Figure 4.57) – The *Proconsul* index is relatively high, and closest to *Colobus* and *Macaca.* The great apes have equal means.

A

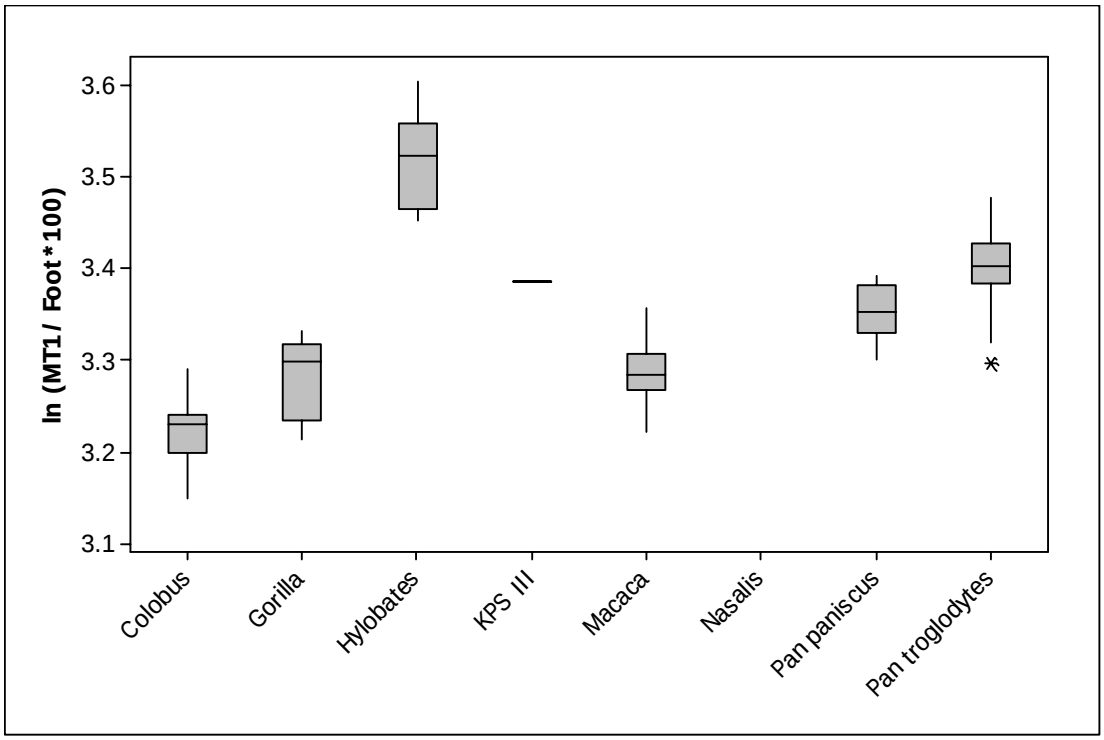

B

n		*Colobus*	*Gorilla*	*Hylobates*	*Macaca*	*Nasalis*	*P. pansicus*
14	*Colobus*						
16	*Gorilla*						
12	*Hylobates*						
29	*Macaca*		=				
x	*Nasalis*						
13	*P. pansicus*						
106	*P. troglodytes*						
R-Sq = 80.90%, F = 155.91, P = 0.00							

Figure 4.58. Adult MT1/ Foot box-plots and ANOVA.

MT1/ Foot (Figure 4.58) – Here *Gorilla* is grouped with *Macaca* highlighting their similar terrestrial hallux proportions. All others are significantly different. KPS III falls right in the middle like *Pan*.

A

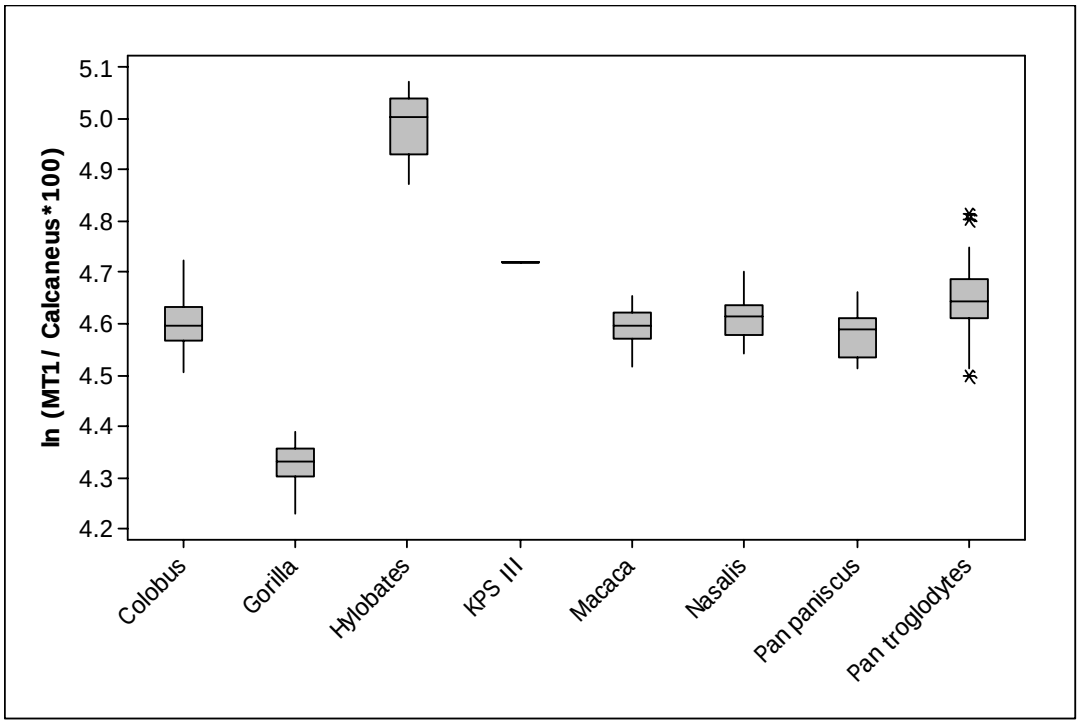

B

n		*Colobus*	*Gorilla*	*Hylobates*	*Macaca*	*Nasalis*	*P. pansicus*
24	*Colobus*						
18	*Gorilla*						
12	*Hylobates*						
29	*Macaca*	=					
10	*Nasalis*	=			=		
15	*P. pansicus*	=			=	=	
109	*P. troglodytes*					=	
R-Sq = 84.79%, F = 195.1, P = 0.00							

Figure 4.59. Adult MT1/ Calcaneus box-plots and ANOVA.

MT1/ Calcaneus (Figure 4.59) – *Proconsul* plots with those groups showing moderate indices for hallucal metatarsal length versus calcaneus length. *Gorilla* and *Hylobate*s fall out at the extremes illustrating the differences in proportions between the gibbon (long halluxed/ short calcaneus) and the gorilla (short halluxed, long calcaneus).

A

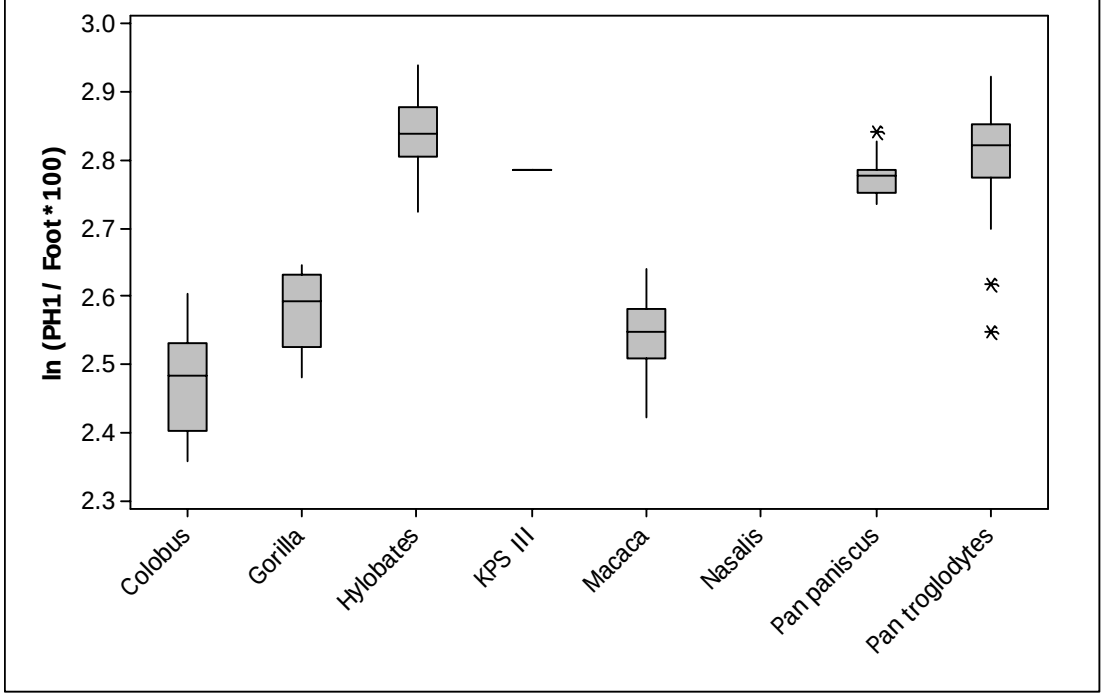

B

n		*Colobus*	*Gorilla*	*Hylobates*	*Macaca*	*Nasalis*	*P. pansicus*
12	*Colobus*						
16	*Gorilla*						
12	*Hylobates*						
28	*Macaca*		=				
x	*Nasalis*						
13	*P. pansicus*			=			
105	*P. troglodytes*			=			=
R – Sq = 84.10%, F = 190.44, P = 0.00							

Figure 4.60. Adult PH1/ Foot box-plots and ANOVA.

PH1/ Foot (Figure 4.60) – *Hylobates, Pan* and *Proconsul* have the longest first proximal phalanx relative to foot length. Again, gorillas and macaques have equal means.

A

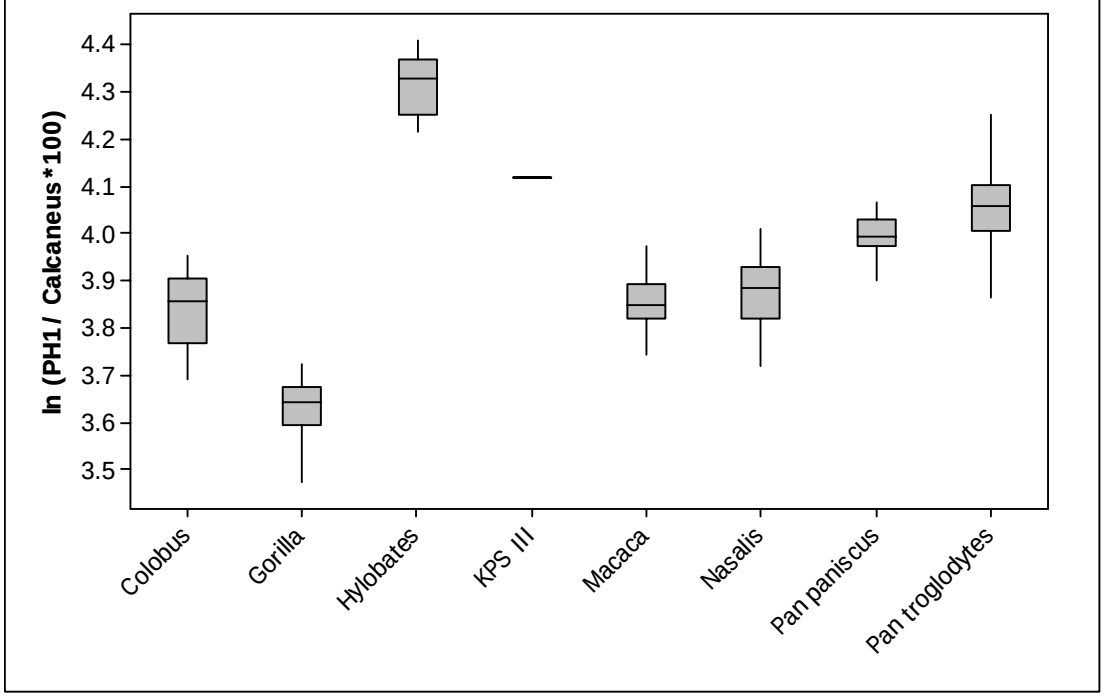

B

n		*Colobus*	*Gorilla*	*Hylobates*	*Macaca*	*Nasalis*	*P. pansicus*
12	*Colobus*						
18	*Gorilla*						
12	*Hylobates*						
28	*Macaca*	=					
10	*Nasalis*	=			=		
13	*P. pansicus*						
107	*P. troglodytes*						=
R – Sq = 84.85%, F = 180.14, P = 0.00							

Figure 4.61. Adult PH1/ Calcaneus box-plots and ANOVA.

PH1/ Calcaneus (Figure 4.61) – The monkeys group together, the chimpanzees group together, and the gorillas and gibbons are again isolated at the extremes. *Proconsul* lies chose to the chimpanzees for this index at the upper levels of this ratio but does not show extremes as high as gibbons.

A

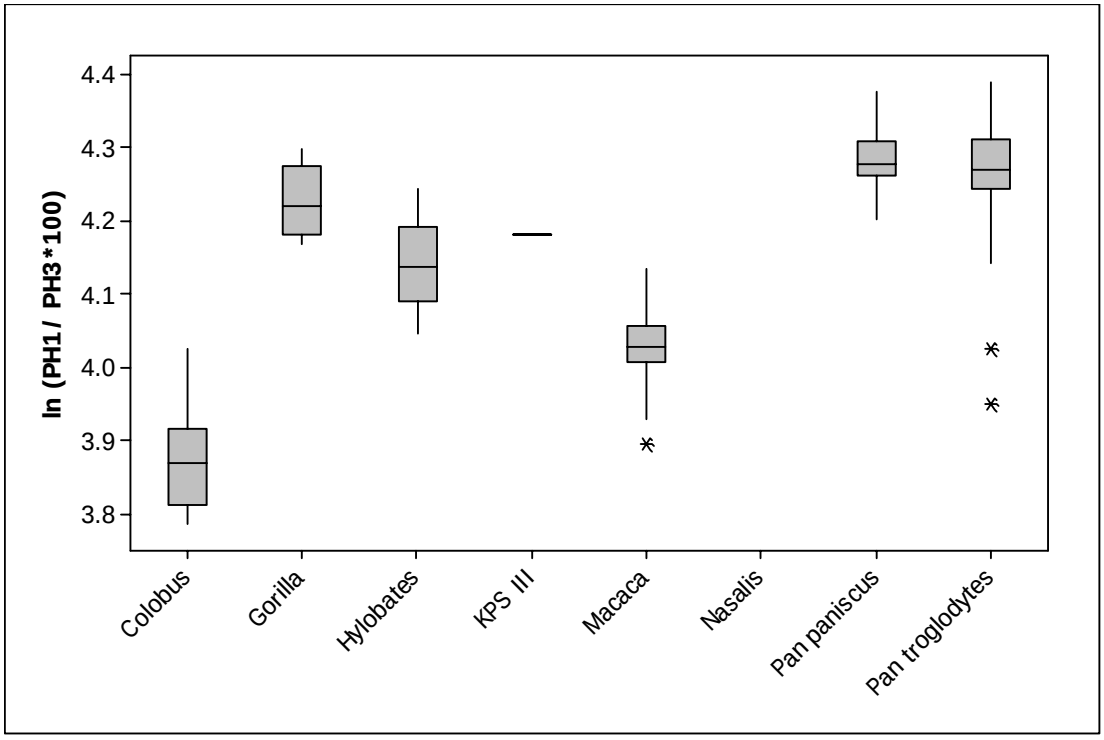

B

n		*Colobus*	*Gorilla*	*Hylobates*	*Macaca*	*Nasalis*	*P. pansicus*
12	*Colobus*						
16	*Gorilla*						
12	*Hylobates*						
28	*Macaca*						
x	*Nasalis*						
13	*P. pansicus*		=				
105	*P. troglodytes*						=
R-Sq = 82.41%, F = 168.63, P = 0.00							

Figure 4.62. Adult PH1/ PH3 box-plots and ANOVA.

PH1/ PH3 (Figure 4.62) – Gorillas and chimpanzees group together with the highest indices. Gibbons and KPS III show a lesser index.

A

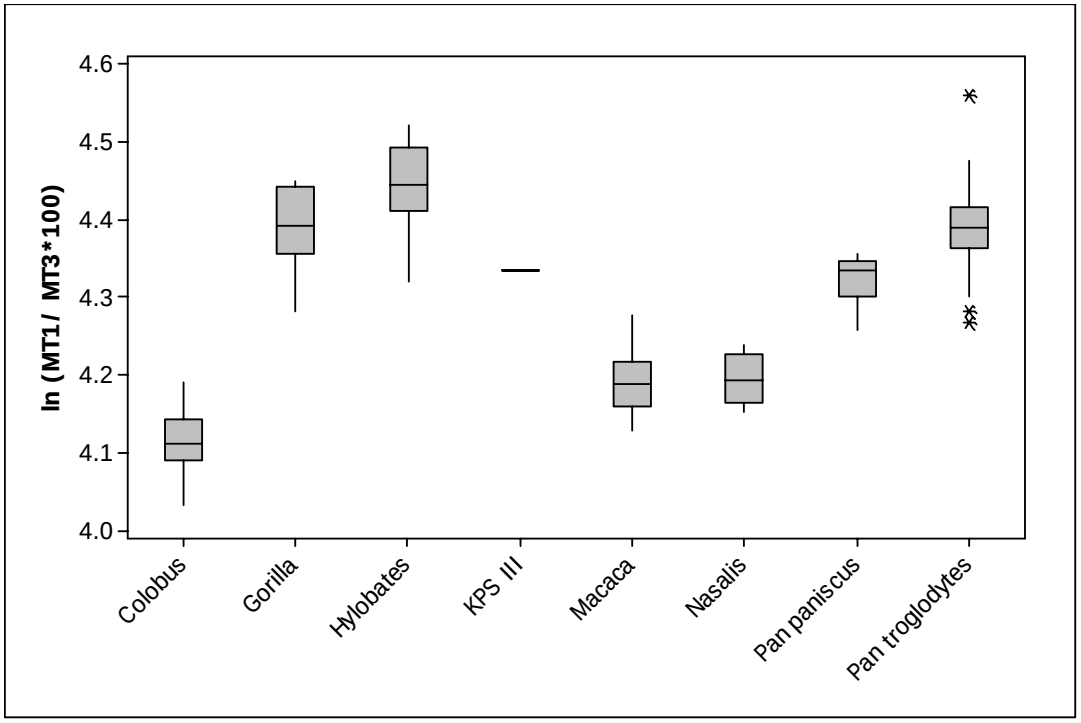

B

n		*Colobus*	*Gorilla*	*Hylobates*	*Macaca*	*Nasalis*	*P. pansicus*
24	*Colobus*						
18	*Gorilla*						
12	*Hylobates*						
29	*Macaca*						
10	*Nasalis*				=		
15	*P. pansicus*						
109	*P. troglodytes*		=				
R-Sq = 87.17%, F = 237.75, P = 0.00							

Figure 4.63. Adult MT1/ MT3 box-plots and ANOVA.

MT1/ MT3 (Figure 4.63) – *Gorilla* and *P. troglodytes* have equal means as do *Macaca* and *Nasalis. Proconsul* overlaps the lesser end of the distribution of gorillas and gibbons and overlaps with both *Pan* species for this index.

Discussion of Bivariate Results

Does a shift in foot proportions from immature to adult ones occur before adult body size is achieved? *Macaca* and *Pan* finish growing just after third molar occlusion, but *Gorilla* continues to grow beyond this life history stage (Leigh and Shea, 1996; Wells and Turnquist, 2001). For all groups, indices of age 4 and 5 individuals are never significantly different, meaning individuals reach fully adult foot proportions by age 4, despite the fact that many are continuing to grow in body size through age 5. So adult foot proportions are reached prior to adult body size for all indices and they are reached even earlier than age group 4 for many indices.

Across the species, age groups 1 and 2 show the highest incidence of significant differences from other age groups which is expected since all three species do not achieve true adult locomotor and behavioral patterns until they become part of age group 2. Age groups 3,4 and 5 represent individuals with adult locomotor behavior in all three modern taxa (Wells and Turnquist, 2001; Doran, 1997).

Are proportions achieving adult form earlier than body size because of locomotor requirements? In the cases where only ages 4 and 5 are the same, proportions are most likely changing as a result of body size. For instance, *Gorilla* shows distinct growth patterns with increasingly longer power arms in relation to calcaneal and pedal load arms for pushing along their increasingly heavy bodies through development (Figures 4.22-4.27). But for many indices, individuals achieve adult proportions by age groups 1 and 2, around the time of first molar eruption and also coinciding with locomotor independence. These indices that show isometry with age are probably linked more closely to locomotor development than body size increase. All three modern taxa tend to already display their

particular MTI1, PH3 and PH1 proportions by age group 1. This observation may emphasize the need for grasping onto mother during the earliest altricial phase of life. However, the observation that *Gorilla* and *Pan* achieve many more aspects of adult foot and hindlimb proportions much earlier in development than *Macaca* indicates that there may be anatomical correlates with differences in life history and behavior between neonates in the groups.

The issue of what is ancestral and what is derived is a confounding factor in the analysis. Changes in *Macaca* proportions may be more dramatic because they might be showing morphological adaptations that diverge more from the ancestral form compared to *Gorilla* and *Pan*, which may have more anatomically primitive or generalized feet. Manley-Buser (1991) found that elevated rates of pedal growth in humans were best explained by the acquisition of derived traits (Gould, 1977). The changes in many of the foot and hindlimb proportions in *M. mulatta* compared to the relative stasis in the two apes, probably signal growth of terrestrially adapted foot proportions, away from that of the primitive form. They also, however, signal fundamentally different growth patterns that are most likely directed by different developmental processes.

The long phalanges of *Proconsul*, resembling *Colobus* and *Pan* proportions, are consistent with an emphasized need for grasping during locomotion. The relationship between the power arm and the calcaneal and pedal load arms in the adult *Proconsul* (III) is a reflection of its small body size, but is also closely aligned with the pattern seen in the three monkey taxa of varying body sizes so it is also indicating monkey-like function.

Rose (1983) observed (based on the available *Proconsul* specimens at the time) that the distal calcaneus is long and the metatarsus connection to the tarsus is narrow.

However, data from KPS III do not support these observations. The anterior (distal) portion of the calcaneus is plotted against calcaneus length for adults and KPS III does not show a pattern that departs from the expected proportions (Figure 4.64).

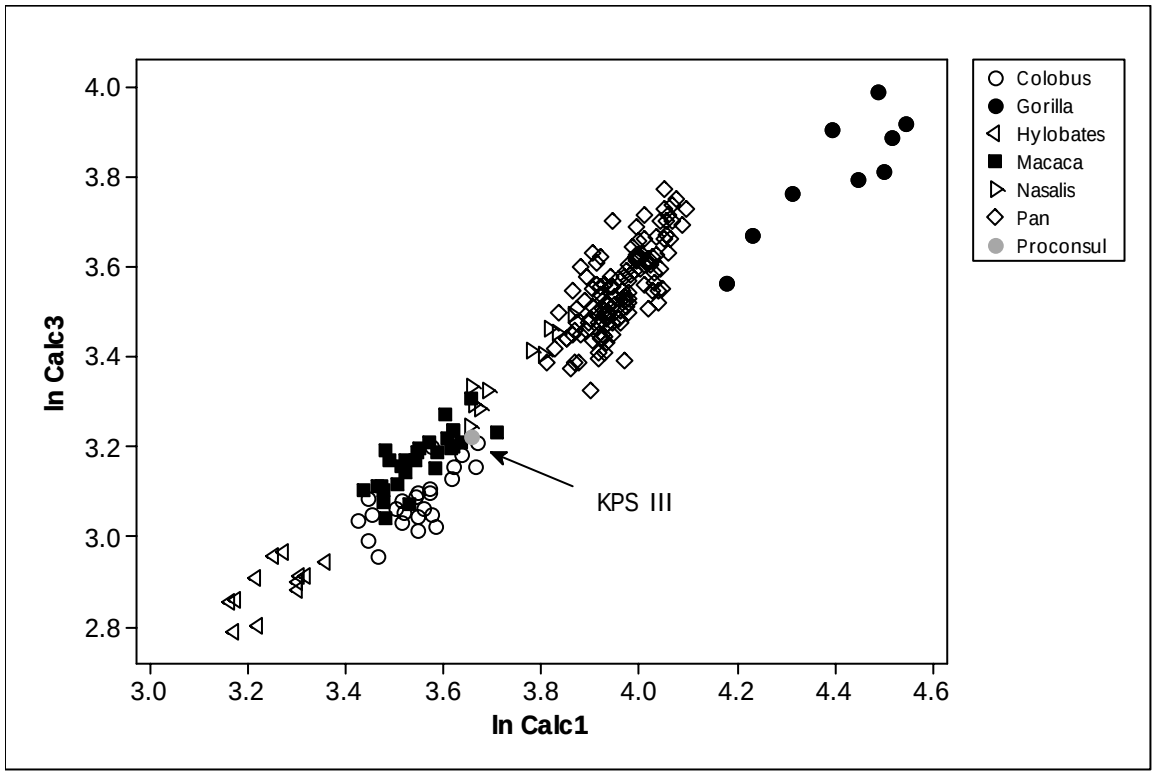

Figure 4.64. Distal calcaneus length versus total calcaneus length for adult sample.

When foot width (the sum of the distal widths of the intermediate cuneiform (ICUN3), lateral cuneiform (LCUN3) and cuboid (CUB3)) is plotted against total foot length KPS III plots with the monkeys and gibbon pattern (Figure 4.65).

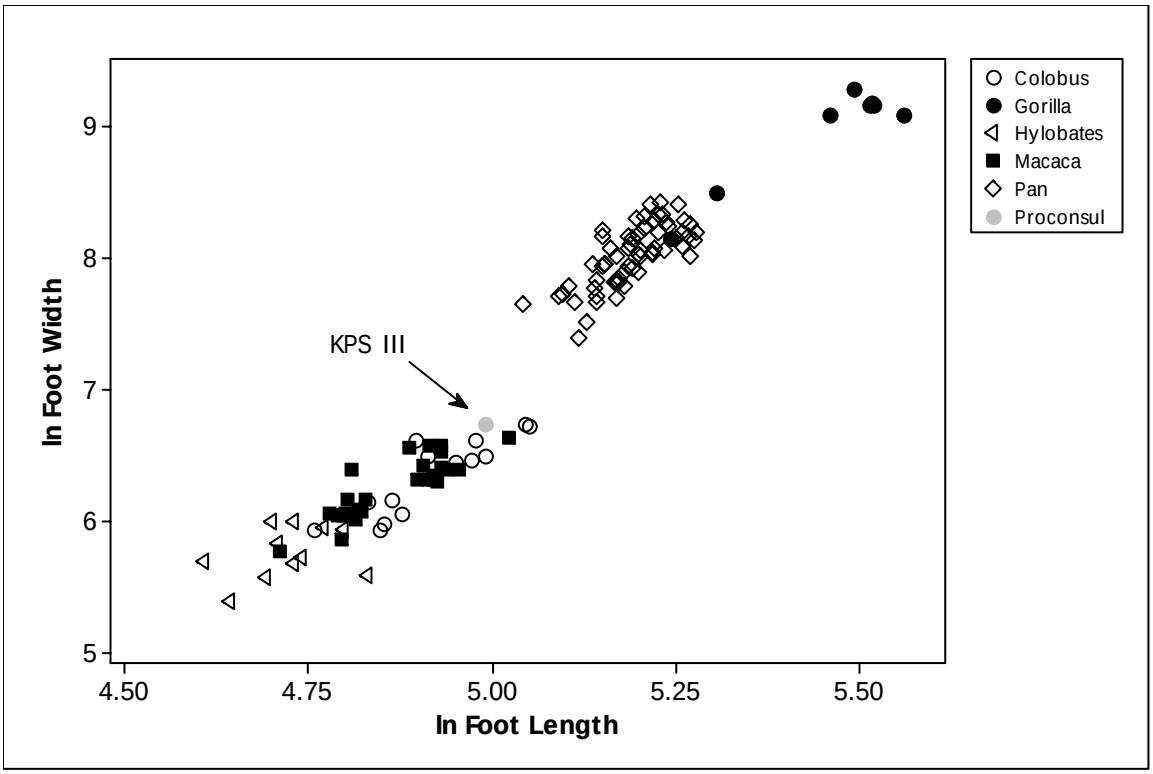

Figure 4.65. Foot width versus foot length for adult sample.

In general, *Proconsul* displays a mixture of features that center on generalized arboreality (Table 4.21). The mechanical units of the foot as well as the overall hindlimb proportions are monkey-like and the relative lengths of MT1, PH1 and PH3 align with arboreal monkeys and apes. The overall findings are consistent with those suggested by Strasser in her 1993 abstract and support the "generalized arboreal quadruped" hypothesis for *Proconsul* locomotion.

The comparison of indices between the various adult taxa show that proportions often differ significantly and they are therefore useful for building a discriminant model in a multivariate analysis to classify *Proconsul*.

Table 4.21. Summary of *Proconsul* comparative proportions.

Index	*Proconsul* is most similar to…	Exceptional observations	Strasser (1993)
Tibia/ Femur	*Macaca, Colobus*	IV - ape	
Tarsus/ Foot	*Macaca, Colobus*	IV - ape	Colobines
MT3/ Foot	*Hylobates, Macaca, Colobus*		Arboreal OWM
MT3/ Calcaneus	*Hylobates, Macaca, Colobus, Nasalis*		
PH3/ Foot	*Pan, Hylobates, Colobus*		Arboreal OWM
PH3/ Calcaneus	*Pan, Colobus*		
Power Arm/ Calcaneal Load Arm	*Colobus, Hylobates, Macaca, Pan*		
Power Arm/ Pedal Load Arm	*Colobus, Macaca*		Colobines
Foot/ Femur	*Macaca*	IV - ape	
MT1/ Foot	*Pan*		
MT1/ Calcaneus	*Pan, Nasalis, Colobus*		
PH1/ Foot	*Hylobates, Pan*		Ape, Hylobates
PH1/ Calcaneus	*Pan*		
PH1/ PH3	*Gorilla, Hylobates, Pan*		
MT1/ MT3	*Hylobates, Gorilla, Pan*	VII - monkey	Arboreal OWM

Multivariate Results

Trial 1 (Figure 4.66) All 20 measures shared by the 6 individuals (KPS plus KNM-RU 2036) were used in the model. Five principal components were used that accounted for 73% of the variation. 100% of the individuals were classified correctly with cross-validation at the family level. All *Proconsul* specimens except KNM-RU 2036 were classified as monkeys/*Nasalis*. RU 2036 was classified as an ape/*Hylobates*. KPS IV falls nearly equally distant from apes and monkeys but is solidly classified as *Nasalis*. The same results occur when five anatomically redundant variables (Calc1, ICun2, ICun4, LCun2, LCun4) are removed (bringing the list of variables closer to 15 which is the recommended maximum).

Trial 2 (Figure 4.67) Traits were picked to include as many age group 1 from the ontogenetic sample as possible. There were very few to choose from and they mostly encompass the metrics of the calcaneus and the metatarsals. Only two principal components were useful but they accounted for 83% of the variation. Only four individuals were misclassified with cross-validation at the family level. KPS I and IV are split between monkey/*Macaca* and ape/*Pan*. RU 2036 was determined monkey/*Macaca* and KPS VIII was placed into ape/ *Pan*.

Trial 3 (Figure 4.68) Traits were picked to maximize features to classify the complete KPS III which includes all metatarsals and both PH1 and PH3. Four principal components account for 74% of the variation were used to build the model that was able to classifiy 100% correctly at the family level with cross-validation. KPS III was grouped with monkey/*Colobus*.

Trial 4 (Figure 4.69) Just the digits were the focus of this trial. Only two principal components making up 89% of the variation were used in the model. The model was able to classify all but two individuals correctly at the family level. KPS I and III were both classified as ape/*Gorilla* .

Trial 5 (Figure 4.70) The same variables were used as in the previous trial but Calc1 was added for a body size parameter. Two principal components were used accounting for 85% of the variation. Only one individual was misclassified with cross-validation at the family level and this time KPS I and III were labeled ape/*Pan*. But KPS I had a 33% probability of clustering with *Macaca*.

Figures 4.66- 4.70. Linear discriminant analysis (LDA) for five trials based on different sets of variables. Metrics were first divided by geometric means. “Sq. Dist.” is the squared distance between that observation to the group centroid or mean vector. “Prob.” is the posterior probability and observations are assigned to the distance with the highest posterior probability.

(A) The first and second principal components plotted with classification line drawn based on the linear discriminant function.

(B) Principal components used in the LDA. Only those with eigenvalues greater than 1 were put into the model.

(C) Results of the LDA grouping sample at the family level. Bold values indicate significant classification for *Proconsul*.

(D) Results of the LDA with groupings of the sample at the genus level. Bold values indicate significant classification for *Proconsul*.

Figure 4.66. Linear Discriminant Analysis: Trial 1.

A

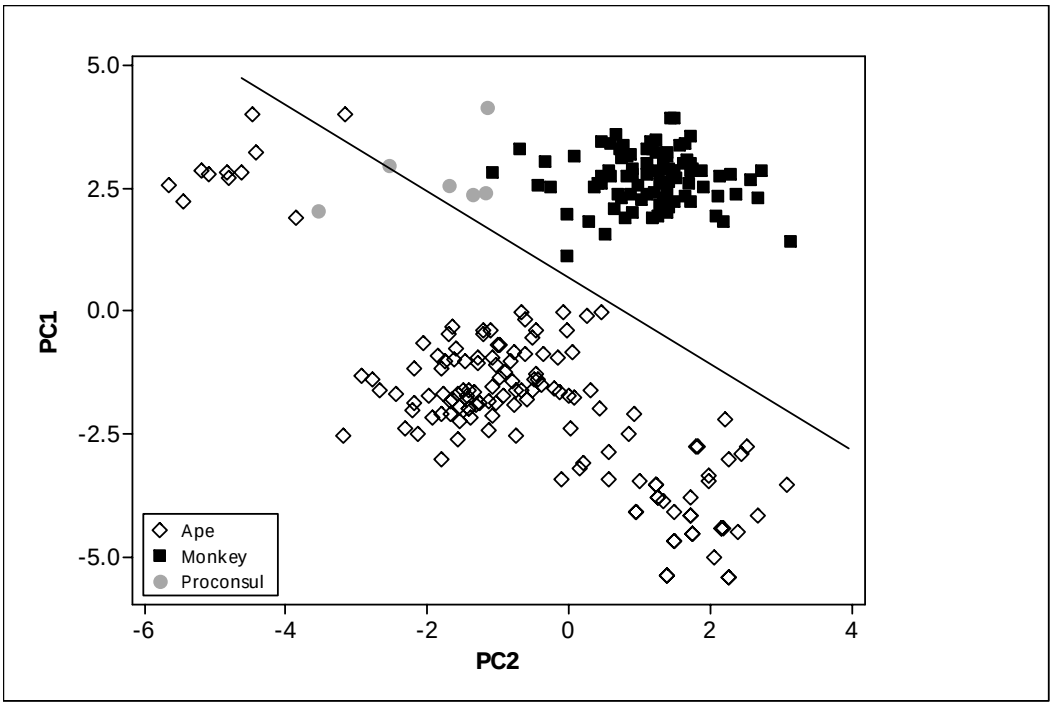

B

Variable	PC1	PC2	PC3	PC4	PC5
Calc1	-0.038	0.467	-0.188	-0.146	0.132
Calc2	-0.307	0.224	-0.047	-0.147	0.065
Calc3	0.181	0.262	-0.269	-0.001	0.121
Calc4	-0.286	-0.151	-0.17	0.087	0.212
Calc8	-0.281	0.188	0.015	-0.216	0.082
Nav1	-0.232	-0.096	0.352	-0.1	-0.206
Nav2	0.194	0.18	0.215	-0.396	-0.318
Mcun1	0.118	-0.356	0.134	-0.218	0.282
Icun1	0.17	-0.247	0.033	0.24	-0.432
Icun2	0.049	-0.074	-0.44	-0.117	-0.533
Icun3	-0.241	-0.213	-0.03	0.263	-0.08
Icun4	-0.259	-0.16	0.012	0.03	-0.062
Lcun1	0.176	-0.123	-0.377	0.307	0.056
Lcun2	0.035	-0.091	-0.512	-0.164	0.122
Lcun3	0.115	0.31	0.121	0.255	-0.148
Lcun4	0.098	0.292	0.148	0.554	0.123
Cub3	-0.296	-0.077	0.066	0.17	0.172
MT3	0.352	0.071	0.109	0.005	0.106
MT2	0.335	-0.085	0.137	-0.042	0.189
MT1	0.263	-0.276	0.038	-0.152	0.277
Eigenvalue	7.1395	3.1234	2.0387	1.2192	1.0495
Proportion	0.357	0.156	0.102	0.061	0.052
Cumulative	0.357	0.513	0.615	0.676	0.729

Figure 4.66. Trial 1 Continued.

C

	Ape	Monkey
Summary of Classification with Cross-validation		
Put into group		
Ape	143	0
Monkey	0	89
Total N	143	89
N Correct	143	89
Proportion	1	1
N=232, N Correct = 232, Proportion Correct = 1.00		
Squared Distance Between Groups		
Ape	0	42.1228
Monkey	42.1228	0
Linear Discriminant Function for Groups		
Constant	-3.1812	-7.8836
PC1	-2.6692	4.1768
PC2	-2.316	3.7093
PC3	-0.0467	0.225
PC4	-0.5496	0.7468
PC5	0.7779	-1.2591
Classification of *Proconsul*		
KPS I		
Sq. Dist.	25.066	**20.059**
Prob.	0.076	**0.924**
KPS III		
Sq. Dist.	23.476	**11.612**
Prob.	0.003	**0.997**
KPS IV		
Sq. Dist.	48.426	**48.187**
Prob.	0.47	**0.53**
KPS VII		
Sq. Dist.	52.195	**20.861**
Prob.	0	**1**
KPS VIII		
Sq. Dist.	22.842	**15.685**
Prob.	0.027	**0.973**
RU 2036		
Sq. Dist.	**19.103**	38.426
Prob.	**1**	0

Figure 4.66. Trial 1 Continued.

D

	Colobus	***Gorilla***	***Hylobates***	***Macaca***	***Nasalis***	***Pan***
Summary of Classification with Cross-validation						
Put into group						
Colobus	16	0	0	5	2	0
Gorilla	0	40	0	0	0	1
Hylobates	0	0	11	0	0	0
Macaca	3	0	0	49	0	0
Nasalis	5	0	0	1	8	0
Pan	0	2	0	0	0	89
Total N	24	42	11	55	10	90
N Correct	16	40	11	49	8	89
Proportion	0.667	0.952	1	0.891	0.8	0.989
N = 232, N Correct = 213, Proportion Correct = 0.918						
Squared Distance Between Groups						
Colobus	0	112.793	75.435	4.585	3.942	46.685
Gorilla	112.793	0	209.264	104.91	117.796	35.085
Hylobates	75.435	209.264	0	84.04	85.935	82.469
Macaca	4.585	104.91	84.04	0	6.617	50.983
Nasalis	3.942	117.796	85.935	6.617	0	49.983
Pan	46.685	35.085	82.469	50.983	49.983	0
Linear Discriminant Function for Groups						
Constant	-10.175	-22.119	-38.697	-10.266	-11.71	-3.554
PC1	6.391	-9.54	7.373	6.201	6.594	-3.074
PC2	1.169	3.843	-10.275	2.359	1.237	-2.189
PC3	1.555	-1.819	2.026	0.196	0.473	0.101
PC4	0.998	-1.087	-3.043	-0.311	2.606	0.35
PC5	-0.46	0.241	1.691	-1.454	-1.132	0.794
Classification of *Proconsul*						
KPS I						
Sq. Dist.	23.784	115.137	54.89	25.351	**16.273**	37.245
Prob.	0.023	0	0	0.01	**0.967**	0
KPS III						
Sq. Dist.	15.576	113.022	52.6	16.116	**9.399**	35.71
Prob.	0.042	0	0	0.032	**0.926**	0
KPS IV						
Sq. Dist.	59.81	166.282	76.439	62.736	**42.131**	70.601
Prob.	0	0	0	0	**1**	0
KPS VII						
Sq. Dist.	31.667	176.064	69.133	34.65	**20.126**	77.698
Prob.	0.003	0	0	0.001	**0.996**	0
KPS VIII						
Sq. Dist.	21.67	122.532	45.169	21.219	**14.964**	39.661
Prob.	0.032	0	0	0.041	**0.927**	0
RU 2036						
Sq. Dist.	48.124	138.589	**35.989**	48.996	38.753	43.549
Prob.	0.002	0	**0.783**	0.001	0.197	0.018

Figure 4.67. Linear Discriminant Analysis: Trial 2.

A

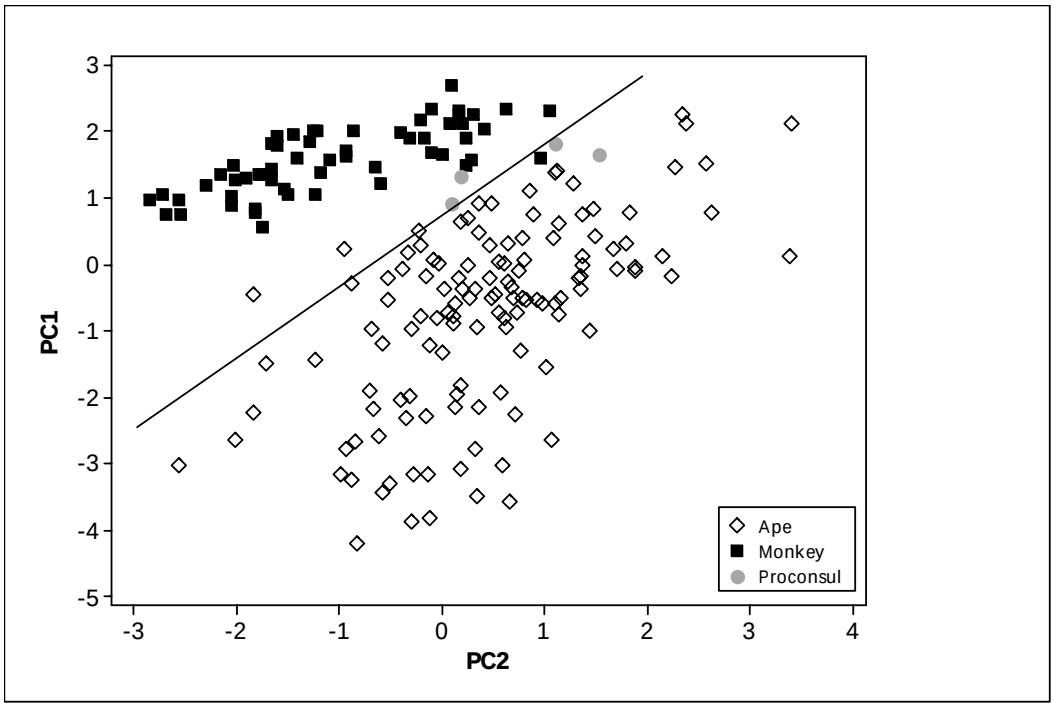

B

Variable	PC1	PC2
Calc2	-0.578	0.208
Calc3	-0.007	-0.699
MT3D	0.557	-0.16
MT2D	0.577	0.189
MT1D	0.149	0.638
Eigenvalue	2.6287	1.5021
Proportion	0.526	0.3
Cumulative	0.526	0.826

Figure 4.67. Trial 2 Continued.

C

	Ape	Monkey
Summary of Classification with Cross-validation		
Put into group		
Ape	124	1
Monkey	3	56
Total N	127	57
N Correct	124	56
Proportion	0.976	0.982
N = 184, N Correct = 180, Proportion Correct = 0.978		
Squared Distance Between Groups		
Ape	0	13.2741
Monkey	13.2741	0
Linear Discriminant Function for Groups		
Constant	-0.6523	-3.1287
PC1	-1.0699	2.3157
PC2	1.13	-2.5198
Classification of *Proconsul*		
KPS I		
Sq. Dist.	3.872	**3.176**
Prob.	0.414	**0.586**
KPS IV		
Sq. Dist.	**5.09**	5.712
Prob.	**0.577**	0.423
KPS VIII		
Sq. Dist.	**4.039**	8.833
Prob.	**0.917**	0.083
RU 2036		
Sq. Dist.	5.309	**2.491**
Prob.	0.196	**0.804**

Figure 4.67. Trial 2 Continued

D

	Gorilla	***Macaca***	***Pan***
Summary of Classification with Cross-validation			
Put into Group			
Gorilla	37	0	2
Macaca	0	56	2
Pan	5	1	81
Total N	42	57	85
N Correct	37	56	81
Proportion	0.881	0.982	0.953
N = 184, N Correct = 174, Proportion Correct = 0.946			
Squared Distance Between Groups			
Gorilla	0	37.555	9.8728
Macaca	37.555	0	13.89
Pan	9.8728	13.89	0
Linear Discriminant Function for Groups			
Constant	-5.3824	-4.5642	-0.4341
PC1	-4.7313	4.0816	-0.517
PC2	1.2875	-2.5854	1.0994
Classification of *Proconsul*			
KPS I			
Sq. Dist.	21.047	3.704	**3.342**
Prob.	0	0.455	**0.545**
KPS IV			
Sq. Dist.	31.089	**5.706**	6.149
Prob.	0	**0.555**	0.445
KPS VIII			
Sq. Dist.	28.006	8.786	**4.624**
Prob.	0	0.111	**0.889**
RU 2036			
Sq. Dist.	26.414	**2.579**	5.319
Prob.	0	**0.797**	0.203

Figure 4.68. Linear Discriminant Analysis: Trial 3.

A

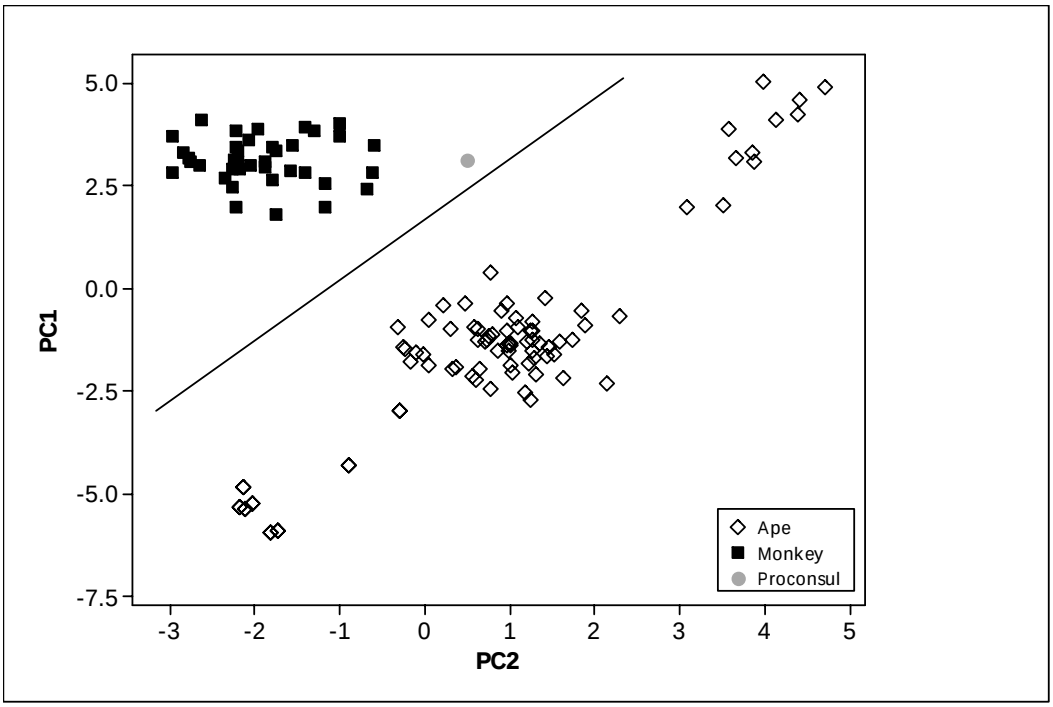

B

Variable	PC1	PC2	PC3	PC4
Calc2	-0.284	-0.175	-0.124	-0.032
Calc3	0.067	-0.347	0.105	-0.3
Calc7	-0.281	0.107	-0.07	-0.094
Calc8	-0.285	-0.15	-0.102	-0.153
Nav1	-0.265	0.084	-0.158	0.186
Mcun1	0.032	0.339	0.028	-0.181
Icun1	0.043	0.202	0.63	0.104
Icun3	-0.253	0.127	0.109	0.158
Lcun1	0.015	-0.11	0.674	-0.075
Lcun3	-0.067	-0.377	-0.006	0.249
Cub1	-0.061	-0.173	0.002	-0.778
Cub3	-0.294	0.07	-0.051	0.107
MT5	0.261	-0.286	-0.101	0.139
MT4	0.306	-0.196	-0.05	0.091
MT3	0.321	-0.136	-0.071	0.059
MT2	0.319	0.068	-0.114	0.049
MT1	0.227	0.311	-0.161	-0.211
PH1	0.082	0.444	-0.09	-0.098
PH3	0.313	0.102	-0.045	-0.03
Eigenvalue	8.7114	3.5547	1.4787	1.2126
Proportion	0.458	0.187	0.078	0.064
Cummulative	0.458	0.645	0.723	0.787

Figure 4.68. Trial 3Continued

C

	Ape	Monkey
Summary of Classification with Cross-validation		
Put into group		
Ape	88	0
Monkey	0	38
Total N	88	38
N Correct	88	38
Proportion	1	1
N = 126, N Correct = 126, Proportion Correct = 1.000		
Squared Distance Between Groups		
Ape	0	78.6355
Monkey	78.6355	0
Linear Discriminant Function for Groups		
Constant	-3.63	-19.055
PC1	-2.785	6.375
PC2	4.087	-9.373
PC3	-0.501	1.125
PC4	-0.612	1.424
Classification of *Proconsul*		
KPS III		
Sq. Dist.	30.092	**16.299**
Prob.	0.001	**0.999**

Figure 4.68. Trial 3 Continued.

D

	Colobus	***Gorilla***	***Hylobates***	***Macaca***	***Pan***
Summary of Classification with Cross-validation					
Put into group					
Colobus	5	0	0	10	0
Gorilla	0	16	0	0	0
Hylobates	0	0	11	0	0
Macaca	7	0	0	16	0
Pan	0	0	0	0	61
Total N	12	16	11	26	61
N Correct	5	16	11	16	61
Proportion	0.417	1	1	0.615	1
N = 126, N Correct = 109, Proportion Correct = 0.865					
Squared Distance Between Groups					
Colobus	0	189.732	89.292	0.359	89.754
Gorilla	189.732	0	240.52	176.972	47.721
Hylobates	89.292	240.52	0	94.788	74.622
Macaca	0.359	176.972	94.788	0	85.204
Pan	89.754	47.721	74.622	85.204	0
Linear Discriminant Function for Groups					
Constant	-22.074	-34.306	-31.723	-20.406	-4.046
PC1	9.645	-12.574	7.552	8.879	-3.888
PC2	-6.564	-2.276	9.239	-6.992	3.204
PC3	2.101	-3.584	2.165	1.792	-0.677
Classification of *Proconsul*					
KPS III					
Sq. Dist.	**15.922**	190.296	32.852	18.618	62.402
Prob.	**0.794**	0	0	0.206	0

Figure 4.69. Linear Discriminant Analysis: Trial 4.

A

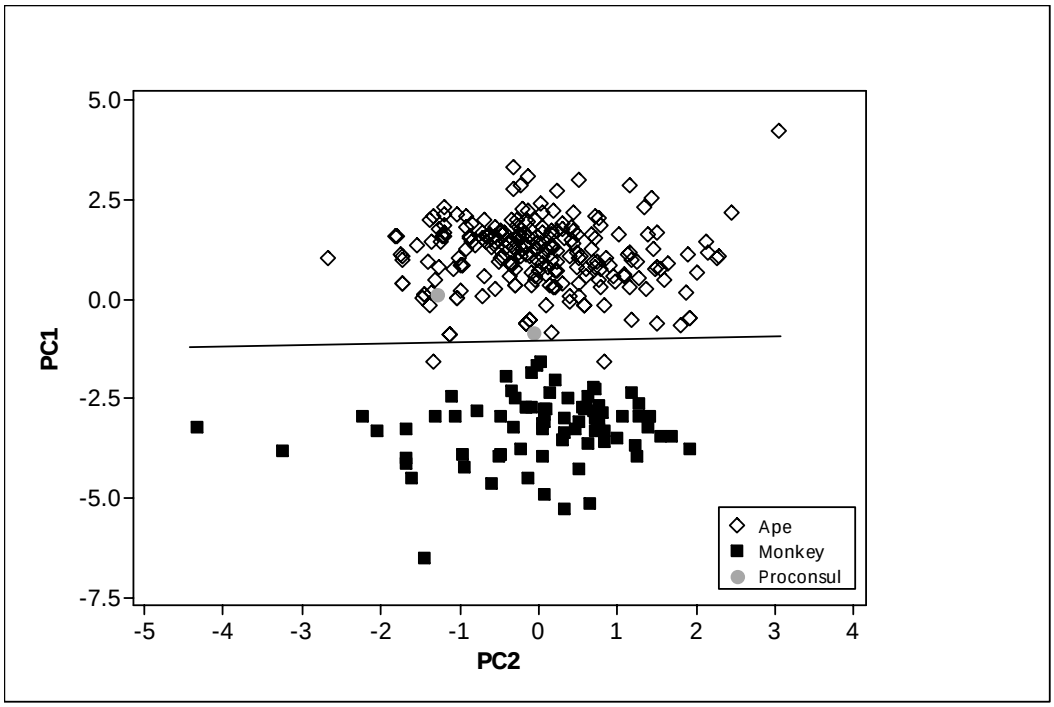

B

Variable	PC1	PC2
MT5	-0.43	-0.191
MT4	-0.469	0.059
MT3	-0.439	0.195
MT2	0.166	0.935
MT1	0.418	-0.079
PH1	0.447	-0.204
Eigenvalue	4.33	0.9839
Proportion	0.722	0.164
Cumulative	0.722	0.886

C

	Ape	Monkey
Summary of Classification with Cross-validation		
Put into group		
Ape	226	0
Monkey	2	79
Total N	228	79
N Correct	226	79
Proportion	0.991	1
N = 307, N Correct = 305, Proportion Correct = 0.993		
Squared Distance Between Groups		
Ape	0	26.285
Monkey	26.285	0
Linear Discriminant Function for Groups		
Constant	-0.8735	-7.2396
PC1	1.5558	-4.479
PC2	-0.039	0.1298
Classification of *Proconsul*		
KPS I		
Sq. Dist.	**5.204**	8.109
Prob.	**0.81**	0.19
KPS III		
Sq. Dist.	**2.962**	17.863
Prob.	**0.999**	0.001

Figure 4.69. Trial 4 Continued

D

	Colobus	***Gorilla***	***Hylobates***	***Macaca***	***Nasalis***	***Pan***
Summary of Classification with Cross-validation						
Put into group						
Colobus	10	0	0	1	2	0
Gorilla	0	34	0	0	0	22
Hylobates	0	2	9	0	0	20
Macaca	1	2	0	55	0	0
Nasalis	1	0	0	1	8	0
Pan	0	3	3	0	0	133
Total N	12	41	12	57	10	175
N Correct	10	34	9	55	8	133
Proportion	0.833	0.829	0.75	0.965	0.8	0.76
N = 307, N Correct = 249, Proportion Correct = 0.811						
Squared Distance Between Groups						
Colobus	0	57.118	132.638	9.679	4.304	93.245
Gorilla	57.118	0	16.023	21.884	37.897	4.533
Hylobates	132.638	16.023	0	72.672	103.16	3.512
Macaca	9.679	21.884	72.672	0	7.263	44.844
Nasalis	4.304	37.897	103.16	7.263	0	68.628
Pan	93.245	4.533	3.512	44.844	68.628	0
Linear Discriminant Function for Groups						
Constant	-28.619	-0.072	-7.814	-10.656	-19.533	-2.188
PC1	-12.196	0.013	6.352	-7.42	-9.646	3.379
PC2	-2.237	-0.414	1.327	-0.517	-3.354	0.53
Classification of *Proconsul*						
KPS I						
Sq. Dist.	38.836	**1.893**	27.938	10.918	24.687	11.736
Prob.	0	**0.982**	0	0.011	0	0.007
KPS III						
Sq. Dist.	56.928	**1.092**	19.297	24.119	35.114	6.822
Prob.	0	**0.946**	0	0	0	0.054

Figure 4.70. Linear Discriminant Analysis: Trial 5.

A

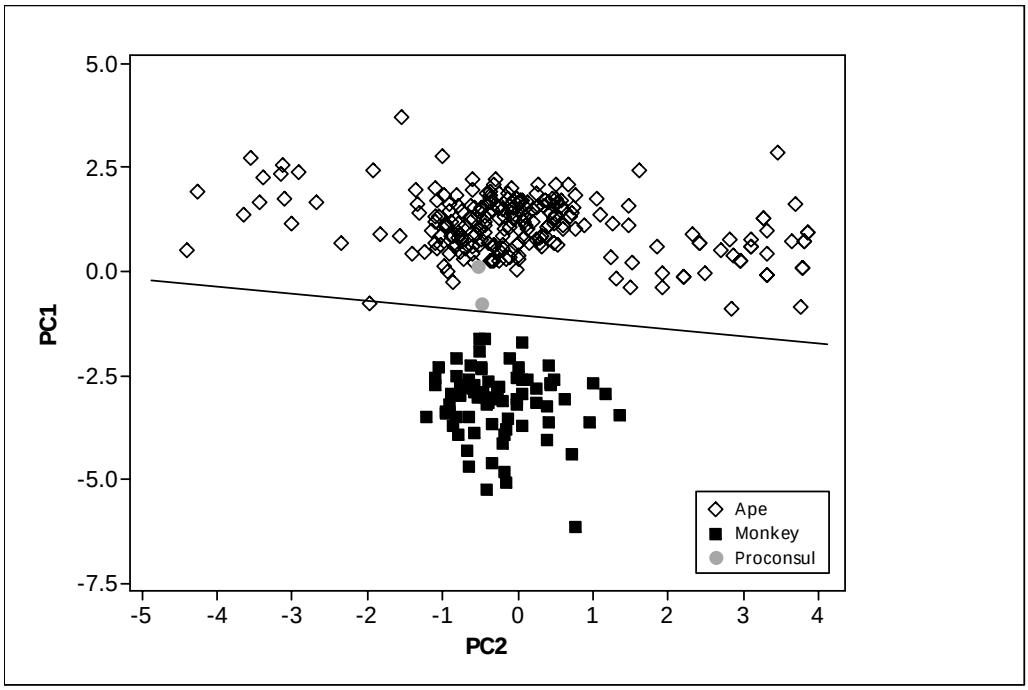

B

Variable	PC1	PC2
Calc1	0.102	0.653
MT5	-0.463	0.113
MT4	-0.479	-0.146
MT3	-0.435	-0.306
MT2	0.074	-0.584
MT1	0.386	-0.293
PH1	0.449	-0.137
Eigenvalue	3.9975	1.9501
Proportion	0.571	0.279
Cumulative	0.571	0.85

C

	Ape	Monkey
Summary of Classification with Cross-validation		
Put into group		
Ape	227	0
Monkey	1	79
Total	228	79
N	227	79
Proportion	0.996	1
N = 301, N Correct = 300, Proportion Correct = .997		
Squared Distance Between Groups		
Ape	0	38.0698
Monkey	38.0698	0
Linear Discriminant Function for Groups		
Constant	-1.267	-10.481
PC1	2.269	-6.528
PC2	0.398	-1.138
Classification of *Proconsul*		
KPS I		
Sq. Dist.	**8.127**	11.225
Prob.	**0.825**	0.175
KPS III		
Sq. Dist.	**2.608**	21.312
Prob.	**1**	0

Figure 4.70. Trial 5 Continued.

D

	Colobus	***Gorilla***	***Hylobates***	***Macaca***	***Nasalis***	***Pan***
Summary of Classification with Cross-validation						
Put into group						
Colobus	11	0	0	1	2	0
Gorilla	0	38	0	0	0	1
Hylobates	0	0	12	0	0	3
Macaca	0	0	0	49	0	0
Nasalis	1	0	0	7	8	0
Pan	0	3	0	0	0	171
Total N	12	41	12	57	10	175
N Correct	11	38	12	49	8	171
Proportion	0.917	0.927	1	0.86	0.8	0.977
N = 301, N Correct = 289, Proportion Correct = 0.941						
Squared Distance Between Groups						
Colobus	0	80.355	151.887	8.583	4.813	90.371
Gorilla	80.355	0	101.84	48.272	46.044	24.796
Hylobates	151.887	101.84	0	90.579	120.459	26.133
Macaca	8.583	48.272	90.579	0	2.659	43.817
Nasalis	4.813	46.044	120.459	2.659	0	57.439
Pan	90.371	24.796	26.133	43.817	57.439	0
Linear Discriminant Function for Groups						
Constant	-28.112	-9.05	-20.74	-10.845	-15.297	-2.108
PC1	-12.347	0.514	6.136	-7.593	-9.033	3.303
PC2	1.251	6.498	-8.867	-0.1	2.202	-1.08
Classification of *Proconsul*						
KPS I						
Sq. Dist.	40.137	27.43	44.241	11.702	20.653	**10.331**
Prob.	0	0	0	0.334	0.004	**0.662**
KPS III						
Sq. Dist.	60.937	25.568	31.573	23.958	35.594	**3.11**
Prob.	0	0	0	0	0	**1**

Discussion of Multivariate Results

When variables taken from throughout the foot are used to build the linear discriminant model (Trials 1 and 3), *Proconsul* is aligned with *Nasalis* and *Colobus.* However, when subsets of variables are chosen to maximize age group participation *Proconsul* is split between *Macaca* and *Pan* and when the variables emphasize digital proportions, the model places *Proconsul* in with the great apes (Table 4.22).

The two individuals in the fourth trial (I and III) were both grouped with *Gorilla* but when calcaneus length was added in trial 5, they were classified as *Pan.* This is probably a result of the added body size component associated with calcaneus length.

Analyses of *Proconsul* immature specimens were not as clear-cut. KPS IV was just as distant from the monkeys as it was from the apes in both trials 1 and 2. RU 2036 was classified most like *Hylobates* in trial 1 but more like *Macaca* in trial 2 when inputs from age 1 and 2 individuals were maximized in building the model. However, it is important to point out that Hylobates was not included in the model for trial 2 since there is no ontogenetic sample for the taxon.

Table 4.22. Summary of multivariate results. (*) Model did not include *Nasalis*.

Individual	Age Group	Classification of *Proconsul*				
		Trial 1	Trial 2*	Trial 3*	Trial 4	Trial 5
KPS IV	1	*Nasalis*	*Macaca/ Pan*			
KPS VII	3	*Nasalis*				
KPS 2036	4	*Hylobates*	*Macaca*			
KPS VIII	4	*Nasalis*	*Pan*			
KPS I	4	*Nasalis*	*Pan/ Macaca*		*Gorilla*	*Pan*
KPS III	5	*Nasalis*		*Colobus*	*Gorilla*	*Pan*

Chapter 5

CROSS-SECTIONAL GEOMETRY OF *PROCONSUL HESELONI* METATARSALS

Introduction

Cross-sectional geometry (CSG) analysis applies engineering beam theory to bones and has been repeatedly substantiated as a method for elucidating their mechanical properties (e.g. Ruff, 1989). Bones experience four types of forces: compression, bending, twisting and shearing (Figure 5.1). Each of these forces produces a distinct stress distribution in the bone and it is hypothesized that each type of stress may be determined by the nature of modeling (periosteal and/or endosteal deposition by osteoblasts or resorption by osteoclasts) and Haversian remodeling (bone turnover) in the bone. There are many intrinsic and extrinsic factors that affect a bone's mechanical

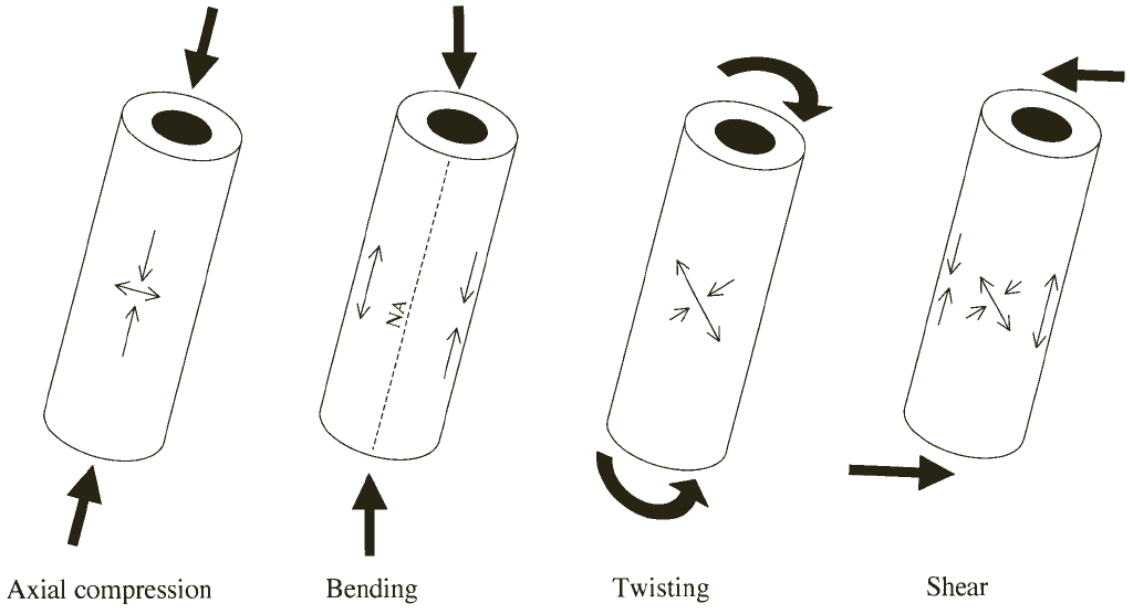

Figure 5.1. Axial compression, bending, twisting and shearing forces on a bone shaft. Thick arrows indicate applied loads and thin ones indicate resulting strain. Modified from Figure 2 in Pearson & Lieberman (2004).

properties in response to loading; these include mineralization, porosity, orientation of collagen fibers, density, and mode, duration and rate of strain (Martin et al., 1998).

The mechanical function of modeling of cortical bone, which is the focus of CSG studies, is much better understood than remodeling. Depositional modeling makes bones stronger, more resistant to stress, and less likely to experience strain. It enlarges the cross-sectional area (CA) of a bone which helps counteract compressive forces by distributing them over large areas, thus reducing stress per unit area. It also increases the second moments of area available for resisting the bending and twisting moments that account for a high proportion of midshaft strains (Bertram & Biewener, 1988; Pearson & Lieberman, 2004). Bone added further away from the axis of bending (increasing the second moment of area) resists bending much more effectively than the same amount of bone added near the axis (Martin et al., 1998). Adding bone by modeling, especially subperiosteally, reduces the strain a given moment generates. Modeling to increase second moments of area in stressed juvenile bones is due to increases in periosteal apposition and also inhibition of endosteal resorption (reviewed in Pearson & Lieberman, 2004).

Since the CA of long bones corresponds to resistance to deformation from axial loading, animals with different locomotor and positional behaviors should show differences in the magnitude and orientation of bone strength. Previous studies on the cross-sectional properties of diaphyses of primate long bones have shown the morphology is useful for distinguishing between locomotor modes (Demes & Jungers, 1993; Kimura, 2003; Schaffler et al., 1985). Usually, in order to distinguish between modes, relative proportions are compared. For instance, Demes and Jungers (1993)

showed that the degree or index of humeral relative to femoral strength in prosimians can be used to differentiate between leapers (more robust femora) and non-leapers (more equal robusticity between the humerus and femur).

Currently there is a debate in the literature about the efficacy of "Wolff's law" - the term commonly used to describe the phenomenon of bone modeling and remodeling as a response to strain. In other words, if a load on a bone increases, the bone will adapt and become stronger to resist that load, and also if the load on a bone decreases, the bone will become weaker.

There are those that have argued against its power and caution against over-interpretation of CSG results (reviewed in Ruff et al., 2006). They cite workers who falsified the strict mathematical interpretation of Wolff's law (the most recent being Cowin, 2001). Still others have shown through *in vivo* strain studies that bone modeling does not necessarily correlate to the axis of maximum bending stress in long bone shafts (Demes et al., 1998, 2001, Lieberman et al., 2004). That is, evidence from external strain gauges placed on the long bones of macaques (Demes et al., 1998) and sheep (Lieberman et al., 2004), indicates that cross-sections were not reinforced in regions of maximum strain during the experiment; the neutral axis did not correlate with the bending axis.

Despite the complications, generally speaking "Wolff's law" still holds: bones *do* adapt to function. Ruff and colleagues (2006) advocate that the robusticity and shape of bone shafts can and should continue to be used to study past and extinct organisms. They propose a change in terminology from "Wolff's law" to "bone functional adaptation" which reflects recent advances (Ruff et al., 2006). Regarding the issues raised by the mismatch of the neutral and bending axes in animals with strain gauges Ruff and

colleagues (2006, p. 490) stated, “Thus, it is probably advisable to continue to report section properties (second moments of area [J] and section moduli [Zx, Zy]) relative to centroidal axes, with the understanding that these are only approximations of true bending rigidity and strength *in vivo*”.

Metatarsal CSG in Primates

To date, there has been only one study on the CSG of human metatarsals (Griffin & Richmond, 2005) and only one including the CSG of metatarsals of non-human primates (Marchi, 2005). Preuschoft’s work in the 1970s anticipated future CSG analyses of primate, especially chimpanzee, metatarsals (Figures 5.2 and 5.3). He described the potential forces affecting the metatarsals of chimpanzees during walking and climbing.

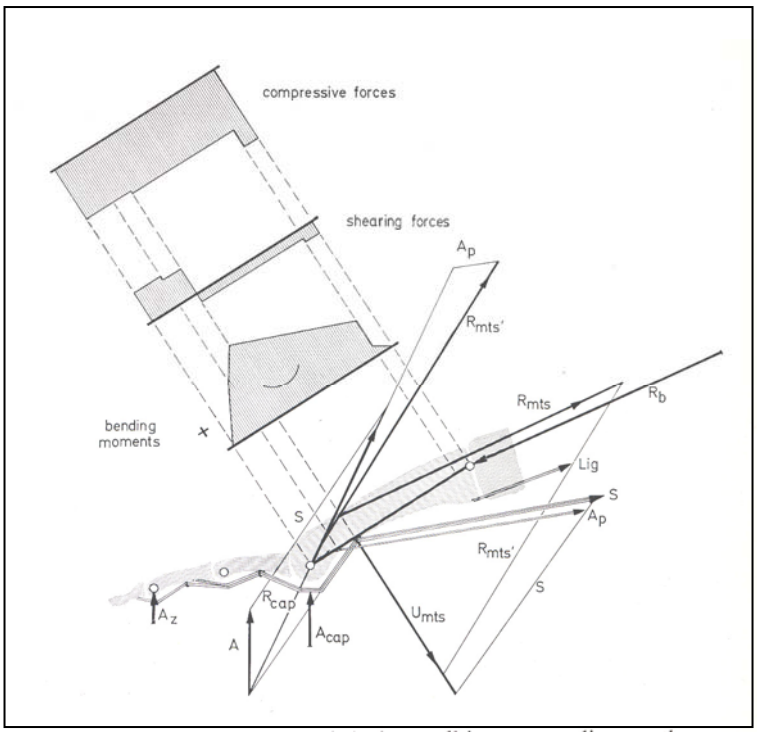

Figure 5.2. Hypothetical forces experienced by a chimpanzee metatarsal during terrestrial walking and standing, with stress diagrams. (Figure 11 from Preuschoft (1970)).

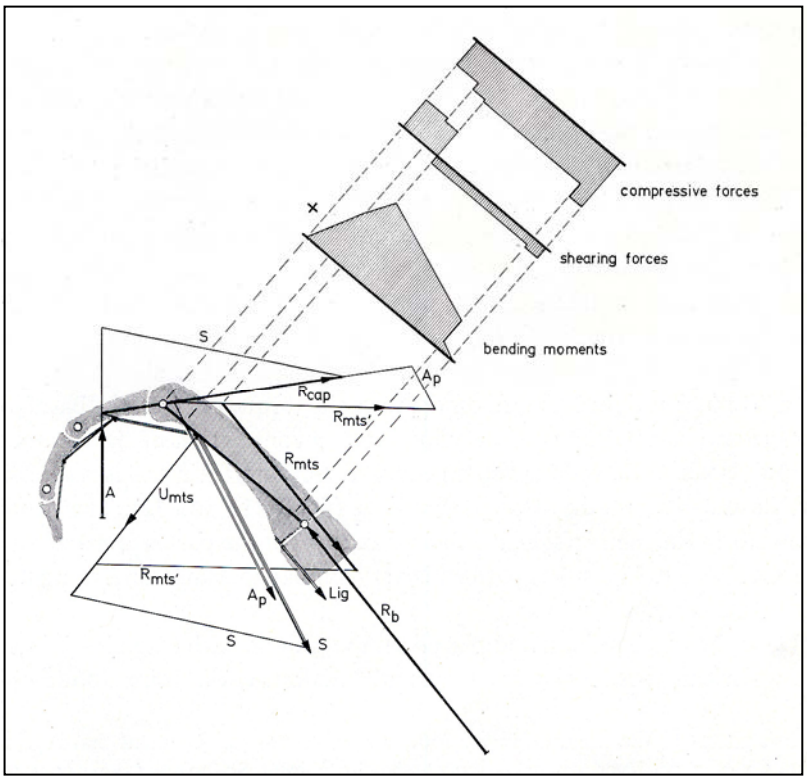

Figure 5.3. Hypothetical forces experienced by a chimpanzee metatarsal during climbing, with stress diagrams. (Figure 10 from Preuschoft (1970)).

Preuschoft's diagrams hypothesize that much of the important action happens at about two thirds of the length of the metatarsal where bending moments are highest and where the axis of the shearing forces (torsional forces) is located. However, diaphyseal midshafts remain the standard for analyses because they are more easily compared between researchers and more accurately reconstructed and analyzed with established techniques. It is most likely that once micro CT becomes more prevalent (that is, when more machines become available and affordable for such analyses), the cross-sectional properties over the length of the entire bone will more commonly be assessed and this

will be true for all cross-sectional geometry studies of other long bones that are capable of fitting inside a microCT machine.

For now, researchers are using midshaft properties to identify adaptations in human and ape metatarsals. Marchi (2005) showed that in adult great apes and humans, the cross-sectional properties of metatarsals are different across the species and, at least for chimpanzees, are consistent with plantar pressure studies by Wunderlich (1999). However, even when corrected for body mass, the CSGs of the metatarsals of gorillas did not fall out with those of chimpanzees who were placed into the same locomotor category (knuckle-walking). Instead, chimpanzees commonly overlapped with orangutans (quadrumanous climbers) and humans (bipeds), not segregating into groups by locomotor category. However, when metatarsal CSG is considered in conjunction with that for the metacarpals, particularly for digits 4 and 5, the relationship of the two becomes a good indicator of general locomotor modes in great apes and humans. Chimpanzees and gorillas have the most robust fourth metacarpal relative to metatarsal, with humans having the least and orangutans falling in the middle. Humans, on the other hand, have the most robust fifth metatarsal, relative to fifth metacarpal as a consequence of freeing the hands from locomotor loads and shifting those loads from four to two limbs.

Ontogeny of Cross-sectional Geometry

The juvenile skeleton is the most affected by mechanical loading; that is, most bone modeling takes place during skeletal growth (Bertram et al., 1991). During normal ontogeny, most bones will grow large and/or thick enough to stay within the zone for their Young's modulus of elasticity on the deformation curve (Currey, 2002). This means

that during ontogeny bones must simultaneously balance the act of growing with the need to remain structurally sound.

Increased strain on the skeleton during development induces more modeling than simply body size increase. The most abundant evidence for this phenomenon comes from the "tennis studies" where the humeri in the racket-wielding arm of elite and habitual tennis players were repeatedly shown to have thicker cortical bone than their antimeres. Humeral asymmetry is heightened in juvenile tennis players and may be accelerated in adults who begin training at a younger age (Bass et al., 2002; Haapasalo et al., 2000; Jones et al., 1977; Kontulainen et al., 2003).

Lieberman and colleagues have argued that modeling, in response to loads, is greatly reduced in adults (Lieberman et al., 2003; Pearson & Lieberman, 2004). They purport that activity in youth determines the manner of bone modeling and hence the adult form. Yet Ruff and colleagues argue that adult activities can also have profound effects on bone modeling. These arguments have major implications for the effects of ontogenetic changes in locomotion on primate long bone cross-sectional properties.

Ruff is one of the few researchers to investigate the correlation between the ontogeny of CSG and primate locomotor behavior (Ruff 2003b, 2003c). Changes in humeral and femoral strength correspond in timing with the onset of bipedalism in human infants (Ruff, 2003c). Baboons show changes in humeral/femoral strength proportions that are not as extreme as those in humans because their changes in locomotion through development are not as extreme (Ruff, 2003b). Changes in trabecular bone are also being shown to correlate with ontogenetic changes in locomotion (Ryan & Krovitz, 2006).

Specific Aims and Hypotheses

Primates undergo changes in locomotor behavior during ontogeny. These changes are accompanied by changes in foot and hindlimb proportions as individuals develop (Chapter 4). There should be changes in the strength properties of the metatarsals through ontogeny since feet are weight and load-bearing organs and forces will increase as the animal's body mass increases. These changes in metatarsal strength properties may or may not be also affected by changes in locomotor behavior during development. Here, the ontogeny of *Macaca mulatta, Pan troglodytes,* and *Proconsul heseloni* metatarsal strength properties are investigated with cross-sectional geometry (CSG) analysis.

The null hypothesis to be tested is that *M. mulatta* and *P. troglodytes*, two catarrhines with different phylogenetic history, body size and locomotor behavior, have the same relative cross-sectional geometry in the metatarsals. Because of the differences in body size and in pedal positional behavior between the more terrestrial foot of *M. mulatta* and the more grasping foot of *P. troglodytes,* there should be differences in strength properties of the metatarsals between the taxa as predicted by Conroy and Rose (1983) and they should also show different patterning among the rays. Most striking should be the relatively greater strength of the first metatarsal in the grasping foot of chimpanzees compared to macaques due to the torsion experienced while the foot is flexed around curved surfaces. Because metatarsals 2-5 are bundled together, the bending (Zx) and torsional (J) strengths will probably not distinguish much. However, bending and torsional properties of the first metatarsal will potentially illuminate differences between the more terrestrial *Macaca* foot, which does not use its first metatarsal much in locomotion on the ground or in the trees, and the more arboreal-like *Pan* foot in which

the first metatarsal is in contact with the substrate on the ground and while grasping branches.

The main goal of the analysis is to better reconstruct foot function and use in *Proconsul heseloni*. The first metatarsal should be stronger in *Proconsul* than in macaques as indicated by the hallucal proportions and the calcaneal morphology which accommodates for a large *m. flexor hallucis longus* (Chapters 3 and 4).

Materials and Methods

Sample

Metatarsals 1-5 were analyzed from a cross-sectional ontogenetic sample of 52 rhesus macaques *Macaca mulatta* and 74 *Pan troglodytes* (Table 5.1). Macaques and chimpanzees are good comparative taxa for the ontogenetic analysis for several reasons. They have different locomotor repertoires within quadrupedalism and both species have been proposed as models for *Proconsul* functional morphology (Li et al., 2002). Macaques are classic terrestrial and arboreal quadrupedal cercopithecoids. Chimpanzees, by comparison, climb and brachiate in the trees and knuckle-walk terrestrially and arboreally. The two species represent a good contrast between a hindlimb driven, mostly terrestrial quadrupedal monkey and a more forelimb reliant quadrupedal ape.

Proconsul heseloni shares similarities with macaques in body size and proportions (Walker & Pickford, 1983; Ruff et al., 1989) and with chimpanzees in hallucal proportions (Strasser, 1993). Since they are located on separate evolutionary branches, macaques and chimpanzees represent distinct phylogenetic categories as well, which is important considering *Proconsul*'s temporal proximity to the split between Old World

monkeys and apes. Most importantly in this case, however, is that relatively large and well-curated skeletal collections exist for macaques and chimpanzees of all ages.

The sample of rhesus macaques was derived entirely from the skeletal collection at The Caribbean Primate Research Center, located at the University of Puerto Rico. This collection was ideal for this study because it contains a large number of complete rhesus macaque skeletons at all developmental stages. The skeletons are derived from a colony of free-ranging monkeys reared in a uniform environment that are all extremely well-documented from long term observation (Rawlins and Kessler, 1986).

The sample of wild-shot chimpanzees was pieced together from collections at the Anthropological Institute in Zurich, the Royal Museum for Central Africa in Tervuren, Belgium, and the Hamann-Todd Collection at the Cleveland Museum of Natural History.

Age Estimation

Dental ages of chimpanzees were determined using the eruption schedules in Dean and Wood (Dean et al., 1981). Macaques at the CPRC all have documented ages at death, but dental eruption stages were noted according to (Kenney, 1975a). In order to compare the extant samples to the fossils, macaque and chimpanzee specimens were placed into age groups according to dental eruption stages (Table 5.2).

Table 5.1. Number of individuals per age group used in the cross-sectional geometry analysis. (*) Metatarsals from both left and right feet were included from KPS I (age group 4) and KPS III (age group 5).

Taxon	**Age Group**					**Total**
	1	**2**	**3**	**4**	**5**	
Macaca mulatta	0	0	8	23	21	52
Pan troglodytes	3	17	13	8	33	74
Proconsul heseloni	1	0	1	3*	1*	6

Table 5.2. Age groups constructed according to dental eruption stages which follow a similar order of eruption timing in both *Macaca mulatta* and *Pan troglodytes* (Cheverud, 1981),

Macaca **Age in years**	***Pan*** **Age in years**	**Tooth Stage**	**Age Group**	**Locomotion**
<1	<3	Only deciduous teeth visible	1	Immature
1-<2.5	3-<6	M1 erupting	2	Transitional
2.5-<4.5	6-<8	Stage 2 complete and M2 erupting	3	Adult
4.5- <7	8- <11	Stage 3 complete and M3 erupting	4	Adult
>7	>11	All teeth in occlusion	5	Adult

Macaca mulatta could not be sampled for age groups 1 and 2 because at these stages of development, the metatarsals are too small to analyze with normal plane film radiography and external molding. MicroCT would be appropriate but it was not available. Chimpanzees, however, were sampled across all five age groups.

The fossil sample consists of five individuals from the KPS site as well as the partial juvenile skeleton, KNM-RU 2036, which is the type specimen of *P. heseloni.* Additional information, beyond dental development stage, was used to group the *Proconsul* individuals (Table 5.3).

Table 5.3. Age group assignments for *Proconsul heseloni* individuals. (*) Sex determined by lower canine shape (Kelley, 1995).

Specimen	**Age and Sex**	**Reason**	**Age Group**
KPS Individual I	subadult male	Some fusion, size	4
KPS Individual III	adult female	Fully fused	5
KPS Individual IV	infant	M1 crown	1
KPS Individual VII	juvenile female	Little fusion, size	3
KPS Individual VIII	subadult female	Some fusion, size	4
KNM-RU 2036	subadult female*	Canines present, third molars erupting, size	4

Body Size Estimation

Body mass standardization is necessary for interpreting functional analyses of postcrania between individuals and taxa (e.g. Jungers, 1985; Ruff et al., 1993). It is particularly important in CSG studies since CSG of long bones is so highly correlated with body weight that it is used as a predictor for body mass (e.g Ruff et al., 1989).

Unfortunately, body weights at death were not recorded for the macaques that died on Cayo Santiago because they decompose quickly in the tropical environment. Likewise, body weights are unknown for most of the chimpanzees in the sample. Adult body masses were calculated using the following equations relating superoinferior femoral head breadth and body mass for African apes and Old World monkeys provided by Ruff (2003a) (Table 5.4).

Pan troglodytes **ln Body Mass = ln FHB * 3.019 – 6.718**

Macaca mulatta **ln Body Mass = ln FHB * 2.389 – 4.541**

Table 5.4. Body Masses estimates based on FHB for adults (Ruff, 2003a) with published estimates for *Proconsul* by Rafferty et al. (1995).

Estimated Body Mass (kg)						
	N	Mean	SE mean	StDev	Minimum	Maximum
M. mulatta	**21**	**7.948**	**0.354**	**1.624**	**5.676**	**10.819**
Female	12	6.753	0.214	0.743	5.676	7.931
Male	9	9.542	0.305	0.915	8.292	10.819
P. troglodytes	**30**	**51.22**	**1.86**	**10.21**	**36.39**	**70.14**
Female	17	48.14	2.43	10.02	36.39	70.14
Male	13	55.26	2.59	9.33	41.49	68.61
Estimated Body Mass (kg) for *Proconsul*						
KPS I			Male	13.6		
KPS III			Female	10.9		
KPS 2036			Female	9.8		

For most of the analysis femoral head breath (FHB) serves as a surrogate for body mass according to methods used by previous workers (e.g. Manley-Buser, 1991; Strasser, 1992; Ruff, 1989) (Figure 5.4). FHB provides a body size variable for the ontogenetic

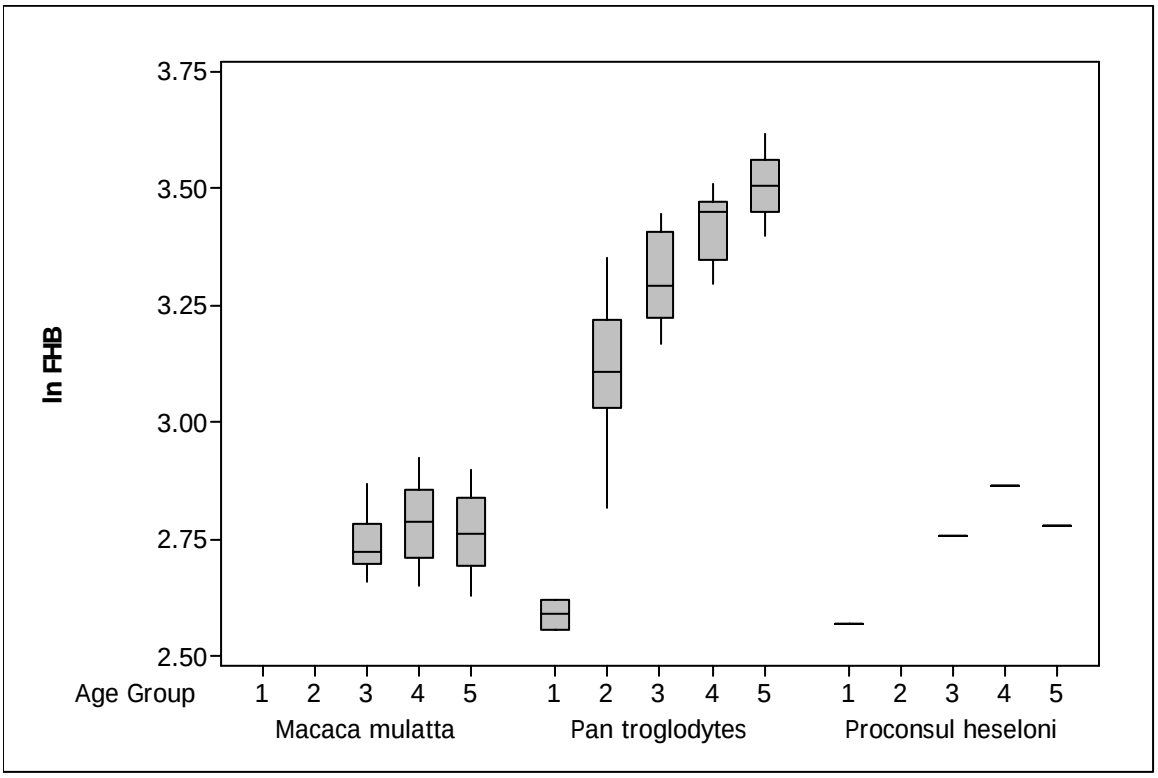

Figure 5.4. Femoral head breadth (transformed by natural log) by age group for each of the taxa.

sample since equations using bones of the hindlimb are not yet available for estimating immature body masses in catarrhines; it is not yet known how the relationship between long bone dimensions and body mass behaves throughout ontogeny. However, parameters to make such estimations may soon be available. Recent work by Raichlen shows that baboons (*Papio cynocephalus*) have a near isometric relationship between hindlimb length and body weight during their first year which includes the transition to locomotor independency (Raichlen, 2004).

Ruff argues that the most appropriate measure of body size in cross-sectional geometry studies of long bones is body weight multiplied by bone length (Ruff, 2003c).

Cross-Sectional Geometry (CSG) Methods

The best method for non-invasive CSG studies is computed tomography (CT) (e.g. Spoor et al., 2000). Although some of the institutions housing comparative primate skeletal material provide medical CT, the resolution of these machines is not sufficient for elucidating CSG of small bones like macaque, *Proconsul*, and immature chimpanzee metatarsals. High resolution micro computed tomography (microCT) offers a solution to this problem, but since it is not widely available and is costly, it was employed solely for imaging the *Proconsul* metatarsals.

Bi-planar radiography combined with latex molding of the external surface serves as an adequate substitute for computed tomography because it approximates true section properties of bone (O'Neill & Ruff., 2004). This technique is known as the latex cast method (LCM). In a methodological study using human femora and tibiae, O'Neill and Ruff (2004) showed that the results produced by LCM correlate strongly to the CSG properties achieved by sectioning bone with very low standard errors and directional bias.

Those working with large samples of museum specimens often prefer LCM, and it has been frequently used for comparative studies of fossil hominin long bone CSG (see O'Neill & Ruff, 2004).

The macaques and chimpanzees in this study were analyzed using the LCM. The method can be summed-up in the following steps: First, to assess the shape of the outer bone surface, molds of the metatarsal midshafts are photographed with a digital camera.

To reconstruct the circumference of the medullary cavity the medial, lateral, dorsal, and plantar cortical thicknesses are measured from the radiographs, corrected for parallax, and then drawn inside the scaled digital photograph of the mold of the outer circumference using the free software ImageJ. These lines dictate the size and placement of the ellipse that serves as the reconstructed medullary cavity. The cross-sectional properties are obtained by running these reconstructed images through a computer program that calculates area and moments.

Details of LCM and the specific procedures used in this study are outlined below.

Step 1: Molding the Midshaft Surface Contour First the length of the metatarsal was measured to locate the midshaft (Figure 5.2). For juveniles with unfused epiphyses, the epiphysis was placed on the end for a measure of total length. If the epiphysis was not present, the length of the epiphysis was estimated using specimens of similar age, size, and sex. The midshaft was marked with a pencil by drawing a line perpendicular to the long axis.

Next, Coltène President® hard putty was wrapped around the midshaft of each metatarsal. Lines were drawn down all four sides and labeled according to anatomical direction (plantar, dorsal, lateral, medial). To make all the orientations uniform, the metatarsals were placed proximal end-down on a grid. The dorsal edge of the proximal articular surface, the frontal plane (FP) (Figure 5.2), was lined up parallel to the line running from the medial to lateral side. (This method of orienting the bone in molding was also used for orientating the bones for x-ray.) Once the putty had set, the molds were cut down the plantar side with a scalpel and removed from the bone.

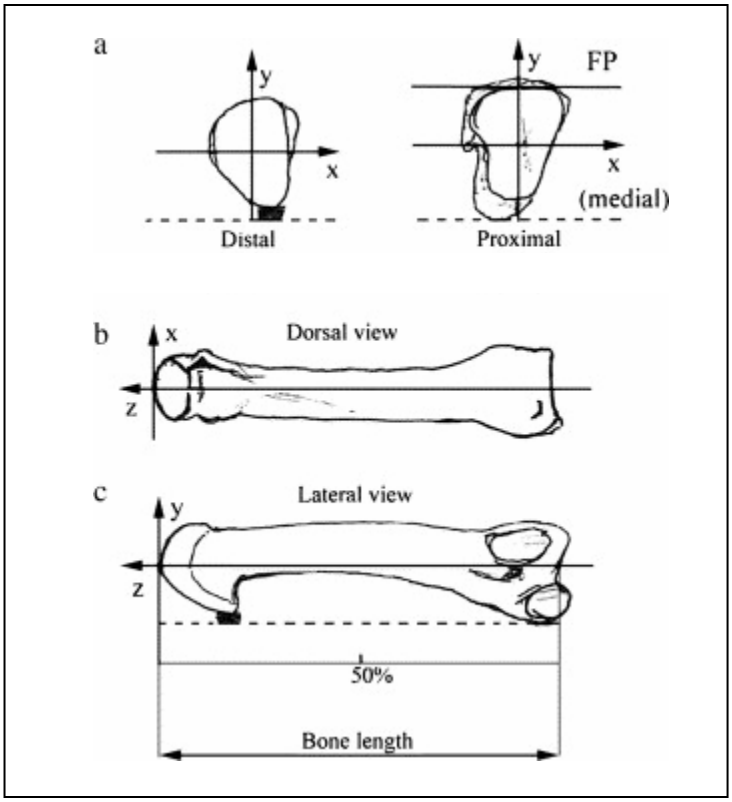

Figure 5.5. Reference axes and orientation for cross-section locations of the metatarsals as illustrated on a human second metatarsal in Figure 2, Marchi (2005): a) view of metatarsal distal and proximal ends; b) dorsal view of the bone; c) lateral view of the bone. 50% is the level at which cross-sectional properties were measured; FP (the frontal plane) passes through the dorsal surface of the proximal end.

Coltène President® putty picks up pencil marks from bone, so the midshaft lines were preserved inside the molds. In the lab, the molds were sliced open with a scalpel, through the midshaft pencil mark inside the mold, visible through the plantar opening. This slice revealed the outer circumference at the midshaft of the metatarsal. Next the molds were laid on a grid with the external lines oriented systematically (dorsal up, medial right), and then they were photographed with a digital camera. The maximum widths of the molds were measured to scale the photographs.

Step 2: Photoshop The digital photographs of the molds were imported into Adobe Photoshop®. Everything outside the inner edge of the mold, which is the circumference of the midshaft, was filled-in with black using the delete function. Then the resulting shape of the cross-section was filled-in with white. After all the images were transformed, they were run through an automated action, or batch file, that assimilated the canvas sizes to equal squares, which is a requirement of the moment calculator program used later.

Step 3: X-Rays The x-rays were taken on multiple machines using various types of film required by each machine. However, in all cases, the x-ray power was optimized to discriminate clearly between the medullary cavity and bone. Furthermore, in all instances the bones were placed either directly on the film, or directly on the thin cassette holding the film. The easiest, most convenient way to arrange the metatarsals for x-ray was to tape them in the proper orientation to a piece of sturdy watercolor paper that was labeled thoroughly and then laid on the film or cassette.

Two orientations were x-rayed for each metatarsal: first the plantar side was oriented down on the film for an image of the medial and lateral cortical bone thicknesses and then the medial side was placed down for an image of the plantar and dorsal cortical bone thicknesses. Orientation for metatarsals 2-5 was dictated by the dorsal edge of the proximal facet, which was laid parallel to the film for the first view and perpendicular in the second. The head determined the orientation of first metatarsal because of the angularity of the proximal facet. So, for the first metatarsal the head was laid flat in the first film and perpendicular in the second.

To measure the x-rays, the films were placed on a light box. Then the length of the metatarsal on the film was measured and the location of the midshaft was marked. A clear piece of acetate marked with a grid was placed on top of the film. Measurements were taken by aligning the longitudinal line of the grid with the long axis of the diaphysis and aligning the perpendicular transverse line with the midshaft and keeping the long axis of the calipers parallel to this line while measuring. The thicknesses of the cortical bone on either side of the medullary cavity and the diameter of the midshaft were recorded.

A measurement error study was performed on 30 chimpanzee metatarsals for seven days, several weeks after the original measurements were taken. The mean absolute range of error for measures of cortical thickness was 0.35 mm, with individual ranges comprising an average of 15.5% of individual means. The mean absolute range of error for measures of midshaft diameter was 0.28 mm, with individual ranges comprising an average of 3.7% of individual means. The midshaft diameter range of error was slightly smaller than that for cortical thickness, probably because the borders are better defined by the x-ray and easier to measure. Endosteal margins are not always sharply defined like the outer cortical surfaces are, causing inconsistencies in identifying this border and resulting in lower measurement precision for cortical thickness than midshaft diameter. Nonetheless, the ranges are similar and predict that any given measurement is about 0.3 mm too large or too small. However, this precision limitation affects cortical measures and diameter measures differently; 0.3 mm is a much larger percent of cortical thickness than it is of the much larger dimension of midshaft diameter. This issue is discussed further in conjunction with parallax, below.

Parallax, or radiographic enlargement of an object, must be accounted for by multiplying all measurements by a correction factor. Parallax is caused by the cone of photons emitted from the x-ray source hitting the object's edges at an angle and thus producing an image on the film that is larger than the actual object. Steps to minimize parallax were taken by positioning the x-ray source far from the film and by placing the bone as close to the film as possible. Fortunately with small bones like metatarsals, parallax is not as pronounced as that seen with radiography of large bones like femora.

Parallax for every bone in every film was assessed. This was done by measuring the midshaft diameter captured by the mold and comparing it to the midshaft diameter on the film. The ratio of these two known measurements (Real midshaft diameter / X-ray midshaft diameter) is used to calculate the unknown real, or "corrected", cortical thickness from the enlarged x-ray datum.

The real cortical thicknesses are calculated according to the equation:

Real (corrected) cortical thickness/ X-ray cortical thickness =
Real midshaft diameter/ X-ray midshaft diameter

Therefore,

Real (corrected) cortical thickness =
X-ray cortical thickness*(Real midshaft diameter / X-ray midshaft diameter)

Normally, each bone is corrected according to its own degree of parallax. Individual variation in parallax exists because bones farther from the center of the film experience an ever-increasing angle of light from the source. Furthermore, different x-ray machines influence parallax uniquely. However, in this study, because the bones and their measurements were so small, the measurement error complicated the relatively low parallax. For example, many measures from the films were smaller than the real bone

dimensions, which should never be the case because parallax enlarges the real dimension. Table 5.5 illustrates this issue where some mean parallax ratios exceed 1.0 when, if measured without error, they should all be less than one.

Table 5.5. Mean, standard deviations of parallax ratio by institution, where parallax is represented by the ratio of mold diameter/x-ray diameter. ML = mediolateral. PD = proximodistal.

Institution	ML Mean	St. Dev.	PD Mean	St. Dev.
RCMA	1.02	0.04	0.99	0.04
Zurich	1.01	0.02	1	0.07
HTB	0.99	0.05	1	0.05
CPRC	1.03	0.04	1.01	0.05

Parallax is often reported as a percentage (e.g. O'Neill, 2004) which is calculated by the following equation (results presented in Table 5.6):

Percent Parallax = (X-ray – Real)/Real*100

Table 5.6. Mean and standard deviations of parallax by institution, where parallax is represented by the percent enlargement. ML = mediolateral. PD = proximodistal.

Institution	ML Mean	St. Dev.	PD Mean	St. Dev.
RCMA	-1.7	3.5	1.3	3.9
Zurich	-0.8	5.7	-0.05	6.8
CMNH	1.2	5.6	-0.1	5.2
CPRC	-2.7	3.5	-0.8	5.1

Considering the effect of measurement error, parallax has a minimal affect on these small measurements. However, it is impossible to comb through thousands of measurements (6 each for 630 metatarsals) and determine which ones are affected more by error or by parallax and then to correct them accordingly. Those that show negative parallax are clearly the victims of measurement error, but it would introduce further bias to "fix" those by re-measuring only those specimens, yet if the entire sample were re-measured, certainly just as many specimens would fall victim to the measurement error problem and show negative parallax.

Since parallax is a relatively minor influence the conventional parallax correction (that is normally applied to much larger bones) was not applied. Correcting measurements by individual runs the risk of grossly over-correcting small measures and under-correcting large ones. Small ones undergo less parallax but risk greater percentages of measurement error. Larger ones experience more parallax but undergo less change due to error.

Instead, the measurements were multiplied by a random parallax index within the first standard deviation around the mean according to their respective institution. This can be accomplished in Microsoft Excel® using the following formula:

Real (corrected) cortical thickness = (x-ray measure)*(RAND()*(b-a)+a)

Where,

a = the minimum first standard deviation below the mean parallax

b = the maximum first standard deviation above the mean parallax

The random assignment of parallax correction is mimicking the random effect of measurement error, thus balancing out its effect on the data in a reasonable way.

Step 4: ImageJ Using the corrected values for cortical thickness, the circumference of the medullary cavity can be reconstructed. Starting with the black and white cross-sectional image from Step 2, a line for each orientation of thickness (medial, lateral, dorsal, plantar) is drawn from the outer cortical circumference into the middle of the cross-section. Because x-ray compresses three-dimensional objects into two-dimensional film, the cortical thicknesses are assumed to represent maximum dimensions. Therefore, the lines for these dimensions are drawn from the most lateral point on each side. A box

is drawn in the center of the cross-section, with sides reaching the terminal points of the lines, to define the area within which the medullary cavity is interpolated. This is done by the final step of drawing an ellipse inside the box. ImageJ is free software available for download from the website http://rsb.info.nih.gov/ij/.

Step 5: IDL The images are analyzed in the moment calculator MOI (Moment of Inertia) written by Dr. Timothy Ryan that runs in the software IDL (Interactive Data Language) produced by RSI®. The user feeds the images and their scales through the MOI program and it calculates their cross-sectional properties by counting the pixels.

Micro-Computed Tomography (microCT) of Fossil Specimens

Because the fossils were too dense to penetrate with normal plane-film x-ray, the *Proconsul* metatarsals had to be analyzed differently, but were done so with the optimal technique that would have been preferred for the rest of the sample. With an XCT Research SA+, a portable microCT machine by Stratec Co., Dr. Masato Nakatsukasa scanned the fossils that were in the appropriate preservation state (Table 5.7). Because the sample was small, both right and left sides were analyzed when available. The metatarsals were oriented the same as they were for the x-rays. These scans were transformed in ImageJ into black and white bone cross-sections and analyzed exactly like the extant sample by running through the moment calculator.

The computer macro produces a set of CSG properties for each image which are listed in Table 5.8.

Table 5.7. *Proconsul* specimens scanned with microCT for the analysis.

Specimen	Right Metatarsals	Left Metatarsals
KPS 1	2,3,4,5	1,2,3,4
KPS 3	1,2,3	2,3,4,5
KPS 4		2,3,4,5
KPS 7		2,3,4
KPS 8	1,2,3,4	
RU 2036		1,2,3

Table 5.8. Cross-sectional properties referenced and analyzed in this study. ML = mediolateral, DP = dorsoplantar.

Abbreviation	Value	Measurement	Units
CA	Cross-sectional area	Axial Loading (tension, compression)	mm^2
I_x	Second moment of area about the x (ML) axis	Sagittal bending rigidity in the DP plane	mm^4
I_y	Second moment of area about the y (DP) axis	Transverse bending rigidity in the ML plane	mm^4
I_{max}	Maximum second moment of area	Maximum bending rigidity	mm^4
I_{min}	Minimum second moment of area	Minimum bending rigidity	mm^4
J ($I_{max} + I_{min}$)	Polar second moment of area	Torsional resistance	mm^4
Z_x	Section modulus about the x (ML) axis	Sagittal bending strength in the DP plane	mm^3
Z_y	Section modulus about the y (DP) axis	Transverse bending strength in the ML plane	mm^3

Statistical Methods

Definitions for the abbreviations of the measurements are located in Table 5.8 and Appendix A. All calculations and statistical procedures were carried out in the software programs Microsoft® Excel and Minitab®.

Scatterplots as well as box-plots showing medians and interquartile ranges provide means to visually assess patterns in the data and to compare them to *Proconsul* (Ruff, 2002).

Least squares (LS) regressions and Pearson's correlation coefficients (R) were calculated for *Macaca* and *Pan* individuals for the bivariate comparisons. Ordinary LS regressions are used as opposed to an alternative that is not yet part of commonly available statistical software packages, reduced major axis (RMA). Slopes derived from the two techniques are very similar when correlation coefficient is close to 1.0 since the RMA slope is equivalent to the LS slope divided by the correlation coefficient (Sokal and Rohlf, 1995). Although RMA takes into account error in both axes, LS regression is appropriate for these data and for these questions because of high correlation between the variables (see below). Not until a more complete sample is collected, both ontogenetically and with additional taxa (which is currently in progress), will it be necessary to test between slopes and therefore between different regression methods. Then, it should be possible to form equations for predicting body mass from metatarsal CSG.

Data were natural log-transformed to maintain linearity of the functions and to avoid the affect of individuals with large body sizes disproportionately affecting the slopes of the regressions (Sokal and Rohlf, 1995).

Results

Means and standard deviations of the cross-sectional properties of the metatarsal midshafts of each species are located in Tables B.13, B.14, and B.15. Pearson's correlation coefficients (R) were calculated for the major CSG variables (CA, J, Zx, Zy) as well as metatarsal lengths, calcaneal length dimensions, units of the foot, body mass estimates, age estimates, and femoral head breadth (Table B.16). All variables were highly correlated at $p = 0.000$ except three comparisons dealing with age. Age does not correlate well with body mass, Zx and Zy probably due to small samples. Body masses were only calculated for adults (age group 5), yet only *Macaca* has known ages in this group, *Pan* individuals were not given age estimates once third molars were in occlusion. Correlation coefficients between CSG variables and FHB are nearly always above 0.90 which justifies the use of ordinary LS regression in the analysis.

Box-plots showing medians and interquartile ranges of metatarsal length by age group in the three taxa illustrate the linear proportions of the feet that need to be considered with the CSG properties (Figures 5.6-5.8). *Macaca* has a much shorter hallux compared to metatarsals 2-5 than *Pan*. The longest metatarsals in *Macaca* (in all represented age groups) are the third and fourth ones, the longest (in all age groups) in *Pan* is the second one. *Proconsul* shows a more *Macaca*-like pattern but with longer metatarsals in general, and most noticeably in the first.

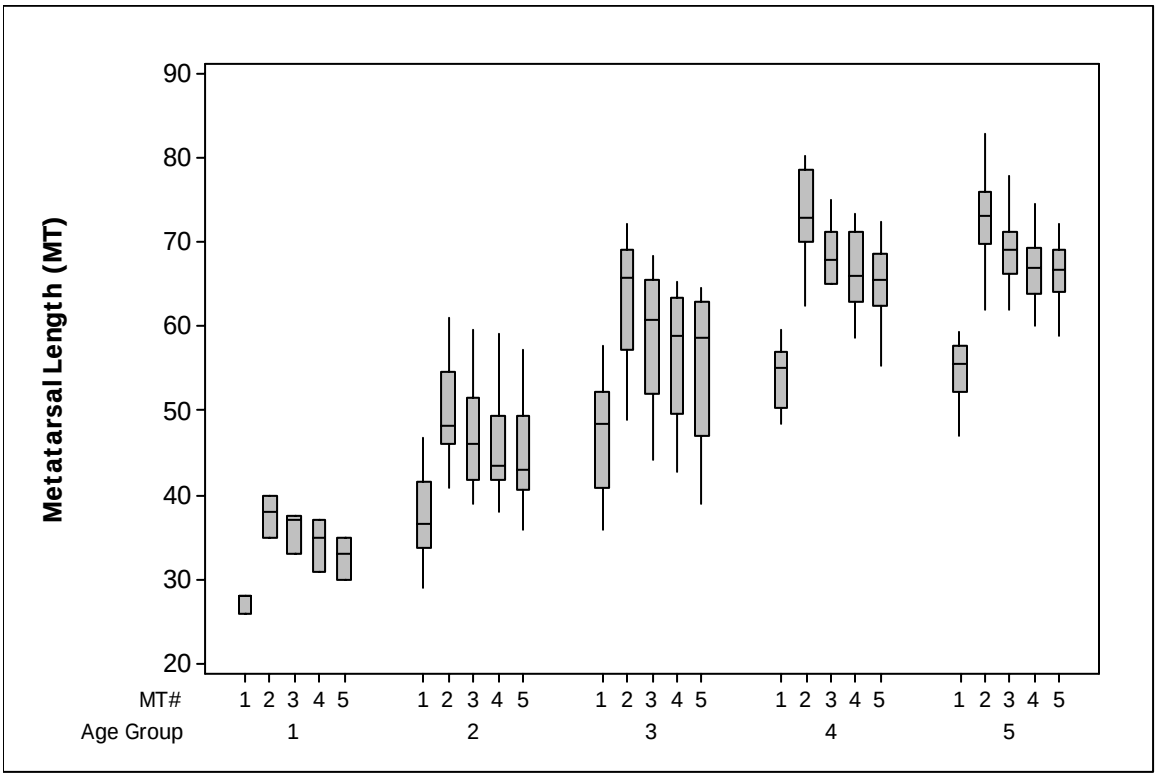

Figure 5.6. Metatarsal lengths by age group for *P. troglodytes.*

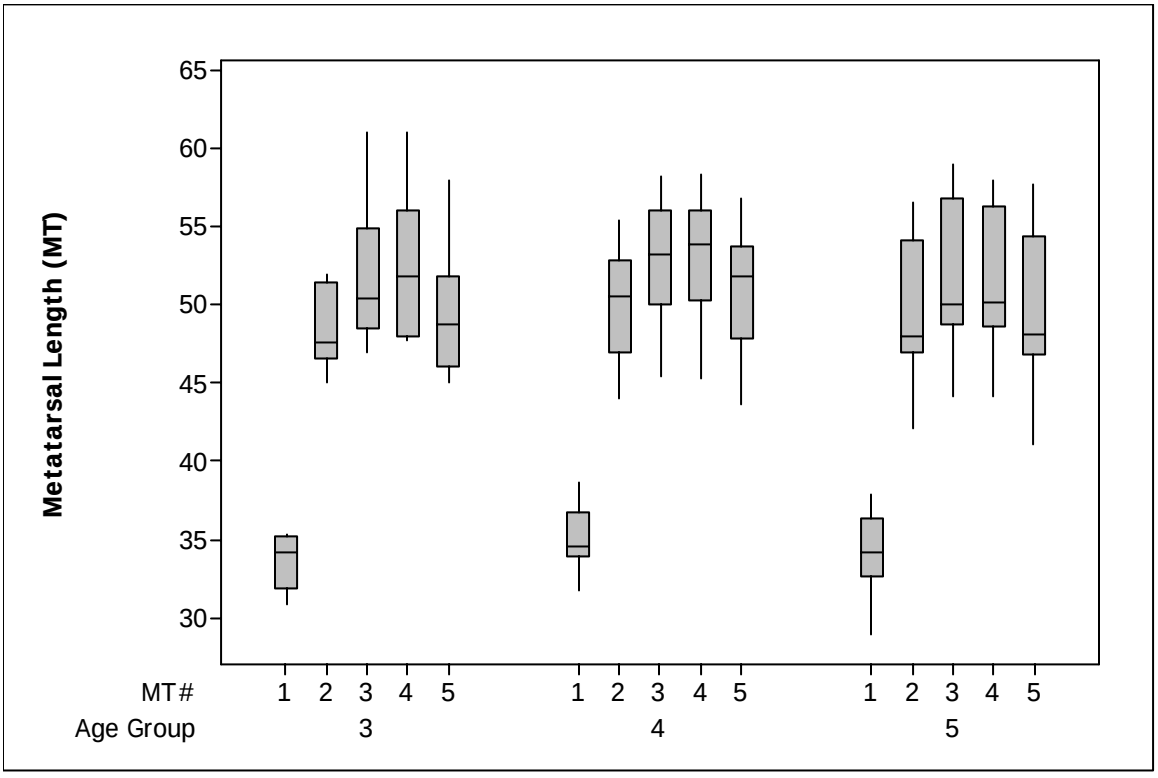

Figure 5.7. Metatarsal lengths by age group for *M. mulatta.*

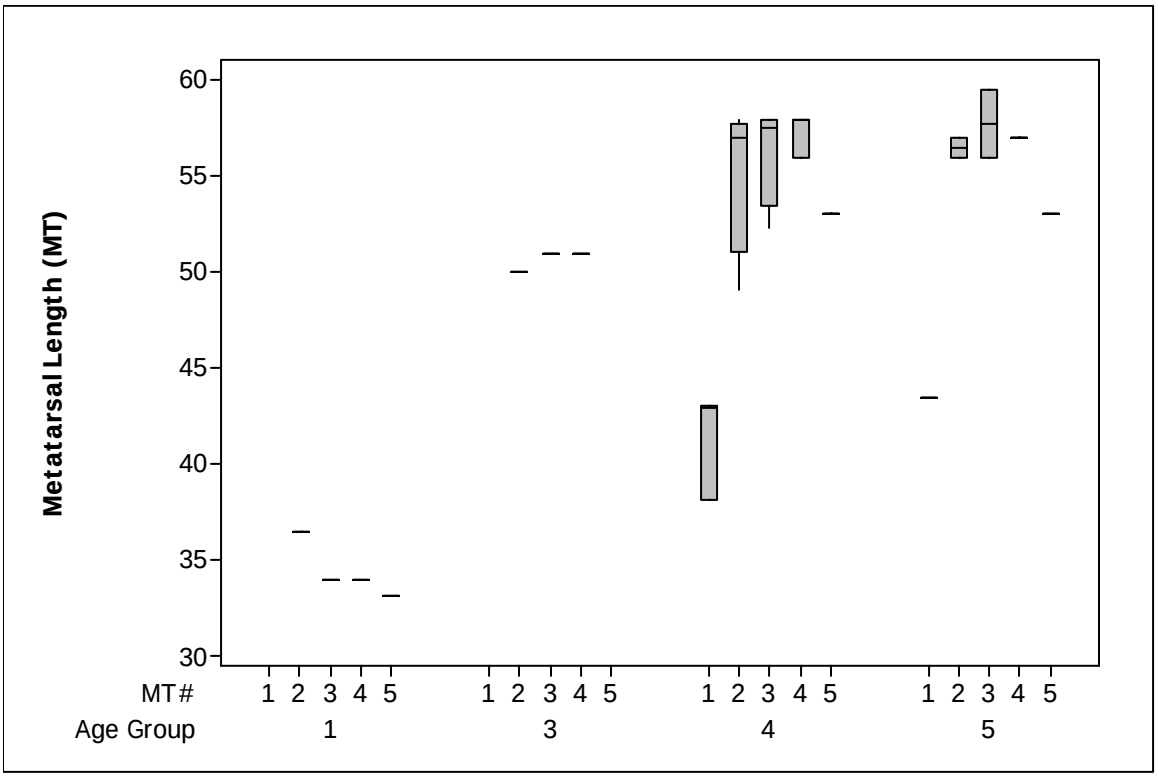

Figure 5.8. Metatarsal lengths by age group for *P. heseloni.*

Box-plots of natural log-transformed J standardized by metatarsal length illustrate the increase in J through ontogeny in the taxa (Figures 5.9-5.11). They also illustrate that patterns are maintained across the age groups within each taxon.

Box-plots of natural log-transformed J and Zx standardized by metatarsal length illustrate the similarities between the magnitude of *Proconsul* and *Macaca* CSG properties in each age group as well as the similarities between J and Zx patterns within groups (Figures 5.12-5.20).

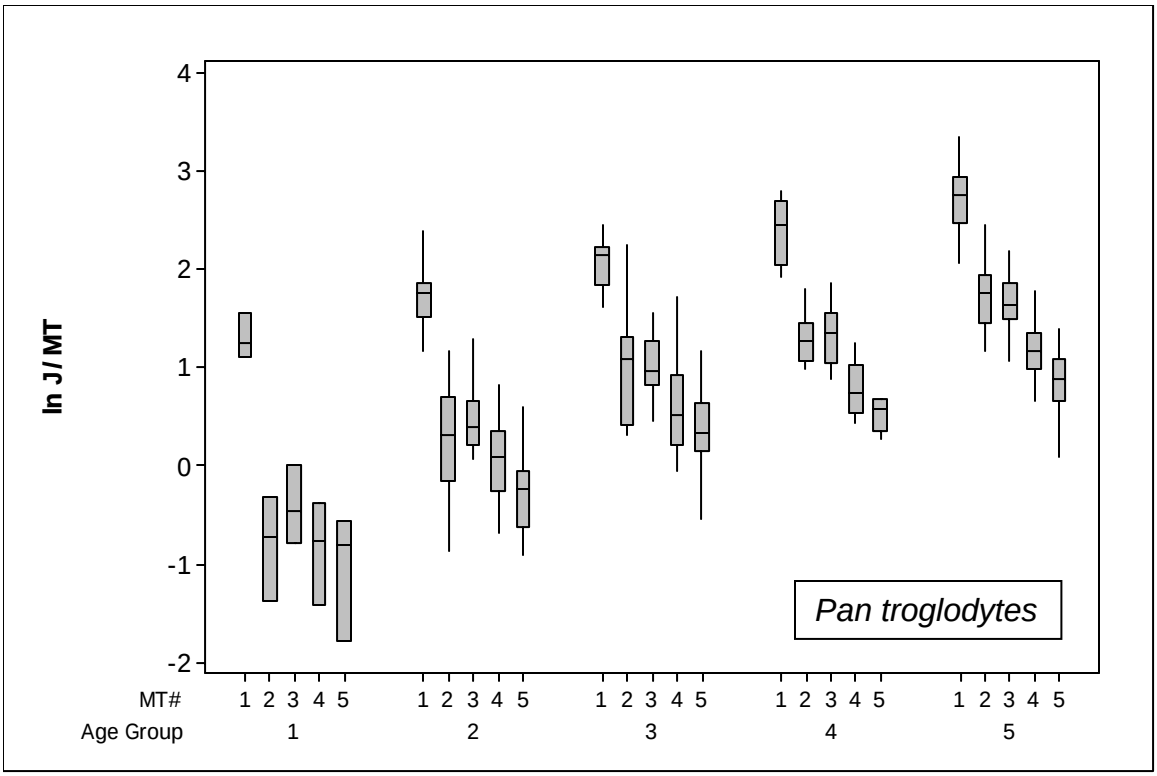

Figure 5.9. Polar second moments of area (J) standardized by metatarsal length for the midshafts of the metatarsals in each age group of *Pan troglodytes*.

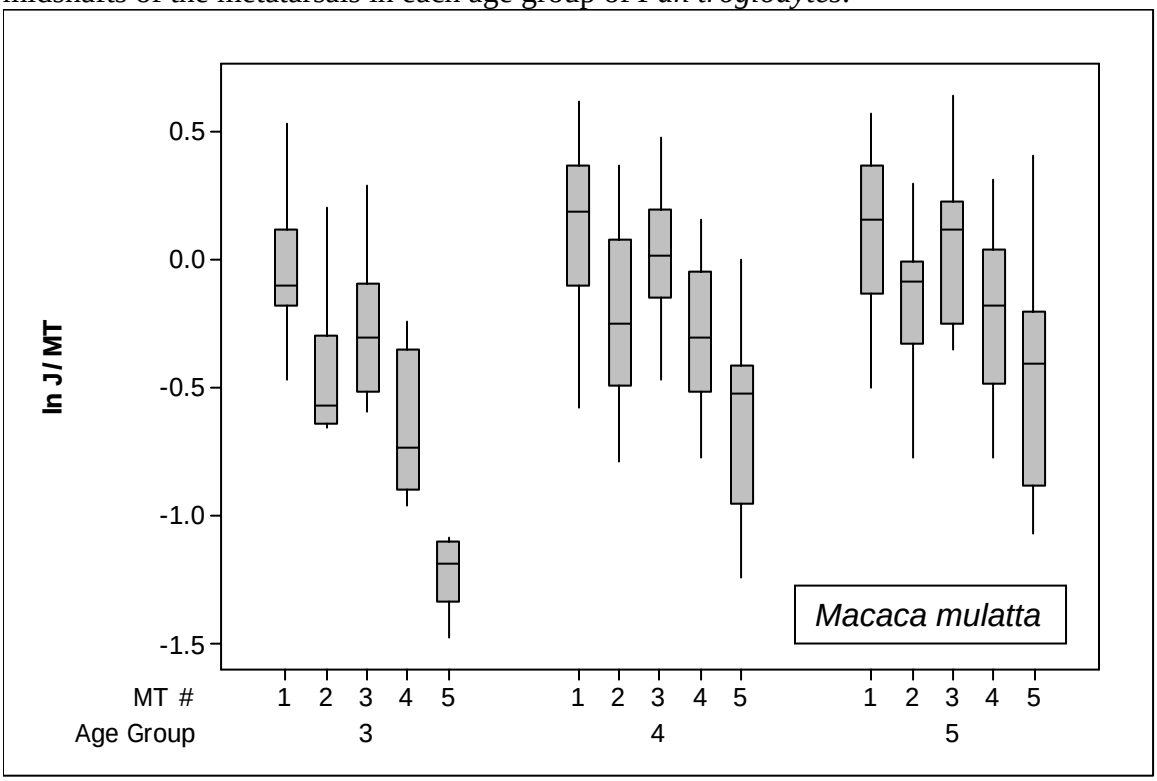

Figure 5.10. Polar second moments of area (J) standardized by metatarsal length for the midshafts of the metatarsals in each age group of *Macaca mulatta*.

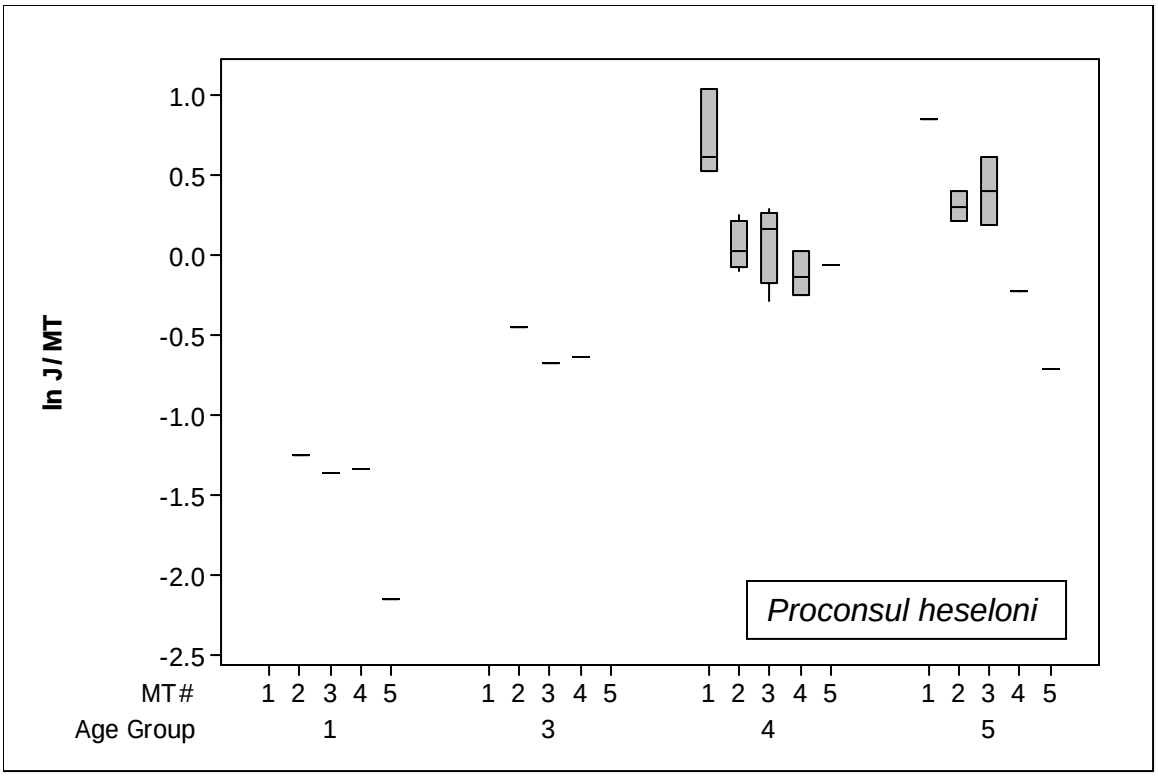

Figure 5.11. Polar second moments of area (J) standardized by metatarsal length for the midshafts of the metatarsals in each age group of *Proconsul heseloni*.

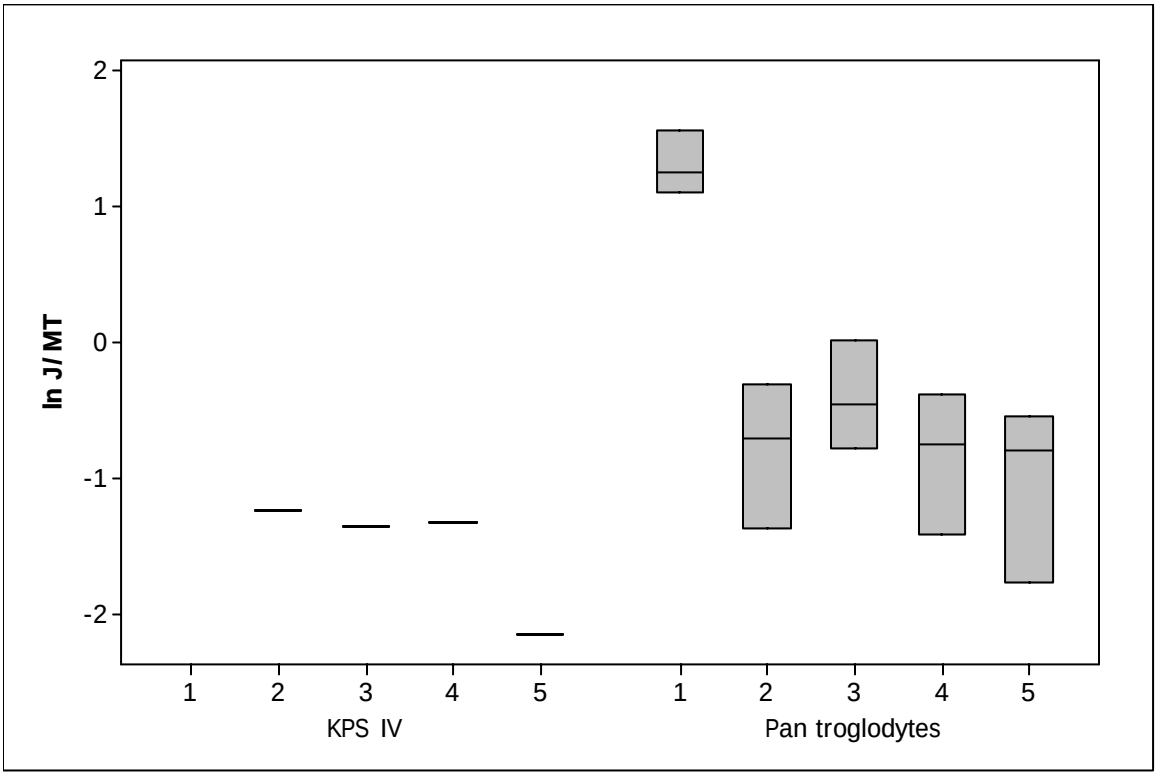

Figure 5.12. Polar second moments of area (J) standardized by metatarsal length for the midshafts of the metatarsals of individuals in age group 1.

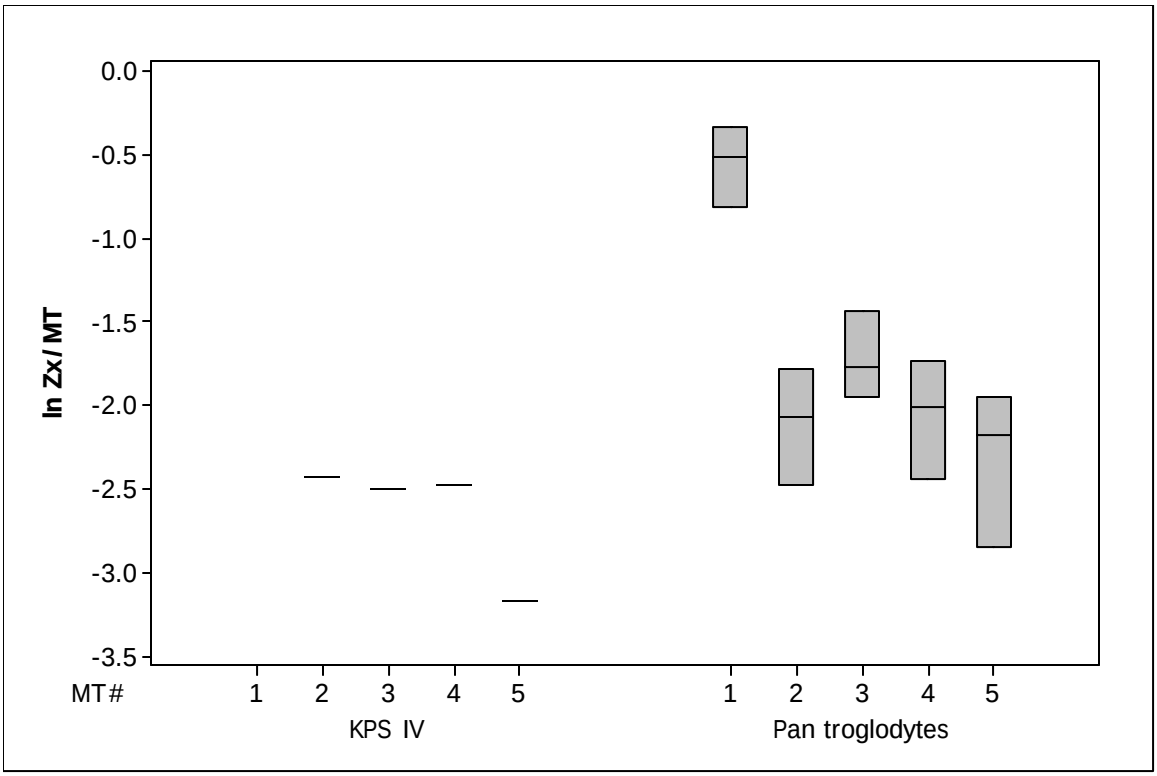

Figure 5.13. Section modulus about the x-axis (Zx) standardized by metatarsal length for the midshafts of the metatarsals of individuals in age group 1.

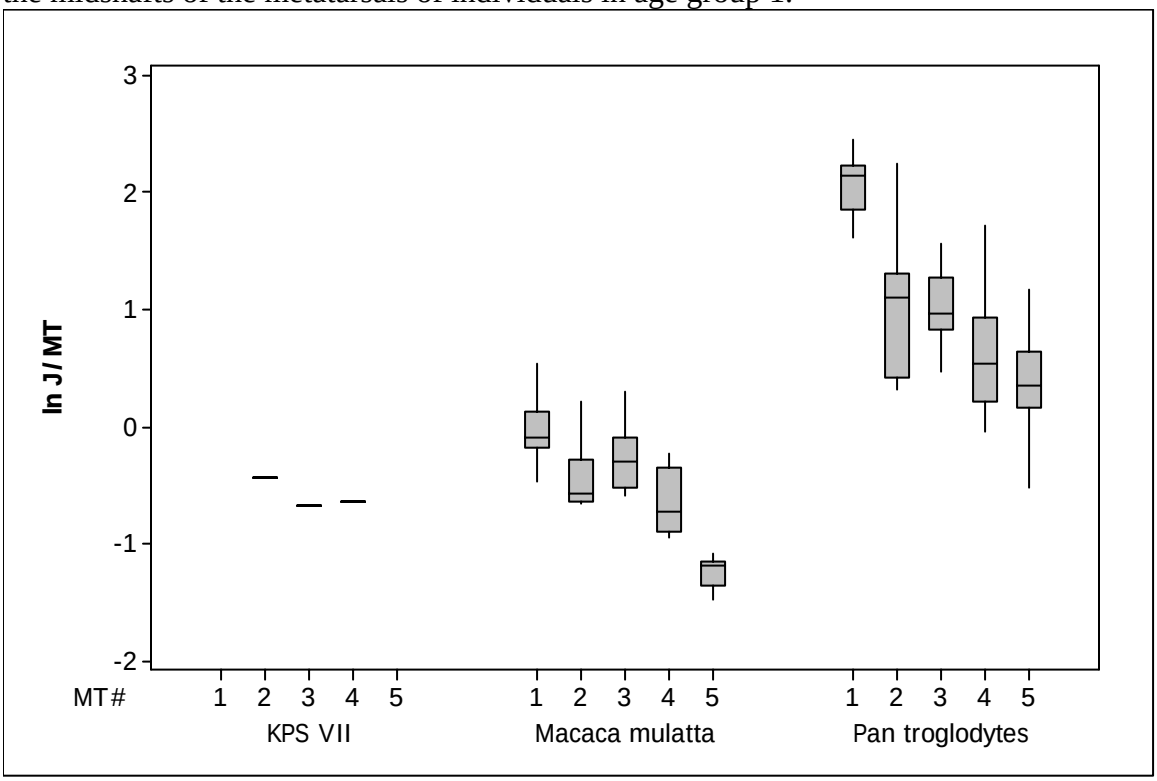

Figure 5.14. Polar second moments of area (J) standardized by metatarsal length for the midshafts of the metatarsals of individuals in age group 3.

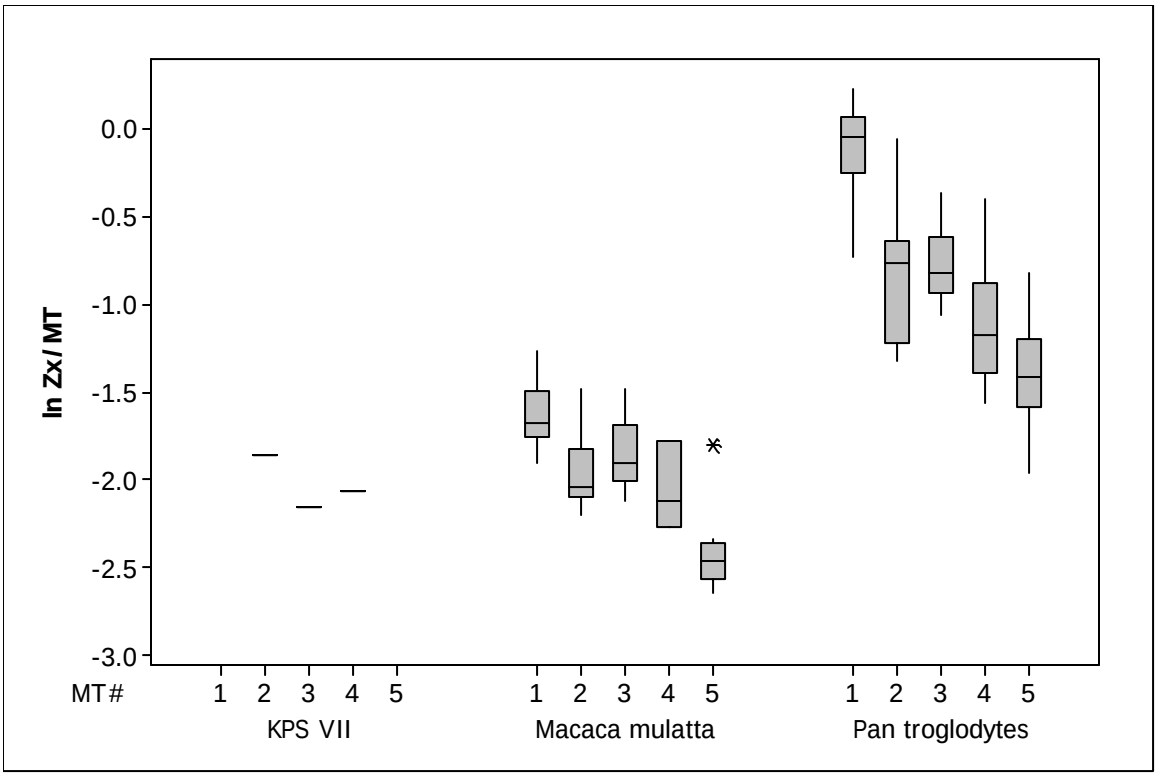

Figure 5.15. Section modulus about the x-axis (Zx) standardized by metatarsal length for the midshafts of the metatarsals of individuals in age group 3.

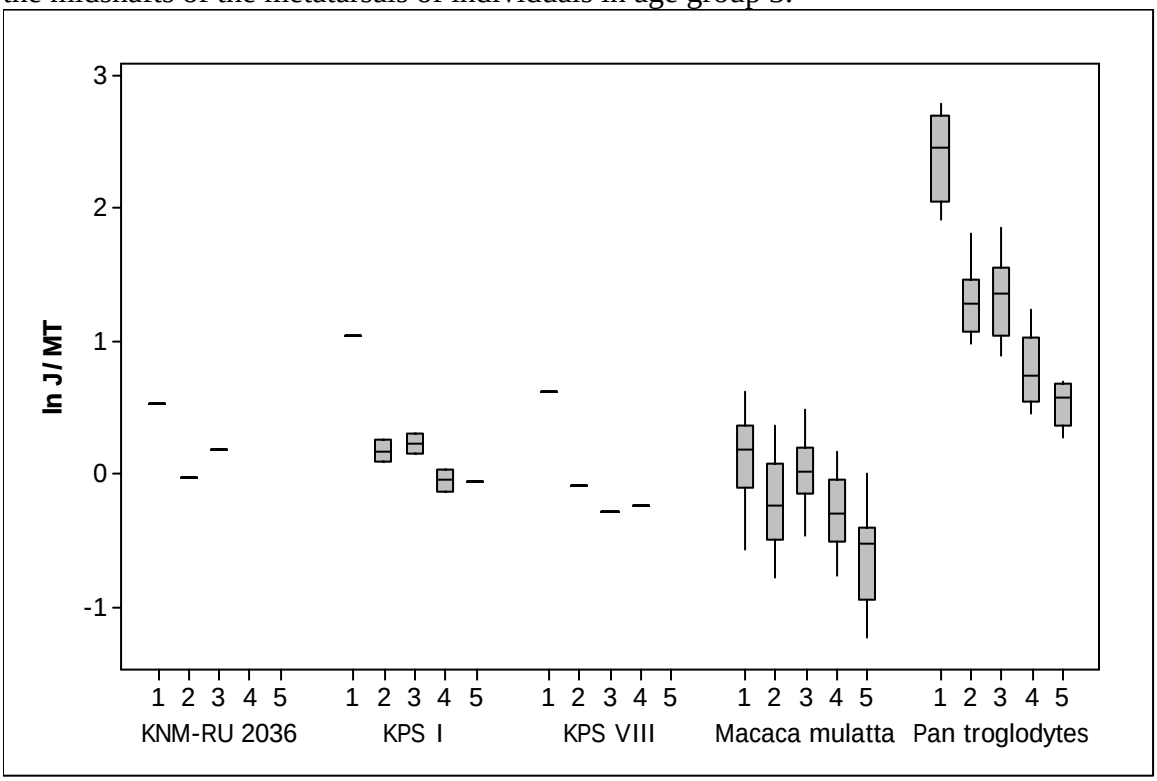

Figure 5.16. Polar second moments of area (J) standardized by metatarsal length for the midshafts of the metatarsals of individuals in age group 4.

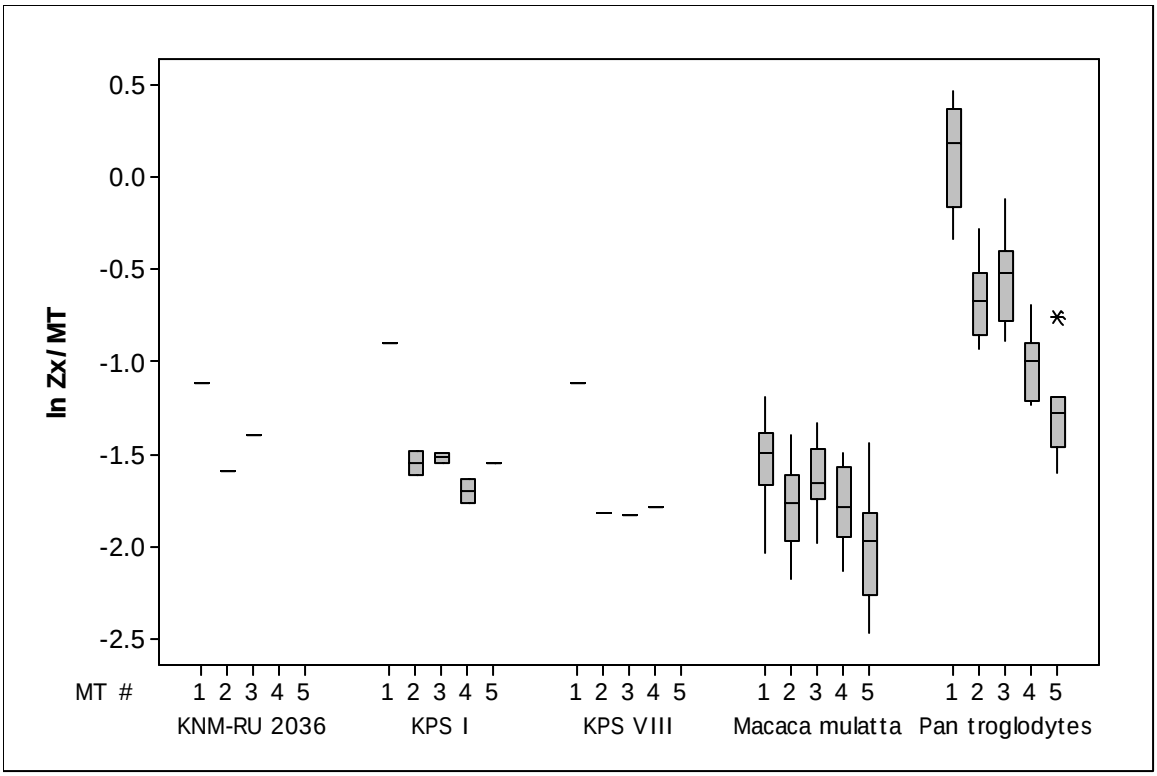

Figure 5.17. Section modulus about the x-axis (Zx) standardized by metatarsal length for the midshafts of the metatarsals of individuals in age group 4.

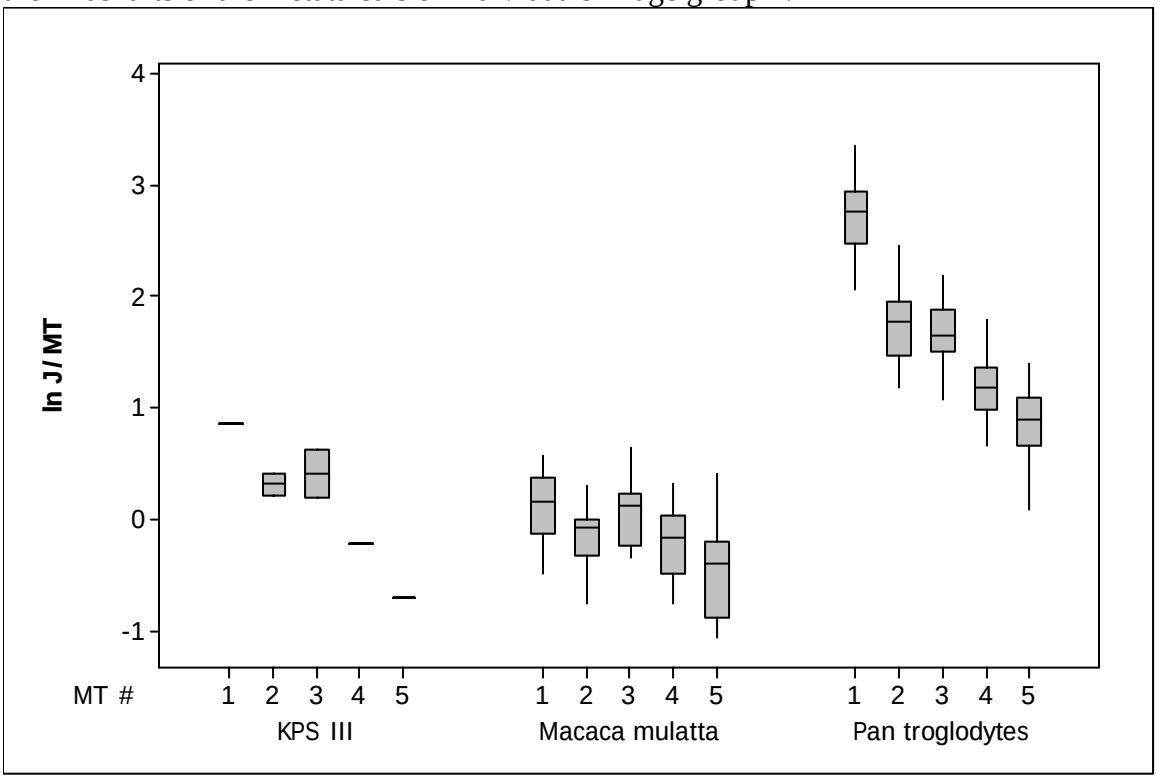

Figure 5.18. Polar second moments of area (J) standardized by metatarsal length for the midshafts of the metatarsals of individuals in age group 5.

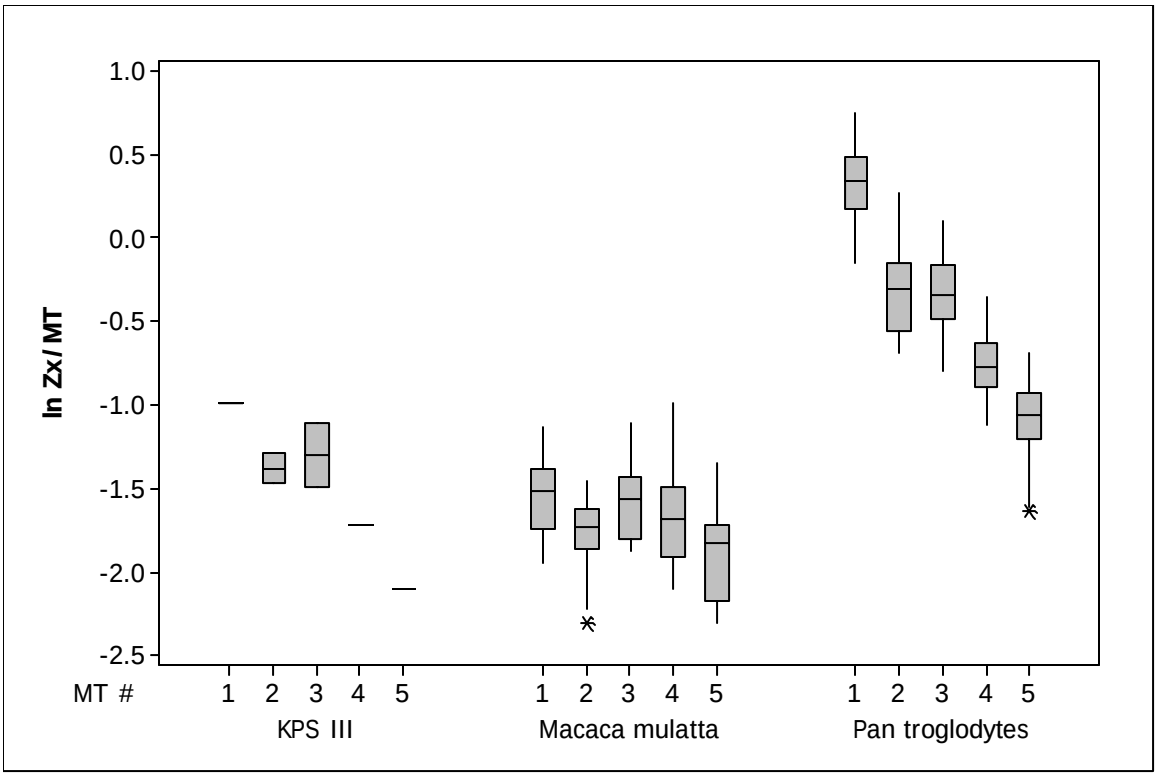

Figure 5.19. Section modulus about the x-axis (Zx) standardized by metatarsal length for the midshafts of the metatarsals of individuals in age group 5.

Plots of ln J and ln Zx standardized by metatarsal length versus FHB for all metatarsals show that the *Proconsul* individuals which have available femoral heads fall in line with *Macaca* for all metatarsals but MT1. Data are presented for CA, J, Zx and Zy in tables B.17-B.19. The *Proconsul* first metatarsal is more resistant to both torsional (J) and bending (Zx) forces than *Macaca* even though it has comparable properties for MT 2-5. MT1 was oriented exactly like MT2-5 for analysis so Zx of MT1 is really Zy, that is, it must be considered the resistance to bending forces in the mediolateral plane because *in vivo* it is rotated medially, in opposition to MT2-5. If age groups 1 and 2 were represented for *Macaca*, the regression would most likely be similar to that of *Proconsul* when the infant KPS IV is present. However, it is expected that *Proconsul* would have larger CSG properties than *Macaca* at these ages. Plots of the rest of the metatarsals show

that *Macac*a and *Proconsul* have relatively higher J and Zx than *Pan* for all metatarsals but MT1.

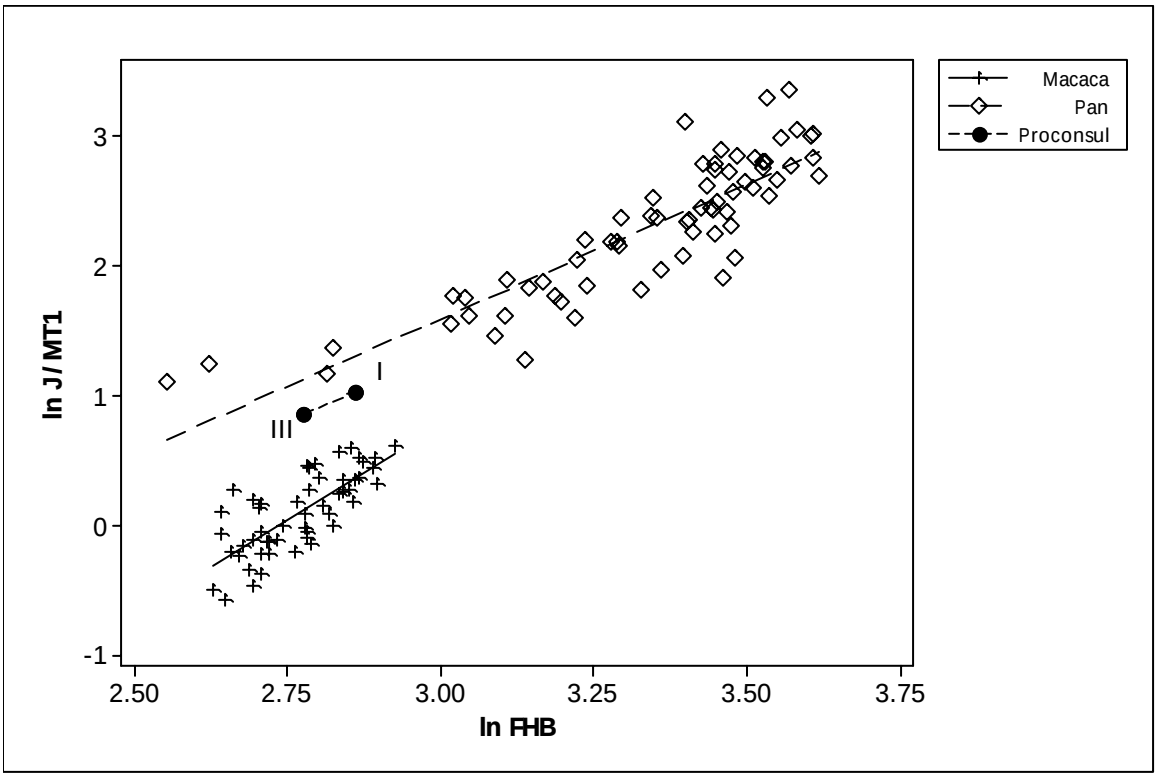

Figure 5.20. J/MT1 versus FHB.

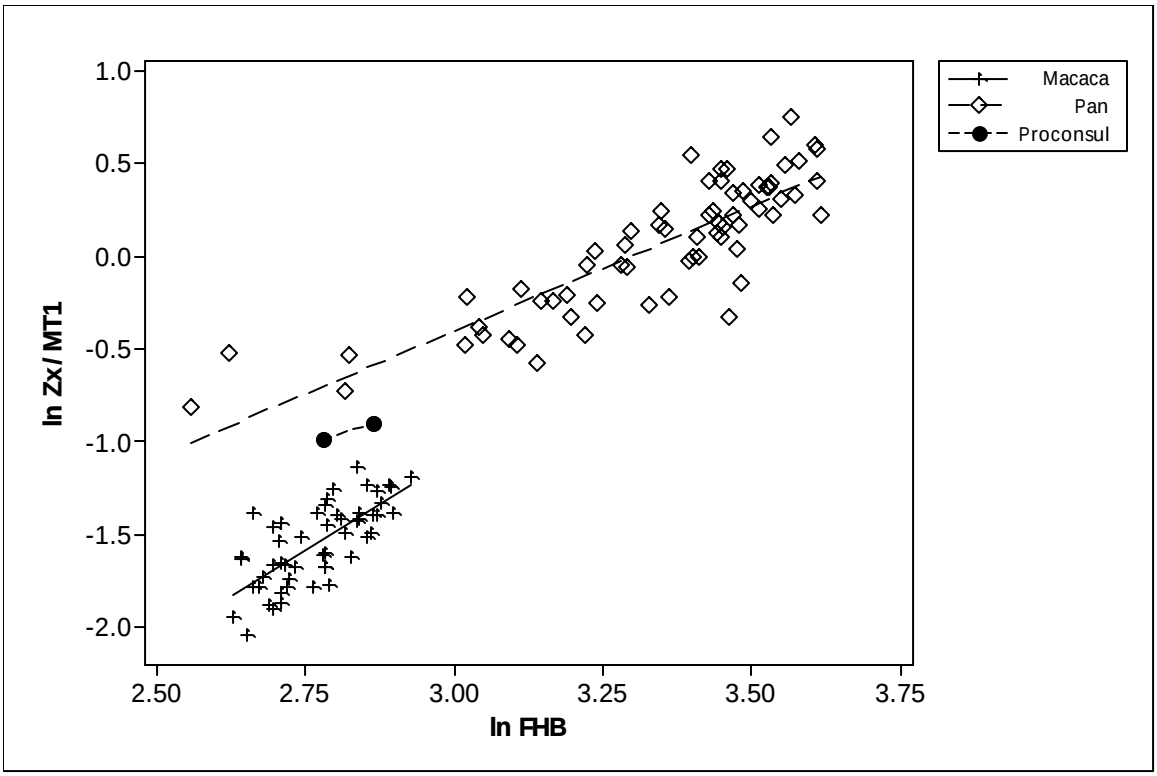

Figure 5.21. Zx/ MT1 versus FHB.

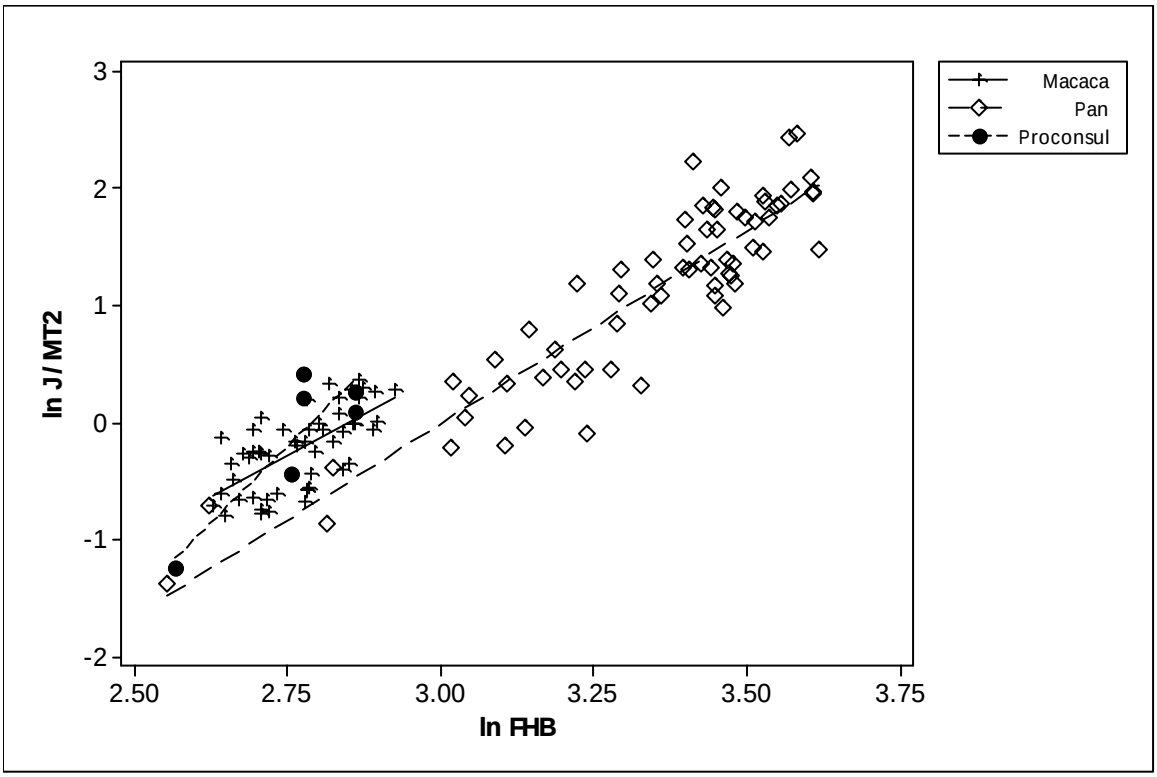

Figure 5.22. J/MT2 versus FHB.

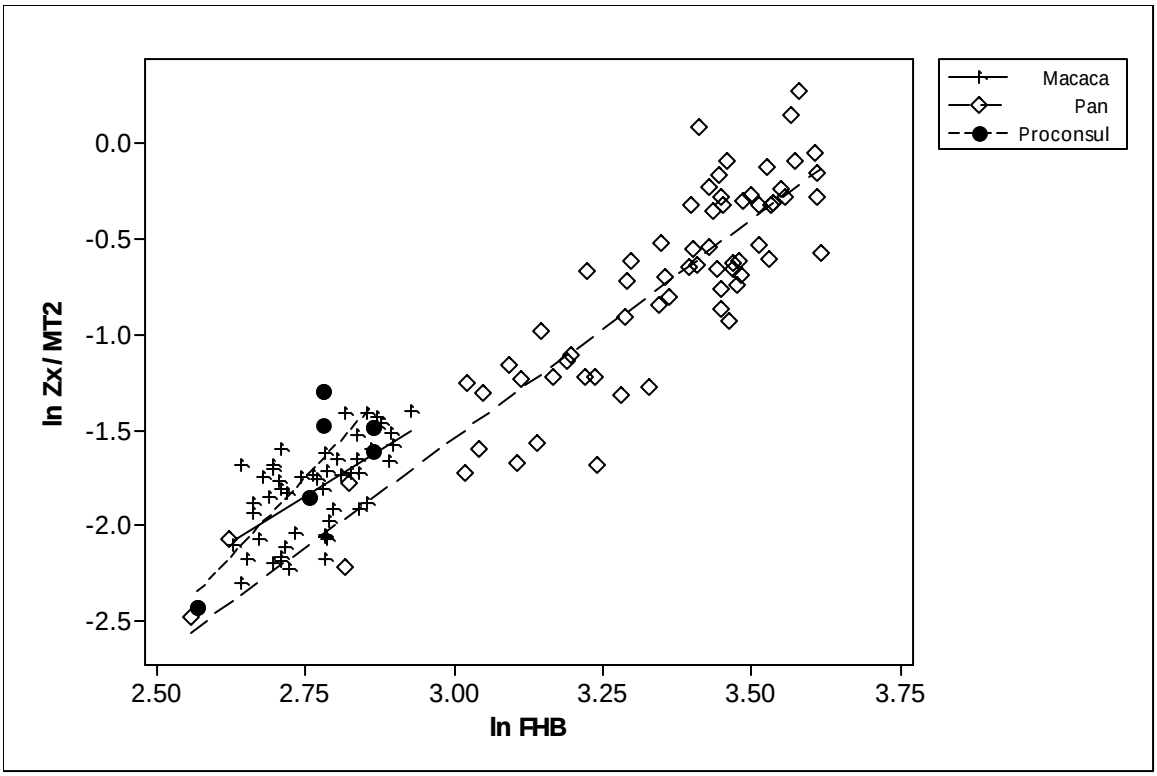

Figure 5.23. Zx/ MT2 versus FHB.

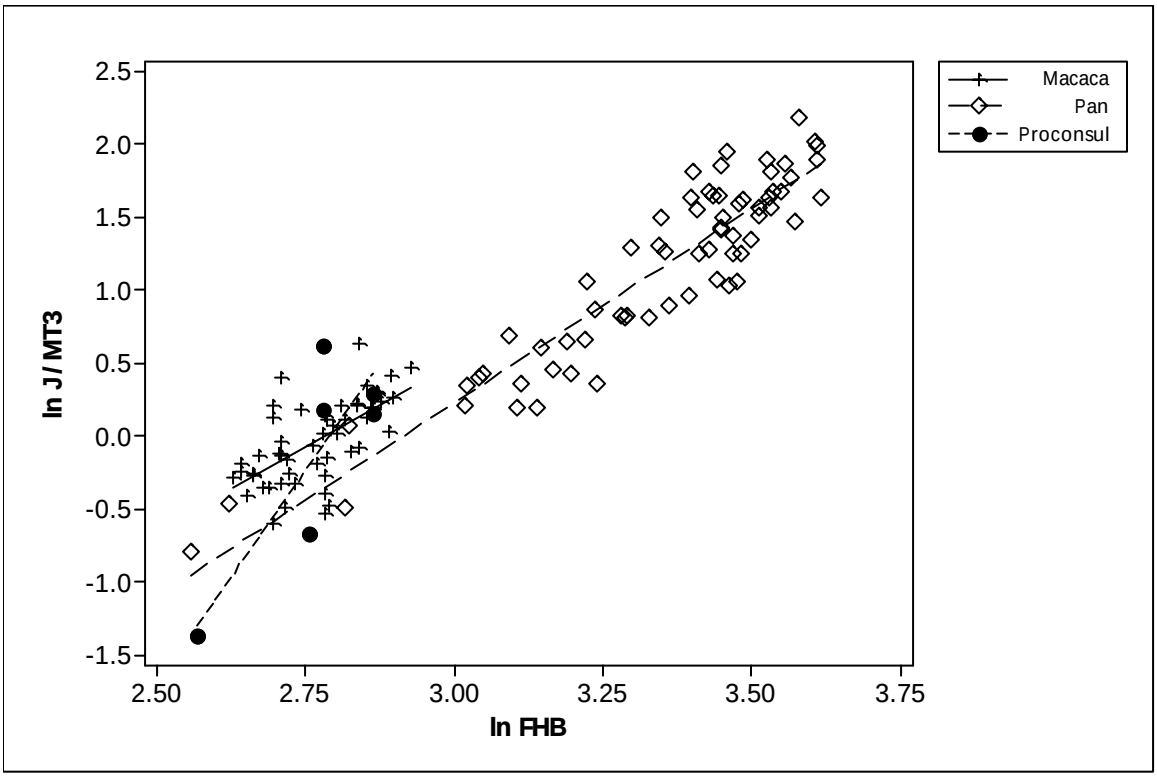

Figure 5.24. J/MT3 versus FHB.

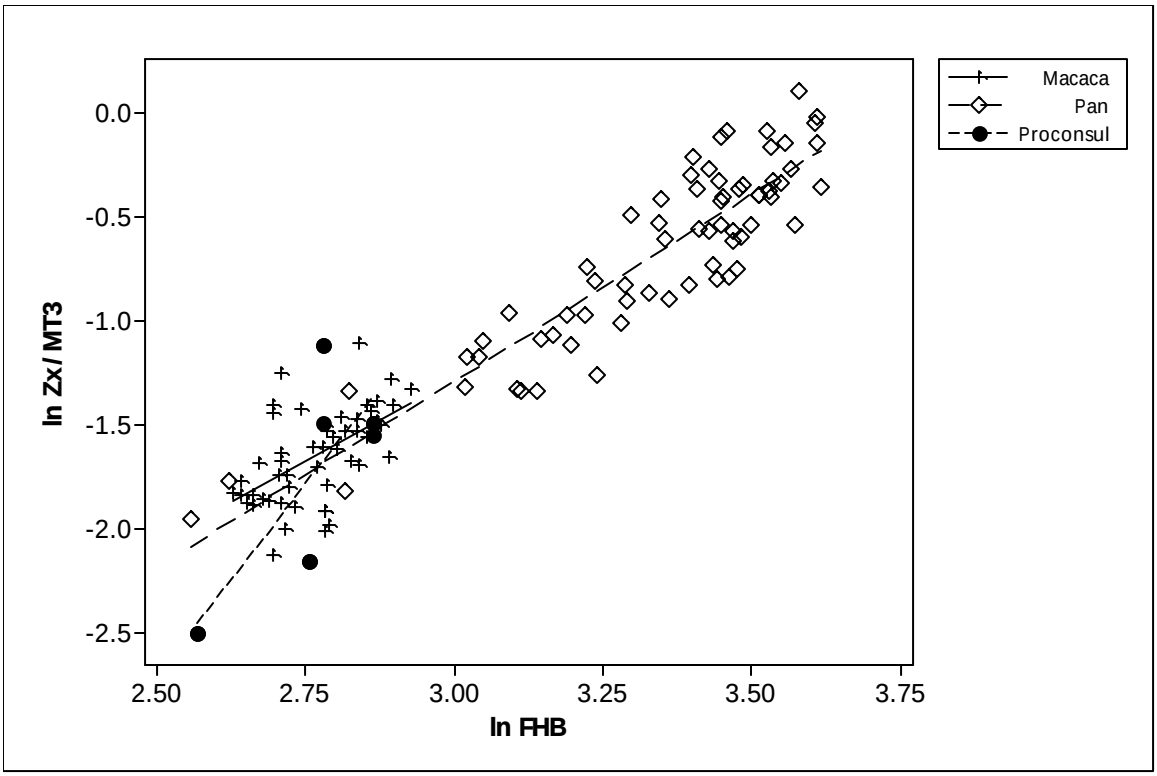

Figure 5.25. Zx/ MT3 versus FHB.

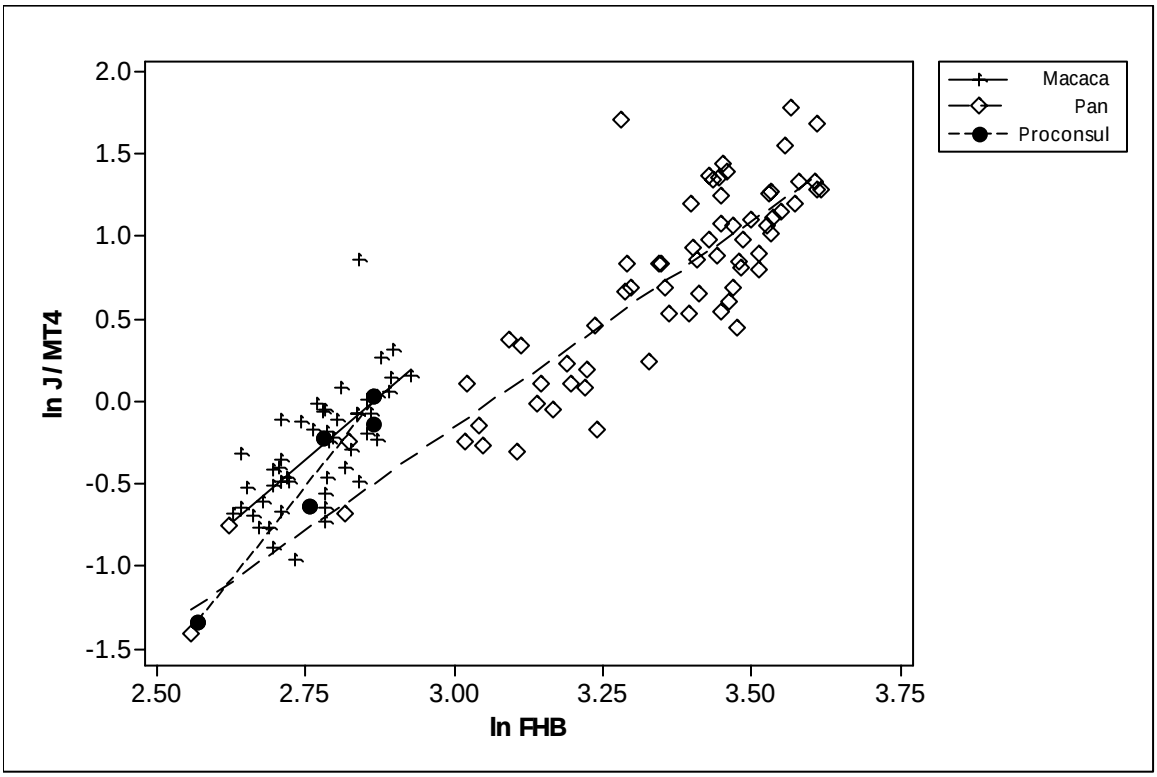

Figure 5.26. J/MT4 versus FHB.

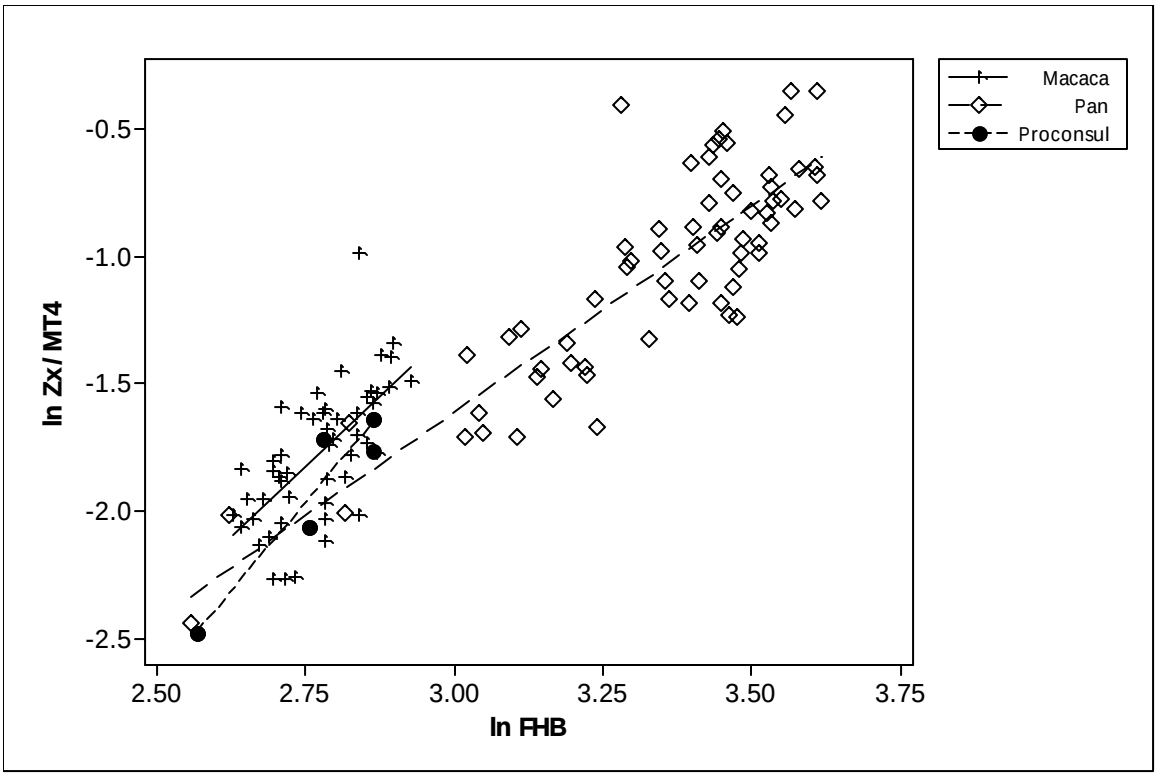

Figure 5.27. Zx/ MT4 versus FHB.

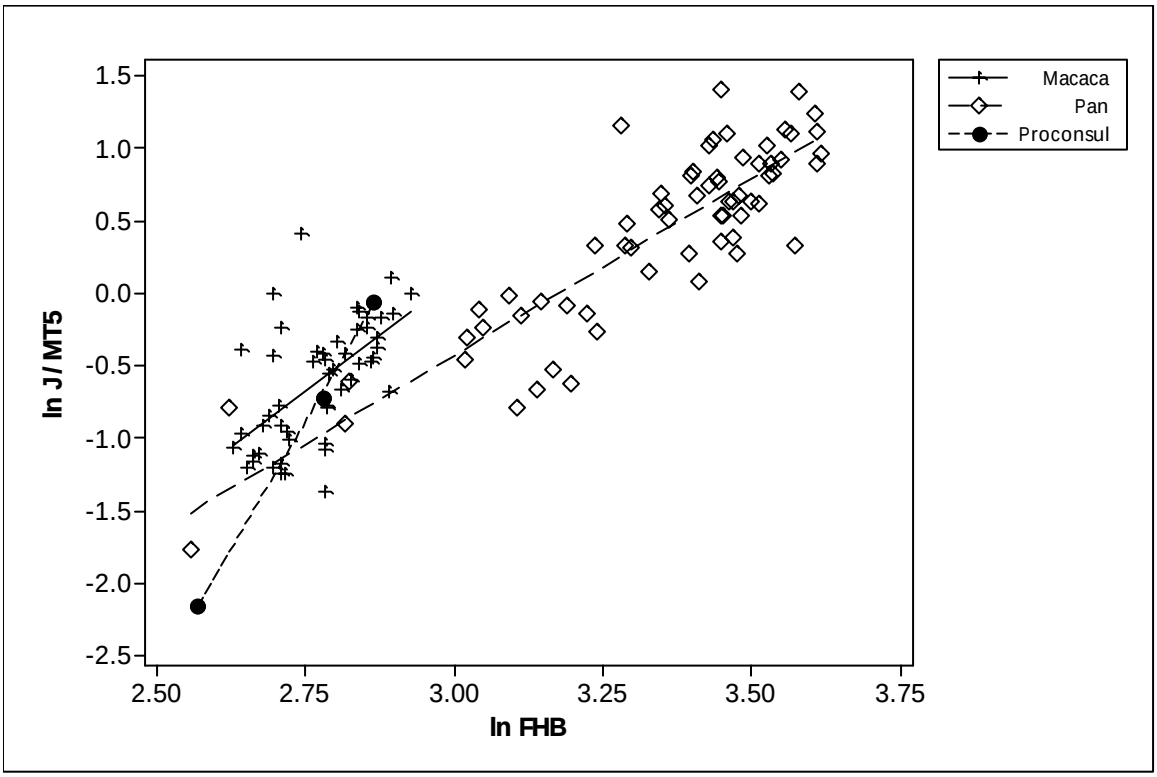

Figure 5.28. J/MT5 versus FHB.

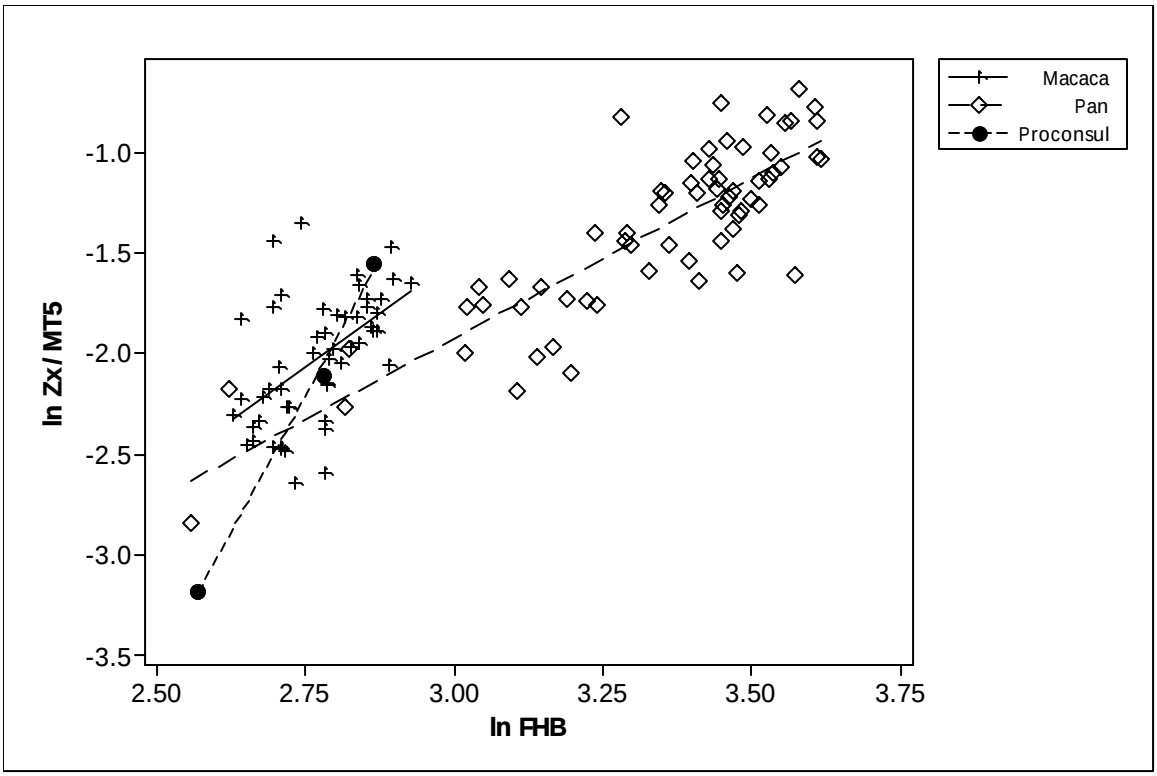

Figure 5.29. Zx/ MT5 versus FHB.

Ratio of Imax to Imin serves as an estimate of roundness of the midshaft. The closer to 1.0, the rounder the midshaft of the metatarsal. As the ratio increases further from 1.0, the metatarsal becomes increasingly flat. By comparing Imax and Imin instead of Ix and Iy, the relative roundness of all the metatarsals can be compared since the orientation of flattening of MT1 (dorsoplantar) is on a different axis than MT2-5 (mediolateral). For *Pan*, the roundest metatarsals are 1 and 5 and 3 is oval. *Macaca* shows the opposite pattern with 3 being the roundest and 1 and 5 being oval. This pattern appears to be consistent through development in *Pan*. *Proconsul* resembles the *Macaca* condition. The patterns of Imin/Imax do not mimic strength property patterns across the metatarsus.

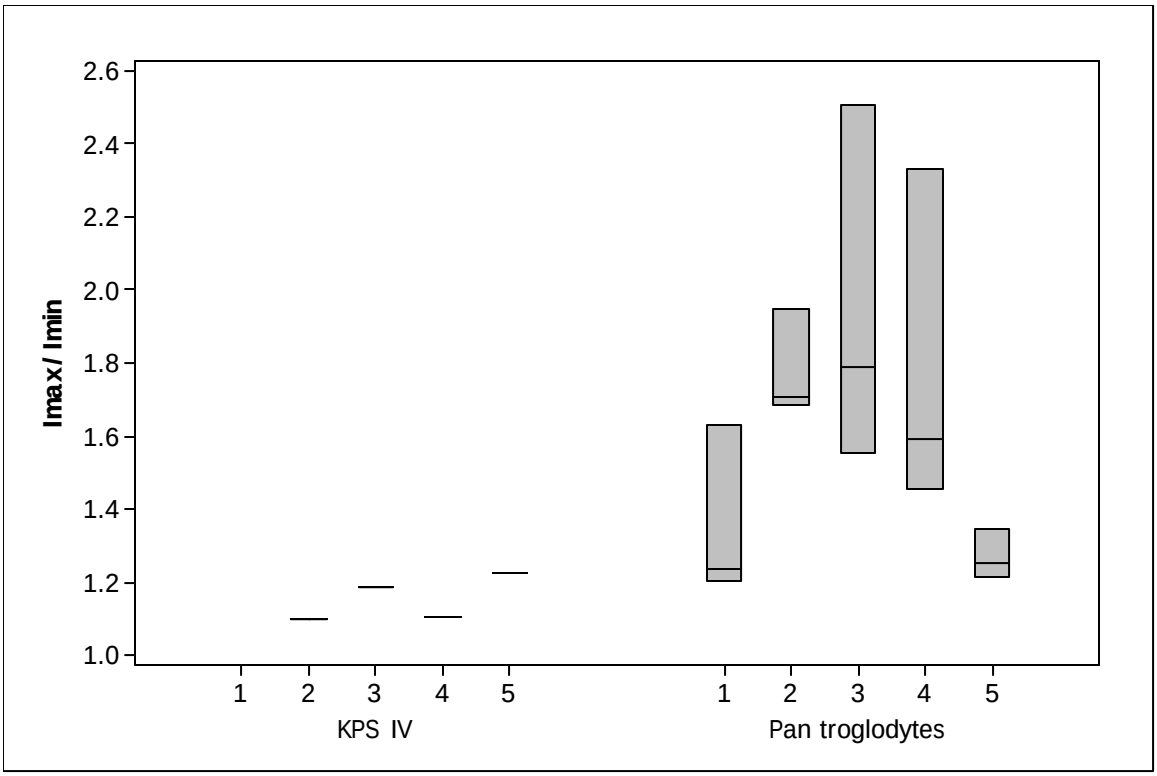

Figure 5.30. Ratio of maximum to minimum second moments of area for metatarsal midshafts (1-5) of individuals in age group 1.

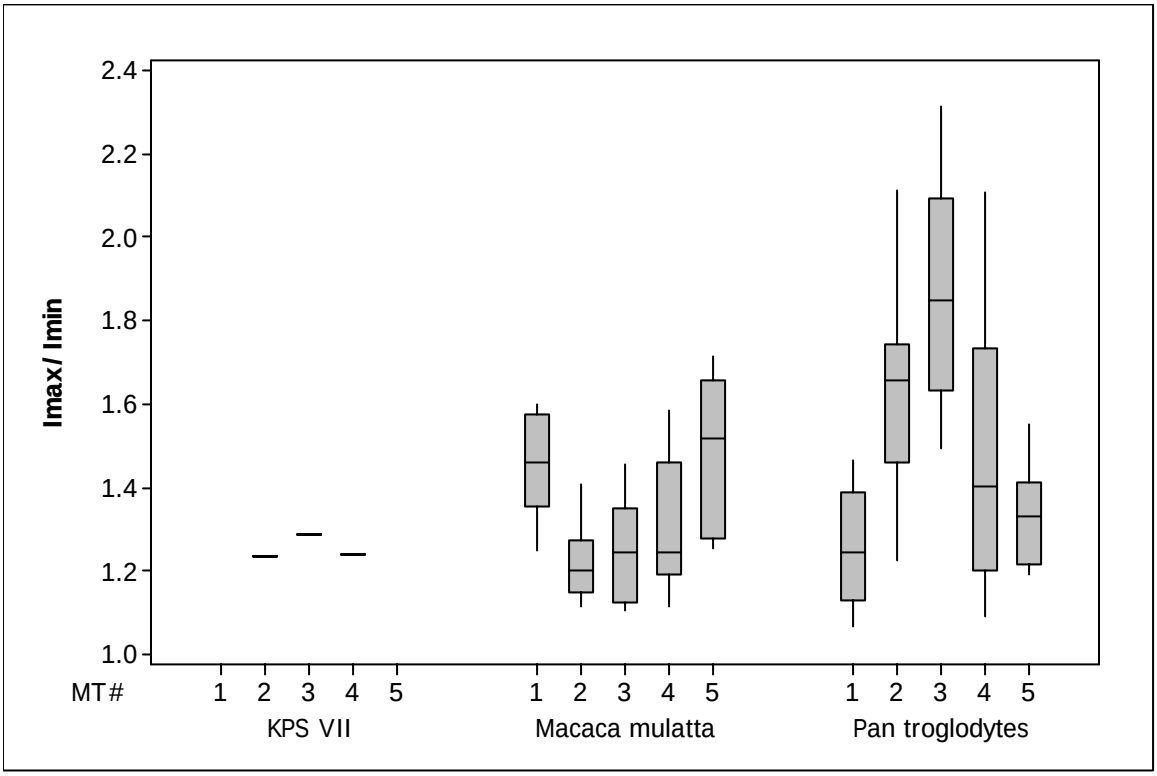

Figure 5.31. Ratio of maximum to minimum second moments of area for metatarsal midshafts (1-5) of individuals in age group 3.

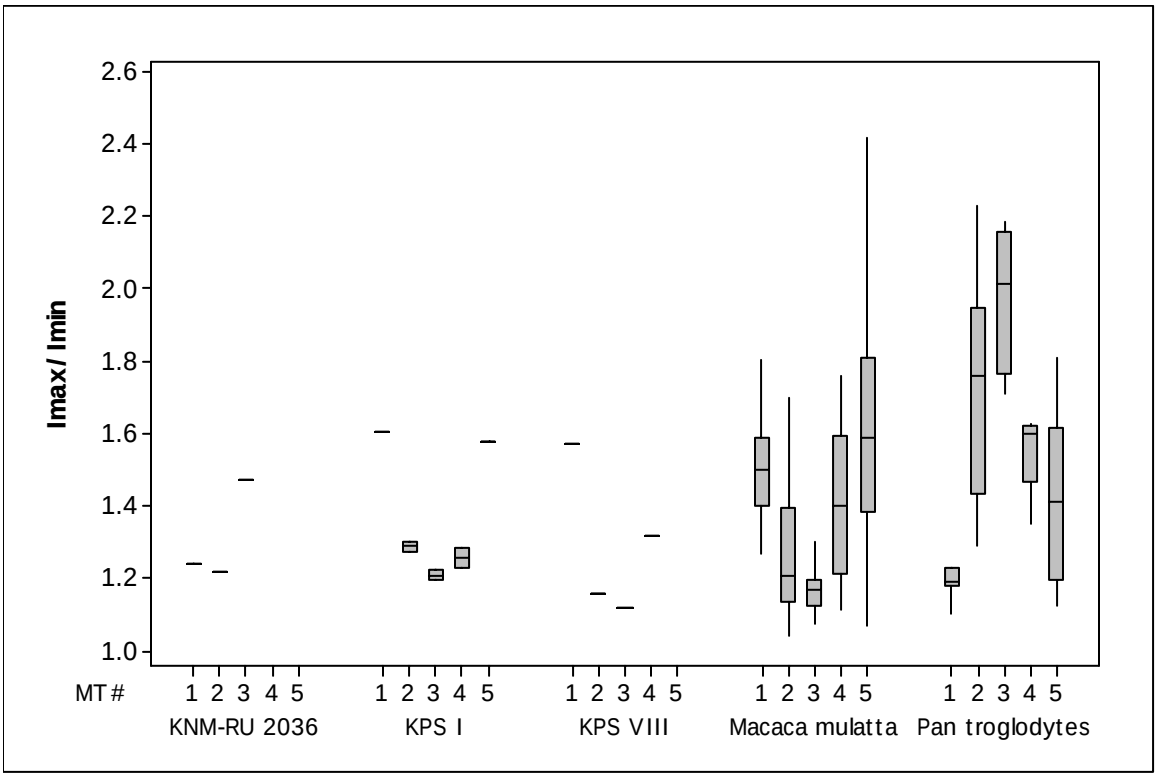

Figure 5.32. Ratio of maximum to minimum second moments of area for metatarsal midshafts (1-5) of individuals in age group 4.

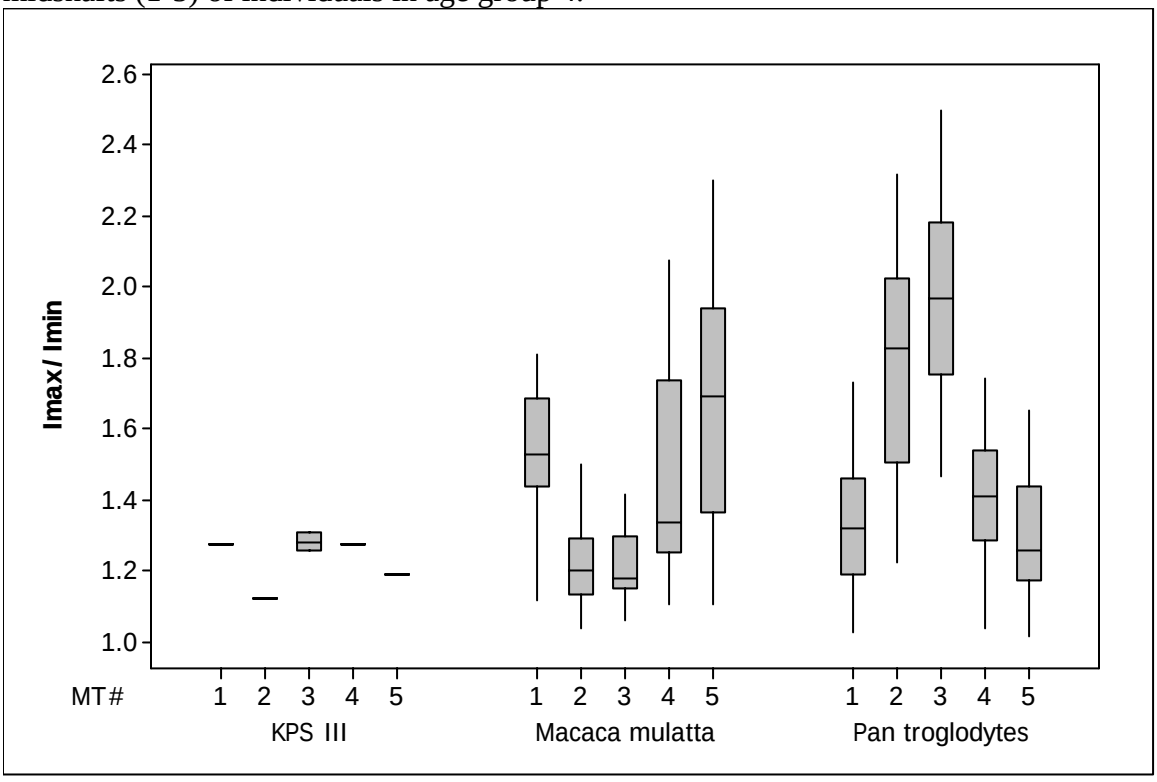

Figure 5.33. Ratio of maximum to minimum second moments of area for metatarsal midshafts (1-5) of individuals in age group 5.

When ratios of Ix/Iy are compared, the orientation of midshaft flattening can be discerned. For this analysis, MT1 was oriented in the same plane as MT 2-5 even though *in vivo* it is rotated medially in opposition to the other metatarsals. *Pan* ratios depart from 1.0 far more than *Macaca* do. In *Macaca*, the hallux is dorsoplantarly flattened, MT2-3 are slightly dorsoplantarly flattened but close to round and MT4-5 are increasingly mediolaterally flattened. *Pan* Ix/Iy mimics exactly the same pattern as Imax/Imin with the MT1 and MT5 being slightly dorsoplantarly flattened and MT2-4 showing mediolateral flattening, especially in MT3. *Proconsul* is showing the *Macaca* patterning, with the exceptions of KPS VII and IV which could be explained by individual variation or could be due to issues with deformation and grouping of fossils within these individuals.

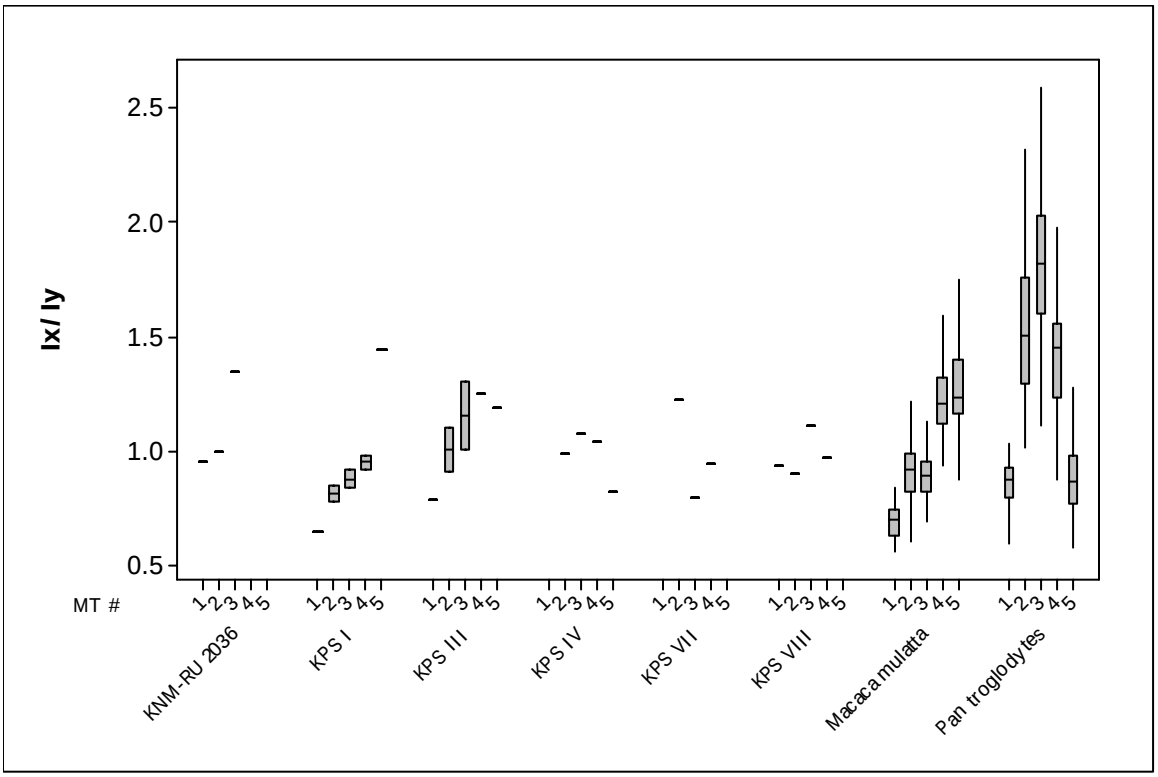

Figure 5.34. Ratio of second moment of area about the x-axis (Ix) to second moment of area about the y-axis (Iy) for metatarsal midshafts in the pooled-age sample.

Discussion

Table 5.9. Error introduced for each method and the cross-sectional properties vulnerable to it.

Method	Error	CSG Affected
Latex Cast Method (LCM) with Bones	Orientation on x-ray	Ix, Iy, Zx, Zy
	Orientation of mold	Ix, Iy, Zx, Zy
	Cutting mold exactly in perpendicular plan to bone shaft	All
	Photographing mold in proper orientation since mold labels are not exact	Ix, Iy, Zx, Zy
	Measuring molds with calipers	All
	Measuring x-rays with calipers	All
	Adapting photo of mold in Photoshop into black and white cross-section	All
	Drawing medullary cavity circumference in Image J	All
MicroCT with Fossils	Taphonomic deformation	All
	Orientation of bone on scanner platform	Ix, Iy, Zx, Zy
	Estimation of midshaft position for bones lacking epiphyses	All
	Adapting scan in Image J	All
	Reconstructing missing fragments	All

Error within methods affects all metatarsals equally, but are comparisons between LCM and microCT supported? Since LCM has been shown to be consistent with direct sectioning of bones for obtaining CSG properties (Stock, 2002; O'Neill and Ruff, 2004), the answer is probably yes, since microCT has such high resolution. Although no study has yet been published comparing results among microCT, medical CT, LCM and direct bone sectioning. However, the results presented here for adult chimpanzees are comparable to those also obtained through LCM by Marchi (2005) and, in turn, his results for humans are comparable to those produced by Griffin and Richmond (2005) with medical CT. Unfortunately it was not possible to get data from the fossils with

normal x-ray as the fossils were too dense to penetrate. And it was not possible to microCT the extant samples either.

The major differences in CSG properties between *Pan* and *Macaca* lie in the hallux and in the relative roundness across the rays. The *Pan* first metatarsal is absolutely stronger in age group 1 than it is in adult *Macaca*. The Macaca-like pattern across MT 2-5 with a stronger hallux is especially evident in the best preserved individuals KPS III and RU 2036.

Like *Macaca*, the *Proconsul* metatarsals are flat and relatively round; they are not curved like *Pan*. Metatarsal curvature probably has a structural relationship (an inverse one) with roundness (Preuschoft, 1970). The metatarsals with the most shaft curvature (always in the dorsoplantar plane) are the ones showing the Imax/Imin ratios furthest from 1.0. Curvature can be quantified directly from the x-ray films and, in the future, it should be considered in conjunction with CSG properties. This is an issue that has not been fully explored in the literature since CSG analyses have been mostly restricted to straight long bones. Non-round shafts may distort assessments of CSG properties (Daegling, 2002), so the structural causes and effects of curvature and roundness deserve to be examined thoroughly.

Despite the elevated strength in the *Proconsul* hallux relative to *Macaca*, the magnitude and patterning of strength is very similar to *Macaca.* Figure 5.35 should be interpreted with caution as individual results from *Proconsul* are being compared with means of *Pan* (n = 33) and *Macaca* (n = 21). However, the similarity between KPS III and the *Pan* pattern is worth pointing out and it is obvious that aside from having similar

cross-sectional area (CA), the *Proconsul* hallux is adapted to withstand stronger forces than the *Macaca* hallux, relative to the rest of the metatarsals.

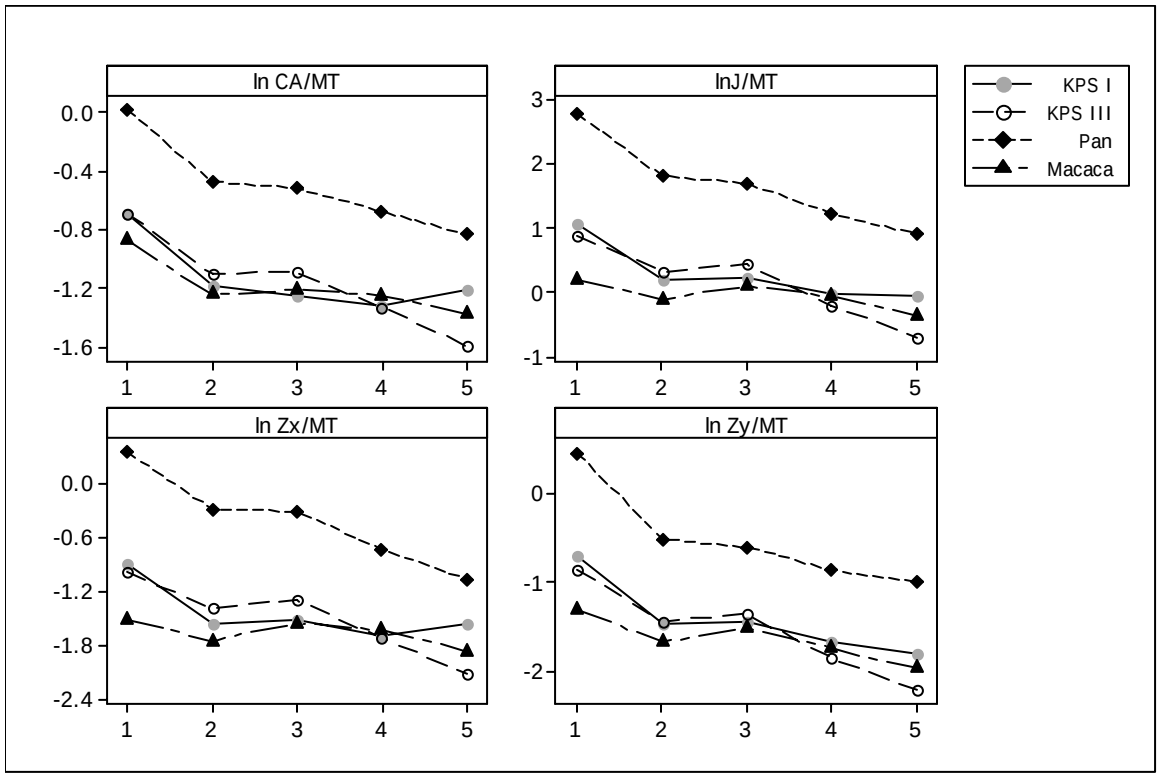

Figure 5.35. Mean cross-sectional properties of the metatarsals of adult (age group 5) *Pan troglodytes* and *Macaca mulatta* with KPS III (adult female) and KPS 1 (subadult male, age group 4).

The pattern of metatarsal CSG across the *Proconsul* foot may reflect the orientation of the functional axis, whether or not it runs through the third metatarsal (as in cercopithecines) or between the first and second (as in platyrrhines, colobines, and hominoids including humans) (Meldrum, 1991). Having the axis of the foot located on the third digit (as opposed to prosimian feet where the axis is on the fourth digit) indicates a lower degree of lateral or peroneal development of the foot and thus implies less use of vertical supports (Walker, 1974). Furthermore a foot with a longer third digit is better for use on horizontal supports, terrestrial or arboreal, because it is symmetrical.

The asymmetrical platyrrhine, colobine and hominoid pattern is to do with arboreality in all but humans which utilize the assymmetrical axis in bipedalism.

Since the pattern of strength properties in *Proconsul* seem to distinguish more between MT1 and the rest of the metatarsals in comparison to *Macaca*, this indicates that the hallux is participating more in locomotion in *Proconsul.* It may also indicate that the functional axis of the foot is not running through the third metatarsal like *Macaca,* that it is located more towards the strong hallux. CSG properties of platyrrhine and colobine metatarsals would help test whether or not this is a valid assumption.

How well does CSG compare with plantar pressure data? Wunderlich (1999) performed plantar pressure studies on *Pan troglodytes* and *Macaca fascicularis* (long-tailed macaques). She compared forces at the metatarsal heads during walking on the ground and on a horizontal pole and her data is plotted with the CSG data for *P. troglodytes* and *M. mulatta* (which can be assumed to have the same locomotion as *M. fascicularis*) (Figures 5.36 and 5.37).

Pressures are distributed more equally across the metatarsals in *Macaca* than in *Pan* which has the highest peak plantar pressure at MT1 on the ground and at MT2 on the pole. *M. fascicularis* has the highest peak plantar pressure at the third metatarsal while walking both on the ground and on a pole.

CSG properties across the metatarsals in *Pan* align with peak plantar pressure while walking on the ground and those for *Macaca* align with both ground and pole walking. The results for *Pan* are indicating that ground reaction force is driving adaptation in the metatarsals rather than muscular force endured during climbing. The first metatarsal is enduring greater forces while walking terrestrially than while climbing.

Forces on the first distal phalanx were as high as MT2 and MT3 for *Pan* on the pole, but forces on MT1 were not as high (Wunderlich, 1999).

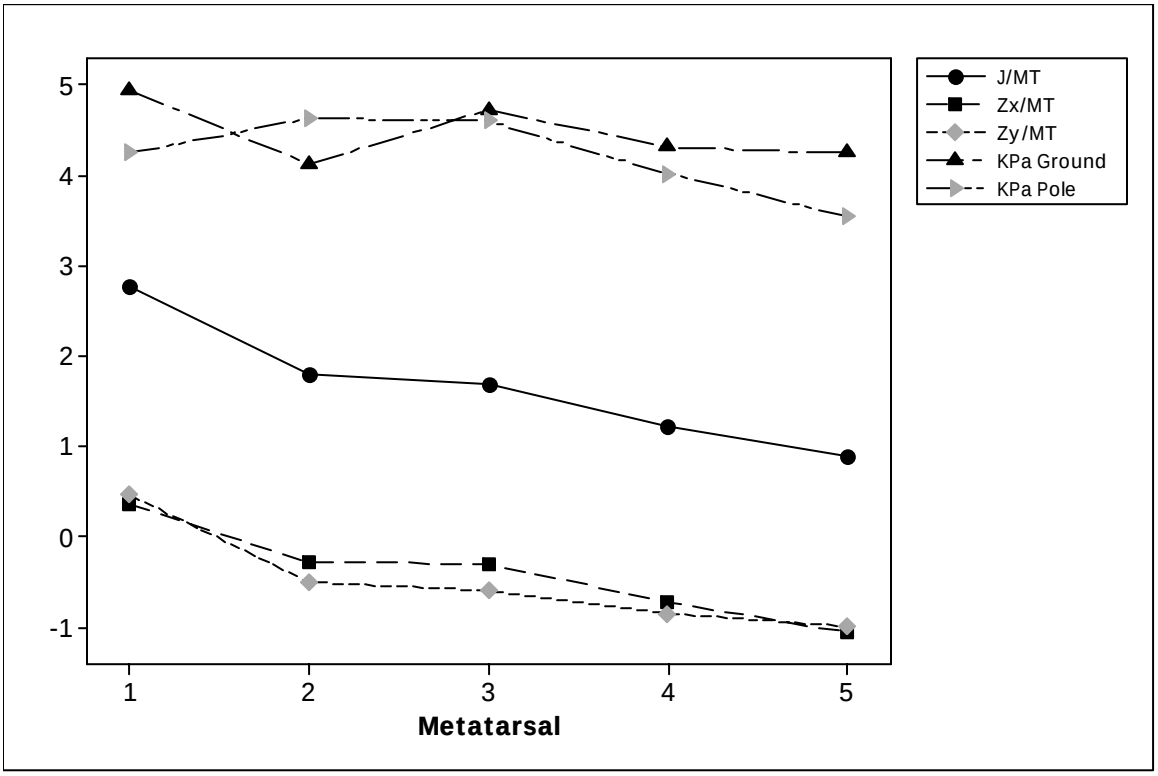

Figure 5.36. Cross-sectional properties of *Pan troglodytes* metatarsals and average regional peak plantar pressure (KPa) for walking on the ground and on a pole, estimated from Figures 3.7a and 3.8a in Wunderlich (1999). All data are natural log-transformed.

Proconsul heseloni body mass is between 10-12 kg and the two male *Pan troglodytes* used by Wunderlich, if normal, averaged about 60 kg (data were not available). Ground reaction forces for *Pan* will be much larger, so it is not necessarily true that the *Proconsul* hallux is strong to endure ground reaction forces while walking terrestrially like *Pan*. It is probable that the long hallux was enduring more ground reaction forces than the short hallux of *Macaca*, but it is also likely that the hallux was also enduring relatively large muscular forces during climbing.

Since *Macaca* uses much of the same positioning when walking regardless if whether it is on the ground or on a pole, it is not possible from these CSG data to determine whether strength of the metatarsals are a response to walking on the ground or on the pole.

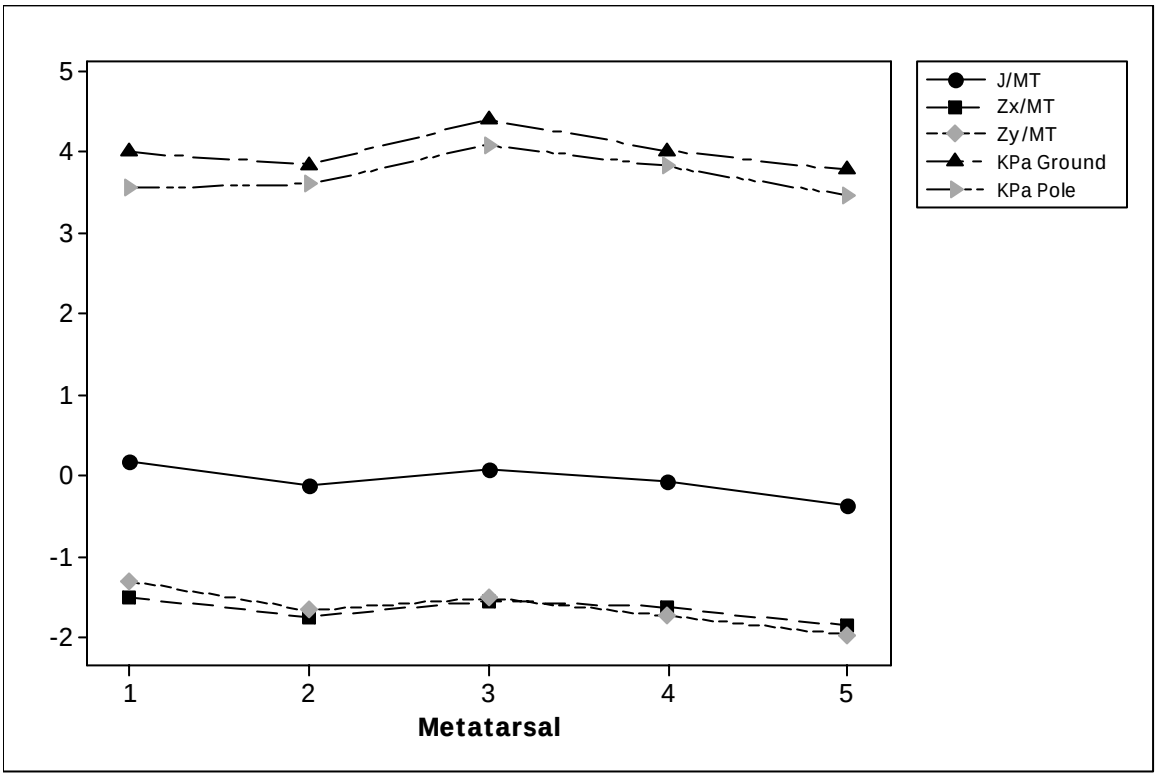

Figure 5.37. Cross-sectional properties of *Macaca mulatta* metatarsals and average regional peak plantar pressure (KPa) for *Macaca fascicularis* while walking on the ground and on a pole, estimated from Figures 3.13a and 3.14a in Wunderlich (1999). All data are natural log-transformed.

Collection of plantar pressures while climbing vertical poles or from other species such as cebids and colobines may completely change these interpretations as they may better explain the high CSG properties of the MT1 in *Pan* and *Proconsul.*

Chapter 6

SUMMARY, CONCLUSIONS & FUTURE RESEARCH

Comparative anatomy and proportions of the *Proconsul heseloni* pedal remains from the Kaswanga Primate Site describe a primate with a foot and hindlimb adapted for an arboreal life like that of certain cercopithecoids. These results support earlier interpretations made on much less abundant fossil evidence (Langdon, 1986). The older individuals in particular (KPS VIII (subadult female, age group 4); KPS I (subadult male, age group 4); KPS III (adult female, age group 5)) show similar mixtures of a monkey-like tarsus combined with an ape-like metatarsus. Furthermore, cross-sectional geometry analyses also support the generalized arboreal quadruped hypothesis.

The biomechanical units of the *Proconsul* foot most closely approximate similarly sized Old World monkeys and the hallucal proportions most closely resemble arboreal Old World monkeys and apes. With reference to the comparative samples used in this study, the cross-sectional geometry of the *Proconsul* metatarsals is mostly similar to that of *Macaca mulatta* except their halluxes have stronger resistance to torsional and bending forces, approaching that of *Pan.* The pattern of metatarsal cross-sectional geometry (CSG) seen in *Proconsul* may turn out to be the same as that of more arboreal cercopithecoids like *Nasalis* and *Colobus*. The linear foot proportions and the relative strength of the hallux for KNM-RU 2036 support conclusions drawn from CSG analysis of the humerus and femur that find it most similar to modern colobines (Ruff, 2002).

Implications for *Proconsul* Behavior and Life History

Faster growing hindlimbs relative to forelimbs have already been observed in *M. mulatta* (Trotter et al., 1975; Turnquist and Wells, 1994), and additional analyses of the proportions of the feet here support this observation. Many primates besides *M. mulatta* (Figure 6.1) are born with large hands and feet, and experience negative allometric growth in these elements relative to some measure of body size (e.g. *Cebus, Ateles, Saimiri, Propithecus*) (Lawler, 2006). Large feet may develop early so young animals may navigate substrates used by mature animals before they reach adult body size (Jungers and Fleagle, 1980), but the young of other non-arboreal mammals also seem to have large feet, so this hypothesis may not be true.

Figure 6.1. *Macaca mulatta* juvenile on Cayo Santiago with characteristically large feet. Photograph by the author.

The drastic difference between the growth in some *Macaca* hindlimb proportions compared to those of *Gorilla* and *Pan* is signaling different developmental mechanisms. The primitive condition for these three taxa is most likely the *Macaca* condition since it is shared by lemurs and New World monkeys. If large infant feet are primitive, then the derived condition, that of *Gorilla* and *Pan*, is for them to be born with adult foot proportions or small feet.

The adaptation for such large feet so early in development could also be linked to mother-infant behavior. Both macaque and ape infants cling to their mothers early in life. Apes carry and position their bodies with a more upright trunk (Fleagle, 1999) and are likely to be more versatile in their arm positions than macaques. Macaques may use their hindlimbs much more than their forelimbs for clinging to their mothers since macaques are hindlimb driven primates in the first place (Turnquist & Wells, 1994). Larger feet would certainly help a more hindlimb reliant monkey to extend its legs around the mother's belly to cling better while she walks - the same way they would help in grasping arboreal supports that adults are able to use.

How the mothers hold on to the infants is just as important as how the infants cling to their mothers. Chimpanzee and gorilla mothers use their forelimbs to assist clinging infants (see, e.g. Fossey, 1983). And it is probable that macaque mothers hold on much less frequently to their offspring with their forelimbs since they are relying on them more for their own positioning and locomotion. If macaque infants are very literally clinging for their lives to their mothers, then strong, long feet would be a useful adaptation.

Gorillas and chimpanzees spend much longer as dependents on their mothers than macaques (Fleagle, 1999). Perhaps because the ape strategy is not to grow up quickly like macaques, but to grow up slowly with more maternal investment, there is no longer selection for accelerated pedal growth so early on in development. Perhaps in apes, maternal investment has taken the place of needing big feet to cling to mother or to walk like an adult.

The widespread negative allometric growth of the feet in non-hominoid primates is suggested to be maintained by selection acting on foot size in young animals (Lawler, 2006), so a major change in selective pressures for infant foot size and its behavioral correlates occurred with the evolution of the apes. Either selection was released from favoring large infant feet and chimpanzee and gorilla infants are accommodating by clinging better with hands, or selection favored small infant feet.

Body proportions that increase altriciality in the locomotion and positional behavior of infant hominoids are not only connected to increased learning period and intelligence but are also going to affect the dietary habits and social interaction of the mothers. It has been shown that chimpanzee mothers with clinging infants can attain normal daily ranges, but those with older, larger, cotraveling juvenile offspring may be geographically constrained (Pontzer & Wrangham, 2006).

The growth pattern in *Macaca* looks like one where the distal segment of the limb is experiencing an extended period of outgrowth during development. Then this accelerated growth in the foot is brought down to a slower pace after infancy, as normal ontogenetic scaling brings the femur and the calcaneus to adult proportions.

Differential growth rates, which for feet are normally considered in relation to hands, are a major cause of primate limb proportion variation (Chiu and Hamrick, 2002). The loss, gain or rearrangement of *cis*-modules that regulate the spatial and temporal expression of HOX genes for foot development is probably what is affecting phenotypic evolution in the primates (Chiu and Hamrick, 2002; Hallgrimsson et al., 2002; Richardson et al., 2004). Indian hedgehog (Ihh) has been identified as a master regulator of bone development (Kronenberg, 2003). It coordinates the proliferation and differentiation of cartilage cells at the growth plate and mutations in its regulatory regime could be responsible for the derived pre- or peri-natal slow-down of foot growth in great apes.

For now, it appears as though *Proconsul* did not have large feet at birth and may have had a similar condition to chimpanzees and gorillas.

Problematic *Proconsul heseloni* Individuals

KPS IV (infant, age group 1)

This individual grouped with apes more often than many of the others in the analyses of proportions and did not show the ape pattern of CSG across the rays. Several confounding factors need to be more thoroughly investigated in order to sort out these results.

The tarsals of the infant KPS IV are much better formed than similarly-aged monkeys and apes. The bones are not as amorphous and under-developed in appearance as chimpanzees and macaques of the same dental ages. Perhaps *Proconsul* developed earlier than the extant taxa. This may explain its higher than expected proportional

indices. However, is it also possible that KPS IV is not 1.2 years old as predicted by tooth enamel growth. That is, the foot bones which were associated with one another *in situ*, may not be correctly assigned to the teeth which were not associated. The possibility of a mismatch explains some of the unexpected results and patterning and is the most parsimonious explanation. But there are other possibilities that need to be considered.

Clearly, taphonomic deformation could be hampering accurate results, but perhaps *Proconsul* grows very differently from *Macaca, Gorilla* and *Pan.* Another possibility is that KPS IV is a young *Proconsul nyanzae*. It shows larger proportions than expected for its age which is what the bigger species from Rusinga Island would presumably show. However, when KPS IV is assigned to older age groups, the growth trajectories are no more similar or dissimilar to the comparative samples (not shown).

Moreover, Beynon and colleagues (1998) posited that *P. nyanzae* may grow differently from *P. heseloni*. This explanation, however, would not account for the perceived disconnect between dental age and tarsal development.

Another, albeit remote, possibility is that KPS IV belongs to an unknown, more ape-like species than the other individuals. However, there are only *Proconsul* teeth present at the site, which makes the presence of an unknown ape-like species a very slim possibility. In this new light, a more detailed re-evaluation and possible reassignment of the bones to individuals, as well as the discovery of immature *P. nyanzae* skeletons will both be helpful for solving this issue.

Until the younger comparative sample is augmented, the CSG of the KPS IV metatarsals were only compared to infant *Pan.* Without the hallux midshaft properties (which were unattainable with microCT), all that is discernable is that the CSG properties

are lower in magnitude than expected for average *Pan*, but this is expected for smaller-bodied *Proconsul*.

KPS VII (juvenile, age group 3)

KPS VII often showed proportions associated with the calcaneus and the third metatarsal that differed from, or caused it to stray from the patterning of, the other *Proconsuls*. The left calcaneus is the best preserved of the two and shows damage at the tuber. Perhaps due to deformation, the length measurement is not quite as long as it should be, but it appears as though a good measure of calcaneus length has been made and is employed here. The third metatarsal measure is estimated from fragments and is seemingly too long. Aside from errors in reconstructing the third metatarsal, it is also very possible that since this individual's feet were not associated *in situ*, perhaps some bones of this individual were grouped incorrectly. Now that the metrics have been analyzed and this individual appears to be anomalous in many respects, the problem should be sorted out with the collection in Nairobi.

Suggestions for Future Research

Functional Morphology

The exquisite preservation and the abundance of repeated elements in the KPS collection provide a wonderful opportunity to perform detailed functional analyses on the tendon, ligament and muscle attachment sites and also on the joint surfaces of these *Proconsul* foot bones. Three-dimensional morphometrics could be a way to quantify overall shape and joint surface morphology of the tarsals in order to compare shape to living taxa and to reconstruct function. Many of the KPS elements are deformed from

taphonomic processes during fossilization which would make three-dimensional analyses difficult for most of the bones without first implementing a reconstructive technique. However, there are a plethora of associated and isolated tarsal bones of *Proconsul* and other Miocene primates in Kenya, many of which are perfectly preserved with no deformation, including KNM-RU 2036.

The metatarsal curvature of the ontogenetic samples of macaques and chimpanzees can be assessed from the radiographs taken for the CSG study, making it possible to test Preuschoft's (1970) prediction that there is correlation between metatarsal curvature and CSG. It is obvious to the naked eye that *Pan troglodytes* metatarsals are curvier than those of *M. mulatta* and, relative to body size and metatarsal length, they are also stronger. There is variation in curvature across the rays in both taxa and the hypothesis should be tested that curvature and strength properties (particularly in the plane of the curvature) are correlated.

Comparative Sample

In order to test the behavioral hypotheses for enlarged macaque infant feet, the cross-sectional geometry of infant macaque metatarsals and a larger sample of infant chimpanzee metatarsals should be analyzed. Infant chimpanzees were poorly sampled in this study because few were available at institutions where x-ray was available. The best collection of infant chimpanzees is located at the Powell-Cotton Museum where there is no x-ray imaging equipment. Macaques in age groups 1 and 2 were not analyzed in this study because they were too small for plane-film x-ray and will require borrowing

specimens from the Cayo Santiago collection to scan with microCT (currently in progress).

If infant macaques are using their feet like adults, then - according to "Wolff's law" or "bone functional adaptation" - their metatarsal CSG properties should be relatively stronger when compared with adults than infant chimpanzee metatarsals or macaque metatarsal CSG properties should be exceedingly stronger in the feet than the hands compared to chimpanzee infants.

Since neither *Macaca mulatta* nor *Pan troglodytes* are extremely arboreal in their locomotor adaptations they may be considered by some to be too highly terrestrial to compare fairly with *Proconsul,* especially as the only two models. Furthermore, both chimpanzees and macaques are derived compared to *Proconsul* and it has been proposed that some New World monkeys, like many cebids that are generalized arboreal quadrupeds, may represent closer functional analogues to *Proconsul.*

To test the suggestions of Rose (1983) and others that *Proconsul* postcrania, particularly the feet, may be adapted for a similar locomotor repertoire to that used by cebids, the proportions, growth and particularly the CSG of cebid foot bones need to be analyzed and compared to *Proconsul.* Although they are phylogenetically distant from *Proconsul* (having diverged from the catarrhines about 15 million years prior to the existence of *Proconsul*), some New World monkeys may be good models for a monkey that uses its feet like an ape. It may be best to consider apes as using their feet like cebids, with many Old World monkeys displaying derived traits. The CSG properties of cebid metatarsals were not analyzed in this study because ontogenetic samples are difficult to find, but finding such samples is the next step in the larger project. Even without growth

data, an adult cebid sample would be highly informative. The CSG of a New World monkey would also help discern scaling and functional patterns among the other taxa while allowing a wider phylogenetic perspective.

Furthermore, if the metatarsal CSG through ontogeny of gorillas were analyzed, it would be possible to study the effect of more exaggerated body size increase on the development of metatarsal cortical bone strength properties. It is also important to glean CSG data from a more arboreal Old World monkey, something more similar to the proportions of *Proconsul* like *Nasalis* or *Colobus*.

A broader comparative sample will aid in teasing apart, cladistically, primitive from derived traits of the foot and hindlimb. The mosaic of features in *Proconsul* contain more information about evolution than simply how the animal moved about 18 million years ago.

Evolution of Hominin Foot and Bipedalism

Analyzing the morphology of extant apes and monkeys to reconstruct the evolution of feet through the catarrhines, especially that of the pre-bipedal ancestors to hominins, is what most researchers interested in human foot evolution have done (e.g. Morton, 1922, 1924; Manley-Buser, 1991). There are very few foot fossils from early in the hominin record with which to work on reconstructing foot evolution, and even those are normally isolated bones. The KPS *Proconsul* feet represent the earliest complete feet in the hominoid lineage. Not only will the results here help toward establishing an evolutionary trajectory of the evolution of the bipedal hominin foot, but the data collected

on modern feet (both linear metrics as well as cross-sectional geometry) will be useful for interpreting other fossil pedal remains from species in the later Miocene and Pliocene.

If there is a correlation between metatarsal strength and the transition to bipedalism in infants, that transition may be studied in hominins. There is a change in humeral to femoral strength proportions as well as in long bone trabecular structures corresponding to the adoption of bipedalism in infants (Ruff, 2003b; Ryan and Krovitz, 2006). It is possible that early hominin species made the transition earlier since there is growing evidence from tooth microstructure that they grew up faster than modern humans did (Dean et al., 2001). When humans are analyzed the same way macaques, gorillas, and chimpanzees have been analyzed here, it will be possible to compare ontogeny of hindlimb proportions and also metatarsal strength with that of the juvenile *A. afarensis* partial skeleton from Dikika, Ethiopia (Alemseged et al., 2006).

Remaining Questions

A major confounding factor in reconstructing *Proconsul* locomotion may be its lack of a tail (Ward & Walker, 1991; Nakatsukasa et al., 2004). *Proconsul's* generic arboreal skeletal morphology is often compared to cebids like *Ateles* and *Alouatta* but these monkeys use their long prehensile tail in their predominantly below-branch suspensory behavior. It may be that the morphological mosaic that makes Miocene hominoids unique compared to living taxa is just as much due to phylogeny as to accommodations made by a highly arboreal primate that does not have the aid of a tail to navigate in the trees. So far, such accommodations for maintaining balance on arboreal

supports without the aid of a tail have been suggested to have evolved in the hominoid elbow (Larson & Stern, 2005).

There are also remaining questions surrounding the difference in body size of the different *Proconsul* species. The current consensus is that *P. heseloni* shares functional morphology throughout the skeleton with the much larger *P. nyanzae.* Larger animals tend to have straighter limbs and move with more erect posture, while smaller ones are able to tolerate crouched limb postures due to the smaller ratio of extensor muscle moment arms (EMA) versus the ground reaction force moment arm (Polk, 2002). If body size within *Proconsul* ranges large enough to affect EMA and hence differences in crouched or erect limb postures, then these postures may be evident in the functional morphology of the limb. Since, so far, no one has identified any differences in functional morphology between the species, EMA differences have not been estimated either.

Conclusion

The nature and patterning of the *Proconsul* skeletal mosaic may provide insights into the process of evolution. After an in-depth analysis of the *Proconsul* pelvis and vertebral column, Carol Ward (1991) observed that *Proconsul* does not show the axial adaptations consistent with versatile arboreality like that seen in the apes, yet its limb mobility, especially at the hip, and its powerful grasping hands and feet (which is supported here) indicate arboreal adaptations. So perhaps this mosaic we are witnessing in *Proconsul* with a pronograde quadrupedally adapted axial skeleton supported by more mobile limbs is the result of early stages of natural selection preferring arboreal adaptations (Ward, 1991). Whether or not these arboreal adaptations are signaling a shift

to ape-like arboreality or a shift in the nature of arboreality within the broader catarrhine lineage is not yet evident from the foot and hindlimb analysis here.

The interesting morphological mix that is apparent in the *Proconsul* foot and throughout the entire *Proconsul* skeleton caused Rose to suggest we should not strive to determine whether *Proconsul* is monkey-like or ape-like. According to Rose (1983) it is neither: it is simply Miocene hominoid-like and we should be comparing living primates to the Miocene ones rather than the other way around. However, the only way to bring an 18 million-year-old extinct animal back to life is to understand the mechanics of its anatomy with the help of extant animals with known locomotor behaviors.

The collection from the Kaswanga Primate Site provides an unusual amount of fossil foot material so that the state of preservation, the comparative anatomy, the proportions, and the metatarsal cross-sectional geometry could be described and analyzed. When added to the body of research on the *Proconsul* foot and overall skeletal function, these findings contribute to the reconstruction of *Proconsul* paleobiology: its locomotion and positional behavior, with implications for life history and phylogeny. Comparisons across a wider range of taxa will contribute knowledge towards this goal, and so will the identification of the genetic regulators of limb growth and their timing during development. Of course, the discovery of more hominoid fossils will most definitely aid in pinning down *Proconsul's* evolutionary and bodily position in the tree.

LITERATURE CITED

Aiello L, Wood B, Key C, Lewis M. 1999. Morphological and taxonomic affinities of the Olduvai ulna (OH 36). American Journal of Physical Anthropology 109*:*89-110.

Alberch P. 1990. Natural selection and developmental constraints: External versus internal determinants of order in nature. In CJ DeRousseau (ed): Primate life History and Evolution. New York: Wiley-Liss, pp. 15-35.

Alemseged Z, Spoor F, Kimbel WH, Bobe R, Geraads D, Reed D, Wynn JG. 2006. A juvenile early hominin skeleton from Dikika, Ethiopia. Nature 443: 296-301.

Andrews P. 1981. A short history of Miocene field palaeontology in Western Kenya. Journal of Human Evolution 10*:*3-9.

Andrews P. 1985. Family group systematics and evolution among catarrhine primates. In Delson E (ed): Ancestors: The Hard Evidence. New York: Alan R. Liss, pp. 14-22.

Andrews PJ, Martin L. 1987.Cladistic relationships of extant and fossil hominoids. J Hum Evol 16: 101-118.

Andrews P, Van Couvering JA. 1975. Palaeoenvironments in the East African Miocene. In FS Szalay (ed.): Approaches to Primate Paleobiology. Basel: Karger, pp. 62-103.

Bacon AM. 1994. New correlations between knee and ankle in Miocene and Plio-Pleistocene primates. Current Primatology 1*:*273-283.

Balakrishnamma S, Ganapathiraju A. 2003. Linear Discriminant Analysis – A Brief Tutorial: Institute for Signal and Information Processing.

Barnett CH, Napier JA. 1952. The axis of rotation at the ankle joint. J. Anat. 86*:*1-9.

Barnicot NA, Hardy R. 1955. The position of the hallux in west Africans. J. Anat. 89*:*355-361.

Bass S, Saxon L, Daly R, Turner C, Robling A, Seeman E, Stuckey S. 2002. The effect of mechanical loading on the size and shape of bone in pre-, peri, and postpubertal girls: a study in tennis players. Journal of Bone Mineral Research 17*:*2274-2280.

Beard, K. C., M. F. Teaford and A. Walker. 1993. New hand bones of the early Miocene hominoid *Proconsul* and their implications for the evolution of the hominoid wrist. Pp. 387-403 in Hands of Primates (H. Preuschoft and D. J. Chivers, eds.). Springer-Verlag, Vienna.

Begun DR. 2002. European hominoids. In WC Hartwig (ed.): The Primate Fossil Record. Cambridge: Cambridge University Press, pp. 339-368.

Begun DR, Teaford MF, Walker A. 1994. Comparative and functional anatomy of *Proconsul* phalanges from the Kaswanga Primate Site, Rusinga Island, Kenya. Journal of Human Evolution 26*:*89-165.

Bertram JEA, Biewener AA. 1988. Bone curvature: Sacrificing strength for load predictability. J. Theor. Biol. 131*:*75-92.

Bertram JEA, and Swartz SM. 1991. The law of bone trasformation: a case of crying Wolff? Biol Rev 66*:*245-273.

Beynon AD, Dean MC, Leakey MG, Reid DJ, and Walker A. 1998. Comparative dental development and microstructure of *Proconsul* teeth from Rusinga Island, Kenya. Journal of Human Evolution 35*:*163-209.

Bloch J, Boyer D. 2002. Grasping Primate Origins. Science 298*:*1606-1610.

Brain CK. 1981. The Hunters or the Hunted? Chicago: Chicago University Press.

Cant JGH. 1986. Locomotion and feeding postures of spider and howling monkeys: Field study and evolutonary interpretation. Folia Primatologica 46*:*1-14.

Carlson KJ, Pickering TR. 2003. Intrinsic qualities of primate bones as predictors of skeletal element representation in modern and fossil carnivore feeding assemblages. Journal of Human Evolution 44*:*431-450.

Cartmill M. 1972. Arboreal adaptations and the origin of the order Primates. In Tuttle R (ed): The Functional and Evolutionary Biology of Primates. Chicago: Aldine-Atherton, pp. 97-122.

Cartmill M. 1974. Pads and claws in arboreal locomotion. In Jenkins FA (ed): Primate Locomotioin. New York: Academic Press, pp. 45-83.

Cheverud J, M. 1981. Epiphyseal union and dental eruption in *Macaca mulatta*. American Journal of Physical Anthropology 56*:*157-167.

Chiu C, Hamrick MW. 2002. Evolution and development of the primate limb skeleton. Evol Anthropol 11: 94-107.

Conroy GC, Rose MD. 1983. The evolution of the primate foot from the earliest primates to the Miocene hominoids. Foot & Ankle 3*:*342-364.

Cowin SC. 2001. Mechanics of materials. In Cowin SC (ed): Bone biomechanics handbook, 2nd ed. Boca Raton: CRC Press.

Currey JD. 2002. Bones: structure and mechanics. Princeton: Princeton University Press.

Daegling DJ. 2002. Estimation of torsional rigidity in primate long bones. J Hum Evol 42: 229-39.

Dagosto M. 1988. Implications of postcranial evidence for the origin of euprimates. Journal of Human Evolution 17*:*35-57.

Dagosto M. 1983. Postcranium of *Adapis parisiensis* and *Leptadapis magnus* (Adapiformes, Primates): adaptations and phylogenetic significance. Folia Primatol 41: 49-101.

Day MH, Wood BA. 1969. Hominoid tali from East Africa.Nature 222: 591-592.

Day MH, Napier JA. 1964. Fossil foot bones. Nature 201*:*969-970.

Dean MC, Wood BA. 1981. Developing pongid dentition and its use for aging individual crania in comparative cross-sectional growth studies. Folia Primatologica 36*:*111-127.

Dean C, Leakey MG, Reid D, Schrenk F, Schwartz GT, Stringer C, and Walker A. 2001. Growth processes in teeth distinguish modern humans from *Homo erectus* and earlier hominins. Nature 414: 628-631.

Decker RL, Szalay FS. 1974. Origins, evolution and function of the tarsus in late Cretaceous eutherians and Paleocene primates. In FA Jenkins (ed.): Primate Locomotion. New York: Academic Press, pp. 261-292.

Demes B, and Jungers WL. 1993. Long bone cross-sectional dimensions, locomotor adaptations and body size in prosimian primates. Journal of Human Evolution 25*:*57-74.

Demes B, Stern JT, Hausman MR, Larson SG, McLeod KJ, Rubin CT. 1998. Patterns of strain in the macaque ulna during functional activity. Am J phys Anthropol 106:87-100.

Demes B, Qin Y-X, Stern JT, Larson SG, Rubin CT. 2001. Patterns of strain in the macaque tibia during functional activity . Am J Phys anthropol 116: 257-265.

DeRousseau CJ. 1985a. Aging in the musculoskeletal system of rhesus monkeys. II. Degenerative joint disease. Am J Phys Anthropol 67:177-184.

DeRousseau CJ. 1985b. Aging in the musculoskeletal system of rhesus monkeys. III. Bone loss. Am J Phys Anthropol 68:157-167.

Doran DM. 1993. Comparative locomotor behavior of chimpanzees and bonobos: The influence of morphology on locomotion. American Journal of Physical Anthropology 91:83-98.

Doran DM. 1997. Ontogeny of locomotion in mountain gorillas and chimpanzees. Journal of Human Evolution 32:323-344.

Drake RE, Van Couvering JA, Pickford MH, Curtis GH, Harris JA. 1988. New chronology for the Early Miocene mammalian faunas of Kisingiri, Western Kenya. J Geological Society 145(3): 479-491.

Duren DL. 2001. Physeal orientation, form and function: relationships with primate locomotor behavior. Dissertation, Kent State University.

Elftman HO, Manter JT. 1935. The evolution of the human foot with special reference to the joints. J. Anat. Lond. 70:56-67.

Falk D. 1983. A reconsideration of the endocast of *Proconsul africanus*: implications for primate brain evolution. In Ciochon RL, Corruncini RS (eds): New Interpretations of Ape and Human Ancestry. New York: Plenum Press, pp. 239-248.

Fleagle JB. 1976. Locomotion and posture of the Malayan siamang and implications for hominoid evolution. Folia Primatologica 26:245-269.

Fleagle JB. 1999. Primate Adaptation and Evolution, second edition. San Diego: Academic Press.

Fossey D. 1983. Gorillas in the Mist. Boston: Houghton-Mifflin.

Gavan JA. 1967. Eruption of primate deciduous dentition: A comparative study. J Dent Res 46:984-988.

Gebo DL. 1988. Foot morphology and locomotor adaptations in Eocene primates. Folia Primatol 50: 3-41.

Gebo DL. 1992. Plantigrady and foot adaptation in African apes: implications for hominid evolution. American Journal of Physical Anthropology 89:29-58.

Gebo DL. 1993. Functional morphology of the foot in primates. In DL Gebo (ed.): Postcranial adaptation in nonhuman primates. Dekalb: Northern Illinois University Press, pp. 175-196.

Gebo DL, Dagosto M, Rose MD. 1991. Foot morphology and evolution in early Eocene *Cantius*. Am J Phys Anthropol 86: 51-73.

Gebo DL, MacLatchy L, Kityo LR Deino A, Kingston J. 1997.A hominoid genus from the Early Miocene of Uganda. Science 276: 401-4.

Gebo DL, Dagosto M, Beard KC, Qi T. 2001. Middle Eocene primate tarsals from China: Implications for haplorhine evolution. American Journal of Physical Anthropology 116*:*83-107.

Gebo DL, Dagosto M, Beard KC, Qi T, Wang J. 2000. The oldest known anthropoid postcranial fossils and the early evolution of higher primates. Nature 404*:*275-278.

Goodall JG. 1962. Nest building behavior in the free ranging chimpanzee. Annals of the New York Academy of Sciences 102*:*455-467.

Goodall JG. 1965. Chimpanzees of the Gombe Stream Reserve. In I Devore (ed.): Primate Behavior. New York: Hold, Rinehart and Winston, pp. 425-473.

Goodall JG. 1986. The Chimpanzees of Gombe. Cambridge, Ma: Belknap Press of Harvard University Press.

Gould SJ. 1966. Allometry and size in ontogeny and phylogeny. Biological Reviews 41:587-640.

Gould SJ. 1977. Ontogeny and Phylogeny.Cambridge: Harvard University Press.

Gregory WK. 1920. On the structure and relations of *Notharctus*, an American Eocene primate. Mem. Amer. Mus. Nat. Hist. 3*:*51-243.

Griffin NL, Richmond BG. 2005. Cross-sectional geometry of the human forefoot. Bone 37*:*23-260.

Haapasalo H, Kontulainen S, Sievanen H, Kannus P, Jarvinen M, Vuori I. 2000. Exercise-induced bone gain is due to enlargement in bone size without a change in volumetric bone density: a peripheral quantitative computed tomography study of the upper arms of male tennis players. Bone 27*:*351-357.

Hallgrimsson B, Willmore K, Hall BK. 2002. Canalization, developmental stability, and morphological integration in primate limbs. Yrbk Phys Anthropol 45: 131-158.

Harrison T. 1982. Small-Bodied Apes from the Miocene of East Africa. Ph.D. thesis, University of London.

Harrison T. 1987. The phylogenetic relationships of the early catarrhine primates: a review of the current evidence. J Hum Evol 16: 41-80.

Harrison T. 1989. New postcranial remains of *Victoriapithecus* from the middle Miocene of Kenya. Journal of Human Evolution 18*:*3-54.

Harrison T. 1993. Cladistic concepts and the species problem in hominoid evolution. In Kimbel WH, Martin LB (eds): Species, Species Concepts, and Primate Evolution. New York: Plenum Press, 345-371.

Harrison T. 2002. Late Oligocene to middle Miocene catarrhines from Afro-Arabia. In Hartwig W (ed): The Primate Fossil Record. Cambridge: Cambridge University press, P 311-338.

Hildebrand M. 1988. Analysis of Vertebrate Structure, 3rd edition. New York: John Wiley & Sons, Inc.

Hopwood AT. 1933. Miocene primates from Kenya. J. Linn. Soc. London, Zool. 38*:*437-464.

Hunt KD. 2004. The special demands of great ape locomotion and posture. In AE Russon and DR Begun (eds.): The Evolution of Thought: Evolutionary Origins of Great Ape Intelligence. Cambridge: Cambridge University Press, pp. 172-189.

Inouye SE. 1992. Ontogeny and allometry of African ape manual rays. Journal of Human Evolution 23*:*102-138.

Inouye SE. 1994. Ontogeny of knuckle-walking hand postures in African apes. Journal of Human Evolution 26*:*459-485.

Ishida H, Kunimatsu Y, Takano T, Nakano Y, Nakatsukasa M. 2004. *Nacholapithecus* skeleton from the middle Miocene of Kenya. Journal of Human Evolution 46*:*69-103.

Jones H, Priest J, Hayes W, Tichenor C, Nagel D. 1977. Humeral hypertophy in response to exercise. Journal of Bone and Joint Surgery 59*:*204-208.

Jungers WL. 1985. Size and scaling in primate biology. New York: Plenum Press.

Jungers WL, Fleagle JG. 1980. Postnatal growth allometry of the extremeties in *Cebus albifrons* and *Cebus apella*: a longitudinal and comparative study. Am J Phys Anthropol 53: 471-478.

Jungers WL, Falsetti A, and Wall C. 1995. Shape, relative size and size-adjustments in morphometrics. Yearbook of Physical Anthropology 38*:*137-161.

Kay RF. Ungar PS. 1997. Dental evidence for diet in some Miocene catarrhines with comments on the effects of phylogeny on the interpretation of adaptation. In

Function, Phylogeny, and Fossils: Miocene Hominoid Evolution and Adaptations. Begun DR, Ward CV, Rose MD. New York: Plenum Press, pp. 131-151.

Keith A. 1923. Man's posture: Its evolution and disorders. Brit Med J 1*:*451-454, 499-502, 545-548, 587-590, 624-626, 669-672.

Keith A. 1929. The history of the human foot and its bearing on orthopaedic practice. Journal of Bone and Joint Surgery 9*:*10-32.

Kelley J. 1995. Sex Determination in Miocene catarrhine primates. American Journal of Physical Anthropology 96*:*391-417.

Kelley J. 1997. Paleobiological and phylogenetic significance of life history in Miocene hominoids. In Begun DR, Ward CV, Rose MC (eds): Function, Phylogeny, and Fossils: Miocene Hominoid Evolution and Adaptation. New York: Plenum Press, pp. 173-208.

Kenney EB. 1975. Development and eruption of teeth in Rhesus. In GH Bourne (ed.): The Rhesus Monkey, Volume 1: Anatomy and Physiology. New York: Academic Press, pp. 145-167.

Kimura T. 2003. Differentiation between fore-and hindlimb bones and locomotor behaviour in primates. Folia Primatologica 74*:*17-32.

Kontulainen S, Sievanen H, Kannus P, Pasanen M, Vuori I. 2003. Effect of long-term impact-loading on mass, size, and estimated strength of humerus and radius of female raquet-sports players: a peripheral quantitative computed tomography study between young and old starters and controls. Journal of Bone Mineral Research 18*:*352-359.

Kronenberg HM. 2003. Developmental regulation of the growth plate. Nature 423:332-336.

Kuykendall KL. 1996. Dental development in chimpanzees (*Pan troglodytes*): the timing of tooth calcification stages. Am J Phys Anthropol 99: 135–157.

Kuykendall KL, Conroy GC. 1996. Permanent tooth calcification in chimpanzees (*Pan troglodytes*): Patterns and polymorphisms. Am J Phys Anthropol 99(1): 159-174.

Langdon JH. 1986. Functional morphology of the Miocene hominoid foot. Basel: Karger.

Larson SG, Stern JT. 2005. Maintenance of above-branch balance during primate arboreal quadrupedalism: Coordinated use of forearm rotators and tail motion. Am J Phys Anthropol 129(1): 71-81.

Lawler RR. 2006. Sifaka positional behavior: Ontogenetic and quantitative genetic approaches. Am J Phys Anthropol: in press.

Le Gros Clark WE, Leakey LSB. 1951. The Miocene Hominoidea of East Africa: Fossil Mammals of East Africa. London: British Museum of Natural History, pp. 1-117.

Leakey MG, Walker A. 1997. *Afropithecus* function and phylogeny. In DR Begun and E al. (eds.): Function, Phylogeny, and Fossils: Miocene Hominoid Evolution and Adaptations. New York: Plenum Press.

Leakey RE, Leakey MG, Walker A. 1988. Morphology of *Afropithecus turkanensis* from Kenya. American Journal of Physical Anthropology 76*:*289-307.

Leigh SR, Setchell JM, Buchanan LS. 2005. Ontogenetic bases of canine dimorphism in anthropoid primates. American Journal of Physical Anthropology 127*:*296-311.

Leigh SR, Shea BT. 1995. Ontogeny and the evolution of adult body size dimorphism in apes. American Journal of Primatology 36*:*37-60.

Leigh SR, Shea BT. 1996. Ontogeny of body size variation in African apes. American Journal of Physical Anthropology 99*:*43-66.

Lewis OJ. 1972. The evolution of the hallucial tarsometatarsal joint of the Anthropoidea. American Journal of Physical Anthropology 37*:*13-34.

Lewis OJ. 1980. The joints of the evolving foot. Part III. The fossil evidence. J. Anat. 131*:*275-298.

Lewis OJ. 1989. Functional morphology of the evolving hand and foot. Oxford: Clarendon Press.

Li Y, Crompton RH, Gunther M, Wang W, Savage R. 2002. Reconstructing the mechanics of quadrupedalism in an extinct hominoid. Z. Morphol. Anthropol. 83*:*265-274.

Lieberman D, Pearson O, Polk JD, Demes B, Crompton A. 2003. Optimization of bone growth and remodeling in response to loading in tapered mammalian limbs. Journal of Experimental Biology 206*:*3125-3138.

Lieberman DE, Polk JD, Demes B. 2004. Predicting long bone loading from cross sectional geometry. Am J Phys Anthropol 123(2): 156-171.

Lisowski FP. 1967. Angular growth changes and comparisons in the primate talus. Folia Primatologica 7*:*81-97.

Lockwood C, Richmond B, Jungers WL, Kimbel WH. 1996. Randomization procedures and sexual dimorphism in *Australopithecus afarensis*. Journal of Human Evolution 31*:*537-548.

Lovejoy CO, Cohn MF, White TD. 1999. Morphological analysis of the mammalian postcranium: a devlopmental perspective. Proc National Acad Sci (U.S.) 96: 13247-13252.

Luo Z-X, Ji Q, Wible JR, Yuan C-X. 2003. An early Cretaceous tribosphenic mammal and metatherian evolution. Science 302*:*1934-1940.

MacLatchy L, Gebo D, Kityo R, Pilbeam D. 2000. Postcranial functional morphology of *Morotopithecus bishopi*, with implications for the evolution of modern ape locomotion. J Hum Evol 39(2): 159-83.

MacLatchy L, Rossie JB. 2005. The Napak Hominoid: Still *Proconsul major*. In D Lieberman, R Smith and J Kelley (eds): Interpreting the Past: Essays on Human, Primate, and Mammal Evolution in Honor of David Pilbeam. Boston: Brill Academic Publishers, Inc., pp. 15-28.

Madar SI, Rose MD, Kelley J, MacLatchy L, Pilbeam D. 2002. New *Sivapithecus* postcranial specimens from the Siwaliks of Pakistan. Journal of Human Evolution 42*:*705-752.

Malenky RK, Kuroda S, Vineberg EO. 2004. The significance of terrestrial herbaceous foods for bonobos, chimpanzees and gorillas. In RW Wrangham, WC McGrew, FB de Waal and PG Heltne (eds.): Chimpanzee Cultures. Cambridge, MA: Harvard University Press.

Manley-Buser KA. 1991. A Heterochronic Study of the Hominoid Foot, University of California, Davis.

Marchi D. 2005. The cross-sectional geometry of the hand and foot bones of the Hominoidea and its relationship to locomotor behavior. Journal of Human Evolution 49*:*743-761.

Martin RD. Towards a new definition of Primates. Man 3: 377-401.

Martin RB, Burr DB, Sharkey NA. 1998. Skeletal Tissue Mechanics. New York: Springer-Verlag, Inc.

Maynard-Smith J, Savage R. 1956. Some locomotory adaptations in mammals. J Linn Soc Zool 42: 603-622.

McCrossin ML, Benefit BR. 1997. On the relationships and adaptations of *Kenyapithecus*, a large-bodied hominoid from the middle Miocene of eastern

Africa. In DR Begun, CV Ward and MD Rose (eds.): Function, Phylogeny, and Fossils: Miocene Hominoid Evolution and Adaptation. New York: Plenum Press, pp. 241-267.

McCrossin ML, Benefit BR, Gitau SN, Palmer AK, Blue KT. 1998. Fossil evidence for the origins of terrestriality among Old World higher primates. In E Strasser, JB Fleagle, AL Rosenberger and H McHenry (eds.): Primate Locomotion. New York: Plenum Press, pp. 353-396.

McHenry HM, Corruccini RS. 1983. The wrist of *Proconsul africanus* and the origin of hominoid postcranial adaptations. In Ciochon RL, Corruccini RS (eds): New Interpretations of Ape and Human Ancestry. New York: Plenum Press, pp. 353-367.

Meldrum D. 1991. Kinematics of the cercopithecine foot on arboreal and terrestrial substrates with implications for the interpretation of hominid terrestrial adaptations. American Journal of Physical Anthropology 84*:*273-289.

Morton DJ. 1922. Evolution of the human foot, I. American Journal of Physical Anthropology 5*:*305-336.

Morton DJ. 1924a. The evolution of the human foot, II. American Journal of Physical Anthropology 7*:*1-52.

Morton DJ. 1924b. Evolution of the longitudinal arch of the human foot. Journal of Bone and Joint Surgery 6*:*56-90.

Morton DJ. 1926. Evolution of man's erect posture. Preliminary report. J. Morphol. Physiol. 43*:*147-149.

Morton DJ. 1927. Human origin: Correlation of previous studies of primate feet and posture with other morphologic evidence. American Journal of Physical Anthropology 10*:*173-203.

Mosimman J. 1970. Size allometry: size and shape variables with characteristics of the log normal and generalized gamma distributions. J. Am. Stat. Assoc. 655*:*930-945.

Mosimann J, James FC. 1979. New statistical methods for allometry with application to Florida red-winged blackbirds. Evoution 33(1): 444-59.

Moyà-Solà S, Köhler M, Alba DM, Casanovas-Vilar I, Galindo J. 2004. *Pierolapithecus catalaunicus*, a New Middle Miocene Great Ape from Spain. Science 306 (5700): 1339 - 1344.

Musiba C, Tuttle RL, Hallgrimsson B, Webb D. 1997. Swift and sure-footed on the savanna: a study of Hadzabe gaits and feet in northern Tanzania. Am. J. Hum. Biol. 9*:*303-321.

Nakatsukasa M, Kunimatsu Y, Nakano Y, Takano T, Ishida H. 2003. Comparative and functional anatomy of phalanges in *Nacholapithecus kerioi*, a Middle Miocene hominoid from northern Kenya. Primates 44*:*371-412.

Nakatsukasa M, Ward CV, Walker A, Teaford MF, Kunimatsu Y, Ogihara N. 2004. Tail loss in *Proconsul heseloni*. Journal of Human Evolution 46*:*777-784.

Napier JA, Davis PR. 1959. The forelimb skeleton and associated remains of *Proconsul africanus*. Fossil Mammals of Africa (Br. Mus. Nat. Hist.) 16*:*1-70.

Nishida T, Takasaki H, TakahataY. 1990. Demography and reproductive profiles. In T Nishida (ed.): The Chimpanzees of the Mahale Mountains: Sexual and Life History Strategies. Tokyo: University of Tokyo Press, pp. 63-97.

O'Neill MC, Ruff CB. 2004. Estimating human long bone cross-sectional geometric properties: a comparison of noninvasive methods. Journal of Human Evolution 47*:*221-235.

Patterson T. 1979. The behavior of a group of captive pygmy chimpanzees (*Pan paniscus*). Primates 20*:*341-354.

Pearson O, Lieberman D. 2004. Aging of Wolff's "Law": Ontogeny and responses to mechanical loading in cortical bone. Yearbook of Physical Anthropology 47*:*63-99.

Pickering TR. 2001. Taphonomy of the Swartkrans hominid postcrania and its bearing on issues of meat-eating and fire management. In HT Bunn (ed.): Meat-eating and Human Evolution. Oxford: Oxford University Press, pp. 33-51.

Pickford M. 1986. Cainozoic Paleontolgical Sites of Western Kenya. Munchner Geowissenschaftliche Abhandlungen (A) 8*:*1-151.

Pickford M, Senut B, Gommery D. 1999. Sexual dimorphism in *Morotopithecus bishopi*, an Early Middle Miocene hominoid from Uganda and a reassessment of its geological and biological contexts. In: Andrews P, Banham P (Eds) Late Cenozoic Environments and Hominid Evolution: a tribute to Bill Bishop. Geological Society, London, pp. 27-38.

Pilbeam D, Young NM. 2004. Hominoid Evolution: Synthesizing Disparate Data. C.R.Palevol. 3*:*303-319.

Polk JD. 2002. Adaptive and phylogenetic influences on musculoskeletal design in cercopithecine primates. Journal of Experimental Biology 205*:*3399-3412.

Pontzer H, Wrangham RW. 2004. Climbing and the daily energy cost of locomotion in wild chimpanzees: implications for hominoid locomotor evolution. J Hum Evol 46: 315–333.

Pontzer H, Wrangham RW. 2006. Ontogeny of ranging in wild chimpanzees. Int J Primatol 27(1): 295-309.

Portmann A. 1990. A zoologist looks at humankind. New York: Columbia University Press.

Preuschoft H. 1970. Functional anatomy of the lower extremity. In: Bourne (ed): The chimpanzee, vol. 3. Basel: Karger. p 221–294.

Preuschoft H. 1973. Body posture and locomotion in some east African Miocene Dryopithecinae. In MH Day (ed.): Human Evolution (Symposium of the Society of the Study of Human Biology, Volume XI). London: Taylor and Francis, pp. 13-46.

Pusey AE. 1983. Mother-offspring relationships in chimpanzees after weaning. Animal Behavior 31*:*363-377.

Pusey AE. 1990. Behavioural changes at adolescence in chimpanzees. Behavior 115*:*203-246.

Rae TC. 1993. Early Miocene hominoid evolution: phylogenetic considerations. Am J PhysAnthropol Suppl. 16: 161.

Rae TC. 1997. The early evolution of the hominoid face. In DR Begun, CV Ward and MD Rose (eds.): Function, Phylogeny, and Fossils: Miocene Hominoid Evolution and Adaptations. New York: Plenum Press, pp. 59-78.

Rafferty KL, Walker A, Ruff CB, Rose MD, Andrews P. 1995. Postcranial estimates of body weights in *Proconsul*, with a note on a distal tibia of *Proconsul major* from Napak, Uganda. American Journal of Physical Anthropology 97*:*391-402.

Raichlen DA. 2004. Ontogeny of limb mass distribution in infant baboons (*Papio cynocephalus*). Journal of Human Evolution 49*:*452-467.

Rawlins RG, Kessler MJ (eds). 1986. The Cayo Santiago Macaques: History, behavior and biology. Albany: State University of New York Press.

Remis MJ. 1995. Effects of body size and social context on the arboreal activites of lowland gorillas in the Central African Republic. Am J Phys Anthropol 97*:*413-433.

Richardson MK, Jeffery JE, Tabin CJ. 2004. Proximodistal patterning of the limb: insights from evolutionary morphology. Evolution & Development 6:1-5.

Richmond BG, Fleagle JG, Kappelman J, Swisher CC. 1998. First hominoid from the Miocene of Ethiopia and the evolution of the catarrhine elbow. Am J Phys Anthrol 105: 257-77.

Rose MD. 1983. Miocene hominoid postcranial morphology: Monkey-like, ape-like, neither, or both? In RL Ciochon and RS Corruccini (eds.): New Interpretations of Ape and Human Ancestry. New York: Plenum Press, pp. 405-417.

Rose MD. 1988. Another look at the anthropoid elbow. J Hum Evol 17: 193-224.

Rose MD. 1993. Locomotor anatomy of Miocene hominoids. In DL Gebo (ed.): Postcranial Adaptation in Nonhuman Primates. Dekalb: NIU Press, pp. 252-272.

Rose MD. 1994. Quadrupedalism in some Miocene catarrhines. Journal of Human Evolution 26*:*387-411.

Rose MD. 1996. Functional morphological similarities in the locomotor skeleton of Miocene catarrhines and platyrhine monkeys. Folia Primatologica 66*:*7-14.

Rossie JB, Simons EL, Gauld SC, Rasmussen DT. 2002. Paranasal sinus anatomy of *Aegyptopithecus*: Implications for hominoid origins. Proc Natl Acad Sci 99*:*8454-8456.

Rowe N. 1996. The Pictorial Guide to Living Primates. Charlestown, Rhode Island: Pogonias Press.

Ruff CB. 1989. New approaches to structural evolution of limb bones in primates. Folia Primatologica 53*:*142-159.

Ruff CB. 2002. Long bone articular and diaphyseal structure in Old World monkeys and apes, I: Locomotor effects. Am J Phys Anthropol 119:305-342.

Ruff CB. 2003a. Long bone articular and diaphyseal structure in Old World monkeys and apes, II: body mass estimation. American Journal of Physical Anthropology 120*:*16-37.

Ruff CB. 2003b. Ontogenetic adaptation to bipedalism: age changes in femoral to humeral length and strength proportions in humans, with a comparison to baboons. J Hum Evol 45: 317-349.

Ruff CB. 2003c. Growth in bone strength, body size, and muscle size in a juvenile longitudinal sample. Bone 33: 317-329.

Ruff CB, Walker A, Teaford MF. 1989. Body mass, sexual dimorphism and femoral proportions of *Proconsul* from Rusinga and Mfangano Islands, Kenya. Journal of Human Evolution 18:515-536.

Ruff CB, Holt B, Trinkhaus E. 2006. Who's afraid of the big bad Wolff?: "Wolff's law" and bone functional adaptation. Am J Phys Anthropol 129(4): 484-498.

Ryan TM, Krovitz GE. 2006. Trabecular bone ontogeny in the human proximal femur. Journal of Human Evolution 51(6): 591-602.

Sarmiento E. 1983. The significance of the heel process in anthropoids. Int. J. Primatol. 4:127-152.

Sarmiento E. 1988. Anatomy of the hominoid wrist joint: its evolutionary and functional implications. Int. J. Primatol. 9:281.

Schaffler MB, Burr DB, Jungers WL, Ruff CB. 1985. Structural and mechanical indicators of limb specialization in primates. Folia Primatologica 45:61-75.

Schultz A. 1926. Fetal growth of man and other primates. Quart. Rev. Biol. 1:465-521.

Schultz A. 1930. The skeleton of the trunk and limbs of higher primates. Human Biology 2:303-438.

Schultz A. 1963a. Relations between the lengths of the main parts of the foot skeleton in primates. Folia Primatologica 1:150-171.

Schultz A. 1963b. The relative lengths of the foot skeleton and its main parts in primates. Symp. Zool. Soc., London 10:199-206.

Seiffert ER, Simons EL. 2001. Astragalar morphology of late Eocene anthropoids from the Fayum Depression (Egypt) and the origin of catarrhine primates. Journal of Human Evolution 41:577-606.

Senut B, Pickford M, Gommery D, Kunimatsu Y. 2000. Un nouveau genre d'hominoide du Miocene inferieur d'Afrique orientale: *Ugandapithecus major* (Le Gros Clark and Leakey, 1950). Comptes Rendus de l'Academie des Sciences Paris 331:227-233.

Sherwood RJ, Ward S, Hill A, Duren DL, Brown B, Downs W. 2002. Preliminary description of the *Equatorius africanus* partial skeleton KNM-TH 28860 from

Kipsaramon, Tugen Hills, Baringo District, Kenya. Journal of Human Evolution 42:63-73.

Simpson GG. 1940. Studies of the earliest primates. Bulletin of the American Museum of Natural History 77: 185-212.

Smith BH. 1994. Sequence of emergence of the permanent teeth in *Macaca, Pan, Homo,* and *Australopithecus*: Its evolutionary significance. Am J Hum Biol 6(1):61-76.

Sokal RR, Rohlf FJ. 1995. Biometry, 3rd edition. New York: W.H. Freeman and Co.

Stauffer RL, Walker A, Ryder OA, Lyons-Weiler M, and Hedges SB. 2001. Human and Ape Molecular Clocks and Constraints on Paleontological Hypotheses. J Heredity 92:469-474.

Steiper M, Young NM, Sukarna T. 2004. Genomic data support the hominoid slowdown and a Middle Oligocene estimate for the hominoid-cercopithecoid divergence. Proceedings of the National Academy of Sciences USA 101:17021-17026.

Stock JT. 2002. A test of two methods of radiogrpahically deriving long bone cross-sectional properties compared to direct sectioning of the diaphysis. Int J Osteoarchaeology 12: 335-342.

Strasser E. 1988. Pedal evidence for the origin and diversification of cercopithecid clades. Journal of Human Evolution 17:225-245.

Strasser E. 1992. Hindlimb proportions, allometry, and biomechanics in Old World monkeys (Primates, Cercopithecidae). American Journal of Physical Anthropology 87:187-214.

Strasser E. 1993. Kaswanga *Proconsul* foot proportions. American Journal of Physical Anthropology Supplement 16:191.

Strasser E. 1994. Relative development of the hallux and pedal digit formulae in Cercopithecidae. Journal of Human Evolution 26:413-440.

Straus WL. 1927. Growth of the human foot and its evolutionary significance. Contrib. Embryol. Carneg. Inst. 19:93-134.

Straus WL. 1949. The riddle of man's ancestry. Quart. Rev. Biol. 24:200-223.

Susman RL. 1983. Evolution of the human foot: Evidence from Plio-Pleistocene hominids. Foot & Ankle 3:365-376.

Sussman RW. 1991. Primate origins and the evolution of angiosperms. Am J Primatol 23: 209-233.

Szalay FS. 1977. Constructing primate phylogenies: A search for testable hypotheses with maximum empirical content. Journal of Human Evolution 6*:*3-18.

Szalay FS, Dagosto M. 1988. Evolution of hallucial grasping in the primates. Journal of Human Evolution 17*:*1-33.

Szalay FS, Delson E. 1979. Evolutionary History of the Primates. New York: Academic Press.

Szalay FS, Langdon JH. 1986. The foot of *Oreopithecus*: an evolutionary assessment. Journal of Human Evolution 15*:*585-621.

Taylor AB. 1997. Relative growth, ontogeny, and sexual dimorphism in *gorilla* (*Gorilla gorilla gorilla* and *G. g. beringei*): Evolutionary and ecological considerations. Am J Primat 43(1): 1-31.

Teaford MF, Walker A, Mugaisi G. 1993. Species discrimination in *Proconsul* from Rusinga and Mfangano Islands, Kenya. In Species, Species Concepts, and Primate Evolution. WH Kimbel, LB Martin, eds. New York: Plenum Press. pp. 373-392.

Trinkaus E. 2005. Anatomical evidence for the antiquity of human footwear use. Journal of Archaeological Science 32*:*1515-1526.

Trotter M, Hixon BB, Deaton SS. 1975. Sequential changes in weight of the skeleton and in length of long limb bones of *Macaca mulatta.* Am J Phys Anthropol 43: 79-94.

Turnquist JE, Wells JP. 1994. Ontogeny of locomotion in rhesus macaques (*Macaca mulatta*): I. Early Postnatal ontogeny of the musculoskeletal system. J Hum Evol 26: 487-99.

Tuttle RL. 1970. Postural, propulsive, and prehensile capabilities in the cheiridia of chimpanzees and other great apes. The Chimpanzee 2*:*167-253.

Tuttle RL. 1986. Apes of the World. Their Social Behavior, Communication, Mentality and Ecology. Noyes: Park Ridge, NJ.

Ungar PS, Kay RF. 1995. The dietary adaptations of European Miocene catarrhines. Proc Nat Acad Sci (U.S.) 92: 5479-5481.

Van Couvering JA, Miller JA. 1969. Miocene stratigraphy and age determinations, Rusinga Island, Kenya. Nature 221*:*628-632.

Volkov T. 1903. Variations squelettiques du pied chez les primates et dans les races humaines. Bull. Soc. Anthrop., Paris 4*:*632-708.

Volkov T. 1904. Variations squelettiques du pied chez les primates et dans les races humaines. Bull. Soc. Anthrop., Paris 5*:*1-50, 201-331.

Walker A. 1974. Locomotor adaptation in past and present prosimian primates. In FA Jenkins (ed.): Primate Locomotion. New York: Academic Press, pp. 349-381.

Walker A. 1997. *Proconsul* Function and Phylogeny. In DR Begun and et al. (eds.): Function, Phylogeny, and Fossils: Miocene Hominoid Evolution and Adaptation. New York: Plenum Press, pp. 209-224.

Walker A. 2006. Taphonomy and site formation of two early Miocene sites on Rusinga Island, Kenya. In TR Pickering, K Schick and N Toth (eds.): African Taphonomy: A Tribute to the Career of C.K. "Bob" Brain. Bloomington, IN: Stone Age Press.

Walker A, Pickford M. 1983. New postcranial fossils of *Proconsul africanus* and *Proconsul nyanzae*. In RL Ciochon and RS Corruccini (eds.): New Interpretations of Ape and Human Ancestry. New York: Plenum, pp. 211-238.

Walker A, Shipman P. 2005. The Ape in the Tree. Cambridge, Mass.: Belknap Press.

Walker A, Teaford MF. 1988. The Kaswanga Primate Site: An Early Miocene hominoid site on Rusinga Island, Kenya. Journal of Human Evolution 17*:*539-544.

Walker A, Teaford MF, Martin LB, Andrews P. 1993. A new species of *Proconsul* from the early Miocene of Rusinga/ Mfangano Islands, Kenya. Journal of Human Evolution 25*:*43-56.

Ward CV. 1991. The Functional Anatomy of the Lower Back and pelvis of the Miocene Hominoid *Proconsul nyanzae* from the Miocene of Mfangano Island, Kenya. Ph.D. Dissertation, The Johns Hopkins University.

Ward CV. 1998. *Afropithecus, Proconsul,* and the primitive hominoid skeleton. In E Strasser, JB Fleagle, A Rossenberger and H McHenry (eds.): Primate Locomotion: Recent Advances. New York: Plenum Press, pp. 337-352.

Ward CV, Ruff CB, Walker A, Teaford MF, Rose MD, Nengo IO. 1995. Functional morphology of *Proconsul* patellas from Rusinga Island, Kenya, with implications for other Miocene-Pliocene catarrhines. Journal of Human Evolution 29*:*1-20.

Ward CV, Walker A. 1991. *Proconsul* did not have a tail. Journal of Human Evolution 21*:*215-220.

Ward CV, Walker A, Teaford MF, Odhiambo I. 1993. Partial skeleton of *Proconsul nyanzae* from Mfangano Island, Kenya. American Journal of Physical Anthropology 90*:*77-111.

Ward S, Brown B, Hill A, Kelly J, Downs W. 1999. *Equatorius*: A new hominoid genus from the middle Miocene of Kenya. Science 285*:*1381-1386.

Ward SC, Duren DL. 2002. Middle and late Miocene African hominoids. In WC Hartwig (ed.): The Primate Fossil Record. Cambridge: Cambridge University Press, pp. 385-397.

Weidenreich F. 1923. Evolution of the human foot. American Journal of Physical Anthropology 26*:*473-487.

Wells JP, Turnquist JE. 2001. Ontogeny of locomotion in rhesus macaques (*Macaca mulatta*): II. Postural and locomotor behavior and habitat use in a free-ranging colony. Am J Phys Anthropol 115: 80-94.

Winkler LA. 1996. Appearance of ossification centers of the lower arm, wrist, lower leg, and ankle in immature orangutans and chimpanzees with an assessment of the relationship of ossification to dental development. Am J Phys Anthropol 99(1): 191-203.

Wood B. 1973. Locomotor affinities of hominoid tali from Kenya. Nature 246*:*45-46.

Wunderlich RE. 1999. Pedal form and plantar pressure distribution in anthropoid primates. Ph.D. thesis, State University of New York at Stony Brook.

Young NM, MacLatchy L. 2004. The phylogenetic position of *Morotopithecus*. Journal of Human Evolution 46: 163-184.

APPENDIX A

ABBREVIATIONS FOR MEASUREMENTS AND QUANTITIES ANALYZED IN THIS STUDY

Abbreviations and explanations of measurements, indices, and biomechanical properties are listed here. Langdon (1986) standardized many of the foot metrics used here and his notation is included in parentheses.

LINEAR MEASURES

CALCANEUS
Calc1 Length (CA1) (= "**Calcaneus**")
Calc2 Posterior Length (CA2)
Calc3 Anterior length (CA3)
Calc4 Length of posterior talar facet in plane of calcaneus (CA4)
Calc5 Total Length of posterior talar facet (CA5)
Calc6 Posterior talar facet breadth (CA6)
Calc7 Tuberosity height (CA7)
Calc8 Tuberosity Width (CA8)

TALUS
Talus1 Length (TA1)
Talus2 Total length with lateral tubercle (TA2)
Talus3 Trochlear Breadth (TA3)
Talus4 Breadth of Ridges (TA4)
Talus5 Lateral crest length (TA5)
Talus6 Head breadth (TA6)
Talus7 Length of head and neck (TA7)

NAVICULAR
Nav1 Width (greatest length) (NA1)
Nav2 Length (Thickness at medial cuneiform articulation) (NA2)
Nav3 Medial thickness (NA3)
Nav4 Lateral thickness (NA4)

MEDIAL CUNEIFORM
MCun1 Length (MC1)

INTERMEDIATE CUNEIFORM
ICun1 Medial length (IC1)
ICun2 Lateral length (IC2)
ICun3 Distal width (IC3)
ICun4 Proximal width (IC3)

LATERAL CUNEIFORM
LCun1 Medial length (LC1)
LCun2 Lateral length (LC2)
LCun3 Distal width (LC3)
LCun4 Proximal width (LC4)

CUBOID
Cub1 Medial length (CU1)
Cub2 Lateral length (CU2)
Cub3 Distal width (CU3)
Cub4 Proximal width (CU4)

5TH METATARSAL
MT5 Total Length (5MT1)
MT5D Length without epiphysis (5MT2)

4TH METATARSAL
MT4 Total Length (4MT1)
MT4D Length without epiphysis (4MT2)

3RD METATARSAL
MT3 Total length (3MT1)
MT3D Length without epiphysis (3MT2)

2ND METATARSAL
MT2 Total length (2MT1)
MT2D Length without epiphysis (2MT2)

1ST METARSAL
MT1 Total Length (1MT1)
MT1D Length without epiphysis (1MT2)

PROXIMAL PHALANGES
PH1 Length of 1 (PH1)
PH2 Length of 2 (PH2)
PH3 Length of 3 (PH3)
PH4 Length of 4 (PH4)
PH5 Length of 5 (PH5)

FEMUR
FemurL Total Length (F1)
FemurLD Length without epiphyses (F2)
Femur = FemurL and FemurLD
FHB Superoinferior width of femoral head (F4)

BodyMass – estimated body mass using data and equations from Ruff (2003)

TIBIA
TibL Total length (T1)
TibLa Length without malleolus (T2)
Tibia = TibL and TibLa
TibLD Length without epiphyses (T3)

FIBULA
FibL Total Length (F1)
FibLD Length without epiphyses (F2)

COMPOSITE MEASUREMENTS

Tarsus = Calc1 + Cub1
Power Arm = Calc2 – ½ Calc4
CalcLoad or **Calcaneal Load Arm** = Calc3 – ½ Calc4
Foot Width = ICun3 + LCun3 + Cub3
PedLoad or **Pedal Load Arm**
Mature = Calc3 – ½ Calc4 + Cub1 + MT3
Immature = Calc3 – ½ Calc4 + Cub1 + MT3D
Foot or **Foot Length**
Mature = Calc1 + Cub1 + MT3 + PH3
Immature = Calc1 + Cub1 + MT3D + PH3

INDICES

Tibia/ Femur = TibLa/FemurL and TibLD/FemurLD
Tarsus/ Foot = Tarsus/Foot
MT3/ Foot = MT3/Foot and MT3D/Foot
MT3/ Calcaneus = MT3/Calc1 and MT3D/Calc1
PH3/Foot = PH3/Foot
PH3/ Calcaneus = PH3/Calc1
Power Arm/ Calcaneal Load Arm = Power Arm/CalcLoad
Power Arm/ Pedal Load Arm = Power Arm/PedLoad
Foot/ Femur = Foot/ FemurL and Foot/FemurLD
MT1/ Foot = MT1/Foot and MT1D/Foot
MT1/ Calcaneus = MT1/Calc1 and MT1D/Calc1
PH1/ Foot = PH1/Foot
PH1/ Calcaneus = PH1/Calc1
PH1/ PH3 = PH1/PH3
MT1/ MT3 = MT1/MT3 and MT1D/MT3D

CROSS-SECTIONAL GEOMETRY

CA	Cross-sectional area
Ix	Second moment of area about the x (ML) axis
Iy	Second moment of area about the y (DP) axis
Imax	Maximum second moment of area
Imin	Minimum second moment of area
J	Polar second moment of area (Imax + Imin**)**
Zx	Section modulus about the x (ML) axis
Zy	Section modulus about the y (DP) axis

CA/MT1 = CA of MT1 divided by the length of MT1 (and so on for CA/MT2, etc)
J/MT1 = J of MT1 divided by the length of MT1 (and so on for J/MT2, etc)
Zx/MT1 = Zx of the first metatarsal divided by the length of the first metatarsal (and so on for Zx/MT2, etc)
Zy/MT1 = Zy of the first metatarsal divided by the length of the first metatarsal (and so on for Zy/MT2, etc)

APPENDIX B

STATISTICAL DATA TABLES

Table B.1. Pearson Correlations for metrics of entire extant sample (pooled ages). Starred bold values are not significantly correlated for $p < 0.05$. (H_o = variables are uncorrelated.) Dashes indicate insufficient data.

	Calc1	Calc2	Calc3	Calc4	Calc5	Calc6	Calc7
Calc2	0.9908						
Calc3	0.95636	0.93774					
Calc4	0.9053	0.92194	0.94057				
Calc5	0.93054	0.94997	0.94307	0.99217			
Calc6	0.95254	0.96458	0.94653	0.96841	0.97272		
Calc7	0.94013	0.95312	0.93949	0.96446	0.96635	0.95977	
Calc8	0.97022	0.9749	0.94634	0.94291	0.94279	0.9664	0.95391
Talus1	0.96845	0.9689	0.96724	0.95773	0.96276	0.96563	0.97353
Talus2	0.95387	0.95948	0.94314	0.93545	0.97126	0.95945	0.97436
Talus3	0.94683	0.95285	0.93872	0.93714	0.95747	0.97183	0.95408
Talus4	0.92114	0.9199	0.89966	0.87582	0.90851	0.93036	0.90684
Talus5	0.96316	0.96668	0.9579	0.95435	0.95465	0.9643	0.97258
Talus6	0.9371	0.94912	0.93203	0.9466	0.96848	0.97213	0.9643
Talus7	0.94455	0.94597	0.92609	0.9078	0.9514	0.95355	0.94606
Nav1	0.91071	0.91902	0.90491	0.9086	0.92769	0.92894	0.94815
Nav2	0.87239	0.87063	0.82655	0.78302	0.8334	0.85057	0.85975
Nav3	0.88525	0.89752	0.86108	0.88084	0.88128	0.8905	0.9053
Nav4	0.39922	0.36895	0.39241	0.28382	0.27687	0.30374	0.35626
MCun1	0.8963	0.90771	0.90972	0.92294	0.94228	0.92792	0.94909
ICun1	0.85885	0.86424	0.86722	0.85385	0.892	0.88272	0.90707
ICun2	0.90844	0.91034	0.89616	0.86887	0.90856	0.90436	0.92477
ICun3	0.92562	0.93846	0.90699	0.91437	0.95534	0.95261	0.9605
ICun4	0.92561	0.9382	0.91026	0.92273	0.9449	0.94084	0.95293
LCun1	0.90961	0.91491	0.913	0.90627	0.93287	0.92766	0.94505
LCun2	0.93991	0.9439	0.92283	0.90808	0.93339	0.93374	0.94523
LCun3	0.9255	0.92004	0.91094	0.86832	0.90971	0.91209	0.93492
LCun4	0.92442	0.92358	0.9105	0.89419	0.91677	0.92282	0.92931
Cub1	0.95561	0.9525	0.92735	0.88695	0.92304	0.93721	0.94697
Cub2	0.43141	0.3953	0.41125	0.30599	0.24628	0.24271	0.34007
Cub3	0.93857	0.95204	0.93268	0.96248	0.96564	0.95854	0.97624
Cub4	0.94724	0.95063	0.93758	0.92236	0.95157	0.95625	0.97151
MT5	0.86898	0.85001	0.83054	0.74875	0.80143	0.80687	0.84784
MT5D	0.89063	0.8643	0.8828	0.79141	0.80549	0.77095	0.85314
MT4	0.82671	0.80874	0.78798	0.70225	0.76008	0.76293	0.81021
MT4D	0.84528	0.81362	0.84736	0.73211	0.75398	0.71969	0.80997
MT3	0.82287	0.80953	0.80486	0.73727	0.79478	0.78371	0.83581
MT3D	0.80972	0.78662	0.80146	0.70749	0.74373	0.70368	0.81211
MT2	0.84502	0.85333	0.85372	0.84795	0.88959	0.8545	0.91585
MT2D	0.83948	0.82754	0.8437	0.7917	0.85255	0.80978	0.88651

MT1	0.84578	0.85945	0.86461	0.87517	0.90611	0.8645	0.93112
MT1D	0.8898	0.90047	0.89716	0.89355	0.93005	0.90058	0.94623
PH1	0.80904	0.83014	0.84654	0.89068	0.90086	0.85093	0.91459
PH2	0.84957	0.85564	0.85505	0.85096	0.86953	0.83362	0.90079
PH3	0.83938	0.84637	0.84819	0.8544	0.87326	0.83648	0.89779
PH4	0.84436	0.85143	0.8498	0.85705	0.87932	0.8435	0.89951
PH5	0.80997	0.80066	0.79796	0.74553	0.76435	0.74236	0.81668
FemurL	0.9072	0.91733	0.90099	0.90657	0.92916	0.91666	0.951
FemurLD	0.92275	0.94207	0.87596	0.88433	0.83855	0.83003	0.87164
FHB	0.95995	0.9717	0.94629	0.95768	0.97371	0.9794	0.96917
BodyMass	0.92994	0.95081	0.92337	0.96427	0.97667	0.9727	0.97888
TibL	0.89292	0.89498	0.8798	0.8554	0.88814	0.87186	0.92918
TibLa	0.89587	0.89886	0.8799	0.85764	0.90142	0.89677	0.93466
TibLD	0.95493	0.92404	0.92791	0.83609	0.79792	0.7696	0.85795
FibL	0.86431	0.86676	0.84899	0.82178	0.86219	0.85039	0.90795
FibLD	0.91069	0.88384	0.89765	0.8103	0.79554	0.75723	0.85289

	Calc8	**Talus1**	**Talus2**	**Talus3**	**Talus4**	**Talus5**	**Talus6**
Talus1	0.96291						
Talus2	0.94967	0.98842					
Talus3	0.96369	0.96758	0.95157				
Talus4	0.92658	0.94157	0.92665	0.94327			
Talus5	0.96239	0.98636	0.9793	0.95873	0.91722		
Talus6	0.95326	0.96512	0.9558	0.97024	0.94126	0.95594	
Talus7	0.94659	0.98717	0.97755	0.92894	0.90391	0.95379	0.92246
Nav1	0.92162	0.93736	0.94091	0.89672	0.81203	0.95629	0.88634
Nav2	0.88984	0.85391	0.84427	0.78926	0.78181	0.87437	0.7933
Nav3	0.89395	0.89587	0.89312	0.87851	0.8079	0.90336	0.86421
Nav4	0.3631	0.35292	0.31647	0.32946	0.41233	0.35047	0.37262
MCun1	0.91257	0.95136	0.94841	0.90549	0.84729	0.94645	0.90993
ICun1	0.859	0.89823	0.90044	0.85249	0.82061	0.9085	0.86631
ICun2	0.91097	0.92332	0.91634	0.88046	0.84125	0.94089	0.88248
ICun3	0.93511	0.95801	0.96179	0.9257	0.8922	0.96005	0.93215
ICun4	0.93117	0.95885	0.95939	0.93094	0.8867	0.95771	0.93807
LCun1	0.9143	0.94974	0.94088	0.9118	0.88041	0.94469	0.9107
LCun2	0.93944	0.95938	0.95124	0.92629	0.89625	0.95855	0.92106
LCun3	0.91728	0.94008	0.94334	0.88375	0.85442	0.95624	0.88271
LCun4	0.91812	0.94301	0.94321	0.9094	0.87807	0.94143	0.91811
Cub1	0.95303	0.96201	0.9499	0.92175	0.89898	0.96152	0.91773
Cub2	0.31959	0.36661	0.41429	0.29199	0.2984	0.37274	0.30073
Cub3	0.94422	0.97572	0.97777	0.95764	0.91418	0.97	0.95844
Cub4	0.95536	0.97596	0.96706	0.94031	0.90386	0.97882	0.94134
MT5	0.82674	0.84392	0.84733	0.77774	0.74782	0.86411	0.77624
MT5D	0.81437	0.88194	0.89073	0.7916	0.80798	0.8999	0.81083
MT4	0.78224	0.79923	0.81855	0.72343	0.70339	0.82719	0.73263
MT4D	0.77267	0.84483	0.85707	0.7379	0.773	0.85299	0.75203
MT3	0.79156	0.81105	0.83222	0.7406	0.71049	0.84196	0.75576
MT3D	0.75084	0.81677	0.83572	0.71834	0.72168	0.83847	0.72647

MT2	0.83535	0.88848	0.90421	0.8251	0.77291	0.9043	0.84343
MT2D	0.83131	0.8603	0.86402	0.78277	0.79326	0.90555	0.80706
MT1	0.84368	0.89582	0.90741	0.84048	0.76934	0.90949	0.86341
MT1D	0.90044	0.93841	0.9377	0.88883	0.87454	0.93905	0.91299
PH1	0.82159	0.8791	0.89212	0.84291	0.77309	0.88147	0.86829
PH2	0.83233	0.87923	0.89133	0.82542	0.77121	0.89188	0.83844
PH3	0.81944	0.87456	0.88717	0.82679	0.77388	0.88002	0.84239
PH4	0.82478	0.87718	0.88914	0.83056	0.77184	0.88184	0.84668
PH5	0.76403	0.8017	0.81732	0.73435	0.69761	0.82782	0.74467
FemurL	0.8997	0.93808	0.94077	0.90027	0.84809	0.94089	0.90818
FemurLD	0.87555	0.87781	0.92467	0.9024	0.91406	0.90568	0.90832
FHB	0.97003	0.97602	0.96967	0.97246	0.92601	0.97343	0.9706
BodyMass	0.95378	0.96608	0.96129	0.96266	0.88158	0.97415	0.95821
TibL	0.87358	0.91521	0.9206	0.85185	0.8018	0.93101	0.85452
TibLa	0.89327	0.91029	0.91184	0.86632	0.80972	0.92607	0.86999
TibLD	0.84548	0.94222	0.95192	0.87698	0.91929	0.95556	0.85799
FibL	0.85037	0.88002	0.88708	0.82486	0.76319	0.90402	0.82773
FibLD	0.80905	0.91475	0.91377	0.8132	0.8492	0.9317	0.8176

	Talus7	**Nav1**	**Nav2**	**Nav3**	**Nav4**	**MCun1**	**ICun1**
Nav1	0.89713						
Nav2	0.83471	0.86976					
Nav3	0.87162	0.93031	0.864				
Nav4	0.30669	0.28234	0.53132	0.27691			
MCun1	0.91547	0.94416	0.82841	0.90322	0.29184		
ICun1	0.85427	0.90563	0.82168	0.86628	0.34063	0.91606	
ICun2	0.87412	0.91815	0.85464	0.87978	0.33823	0.91067	0.89702
ICun3	0.92868	0.92696	0.84318	0.89058	0.2809	0.93679	0.91216
ICun4	0.92814	0.93635	0.86083	0.89093	0.28454	0.94338	0.9142
LCun1	0.91593	0.89368	0.80092	0.86498	0.34734	0.9271	0.89703
LCun2	0.92472	0.9124	0.84448	0.88659	0.32225	0.93384	0.88014
LCun3	0.90179	0.94309	0.87149	0.88251	0.37145	0.9271	0.89852
LCun4	0.91773	0.91364	0.85198	0.86523	0.34953	0.91484	0.88784
Cub1	0.92731	0.91854	0.88325	0.89917	0.40742	0.92255	0.87965
Cub2	0.35756	0.41862	0.52395	0.38601	0.37924	0.4199	0.43106
Cub3	0.95265	0.94809	0.8572	0.89357	0.33061	0.95425	0.91206
Cub4	0.93907	0.93906	0.8584	0.90161	0.35608	0.94175	0.90158
MT5	0.80464	0.87154	0.85628	0.83269	0.40184	0.82269	0.82085
MT5D	0.86501	0.87899	0.87899	0.83558	0.37213	0.8776	0.85563
MT4	0.77047	0.849	0.84379	0.80458	0.37997	0.80627	0.81236
MT4D	0.83502	0.83844	0.86667	0.81261	0.44047	0.84797	0.82053
MT3	0.77439	0.87135	0.8421	0.81842	0.33626	0.83912	0.83968
MT3D	0.80261	0.80554	0.7989	0.78626	0.33357	0.81886	0.79968
MT2	0.84204	0.91882	0.82439	0.85235	0.26309	0.91833	0.88787
MT2D	0.84381	0.81591	0.76421	0.82537	0.28263	0.85392	0.80333
MT1	0.84249	0.92533	0.79735	0.84694	0.242	0.93205	0.88768
MT1D	0.91465	0.88305	0.79029	0.81524	**0.20315***	0.94181	0.88535
PH1	0.83662	0.88703	0.74992	0.83209	0.29152	0.91866	0.87846

PH2	0.84127	0.90654	0.82328	0.85381	0.35457	0.90544	0.88715
PH3	0.83804	0.90132	0.80219	0.84116	0.32847	0.90688	0.88926
PH4	0.84152	0.89858	0.79952	0.838	0.32703	0.90178	0.88115
PH5	0.76654	0.84289	0.82217	0.80313	0.44645	0.80598	0.81458
FemurL	0.90141	0.9392	0.83381	0.89787	0.2857	0.9432	0.91223
FemurLD	0.87073	0.91084	0.7787	0.7706	0.52207	0.90533	0.82508
FHB	0.94986	0.92787	0.82078	0.89726	0.29948	0.93459	0.88225
BodyMass	0.9203	0.96494	0.82882	0.93384	0.29699	0.948	0.887
TibL	0.87329	0.94404	0.85724	0.89332	0.29059	0.92557	0.90083
TibLa	0.8651	0.93456	0.84855	0.88947	0.29707	0.91353	0.89329
TibLD	0.9262	0.90507	0.84571	0.89903	0.68503	0.92135	0.91093
FibL	0.8383	0.92454	0.85105	0.8758	0.30155	0.89904	0.88031
FibLD	0.89694	0.84797	0.74118	0.74241	0.40713	0.89374	0.88402

	ICun2	**ICun3**	**ICun4**	**LCun1**	**LCun2**	**LCun3**	**LCun4**
ICun3	0.90964						
ICun4	0.91781	0.96854					
LCun1	0.91928	0.92685	0.90777				
LCun2	0.93062	0.94008	0.93327	0.9457			
LCun3	0.9183	0.92855	0.92558	0.9108	0.94208		
LCun4	0.88567	0.9323	0.91683	0.90721	0.91567	0.94673	
Cub1	0.92675	0.92689	0.93536	0.92688	0.96361	0.94054	0.91142
Cub2	0.4802	0.38203	0.37908	0.39157	0.46157	0.52386	0.39977
Cub3	0.92523	0.96041	0.95206	0.95607	0.95323	0.94141	0.93656
Cub4	0.9214	0.94865	0.94589	0.94303	0.95689	0.94301	0.93673
MT5	0.84045	0.83546	0.82146	0.8171	0.82738	0.90105	0.87278
MT5D	0.8669	0.84875	0.85485	0.833	0.88455	0.92553	0.86582
MT4	0.8202	0.81008	0.80734	0.78503	0.7981	0.88295	0.85242
MT4D	0.82869	0.81136	0.81428	0.80623	0.85503	0.91579	0.82993
MT3	0.83938	0.83273	0.82921	0.7992	0.81228	0.89355	0.85883
MT3D	0.79031	0.78763	0.79292	0.7681	0.80479	0.8917	0.81382
MT2	0.88226	0.90418	0.89851	0.86874	0.87236	0.91407	0.88912
MT2D	0.76581	0.81251	0.86427	0.81848	0.85226	0.86592	0.88339
MT1	0.89458	0.90475	0.89506	0.88653	0.8907	0.90788	0.86182
MT1D	0.85126	0.91228	0.89868	0.92588	0.92517	0.89388	0.90109
PH1	0.84561	0.87646	0.87222	0.86954	0.86304	0.86177	0.84849
PH2	0.87005	0.88681	0.88204	0.85402	0.87282	0.89919	0.85417
PH3	0.86303	0.87354	0.87057	0.85511	0.86442	0.89303	0.8621
PH4	0.85721	0.87092	0.86556	0.85389	0.86313	0.89228	0.86121
PH5	0.81345	0.78603	0.79597	0.77257	0.79893	0.8652	0.791
FemurL	0.9001	0.93547	0.92589	0.90448	0.91865	0.91972	0.90575
FemurLD	0.81413	0.90433	0.87073	0.89142	0.86459	0.81996	0.88988
FHB	0.90476	0.95261	0.94751	0.92558	0.94541	0.90923	0.92343
BodyMass	0.93483	0.9505	0.94818	0.92215	0.94368	0.92313	0.90104
TibL	0.89884	0.91456	0.90747	0.87938	0.89721	0.92586	0.89393
TibLa	0.88924	0.91035	0.90338	0.87022	0.88798	0.91334	0.89101
TibLD	0.86319	0.92636	0.90663	0.93149	0.92492	0.92301	0.92296
FibL	0.87896	0.88968	0.87759	0.84954	0.86743	0.90169	0.87258

FibLD	0.83948	0.87599	0.8708	0.87062	0.8944	0.90551	0.87973

	Cub1	**Cub2**	**Cub3**	**Cub4**	**MT5**	**MT5D**	**MT4**
Cub2	0.50985						
Cub3	0.94914	0.29244					
Cub4	0.9627	0.43268	0.98245				
MT5	0.84667	0.56437	0.84565	0.8682			
MT5D	0.89064	0.6242	0.84467	0.87944	0.98662		
MT4	0.8179	0.61216	0.80664	0.83408	0.98165	0.97226	
MT4D	0.86005	0.62939	0.79381	0.83631	0.96705	0.98175	0.97706
MT3	0.8273	0.59957	0.82916	0.84876	0.96731	0.96306	0.98691
MT3D	0.81159	0.598	0.78775	0.80805	0.92457	0.97466	0.93986
MT2	0.86693	0.51402	0.9132	0.90152	0.91553	0.94259	0.92253
MT2D	0.83488	0.44326	0.87833	0.85406	0.84741	0.92895	0.95136
MT1	0.87586	0.46783	0.92928	0.90787	0.86833	0.92826	0.86726
MT1D	0.89135	0.31136	0.94757	0.93208	0.93774	0.90562	0.92944
PH1	0.83505	0.39899	0.90705	0.8811	0.77697	0.84136	0.77921
PH2	0.86743	0.55989	0.88764	0.88951	0.89461	0.93826	0.90638
PH3	0.8566	0.52252	0.88893	0.88764	0.90267	0.93035	0.91283
PH4	0.85455	0.52092	0.89191	0.88941	0.91243	0.92949	0.91951
PH5	0.81551	0.64534	0.79529	0.82143	0.90959	0.95301	0.91426
FemurL	0.91379	0.43105	0.946	0.94098	0.87329	0.88233	0.85796
FemurLD	0.8486	**0.14448***	0.85031	0.90789	0.81342	0.77742	0.74487
FHB	0.9416	0.3313	0.96755	0.95828	0.80624	0.83953	0.76454
BodyMass	0.93403	0.36814	0.97033	0.9557	0.83005	**0.41426***	0.80862
TibL	0.90007	0.51275	0.92333	0.92207	0.92358	0.92953	0.91801
TibLa	0.89163	0.46062	0.92744	0.91734	0.92153	0.91669	0.91584
TibLD	0.93045	0.4337	0.8411	0.93277	0.9041	0.92978	0.8873
FibL	0.87158	0.53002	0.89728	0.89613	0.92006	0.94007	0.91824
FibLD	0.89608	0.33215	0.84801	0.89882	0.92463	0.93542	0.92492

	MT4D	**MT3**	**MT3D**	**MT2**	**MT2D**	**MT1**	**MT1D**
MT3	0.97112						
MT3D	0.99035	0.96064					
MT2	0.95561	0.95212	0.94231				
MT2D	0.91802	0.85954	0.91588	0.88609			
MT1	0.93857	0.90594	0.92034	0.96804	0.86105		
MT1D	0.88997	0.93715	0.88597	0.95561	0.91738	0.99297	
PH1	0.80031	0.82717	0.81041	0.91922	0.84886	0.94694	0.96195
PH2	0.92837	0.93186	0.92376	0.94883	0.91751	0.94869	0.9525
PH3	0.91098	0.93688	0.91488	0.95248	0.91405	0.95247	0.97217
PH4	0.91293	0.93729	0.9156	0.94883	0.914	0.94595	0.97142
PH5	0.9488	0.9131	0.94085	0.87632	0.88663	0.85048	0.8667
FemurL	0.82927	0.88539	0.82492	0.9454	0.85359	0.95379	0.94357
FemurLD	0.76889	0.85971	0.77829	0.96832	0.8909	0.99277	0.94563
FHB	0.77567	0.78257	0.75527	0.86717	0.81247	0.88844	0.90978
BodyMass	**0.45202***	0.85138	**0.47786***	0.93529	**-0.1685***	0.95052	**-0.448***
TibL	0.90494	0.93572	0.89313	0.96116	0.85826	0.95837	0.93875

TibLa	0.88972	0.934	0.87664	0.9565	0.8406	0.95311	0.93611
TibLD	0.9272	0.93135	0.9351	0.9756	0.9834	0.97624	0.97429
FibL	0.93064	0.93691	0.9242	0.95081	0.84228	0.94347	0.92853
FibLD	0.92481	0.94071	0.91701	0.94708	0.97856	0.93871	0.95285

	PH1	**PH2**	**PH3**	**PH4**	**PH5**	**FemurL**	**FemurLD**
PH2	0.94178						
PH3	0.94772	0.97902					
PH4	0.94474	0.97501	0.99072				
PH5	0.8467	0.9408	0.93383	0.93759			
FemurL	0.93124	0.94327	0.94498	0.94559	0.86526		
FemurLD	0.91208	0.88595	0.91153	0.90925	0.77276	0.94456	
FHB	0.87494	0.86603	0.86346	0.86952	0.77733	0.94047	0.92524
BodyMass	0.89136	0.91717	0.88611	0.88303	0.80899	0.9717	---
TibL	0.9012	0.95484	0.95192	0.95208	0.89506	0.97591	0.80013
TibLa	0.88954	0.94827	0.94584	0.94638	0.88245	0.97278	0.81819
TibLD	0.91015	0.96612	0.97634	0.96493	0.90238	0.97479	0.93624
FibL	0.87591	0.93985	0.94192	0.94303	0.89113	0.95498	0.93516
FibLD	0.87763	0.95712	0.95881	0.94951	0.90393	0.91698	0.9153

	FHB	**BodyMass**	**TibL**	**TibLa**	**TibLD**	**FibL**
BodyMass	0.99679					
TibL	0.89948	0.95538				
TibLNoMa	0.90435	0.94775	0.99851			
TibLD	0.90422	---	0.99494	0.99649		
FibL	0.87198	0.93207	0.98726	0.98502	0.98948	
FibLD	0.85399	**0.32688***	0.98476	0.98297	0.99666	0.91511

Table B.2. Regression statistics for log-transformed metrics and indices of the ontogenetic sample of *Gorilla gorilla*.

Gorilla gorilla								
Measure or Index	**Predictor**	**n**	**LS slope**	**SE**	**y-int**	**R**	**P**	**Sig**
Calc1	FHB	65	0.859	0.028	1.058	0.951	0.000	*
Calc2	FHB	65	1.022	0.033	0.162	0.945	0.000	*
Calc3	FHB	65	0.694	0.030	1.124	0.894	0.000	*
Calc4	FHB	65	0.832	0.032	0.023	0.884	0.000	*
Calc8	FHB	65	0.963	0.039	-0.339	0.910	0.000	*
Nav1	FHB	48	1.796	0.118	-3.059	0.905	0.000	*
Nav2	FHB	45	1.288	0.071	-2.246	0.872	0.000	*
MCun1	FHB	54	1.010	0.045	-0.841	0.917	0.000	*
ICun1	FHB	54	0.961	0.055	-1.133	0.871	0.000	*
ICun2	FHB	54	1.336	0.081	-2.627	0.860	0.000	*
ICun3	FHB	54	1.036	0.047	-1.292	0.912	0.000	*
ICun4	FHB	54	1.115	0.065	-1.612	0.828	0.000	*
LCun1	FHB	60	0.863	0.052	-0.563	0.846	0.000	*
LCun2	FHB	60	1.117	0.050	-1.290	0.859	0.000	*
LCun3	FHB	60	1.228	0.043	-1.854	0.926	0.000	*
LCun4	FHB	60	0.996	0.053	-1.255	0.860	0.000	*
Cub3	FHB	64	1.130	0.036	-1.057	0.915	0.000	*
MT3	FHB	49	0.833	0.050	1.128	0.895	0.000	*
MT2	FHB	54	0.827	0.042	1.199	0.897	0.000	*
MT1	FHB	55	0.883	0.048	0.701	0.884	0.000	*
PH1	FHB	62	0.855	0.038	0.106	0.890	0.000	*
PH3	FHB	57	0.694	0.026	1.110	0.925	0.000	*
Femur	FHB	65	0.842	0.024	2.594	0.946	0.000	*
Tibia	FHB	61	0.942	0.029	2.046	0.955	0.000	*
Tarsus	FHB	64	0.942	0.025	1.042	0.947	0.000	*
Power Arm	FHB	65	1.079	0.039	-0.294	0.942	0.000	*
Calcaneal Load Arm	FHB	65	0.645	0.035	0.982	0.878	0.000	*
Tibia/ Femur	Age	30	0.000	0.020	4.361	0.013	0.944	ns
	FHB	48	0.025	0.019	4.284	0.185	0.209	ns
Tarsus/ Foot	Age	38	0.004	0.013	3.789	0.325	0.046	*
	FHB	54	0.072	0.015	3.571	0.562	0.000	*
MT3/ Foot	Age	41	0.008	0.021	3.460	0.373	0.016	*
	FHB	57	0.039	0.022	3.369	0.231	0.083	ns
MT3/ Calcaneus	Age	47	0.004	0.005	4.544	0.113	0.452	ns
	FHB	65	-0.002	0.031	4.566	-0.008	0.947	ns
PH3/ Foot	Age	41	-0.020	0.003	3.156	-0.790	0.000	*
	FHB	57	-0.197	0.016	3.718	-0.857	0.000	*
PH3/ Calcaneus	Age	41	-0.021	0.003	4.228	-0.675	0.000	*
	FHB	57	-0.229	0.024	4.893	-0.782	0.000	*
Power Arm/ Calcaneal Load Arm	Age	47	0.048	0.007	4.528	0.724	0.000	*
	FHB	65	0.435	0.049	3.329	0.747	0.000	*
Power Arm/ Pedal Load Arm	Age	46	0.028	0.005	3.288	0.633	0.000	*
	FHB	64	0.289	0.035	2.465	0.722	0.000	*
Foot/ Femur	Age	29	-0.007	0.003	4.237	-0.374	0.045	*

	FHB	45	-0.030	0.027	4.301	-0.170	0.264	ns
MT1/ Foot	Age	41	0.000	0.003	3.278	-0.006	0.969	ns
	FHB	57	0.002	0.019	3.273	0.012	0.929	ns
MT1/ Calcaneus	Age	46	-0.005	0.004	4.371	-0.181	0.229	ns
	FHB	64	-0.049	0.023	4.513	-0.260	0.038	*
PH1/ Foot	Age	40	-0.004	0.004	2.613	-0.142	0.383	ns
	FHB	56	-0.028	0.029	2.689	-0.131	0.335	ns
PH1/ Calcaneus	Age	44	-0.005	0.005	3.685	-0.166	0.281	ns
	FHB	62	-0.060	0.034	3.861	-0.224	0.079	ns
PH1/ PH3	Age	40	0.016	0.005	4.063	0.473	0.002	*
	FHB	56	0.168	0.029	3.579	0.617	0.000	*
MT1/ Mt3	Age	47	-0.009	0.003	4.429	-0.397	0.006	*
	FHB	65	-0.043	0.020	4.534	-0.254	0.041	*

Table B.3 Regression statistics for log-transformed metrics and indices of the ontogenetic sample of *Macaca mulatta.*

Macaca mulatta								
Measure or Index	**Predictor**	**N**	**LS slope**	**SE**	**Y-INT**	**R**	**P**	**Sig**
Calc1	FHB	114	0.853	0.018	1.181	0.697	0.000	*
Calc2	FHB	114	1.067	0.027	0.074	0.754	0.000	*
Calc3	FHB	114	0.638	0.027	1.409	0.593	0.000	*
Calc4	FHB	114	0.809	0.039	-0.001	0.651	0.000	*
Calc8	FHB	114	1.029	0.029	-0.526	0.743	0.000	*
Nav1	FHB	107	1.206	0.035	-0.511	0.666	0.000	*
Nav2	FHB	107	1.289	0.055	-1.490	0.590	0.000	*
MCun1	FHB	109	0.791	0.034	0.147	0.585	0.000	*
ICun1	FHB	104	0.928	0.045	-0.650	0.585	0.000	*
ICun2	FHB	104	0.836	0.060	-0.563	0.506	0.000	*
ICun3	FHB	104	0.976	0.041	-0.918	0.649	0.000	*
ICun4	FHB	104	1.076	0.050	-1.237	0.682	0.000	*
LCun1	FHB	108	0.747	0.036	0.025	0.538	0.000	*
LCun2	FHB	108	0.982	0.034	-0.488	0.643	0.000	*
LCun3	FHB	108	1.096	0.036	-0.870	0.676	0.000	*
LCun4	FHB	108	0.898	0.033	-0.629	0.653	0.000	*
Cub3	FHB	109	0.924	0.032	-0.298	0.618	0.000	*
MT3	FHB	61	0.790	0.061	1.768	0.127	0.000	*
MT2	FHB	58	0.747	0.063	1.840	0.117	0.000	*
MT1	FHB	61	0.742	0.075	1.481	0.144	0.000	*
PH1	FHB	111	1.029	0.041	-0.100	0.787	0.000	*
PH3	FHB	110	0.966	0.038	0.660	0.786	0.000	*
Femur	FHB	100	1.306	0.058	1.523	0.713	0.000	*
Tibia	FHB	78	0.923	0.074	2.487	0.442	0.000	*
Tarsus	FHB	109	0.905	0.021	1.350	0.650	0.000	*
Power Arm	FHB	114	1.157	0.036	-0.435	0.755	0.000	*
Calcaneal Load Arm	FHB	114	0.601	0.031	1.295	0.549	0.000	*
Tibia/ Femur	Age	113	-0.009	0.001	4.562	-0.697	0.000	*
	FHB	112	-0.116	0.013	4.825	-0.648	0.000	*
Tarsus/ Foot	Age	106	-0.014	0.001	3.716	-0.792	0.000	*
	FHB	106	-0.201	0.027	4.185	-0.586	0.000	*
MT3/ Foot	Age	108	0.013	0.001	3.606	0.752	0.000	*
	FHB	108	0.160	0.022	3.238	0.581	0.000	*
MT3/ Calcaneus	Age	113	0.028	0.002	4.794	0.841	0.000	*
	FHB	113	0.309	0.030	4.108	0.696	0.000	*
PH3/ Foot	Age	106	0.002	0.001	3.107	0.129	0.189	ns
	FHB	106	-0.044	0.022	3.235	-0.196	0.044	*
PH3/ Calcaneus	Age	110	0.014	0.002	4.320	0.607	0.000	*
	FHB	110	0.085	0.032	4.160	0.250	0.008	*
Power Arm/ Calcaneal Load Arm	Age	115	0.043	0.004	4.149	0.751	0.000	*
	FHB	114	0.556	0.047	2.875	0.745	0.000	*
Power Arm/ Pedal Load Arm	Age	109	0.011	0.002	2.904	0.430	0.000	*
	FHB	109	0.250	0.033	2.284	0.594	0.000	*
Foot/ Femur	Age	100	-0.023	0.002	4.466	-0.823	0.000	*

	FHB	100	-0.309	0.034	5.181	0.073	0.000	*
MT1/ Foot	Age	105	0.012	0.002	3.186	0.577	0.000	*
	FHB	105	0.092	0.032	2.999	0.269	0.005	*
MT1/ Calcaneus	Age	113	0.026	0.002	4.386	0.775	0.000	*
	FHB	113	0.232	0.036	3.895	0.520	0.000	*
PH1/ Foot	Age	107	0.004	0.002	2.508	0.165	0.089	ns
	FHB	107	-0.030	0.038	2.608	-0.076	0.434	ns
PH1/ Calcaneus	Age	111	0.019	0.002	3.704	0.628	0.000	*
	FHB	111	0.159	0.038	3.369	0.376	0.000	*
PH1/ PH3	Age	109	0.005	0.002	3.988	0.282	0.003	*
	FHB	109	0.080	0.026	3.799	0.289	0.002	*
MT1/ MT3	Age	113	-0.002	0.001	4.198	-0.145	0.127	ns
	FHB	113	-0.077	0.027	4.393	-0.399	0.000	*

Table B.4. Regression statistics for log-transformed metrics and indices of the ontogenetic sample of *Pan troglodytes*.

Pan troglodytes								
Measure or Index	**Predictor**	**N**	**LS slope**	**SE**	**Y-INT**	**R**	**P**	**Sig**
Calc1	FHB	207	0.835	0.016	1.041	0.907	0.000	*
Calc2	FHB	207	1.010	0.020	0.107	0.916	0.000	*
Calc3	FHB	207	0.724	0.021	1.030	0.860	0.000	*
Calc4	FHB	207	0.909	0.029	-0.159	0.812	0.000	*
Calc8	FHB	207	0.940	0.032	-0.346	0.882	0.000	*
Nav1	FHB	172	1.828	0.091	-2.829	0.711	0.000	*
Nav2	FHB	170	1.431	0.094	-2.619	0.699	0.000	*
MCun1	FHB	197	0.935	0.031	-0.395	0.796	0.000	*
ICun1	FHB	188	1.084	0.050	-1.384	0.758	0.000	*
ICun2	FHB	186	1.165	0.052	-1.845	0.715	0.000	*
ICun3	FHB	186	1.146	0.044	-1.591	0.793	0.000	*
ICun4	FHB	150	1.344	0.069	-2.310	0.772	0.000	*
LCun1	FHB	202	0.742	0.029	-0.045	0.757	0.000	*
LCun2	FHB	202	0.887	0.027	-0.392	0.773	0.000	*
LCun3	FHB	201	1.196	0.032	-1.577	0.817	0.000	*
LCun4	FHB	155	0.861	0.041	-0.695	0.769	0.000	*
Cub3	FHB	93	1.094	0.041	-0.769	0.788	0.000	*
MT3	FHB	190	0.978	0.030	0.798	0.802	0.000	*
MT2	FHB	184	0.928	0.030	1.043	0.800	0.000	*
MT1	FHB	186	0.959	0.026	0.649	0.820	0.000	*
PH1	FHB	199	0.889	0.027	0.290	0.868	0.000	*
PH3	FHB	197	0.815	0.023	0.877	0.887	0.000	*
Femur	FHB	206	0.882	0.020	2.572	0.873	0.000	*
Tibia	FHB	182	0.997	0.028	1.964	0.846	0.000	*
Tarsus	FHB	202	0.896	0.017	1.146	0.841	0.000	*
Power Arm	FHB	204	1.044	0.026	-0.325	0.919	0.000	*
Calcaneal Load Arm	FHB	204	0.645	0.022	0.961	0.829	0.000	*
Tibia/ Femur	Age	98	-0.003	0.002	4.413	-0.172	0.090	ns
	FHB	190	-0.005	0.011	4.409	-0.033	0.655	ns
Tarsus/ Foot	Age	92	0.002	0.002	3.684	0.092	0.384	ns
	FHB	192	-0.018	0.013	3.744	-0.101	0.163	ns
MT3/ Foot	Age	92	0.004	0.002	3.575	0.181	0.085	ns
	FHB	192	0.057	0.012	3.419	0.331	0.000	*
MT3/ Calcaneus	Age	113	0.012	0.003	4.737	0.348	0.000	*
	FHB	207	0.119	0.020	4.442	0.388	0.000	*
PH3/ Foot	Age	92	-0.010	0.003	3.195	-0.311	0.003	*
	FHB	192	-0.053	0.015	3.319	-0.246	0.001	*
PH3/ Calcaneus	Age	104	-0.012	0.004	4.428	-0.322	0.001	*
	FHB	197	-0.019	0.021	4.438	-0.065	0.367	ns
Power Arm/ Calcaneal Load Arm	Age	111	0.045	0.005	4.311	0.663	0.000	*
	FHB	204	0.399	0.036	3.319	0.620	0.000	*
Power Arm/ Pedal Load Arm	Age	94	0.022	0.005	2.988	0.394	0.000	*
	FHB	195	0.226	0.030	2.411	0.488	0.000	*
Foot/ Femur	Age	83	-0.001	0.003	4.175	-0.028	0.802	ns

	FHB	183	-0.049	0.020	4.319	-0.218	0.003	*
MT1/ Foot	Age	90	0.000	0.003	3.386	0.018	0.865	ns
	FHB	189	0.019	0.014	3.332	0.100	0.169	ns
MT1/ Calcaneus	Age	113	0.005	0.003	4.567	0.153	0.107	ns
	FHB	207	0.074	0.020	4.376	0.254	0.000	*
PH1/ Foot	Age	90	0.002	0.005	2.776	0.044	0.684	ns
	FHB	189	0.027	0.023	2.710	0.087	0.232	ns
PH1/ Calcaneus	Age	105	0.000	0.004	4.007	0.006	0.953	ns
	FHB	199	0.055	0.024	3.850	0.161	0.023	*
PH1/ PH3	Age	101	0.012	0.003	4.183	0.362	0.000	*
	FHB	193	0.081	0.020	3.992	0.301	0.000	*
MT1/ Mt3	Age	111	-0.006	0.002	4.438	-0.235	0.013	*
	FHB	205	-0.050	0.014	4.563	-0.235	0.001	*

Table B.5. Regression statistics for *Colobus* hindlimb metrics versus femoral head breadth (FHB).

Colobus						
n=24	**LS slope**	**SE**	**y-int**	**R**	**P**	**Sig**
Calc1	0.90064	0.1405	1.03153	0.807	0	*
Calc2	0.964981	0.1974	0.394663	0.722	0.000	*
Calc3	0.65487	0.1974	1.25445	0.616	0.001	*
Calc4	0.07282	0.3834	2.03915	0.040	0.851	ns
Calc8	0.848798	0.2206	-0.01869	0.634	0.001	*
Nav1	1.1074	0.1709	-0.18439	0.810	0.000	*
Nav2	0.665242	0.3269	0.255447	0.398	0.054	ns
MCun1	1.45276	0.2666	-1.65885	0.765	0.000	*
ICun1	0.19189	0.3193	1.43878	0.130	0.554	ns
ICun2	-0.36121	0.4752	2.66432	-0.160	0.455	ns
ICun3	0.946278	0.258	-0.86054	0.616	0.001	*
ICun4	0.09819	0.305	1.44772	0.068	0.751	ns
LCun1	0.54032	0.2837	0.620654	0.376	0.070	ns
LCun2	0.768833	0.3423	0.040252	0.432	0.035	*
LCun3	1.05302	0.2187	-0.77003	0.716	0.000	*
LCun4	0.467999	0.2507	0.65291	0.370	0.075	ns
Cub3	0.904131	0.292	-0.1002	0.551	0.005	*
MT3	0.97917	0.1544	1.29766	0.804	0.000	*
MT2	1.05781	0.1778	1.00081	0.785	0.000	*
MT1	1.10906	0.1993	0.44474	0.765	0.000	*
Power Arm	1.24966	0.2448	-0.64413	0.736	0.000	*
CalcLoad	0.845478	0.2336	0.476796	0.611	0.002	*
PedLoad	0.92739	0.1478	1.86389	0.801	0.000	*
Foot	0.92625	0.1817	2.3296	0.827	0.000	*
Tarsus	0.87462	0.1497	1.41096	0.780	0.000	*
PH1	1.25112	0.4267	-0.70926	0.680	0.015	*
PH3	0.931111	0.2339	0.912125	0.754	0.002	*
FemurL	0.90022	0.1289	2.74558	0.83	0	*
TibiaLa	1.00545	0.1561	2.34585	0.808	0	*

Table B.6. Regression statistics for *Gorilla* hindlimb metrics versus femoral head breadth (FHB).

Gorilla gorilla						
n= 18	**LS slope**	**SE**	**y-int**	**R**	**P**	**Sig**
Calc1	0.81652	0.09317	1.26886	0.910	0.000	*
Calc2	0.919279	0.09803	0.616019	0.920	0.000	*
Calc3	0.70023	0.1441	1.12736	0.772	0.000	*
Calc4	0.856386	0.07257	-0.02827	0.947	0.000	*
Calc8	1.23681	0.1076	-1.32083	0.944	0.000	*
Nav1	0.913118	0.09642	0.372772	0.921	0.000	*
Nav2	1.04158	0.1622	-1.26171	0.849	0.000	*
MCun1	0.684351	0.08114	0.43453	0.904	0.000	*
ICun1	0.783227	0.1716	-0.45088	0.752	0.000	*
ICun2	0.906269	0.1377	-0.95749	0.855	0.000	*
ICun3	0.792403	0.1054	-0.31651	0.883	0.000	*
ICun4	0.678089	0.1448	0.104133	0.760	0.000	*
LCun1	1.0561	0.1528	-1.2759	0.866	0.000	*
LCun2	0.962199	0.1523	-0.66402	0.845	0.000	*
LCun3	0.900108	0.1154	-0.58259	0.890	0.000	*
LCun4	0.685739	0.1206	-0.04534	0.818	0.000	*
Cub3	0.985791	0.08871	-0.47293	0.941	0.000	*
MT3	0.59084	0.0735	2.07037	0.895	0.000	*
MT2	0.56227	0.04406	2.23714	0.954	0.000	*
MT1	0.60252	0.05751	1.80951	0.934	0.000	*
Power Arm	0.934702	0.1124	0.325567	0.901	0.000	*
CalcLoad	0.62971	0.1946	1.05838	0.629	0.005	*
PedLoad	0.7006	0.1049	2.22725	0.858	0.000	*
Foot	0.74204	0.09592	2.58819	0.900	0.000	*
Tarsus	0.88779	0.1142	1.2851	0.889	0.000	*
PH1	0.49399	0.1104	1.52586	0.746	0.000	*
PH3	0.47299	0.09588	1.98076	0.797	0	*
FemurL	0.59616	0.06426	3.56564	0.918	0	*
TibiaLa	0.65162	0.08933	3.14415	0.877	0	*

Table B.7. Regression statistics for *Hylobates* hindlimb metrics versus femoral head breadth (FHB).

Hylobates lar						
n= 12	**LS slope**	**SE**	**y-int**	**R**	**P**	**Sig**
Calc1	0.63243	0.3175	1.49101	0.533	0.074	ns
Calc2	0.970525	0.3315	0.078005	0.679	0.015	*
Calc3	0.50285	0.279	1.48794	0.495	0.102	ns
Calc4	0.603436	0.4333	0.496589	0.403	0.194	ns
Calc8	1.52205	0.6118	-2.09335	0.618	0.032	*
Nav1	0.6009	0.4041	1.12975	0.426	0.168	ns
Nav2	0.688687	0.2518	-0.04199	0.654	0.021	*
MCun1	0.65246	0.2512	0.596092	0.635	0.027	*
ICun1	0.94647	0.5527	-0.73809	0.476	0.118	ns
ICun2	-0.05684	0.6019	1.7827	-0.030	0.927	ns
ICun3	0.619628	0.5671	0.010921	0.327	0.300	ns
ICun4	0.848615	0.3698	-0.66815	0.587	0.045	*
LCun1	0.772663	0.5764	-0.21486	0.408	0.213	ns
LCun2	0.430637	0.5554	0.956876	0.250	0.458	ns
LCun3	0.679767	0.2682	-0.06479	0.645	0.032	*
LCun4	0.93505	0.3283	-1.08509	0.688	0.019	*
Cub3	0.487025	0.3972	0.825709	0.362	0.248	ns
MT3	0.5851	0.5078	2.17141	0.342	0.276	ns
MT2	0.62663	0.4027	2.11018	0.441	0.151	ns
MT1	0.18475	0.4325	3.12534	0.134	0.678	ns
Power Arm	1.11832	0.4681	-0.65504	0.603	0.038	*
CalcLoad	0.47888	0.2865	1.27238	0.467	0.126	ns
PedLoad	0.61019	0.3383	2.54413	0.495	0.101	ns
Foot	0.6599	0.292	2.88706	0.582	0.047	*
Tarsus	0.691	0.2617	1.69055	0.641	0.025	*
PH1	-0.06405	0.3518	3.14233	-0.057	0.859	ns
PH3	0.71837	0.1738	1.42519	0.794	0.002	*
FemurL	0.5861	0.286	3.67374	0.544	0.068	ns
TibiaLa	0.78089	0.357	2.95679	0.569	0.054	ns

Table B.8. Regression statistics for *Macaca* hindlimb metrics versus femoral head breadth (FHB).

Macaca mulatta						
n= 29	**LS slope**	**SE**	**y-int**	**R**	**P**	**Sig**
Calc1	0.63356	0.07784	1.79939	0.843	0.000	*
Calc2	0.824525	0.07861	0.776679	0.896	0.000	*
Calc3	0.39777	0.1054	2.07094	0.588	0.001	*
Calc4	0.613548	0.1406	0.558524	0.643	0.000	*
Calc8	0.936705	0.1166	-0.23575	0.840	0.000	*
Nav1	0.786809	0.07288	0.664733	0.901	0.000	*
Nav2	0.775784	0.1277	-0.06916	0.760	0.000	*
MCun1	0.35551	0.109	1.35214	0.532	0.003	*
ICun1	0.582305	0.1293	0.30591	0.662	0.000	*
ICun2	0.395798	0.2022	0.64299	0.358	0.061	ns
ICun3	0.730355	0.1046	-0.21688	0.808	0.000	*
ICun4	0.741862	0.1826	-0.28099	0.623	0.000	*
LCun1	0.527634	0.1199	0.623093	0.661	0.000	*
LCun2	0.557184	0.1241	0.690939	0.668	0.000	*
LCun3	0.588715	0.1165	0.543747	0.711	0.000	*
LCun4	0.667882	0.1255	0.01815	0.729	0.000	*
Cub3	0.921019	0.1177	-0.28257	0.833	0.000	*
MT3	0.80173	0.09124	1.74295	0.861	0.000	*
MT2	0.79119	0.08565	1.72642	0.872	0.000	*
MT1	0.76869	0.07816	1.41621	0.884	0.000	*
Power Arm	0.886055	0.09206	0.351774	0.880	0.000	*
CalcLoad	0.34854	0.1431	1.98248	0.424	0.022	*
PedLoad	0.66945	0.07685	2.57957	0.859	0.000	*
Foot	0.68645	0.0715	2.96299	0.879	0.000	*
Tarsus	0.62529	0.06659	2.12785	0.875	0.000	*
PH1	0.719221	0.1175	0.811241	0.768	0.000	*
PH3	0.5757	0.09381	1.78811	0.763	0.000	*
FemurL	0.90023	0.09047	2.68344	0.886	0	*
TibiaLa	0.82603	0.1055	2.78035	0.838	0	*

Table B.9. Regression statistics for *Nasalis* hindlimb metrics versus femoral head breadth (FHB). Dashes indicate insufficient data.

Nasalis larvatus						
n= 10	**LS slope**	**SE**	**y-int**	**R**	**P**	**Sig**
Calc1	0.64752	0.1233	1.80187	0.881	0.001	*
Calc2	0.791208	0.1465	0.809857	0.886	0.001	*
Calc3	0.60271	0.1633	1.56542	0.794	0.006	*
Calc4	0.944584	0.2511	-0.41635	0.799	0.006	*
Calc8	0.971109	0.2202	-0.45856	0.842	0.002	*
Nav1	0.873921	0.1131	0.463959	0.939	0.000	*
Nav2	0.887518	0.1572	-0.51748	0.894	0.000	*
MCun1	0.699152	0.1371	0.43879	0.874	0.001	*
ICun1	1.0233	0.2567	-0.87231	0.816	0.004	*
ICun2	1.09258	0.251	-1.33078	0.839	0.002	*
ICun3	0.724869	0.1394	-0.09155	0.878	0.001	*
ICun4	1.07058	0.2114	-1.31394	0.873	0.001	*
LCun1	0.688272	0.1635	0.264159	0.830	0.003	*
LCun2	0.834935	0.1095	-0.09376	0.938	0.000	*
LCun3	0.841323	0.2264	-0.16074	0.796	0.006	*
LCun4	0.797301	0.203	-0.22653	0.811	0.006	*
Cub3	0.73073	0.1947	0.351943	0.799	0.006	*
MT3	0.79878	0.1079	1.76938	0.934	0.000	*
MT2	0.69642	0.1711	1.9715	0.821	0.004	*
MT1	0.84757	0.04431	1.21182	0.989	0.000	*
Power Arm	0.7459	0.1429	0.680705	0.879	0.001	*
CalcLoad	0.5216	0.1674	1.59467	0.740	0.014	*
PedLoad	0.72825	0.1133	2.4426	0.915	0.000	*
Foot	---	---	---	---	---	---
Tarsus	0.67379	0.12	2.01305	0.893	0.001	*
PH1	0.64345	0.2267	1.08652	0.708	0.022	*
PH3	---	---	---	---	---	---
FemurL	0.73039	0.06499	3.22619	0.970	0	*
TibiaLa	0.80002	0.05708	2.89443	0.980	0	*

Table B.10. Regression statistics for *Pan paniscus* hindlimb metrics versus femoral head breadth (FHB).

Pan paniscus						
n= 15	**LS slope**	**SE**	**y-int**	**R**	**P**	**Sig**
Calc1	0.46319	0.2005	2.35181	0.540	0.038	*
Calc2	0.39759	0.1932	2.28282	0.496	0.060	ns
Calc3	0.68623	0.349	1.14074	0.479	0.071	ns
Calc4	0.717834	0.3806	0.455943	0.464	0.082	ns
Calc8	0.26643	0.3761	1.98713	0.193	0.491	ns
Nav1	0.908069	0.282	0.388947	0.666	0.007	*
Nav2	0.32199	0.4542	1.38809	0.193	0.491	ns
MCun1	0.21188	0.3118	2.09931	0.185	0.509	ns
ICun1	0.23878	0.5437	1.64746	0.121	0.668	ns
ICun2	0.748807	0.5193	-0.41683	0.371	0.173	ns
ICun3	0.31515	0.6845	1.33801	0.127	0.653	ns
ICun4	0.20879	0.6362	1.64812	0.091	0.748	ns
LCun1	0.555695	0.3458	0.635459	0.407	0.132	ns
LCun2	0.29735	0.256	1.56171	0.307	0.266	ns
LCun3	-0.04793	0.4041	2.69931	-0.033	0.907	ns
LCun4	0.23351	0.4281	1.52205	0.150	0.907	ns
Cub3	0.775612	0.4265	0.212256	0.450	0.092	ns
MT3	0.41541	0.2588	2.77007	0.407	0.132	ns
MT2	0.44556	0.2874	2.7492	0.395	0.145	ns
MT1	0.36615	0.2942	2.65804	0.326	0.235	ns
Power Arm	0.29404	0.1963	2.3612	0.384	0.158	ns
CalcLoad	0.675481	0.3975	0.847067	0.426	0.113	ns
PedLoad	0.43794	0.2487	3.18252	0.439	0.102	ns
Foot	0.41537	0.2336	3.74023	0.473	0.103	ns
Tarsus	0.39717	0.1809	2.88162	0.520	0.047	*
PH1	0.34679	0.2968	2.14778	0.332	0.267	ns
PH3	0.48496	0.3385	1.99215	0.397	0.180	ns
FemurL	0.59083	0.1854	3.63016	0.662	0.007	*
TibiaLa	0.64489	0.2342	3.21983	0.607	0.016	*

Table B.11. Regression statistics for *Pan troglodytes* hindlimb metrics versus femoral head breadth (FHB).

Pan troglodytes						
n= 107	**LS slope**	**SE**	**y-int**	**R**	**P**	**Sig**
Calc1	0.65373	0.06918	1.68082	0.683	0.000	*
Calc2	0.65618	0.07782	1.353	0.641	0.000	*
Calc3	0.859191	0.1075	0.555846	0.621	0.000	*
Calc4	0.91546	0.1294	-0.18754	0.576	0.000	*
Calc8	0.569021	0.1175	0.948137	0.518	0.000	*
Nav1	0.6939	0.07229	1.14966	0.694	0.000	*
Nav2	0.482656	0.2057	0.699317	0.226	0.021	*
MCun1	0.51196	0.09519	1.08597	0.472	0.000	*
ICun1	0.475596	0.1442	0.754045	0.312	0.001	*
ICun2	0.536913	0.1278	0.356399	0.386	0.000	*
ICun3	0.472325	0.1307	0.767	0.338	0.000	*
ICun4	0.551397	0.1455	0.461258	0.361	0.000	*
LCun1	0.33958	0.1188	1.35132	0.272	0.005	*
LCun2	0.506189	0.1002	0.931041	0.448	0.000	*
LCun3	0.508887	0.1103	0.825099	0.416	0.000	*
LCun4	0.651239	0.1166	0.032645	0.495	0.000	*
Cub3	0.66808	0.1399	0.709963	0.572	0.000	*
MT3	0.56717	0.07614	2.24116	0.594	0.000	*
MT2	0.5357	0.07042	2.42001	0.604	0.000	*
MT1	0.46892	0.0707	2.36742	0.551	0.000	*
Power Arm	0.56308	0.1004	1.36839	0.487	0.000	*
CalcLoad	0.815796	0.1159	0.36354	0.574	0.000	*
PedLoad	0.59241	0.06608	2.65022	0.664	0.000	*
Foot	0.57431	0.05807	3.20201	0.703	0.000	*
Tarsus	0.64104	0.06364	2.03667	0.706	0.000	*
PH1	0.4105	0.09432	1.98009	0.399	0.000	*
PH3	0.45815	0.08083	2.14829	0.493	0.000	*
FemurL	0.44228	0.05837	4.12683	0.6	0	*
TibiaLa	0.46256	0.07322	3.84393	0.534	0	*

Table B.12. Regression statistics of pooled adults in the bivariate analysis vs. femoral head breadth (FHB).

ALL ADULTS						
n=217	**LS slope**	**SE**	**y-int**	**R**	**P**	**Sig**
Calc1	0.72422	0.01815	1.47309	0.94	0	*
Calc2	0.949988	0.0179	0.36204	0.965	0	*
Calc3	0.65346	0.01768	1.28052	0.931	0	*
Calc4	1.02998	0.01758	-0.61436	0.971	0	*
Calc8	0.959643	0.01932	-0.37203	0.967	0	*
Nav1	0.978823	0.01034	0.14615	0.989	0	*
Nav2	0.554921	0.02499	0.491586	0.837	0	*
MCun1	0.678603	0.01245	0.494256	0.967	0	*
ICun1	0.636101	0.01923	0.189396	0.917	0	*
ICun2	0.755121	0.01984	-0.40382	0.935	0	*
ICun3	0.87414	0.01692	-0.63003	0.963	0	*
ICun4	0.906285	0.01842	-0.77765	0.961	0	*
LCun1	0.645308	0.01725	0.293093	0.933	0	*
LCun2	0.716927	0.01567	0.203979	0.954	0	*
LCun3	0.687448	0.01968	0.206621	0.925	0	*
LCun4	0.659294	0.02269	0.023403	0.899	0	*
Cub3	0.9701	0.01889	-0.38054	0.972	0	*
MT3	0.36643	0.01425	2.94555	0.871	0	*
MT2	0.49945	0.01067	2.53771	0.955	0	*
MT1	0.58038	0.0114	1.95914	0.962	0	*
Power Arm	0.924494	0.02356	0.161682	0.938	0	*
CalcLoad	0.52925	0.02153	1.38174	0.862	0	*
PedLoad	0.4527	0.01325	3.14961	0.921	0	*
Foot	0.53169	0.01169	3.35976	0.958	0	*
Tarsus	0.71311	0.01588	1.81907	0.952	0	*
PH1	0.69556	0.02036	0.936166	0.926	0	*
PH3	0.41461	0.01332	2.27939	0.917	0	*
FemurL	0.60719	0.009457	3.54986	0.975	0	*
TibiaLa	0.49475	0.01058	3.73825	0.956	0	*

Table B.13. Cross-sectional properties of *Proconsul heseloni* metatarsal midshafts. (*) These specimens had fractures at the midshaft that required small portions of the cross-section to be reconstructed in Photoshop®.

Specimen	Side	MT#	MTL	CA	Ix	Iy	Imax	Imin	J	Zx	Zy
KNM-RU 2036	L	1	38.1	15.78	31.66	33.35	35.96	29.05	65.01	12.42	12.37
KNM-RU 2036	L	2	49.1	15.34	23.75	23.85	26.11	21.49	47.60	9.94	9.48
KNM-RU 2036	L	3	52.3	17.75	36.08	26.85	37.47	25.47	62.94	12.96	11.38
KPS 1	L	1	42.9	21.52	47.56	73.95	74.85	46.68	121.53	17.47	21.19
KPS 1	L	2	57	16.45	28.58	33.71	34.90	27.40	62.30	11.32	12.22
KPS 1*	L	3	58	15.57	32.09	35.20	36.99	30.31	67.30	12.26	12.97
KPS 1	L	4	58	14.51	24.97	25.56	28.40	22.13	50.52	9.89	10.23
KPS 1	R	2	57	18.14	32.24	41.43	41.66	32.01	73.67	12.93	14.01
KPS 1	R	3	58	17.17	35.46	42.40	42.40	35.46	77.87	13.05	14.39
KPS 1	R	4	58	16.27	28.75	31.38	33.15	26.98	60.13	11.25	11.68
KPS 1	R	5	53	15.81	29.34	20.40	30.44	19.31	49.75	11.22	8.76
KPS 3	L	2	57	18.13	33.61	36.94	37.32	33.23	70.55	13.04	13.20
KPS 3	L	3	59.5	17.58	35.90	35.84	39.92	31.83	71.75	13.43	13.48
KPS 3	L	4	57	14.96	25.42	20.32	25.62	20.11	45.73	10.23	8.97
KPS 3	L	5	53	10.73	14.09	11.84	14.10	11.83	25.93	6.42	5.84
KPS 3	R	1	43.5	21.79	45.29	57.66	57.68	45.30	102.98	16.19	18.51
KPS 3	R	2	56	19.33	44.04	40.16	44.49	39.73	84.22	15.35	13.72
KPS 3*	R	3	56	21.10	58.99	45.17	59.00	45.19	104.19	18.36	16.33
KPS 4	L	2	36.5	6.67	5.23	5.28	5.50	5.01	10.51	3.21	3.04
KPS 4*	L	3	34	6.61	4.51	4.20	4.73	3.98	8.71	2.79	2.61
KPS 4	L	4	34	7.01	4.55	4.38	4.68	4.25	8.93	2.85	2.82
KPS 4	L	5	33.1	4.79	1.73	2.11	2.11	1.72	3.84	1.38	1.52
KPS 7*	L	2	50	11.80	17.64	14.40	17.70	14.35	32.04	7.82	6.88
KPS 7	L	3	51	11.48	11.55	14.51	14.66	11.39	26.06	5.89	6.64
KPS 7	L	4	51	11.94	13.07	13.83	14.89	12.00	26.89	6.48	6.54
KPS 8*	R	1	43	19.29	38.49	41.34	48.82	31.03	79.85	14.04	14.25
KPS 8	R	2	58	13.33	25.09	27.97	28.46	24.60	53.06	9.43	10.66
KPS 8	R	3	57	13.12	22.59	20.44	22.73	20.31	43.04	9.09	8.91
KPS 8	R	4	56	13.65	21.49	22.25	24.86	18.87	43.73	9.35	9.44

Table B.14 Cross-sectional properties (means and standard deviations) of *Macaca mulatta* metatarsal midshafts.

	Age Group	N		MTL	CA	Ix	Iy	Imax	Imin	J	Zx	Zy
MT1	3	8	MEAN	34.2	12.0	14.5	20.3	20.5	14.3	34.8	6.9	8.1
			STDEV	*3.2*	*1.7*	*6.5*	*8.4*	*8.3*	*6.6*	*14.8*	*2.0*	*2.4*
	4	23	MEAN	34.7	14.3	17.2	25.2	25.4	16.9	42.4	7.8	9.6
			STDEV	*2.5*	*2.3*	*5.9*	*8.5*	*8.5*	*5.9*	*14.2*	*2.0*	*2.4*
	5	21	MEAN	34.3	14.2	16.6	24.2	24.6	16.2	40.8	7.6	9.3
			STDEV	*2.5*	*2.4*	*5.9*	*8.4*	*8.5*	*5.8*	*14.0*	*2.1*	*2.4*
MT2	3	8	MEAN	49.3	11.8	16.3	17.8	18.5	15.6	34.1	7.2	7.7
			STDEV	*4.5*	*2.2*	*8.2*	*7.9*	*8.3*	*7.8*	*16.1*	*2.6*	*2.5*
	4	23	MEAN	50.2	14.3	20.5	23.3	24.7	19.2	43.8	8.7	9.3
			STDEV	*3.3*	*2.7*	*7.6*	*10.2*	*10.4*	*7.0*	*17.2*	*2.5*	*2.9*
	5	21	MEAN	50.0	14.4	20.6	23.6	24.4	19.8	44.2	8.7	9.4
			STDEV	*4.0*	*2.4*	*7.1*	*8.5*	*8.6*	*6.8*	*15.2*	*2.3*	*2.5*
MT3	3	8	MEAN	51.8	12.3	18.5	22.9	23.1	18.4	41.5	8.3	9.2
			STDEV	*4.6*	*2.0*	*7.5*	*10.0*	*10.2*	*7.3*	*17.4*	*2.5*	*2.7*
	4	23	MEAN	53.0	15.1	25.7	29.2	29.6	25.3	54.9	10.6	11.4
			STDEV	*3.9*	*2.2*	*7.5*	*8.8*	*8.8*	*7.4*	*16.2*	*2.4*	*2.6*
	5	21	MEAN	52.2	15.5	27.5	29.5	31.2	25.8	57.0	11.1	11.5
			STDEV	*4.3*	*2.5*	*10.5*	*9.6*	*11.1*	*8.9*	*19.9*	*3.1*	*2.9*
MT4	3	8	MEAN	52.4	10.9	15.0	13.2	16.2	12.0	28.2	6.8	6.4
			STDEV	*4.7*	*1.6*	*5.8*	*4.5*	*6.5*	*3.7*	*10.2*	*1.9*	*1.6*
	4	23	MEAN	53.2	13.9	23.0	18.8	24.3	17.4	41.8	9.3	8.3
			STDEV	*3.8*	*2.3*	*7.4*	*6.5*	*8.2*	*5.8*	*13.7*	*2.3*	*2.1*
	5	21	MEAN	51.8	14.8	26.3	21.6	28.8	19.1	47.9	10.1	9.1
			STDEV	*4.2*	*3.3*	*13.8*	*11.3*	*17.2*	*8.2*	*24.9*	*3.6*	*3.4*
MT5	3	8	MEAN	49.6	8.8	9.8	7.8	10.7	7.0	17.6	4.7	4.2
			STDEV	*4.2*	*1.9*	*5.9*	*4.5*	*6.7*	*3.6*	*10.3*	*2.0*	*1.7*
	4	23	MEAN	50.9	12.1	17.0	13.1	18.6	11.5	30.1	7.2	6.3
			STDEV	*3.8*	*2.3*	*7.1*	*5.4*	*7.8*	*4.5*	*11.9*	*2.2*	*1.9*
	5	21	MEAN	50.0	12.5	19.0	15.3	21.3	13.0	34.3	7.8	7.0
			STDEV	*4.5*	*2.5*	*8.5*	*6.9*	*9.3*	*6.3*	*15.1*	*2.5*	*2.3*

Table B.15. Cross-sectional properties (means and standard deviations) of *Pan troglodytes* metatarsal midshafts.

	Age Group	N		MTL	CA	Ix	Iy	Imax	Imin	J	Zx	Zy
MT1	1	2	MEAN	27.0	15.2	37.8	49.8	51.0	36.6	87.6	13.9	15.2
			STDEV	*1.4*	*0.4*	*7.9*	*3.8*	*2.2*	*6.3*	*4.1*	*2.1*	*0.2*
	2	17	MEAN	37.4	27.0	109.5	126.0	129.9	105.4	235.3	29.3	31.4
			STDEV	*5.3*	*7.9*	*60.2*	*59.3*	*62.2*	*56.9*	*118.4*	*11.6*	*11.6*
	3	11	MEAN	45.8	38.0	183.3	207.4	214.3	176.1	390.4	44.5	47.4
			STDEV	*6.4*	*8.1*	*68.3*	*67.0*	*71.5*	*63.0*	*133.3*	*12.7*	*12.2*
	4	8	MEAN	54.1	50.3	298.0	332.5	344.0	285.6	629.6	63.6	68.0
			STDEV	*3.9*	*9.3*	*114.0*	*100.6*	*112.4*	*97.9*	*209.4*	*18.8*	*17.0*
	5	33	MEAN	54.9	56.0	397.7	489.8	506.6	380.6	887.2	78.0	86.7
			STDEV	*3.2*	*9.2*	*116.0*	*183.7*	*181.7*	*118.5*	*293.2*	*17.7*	*23.4*
MT2	1	2	MEAN	37.5	7.3	7.8	5.8	8.6	5.1	13.6	3.9	3.4
			STDEV	*3.5*	*0.5*	*2.0*	*2.9*	*3.1*	*1.9*	*4.9*	*0.8*	*1.3*
	2	17	MEAN	50.1	18.2	44.0	33.6	47.1	30.5	77.6	14.4	12.4
			STDEV	*5.3*	*6.0*	*27.7*	*21.3*	*29.7*	*19.1*	*48.5*	*6.8*	*5.8*
	3	11	MEAN	62.2	27.7	97.6	65.8	101.7	61.7	163.4	26.0	21.1
			STDEV	*7.2*	*6.5*	*47.0*	*32.5*	*49.7*	*29.6*	*78.1*	*9.5*	*7.7*
	4	8	MEAN	73.0	37.1	167.3	111.1	176.4	101.9	278.3	38.7	31.4
			STDEV	*5.8*	*7.0*	*62.3*	*33.8*	*67.3*	*29.9*	*95.4*	*10.2*	*6.7*
	5	33	MEAN	73.1	45.3	276.7	166.5	281.3	161.8	443.1	55.0	43.9
			STDEV	*4.4*	*7.7*	*100.7*	*63.4*	*101.2*	*61.7*	*157.9*	*15.0*	*12.2*
MT3	1	2	MEAN	35.3	8.5	12.3	6.6	12.4	6.5	18.9	5.4	4.0
			STDEV	*3.2*	*0.1*	*0.4*	*2.3*	*0.3*	*2.3*	*2.7*	*0.2*	*0.9*
	2	17	MEAN	46.8	17.6	53.2	31.2	54.1	30.3	84.4	16.2	12.3
			STDEV	*5.7*	*5.5*	*29.4*	*21.0*	*30.5*	*19.9*	*49.9*	*7.0*	*5.9*
	3	11	MEAN	57.2	26.7	104.0	60.1	107.1	57.1	164.2	27.4	20.4
			STDEV	*7.8*	*6.0*	*44.9*	*28.9*	*46.2*	*27.7*	*72.5*	*9.2*	*7.2*
	4	8	MEAN	67.2	34.0	176.2	93.4	178.8	90.7	269.6	40.2	29.1
			STDEV	*5.8*	*6.7*	*72.3*	*35.9*	*72.6*	*35.2*	*107.1*	*12.7*	*8.6*
	5	33	MEAN	68.7	40.9	241.2	131.2	246.2	126.2	372.4	50.6	37.6
			STDEV	*4.2*	*6.0*	*72.8*	*38.9*	*73.3*	*38.0*	*108.0*	*12.1*	*8.3*
MT4	1	2	MEAN	33.0	6.7	7.2	4.3	7.3	4.2	11.5	3.6	2.8
			STDEV	*2.8*	*0.2*	*1.9*	*2.4*	*1.9*	*2.4*	*4.3*	*0.8*	*1.0*
	2	17	MEAN	45.5	15.2	33.4	21.8	33.9	21.3	55.2	11.3	9.3
			STDEV	*5.8*	*4.1*	*18.3*	*11.9*	*18.1*	*12.1*	*29.9*	*4.6*	*3.6*
	3	11	MEAN	55.4	22.8	65.6	53.0	68.9	49.7	118.6	19.4	17.1
			STDEV	*7.9*	*7.0*	*42.5*	*48.1*	*49.1*	*40.4*	*88.7*	*9.7*	*10.1*
	4	8	MEAN	66.3	27.7	91.1	60.3	93.0	58.4	151.4	24.4	19.9
			STDEV	*4.9*	*5.0*	*32.2*	*22.9*	*33.1*	*21.9*	*54.3*	*6.1*	*5.2*
	5	33	MEAN	66.6	33.7	127.9	96.5	130.0	94.4	224.4	32.0	28.3
			STDEV	*4.0*	*5.1*	*36.3*	*33.2*	*37.2*	*32.3*	*67.8*	*7.3*	*7.2*
MT5	1	2	MEAN	31.5	5.7	4.5	5.1	5.3	4.3	9.6	2.7	2.8
			STDEV	*2.1*	*1.0*	*2.3*	*3.3*	*3.1*	*2.5*	*5.6*	*1.0*	*1.2*
	2	17	MEAN	44.6	13.3	19.4	21.8	23.0	18.2	41.3	8.1	8.8
			STDEV	*6.0*	*3.8*	*12.2*	*13.9*	*13.7*	*12.2*	*25.8*	*3.6*	*4.1*
	3	11	MEAN	54.5	20.4	39.6	50.3	51.0	38.9	89.9	14.3	16.4

			STDEV	*9.4*	*6.4*	*24.2*	*28.4*	*28.3*	*24.3*	*52.5*	*6.6*	*7.4*
	4	8	MEAN	65.1	26.1	56.5	75.0	76.4	55.1	131.5	18.9	22.0
			STDEV	*5.1*	*6.3*	*29.2*	*39.6*	*39.4*	*29.4*	*68.2*	*6.7*	*8.0*
	5	33	MEAN	66.8	29.0	78.1	86.0	92.6	71.6	164.1	23.2	24.7
			STDEV	*4.1*	*4.8*	*24.6*	*27.7*	*29.1*	*22.4*	*49.9*	*5.6*	*6.1*

Table B.16. Pearson's correlation coefficients (R) for the age- and taxon-pooled sample used in the cross-sectional geometry analysis (all ages and all three taxa: *Macaca*, *Pan* and *Proconsul*). All significant with p = 0.000 except three instances (bold, with p-value in parentheses).

	Age	Calc1	Calc2	Calc3	FHB	BodyMass
Calc1	0.391					
Calc2	0.375	0.986				
Calc3	0.333	0.959	0.945			
FHB	0.246	0.948	0.967	0.923		
BodyMass	**0.209 (0.364)**	0.97	0.967	0.957	0.987	
Tarsus	0.368	0.996	0.983	0.949	0.946	0.969
PowerArm	0.414	0.979	0.989	0.915	0.941	0.952
CalcLoad	0.354	0.912	0.875	0.972	0.839	0.926
Foot	0.444	0.966	0.942	0.925	0.881	0.956
MTL1	0.337	0.96	0.965	0.931	0.929	0.933
CA1	0.232	0.929	0.952	0.92	0.953	0.937
J1	0.218	0.889	0.904	0.884	0.909	0.92
Zx1	**0.190 (0.073)**	0.917	0.938	0.911	0.947	0.95
Zy1	**0.199 (0.061)**	0.905	0.925	0.898	0.932	0.926
MTL2	0.466	0.964	0.957	0.909	0.906	0.943
CA2	0.412	0.924	0.934	0.914	0.927	0.934
J2	0.361	0.853	0.858	0.847	0.861	0.897
Zx2	0.356	0.884	0.892	0.876	0.896	0.913
Zy2	0.406	0.891	0.896	0.884	0.889	0.914
MTL3	0.537	0.908	0.874	0.85	0.786	0.915
CA3	0.446	0.937	0.938	0.917	0.927	0.943
J3	0.378	0.898	0.895	0.885	0.895	0.934
Zx3	0.381	0.913	0.916	0.899	0.918	0.94
Zy3	0.451	0.915	0.907	0.901	0.893	0.935
MTL4	0.533	0.882	0.841	0.824	0.741	0.893
CA4	0.479	0.925	0.927	0.896	0.898	0.918
J4	0.372	0.873	0.874	0.844	0.849	0.895
Zx4	0.426	0.9	0.902	0.872	0.878	0.897
Zy4	0.409	0.883	0.88	0.852	0.844	0.889
CA5	0.478	0.927	0.926	0.904	0.894	0.922
J5	0.395	0.886	0.884	0.866	0.862	0.904
Zx5	0.456	0.903	0.897	0.885	0.868	0.905
Zy5	0.408	0.906	0.91	0.883	0.888	0.906

	Tarsus	PowerArm	CalcLoad	Foot	MTL1	CA1
PowerArm	0.976					
CalcLoad	0.898	0.867				
Foot	0.969	0.946	0.904			
MTL1	0.961	0.951	0.874	0.949		
CA1	0.93	0.926	0.844	0.887	0.933	

J1	0.883	0.88	0.821	0.851	0.883	0.962
Zx1	0.916	0.909	0.835	0.873	0.915	0.985
Zy1	0.901	0.899	0.828	0.86	0.899	0.978
MTL2	0.964	0.958	0.861	0.964	0.975	0.918
CA2	0.921	0.908	0.846	0.901	0.916	0.96
J2	0.843	0.83	0.783	0.834	0.847	0.902
Zx2	0.877	0.863	0.807	0.862	0.877	0.928
Zy2	0.882	0.869	0.821	0.871	0.882	0.922
MTL3	0.912	0.891	0.842	0.952	0.918	0.81
CA3	0.937	0.921	0.86	0.925	0.925	0.956
J3	0.893	0.875	0.831	0.879	0.883	0.931
Zx3	0.91	0.893	0.839	0.89	0.902	0.943
Zy3	0.914	0.892	0.858	0.904	0.893	0.924
MTL4	0.886	0.863	0.828	0.937	0.887	0.77
CA4	0.922	0.914	0.84	0.923	0.919	0.93
J4	0.867	0.861	0.789	0.87	0.866	0.886
Zx4	0.895	0.889	0.816	0.895	0.894	0.909
Zy4	0.877	0.87	0.801	0.881	0.868	0.876
CA5	0.925	0.918	0.865	0.915	0.918	0.939
J5	0.884	0.876	0.828	0.879	0.88	0.918
Zx5	0.901	0.889	0.85	0.895	0.892	0.914
Zy5	0.907	0.902	0.84	0.894	0.901	0.932

	J1	**Zx1**	**Zy1**	**MTL2**	**CA2**	**J2**
Zx1	0.987					
Zy1	0.995	0.992				
MTL2	0.886	0.903	0.895			
CA2	0.947	0.956	0.951	0.914		
J2	0.933	0.92	0.922	0.847	0.969	
Zx2	0.939	0.937	0.934	0.874	0.983	0.993
Zy2	0.945	0.937	0.937	0.883	0.981	0.99
MTL3	0.787	0.795	0.785	0.96	0.841	0.785
CA3	0.918	0.941	0.926	0.929	0.973	0.919
J3	0.928	0.936	0.925	0.895	0.956	0.942
Zx3	0.928	0.945	0.931	0.907	0.964	0.936
Zy3	0.916	0.925	0.914	0.91	0.951	0.918
MTL4	0.747	0.752	0.744	0.938	0.808	0.747
CA4	0.911	0.925	0.916	0.931	0.949	0.898
J4	0.899	0.901	0.894	0.881	0.903	0.882
Zx4	0.903	0.915	0.904	0.907	0.923	0.886
Zy4	0.888	0.889	0.884	0.887	0.896	0.868
CA5	0.906	0.918	0.914	0.927	0.941	0.877
J5	0.91	0.911	0.909	0.891	0.92	0.884
Zx5	0.905	0.907	0.906	0.904	0.925	0.88
Zy5	0.905	0.917	0.913	0.91	0.923	0.871

	Zx2	**Zy2**	**MTL3**	**CA3**	**J3**	**Zx3**
Zy2	0.987					

MTL3	0.804	0.82				
CA3	0.94	0.941	0.866			
J3	0.949	0.949	0.834	0.977		
Zx3	0.95	0.947	0.835	0.983	0.992	
Zy3	0.931	0.94	0.865	0.981	0.989	0.98
MTL4	0.764	0.786	0.991	0.835	0.799	0.799
CA4	0.913	0.923	0.878	0.957	0.932	0.935
J4	0.885	0.901	0.829	0.906	0.908	0.9
Zx4	0.898	0.909	0.852	0.93	0.92	0.918
Zy4	0.873	0.894	0.844	0.903	0.897	0.889
CA5	0.897	0.901	0.873	0.967	0.94	0.944
J5	0.895	0.897	0.838	0.944	0.949	0.938
Zx5	0.891	0.9	0.859	0.952	0.945	0.941
Zy5	0.891	0.89	0.846	0.949	0.939	0.935

	Zy3	**MTL4**	**CA4**	**J4**	**Zx4**	**Zy4**
MTL4	0.835					
CA4	0.936	0.854				
J4	0.904	0.802	0.977			
Zx4	0.92	0.825	0.989	0.991		
Zy4	0.904	0.818	0.976	0.993	0.985	
CA5	0.948	0.849	0.959	0.919	0.936	0.923
J5	0.947	0.809	0.935	0.924	0.928	0.922
Zx5	0.952	0.835	0.947	0.928	0.936	0.93
Zy5	0.942	0.816	0.938	0.915	0.927	0.918

	CA5	**J5**	**Zx5**
J5	0.979		
Zx5	0.987	0.99	
Zy5	0.984	0.991	0.981

Table B.17. Regression statistics for cross-sectional geometry properties of *Pan troglodytes* metatarsal midshafts against femoral head breadth (FHB).

***Pan troglodytes* (Age Groups 1-5)**							
	N	**LS slope**	**SE**	**y-int**	**R**	**R-Sq**	**P**
CA/MT1	68	0.7656	0.07041	-2.6985	0.80	64.2	0.000
J/MT1	68	2.0806	0.1429	-4.6452	0.87	76.3	0.000
Zx/MT1	68	1.356	0.1011	-4.4707	0.85	73.1	0.000
Zy/MT1	68	1.3589	0.1089	-4.3919	0.84	70.2	0.000
CA/MT2	67	3.4195	0.1952	-10.8232	0.91	82.5	0.000
J/MT2	67	3.2989	0.1817	-9.9101	0.91	83.5	0.000
Zx/MT2	67	2.2946	0.1415	-8.4265	0.90	80.2	0.000
Zy/MT2	67	2.1761	0.1314	-8.2305	0.90	80.8	0.000
CA/MT3	68	1.0366	0.07402	-4.1978	0.86	74.8	0.000
J/MT3	68	2.6672	0.1317	-7.7704	0.93	86.1	0.000
Zx/MT3	68	1.7983	0.1041	-6.684	0.90	81.9	0.000
Zy/MT3	68	1.7872	0.1059	-6.9393	0.90	81.2	0.000
CA/MT4	68	0.9688	0.07276	-4.1161	0.85	72.9	0.000
J/MT4	68	2.5031	0.162	-7.6661	0.88	78.3	0.000
Zx/MT4	68	1.6251	0.1172	-6.4885	0.86	74.4	0.000
Zy/MT4	68	1.7062	0.1297	-6.9252	0.85	72.4	0.000
CA/MT5	66	0.9036	0.08355	-4.0284	0.80	64.6	0.000
J/MT5	66	2.4467	0.1678	-7.7657	0.88	76.9	0.000
Zx/MT5	66	1.597	0.1226	-6.7161	0.85	72.6	0.000
Zy/MT5	66	1.6034	0.1278	-6.6517	0.84	71.1	0.000

Table B.18. Regression statistics for cross-sectional geometry properties of *Pan troglodytes* metatarsal midshafts against femoral head breadth (FHB) for age groups 3-5 only.

***Pan troglodytes* (Age groups 3-5)**							
	N	**LS slope**	**SE**	**y-int**	**R**	**R-Sq**	**P**
CA/MT1	49	0.7505	0.1834	-2.638	0.51	26.3	0.000
J/MT1	49	2.635	0.3559	-6.543	0.73	53.8	0.000
Zx/MT1	49	1.7011	0.2546	-5.654	0.70	48.7	0.000
Zy/MT1	49	1.6979	0.2798	-5.551	0.66	43.9	0.000
CA/MT2	48	3.6608	0.4773	-11.63	0.75	56.1	0.000
J/MT2	48	3.5439	0.4517	-10.73	0.76	57.2	0.000
Zx/MT2	48	2.3808	0.3567	-8.708	0.70	49.2	0.000
Zy/MT2	48	2.3579	0.3378	-8.851	0.72	51.4	0.000
CA/MT3	49	0.9187	0.1826	-3.78	0.59	35.0	0.000
J/MT3	49	2.8165	0.3293	-8.268	0.78	60.9	0.000
Zx/MT3	49	1.8995	0.2626	-7.022	0.73	52.7	0.000
Zy/MT3	49	1.8524	0.2693	-7.156	0.71	50.2	0.000
CA/MT4	49	0.875	0.1922	-3.785	0.55	30.6	0.000
J/MT4	49	2.5235	0.4244	-7.723	0.65	42.9	0.000
Zx/MT4	49	1.5945	0.3084	-6.376	0.60	36.3	0.000
Zy/MT4	49	1.6335	0.3446	-6.664	0.57	32.3	0.000
CA/MT5	47	0.6632	0.2221	-3.188	0.41	16.5	0.005
J/MT5	47	2.3036	0.429	-7.251	0.62	39.0	0.000
Zx/MT5	47	1.5863	0.3215	-6.67	0.59	35.1	0.000
Zy/MT5	47	1.2508	0.3279	-5.419	0.49	24.4	0.000

Table B.19. Regression statistics for cross-sectional geometry properties of *Macaca mulatta* metatarsal midshafts against femoral head breadth (FHB).

***Macaca mulatta* (Age groups 3-5)**							
	N	**LS slope**	**SE**	**y-int**	**R**	**R-Sq**	**P**
CA/MT1	51	1.0019	0.1799	-3.69	0.62	38.3	0.000
J/MT1	51	2.8788	0.3581	-7.87	0.75	56.4	0.000
Zx/MT1	51	2.0063	0.2653	-7.1	0.73	53.4	0.000
Zy/MT1	51	1.9723	0.2725	-6.81	0.72	51.2	0.000
CA/MT2	51	2.7879	0.4452	-8.71	0.66	44.0	0.000
J/MT2	51	2.7694	0.4494	-7.9	0.66	43.2	0.000
Zx/MT2	51	1.9294	0.3412	-7.15	0.62	39.0	0.000
Zy/MT2	51	1.8653	0.3557	-6.91	0.60	35.5	0.000
CA/MT3	51	0.7454	0.2063	3.339	0.45	20.7	0.000
J/MT3	51	2.2991	0.3933	-6.4	0.64	40.6	0.000
Zx/MT3	51	1.5785	0.3269	-6.02	0.56	31.8	0.000
Zy/MT3	51	1.5551	0.2758	-5.89	0.62	38.9	0.000
CA/MT4	51	0.9132	0.2563	-3.88	0.46	20.9	0.000
J/MT4	51	3.1207	0.4568	-8.94	0.70	49.3	0.000
Zx/MT4	51	2.2126	0.3582	-7.91	0.66	43.8	0.000
Zy/MT4	51	2.0859	0.3379	-7.66	0.66	43.7	0.000
CA/MT5	51	1.0399	0.2954	-4.35	0.45	20.2	0.001
J/MT5	51	3.1083	0.6067	-9.22	0.59	34.9	0.000
Zx/MT5	51	2.1551	0.4754	-7.99	0.54	29.1	0.000
Zy/MT5	51	2.1936	0.4611	-8.22	0.56	31.2	0.000

APPENDIX C

RAW LINEAR MEASURES OF ALL SPECIMENS IN THE MODERN COMPARATIVE SAMPLE

Specimens are grouped by taxon in alphabetical order and are listed here with the starting page indicated: *Colobus* (p. 322), *Gorilla* (p. 326), *Hylobates* (p. 336), *Macaca* (p. 339), *Nasalis* (p. 356), *Pan paniscus* (p. 358), *Pan troglodytes* (p. 361). Abbreviations are defined in Appendix A. Blank cells indicate unattainable measures due to missing bones, fused bones, or glued epiphyses or they indicate the measure was not recorded (as is the case for specimens examined early in the study). Measurements of long bone lengths were taken with an osteometric board and all others were taken with digital calipers. Data for the measures Talus3, Talus4, Talus7, Nav3, and Nav4 are not included out of concern for their repeatability (which is why they are also not thoroughly incorporated into the dissertation analyses). Measurements are in millimeters.

Age
For *Macaca mulatta*, age is precisely the age-at-death reported by the workers at Cayo Santiago, but for the rest of the ontogenetic samples it is based on the author's assessment of tooth eruption (Dean & Wood, 1981) and is estimated to the whole or half year in most cases. Individuals are labeled "adult" if third molars are in occlusion.

Age Group
The individuals were assigned to groups according to dental eruption stage for cross-species comparisons. Definition for these groups is located in Table 4.4.

Location
CPRC = Caribbean Primate Research Center, University of Puerto Rico
HT B = Hamman-Todd Collection, Cleveland Museum of Natural History
MCZ = Museum of Comparative Zoology, Harvard University
NMK = National Museums of Kenya
PCM = Powell-Cotton Museum, Birchington, Kent, England
RMCA = Royal Museum of Central Africa, Tervurent, Belgium
Zurich = University of Zurich

Author's Important Note
Because of the magnitude of the dataset, errors were discovered and either repaired or discarded before the dissertation analysis. However, it it is probable that some data may still be reported incorrectly. Please be aware of this small and completely unintentional potential for error. If it is impossible to check a suspicious or outlying measure against the real specimen, please discard it from the analysis.

Taxon	*Colobus angolensis*	*Colobus angolensis*	*Colobus angolensis*	*Colobus angolensis*	*Colobus angolensis*	*Colobus badius (red)*	*Colobus badius (red)*	*Colobus badius (red)*
Location	RMCA	RMCA	RMCA	RMCA	RMCA	RMCA	RMCA	RMCA
Specimen	91086	25476	25523	18232	28674	33101	33099	33102
Sex	Female	Male	Male	Male	Male	Female	Female	Female
Age	Adult	Adult	Adult	Adult	Adult	Adult	Adult	Adult
Age Group	5	5	5	5	5	5	5	5
Calc1	31.3	33.5	36.0	38.9	34.7	33.7	31.6	33.6
Calc2	18.8	21.0	24.9	23.5	20.7	20.1	20.6	20.8
Calc3	21.8	21.8	20.6	23.5	22.2	21.2	21.1	20.8
Calc4	8.5	8.9	11.6	10.4	8.0	9.2	12.2	7.5
Calc5	9.5	10.6			9.8	10.2		9.8
Calc6	8.7	8.5			9.0	9.5		10.5
Calc7	18.2	17.2	16.5	17.1	18.3	16.6	16.8	16.6
Calc8	11.2	10.3	11.3	10.5	10.7	9.6	9.9	10.1
Talus1	25.4	25.1	26.2	26.9	26.0	25.0	24.6	25.2
Talus2	25.8	25.6	26.2	26.9	27.1	24.8	24.6	25.3
Talus5	13.8	13.7	14.7	14.7	14.7	14.0	14.4	14.5
Talus6	11.4	11.1	12.9	12.5	11.7	11.7	11.3	11.5
Nav1	17.4	17.7	19.5	19.9	19.2	17.2	15.4	17.7
Nav2	8.3	8.0	9.0	9.3	8.9	8.2	7.5	7.9
MCun1	11.7	11.2	11.9	10.9	11.7	10.6	9.3	11.4
ICun1	7.6	8.3	8.0	7.1	7.3	7.3	7.7	7.3
ICun2	5.5	6.4	6.3	6.2	6.1	4.8	5.9	5.7
ICun3	6.3	6.1	6.7	6.1	6.5	6.3	5.8	5.1
ICun4	6.2	5.3	4.9	4.5	5.9	5.3	6.1	6.1
LCun1	8.9	8.7	9.7	8.9	9.3	8.3	9.0	8.7
LCun2	9.6	9.6	10.3	9.9	9.3	10.2	9.4	8.7
LCun3	8.9	8.3	9.2	9.0	9.5	8.4	8.7	8.7
LCun4	6.3	6.7	7.6	7.2	8.0	7.3	6.1	7.2
Cub1	12.4	13.0	12.6	14.8	12.0	11.3	11.4	11.8
Cub2	7.4	7.3	7.6	8.0	7.2	7.6	5.7	8.2
Cub3	12.4	11.9	12.1	11.8	12.1	9.0	9.4	9.6
Cub4	13.0	13.8	11.9	12.4	13.8	11.0	11.6	11.5
MT5	57.7	56.6	60.6	57.1	58.0	53.1	52.2	55.8
MT5D								
MT4	56.7	58.8	61.3	57.8	57.6	55.6	52.7	56.8
MT4D								
MT3	54.7	57.1	58.9	57.0	54.9	53.0	51.4	54.2
MT3D								

MT2	52.9	53.9	55.7	54.5	50.4	48.6	46.8	45.8
MT2D								
MT1	35.3	36.0	39.0	36.4	34.4	31.8	30.3	30.6
MT1D								
PH1			17.4	16.8	18.1	14.9	13.7	14.2
PH2			29.9	26.5	27.4	25.0	24.8	25.3
PH3			37.6	33.5	32.3	31.6	31.0	31.6
PH4			36.5	34.7	31.9	31.6	31.6	31.0
PH5			29.1	27.0	26.7	24.6	26.0	24.4
FemurL	192	193	203	203	190	181	174	180
FemurLD								
FHB	16.1	15.7	16.3	17.1	15.6	16.4	14.7	15.9
TibL	169	171	189	185	181	165	160	167
TibLa	166	167	186	180	176	160	155	162
TibLD								
FibL	161	163		173	168	154	151	157
FibLD								

Taxon	***Colobus badius (red)***	***Colobus badius (red)***	***Colobus badius (red)***	***Colobus badius (red)***	***Colobus guereza***	***Colobus guereza***	***Colobus guereza***	***Colobus guereza***
Location	RMCA	RMCA	RMCA	RMCA	RMCA	RMCA	RMCA	RMCA
Specimen	18402	37643	33090	5988	5897	5896	2157	27259
Sex	Female	Female	Male	Male	Female	Female	Female	Male
Age	Adult	Adult	Adult	Adult	Adult	Adult	Adult	Adult
Age Group	5	5	5	5	5	5	5	5
Calc1	31.3	33.2	30.7	35.6	35.7	34.6	32.0	37.2
Calc2	19.9	19.8	19.5	21.3	23.6	23.1	20.6	23.4
Calc3	19.9	21.4	20.8	24.5	21.1	21.0	19.3	22.9
Calc4	9.2	10.7	10.1	9.6	8.9	8.5	8.5	9.1
Calc5				10.7	11.9	10.5	9.1	10.7
Calc6				10.8	9.8	10.0	9.4	9.8
Calc7	15.3	15.7	15.1	17.4	16.9	18.0	14.3	16.8
Calc8	7.9	10.5	9.3	10.8	10.8	10.8	10.9	10.0
Talus1	23.5	26.6	25.8	27.6	27.1	26.4	25.1	29.5
Talus2	23.5	26.6	25.8	27.1	27.1	26.3	24.9	28.8
Talus5	11.2	13.9	14.5	15.1	15.4	15.9	14.4	16.2
Talus6	11.2	11.4	11.2	12.6	12.7	12.6	12.0	12.0
Nav1	17.2	16.3	16.6	18.9	18.0	18.6	16.0	18.6
Nav2	7.4	7.4	6.7	8.4	9.7	9.6	8.0	8.5
MCun1	8.7	6.9	9.3	11.6	12.3	10.7	8.7	10.1

ICun1	4.8	6.2	6.7	6.1	7.1	7.6	6.4	7.0
ICun2	5.4	4.9	5.7	3.7	5.0	5.5	4.5	4.9
ICun3	4.8	4.9	5.4	5.8	5.7	5.8	5.7	5.9
ICun4	4.8	5.3	5.4	5.9	6.3	6.2	5.6	6.3
LCun1	7.4	6.6	8.2	7.9	7.6	8.2	7.3	8.9
LCun2	7.9	7.7	8.4	8.1	8.4	8.7	6.8	9.6
LCun3	7.9	7.4	7.4	8.6	8.8	8.9	7.8	8.8
LCun4	7.5	6.8	6.3	8.0	6.7	7.2	7.1	6.4
Cub1	12.0	11.8	10.4	12.2	13.6	12.4	10.9	12.7
Cub2	5.7	7.2	6.9	8.6	6.1	6.8	6.2	7.8
Cub3	10.4	10.4	9.6	11.4	12.5	12.2	10.7	11.9
Cub4	11.4	11.7	11.8	12.2	14.7	13.4	12.8	13.7
MT5	52.5	55.8	49.3	58.3	57.2	56.8	51.9	59.4
MT5D								
MT4	53.0	52.1	48.0	57.6	57.9	58.9	53.3	59.9
MT4D								
MT3	52.5	50.5	47.5	55.5	57.7	56.9	52.1	58.0
MT3D								
MT2	47.1	46.3	43.9	51.0	54.6	52.9	49.9	52.3
MT2D								
MT1	31.5	32.4	28.6	34.5	35.9	34.3	31.1	33.6
MT1D								
PH1	15.4	15.3	12.3					
PH2	24.6	25.6	22.2					
PH3	32.3	31.7	27.9					
PH4	33.3	31.9	29.2					
PH5	26.0	24.4	22.5					
FemurL	177	178	167	195	191	185	181	198
FemurLD								
FHB	14.3	15.4	15.1	16.4	16.3	16.1	15.2	16.5
TibL	162	161	153	170	184	182	169	184
TibLa	159	157	150	165	177	177	165	180
TibLD								
FibL	156	153	144	158			162	174
FibLD								

Taxon	***Colobus guereza***	***Colobus g. occidentalis***	***Colobus g. occidentalis***	***Colobus g. occidentalis***	***Colobus g. occidentalis***	***Colobus g. occidentalis***	***Colobus g. occidentalis***	***Colobus g. occidentalis***
Location	RMCA	PCM	PCM	PCM	PCM	PCM	PCM	PCM
Specimen	2155	MER. ??	MER. 66	MER. 277	MER. 107	MER. 303	MER. 749	MER. 830

Sex	Male	Female	Female	Female	Male	Male	Male	Male
Age	Adult	Adult	Adult	Adult	Adult	Adult	Adult	Adult
Age Group	5	5	5	5	5	5	5	5
Calc1	35.6	34.7	34.5	37.3	35.1	37.9	39.2	35.6
Calc2	23.0	22.9	22.7	23.1	23.6	24.1	24.9	22.3
Calc3	22.2	20.4	21.9	23.5	21.4	24.1	24.8	22.3
Calc4	8.8	9.2	9.5	9.5	9.3	10.1	10.4	9.6
Calc5	10.1	11.6	11.7	10.6	11.3	12.2	12.0	11.8
Calc6	9.8	9.4	9.7	10.5	10.1	11.2	11.0	9.6
Calc7	16.9	17.2	16.1	17.0	16.0	20.4	17.7	17.5
Calc8	11.4	11.0	10.2	10.7	11.3	11.3	10.9	11.1
Talus1	27.2	27.1	26.6	28.5	28.9	29.4	29.7	27.9
Talus2	27.7	26.9	26.6	28.1	28.9	30.1	29.9	28.9
Talus5	15.7	15.2	15.2	15.3	16.2	17.0	17.0	15.1
Talus6	13.4	13.3	12.3	12.6	13.0	14.2	15.0	13.0
Nav1	18.5	18.1	18.2	19.1	19.8	21.7	20.9	19.9
Nav2	8.7	7.1	7.4	9.0	8.1	8.3	10.0	8.2
MCun1	10.1	11.7	11.8	13.0	11.6	12.7	12.7	11.3
ICun1	7.1	6.4	8.0	7.4	7.1	7.3	8.1	7.3
ICun2	5.4	5.3	4.0	4.5	4.8	5.6	5.0	5.7
ICun3	6.1	6.6	6.2	5.7	6.3	5.9	7.0	6.3
ICun4	5.4	5.8	5.5	5.4	5.4	6.0	5.5	5.7
LCun1	8.5	8.2	8.5	8.9	8.1	8.4	9.6	8.7
LCun2	7.5	8.8	9.4	8.6	8.7	10.0	9.9	9.6
LCun3	8.4	8.7	8.8	10.1	8.7	10.8	10.2	9.1
LCun4	7.3	7.4	6.9	7.2	7.2	8.3	7.0	7.0
Cub1	13.3	11.6	13.0	13.5	12.4	13.5	13.8	12.9
Cub2	7.0	7.7	7.6	10.2	8.1	10.2	9.7	7.9
Cub3	11.8	11.6	11.0	11.5	11.5	13.2	11.8	12.2
Cub4	13.9	13.5	14.0	13.3	13.8	16.2	15.1	14.1
MT5	57.8	56.7	60.0	61.6	62.8	62.9	64.4	57.8
MT5D								
MT4	59.6	56.3	61.6	63.2	60.4	65.9	65.1	60.1
MT4D								
MT3	58.3	55.0	60.2	61.7	59.1	64.6	64.4	59.1
MT3D								
MT2	55.0	51.5	55.5	56.9	55.6	60.3	57.8	55.2
MT2D								
MT1	34.4	34.3	35.3	37.5	35.6	39.6	40.4	37.8
MT1D								
PH1		17.3			17.9		19.1	
PH2		27.5		26.8	27.1	30.3	30.2	
PH3		34.6		34.5	34.7	39.4	38.4	
PH4		34.4		34.5	34.5	39.4		
PH5		27.9		27.3	28.1	31.2	30.2	
FemurL	200	191	200	211	198	210	213	209
FemurLD								

FHB	16.6	17.7	16.8	17.2	17.1	18.3	17.9	17.3
TibL	179	178	178	195	185	202	202	195
TibLa	172	174	173	191	180	197	197	192
TibLD								
FibL	168	168	169	186	172	191	187	184
FibLD								

Taxon	***Gorilla gorilla gorilla***							
Location	RMCA	PCM	PCM	RMCA	PCM	PCM	PCM	PCM
Specimen	12675	M756	CAMI224	35274	M690 S1	M99	M333	M141
Sex	?	Male	Male	Male	Male	Male	Female	Male
Age	0.5	0.8	1.3	1.5	2.0	2.3	2.5	2.5
Age Group	1	1	1	1	1	1	1	1
Calc1	31.2	28.8	35.4	32.4	38.2	36.5	39.3	37.7
Calc2	20.6	19.0	23.0	20.2	23.7	22.8	26.7	24.3
Calc3	19.6	17.0	24.8	23.3	25.8	26.0	24.3	23.1
Calc4	10.8	7.9	11.6	10.3	11.3	12.3	12.8	9.9
Calc5	10.8	9.2	12.1	11.6	12.4	13.9	14.8	11.9
Calc6	10.0	8.8	11.8	11.3	11.7	15.0	15.0	11.5
Calc7	14.2	13.0	16.8	15.4	16.8	16.8	16.8	15.4
Calc8	9.9	8.2	11.3	11.2	12.7	14.5	14.5	12.3
Talus1	16.1	19.3	20.3	22.8	26.9	21.4	28.5	25.1
Talus2	16.1	19.3	20.3	22.8	26.9	21.4	28.5	25.1
Talus5				11.4				
Talus6	12.8	12.0	14.9	13.8	15.8	15.5	17.5	15.2
Nav1								
Nav2								
MCun1							10.4	
ICun1								
ICun2								
ICun3								
ICun4								
LCun1					6.5		8.3	8.0
LCun2					6.5		8.5	9.0
LCun3					6.0		7.4	6.1
LCun4					4.7		5.2	5.7
Cub1		7.7	8.6	10.7	11.0	11.2	13.5	12.7
Cub2		1.4	3.0	3.0	3.2	3.4	5.5	4.4
Cub3		6.5	8.3	9.1	11.0	9.8	12.6	11.4
Cub4		7.1	8.3	10.2	12.3	12.0	12.6	11.8
MT5							41.1	
MT5D	27.5	27.0	29.6	31.9	34.1	34.0	36.6	32.1
MT4							42.1	
MT4D	27.9	28.4	29.9	31.8	34.3	34.5	37.0	33.9
MT3							41.4	
MT3D	28.1	29.1	30.1	33.1	34.2	35.1	36.8	35.0

MT2							45.3	
MT2D	31.3	30.7	32.1	36.2	36.0	37.0	39.6	36.8
MT1								29.7
MT1D	24.0	23.1	25.0	27.3	26.3	30.3	32.9	28.4
PH1		10.9	14.2		13.9	15.3	16.2	14.1
PH2		17.0	19.8		20.6	23.6	24.0	22.0
PH3		19.2	22.0		23.9	27.4	27.2	25.2
PH4		19.1	22.2		23.5	26.4	26.2	24.4
PH5		15.0	20.1		18.5	20.7	22.1	18.0
FemurL	123	124	140	145	155	173	192	167
FemurLD		115		131				
FHB	11.0	14.1	17.7	17.1	19.1	19.2	22.7	19.3
TibL			112		126	137	151	140
TibLa								
TibLD	99	93	103	109	120		144	
FibL							136	
FibLD	89	84	95	95	108	107	128	117

Taxon	***Gorilla gorilla gorilla***							
Location	PCM	PCM	PCM	RMCA	PCM	PCM	PCM	PCM
Specimen	M471	M880	M119 S3	808	M29	M98	M625	M828
Sex	Male	Male	Male	Female	Female	Female	Female	Female
Age	3.0	3.0	3.5	3.5	3.8	3.8	4.0	4.0
Age Group	2	2	2	2	2	2	2	2
Calc1	43.5	47.3	47.9	43.1	45.1	48.5	43.3	37.6
Calc2	30.6	31.8	33.8	32.7	30.2	37.0	30.4	24.8
Calc3	28.1	31.1	33.2	23.5	30.1	27.2	29.7	26.1
Calc4	14.8	15.7	18.4	14.2	16.2	14.1	17.2	14.1
Calc5	16.6	17.9	21.7	15.7	17.4	17.1	18.3	14.7
Calc6	15.3	15.5	19.5	14.5	15.4	15.3	15.4	14.9
Calc7	21.3	22.4	26.0	18.9	21.2	22.3	23.7	18.6
Calc8	15.6	17.4	18.5	12.9	14.5	19.3	15.3	14.3
Talus1	29.5	32.4	36.8	30.9	31.4	34.7	31.6	25.2
Talus2	29.5	32.4	36.8	30.9	31.4	34.7	31.6	25.2
Talus5				16.8		19.8	16.2	
Talus6	19.0	20.6	23.7	17.8	18.7	19.8	18.7	16.9
Nav1				11.4		16.0		
Nav2						6.9		
MCun1		9.7	13.0	10.3	12.2	13.1		
ICun1	6.6		9.4	7.2	6.8	8.0	6.4	
ICun2	5.0		6.8	6.9	3.8	6.5	5.6	
ICun3	7.2		8.8	7.1	8.1	8.4	8.1	
ICun4	7.2		8.5	7.2	6.7	7.6	7.1	
LCun1	9.0	9.1	11.7	10.1	8.8	9.4	9.0	8.2
LCun2	9.9	11.0	12.5	10.5	10.9	12.2	9.4	7.5
LCun3	7.8	9.0	9.9	8.3	9.3	8.7	7.9	6.5
LCun4	7.5	8.5	8.0	6.4	8.1	8.8	6.6	6.6

Cub1	13.8	15.3	17.0	14.5	13.9	16.3	14.1	11.8
Cub2	5.0	5.7	4.5	4.3	4.0	5.1	2.6	3.6
Cub3	12.7	13.6	16.4	12.5	13.5	15.9	15.0	10.0
Cub4	14.5	15.6	17.0	13.0	15.0	17.8	15.1	12.0
MT5	41.8	47.0		37.2		47.3	45.3	
MT5D	37.4	40.8	43.3	33.5	39.3	41.3	39.0	35.8
MT4		47.4	49.6	37.3	50.0	50.0	46.1	
MT4D	37.8	41.0	44.0	32.4	43.1	42.2	39.0	35.8
MT3				37.6	50.5	50.4	45.9	
MT3D	36.6	41.6	43.4	32.5	43.5	41.6	39.1	36.0
MT2	43.7	50.5		41.4	54.9	52.4	51.0	
MT2D	38.1	45.1	45.5	36.8	46.2	45.1	41.8	37.1
MT1		36.0	39.2	31.0	36.7	38.8	38.0	
MT1D	31.1	35.3	38.1	29.1	34.9	37.4	35.1	28.3
PH1	15.9	18.3	20.1	20.2	18.4		18.4	14.1
PH2	27.3	25.9	25.4	24.2	24.4		24.6	19.7
PH3	27.5	29.9	28.3	26.4	28.1	31.9	28.7	25.4
PH4	26.8	28.5	26.7	26.0		29.8	28.7	22.1
PH5	24.3	21.4	21.5	21.1	20.1	22.9	23.2	19.3
FemurL	186	192	230	191	210	214	193	192
FemurLD							185	
FHB	23.2	25.6	30.2	26.8	26.8	28.4	26.8	23.7
TibL	152	160	177	152	166	175		154
TibLa				142				
TibLD					155	156	145	
FibL	128	139		135				135
FibLD		132	145	117	141		128	128

Taxon	***Gorilla gorilla gorilla***							
Location	RMCA	PCM	PCM	RMCA	PCM	PCM	PCM	PCM
Specimen	834	CAMI14	M689	1002	FC114	M35	M57	M464
Sex	Female	Female	Male	Male	Female	Female	Female	Male
Age	7.0	7.3	7.3	7.5	8.0	9.0	9.0	9.0
Age Group	3	3	3	3	4	4	4	4
Calc1	65.9	61.0	70.7	70.5	54.0	70.0	69.0	77.9
Calc2	51.4	44.5	52.6	53.4	38.2	53.1	49.8	58.2
Calc3	38.3	35.6	42.6	42.4	33.6	41.6	40.0	45.4
Calc4	20.8	18.4	23.0	25.5	19.3	22.6	21.5	24.0
Calc5	23.8	21.0	25.3	27.4	21.7	24.3	25.1	28.4
Calc6	21.5	19.3	23.6	25.9	21.5	24.6	22.3	26.3
Calc7	31.6	31.5	37.0	35.5	23.9	38.9	37.5	38.6
Calc8	19.7	19.6	25.0	28.0	18.1	25.1	24.6	27.6
Talus1	46.2	41.8	55.5	52.2	43.3	54.8	50.1	55.6
Talus2	49.9	44.9	55.5	56.2	45.4	57.8	53.6	58.8
Talus5	28.4	23.4	31.5	31.1	27.8	33.1	29.8	35.4
Talus6	27.1	25.1	30.3	28.2	23.0	30.1	27.2	30.4
Nav1	34.6	35.8	30.1	39.9	36.6	45.1	40.3	41.6

Nav2	12.1	9.2	11.8	13.0	9.6	14.2	11.6	14.3
MCun1	17.6	17.7	17.5	17.4	15.9	19.8	18.2	20.5
ICun1	12.4	10.5	11.8	13.7	11.2	11.9	11.2	11.5
ICun2	10.5	10.1	11.1	9.7	8.9	11.6	9.2	9.8
ICun3	11.4	10.6	13.3	11.9	12.5	12.5	12.0	14.2
ICun4	12.9	11.0	14.1	12.8	9.9	13.5	10.7	13.7
LCun1	12.4	12.8	16.3	10.9	12.9	14.6	14.5	13.8
LCun2	16.8	15.2	19.3	18.4	14.0	18.1	12.5	20.5
LCun3	13.3	13.0	13.7	14.7	13.9	16.7	14.7	16.0
LCun4	9.2	10.3	11.9	10.9	10.8	11.9	11.6	15.2
Cub1	21.0	19.7	26.1	26.4	18.6	25.8	21.6	24.8
Cub2	7.1	5.6	11.9	8.5	6.3	8.2	6.9	8.3
Cub3	18.8	19.7	23.1	22.9	19.4	25.6	24.0	27.6
Cub4	19.9	19.4	23.2	25.0	19.8	26.5	24.5	28.0
MT5	61.5	61.6	64.9	64.5	57.9	70.5	74.9	77.8
MT5D	54.2	57.0	57.1	56.0	50.8			67.7
MT4	59.0	62.4	67.2		55.6	65.5	72.9	
MT4D	49.9	54.8	58.5	51.8	46.5			63.6
MT3	60.2	59.3	67.1	61.9	56.4	64.9	74.5	73.5
MT3D	51.2	49.6	56.9	51.3	46.3			60.5
MT2	62.7	63.1	72.4	65.3	61.3	69.0	78.4	78.5
MT2D	54.6	54.9	61.7	55.1	50.7			66.2
MT1	48.6	48.3	53.3	48.3	41.8	54.5	58.2	54.5
MT1D	45.3	44.8	49.9	46.2	40.2			50.6
PH1	28.0	24.2	26.1	25.0	20.3	27.3	28.1	28.5
PH2		31.0	36.2		30.4	35.1	37.8	37.6
PH3		40.3	38.6		34.2	38.8	42.3	41.6
PH4		35.3	36.8		32.5	37.0	39.7	40.9
PH5		30.2	27.3		25.2	31.2	32.5	33.6
FemurL	315	265	303	320	250	320	350	348
FemurLD								
FHB	41.9	33.8	39.7	47.7	35.5	42.8	40.0	46.9
TibL	246	212	243	267	211	256	290	289
TibLa	233	203	239	252	200	244	279	273
TibLD								
FibL	221	191	219	232	188	225	265	258
FibLD								

Taxon	***Gorilla gorilla gorilla***							
Location	PCM	PCM	PCM	PCM	PCM	PCM	PCM	PCM
Specimen	M847 S2	M160	M667	M841	M180 S1	M387	M985	M674
Sex	Male	Female	Female	Female	Female	Female	Female	Male
Age	5.5	6.0	6.0	6.0	7.0	7.0	7.0	7.0
Age Group	2	3	3	3	3	3	3	3
Calc1	56.5	61.7	58.8	57.3	59.8	62.3	66.4	60.1

Calc2	40.9	45.9	40.9	42.6	43.0	47.2	50.5	42.9
Calc3	35.5	35.3	35.9	33.7	35.4	35.1	35.7	37.4
Calc4	21.0	19.1	18.1	17.5	19.3	18.7	19.7	19.2
Calc5	23.3	22.8	21.0	20.1	21.1	22.9	22.0	22.0
Calc6	20.0	19.4	22.8	19.7	17.9	21.4	19.7	23.2
Calc7	27.3	28.8	26.5	28.9	29.0	26.0	29.2	33.5
Calc8	20.2	19.7	19.5	20.9	21.9	21.4	20.1	23.9
Talus1	40.5	45.4	45.0	42.0	44.7	47.3	48.0	47.1
Talus2	41.4	48.4	44.6	43.6	48.9	48.3	50.7	46.9
Talus5	19.5	25.6	27.8	23.7	23.6	27.6	27.7	28.5
Talus6	25.0	25.6	25.5	24.4	23.3	26.3	25.1	28.3
Nav1	14.6	29.7	29.3	28.1	28.1	28.8	33.3	29.8
Nav2		11.0	10.5	9.9	9.9	10.8	12.1	10.6
MCun1	14.0	15.5	15.5	15.2	14.4	14.9	17.6	16.6
ICun1	8.9	10.5	8.8	9.1	9.1	9.5	10.2	9.3
ICun2	8.2	7.3	8.0	8.0	7.8	9.3	12.3	9.1
ICun3	9.3	11.1	11.5	10.2	10.3	11.3	11.7	11.3
ICun4	7.6	11.4	10.7	8.7	10.6	10.8	12.7	12.7
LCun1	13.5	12.2	12.3	11.1	13.4	11.9	15.4	12.2
LCun2	14.8	13.8	14.9	14.7	15.5	17.5	17.4	14.2
LCun3	10.6	13.8	12.3	12.7	12.1	14.4	13.5	12.4
LCun4	9.3	10.8	10.9	9.5	9.2	10.6	7.9	10.3
Cub1	18.4	20.0	19.4	17.9	20.7	19.9	23.5	18.6
Cub2	6.4	8.6	6.5	5.7	6.6	6.8	6.8	6.6
Cub3	17.7	19.5	19.0	17.6	20.1	20.6	22.3	20.3
Cub4	18.9	18.8	21.9	20.2	21.1	22.1	22.3	20.2
MT5		60.8	54.5	59.7		67.1	63.9	56.8
MT5D	52.8	53.8	47.1	53.9	56.1	60.0	56.2	51.0
MT4	60.2	61.2	55.9	62.0		66.9	64.1	60.4
MT4D	52.5	50.8	46.7	54.5	54.0	58.2	54.7	52.4
MT3	59.7	60.3	56.0	62.9		67.9	62.5	59.3
MT3D	51.2	50.8	46.0	54.7	53.5	58.9	52.4	51.2
MT2	64.3	62.4	59.2	65.4		69.4	66.4	63.9
MT2D	55.7	53.6	48.8	56.1	58.2	58.6	54.2	53.8
MT1	43.4	48.9	42.1	46.2		49.0	49.5	43.9
MT1D	41.6	46.1	39.1	44.4	43.8	47.2	46.9	41.4
PH1	20.2	24.4	19.7	22.8	19.5	25.8	24.1	21.5
PH2	30.1	32.0	25.3	33.5	31.5	34.6	34.0	31.5
PH3	33.6	34.5	31.3	37.0	33.9	38.9		34.1
PH4	32.6	34.0	31.8	35.3	32.1	38.7	35.8	34.9
PH5	26.0	26.2	21.6	27.3	24.6	30.4	29.8	26.2
FemurL	257	265	244	275	208	284	277	278
FemurLD								
FHB	31.3	35.1	34.6	34.3	34.8	38.3	37.9	36.9
TibL	211	220	204	235	228	225	228	215
TibLa	206	208	193	223	218	216	216	209
TibLD								
FibL	185	193	182	198	199	190		193

FibLD	173			189		179		

Taxon	***Gorilla gorilla gorilla***							
Location	RMCA	PCM	PCM	RMCA	PCM	PCM	PCM	PCM
Specimen	834	CAMI14	M689	1002	FC114	M35	M57	M464
Sex	Female	Female	Male	Male	Female	Female	Female	Male
Age	7.0	7.3	7.3	7.5	8.0	9.0	9.0	9.0
Age Group	3	3	3	3	4	4	4	4
Calc1	65.9	61.0	70.7	70.5	54.0	70.0	69.0	77.9
Calc2	51.4	44.5	52.6	53.4	38.2	53.1	49.8	58.2
Calc3	38.3	35.6	42.6	42.4	33.6	41.6	40.0	45.4
Calc4	20.8	18.4	23.0	25.5	19.3	22.6	21.5	24.0
Calc5	23.8	21.0	25.3	27.4	21.7	24.3	25.1	28.4
Calc6	21.5	19.3	23.6	25.9	21.5	24.6	22.3	26.3
Calc7	31.6	31.5	37.0	35.5	23.9	38.9	37.5	38.6
Calc8	19.7	19.6	25.0	28.0	18.1	25.1	24.6	27.6
Talus1	46.2	41.8	55.5	52.2	43.3	54.8	50.1	55.6
Talus2	49.9	44.9	55.5	56.2	45.4	57.8	53.6	58.8
Talus5	28.4	23.4	31.5	31.1	27.8	33.1	29.8	35.4
Talus6	27.1	25.1	30.3	28.2	23.0	30.1	27.2	30.4
Nav1	34.6	35.8	30.1	39.9	36.6	45.1	40.3	41.6
Nav2	12.1	9.2	11.8	13.0	9.6	14.2	11.6	14.3
MCun1	17.6	17.7	17.5	17.4	15.9	19.8	18.2	20.5
ICun1	12.4	10.5	11.8	13.7	11.2	11.9	11.2	11.5
ICun2	10.5	10.1	11.1	9.7	8.9	11.6	9.2	9.8
ICun3	11.4	10.6	13.3	11.9	12.5	12.5	12.0	14.2
ICun4	12.9	11.0	14.1	12.8	9.9	13.5	10.7	13.7
LCun1	12.4	12.8	16.3	10.9	12.9	14.6	14.5	13.8
LCun2	16.8	15.2	19.3	18.4	14.0	18.1	12.5	20.5
LCun3	13.3	13.0	13.7	14.7	13.9	16.7	14.7	16.0
LCun4	9.2	10.3	11.9	10.9	10.8	11.9	11.6	15.2
Cub1	21.0	19.7	26.1	26.4	18.6	25.8	21.6	24.8
Cub2	7.1	5.6	11.9	8.5	6.3	8.2	6.9	8.3
Cub3	18.8	19.7	23.1	22.9	19.4	25.6	24.0	27.6
Cub4	19.9	19.4	23.2	25.0	19.8	26.5	24.5	28.0
MT5	61.5	61.6	64.9	64.5	57.9	70.5	74.9	77.8
MT5D	54.2	57.0	57.1	56.0	50.8			67.7
MT4	59.0	62.4	67.2		55.6	65.5	72.9	
MT4D	49.9	54.8	58.5	51.8	46.5			63.6
MT3	60.2	59.3	67.1	61.9	56.4	64.9	74.5	73.5
MT3D	51.2	49.6	56.9	51.3	46.3			60.5
MT2	62.7	63.1	72.4	65.3	61.3	69.0	78.4	78.5
MT2D	54.6	54.9	61.7	55.1	50.7			66.2
MT1	48.6	48.3	53.3	48.3	41.8	54.5	58.2	54.5
MT1D	45.3	44.8	49.9	46.2	40.2			50.6
PH1	28.0	24.2	26.1	25.0	20.3	27.3	28.1	28.5
PH2		31.0	36.2		30.4	35.1	37.8	37.6

PH3		40.3	38.6		34.2	38.8	42.3	41.6
PH4		35.3	36.8		32.5	37.0	39.7	40.9
PH5		30.2	27.3		25.2	31.2	32.5	33.6
FemurL	315	265	303	320	250	320	350	348
FemurLD								
FHB	41.9	33.8	39.7	47.7	35.5	42.8	40.0	46.9
TibL	246	212	243	267	211	256	290	289
TibLa	233	203	239	252	200	244	279	273
TibLD								
FibL	221	191	219	232	188	225	265	258
FibLD								

Taxon	***Gorilla gorilla gorilla***							
Location	RMCA	PCM	PCM	PCM	PCM	PCM	PCM	HT B
Specimen	881	M847 S1	ZVI30	ZIII31	M204	M505	M717	1999
Sex	Female	Female	Male	Male	Male	Male	Male	Female
Age	9.0	10.0	10.0	10.0	10.0	10.0	10.0	Adult
Age Group	4	4	4	4	4	4	4	5
Calc1	66.5	68.6	75.6	95.6	89.6	77.9	77.3	68.7
Calc2	49.6	54.2	57.3	74.7	66.7	60.0	56.5	52.2
Calc3	36.2	34.0	42.4	54.7	52.6	46.0	44.8	39.3
Calc4	17.4	20.1	23.8	30.5	27.0	26.8	23.3	21.5
Calc5	24.9	22.6	31.5	36.8	31.4	29.6	26.9	23.1
Calc6	20.1	23.1	29.6	28.8	27.1	28.8	24.9	22.8
Calc7	26.9	32.9	40.3	44.2	45.7	42.2	39.4	38.7
Calc8	21.2	23.2	33.8	31.3	28.6	29.1	28.8	26.5
Talus1	45.8	50.1	53.6	62.8	63.7	60.3	55.6	52.2
Talus2	47.7	53.0	57.6	67.8	68.9	62.9	61.5	48.9
Talus5	23.6	30.4	32.8	37.9	41.4	39.2	33.4	32.0
Talus6	25.6	28.1	31.2	37.1	34.4	32.6	29.5	26.8
Nav1	36.5	42.5	42.6	54.1	50.8	40.5	45.3	42.0
Nav2	12.5	12.6	14.7	15.3	15.9	14.3	13.5	14.3
MCun1	15.9	20.3	19.9	24.8	21.9	20.7	20.2	18.4
ICun1	10.4	13.4	12.6	16.9	14.9	11.6	11.8	12.1
ICun2	9.5	9.9	13.4	15.3	14.4	11.6	11.5	10.5
ICun3	12.2	14.2	12.3	15.1	15.5	14.8	14.9	14.0
ICun4	11.9	13.7	11.1	15.1	15.7	13.5	14.8	12.8
LCun1	10.8	14.9	13.7	18.2	16.6	15.7	13.9	13.9
LCun2	15.2	20.1	18.4	19.2	21.5	18.8	17.7	18.1
LCun3	12.4	18.5	17.9	20.8	18.9	17.6	18.4	15.0
LCun4	9.1	11.7	12.9	17.4	13.7	13.1	12.8	12.6
Cub1	23.1	24.8	25.4	24.9	27.3	26.5	26.9	23.4
Cub2	9.4	8.5	9.1	8.0	12.5	10.9	12.2	7.7
Cub3	16.9	24.7	25.2	29.7	27.2	27.3	26.0	23.1
Cub4	20.3	23.6	25.4	29.6	29.6	29.8	26.3	25.9
MT5		73.4	77.6	94.6	94.8	73.2	76.2	73.6
MT5D	56.0				84.4	63.4	67.9	

MT4	61.9	72.7	73.1	93.0	88.1	72.7	76.5	67.7
MT4D	53.2				75.7	61.9	64.8	
MT3		73.4	73.7	92.5	86.2	72.7	75.7	67.9
MT3D	53.5				73.6	62.2	63.3	
MT2	66.1	76.1	75.7	94.9	86.9	73.4	77.9	73.9
MT2D	57.8				75.5	62.4	64.8	
MT1	48.3	58.9	56.6	75.3	64.3	58.0	53.8	54.8
MT1D	44.5				60.1	54.2	48.9	
PH1	24.3	29.1	31.2	37.6	32.2	29.4	26.3	28.4
PH2		39.9	38.1	45.6	41.6	36.3	39.0	37.5
PH3		42.9	41.8	50.6	47.1	41.3	43.1	41.5
PH4		42.2	40.6	51.1	45.5	40.9	41.9	39.4
PH5		33.1	33.1	39.8	37.3	33.6	33.8	31.6
FemurL	311	316	340	375	380	327	340	314
FemurLD								
FHB	40.7	40.4	45.2	50.4	51.6	47.0	44.9	38.4
TibL	241	270	290	335	318	266	281	259
TibLa	227	258	277	317	302	251	267	249
TibLD								
FibL	212	236		297	283	242	247	230
FibLD								

Taxon	***Gorilla gorilla gorilla***							
Location	HT B	HT B	HT B	HT B	HT B	PCM	PCM	PCM
Specimen	2069	2767	2745	2826	2000	M688	M687	M690 S2
Sex	Female	Male	Male	Male	Male	Female	Male	Male
Age	Adult	Adult	Adult	Adult	Adult	Adult	Adult	Adult
Age Group	5	5	5	5	5	5	5	5
Calc1	74.6	88.8	80.9	91.2	94.0	65.2	85.3	89.9
Calc2	56.0	65.6	60.3	72.0	72.4	50.5	67.7	74.5
Calc3	43.1	54.1	49.7	48.8	50.4	35.3	44.5	45.3
Calc4	23.7	29.0	25.7	29.7	27.0	21.1	27.5	30.0
Calc5	28.1	30.7	30.4	30.9	30.0	24.8	31.2	33.3
Calc6	23.3	29.1	27.1	30.6	28.9	20.0	29.9	28.6
Calc7	40.9	47.5	47.6	54.3	49.3	32.4	43.0	48.9
Calc8	24.1	33.6	35.0	37.5	32.9	21.8	34.5	34.2
Talus1	55.8	66.6	60.5	65.9	69.1	48.4	59.5	59.8
Talus2	53.4	63.5	64.8	63.6	65.9	51.6	63.2	65.3
Talus5	32.8	42.5	40.0	43.4	41.0	31.3	38.6	39.7
Talus6	28.7	32.6	33.6	36.0	35.2	25.7	34.1	33.5
Nav1	42.0	51.7	51.2	55.1	56.8	37.2	48.0	53.3
Nav2	12.0	15.9	15.1	17.7	19.6	11.4	16.6	17.7
MCun1	18.2	23.2	22.0	22.4	24.1	18.9	23.1	22.5
ICun1	11.1	15.7	14.5	12.8	13.7	9.5	14.1	13.2
ICun2	11.4	14.1	12.4	13.3	14.1	9.1	14.2	13.6
ICun3	13.1	15.3	15.7	15.7	16.1	12.2	16.9	18.8
ICun4	13.8	13.7	16.9	16.1	17.0	12.3	17.4	15.7

LCun1	14.1	20.5	15.8	18.2	17.6	11.4	16.6	18.1
LCun2	17.5	23.1	20.5	21.4	24.2	15.2	24.5	23.3
LCun3	15.6	19.6	20.3	18.8	18.4	13.4	20.0	19.0
LCun4	11.4	12.5	15.1	14.2	13.7	10.8	15.1	14.7
Cub1	23.3	30.4	29.2	29.9	35.5	18.2	31.7	28.2
Cub2	8.5	7.3	11.4	10.4	15.0	6.8	10.4	11.4
Cub3	23.5	31.6	27.7	32.9	29.9	21.2	28.4	30.0
Cub4	23.4	34.2	32.6	33.7	33.4	22.4	31.5	28.8
MT5	73.7	88.8	81.3	90.6	90.0	70.9	82.8	90.1
MT5D								
MT4	67.5	78.8	78.6	84.0	84.2	67.8	82.3	82.8
MT4D								
MT3	67.5	79.6	78.3	81.3	83.1	67.2	86.0	79.7
MT3D								
MT2	73.3	83.7	81.5	86.8	88.4	70.8	82.8	89.2
MT2D								
MT1	57.8	67.6	61.4	67.4	64.5	52.5	62.3	67.8
MT1D								
PH1	28.8	33.0	32.8	34.4	32.0	25.5	32.5	29.0
PH2		44.1	40.8	44.2	42.3	34.8	42.1	42.4
PH3		50.5	46.4	46.7	47.1	38.7	44.9	44.8
PH4		49.0	44.7	47.3	45.4	38.4	43.4	44.3
PH5		41.0	36.6	42.1	36.9	30.5	35.5	35.8
FemurL	303	380	341	386	380	315	347	377
FemurLD								
FHB	38.4	50.0	49.8	53.4	49.1	38.1	48.6	54.6
TibL	262	330	281	332	320	264	290	330
TibLa	250	319	268	320	306	253	274	315
TibLD								
FibL	239	291	250	300	281	240	257	299
FibLD								

Taxon	***Gorilla gorilla gorilla***								
Location	PCM	HT B	HT B	PCM	PCM	HT B	HT B	HT B	HT B
Specimen	M688	1999	2069	M687	M690 S2	2767	2745	2826	2000
Sex	Female	Female	Female	Male	Male	Male	Male	Male	Male
Age	Adult	Adult	Adult	Adult	Adult	Adult	Adult	Adult	Adult
Age Group	5	5	5	5	5	5	5	5	5
Calc1	65.2	68.7	74.6	85.3	89.9	88.8	80.9	91.2	94.0
Calc2	50.5	52.2	56.0	67.7	74.5	65.6	60.3	72.0	72.4
Calc3	35.3	39.3	43.1	44.5	45.3	54.1	49.7	48.8	50.4
Calc4	21.1	21.5	23.7	27.5	30.0	29.0	25.7	29.7	27.0
Calc5	24.8	23.1	28.1	31.2	33.3	30.7	30.4	30.9	30.0
Calc6	20.0	22.8	23.3	29.9	28.6	29.1	27.1	30.6	28.9
Calc7	32.4	38.7	40.9	43.0	48.9	47.5	47.6	54.3	49.3
Calc8	21.8	26.5	24.1	34.5	34.2	33.6	35.0	37.5	32.9
Talus1	48.4	52.2	55.8	59.5	59.8	66.6	60.5	65.9	69.1

Talus2	51.6	48.9	53.4	63.2	65.3	63.5	64.8	63.6	65.9
Talus5	31.3	32.0	32.8	38.6	39.7	42.5	40.0	43.4	41.0
Talus6	25.7	26.8	28.7	34.1	33.5	32.6	33.6	36.0	35.2
Nav1	37.2	42.0	42.0	48.0	53.3	51.7	51.2	55.1	56.8
Nav2	11.4	14.3	12.0	16.6	17.7	15.9	15.1	17.7	19.6
MCun1	18.9	18.4	18.2	23.1	22.5	23.2	22.0	22.4	24.1
ICun1	9.5	12.1	11.1	14.1	13.2	15.7	14.5	12.8	13.7
ICun2	9.1	10.5	11.4	14.2	13.6	14.1	12.4	13.3	14.1
ICun3	12.2	14.0	13.1	16.9	18.8	15.3	15.7	15.7	16.1
ICun4	12.3	12.8	13.8	17.4	15.7	13.7	16.9	16.1	17.0
LCun1	11.4	13.9	14.1	16.6	18.1	20.5	15.8	18.2	17.6
LCun2	15.2	18.1	17.5	24.5	23.3	23.1	20.5	21.4	24.2
LCun3	13.4	15.0	15.6	20.0	19.0	19.6	20.3	18.8	18.4
LCun4	10.8	12.6	11.4	15.1	14.7	12.5	15.1	14.2	13.7
Cub1	18.2	23.4	23.3	31.7	28.2	30.4	29.2	29.9	35.5
Cub2	6.8	7.7	8.5	10.4	11.4	7.3	11.4	10.4	15.0
Cub3	21.2	23.1	23.5	28.4	30.0	31.6	27.7	32.9	29.9
Cub4	22.4	25.9	23.4	31.5	28.8	34.2	32.6	33.7	33.4
MT5	70.9	73.6	73.7	82.8	90.1	88.8	81.3	90.6	90.0
MT5D									
MT4	67.8	67.7	67.5	82.3	82.8	78.8	78.6	84.0	84.2
MT4D									
MT3	67.2	67.9	67.5	86.0	79.7	79.6	78.3	81.3	83.1
MT3D									
MT2	70.8	73.9	73.3	82.8	89.2	83.7	81.5	86.8	88.4
MT2D									
MT1	52.5	54.8	57.8	62.3	67.8	67.6	61.4	67.4	64.5
MT1D									
PH1	25.5	28.4	28.8	32.5	29.0	33.0	32.8	34.4	32.0
PH2	34.8	37.5		42.1	42.4	44.1	40.8	44.2	42.3
PH3	38.7	41.5		44.9	44.8	50.5	46.4	46.7	47.1
PH4	38.4	39.4		43.4	44.3	49.0	44.7	47.3	45.4
PH5	30.5	31.6		35.5	35.8	41.0	36.6	42.1	36.9
FemurL	315	314	303	347	377	380	341	386	380
FemurLD									
FHB	38.1	38.4	38.4	48.6	54.6	50.0	49.8	53.4	49.1
TibL	264	259	262	290	330	330	281	332	320
TibLa	253	249	250	274	315	319	268	320	306
TibLD									
FibL	240	230	239	257	299	291	250	300	281
FibLD									

Taxon	*Hylobates lar lar*	*Hylobates lar lar*	*Hylobates lar lar*	*Hylobates lar lar*	*Hylobates lar lar*	*Hylobates lar lar*
Location	MCZ	MCZ	MCZ	MCZ	MCZ	MCZ
Specimen	MCZ 41552	MCZ 41547	MCZ 41543	MCZ 41534	MCZ 41529	MCZ 41501
Sex	Female	Female	Female	Male	Male	Male
Age	Adult	Adult	Adult	Adult	Adult	Adult
Age Group	5	5	5	5	5	5
Calc1	25.0	24.9	28.8	27.6	27.2	23.8
Calc2	15.7	15.5	18.7	17.6	17.5	15.8
Calc3	16.4	18.4	18.9	18.4	18.2	16.3
Calc4	7.7	9.0	9.1	8.8	9.6	8.2
Calc5	7.7	9.8	9.7	9.8	10.2	8.9
Calc6	8.1	7.8	8.4	7.8	8.1	7.5
Calc7	17.1	14.6	19.0	17.7	17.9	13.9
Calc8	11.0	8.2	9.9	9.5	9.0	7.5
Talus1	22.0	20.3	22.4	22.4	21.9	19.9
Talus2	22.0	20.9	22.3	21.8	21.9	20.0
Talus5	13.7	12.9	13.3	14.6	14.4	13.3
Talus6	10.7	9.1	10.6	10.1	11.1	9.0
Nav1	17.0	16.6	16.8	17.9	18.5	16.1
Nav2	6.5	6.6	7.4	6.9	6.4	6.8
MCun1	11.4	11.0	12.1	11.5	11.4	10.5
ICun1	6.8	7.5	6.0	6.8	7.4	6.7
ICun2	4.6	5.4	4.4	4.9	4.8	4.4
ICun3	5.5	6.2	5.0	6.0	6.5	5.1
ICun4	5.3	5.3	5.9	5.7	5.8	5.3
LCun1	7.1	6.9	6.7	7.7	7.5	6.0
LCun2	8.3	8.0	8.4	8.8	9.3	7.2
LCun3	6.4	6.4	6.6	6.8	6.6	5.9
LCun4	4.2	4.7	5.0	4.7	4.8	4.7
Cub1	11.9	11.9	11.2	11.8	11.3	10.3
Cub2	7.0	8.1	7.0	7.5	7.6	6.6
Cub3	8.4	8.6	8.0	9.9	9.0	8.8
Cub4	9.8	9.2	9.8	9.8	11.2	9.3
MT5	39.4	37.1	43.0	37.3	43.0	38.3
MT5D						
MT4	42.3	41.4	47.4	41.8	47.7	42.5
MT4D						
MT3	45.0	42.5	52.1	43.6	50.8	44.1
MT3D						

MT2	47.2	45.6	55.3	46.3	53.5	45.7
MT2D						
MT1	37.8	35.0	44.3	36.0	40.6	37.7
MT1D						
PH1	19.6	19.8	21.1	18.6	18.5	18.4
PH2	29.2	29.2	30.1	27.7	28.8	25.3
PH3	31.3	31.7	33.3	30.3	32.1	31.0
PH4	30.0	29.7	33.1	29.1	29.5	28.7
PH5	27.5	26.3	28.8	26.6	21.9	19.1
FemurL	209	202	225	202	210	203
FemurLD						
FHB	16.3	16.8	17.1	17.0	17.2	16.2
TibL	178	170	202	168	190	171
TibLa	173	166	198	162	185	168
TibLD						
FibL	168	160	191	155	179	163
FibLD						

Taxon	***Hylobates lar lar***	***Hylobates lar mulleri***	***Hylobates lar mulleri***	***Hylobates lar mulleri***	***Hylobates lar mulleri***	***Hylobates lar mulleri***
Location	MCZ	MCZ	MCZ	MCZ	MCZ	MCZ
Specimen	MCZ 41495	MCZ 37373	MCZ 37378	MCZ 37383	MCZ 37374	MCZ 37380
Sex	Male	Female	Female	Female	Male	Male
Age	Adult	Adult	Adult	Adult	Adult	Adult
Age Group	5	5	5	5	5	5
Calc1	27.3	25.8	27.2	23.9	23.7	26.4
Calc2	16.9	16.0	16.5	14.3	14.4	16.1
Calc3	18.4	19.2	17.9	17.4	17.4	19.4
Calc4	9.5	9.4	8.5	7.8	9.3	9.7
Calc5	9.9	10.5	9.3	8.3	9.4	10.9
Calc6	9.0	8.8	7.2	6.8	6.7	7.3
Calc7	17.7	16.5	15.7	14.5	13.4	14.3
Calc8	9.1	9.4	7.4	6.9	7.8	8.4
Talus1	22.2	23.1	20.5	19.7	20.2	22.8
Talus2	22.3	23.1	20.5	19.7	20.2	22.8
Talus5	13.9	14.8	12.3	12.4	12.7	14.4
Talus6	10.5	10.9	10.7	8.8	9.3	10.7
Nav1	18.2	15.5	17.4	14.5	14.9	15.6
Nav2	6.5	6.9	6.2	5.9	6.4	6.2
MCun1	11.9	11.3	11.1	10.5	10.0	12.0

ICun1	6.0	8.2	6.2	5.6	7.3	6.3
ICun2	5.0	6.4	5.1	5.1	5.6	5.4
ICun3	5.4	6.3	6.4	4.7	5.9	5.6
ICun4	4.9	6.0	6.1	4.7	5.3	5.5
LCun1		8.1	7.5	5.7	7.3	6.7
LCun2		10.5	9.2	8.0	9.1	8.9
LCun3		6.3	6.3	5.5	6.2	6.0
LCun4		4.9	4.8	4.4	3.8	4.7
Cub1	11.3	12.1	11.7	10.3	10.0	12.4
Cub2	5.9	8.2	8.3	5.9	7.2	8.6
Cub3	8.7	10.1	9.6	8.5	8.1	9.2
Cub4	8.7	11.6	10.3	9.4	9.4	10.6
MT5	38.4	35.1	41.3	37.6	34.3	38.8
MT5D						
MT4	42.6	38.3	45.4	39.7	37.8	41.5
MT4D						
MT3	50.1	40.8	47.8	41.5	38.3	43.9
MT3D						
MT2	47.2	44.6	50.4	45.4	41.6	47.3
MT2D						
MT1	37.7	35.3	42.2	38.2	34.5	39.3
MT1D						
PH1	19.8	17.9	21.5	19.7	17.7	20.2
PH2	27.2	27.1	29.8	26.6	25.1	30.1
PH3	29.5	31.3	31.5	28.2	28.3	31.9
PH4	27.9	28.4	30.3	27.2	26.1	30.7
PH5	19.9	25.1	24.2	21.7	24.0	22.5
FemurL	192	207	216	187	186	189
FemurLD						
FHB	15.7	17.3	15.4	14.8	14.9	16.8
TibL	163	178	188	163	157	174
TibLa	157	173	182	159	151	169
TibLD						
FibL	155	169	176	152	148	162
FibLD						

Taxon	***Macaca mulatta***							
Location	CPRC	CPRC	CPRC	CPRC	CPRC	CPRC	CPRC	CPRC
Specimen	468	476	492	506	462	485	449	474
Sex	Male	Female	Male	Female	Male	Male	Female	Female
Age	0.0	0.1	0.1	0.2	0.3	0.3	0.6	0.6
Age Group	1	1	1	1	1	1	1	1
Calc1	14.3	16.3	15.9	18.8	18.1	20.3	21.4	20.6
Calc2	7.3	8.6	8.3	9.6	9.4	10.5	11.9	11.1
Calc3	11.7	12.6	12.2	14.3	16.1	15.8	15.3	15.1
Calc4	4.1	4.0	3.5	4.5	6.9	5.2	5.7	5.0
Calc5	4.1	4.2	3.8	4.9	6.9	5.2	6.1	5.4
Calc6	3.7	3.7	4.2	4.4	4.2	4.9	5.4	5.1

Calc7	5.7	5.8	6.6	7.5	7.4	8.6	8.7	9.0
Calc8	3.6	3.9	4.4	4.5	4.8	5.0	5.5	6.2
Talus1	10.3	12.5	12.1	14.1	13.1	15.5	16.3	16.1
Talus2	10.3	12.5	12.1	14.1	13.1	15.5	16.3	16.1
Talus5		5.8	5.6	6.9	5.6	7.8	8.0	8.2
Talus6	4.6	5.2	5.5	6.1	6.1	6.9	6.9	6.7
Nav1								8.0
Nav2								4.1
MCun1					4.5		6.1	6.1
ICun1							3.6	3.8
ICun2							3.3	3.4
ICun3							3.6	3.6
ICun4							3.1	3.1
LCun1					3.9		5.5	5.4
LCun2					3.9		5.2	5.7
LCun3					3.6		4.9	4.3
LCun4					2.7		3.9	4.0
Cub1					4.4		7.1	6.7
Cub2					1.8		4.3	3.8
Cub3					4.6		5.9	5.8
Cub4					4.8		6.6	6.5
MT5								
MT5D		18.0	16.2	19.6	19.0	21.7	22.8	21.9
MT4								
MT4D		19.0	18.2	22.1	21.5	23.3	25.2	24.4
MT3								
MT3D		19.1	18.7	22.4	22.1	23.5	26.0	24.5
MT2								
MT2D		17.1	17.1	21.4	20.7	23.1	24.3	23.2
MT1								
MT1D		13.8	13.1	15.0	15.6	17.3	17.3	16.5
PH1			7.1	8.4	7.4	9.4		8.8
PH2			12.7	14.1		15.6		14.8
PH3			13.3	15.0		16.1		15.6
PH4			13.6	14.4		15.3		15.0
PH5			12.8	13.8		14.9		13.0
FemurL								
FemurLD	50	57	58	64	64	71	75	78
FHB		6.0	6.6	7.2	7.1	8.8	9.2	9.2
TibL								
TibLa								
TibLD	47	56	56	62	62	70	73	75
FibL								
FibLD	44	51	52	57	58	66	69	71

Taxon	***Macaca mulatta***							
Location	CPRC	CPRC	CPRC	CPRC	CPRC	CPRC	CPRC	CPRC
Specimen	475	473	464	477	615	613	549	479

Sex	Male	Male	Male	Female	Male	Male	Male	Male
Age	0.8	0.9	0.9	1.0	1.0	1.0	1.0	1.0
Age Group	1	1	1	1	2	2	2	2
Calc1	22.8	25.9	25.2	24.2	22.2	23.9	26.1	24.0
Calc2	12.1	13.5	13.8	12.8	11.8	13.0	13.8	13.8
Calc3	18.2	20.7	19.9	18.3	18.1	18.6	21.3	18.7
Calc4	6.7	7.6	7.9	7.2	7.4	7.6	7.7	7.7
Calc5	7.6	8.2	8.0	7.6	7.8	8.0	8.5	8.6
Calc6	5.8	6.6	6.0	6.0	5.5	6.0	6.7	6.1
Calc7	8.9	10.5	10.7	9.6	9.8	9.7	10.0	12.3
Calc8	5.4	7.3	6.8	6.1	5.8	6.7	7.7	7.4
Talus1	17.4	20.4	19.6	18.9	16.7	19.2	21.0	19.0
Talus2	17.4	20.4	19.6	18.9	16.7	19.2	21.0	19.0
Talus5	8.9	9.9	8.9	9.4	8.0	9.4	10.0	9.7
Talus6	7.8	8.7	8.4	7.9	7.6	8.1	8.6	8.9
Nav1	8.7	10.9	10.6	10.0	8.5	9.8	11.9	10.5
Nav2	3.4	5.0	4.5	4.6	4.1	4.2	5.3	4.3
MCun1	6.4	8.3	8.4	7.6	6.9	8.0	8.5	8.2
ICun1	4.0	5.3	4.9	4.3			5.3	
ICun2	3.4	4.4	3.8	3.7			4.5	
ICun3	3.6	4.3	4.2	3.9			4.5	
ICun4	3.1	4.1	3.7	3.4			4.2	
LCun1	5.3	6.5	6.4	5.9	5.5	6.0	6.3	6.4
LCun2	5.5	6.8	6.5	6.0	5.5	6.5	6.5	6.7
LCun3	5.3	6.0	5.6	5.3	4.8	5.4	6.0	6.2
LCun4	4.3	5.1	4.7	4.4	4.2	4.4	5.1	5.0
Cub1	7.1	9.3	8.7	8.3		8.8	9.2	8.6
Cub2	4.5	6.2	4.3	5.5		4.9	6.4	4.9
Cub3	5.8	6.9	6.5	6.3		6.9	6.7	6.6
Cub4	6.1	7.9	7.9	7.6		7.1	8.0	7.6
MT5								
MT5D	24.6	28.5	28.4	26.6	25.5	26.7	28.7	25.6
MT4								
MT4D	27.0	30.6	31.0	28.6	27.9	29.0	30.5	28.4
MT3								
MT3D	27.7	31.2	31.3	28.5	28.0	29.3	30.6	28.7
MT2								
MT2D	26.8	29.0	30.3	27.1	26.1	27.8	29.9	27.9
MT1								
MT1D	18.8	19.9	21.1	18.8	19.5	18.6	20.8	19.5
PH1	9.7	10.2	10.6	9.5	9.1	8.5	9.7	10.3
PH2	16.6	17.6	17.2	17.7		16.3	16.9	18.0
PH3	17.9	20.3	19.1	18.8	18.0	17.9	18.4	18.9
PH4	16.9	20.1	17.7	18.0		16.7	17.6	18.4
PH5	15.9	16.3	16.4	16.7		15.6	16.5	18.0
FemurL		105		98			108	100
FemurLD	86	94	96	90	89	93	98	91
FHB	10.3	11.0	11.0	10.6	10.4	10.7	11.6	10.8

TibL								
TibLa								
TibLD	80	93	92	88	83	91	95	88
FibL								
FibLD	76	86	88	82	80	86	89	81

Taxon	***Macaca mulatta***							
Location	CPRC	CPRC	CPRC	CPRC	CPRC	CPRC	CPRC	CPRC
Specimen	537	481	592	501	471	472	522	3692
Sex	Male	Female	Male	Female	Female	Female	Female	Male
Age	1.1	1.1	1.7	1.8	1.8	1.8	1.9	2.1
Age Group	2	2	2	2	2	2	2	2
Calc1	24.4	25.8	28.1	26.2	29.2	28.2	29.4	26.8
Calc2	13.4	13.6	16.0	13.9	15.0	16.3	15.9	13.9
Calc3	20.2	21.2	21.8	20.3	21.0	19.1	21.4	20.8
Calc4	8.0	7.1	8.9	7.9	6.9	7.6	8.5	7.9
Calc5	8.7	7.9	9.6	8.6	7.6	8.8	9.5	8.5
Calc6	6.8	6.4	7.4	6.9	6.2	7.1	7.8	6.6
Calc7	10.7	12.2	12.4	11.9	12.6	13.4	11.6	10.8
Calc8	7.3	7.4	8.0	7.5	8.8	7.9	8.3	7.8
Talus1	20.0	21.3	23.8	22.7	23.0	24.1	22.7	21.5
Talus2	20.0	21.3	23.8	22.7	23.0	24.1	22.7	21.5
Talus5	10.5	10.8	11.6	11.6	11.7	12.5	12.2	11.5
Talus6	8.9	8.4	9.1	8.9	9.1	9.6	9.6	9.2
Nav1	10.6	11.6	13.1	12.9	13.9	14.6	14.1	
Nav2	4.2	5.5	5.8	7.3	6.9	7.5	7.2	
MCun1	7.9	8.4	8.7	9.2	8.8	9.1	9.3	8.5
ICun1	4.6	5.3	5.2	6.0	6.2	6.4	6.2	
ICun2	4.1	4.5	4.5	4.9	5.2	5.8	5.4	
ICun3	4.0	4.4	4.6	4.7	5.1	5.3	5.4	
ICun4	4.0	3.8	4.5	4.5	4.5	4.9	5.0	
LCun1	6.4	6.8	6.7	7.4	7.0	7.2	7.3	6.9
LCun2	6.6	6.8	6.6	7.5	8.0	8.4	7.8	7.2
LCun3	5.7	6.5	6.8	7.1	7.0	6.8	7.3	6.3
LCun4	4.6	5.0	5.1	5.1	5.3	5.5	5.3	5.4
Cub1	9.2	10.0	10.6	10.6	11.4	11.0	10.8	10.5
Cub2	6.0	6.7	5.8	7.1	7.7	7.8	6.9	6.8
Cub3	7.1	6.9	9.0	7.8	8.7	8.5	8.2	7.7
Cub4	7.9	8.8	9.3	9.9	9.5	9.2	10.6	9.2
MT5								
MT5D	26.9	28.9	32.4	31.9	33.5	34.6	35.0	31.2
MT4								
MT4D	29.0	30.1	34.4	34.4	34.9	35.9	36.4	33.3
MT3								
MT3D	28.6	30.1	34.1	33.5	34.6	35.8	35.5	33.2
MT2								
MT2D	27.8	28.5	32.6	33.0	32.5	33.9	34.6	31.3
MT1								

MT1D	19.7	20.7	22.3	22.1	22.6	22.8	24.2	21.6
PH1	9.7	10.8	10.5	11.5	11.5	11.7	12.4	10.2
PH2	15.8	17.3	18.6	18.4	18.3	19.3	19.4	
PH3	17.8	18.9	20.4	21.3	20.1	21.9	22.2	19.4
PH4	17.0	17.9	19.1	20.5	19.3	20.4	21.5	
PH5	15.9	16.6	18.1	18.7	17.7	18.6	19.3	
FemurL	99	105	124	115	118	128	127	
FemurLD	89	96	114	105	109	117	114	111
FHB	11.3	11.9	12.9	13.0	12.7	14.2	14.0	11.9
TibL							120	
TibLa							114	
TibLD	85	93	108	102	102	114	108	103
FibL								
FibLD	82	88	102	96	96	108	102	97

Taxon	***Macaca mulatta***							
Location	CPRC	CPRC	CPRC	CPRC	CPRC	CPRC	CPRC	CPRC
Specimen	486	642	458	676	443	446	490	510
Sex	Female	Female	Female	Male	Female	Female	Male	Male
Age	2.1	2.1	2.5	2.5	4.0	4.0	4.0	4.4
Age Group	2	2	2	2	3	3	3	3
Calc1	30.5	29.6	29.8	32.0	34.8	31.7	35.6	38.4
Calc2	17.1	15.8	17.3	17.2	20.6	19.2	20.8	24.2
Calc3	21.5	21.6	19.8	24.0	23.0	21.4	24.9	26.9
Calc4	8.0	8.1	8.5	9.0	9.0	7.6	9.1	11.4
Calc5	8.0	8.4	8.9	9.5	9.2	8.5	10.1	12.5
Calc6	7.8	7.2	7.5	8.1	9.4	8.0	8.4	10.1
Calc7	13.0	12.3	12.7	12.6	12.5	14.2	13.7	15.9
Calc8	8.7	8.5	8.1	8.9	9.1	9.2	9.8	10.9
Talus1	23.2	23.4	23.3	25.5	25.3	23.9	26.2	29.2
Talus2	23.3	23.4	23.3	25.5	25.3	23.9	26.2	29.2
Talus5	12.4	13.2	13.3	13.8	14.7	13.3	14.5	17.5
Talus6	9.4	9.7	9.9	10.8	10.9	10.5	11.7	12.8
Nav1	14.5	14.2	15.4	15.2	17.0	14.4	17.9	19.1
Nav2	6.8	6.8	6.4	7.0	7.4	8.2	8.5	8.9
MCun1	9.3	10.0	9.2		10.1	9.3	11.0	12.1
ICun1	5.9	5.9	6.4	6.2	6.6	6.1	7.1	8.4
ICun2	4.8	5.6	5.9	5.2	5.6	5.5	6.3	6.6
ICun3	4.4	5.0	4.9	5.6	5.5	5.1	6.2	7.5
ICun4	4.7	4.7	4.7	4.9	5.6	5.4	5.8	6.7
LCun1	7.2	7.8	7.7	7.4	7.8	7.6	8.5	9.2
LCun2	7.6	7.8	7.2	7.9	9.0	8.8	10.3	10.1
LCun3	6.2	6.9	7.3	7.4	8.1	7.6	9.8	9.8
LCun4	5.0	5.3	5.5	6.1	5.9	5.6	7.3	7.2
Cub1	10.9	10.9	11.0	11.7	12.7	11.1	13.0	13.9
Cub2	7.0	6.8	7.4	7.3	8.8	8.8	9.0	10.3
Cub3	8.4	8.9	8.7	8.8	10.3	8.6	10.4	10.9
Cub4	10.2	10.2	9.8	10.0	12.6	10.7	12.5	13.8
MT5					51.3			

MT5D	36.9	35.4	39.9	38.0	46.7	40.7	47.6	53.2
MT4					52.2			
MT4D	39.0	37.6	40.4	39.4		42.9	50.4	54.3
MT3					51.6			
MT3D	39.5	38.7	40.0	39.1		41.8	50.2	54.4
MT2					49.9			
MT2D	37.1	36.6	37.7	37.9		39.6	47.2	54.3
MT1					33.7	30.8		
MT1D	24.9	24.3	26.8	25.6		30.8	31.8	36.7
PH1	13.0	12.1	13.4	12.8	16.1	17.3	14.5	17.8
PH2	21.0	20.3	21.6	21.3	24.2	25.8	25.8	28.0
PH3	23.5	22.3	23.6	23.7	27.7	27.1	27.2	31.0
PH4	21.8	21.1	22.7	22.0	26.4	27.6	26.3	28.2
PH5	20.5	19.7	21.6	20.5	25.1	25.2	24.9	27.4
FemurL	130	132	136	135	169	156	174	183
FemurLD	120	121	125	124	160	148	156	166
FHB	13.5	13.6	14.0	13.8	16.2	15.4	16.2	17.6
TibL			135		157	147	161	178
TibLa			130		153	141	156	173
TibLD	119	116	124	116		135	147	163
FibL			127				153	166
FibLD	113	110	118	110	139	126	142	155

Taxon	***Macaca mulatta***							
Location	CPRC	CPRC	CPRC	CPRC	CPRC	CPRC	CPRC	CPRC
Specimen	519	545	565	585	794	552	3003	562
Sex	Female	Female	Female	Female	Male	Female	Female	Male
Age	3.2	3.4	4.2	4.4	2.5	2.6	2.6	2.8
Age Group	3	3	3	3	3	3	3	3
Calc1	31.6	34.3	31.9	33.4	29.6	31.0	28.7	34.1
Calc2	18.4	20.3	19.1	19.8	16.2	16.3	15.8	18.0
Calc3	21.8	23.9	22.5	24.0	23.6	23.9	21.1	25.2
Calc4	9.0	7.7	8.4	8.6	9.2	8.5	7.3	8.8
Calc5	9.6	8.7	9.0	9.2	9.8	9.4	8.3	9.2
Calc6	9.1	8.4	8.6	7.5	7.5	7.3	7.6	7.9
Calc7	13.4	15.2	13.3	14.2	12.9	12.9	12.1	13.9
Calc8	8.4	9.5	9.7	9.4	8.9	8.6	8.6	9.8
Talus1	24.0	24.1	23.9	24.3	24.5	23.9	22.8	25.7
Talus2	24.0	24.1	23.9	24.3	24.5	23.9	22.8	25.7
Talus5	13.7	13.3	13.7	13.7	13.6	13.4	13.1	14.0
Talus6	10.9	10.8	10.7	11.4	10.0	10.4	9.4	10.8
Nav1	15.8	15.4	15.4	15.7	14.7	14.9	14.2	15.9
Nav2	7.5	8.3	6.9	8.3	6.8	6.8	7.2	8.1
MCun1	10.1	10.7	9.4	10.2	10.3	8.7	9.3	10.3
ICun1	6.5	7.6	5.7	6.2	5.9	6.4	6.1	5.9
ICun2	5.8	5.7	5.4	5.5	5.4	5.3	4.8	5.3
ICun3	5.7	6.6	5.3	5.2	5.2	5.4	5.0	5.6
ICun4	5.2	5.3	5.4	5.1	5.1	5.0	4.9	5.2

LCun1	7.9	8.3	7.3	7.6	7.9	7.6	7.5	7.8
LCun2	9.1	9.1	9.0	8.5	8.2	8.5	7.7	9.6
LCun3	7.8	8.1	8.2	7.9	7.2	7.3	7.6	8.0
LCun4	5.9	5.9	5.9	6.1	5.8	5.5	5.5	6.5
Cub1	11.7	11.8	11.3	11.9	11.1	10.7	11.7	12.6
Cub2	8.1	7.3	7.9	8.8	7.6	7.1	6.4	8.5
Cub3	8.9	8.6	8.7	8.8	8.9	9.2	8.5	8.8
Cub4	11.0	10.3	10.4	11.1	10.7	9.4	10.2	11.6
MT5		45.8	47.7	49.8				
MT5D	42.4	41.4	44.0	46.2	34.0	37.1	35.3	40.9
MT4		47.7	50.1	51.8				
MT4D	44.8	43.5	45.5	47.5	36.1	39.7	38.7	43.0
MT3	49.8	48.1	50.3	50.6				
MT3D	45.2	43.3	45.9	46.3	35.9	38.9	38.5	43.3
MT2		46.5	46.9	48.3				
MT2D	43.6	41.7	42.3	44.2	35.9	38.2	36.0	41.8
MT1	31.9	31.8	34.6	35.3				
MT1D	28.4		30.3	31.3	23.7	25.6	24.9	27.0
PH1	14.6	14.1	15.2	15.0	11.2	12.8	12.0	12.9
PH2					19.9	21.3		22.5
PH3	25.7	26.0	28.2	27.9	22.0	23.4	21.9	24.7
PH4					21.5	21.8		23.5
PH5					19.3	19.7		21.7
FemurL	156	159	161	161		141		152
FemurLD	141	143			117	130	122	139
FHB	15.1	15.0	14.3	14.8	13.3	13.7	13.9	15.2
TibL		151	150	149		134		
TibLa		145	144	144		129		
TibLD	137			136	109	122	117	129
FibL			137					
FibLD	131	128		130	100	115	112	121

Taxon	***Macaca mulatta***							
Location	CPRC	CPRC	CPRC	CPRC	CPRC	CPRC	CPRC	CPRC
Specimen	561	831	784	509	595	507	511	640
Sex	Male	Male	Male	Male	Male	Female	Female	Male
Age	2.9	3.0	3.0	3.4	3.4	3.5	3.5	3.6
Age Group	3	3	3	3	3	3	3	3
Calc1	31.8	33.5	32.2	34.6	37.7	29.7	32.7	32.0
Calc2	17.9	18.8	17.3	20.1	21.4	17.5	19.6	18.9
Calc3	24.8	25.1	24.0	23.5	26.8	20.9	21.9	23.8
Calc4	8.9	9.7	9.7	9.0	9.6	7.0	8.1	8.9
Calc5	9.9	10.2	10.7	9.9	10.2	8.4	9.4	9.6
Calc6	8.4	8.1	8.9	8.8	9.3	7.1	8.1	8.6
Calc7	13.9	13.8	14.5	15.2	15.7	13.3	14.9	13.9
Calc8	9.3	9.2	9.9	10.4	10.4	8.7	9.4	9.4
Talus1	25.5	26.3	26.3	26.1	27.9	23.1	25.3	25.2
Talus2	25.5	26.3	26.3	26.1	27.9	23.1	25.3	25.2

Talus5	14.4	15.2	14.3	14.7	16.5	13.1	14.9	14.4
Talus6	11.3	12.1	10.3	10.5	11.9	10.4	11.2	10.5
Nav1	16.7	16.4	16.3	16.3	18.2	14.9	16.3	15.6
Nav2	8.1	7.9	7.0	7.8	9.0	7.2	7.4	7.3
MCun1	10.4	9.9	10.3	10.0	11.2	9.6	10.0	10.0
ICun1	6.7	6.5	6.2	7.0	7.3	5.9	6.8	6.1
ICun2	5.9	5.2	5.5	5.0	5.8	5.6	6.0	5.4
ICun3	5.7	5.4	5.8	5.5	6.1	5.5	5.6	5.3
ICun4	5.7	4.7	5.6	5.1	6.4	5.3	5.4	5.3
LCun1	7.8	8.3	8.6	7.6	9.3	7.8	8.4	7.2
LCun2	9.0	8.5	8.4	9.9	10.2	8.1	8.8	8.8
LCun3	8.4	8.1	8.7	8.6	9.3	7.6	8.5	8.2
LCun4	6.1	6.1	6.4	6.3	6.5	5.6	6.0	6.3
Cub1	12.7	11.8	11.9	13.0	13.3	12.0	12.3	12.4
Cub2	7.3	7.9	8.1	9.1	9.6	8.0	9.2	7.6
Cub3	9.8	9.2	8.9	9.4	9.4	8.5	8.1	9.4
Cub4	12.2	10.9	10.9	11.5	11.8	10.3	11.5	11.6
MT5								
MT5D	40.9	41.6	38.0	45.1	45.8	38.2	41.7	41.2
MT4								
MT4D	41.7	44.0	40.5	46.0	48.7	42.5	42.9	43.1
MT3								
MT3D	41.6	43.4	40.9	46.5	48.7	43.1	43.9	43.0
MT2								
MT2D	40.5	42.5	40.7	43.4	46.1	37.8	40.5	39.9
MT1								
MT1D	26.5	27.7	26.7	29.8	31.0	28.2	28.1	27.2
PH1	13.6	13.7	13.5	14.6	15.1	15.5	14.7	13.7
PH2	21.7	23.0	21.8	25.2	24.0	25.5	23.6	23.4
PH3	24.3	25.0	23.8	27.7	26.2	27.2	24.8	25.4
PH4	23.3	24.1	22.8	26.6	25.1	25.5	23.9	23.7
PH5	21.2	22.2	21.3	24.1	23.0	25.4	23.0	22.5
FemurL	143	147	145	155	165	150	152	151
FemurLD	130	136	133	43	153			135
FHB	15.6	15.6	15.0	16.3	16.4	14.6	15.6	15.6
TibL	135			149		140	143	
TibLa	129			144		135	139	
TibLD	122	129	123	135	145	128	131	130
FibL						132	135	
FibLD	115	120	116	127	137	120	125	124

Taxon	***Macaca mulatta***							
Location	CPRC	CPRC	CPRC	CPRC	CPRC	CPRC	CPRC	CPRC
Specimen	600	797	513	466	538	520	521	1230
Sex	Male	Male	Female	Female	Male	Female	Male	Female
Age	3.7	3.8	3.9	3.9	4.1	4.4	4.4	5.6
Age Group	3	3	3	3	3	3	3	4
Calc1	33.5	34.0	31.3	33.5	36.7	32.5	38.5	33.2

Calc2	19.2	20.0	19.5	21.2	21.8	19.2	23.8	20.1
Calc3	24.5	23.4	21.6	21.7	25.6	22.2	24.0	22.7
Calc4	9.2	9.3	8.5	8.8	9.7	8.3	10.3	8.8
Calc5	9.7	9.8	9.2	9.5	10.7	9.3	11.7	9.5
Calc6	8.6	8.9	7.6	7.8	9.4	8.2	10.3	8.4
Calc7	14.4	15.0	12.0	14.4	15.6	13.4	16.8	14.0
Calc8	9.6	10.2	9.4	9.5	10.4	8.8	10.8	9.0
Talus1	25.4	26.1	24.2	24.8	26.5	24.3	27.5	24.7
Talus2	25.4	26.1	24.2	24.8	26.5	24.3	27.5	24.7
Talus5	14.3	15.5	13.9	14.7	15.9	13.8	16.6	14.4
Talus6	10.7	11.7	11.1	11.1	12.1	10.3	12.7	10.5
Nav1	16.5	17.4	15.6	16.7	17.2	15.5	19.6	15.8
Nav2	7.6	7.9	7.2	7.4	7.8	7.5	9.0	7.7
MCun1	10.5	10.3	9.9	10.6	10.7	10.3	11.7	9.1
ICun1	6.8	6.4	6.1	7.2	7.3	6.2	7.1	6.2
ICun2	6.0	5.3	5.8	6.0	6.2	5.4	5.8	5.4
ICun3	5.6	6.1	5.3	6.0	6.4	5.4	6.7	5.7
ICun4	5.6	5.7	5.4	5.6	5.5	5.1	6.3	5.9
LCun1	8.1	8.5	6.9	8.5	8.5	7.6	9.4	7.5
LCun2	9.1	9.0	8.6	9.1	9.9	9.0	9.9	8.7
LCun3	9.1	9.1	7.5	9.3	9.0	8.4	10.0	8.2
LCun4	6.4	6.5	5.8	6.6	6.8	5.5	7.2	6.1
Cub1	12.5	12.2	11.1	12.4	13.3	12.8	14.1	11.4
Cub2	8.5	7.5	8.1	8.0	9.0	8.2	9.9	6.7
Cub3	8.9	10.4	8.1	9.5	10.3	8.2	10.4	8.8
Cub4	11.0	12.0	10.6	11.0	12.4	10.7	12.3	10.7
MT5								47.9
MT5D	41.6	43.8	40.5	42.4	47.4	43.6	48.2	
MT4								50.3
MT4D	44.2	45.8	43.6	44.3	49.4	45.9	48.1	
MT3								50.0
MT3D	44.2	45.5	43.5	44.6	49.4	45.9	48.5	
MT2								46.9
MT2D	41.0	43.9	41.2	42.5	47.3	42.9	48.2	
MT1								34.5
MT1D	26.9	28.6	28.5	28.7	31.7	32.5	31.3	
PH1	13.6	14.6	15.0	14.7	15.7	15.1	15.9	15.2
PH2	22.5		23.1	22.9	25.4	24.5	26.3	25.7
PH3	24.8	26.3	25.3	25.8	27.3	27.1	27.6	27.9
PH4	23.4		23.5	24.5	25.6	25.7	26.8	26.9
PH5	21.9		22.1	23.4	25.1	24.2	25.2	25.4
FemurL	148	164	161	158	169	161	180	173
FemurLD	135	147	148	142	150		160	
FHB	15.9	16.2	14.6	15.2	16.5	14.6	17.2	15.0
TibL		155	146	148	158	152	168	161
TibLa		151	142	143	153	147	164	156
TibLD	127	142	134	135	144	140	152	
FibL			135			143	155	151

FibLD	120	137	127	129	137	134	143	139

Taxon	***Macaca mulatta***							
Location	CPRC	CPRC	CPRC	CPRC	CPRC	CPRC	CPRC	CPRC
Specimen	438	451	453	469	470	488	494	518
Sex	Male	Male	Female	Male	Male	Male	Female	Female
Age	6.5	4.6	5.2	6.7	6.6	4.9	5.2	4.5
Age Group	4	4	4	4	4	4	4	4
Calc1	36.3	34.9	31.6	40.9	38.8	36.9	32.8	34.1
Calc2	23.0	22.1	19.0	24.1	24.3	22.1	19.3	20.1
Calc3	24.5	23.4	21.6	26.3	25.6	26.6	20.9	23.5
Calc4	10.4	10.4	8.4	9.9	10.7	11.4	8.2	9.4
Calc5	10.9	11.0	9.4	10.1	11.4	12.0	8.7	10.5
Calc6	9.3	8.3	7.9	9.5	10.2	8.7	8.3	8.2
Calc7	15.7	16.1	13.8	18.3	17.2	15.8	12.8	14.0
Calc8	11.5	10.0	9.6	13.0	11.7	10.1	9.6	8.7
Talus1	27.8	26.1	24.6	28.4	29.9	27.1	23.9	24.7
Talus2		26.1	24.6	28.4	29.9	27.1	23.9	24.7
Talus5	16.5	15.0	14.6	16.0	17.1	15.3	13.5	13.7
Talus6	12.6	11.8	10.9	11.5	12.7	11.8	11.6	10.5
Nav1	18.7	16.4	16.0	17.5	18.8	17.5	16.0	15.4
Nav2	7.6	7.8	7.8	8.1	8.5	8.3	7.4	7.0
MCun1	11.4	10.6	9.2	11.2	11.4	10.4	9.3	9.7
ICun1	7.6	7.0	6.3	7.0	8.1	7.1	6.4	6.8
ICun2	6.0	4.7	5.8	5.8	6.0	6.8	5.6	5.5
ICun3	6.7	6.8	5.2	6.1	7.1	6.4	5.6	5.3
ICun4	6.6	5.8	4.8	5.9	6.1	5.3	5.5	5.5
LCun1	8.2	7.3	7.4	8.3	9.4	9.6	7.5	6.8
LCun2	10.4	9.9	8.5	10.0	10.0	10.0	9.2	8.7
LCun3	9.5	9.5	7.9	8.7	9.5	9.5	8.1	8.6
LCun4	7.3	6.9	5.8	6.4	6.9	6.5	5.7	6.1
Cub1	13.1	13.3	13.1	14.9	15.0	13.8	12.2	11.4
Cub2	9.8	9.2	8.7	9.8	9.3	9.0	9.2	8.5
Cub3	10.1	9.6	8.6	10.2	10.9	10.1	8.5	8.9
Cub4	11.9	11.1	11.6	12.6	13.0	12.5	10.7	10.5
MT5	53.7		45.2	55.7	55.3	51.4	43.7	
MT5D		48.1						41.3
MT4	56.3		47.7	57.6	57.7	53.8	45.3	
MT4D		50.3						44.5
MT3	55.9		47.0	57.7	58.2	53.2	45.4	48.1
MT3D		50.3						42.9
MT2	52.5		45.3	53.9	55.4	50.5	44.0	
MT2D		47.9						43.4
MT1	37.2		31.7	36.4	36.7	34.4	32.5	
MT1D		30.5						29.9
PH1	16.9	15.9	14.2	17.4	18.2	16.2	15.0	14.8
PH2	28.2	27.9	23.1	27.6	28.9	26.5	25.7	25.6
PH3	30.3	30.2	26.0	29.9	31.0	29.4	28.1	27.5

PH4	28.7	28.6	25.0	29.1	29.7	28.4	27.0	25.9
PH5	26.2	27.4	22.7	27.3	28.7	26.3	23.9	25.4
FemurL	190	177	168	189	200	188	154	161
FemurLD		170	160					
FHB	17.6	16.2	15.0	17.1	18.7	16.9	14.8	14.5
TibL	178	166	151	174	180	167	145	147
TibLa	172	161	145	169	174	161	140	142
TibLD		151						135
FibL	165	155	141	164	169	158	137	136
FibLD		144				147		127

Taxon	***Macaca mulatta***							
Location	CPRC	CPRC	CPRC	CPRC	CPRC	CPRC	CPRC	CPRC
Specimen	526	528	540	571	572	576	577	581
Sex	Male	Male	Male	Male	Female	Male	Female	Male
Age	5.4	6.6	5.7	6.0	6.1	6.0	6.9	6.0
Age Group	4	4	4	4	4	4	4	4
Calc1	34.9	38.2	35.9	35.5	33.8	39.1	32.3	35.0
Calc2	21.4	23.4	22.6	21.3	20.7	23.8	18.9	20.8
Calc3	22.3	24.1	24.8	27.1	24.0	27.9	23.1	25.3
Calc4	9.2	9.9	10.3	8.8	9.7	9.9	8.8	9.3
Calc5	10.3	11.1	11.3	9.3	10.2	11.0	9.9	10.2
Calc6	8.0	9.9	9.8	11.4	8.6	9.7	7.8	9.4
Calc7	14.1	15.9	14.9	17.0	14.9	15.6	13.9	14.6
Calc8	10.2	10.9	10.9	12.5	9.5	10.8	9.5	10.5
Talus1	26.2	27.9	27.7	27.1	25.8	28.1	24.4	25.5
Talus2	26.2	27.9	27.7	27.1	25.8	28.1	24.3	25.5
Talus5	16.0	16.4	16.2	17.0	14.8	16.3	14.3	14.2
Talus6	11.5	12.0	11.7	12.5	12.6	11.9	10.3	10.6
Nav1	17.2	17.8	17.8	17.7	16.4	18.1	16.5	17.1
Nav2	8.5	9.3	8.9	7.5	7.8	9.6	8.0	7.9
MCun1	9.6	10.5	10.9	10.4	10.4	11.0	10.3	9.9
ICun1	6.9	6.6	6.8	7.8	6.7	7.8	6.4	7.0
ICun2	5.7	5.9	5.8	6.7	6.4	7.0	5.7	6.1
ICun3	5.9	6.1	5.9	6.1	5.7	6.9	5.4	6.2
ICun4	5.2	6.5	6.1	6.2	5.1	6.3	5.1	6.5
LCun1	7.9	8.2	8.5	8.4	8.3	8.7	7.0	8.2
LCun2	9.4	10.1	9.9	9.7	8.8	10.6	8.6	10.0
LCun3	8.4	9.8	9.2	9.6	8.2	9.5	8.3	9.1
LCun4	6.4	6.8	6.9	6.8	5.9	6.8	6.0	6.5
Cub1	12.9	13.1	12.7	12.5	13.0	14.1	12.0	12.6
Cub2	9.6	10.0	10.0	9.0	9.0	10.7	8.3	9.4
Cub3	9.6	9.9	10.3	10.3	9.4	11.0	8.6	9.0
Cub4	12.1	12.6	12.5	12.1	11.5	13.1	11.3	11.5
MT5	49.4	56.0	52.9	53.1	48.4	54.0	45.1	51.1
MT5D								
MT4	50.9	58.3	53.4	55.9	51.2	55.8	47.3	54.8
MT4D								

MT3	50.5	58.2	52.8	55.8	51.8	55.4	46.7	54.4
MT3D								
MT2	47.6	54.9	46.7	54.0	49.3	51.8	45.8	52.1
MT2D								
MT1	33.2	36.0	34.0	37.9	33.9	37.0	27.2	35.2
MT1D								
PH1	14.9	16.2	16.1	17.5	15.3	17.6	14.5	14.9
PH2	24.9	27.4	26.4	27.9	25.8	29.1	25.0	28.4
PH3	26.7	31.8	29.2	30.2	28.2	31.6	27.5	30.0
PH4	25.2	28.5	28.9	28.5	26.3	29.9	26.0	28.7
PH5	23.8	26.8	26.0	26.9	25.1	28.5	24.6	27.4
FemurL	176	184	177	183	175	191	160	176
FemurLD								
FHB	16.3	18.0	16.7	16.2	15.2	17.5	14.3	16.4
TibL	158	171	167	169	159	171	148	164
TibLa	153	165	161	163	153	166	143	159
TibLD								
FibL		160	156	158	148		140	152
FibLD	138		151					

Taxon	***Macaca mulatta***							
Location	CPRC	CPRC	CPRC	CPRC	CPRC	CPRC	CPRC	CPRC
Specimen	583	586	591	601	614	632	532	559
Sex	Male	Male	Male	Female	Male	Female	Male	Female
Age	5.4	5.3	6.7	5.6	4.7	6.2	4.6	4.8
Age Group	4	4	4	4	4	4	4	4
Calc1	39.7	36.6	36.9	35.6	35.4	32.2	35.9	33.8
Calc2	24.2	22.6	22.7	21.3	21.7	19.6	20.6	19.8
Calc3	28.2	25.5	25.8	25.0	24.5	22.8	23.5	22.9
Calc4	9.9	9.8	10.5	8.9	9.6	8.8	9.6	7.6
Calc5	10.7	10.4	11.4	9.7	10.2	9.3	10.2	8.9
Calc6	9.7	9.6	9.8	8.2	8.8	7.7	8.9	7.6
Calc7	18.1	15.3	15.6	15.8	15.9	13.1	14.6	13.8
Calc8	11.6	11.3	11.2	10.7	10.5	10.1	10.4	9.4
Talus1	28.5	26.0	27.3	26.3	26.6	24.3	26.9	24.1
Talus2	28.5	26.0	27.3	26.3	26.6	24.3	26.9	24.1
Talus5	16.9	15.9	15.9	15.3	15.6	14.2	15.3	13.4
Talus6	12.4	11.0	12.1	12.0	11.8	11.1	11.7	10.0
Nav1	18.5	17.3	18.1	17.5	17.7	15.7	17.1	14.9
Nav2	9.6	8.7	8.1	9.0	8.8	7.5	8.6	7.7
MCun1	10.7	10.3	10.6	10.8	11.0	9.9	10.1	9.6
ICun1	7.6	6.5	7.4	6.7	7.3	6.6	6.8	6.3
ICun2	6.0	5.3	6.5	6.1	5.9	5.6	6.7	5.2
ICun3	7.0	5.7	6.1	6.0	5.8	5.7	7.1	5.3
ICun4	6.8	6.1	5.8	5.3	6.1	5.3	6.4	5.1
LCun1	8.5	8.1	10.0	8.8	8.1	7.8	8.4	7.3
LCun2	10.8	8.4	10.8	9.1	9.5	8.3	10.5	8.9
LCun3	10.2	9.0	10.4	8.3	9.4	8.0	9.2	8.1

LCun4	7.6	7.0	6.9	6.2	6.8	6.0	6.1	6.0
Cub1	14.3	13.0	13.6	13.2	13.0	11.7	12.8	11.7
Cub2	9.4	8.6	9.0	9.3	9.7	8.3	10.0	7.4
Cub3	10.0	11.0	10.5	9.5	10.3	8.4	10.3	9.0
Cub4	12.8	11.8	12.7	11.2	11.5	10.6	12.4	10.5
MT5	56.8	52.5	51.8	49.1	53.3	47.4		41.3
MT5D					48.4		45.9	
MT4	57.2	55.3	53.5	52.0	56.0	48.4		45.4
MT4D					51.5		47.6	
MT3	56.6	54.6	52.6	51.3	56.7	49.5		47.4
MT3D					51.5		48.2	
MT2	53.5	50.0	50.6	50.5	52.9	46.6		
MT2D					47.9		46.4	42.1
MT1	37.9	34.4	35.1	34.7	38.6	34.0		30.9
MT1D							30.8	
PH1	18.8	15.7	17.3	15.5	17.9	16.0	17.6	14.8
PH2			28.3	26.7		24.0	27.0	24.8
PH3	32.9	30.0	30.3	29.4	30.9	28.7	29.6	26.1
PH4			28.9	28.3		27.4	28.3	25.3
PH5			27.7	26.8		25.4	27.0	23.9
FemurL	199	195	188	170	183	167	177	154
FemurLD								
FHB	17.4	16.1	17.4	16.1	17.1	14.1	16.6	14.4
TibL	187	172	169	159		150	161	149
TibLa	182	166	164	153		146	154	145
TibLD					155		146	
FibL	176	159	160	148		137	150	140
FibLD					145		139	130

Taxon	***Macaca mulatta***							
Location	CPRC	CPRC	CPRC	CPRC	CPRC	CPRC	CPRC	CPRC
Specimen	555	634	563	611	454	639	1213	1224
Sex	Female	Female	Male	Female	Female	Female	Male	Female
Age	5.2	5.4	5.4	5.9	6.3	6.6	7.7	8.0
Age Group	4	4	4	4	4	4	5	5
Calc1	31.6	32.2	37.3	33.6	32.9	32.5	36.7	33.8
Calc2	18.5	19.4	22.5	19.5	20.5	19.8	21.6	20.0
Calc3	22.9	21.2	25.8	24.8	21.4	22.2	26.4	23.8
Calc4	8.3	9.2	10.3	9.6	8.5	8.0	9.5	8.4
Calc5	8.6	9.4	11.7	10.0	9.7	9.2	10.0	9.9
Calc6	7.7	8.5	9.8	8.4	9.5	8.3	8.7	8.3
Calc7	13.8	14.2	16.3	14.4	14.4	15.2	15.8	14.6
Calc8	8.8	9.2	10.8	9.9	10.2	10.1	10.2	9.8
Talus1	24.0	24.7	26.2	24.9	24.3	25.5	27.2	24.0
Talus2	24.0	24.7	26.2	24.9	24.3	25.5	27.2	24.0
Talus5	13.5	14.4	16.5	14.3	14.9	14.9	15.2	14.2
Talus6	10.2	11.1	11.8	10.8	10.7	10.6	11.4	10.5
Nav1	15.1	15.9	17.8	16.5	16.0	15.0	17.3	15.9

Nav2	6.9	8.0	7.9	7.5	7.9	7.7	8.9	7.6
MCun1	9.3	9.8	10.7	9.7	10.3	9.9	10.4	10.5
ICun1	6.1	6.4	6.8	7.0	6.9	6.8	7.0	
ICun2	4.9	6.0	6.0	5.3	6.9	5.8	5.8	
ICun3	5.2	6.1	6.2	5.5	6.0	5.5	6.2	
ICun4	5.1	5.3	5.5	5.1	6.0	5.5	5.8	
LCun1	7.7	7.3	8.2	8.3	6.6	8.1	8.4	7.8
LCun2	8.3	8.5	8.8	9.2	9.5	9.6	10.0	9.5
LCun3	7.3	7.8	9.8	8.9	9.0	8.6	9.2	8.7
LCun4	5.3	5.9	7.3	6.0	6.7	6.2	6.5	6.3
Cub1	11.8	12.0	12.6	12.0	11.7	12.5	12.8	11.6
Cub2	8.1	8.2	9.8	8.3	8.5	9.0	8.9	8.4
Cub3	7.8	9.1	10.8	9.0	9.3	9.4	9.6	8.3
Cub4	10.8	10.9	11.1	11.7	11.6	11.2	11.9	10.3
MT5		44.0		48.8	45.4	46.6	53.0	48.6
MT5D	38.5		49.4					
MT4		47.2	54.2	50.4	48.4	48.1	55.2	50.3
MT4D	40.3		47.1					
MT3		49.9		50.0	48.8	48.4	54.7	50.0
MT3D	40.2		51.3					
MT2		47.0		48.0	46.0	47.3	53.0	47.2
MT2D	37.8		49.9					
MT1		32.3		32.2	30.3	31.3	37.2	32.8
MT1D	27.7		32.2					
PH1	14.9	15.4	19.4	15.1	15.3	14.7	18.0	
PH2	23.8		27.7		26.7		29.9	26.4
PH3	25.9		30.7	27.1	28.3	27.2	32.7	28.7
PH4	24.0		28.9		26.8		30.2	27.0
PH5	22.6		28.8		25.4		28.8	
FemurL	152	167	186	168	167	162	190	165
FemurLD								
FHB	14.3	15.4	17.3	14.5	15.1	15.3	16.6	14.0
TibL	146	157	170	157	151	152	174	156
TibLa	139	153	167	151	146	147	168	151
TibLD	133		155					
FibL	135	148		147	144	142	163	147
FibLD	125		146					

Taxon	***Macaca mulatta***							
Location	CPRC	CPRC	CPRC	CPRC	CPRC	CPRC	CPRC	CPRC
Specimen	1591	3453	3525	436	437	439	440	442
Sex	Female	Female	Male	Female	Male	Male	Female	Male
Age	7.9	7.4	7.6	10.5	9.7	7.5	12.0	11.7
Age Group	5	5	5	5	5	5	5	5
Calc1	31.1	32.2	35.5	32.4	35.9	37.2	32.3	34.7
Calc2	18.9	19.9	22.8	19.8	23.3	24.1	20.8	22.0
Calc3	22.2	22.5	24.8	21.0	23.4	24.4	21.7	24.3
Calc4	8.3	9.3	11.0	9.2	10.7	10.5	10.8	10.5

Calc5	9.2	9.7	11.0	9.8	11.9	11.5	10.8	11.0
Calc6	8.5	8.7	10.6	8.1	9.7	10.1	9.5	10.5
Calc7	14.0	15.0	17.1	14.7	16.2	16.6	14.6	17.0
Calc8	9.3	9.5	11.3	9.8	10.9	12.4	10.7	12.3
Talus1	22.8	24.2	25.5	24.4	27.9	27.8	25.1	29.4
Talus2	22.8	24.2	25.5	24.4	27.9	27.8	25.1	29.4
Talus5	12.8	13.9	15.4	14.0	17.6	16.9	15.3	17.4
Talus6	9.6	10.2	11.6	10.1	12.7	12.2	11.8	12.4
Nav1	14.6	15.3	17.5	15.6	18.5	19.0	17.6	19.3
Nav2	6.6	7.6	8.5	6.6	8.7	8.8	7.8	8.7
MCun1	9.2	10.4	11.1	9.2	10.2	10.7	10.7	10.5
ICun1	6.2	6.6	6.5	6.5	6.8	6.7	7.2	7.8
ICun2	4.7	5.4	5.0	5.6	6.3	6.2	6.1	5.2
ICun3	5.2	6.0	6.0	5.7	6.7	6.5	6.4	6.7
ICun4	4.9	5.8	5.8	4.8	6.4	6.8	7.5	6.7
LCun1	6.9	7.6	7.9	7.1	8.6	8.0	8.2	8.8
LCun2	7.6	9.3	9.5	8.4	9.8	10.4	8.6	9.9
LCun3	7.4	8.6	8.6	8.4	8.9	10.3	8.9	9.7
LCun4	5.1	6.2	6.1	5.9	6.8	7.1	7.2	6.8
Cub1	10.3	12.2	12.7	11.4	13.0	12.7	12.9	14.0
Cub2	6.9	7.8	8.6	8.2	8.3	9.3	8.7	9.5
Cub3	8.5	8.5	10.8	8.9	10.4	10.2	10.5	10.8
Cub4	10.3	11.2	12.1	11.3	12.1	13.4	12.3	12.9
MT5	41.1	47.1	56.0	46.6	54.6	56.2	47.2	51.2
MT5D								
MT4	44.1	50.2	56.8	48.9	56.0	58.0	48.9	54.3
MT4D								
MT3	44.1	50.0	56.7	48.8	57.0	58.0	49.5	54.8
MT3D								
MT2	42.1	46.9	54.6	46.9	53.7	55.3	47.3	52.3
MT2D								
MT1	28.9	31.0	36.1	32.4	36.6	36.2	33.8	36.3
MT1D								
PH1	14.5	14.9	17.5	15.2	16.6	16.7	17.2	16.8
PH2	23.8	25.7	29.7	25.8	26.8	28.5	25.1	26.6
PH3	25.7	29.3	31.5	27.7	29.3	30.7	28.0	29.2
PH4	23.9	27.2	30.1	26.2	28.1	29.4	27.9	27.9
PH5	23.3	25.0	28.6	24.6	27.2	27.9	26.3	27.2
FemurL	153	162	187	168	199	188	170	185
FemurLD								
FHB	13.8	14.0	16.5	15.0	18.1	17.1	15.0	18.1
TibL	143	155	172	151	174	172	155	171
TibLa		151	166	146	168	165	150	165
TibLD								
FibL	133	145	160	141	165	163	145	159
FibLD								

Taxon	***Macaca mulatta***

Location	CPRC	CPRC	CPRC	CPRC	CPRC	CPRC	CPRC	CPRC
Specimen	444	447	514	523	531	579	590	644
Sex	Female	Female	Female	Male	Male	Female	Female	Male
Age	9.9	8.0	8.5	8.8	7.5	9.0	8.9	8.2
Age Group	5	5	5	5	5	5	5	5
Calc1	34.1	33.2	32.4	37.9	37.3	32.8	33.6	37.4
Calc2	21.7	20.7	19.6	23.2	22.4	19.6	20.9	22.9
Calc3	21.6	22.6	22.2	24.7	24.6	23.8	23.4	24.5
Calc4	9.9	10.0	9.2	10.1	9.4	8.7	10.1	9.6
Calc5	9.9	10.0	9.9	11.1	10.2	9.4	10.2	10.3
Calc6	8.6	9.3	8.9	9.8	9.3	9.5	9.0	10.0
Calc7	15.0	13.7	14.8	15.5	16.4	15.6	16.0	16.7
Calc8	10.3	9.3	9.9	10.9	10.7	11.3	10.5	11.0
Talus1	25.7	24.2	24.0	26.8	27.4	25.9	25.1	26.9
Talus2	25.7	24.5	24.0	26.8	27.4	25.9	25.1	26.9
Talus5	15.6	14.4	14.1	16.1	16.1	14.8	15.0	15.8
Talus6	11.2	11.2	10.5	12.1	11.5	11.1	11.5	12.0
Nav1	16.7	16.1	15.9	19.0	17.3	17.5	16.7	17.5
Nav2	7.6	7.1	7.6	8.2	8.7	7.1	7.7	7.8
MCun1	10.4	9.8	10.1	10.8	10.7	9.6	11.4	10.4
ICun1	6.6	6.3	6.5	6.5	7.2	6.9	7.4	7.3
ICun2	5.1	5.3	5.4	4.9	6.4	5.5	6.5	5.9
ICun3	6.0	5.5	6.0	6.2	6.4	6.1	6.0	6.3
ICun4	5.5	5.6	5.5	6.8	5.4	6.1	5.8	6.1
LCun1	7.2	7.6	7.9	8.2	7.6		8.8	9.0
LCun2	9.2	8.5	9.2	9.5	9.8		8.7	9.0
LCun3	8.8	8.2	8.3	9.3	9.2		8.0	9.0
LCun4	6.5	6.2	6.0	6.9	6.4		6.4	6.7
Cub1	12.2	11.5	12.5	12.6	13.1	12.2	12.2	12.7
Cub2	9.1	7.6	8.3	8.4	9.9	7.9	7.6	8.0
Cub3	9.1	9.3	8.5	10.4	9.3	9.8	9.9	10.2
Cub4	12.4	11.7	11.2	13.1	12.3	11.7	11.6	12.0
MT5	48.2	47.2	44.8	57.7	53.4	46.7	47.8	55.1
MT5D								
MT4	50.1	48.6	47.4	56.4	57.0	48.5	48.1	56.9
MT4D								
MT3	50.3	48.7	48.2	59.0	57.1	48.9	48.6	57.1
MT3D								
MT2	49.1	45.9	46.4	56.6	54.7	46.7	48.0	53.1
MT2D								
MT1	34.2	31.2	33.3	37.8	36.2	31.6	35.0	37.9
MT1D								
PH1	16.1	15.5	16.7	18.3	16.9	15.1	16.5	16.8
PH2	27.0	26.0	26.3	29.9	28.1	25.4	26.3	28.4
PH3	28.6	28.0	28.5	32.4	30.1	27.8	27.6	29.9
PH4	27.0	26.1	27.2	30.8	28.9	25.8	27.1	28.2
PH5	26.0	24.7	25.9	30.3	27.8	24.6	22.3	27.4
FemurL	167	170	166	203	195	156	166	190

FemurLD								
FHB	15.9	14.6	14.8	17.7	16.2	15.8	15.5	17.3
TibL	155	154	153	190	179	149	157	181
TibLa	149	150	148	183	173	144	151	176
TibLD								
FibL	145	148	143	180	167	139	145	170
FibLD								

Taxon	***Macaca mulatta***							
Location	CPRC	CPRC	CPRC	CPRC	CPRC	CPRC	CPRC	CPRC
Specimen	686	853	627	1243	1573	2029	551	801
Sex	Male	Female	Female	Male	Male	Female	Male	Male
Age	8.4	8.5	7.2	7.2	7.4	7.6	8.1	8.2
Age Group	5	5	5	5	5	5	5	5
Calc1	36.8	32.0	33.9	37.2	37.3	34.6	36.0	38.7
Calc2	22.7	19.0	19.3	23.1	23.2	19.8	21.4	22.6
Calc3	25.0	22.5	23.2	25.4	25.4	23.8	24.3	27.4
Calc4	9.6	8.6	8.3	10.0	10.2	8.1	9.5	10.6
Calc5	10.1	9.1	8.9	10.9	10.7	9.0	10.0	11.0
Calc6	9.4	8.6	8.0	10.0	10.0	8.3	7.7	9.0
Calc7	17.1	13.8	14.6	16.2	17.0	15.8	16.7	17.0
Calc8	11.4	9.2	9.5	11.5	13.5	9.5	11.3	11.4
Talus1	25.5	24.1	24.1	27.4	28.5	24.5	26.3	28.2
Talus2	25.5	24.1	24.1	27.4	28.5	24.5	26.3	28.2
Talus5	15.6	14.2	13.0	16.3	17.3	14.6	15.4	17.1
Talus6	12.2	10.7	12.0	12.5	12.3	10.3	11.8	12.5
Nav1	17.6	15.8	16.0	19.2	18.2	16.0	18.5	18.6
Nav2	8.7	7.7	7.3	8.8	8.8	7.5	8.6	9.3
MCun1	10.4	10.3	9.6	10.4	11.2	9.1	10.4	11.3
ICun1	7.6	6.3	6.5	7.1	7.9	6.0	6.5	7.9
ICun2	6.3	5.4	5.6	5.6	6.2	5.6	6.0	7.2
ICun3	6.6	5.3	5.8	5.9	6.6	5.5	6.9	6.6
ICun4	6.1	5.3	6.0	6.1	5.8	5.3	6.5	6.4
LCun1	8.2	7.1		8.5	8.8	8.3	7.9	9.0
LCun2	9.8	8.6		9.9	9.7	8.9	9.7	10.7
LCun3	9.3	7.7		9.4	9.4	7.8	8.8	9.7
LCun4	6.9	5.8		7.3	7.0	5.7	6.8	7.4
Cub1	12.4	11.4	11.6	13.3	14.0	12.4	13.0	14.0
Cub2	8.7	7.5	8.7	8.4	9.4	7.7	10.2	8.9
Cub3	9.9	8.6	8.6	10.8	11.7	9.4	9.1	11.2
Cub4	12.4	11.3	10.8	13.2	12.8	12.2	11.4	13.4
MT5	54.3	47.1	47.4	55.2	53.4	47.7	53.6	53.8
MT5D								
MT4	56.2	48.7	51.1	57.4	53.7	49.3	55.8	54.8
MT4D								
MT3	56.4	49.2	51.8	57.2	53.5	49.2	56.0	54.9
MT3D								
MT2	54.4	47.8	48.7	54.2	50.4	46.8	51.9	53.5

MT2D								
MT1	36.4	33.7	32.8	37.7	36.9	33.2	35.2	35.5
MT1D								
PH1	18.3	16.5	14.3	15.8	18.1	15.3	18.1	18.1
PH2	30.3	26.5	25.4	29.3			27.0	
PH3	32.8	28.5	28.0	32.0	31.4	27.2	29.1	31.1
PH4	31.1	27.2	26.0	30.4			27.5	
PH5	28.8	25.7	26.1	28.7			26.4	
FemurL	197	160	162	195	195	166	179	188
FemurLD								
FHB	17.1	14.7	15.0	16.7	18.1	14.7	16.5	17.0
TibL	180	153	148	181	173	150	168	174
TibLa	185	148	144	177	167	144	164	167
TibLD								
FibL	167	142	138	172	162	142	153	160
FibLD								

Taxon	***Macaca mulatta***	
Location	CPRC	CPRC
Specimen	635	689
Sex	Male	Female
Age	8.4	8.5
Age Group	5	5
Calc1	40.8	32.4
Calc2	25.6	18.2
Calc3	25.3	24.4
Calc4	10.0	9.0
Calc5	11.2	9.7
Calc6	10.0	8.3
Calc7	15.9	14.3
Calc8	11.6	9.4
Talus1	28.6	24.7
Talus2	28.6	24.7
Talus5	16.2	14.1
Talus6	13.0	11.2
Nav1	19.6	15.9
Nav2	9.0	7.6
MCun1	11.3	10.4
ICun1	7.3	6.3
ICun2	6.2	5.9
ICun3	7.2	5.7
ICun4	6.9	5.4
LCun1	8.7	8.0
LCun2	10.6	9.5
LCun3	9.5	8.8
LCun4	7.2	6.3
Cub1	13.7	11.7
Cub2	8.1	8.0

Cub3	11.3	8.5
Cub4	12.5	11.1
MT5	61.4	46.8
MT5D		
MT4	63.1	48.2
MT4D		
MT3	63.2	47.9
MT3D		
MT2	60.2	45.8
MT2D		
MT1	42.1	31.8
MT1D		
PH1	20.0	14.8
PH2	30.8	
PH3	34.1	27.0
PH4	32.6	
PH5	32.2	
FemurL	210	157
FemurLD		
FHB	18.8	13.7
TibL	193	147
TibLa	189	141
TibLD		
FibL	182	139
FibLD		

Taxon	***Nasalis larvatus***				
Location	MCZ	MCZ	MCZ	MCZ	MCZ
Specimen	41555	41560	41559	41562	37326
Sex	Female	Female	Female	Female	Male
Age	Adult	Adult	Adult	Adult	Adult
Age Group	5	5	5	5	5
Calc1	38.9	39.3	40.1	38.5	38.7
Calc2	21.2	23.2	21.5	21.8	22.2
Calc3	27.0	26.7	27.8	25.6	28.0
Calc4	10.4	10.6	9.2	9.3	10.6
Calc5	11.1	10.9	10.3	9.5	11.6
Calc6	10.2	10.7	9.7	9.7	9.9
Calc7	18.7	18.9	18.1	18.6	17.5
Calc8	10.4	10.5	9.7	10.5	10.7
Talus1	29.3	27.9	30.1	28.8	29.2
Talus2	28.6	28.4	29.8	28.7	30.2
Talus5	17.4	16.6	17.2	15.9	16.9
Talus6	12.5	13.1	12.2	12.3	12.4
Nav1	19.9	20.0	20.1	19.4	19.5
Nav2	8.3	7.8	7.6	7.5	7.4
MCun1	11.5	11.2	12.0	11.5	11.8
ICun1	7.9	7.0	8.6	7.7	8.6

ICun2	6.1	6.0	5.8	5.9	6.7
ICun3	7.4	7.2	7.4	7.1	7.7
ICun4	6.3	6.2	5.7	5.6	5.7
LCun1	9.5	9.1	9.6	8.9	10.0
LCun2	10.8	10.0	10.2	9.6	10.3
LCun3	9.9	9.4	9.2	8.8	10.6
LCun4	7.9	7.9	8.0	7.4	8.5
Cub1	13.5	12.7	13.8	12.1	13.2
Cub2	8.8	8.0	8.3	7.8	7.6
Cub3	11.9	12.1	11.1	11.2	11.7
Cub4	14.7	13.7	14.0	13.3	14.2
MT5	60.8	60.2	59.9	57.3	56.5
MT5D					
MT4	63.6	60.0	59.4	57.9	58.0
MT4D					
MT3	62.7	59.2	58.5	56.6	57.5
MT3D					
MT2	56.2	50.5	53.4	52.9	52.9
MT2D					
MT1	39.8	39.2	38.8	39.2	37.7
MT1D					
PH1	18.9	19.0	20.8	17.8	19.4
PH2					
PH3					
PH4					
PH5					
FemurL	207	207	215	210	200
FemurLD					
FHB	18.3	18.5	18.5	18.0	17.1
TibL	188	191	191	185	181
TibLa	182	187	186	182	175
TibLD					
FibL	174	178	176	171	169
FibLD					

Taxon	***Nasalis larvatus***				
Location	MCZ	MCZ	MCZ	MCZ	MCZ
Specimen	37330	41563	41557	38325	7099
Sex	Male	Male	Male	Male	Male
Age	Adult	Adult	Adult	Adult	Adult
Age Group	5	5	5	5	5
Calc1	44.7	45.3	46.1	43.7	47.6
Calc2	26.6	25.7	27.6	25.3	26.5
Calc3	30.2	31.9	31.6	30.4	32.9
Calc4	12.3	13.1	13.4	11.6	12.2
Calc5	13.2	13.9	14.2	12.2	13.2
Calc6	12.0	12.3	13.5	13.7	13.1
Calc7	22.8	23.4	23.8	22.6	19.4

Calc8	13.2	13.7	13.3	11.5	13.4
Talus1	34.1	33.5	34.6	33.1	34.7
Talus2	34.9	34.5	36.9	33.1	34.7
Talus5	20.7	20.1	20.5	20.7	18.3
Talus6	15.4	15.1	15.2	14.3	15.9
Nav1	24.3	24.6	24.4	22.8	24.2
Nav2	9.4	9.7	9.7	8.7	9.6
MCun1	13.4	13.4	13.8	14.1	13.8
ICun1	10.1	10.6	9.6	10.2	10.2
ICun2	7.8	8.0	8.1	7.9	8.2
ICun3	8.8	9.0	9.0	8.5	8.4
ICun4	7.3	7.8	8.2	7.3	6.9
LCun1	11.1	11.5	10.5	11.1	11.3
LCun2	13.1	12.1	12.1	11.7	11.7
LCun3	11.9	12.1	12.3	11.1	11.2
LCun4	9.7	9.3	10.3	8.9	9.6
Cub1	15.6	15.5	15.0	15.1	16.0
Cub2	9.2	10.3	10.4	9.4	8.1
Cub3	13.1	14.0	14.3	13.6	14.7
Cub4	15.6	16.6	16.4	16.1	17.2
MT5	72.3	71.8	70.0	68.7	69.6
MT5D					
MT4	72.3	72.0	72.0	69.1	70.7
MT4D					
MT3	71.3	71.8	69.8	67.4	70.0
MT3D					
MT2	59.8	66.3	63.0	61.6	64.1
MT2D					
MT1	49.2	46.3	46.3	46.0	44.8
MT1D					
PH1	24.7	18.7	23.3	21.4	20.7
PH2					
PH3					
PH4					
PH5					
FemurL	250	245	241	235	243
FemurLD					
FHB	24.0	22.0	21.6	21.8	21.3
TibL	229	223	218	220	222
TibLa	223	217	211	213	217
TibLD					
FibL	211	207	200	204	206
FibLD					

Taxon	***Pan paniscus***							
Location	RMCA	RMCA	RMCA	RMCA	RMCA	RMCA	RMCA	RMCA
Specimen	29060	13201	29040	15293	29045	27698	15296	15295
Sex	Female	Female	Female	Female	Female	Female	Female	Female

Age	Adult	Adult	Adult	Adult	Adult	Adult	Adult	Adult
Age Group	5	5	5	5	5	5	5	5
Calc1	51.0	49.2	53.0	50.3	50.1	53.3	49.6	51.0
Calc2	38.6	36.7	39.0	38.8	37.4	39.6	38.3	38.2
Calc3	33.0	32.4	33.9	29.8	33.1	34.1	31.0	30.9
Calc4	18.4	16.6	20.0	17.0	19.5	19.8	17.8	17.6
Calc5	22.0	20.6	21.6	20.1	22.0	21.8	20.2	19.5
Calc6	17.6	17.7	19.0	17.6	20.5	17.0	16.7	17.9
Calc7	28.3	28.4	29.0	30.4	30.4	29.0	26.1	28.2
Calc8	17.3	16.6	17.3	17.9	17.5	17.8	16.5	20.0
Talus1	39.5	41.6	41.4	40.4	42.9	39.8	39.6	42.3
Talus2	42.1	43.5	43.4	43.5	46.2	45.4	44.3	45.7
Talus5	25.6	24.7	27.8	23.1	25.4	24.8	23.1	23.9
Talus6	19.5	18.7	21.4	20.9	21.3	20.2	20.6	21.4
Nav1	30.1	30.2	35.9	33.2	32.8	31.7	32.1	32.2
Nav2	13.7	10.8	12.9	11.0	13.3	11.3	11.6	11.1
MCun1	17.6	15.2	17.4	16.5	17.2	16.9	16.3	16.6
ICun1	12.6	10.5	12.8	10.9	13.2	10.5	11.6	12.1
ICun2	8.6	8.4	8.9	8.0	9.8	8.9	8.8	6.6
ICun3	11.5	10.4	12.0	10.8	12.7	10.2	8.4	10.9
ICun4	11.8	10.3	11.3	10.5	12.3	10.5	8.6	10.7
LCun1	12.8	11.3	12.8	12.5	13.0	11.9	12.5	11.6
LCun2	14.1	12.6	13.4	12.9	13.2	12.9	13.0	12.6
LCun3	12.8	12.4	12.0	11.7	13.8	12.3	11.8	11.8
LCun4	10.6	9.0	10.8	9.7	11.0	9.4	10.2	9.8
Cub1	18.5	18.6	18.5	18.0	19.3	18.1	17.1	17.8
Cub2	9.3	5.5	5.8	7.5	9.0	5.2	7.0	7.3
Cub3	16.9	16.7	18.6	17.5	18.4	17.4	16.4	16.6
Cub4	17.7	19.3	21.0	20.0	19.1	20.0	17.9	17.7
MT5	63.9	63.9	64.4	62.4	64.0	63.8	60.4	60.9
MT5D								
MT4	66.6	64.6	64.6	63.8	66.0	62.4	62.7	64.1
MT4D								
MT3	66.6	65.9	64.7	65.1	68.9	65.0	63.7	65.8
MT3D								
MT2	74.4	70.2	72.7	70.7	75.9	68.9	68.5	70.3
MT2D								
MT1	51.4	49.5	49.8	49.3	53.0	49.3	46.3	46.4
MT1D								
PH1	28.2		27.6	26.8	28.6	28.2	26.8	28.0
PH2	36.7		40.1	34.8	35.5	35.4	32.9	34.5
PH3	40.4		41.4	37.9	40.2	39.3	36.5	36.7
PH4	39.2		40.6	36.6	35.6	37.5	35.4	36.2
PH5	32.0		30.8	30.0	28.8	29.5	28.8	29.5
FemurL	284	272	299	299	289	290	300	283
FemurLD								
FHB	28.2	30.7	33.0	30.7	30.8	30.1	33.3	30.2

TibL	241	222	247	242	235	238	250	242
TibLa	231	212	235	229	222	229	239	231
TibLD								
FibL	217	205	223	216	213	217	221	222
FibLD								

Taxon	***Pan paniscus***						
Location	RMCA	RMCA	RMCA	RMCA	RMCA	RMCA	RMCA
Specimen	29042	27696	13202	29047	29052	23509	15294
Sex	Female	Male	Male	Male	Male	Male	Male
Age	Adult	Adult	Adult	Adult	Adult	Adult	Adult
Age Group	5	5	5	5	5	5	5
Calc1	51.2	54.2	49.6	58.1	51.7	50.6	50.4
Calc2	36.9	39.8	36.1	42.2	40.0	37.0	37.8
Calc3	33.7	37.5	33.4	39.0	31.5	31.6	31.2
Calc4	18.6	20.4	17.7	21.3	20.0	17.2	17.0
Calc5	21.3	24.9	21.5	23.8	21.9	19.0	18.6
Calc6	18.6	22.0	19.6	22.3	17.3	15.7	17.2
Calc7	30.5	33.8	31.7	34.6	31.5	26.7	29.8
Calc8	18.4	20.2	19.9	20.3	18.7	17.3	18.0
Talus1	40.8	44.7	41.3	48.0	42.4	39.1	40.9
Talus2	43.8	47.9	42.8	53.3	46.8	40.3	44.2
Talus5	24.7	28.2	26.4	28.5	25.1	25.2	23.7
Talus6	21.2	22.7	21.0	24.3	21.9	19.7	20.6
Nav1	34.1	35.6	36.0	38.2	34.9	31.4	32.6
Nav2	12.3	12.7	12.7	13.7	12.4	11.7	10.9
MCun1	16.9	17.5	18.7	18.1	17.5	15.9	15.4
ICun1	12.8	9.8	11.2	13.5	13.3	11.3	11.6
ICun2	7.5	8.8	9.1	10.0	8.4	9.2	8.9
ICun3	11.9	13.9	11.2	13.0	12.4	10.3	10.2
ICun4	10.6	10.5	9.5	13.4	11.6	10.3	8.9
LCun1	12.6	14.4	12.4	14.3	13.9	12.7	12.8
LCun2	13.2	13.5	12.4	14.9	13.9	13.3	12.9
LCun3	13.4	13.3	14.3	13.2	13.7	12.3	11.0
LCun4	10.9	10.5	11.6	10.5	11.1	9.6	9.0
Cub1	17.3	19.8	18.8	19.3	17.4	17.8	17.4
Cub2	6.0	9.3	7.4	7.1	6.8	5.4	7.6
Cub3	17.4	17.2	16.9	22.3	20.6	17.5	16.3
Cub4	19.2	22.0	18.8	21.6	22.2	17.8	18.1
MT5	63.5	69.4	65.1	71.8	67.2	57.2	63.8
MT5D							
MT4	65.1	70.4	62.0	73.5	67.5	58.0	65.4
MT4D							
MT3	66.5	72.6	65.6	73.8	69.1	59.8	64.7
MT3D							
MT2	73.2	79.0	72.3	80.5	72.5	64.2	70.4
MT2D							

MT1	50.7	52.2	50.8	57.6	51.0	46.3	49.7
MT1D							
PH1	27.8	29.5		31.3	30.2	25.0	29.0
PH2	34.6	37.9		40.1	36.8	31.1	32.5
PH3	37.6	40.9		43.4	40.3	34.2	36.4
PH4	36.8	38.1		42.2	39.4	33.3	35.9
PH5	30.1	28.8		34.7	32.5	26.8	30.5
FemurL	282	290	279	310	272	261	294
FemurLD							
FHB	30.2	32.1	30.6	34.5	30.4	29.7	30.6
TibL	236	257	236	268	239	216	247
TibLa	223	245	223	252	229	203	236
TibLD							
FibL	211	232	211	236	217	193	225
FibLD							

Taxon	***Pan troglodytes schweinfurthii***							
Location	RMCA	RMCA	RMCA	RMCA	RMCA	RMCA	RMCA	RMCA
Specimen	10781	13762	2986	302	9584	29076	5894	26494
Sex	Female	?	Male	Female	Male	Male	Male	?
Age	2.5	0.8	0.9	1.0	2.5	3.8	4.5	7.5
Age Group	1	1	1	1	1	2	2	3
Calc1	25.1	20.8	21.2	24.1	26.6	29.2	33.6	53.4
Calc2	15.6	12.8	13.3	15.7	16.7	19.1	21.9	38.3
Calc3	16.4	15.8	14.7	17.8	18.4	22.5	28.8	29.8
Calc4	6.5	7.8	6.4	8.2	8.7	11.8	15.3	16.0
Calc5	7.5	8.0	7.1	9.3	9.6	12.7	15.9	18.8
Calc6	9.0	6.8	7.1	9.0	9.7	12.0	11.4	17.1
Calc7	12.8	9.4	10.0	12.4	12.7	16.3	19.4	29.0
Calc8	8.6	5.8	5.8	8.2	8.8	9.8	10.3	17.0
Talus1	19.5	15.0		20.1	18.0	24.9	27.5	42.4
Talus2	19.5	15.0		20.1	18.0	24.9	27.5	42.7
Talus5	9.8	8.8				12.8	14.7	26.6
Talus6	12.2	8.7		10.8	11.7	13.8	15.3	21.5
Nav1							12.1	34.0
Nav2							6.0	9.0
MCun1						8.3	9.7	18.1
ICun1								11.2
ICun2								8.8
ICun3								10.4
ICun4								12.0
LCun1	5.9					6.6	9.3	12.2
LCun2	6.0					7.5	9.6	14.3
LCun3	5.3					5.5	7.7	13.6
LCun4	5.0					4.5	6.7	9.6
Cub1	8.9					8.4	10.4	18.3
Cub2	3.8					4.3	3.3	4.9
Cub3	7.8					8.8	12.5	21.2

Cub4	8.1					9.8	12.6	20.4
MT5							38.3	
MT5D	29.1	20.2	21.3	22.9	23.6	32.1	33.9	54.5
MT4							39.4	
MT4D	30.7	21.1	23.1	26.2	27.1	32.9	34.2	51.8
MT3							40.6	59.2
MT3D	32.1	22.5	23.8	25.8	29.4	34.1	34.9	51.3
MT2							45.2	
MT2D	34.7	25.4	26.5	28.8	31.8	38.7	39.3	57.4
MT1							31.1	
MT1D	26.9	19.1	21.6	21.9	23.9	29.3	29.2	43.1
PH1	12.7	11.4	13.0	13.1	13.7	16.3		22.6
PH2	19.9	16.2	17.3	16.7	18.6	19.7		30.3
PH3	22.5	17.4	19.1	19.3	20.9	23.9		35.3
PH4	21.8	17.6	18.9	18.5	20.6	23.3		34.8
PH5	15.9	14.0	14.9	13.7	15.0	17.1		
FemurL	143					155	167	260
FemurLD		84	91	113	124			237
FHB	12.9	11.0				16.7	19.2	31.4
TibL	120						137	
TibLa	113						135	
TibLD		75	77	93	106	125		201
FibL							126	
FibLD	104	68	72	89	98	117		184

Taxon	***Pan troglodytes schweinfurthii***						
Location	RMCA	RMCA	RMCA	RMCA	RMCA	RMCA	RMCA
Specimen	29072	5301	5378	23511	29077	458	30676
Sex	Male	Female	?	Male	Male	Female	Male
Age	6.0	7.0	6.8	7.0	10.0	8.0	8.0
Age Group	3	3	3	3	4	4	4
Calc1	38.1	41.2	41.5	43.5	52.4	54.1	57.0
Calc2	27.4	29.4	28.9	30.6	38.9	39.0	42.2
Calc3	26.0	28.3	29.2	29.5	32.6	33.5	36.6
Calc4	15.6	16.2	16.2	14.5	19.2	20.2	21.2
Calc5	18.1	17.8	20.2	17.2	22.5	23.0	23.7
Calc6	13.6	13.5	17.1	15.6	18.4	17.5	16.4
Calc7	23.2	22.5	25.3	21.4	34.1	31.0	33.4
Calc8	13.6	13.0	15.7	13.8	20.5	16.9	16.2
Talus1	34.7	35.5	37.4	35.6	43.3	41.4	42.8
Talus2	34.7	36.3	38.5	35.6	45.8	44.3	47.4
Talus5	19.7	21.2	21.9	21.7	27.6	26.1	26.1
Talus6	17.8	19.3	19.0	19.4	23.8	22.3	23.1
Nav1		25.7	20.4	23.2	37.3	32.2	35.0
Nav2		7.8	8.4	8.5	11.4	10.7	
MCun1	12.7	14.7	14.2	12.8	17.9	16.8	
ICun1	8.1		9.0	11.0	13.3	10.0	11.2

ICun2	5.0		7.7	7.8	8.8	8.8	7.7
ICun3	8.7		9.6	8.9	11.8	10.7	10.8
ICun4	7.1		8.6	7.7	12.4	10.5	9.5
LCun1	9.7	11.0	12.2	11.3	13.3	12.1	13.0
LCun2	10.7	12.4	13.9	12.4	14.5	15.2	15.5
LCun3	8.0	10.7	11.1	10.6	13.4	12.6	14.8
LCun4	7.8	7.7	8.9	8.4	9.2	9.6	10.5
Cub1	13.0	14.1	19.1	15.5	19.8	19.5	19.3
Cub2	1.7	4.7	4.1	3.5	7.0	10.6	7.9
Cub3	15.2	13.2	18.2	15.6	22.1	18.7	21.0
Cub4	16.8	15.6	18.0	15.3	23.1	21.4	19.8
MT5				51.0		69.1	70.1
MT5D	35.7	39.1	46.4	45.9	59.4	69.1	
MT4	42.8			50.4	67.5	72.2	69.3
MT4D	36.8	41.2	44.9	44.8	58.2		
MT3	44.2		50.9	51.2	68.0	71.7	69.7
MT3D	37.3	41.0	44.1	43.9	57.6		
MT2				56.5	73.7	80.3	74.2
MT2D	43.0	47.7	49.7	50.2	63.6	78.6	
MT1				43.3	51.0	54.2	57.4
MT1D	33.9	37.3	41.8	40.3	46.6		
PH1	18.7	23.2			28.2		33.4
PH2	22.7	28.2		25.3	37.0		41.1
PH3	25.3	31.3		30.3	42.0		44.0
PH4	25.0	29.6		29.7	41.0		39.2
PH5	17.9	22.5		23.4	30.6		34.5
FemurL	206	228	226	224	264	284	299
FemurLD	198						
FHB	23.7	25.4	26.9	26.5	32.3	31.5	32.5
TibL	150	184	185	183		234	258
TibLa	144	173		177		224	245
TibLD					201		
FibL			166	168		211	225
FibLD	133	149	154		185		211

Taxon	***Pan troglodytes schweinfurthii***		
Location	RMCA	RMCA	RMCA
Specimen	13716	545	30845
Sex	Male	Female	Female
Age	9.0	Adult	Adult
Age Group	4	5	5
Calc1	54.5	51.6	56.8
Calc2	41.0	37.8	43.0
Calc3	33.6	32.4	33.9
Calc4	19.7	19.1	20.2
Calc5	21.8	21.0	22.7
Calc6	19.2	17.5	19.3

Calc7	31.7	33.2	33.6
Calc8	16.1	18.5	18.6
Talus1	40.9	41.5	46.6
Talus2	43.2	44.3	52.4
Talus5	25.2	25.5	26.9
Talus6	22.1	22.2	24.9
Nav1	32.5	35.6	36.6
Nav2	9.9	12.1	9.8
MCun1	14.3	17.3	19.5
ICun1	10.9	12.3	12.1
ICun2	8.0	10.1	9.5
ICun3	10.3	11.4	11.9
ICun4	8.8	9.9	11.9
LCun1	12.5	11.7	12.6
LCun2	14.5	14.1	14.7
LCun3	14.0	12.3	15.5
LCun4	8.7	10.4	10.9
Cub1	19.1	19.7	19.7
Cub2	7.1	9.1	8.2
Cub3	22.1	19.8	22.3
Cub4	20.5	22.5	23.7
MT5	61.1	63.5	62.1
MT5D			
MT4	60.0	63.4	63.1
MT4D			
MT3	62.1	64.6	65.4
MT3D			
MT2	66.2	68.5	71.1
MT2D			
MT1	51.7	51.9	52.2
MT1D			
PH1		24.6	32.4
PH2		35.6	38.8
PH3		43.9	44.3
PH4		41.1	40.4
PH5			35.3
FemurL	276	281	300
FemurLD			
FHB	31.1	32.5	33.6
TibL	232	230	243
TibLa	222	223	229
TibLD			
FibL	209	217	212
FibLD			199

Taxon	***Pan troglodytes troglodytes***							
Location	Zurich	PCM	PCM	PCM	PCM	HT B	PCM	PCM
Specimen	AS	CAMI2	CAMII3	M465	M475	1848	M152	M475

	1571	02	14		S2			S1
Sex	Female	?	Male	Female	Female		Male	Male
Age	1.8	0.4	0.5	0.8	1.0	1.3	1.3	1.8
Age Group	1	1	1	1	1	1	1	1
Calc1	25.2	24.1	19.5	20.3	24.3	24.0	23.4	24.6
Calc2	15.4	14.6	12.0	12.8	14.7	15.9	14.9	14.9
Calc3	15.4	18.9	14.9	14.6	17.4	19.0	16.4	17.8
Calc4	7.5	7.6	6.3	7.5	7.5	10.5	7.9	8.2
Calc5								
Calc6								
Calc7	12.9							
Calc8	8.6							
Talus1	18.2	18.6	14.0	17.5	18.5		18.2	20.6
Talus2	18.2	18.6		17.5	18.5	21.1	18.2	20.6
Talus5								
Talus6	10.8	10.3	8.2	8.8	14.6	12.1	8.8	10.5
Nav1						15.8		
Nav2						4.8		
MCun1						8.6		
ICun1						4.0		
ICun2								
ICun3								
ICun4								
LCun1						6.5		
LCun2						8.6		
LCun3								
LCun4								
Cub1						7.4		
Cub2						2.1		
Cub3								
Cub4						8.4		
MT5								
MT5D	28.2		21.4	21.6	27.1	27.8	23.4	25.9
MT4								
MT4D	28.5	24.6	22.7	23.6	28.4	27.2	24.1	25.7
MT3						30.3		
MT3D	28.7	25.8	23.5	24.3	29.1	27.3	25.5	25.3
MT2						31.5		
MT2D	32.4	28.2	25.8	26.4	31.5	27.5	27.8	27.6
MT1						24.2		
MT1D	25.7	21.3	21.0	21.0	24.7	23.7	19.9	22.3
PH1	15.1	12.7	12.7		14.2		12.5	12.7
PH2	19.4	19.0	16.6		18.6	17.7	17.2	16.5
PH3	21.5	19.4	18.3		21.3	19.4	20.3	20.4
PH4	21.2	19.0	17.5		21.0	19.9	18.3	18.5
PH5	16.8		13.4		16.9	15.1	14.2	14.5
FemurL	130			104	127	117	113	122

FemurLD	116	100	99	100	115	108	108	113
FHB	13.8				11.3			11.2
TibL	106				107	102		
TibLa						97		
TibLD	98	90	81	86		92	93	95
FibL	96					88		
FibLD	93	83	73	79	93	81	85	86

Taxon	***Pan troglodytes troglodytes***							
Location	PCM	HT B	PCM	HT B	HT B	HT B	HT B	Zurich
Specimen	M777	753	M556 S1	1716	2186	2957	3540	7421
Sex	Female		Female	Female	Female	Female	Male	Female
Age	2.0	2.5	2.5	5.0	3.8	5.5	5.5	4.0
Age Group	1	1	1	2	2	2	2	2
Calc1	28.6	22.9	27.4	34.7	37.0	51.8	36.8	30.0
Calc2	17.8	16.8	17.1	23.9	24.2	33.5	25.4	19.2
Calc3	20.7	17.1	19.3	23.5	27.0	35.3	26.1	21.3
Calc4	9.0	11.1	9.0	12.2	16.5	21.4	15.4	
Calc5								
Calc6								
Calc7								18.3
Calc8								11.8
Talus1	20.8		19.9					26.4
Talus2	20.8	18.4	19.9	28.9	29.4	41.7	32.0	26.4
Talus5								16.1
Talus6	10.5	10.6	10.2	15.2	16.4	21.8	16.9	16.8
Nav1						34.5		
Nav2						10.1		
MCun1			7.4	12.2	13.1	18.4	11.7	10.9
ICun1			5.9	6.3	7.1	9.4	6.6	5.1
ICun2			4.5	5.2	6.5	8.8	5.1	4.6
ICun3			4.4	5.9	6.4	9.8	7.3	6.0
ICun4				7.7	5.1	9.0	5.3	4.8
LCun1	7.2	6.7	5.9	7.8	8.7	12.3	9.3	9.6
LCun2	7.2	7.1	6.7	7.9	11.7	16.5	9.6	9.7
LCun3	6.0	4.3	4.0	7.4	9.6	14.8	8.3	8.5
LCun4				7.6	6.9	9.3	6.8	6.8
Cub1		7.3	8.1	10.7	12.2	21.6	12.2	12.5
Cub2		5.7	2.5	2.6	4.3	7.9	2.8	1.9
Cub3								12.9
Cub4		8.6	8.3	9.1	13.5	19.3	14.7	14.1
MT5				41.7	43.0	57.3		
MT5D	30.6	27.1	28.9		37.0	46.8	36.7	37.8
MT4					41.6	59.1		
MT4D	32.8	27.3	29.5	38.3	39.2	51.4	39.8	39.2
MT3				46.0	46.2	59.5		

MT3D	32.2	28.2	29.3	38.7	40.8	50.4	39.8	39.5
MT2					48.7			50.3
MT2D	37.2	32.0	32.4	43.8	42.9	55.0	42.6	43.9
MT1		24.6			36.7	46.8		
MT1D	28.0		25.8	34.2	34.8	42.8	35.0	34.3
PH1	16.3	13.5	15.6	20.1	20.3	23.4	19.6	19.0
PH2	23.1	18.6	20.3		25.2	30.2	25.8	24.3
PH3	25.8	20.9	22.8		28.4	33.6	30.6	27.7
PH4	25.0	19.9	21.9		26.8	33.3	27.7	26.6
PH5	18.9	15.7	16.3		22.3	25.1	21.4	21.6
FemurL	143	126	133	186	191	247	205	178
FemurLD	136	114	128	173	177	225	188	
FHB		12.4	12.0	20.5	22.0	28.6	24.4	20.9
TibL		106	116			210		149
TibLa						198		148
TibLD	115	100		148	145	184	156	
FibL		100		143		185		131
FibLD	106	94	100		130	166	143	125

Taxon	***Pan troglodytes troglodytes***							
Location	Zurich	Zurich	Zurich	Zurich	Zurich	Zurich	Zurich	Zurich
Specimen	AS 1075	AS 1570	AS 1755	AS 310	PAL 154	PAL 163	PAL 187	PAL 189
Sex	Male	Female	Female	Male	Female	Male	Female	Female
Age	5.0	5.8	5.5	3.8	5.3	5.0	5.8	5.8
Age Group	2	2	2	2	2	2	2	2
Calc1	35.9	42.7	34.6	35.1	41.9	42.9	38.6	43.1
Calc2	23.1	31.4	21.9	23.2	27.9	29.1	26.1	29.9
Calc3	27.7	28.4	27.4	24.6	29.9	32.3	24.8	31.7
Calc4	14.7	16.5	14.7	13.8	16.5	19.3	12.9	17.2
Calc5	15.6	19.0	16.0		17.8	20.7	15.7	19.2
Calc6	13.2	15.0	12.6		14.6	17.2	13.7	17.7
Calc7	20.8	24.7	20.0	19.8	23.7	25.5	17.8	26.6
Calc8	13.7	14.5	12.4	13.3	14.1	17.2	13.1	16.3
Talus1	30.2	36.0	30.5	29.0	33.3	37.8	30.6	35.8
Talus2	30.2	38.0	30.5	29.0	34.2	38.5	30.4	36.5
Talus5	16.4	21.5	17.3	14.2	19.6	22.6	17.6	21.8
Talus6	14.9	16.7	14.5	16.5	17.4	20.5	14.5	22.2
Nav1		22.9	15.1		22.6	22.0	15.9	16.5
Nav2		10.5	5.7		8.1	7.8	6.4	5.9
MCun1	10.8	14.9	11.8		14.2	16.0	11.9	15.6
ICun1	6.7	8.8	6.4		9.1	9.2	6.8	7.2
ICun2	4.9	7.8	6.2		8.4	7.1	6.4	6.8
ICun3	5.1	8.3	6.2		8.8	9.2	6.7	9.4
ICun4	5.1	8.4	5.4		8.9	9.1	6.1	8.3
LCun1	8.2	11.1	8.9		12.1	11.9	9.7	11.3
LCun2	9.8	13.1	9.8		12.8	14.3	11.4	13.7
LCun3	7.5	11.1	8.0		10.9	10.3	9.2	10.9
LCun4	5.8	8.5	5.8		8.2	8.7	6.9	8.6

Cub1	11.7	16.1	11.9		16.0	18.1	14.7	16.1
Cub2	3.3	7.0	4.3		6.0	7.4	2.4	6.5
Cub3	13.4	15.6	13.6		16.3	16.3	14.5	15.4
Cub4	14.0	16.5	13.3		17.3	19.8	15.6	17.1
MT5	42.7	49.7	39.3	40.9	51.6	45.5	43.5	55.1
MT5D	39.1	44.3	35.8	36.8	46.0	42.1	39.3	47.9
MT4	39.8	50.5	42.1	42.6	53.1	48.3	43.6	53.7
MT4D	34.5	43.5	37.0	37.4	46.4	43.8	38.7	46.1
MT3	41.7	53.2	42.0	41.6	54.5	48.5	46.4	53.5
MT3D	36.5	45.9	37.1	37.5	46.6	42.3	40.2	45.9
MT2	45.4	56.4	46.4	46.0	56.9	53.0	48.2	57.3
MT2D	39.8	49.7	41.7	38.9	49.8	48.7	43.0	50.1
MT1	33.7	42.3	34.0	32.4	45.3	41.1	38.4	45.1
MT1D	32.6	39.8	32.8	32.0	43.4	39.9	36.1	41.6
PH1	18.8	23.2	19.1	21.9	23.2	22.3	20.4	20.5
PH2	24.0	29.4	24.5	23.7	26.8	27.1	24.0	28.4
PH3	27.6	32.0	26.2	28.0	32.1	30.3	28.6	32.3
PH4	26.5	30.3	26.0	26.6	30.0	29.0	26.8	31.4
PH5	21.0	23.7	20.0	20.1	21.7	23.3	21.2	25.7
FemurL	183	215	183	278	218	212	189	222
FemurLD								
FHB	22.4	23.2	20.5	21.0	25.6	26.8	23.0	28.3
TibL	150	182	146	143	184	178	156	191
TibLa	145	174	142	140	174	168	149	180
TibLD								
FibL	133	165	133	123	163		141	168
FibLD	124		125	118		142		

Taxon	***Pan troglotyes troglodytes***						
Location	Zurich	Zurich	Zurich	HT B	PCM	HT B	PCM
Specimen	PAL 197	AS 423	PAL 53	1177	M754	829	M657
Sex	Female	Female	Female		Female		Female
Age	4.0	4.0	5.0	3.5	3.5	3.8	3.8
Age Group	2	2	2	2	2	2	2
Calc1	41.4	28.7	34.6	38.3	26.7	34.6	35.8
Calc2	27.5	19.0	21.7	26.6	16.9	22.8	22.9
Calc3	30.5	21.2	22.5	23.9	16.6	27.8	27.0
Calc4	17.0	11.3	10.4	26.4	7.4	16.7	13.7
Calc5	18.2	12.3	12.9				
Calc6	16.2	11.6	12.0				
Calc7	24.8	16.3	20.2				
Calc8	14.6	11.2	13.6				
Talus1	33.1	25.1	30.0		21.1		31.9
Talus2	33.1	25.1	30.0	32.5	21.1	30.0	31.9
Talus5	18.1	13.3	14.9				
Talus6	17.9	13.6	17.4	18.2	12.7	14.6	16.5
Nav1						17.9	15.0
Nav2						3.0	5.8

MCun1	12.1	9.0	11.4	12.9	9.0	12.2	11.7
ICun1	7.8		6.9	7.7		5.2	8.0
ICun2	6.0		5.3	5.4			5.2
ICun3	8.5		6.2	7.4			7.6
ICun4	7.3		5.3				
LCun1	10.0	7.6	9.0	10.0	7.2	9.7	10.0
LCun2	11.3	8.3	10.1	10.8	7.8	10.9	10.6
LCun3	9.6	6.2	8.1	9.5	5.9		7.9
LCun4	7.9	6.0	7.6				
Cub1	14.9	9.7	12.4	13.3	8.7	12.1	11.8
Cub2	2.8	4.7	3.3		3.5	4.8	3.5
Cub3	16.1	10.3	13.1				
Cub4	16.1	10.3	14.0	15.9	9.8	12.5	13.6
MT5	49.2		40.2	46.6	35.9	41.4	44.1
MT5D	44.3	33.1	36.0	43.1	30.7	36.9	40.2
MT4	47.8		43.1	46.1		40.6	
MT4D	42.3	34.2	38.7	41.7	32.0	35.1	41.5
MT3	49.9		43.2	47.7		42.7	49.1
MT3D	43.1	33.8	38.3	41.9	33.3	36.7	41.8
MT2	52.3		47.3	50.2	43.9	46.4	53.2
MT2D	47.5	36.7	42.1	45.1	37.2	40.7	46.3
MT1	40.1		34.1	36.5		32.6	36.8
MT1D	37.9	27.1	32.8	34.7	30.3	31.4	34.9
PH1	21.3	15.6	18.3	20.3	17.6	18.2	20.8
PH2	28.8	21.2	23.8	26.1	22.4	23.4	28.0
PH3	30.3	24.7	28.0	29.9	25.8	26.1	30.8
PH4	28.8	23.5	27.9	27.4	24.9		
PH5	22.2	18.5	21.0	20.9	19.7		21.2
FemurL	203	159	190	220	153	181	204
FemurLD							
FHB	24.3	16.8	22.3		15.4	20.2	22.8
TibL	166	130	154	161	127	141	167
TibLa	159			156		135	163
TibLD							
FibL	149			148	115	124	153
FibLD		110	130		110	116	

Taxon	***Pan troglodytes troglodytes***							
Location	PCM	PCM	HT B	PCM	PCM	PCM	PCM	PCM
Specimen	M674	M403	830	M665	M911	M930	M93	M250
Sex	Female	Male	Male	Female	Female	Female	Male	Male
Age	3.8	3.8	4.0	4.0	4.0	4.0	4.0	4.0
Age Group	2	2	2	2	2	2	2	2
Calc1	33.4	32.6	31.7	30.6	33.1	34.8	38.8	35.3
Calc2	21.1	22.1	19.8	21.0	20.7	23.6	26.9	23.2
Calc3	25.7	24.9	20.7	21.0	26.0	26.7	27.7	24.4
Calc4	12.2	14.1		10.4	12.6	15.4	15.7	11.7
Calc5								

Calc6								
Calc7								
Calc8								
Talus1	24.6	28.8		25.3	29.8	29.4	32.7	30.5
Talus2	24.6	28.8	23.2	25.3	29.8	29.4	32.7	30.5
Talus5								
Talus6	13.5	15.0	11.4	14.0	15.4	15.7	18.8	16.4
Nav1		11.2						
Nav2								
MCun1	9.1	11.4	8.5	10.0	10.7	10.8		11.0
ICun1	6.5	7.5	4.0	5.3		6.2		5.6
ICun2	3.2	6.5		4.6		4.8		4.5
ICun3	6.4	5.9		5.5		5.6		5.6
ICun4		5.9						
LCun1	7.6	9.7	7.1	7.6	8.7	9.6	10.6	8.6
LCun2	8.6	10.0	8.3	8.5	9.1	9.6	10.6	9.6
LCun3	6.6	6.6	6.7	6.4	6.7	6.8	8.2	8.6
LCun4		6.6						
Cub1	8.8	11.9	9.5	10.6	10.8	10.6	13.4	11.7
Cub2	3.6	3.9	5.1	2.3	3.6	3.7	8.8	4.4
Cub3								
Cub4	9.6	12.1	10.2	11.3	11.7	12.0	13.9	11.3
MT5		35.5	34.9	40.6		43.8		43.1
MT5D	33.8	32.6	32.4	35.7	34.8	39.2	38.8	38.9
MT4	40.1	37.9	35.3	43.5	42.7	45.8		45.6
MT4D	35.5	33.5	31.4	37.7	35.9	39.1	40.3	40.5
MT3	41.3	39.0	35.7	45.1		45.6	46.5	44.8
MT3D	35.9	32.5	32.6	38.5	37.3	38.2	40.1	39.2
MT2	43.0		37.2	49.6		48.2	49.4	48.2
MT2D	38.4	35.9	34.9	42.7	42.0	42.6	43.3	43.0
MT1	31.8	33.2	29.2	34.7	34.4	38.0		36.7
MT1D	30.9	31.3		33.6		35.1	36.6	34.3
PH1	16.7	17.5	16.7	18.1	20.2	22.0	20.2	21.0
PH2	21.3	23.6	20.6	22.6	22.2	25.7	25.6	25.4
PH3	24.8	26.3	22.3	26.9	26.3	29.6	28.7	29.1
PH4	24.0	23.5	22.2	26.6	26.0	29.4	27.4	28.3
PH5	19.3	15.8	17.6	19.1	20.1	22.3	19.9	21.1
FemurL	171	178	152	165	184	185	204	182
FemurLD			140					
FHB	17.2	19.4	17.9	18.4	19.8	20.0	24.7	21.4
TibL	137	144		139	155	156	162	154
TibLa		141		137	151		160	150
TibLD			112					
FibL	126		108		132	145		138
FibLD	120	124	100	119	128	137	141	

Taxon	***Pan troglodytes troglodytes***							
Location	PCM	PCM	Zurich	Zurich	Zurich	PCM	PCM	PCM

Specimen	M397	M744	PAL 193	PAL 196	PAL 198	CAMI93	M507	CAMI220
Sex	Male	Male	Female	Female	Female	Female	Female	Male
Age	4.0	4.0	4.0	4.0	4.0	5.0	5.0	5.0
Age Group	2	2	2	2	2	2	2	2
Calc1	36.5	37.6	31.6	33.8	39.3	37.6	38.5	34.3
Calc2	23.1	25.6	21.5	20.5	26.3	23.8	25.3	21.2
Calc3	28.0	28.3	22.5	27.1	27.8	26.3	26.3	22.6
Calc4	13.0	15.6	12.7	13.0	14.8	14.1	14.5	11.4
Calc5			14.1	14.0	15.6			
Calc6			11.6	10.2	12.9			
Calc7			17.0	17.9	18.5			
Calc8			10.6	12.3	13.3			
Talus1	32.3	32.4	26.2	29.6	32.2	33.7	32.9	28.2
Talus2	16.4	32.4	26.2	29.6	32.2	33.7	32.9	28.2
Talus5			15.5	15.6	15.9			
Talus6	18.2	17.8	13.1	13.0	16.8	17.7	18.2	15.5
Nav1	13.9					17.8	12.1	
Nav2	5.8					7.1	5.2	
MCun1	12.1	12.5	9.8	11.5	12.5	12.5	11.9	10.3
ICun1	7.3	6.9	5.5	6.4	7.6	8.1	6.7	
ICun2	6.1	4.6	4.3	6.3	5.8	6.6	4.8	
ICun3	6.7	7.6	5.0	5.4	7.2	8.7	6.6	
ICun4			4.4	4.5	5.6			
LCun1	9.8	7.7	8.6	9.5	10.7	9.2	9.3	7.6
LCun2	10.3	9.7	10.0	11.0	11.8	11.7	9.6	8.5
LCun3	7.2	8.6	6.4	7.3	8.4	9.9	8.1	7.4
LCun4			5.7	6.3	7.5			
Cub1	12.4	14.2	12.1	13.5	14.5	13.4	13.1	11.1
Cub2	4.4	4.7	2.8	1.3	5.3	7.2	5.7	3.7
Cub3			12.2	14.2	15.0			
Cub4	14.2	12.7	12.4	14.7	15.3	14.1	13.2	9.4
MT5	47.1	43.2	39.7	44.2	46.0	40.1		
MT5D	41.5	39.0	36.4	39.4	41.6		39.7	35.2
MT4	46.5	44.5	41.6	45.8	46.2	41.2		40.4
MT4D	40.4	39.2	37.0	41.1	41.0		40.4	34.5
MT3	48.8	47.2	41.6	43.3	47.7	42.0	45.8	
MT3D	42.5	41.0	37.4	38.1	41.4		39.6	34.1
MT2	53.2	52.0	45.5	44.7	53.1	53.6	49.7	
MT2D	46.4	45.0	41.1	38.9	45.8	45.6	43.4	39.1
MT1	37.8	35.2	33.1	37.6	38.8	38.6	34.4	
MT1D			30.7	36.2	36.2			30.6
PH1	19.6	19.6	17.6	20.0	21.0	21.7	18.1	17.1
PH2	25.0	24.8	21.4	22.7	25.2	24.8	24.1	22.8
PH3	28.3	28.9	24.8	25.9	27.9	29.4	28.4	25.2
PH4	27.4	28.3	24.2	25.9	27.0	28.6	27.4	24.6
PH5	20.9	22.0	18.2	19.7	22.0	20.2	21.4	19.3

FemurL	196	190	181	190	202	203	196	181
FemurLD								
FHB	22.5	24.2	19.6	22.5	24.1	23.6	23.9	19.9
TibL	167	157	144	154	165	168	158	151
TibLa	165		139	150	160	161	154	
TibLD								
FibL	141	143	129		143	153	144	138
FibLD	138		123	128	138		136	130

Taxon	***Pan troglodytes troglodytes***							
Location	PCM	PCM	Zurich	PCM	PCM	PCM	PCM	Zurich
Specimen	M60	M876	PAL 221	C195	M259	M453	M675	PAL 192
Sex	Male	Male	Male	Male	Male	Male	Male	Male
Age	5.0	5.0	5.0	5.5	5.5	5.5	5.5	5.5
Age Group	2	2	2	2	2	2	2	2
Calc1	37.4	39.3	35.5	40.6	37.4	36.7	37.1	42.7
Calc2	24.3	26.1	24.7	25.3	25.1	23.7	25.1	29.9
Calc3	29.0	26.3	26.2	27.9	28.2	25.3	27.3	28.2
Calc4	14.7	14.9	16.4	13.1	15.0	12.3	15.3	16.7
Calc5								18.8
Calc6								16.1
Calc7			18.5					22.7
Calc8			11.4					13.7
Talus1	32.0	31.2	31.3	34.8	34.1	32.1	33.5	32.0
Talus2		31.2	31.3	34.8	34.1	32.1	33.5	32.0
Talus5			16.1					18.0
Talus6	18.3	17.4	15.2	20.2	17.0	17.2	19.4	17.2
Nav1	29.5	14.8		16.5	13.4	12.8	11.2	17.0
Nav2	7.9	5.2		4.9	5.5	5.7	5.1	5.6
MCun1	12.2	11.6	11.2	13.2	12.1	12.6	13.2	12.3
ICun1	8.2		5.2		7.2	7.8	6.6	6.6
ICun2	7.2		4.4		5.6	5.3	4.9	5.8
ICun3	4.9		5.4		7.7	7.1	6.6	7.6
ICun4			5.0					6.7
LCun1	9.8	9.6	8.3	12.4	11.1	9.3	8.8	10.2
LCun2	9.8	10.1	9.3	11.8	11.1	11.1	9.3	11.6
LCun3	8.6	8.0	6.5	9.1	8.9	8.1	7.4	8.3
LCun4			6.4					7.0
Cub1	13.6	13.5	12.2	15.4	13.4	12.3	12.6	14.2
Cub2	3.4	10.8	5.8	4.3	3.2	5.7	4.9	2.9
Cub3			10.0					13.3
Cub4	12.4	11.4	11.9	14.2	17.1	13.0	13.3	15.1
MT5	44.1	41.6	37.7	45.1		45.1	46.6	50.4
MT5D	39.3	38.4	36.5	39.8	41.1	39.7	40.5	46.2
MT4	44.5	43.4	38.8	48.8	47.1	47.1	48.9	49.2
MT4D	39.1	37.9	35.2	42.8	41.2	40.8	42.7	44.4

MT3	45.4	44.3	40.8	48.5	50.2	47.4		50.2
MT3D	29.3	38.6	35.4	40.7	42.4	39.7	43.2	44.3
MT2	49.3		45.0	52.1	54.3	53.4	54.5	54.0
MT2D	43.0	44.1	39.5	45.0	46.8	47.0	48.0	48.5
MT1	38.5		32.0	36.6	38.3	39.0	36.9	42.3
MT1D	35.5	34.1	31.1			38.0	34.3	38.6
PH1	20.3	19.5	18.0	21.4	22.2	22.5	19.1	21.0
PH2	25.8	23.9	21.3	25.6	25.2	28.8	25.6	26.2
PH3	30.1	27.5	24.7	29.0	28.9	31.0	29.4	29.3
PH4	28.5	27.0	23.3	30.0	27.8	29.8	28.8	28.8
PH5	22.8	22.3	18.3	23.8	22.2	21.9	22.7	23.7
FemurL	193	195	170	211	202	195	200	205
FemurLD								
FHB	21.9	24.0	20.3	24.9	24.0	22.9	22.4	24.2
TibL	159	164	140	179	159	162	163	166
TibLa	154		132	170	156		161	160
TibLD								
FibL			126	154	147		155	153
FibLD	136	138		146		138	142	

Taxon	***Pan troglodytes troglodytes***							
Location	PCM	HT B	HT B	Zurich	Zurich	Zurich	Zurich	Zurich
Specimen	C214	1773	3541	AS 1687	AS 1736	AS 1744	PAL 130	PAL 134
Sex	Female		Female	Female	Female	Male	Female	Female
Age	5.8	7.0	6.0	6.0	6.5	6.5	7.0	7.5
Age Group	2	3	3	3	3	3	3	3
Calc1	36.0	46.2	44.5	48.7	51.6	40.1	49.4	50.8
Calc2	23.1	30.5	30.6	36.1	37.9	28.7	36.1	35.5
Calc3	26.7	32.1	29.6	31.4	33.5	30.1	32.5	31.0
Calc4	12.7	16.7	15.8	19.0	19.6	18.0	19.0	16.1
Calc5				21.8	22.5	19.2	21.3	18.9
Calc6				16.8	18.5	15.5	18.2	15.3
Calc7				30.6	29.5	24.3	26.9	26.8
Calc8				18.6	18.1	15.0	15.4	14.7
Talus1	30.3			41.4	42.3	34.7	41.6	39.6
Talus2	30.3	37.3	37.3	43.9	46.0	35.5	42.5	42.4
Talus5				24.7	24.8	21.5	24.6	22.0
Talus6	17.0	19.7	19.9	21.3	20.9	17.7	18.6	20.6
Nav1	17.0	25.5	24.5	33.9	34.3	23.9	31.2	31.8
Nav2		8.0	7.6	11.3	11.2	8.8	9.1	9.2
MCun1	13.6	14.7	16.2	17.0	17.2	12.9	16.6	17.1
ICun1	8.4	9.6	10.5	8.8	11.1	8.5	9.5	10.5
ICun2	5.1	5.9	8.1	8.9	9.9	7.7	8.0	8.9
ICun3	8.2	9.3	10.0	9.9	10.0	8.5	10.1	9.8
ICun4		7.7	9.3	9.3	10.2	8.5	9.6	8.4
LCun1	10.1	10.6	11.9	13.7	14.4	11.6	12.5	11.0

LCun2	9.9	13.9	13.9	15.8	16.8	13.0	13.2	13.0
LCun3	8.9	9.1	9.8	13.3	13.8	9.9	11.9	11.9
LCun4		6.9	9.5	9.0	8.6	7.7	9.4	9.0
Cub1	14.6	16.1	15.2	20.0	21.7	15.8	17.1	17.8
Cub2	4.7	5.5	8.3	7.0	9.2	3.8	4.3	8.8
Cub3				19.4	20.2	17.7	20.6	18.7
Cub4	13.4	16.5	13.9	20.4	20.8	18.9	20.8	18.3
MT5		51.6	50.4	64.5	62.5	45.5	58.6	63.0
MT5D	38.3	42.8	41.5	56.9		40.3	52.1	56.7
MT4	44.3	54.2	52.8	63.3	65.4	46.3	59.5	63.6
MT4D		46.5		54.6		40.8	51.3	56.5
MT3	47.0	55.3	54.8	65.0	67.5	49.2	61.8	66.0
MT3D		46.2		55.1		42.0	52.8	57.6
MT2	33.8	59.3	60.0	68.5	71.1	54.1	65.9	69.5
MT2D		51.6		58.5		47.5	57.7	61.6
MT1	35.6	43.2	42.3	53.5	55.3	39.6	48.6	50.2
MT1D	33.8	40.9		50.2		37.4	45.6	47.4
PH1	14.8	26.6	23.6	30.2	30.3	20.7	24.0	26.0
PH2	25.2	34.0	31.0	38.6	34.3	24.2	30.6	32.9
PH3	29.1	35.2	34.0	43.0	41.1	28.3	34.7	38.1
PH4	27.9	36.7	32.5	39.9	38.9	26.7	34.1	36.9
PH5	20.8	29.8	23.5	29.9	30.3	22.3	25.7	27.8
FemurL	181	230	232	255	282	202	255	252
FemurLD		210						
FHB	22.9	27.9	25.0	30.8	30.2	25.1	26.8	26.6
TibL	159	195	199	217	238	165	203	221
TibLa	155	185	190	207	227	156	193	211
TibLD		172						
FibL	146	174	180	194	216	149	185	196
FibLD		154						

Taxon	***Pan troglodytes troglodytes***							
Location	Zurich	PCM	PCM	PCM	PCM	PCM	PCM	PCM
Specimen	PAL 190	M145	M881	M94	M363	M635	M746	M801
Sex	Female	Female	Female	Male	Male	Male	Male	Male
Age	7.0	6.0	6.0	6.0	6.0	6.0	6.0	6.0
Age Group	3	3	3	3	3	3	3	3
Calc1	47.8	45.8	39.6	41.7	33.5	39.4	44.8	40.6
Calc2	34.8	32.3	27.4	26.6	23.0	25.9	29.0	30.6
Calc3	33.3	33.2	29.7	31.3	25.9	26.8	31.7	27.4
Calc4	19.9	17.7	16.0	16.7	15.9	13.2	16.7	17.1
Calc5	21.8						19.9	
Calc6	15.9						16.3	
Calc7	27.9						26.0	
Calc8	17.1						15.3	

Talus1	38.4	39.1	35.6	36.1	29.8	34.5	39.3	35.4
Talus2	42.6	38.0	35.6	36.1	29.8	34.5	39.7	35.4
Talus5	22.1						22.0	
Talus6	18.9	20.4	17.9	20.2	16.6	17.2	21.0	18.8
Nav1	31.8	25.7	18.8	18.6		13.3	26.9	23.5
Nav2	10.8	8.7	6.0	7.0		5.3	7.5	7.2
MCun1	15.7	14.4	15.1	12.3		12.4	16.7	14.7
ICun1	8.9	8.9	8.4	8.4		5.5	9.7	8.9
ICun2	8.3	7.2	7.1	5.8		4.6	8.8	7.3
ICun3	9.1	9.4	9.1	8.0		6.9	9.9	8.4
ICun4	9.5						9.2	
LCun1	12.1	11.4	10.7	11.2	8.3	10.1	12.6	10.3
LCun2	15.3	12.3	11.9	11.8	8.6	10.9	12.9	11.2
LCun3	11.4	11.8	8.8	9.3	6.8	7.8	10.4	8.6
LCun4	8.8						8.4	
Cub1	17.6	15.9	13.5	15.7	11.8	13.5	15.2	15.1
Cub2	8.2	6.0	3.3	5.0	7.6	4.1	6.9	4.5
Cub3	17.9							
Cub4	18.4	17.4	15.8	15.9	11.6	14.6	17.0	16.6
MT5	61.8	52.0		47.7	39.5	44.7	52.9	45.7
MT5D	56.9		43.7		34.2	40.5	47.7	40.0
MT4	60.0	52.3	49.7	48.6	40.0		50.0	47.4
MT4D	53.6		42.4		35.1	40.1	45.2	40.0
MT3	60.9	53.4	52.3	49.3	42.2	46.9	54.2	48.7
MT3D	53.6		44.4		35.8	40.3	47.0	39.8
MT2	67.1	56.6	56.9	54.4	46.8	50.9	58.9	52.1
MT2D	60.1		48.4		40.6	44.2	51.6	43.3
MT1	51.0	42.3	41.3	39.3	34.5	36.3	44.0	39.1
MT1D					32.6	33.9	42.9	37.7
PH1	26.2	26.6	26.3	22.8	16.5	18.1	24.3	22.7
PH2	32.3	32.5	30.8	26.9	23.3	23.7	31.2	27.4
PH3	36.3	27.5	35.0	31.2	26.6	27.7	35.2	31.7
PH4	35.7	34.7	32.7	29.3	24.9	27.3	32.4	31.7
PH5	29.4	27.4	25.1	21.7	19.5	21.0	25.5	22.4
FemurL	267	223	221	213	191	203	228	206
FemurLD								
FHB	29.8	27.0	25.7	25.0	21.9	23.6	25.7	25.5
TibL	220	191	181	185	156	173	196	171
TibLa	210	180	172	177	154	170	185	160
TibLD				177				
FibL	200	175	152	168	139	156	176	156
FibLD			148		136			

Taxon	***Pan troglodytes troglodytes***							
Location	PCM	PCM	PCM	PCM	PCM	PCM	HT B	HT B
Specimen	M274	M805	CAMI118	M382	M454	M636	347	1771
Sex	Female	Female	Male	Female	Female	Male		Female

Age	6.3	6.3	6.3	6.5	6.5	6.5	7.0	7.0
Age Group	3	3	3	3	3	3	3	3
Calc1	38.9	41.4	39.5	44.4	40.8	43.3	50.2	43.2
Calc2	28.2	29.0	27.0	30.4	28.2	29.8	37.6	29.6
Calc3	28.2	31.3	28.6	30.7	27.7	30.9	35.7	30.6
Calc4	17.1	18.0	15.8	17.8	14.5	18.0	24.7	15.6
Calc5				19.7				
Calc6				17.2				
Calc7				25.2				
Calc8				16.5				
Talus1	32.6	33.7	34.9	40.5	34.8	36.7		
Talus2	32.6	36.3	34.9	41.3	34.5	38.4	43.8	36.0
Talus5				22.8				
Talus6	19.2	20.6	18.4	19.9	18.4	19.7	26.8	18.1
Nav1	18.1	26.3	21.2	26.8	19.0	25.2	33.1	26.4
Nav2	5.9	7.9	7.4	7.3	7.3	8.6	6.9	9.4
MCun1	13.1	15.4	13.3	15.3	14.0	14.6	17.5	14.4
ICun1	8.2	9.6	8.6	8.2	9.0	8.2	9.2	7.7
ICun2	7.3	7.1	5.5	8.0	7.8	6.7	7.7	6.9
ICun3	8.4	8.8	7.5	10.3	9.0	7.9	8.8	8.8
ICun4				9.6				8.1
LCun1	11.0	11.7	9.2	11.2	10.9	10.9	11.8	10.7
LCun2	11.4	12.8	9.9	12.4	11.5	11.9	13.7	11.9
LCun3	9.4	11.6	8.6	10.9	9.3	10.6	11.1	10.0
LCun4				9.2				7.7
Cub1	14.0	14.5	13.9	17.2	14.4	15.6	18.8	16.2
Cub2	3.9	6.2	4.8	6.2	7.0	4.2	8.1	6.2
Cub3				16.2				
Cub4	12.1	13.8	13.2	17.6	15.1	16.8	19.7	16.6
MT5		54.6		51.9	48.5	56.0	57.4	50.3
MT5D	42.8	47.9	36.2	45.9	44.2	49.8		45.2
MT4	47.5		40.3	55.0		56.8	56.9	51.7
MT4D	41.3	49.5	34.9	46.4	47.1	49.1		44.3
MT3	48.0	57.4	35.5	57.3	54.9	58.8	57.7	
MT3D	40.8	50.5	28.5	48.6	48.5	50.4		46.6
MT2		62.3	46.1	59.6	57.0	63.3	63.3	52.0
MT2D	44.9	54.2	39.2	51.0	5.1	54.3		46.3
MT1		45.5	34.7	42.5	42.0	44.1	48.5	41.4
MT1D	34.4	44.1	32.8	41.3	40.4	42.0		39.1
PH1	21.7	26.7	18.4	23.4	23.2	24.6	26.1	26.7
PH2	26.1	29.4	23.5	32.0	27.2	30.8	32.9	
PH3	30.4	34.1	29.4	36.6	33.3	34.8	38.4	
PH4	29.5	32.8	26.8	34.6	31.3	33.2	36.4	
PH5	23.2	25.2	20.1	24.3	22.9	25.5	27.5	
FemurL	208	225	189	225	215	226	245	225
FemurLD								
FHB	24.0	24.9	25.1	26.4	25.3	26.0	33.7	25.7

TibL	172	189	158	200	190	193	209	191
TibLa	166	180	150	189	180	182	199	178
TibLD							185	
FibL	148	173		183	172	176	174	172
FibLD	144		125				168	

Taxon	***Pan troglodytes troglodytes***							
Location	HT B	PCM	PCM	PCM	PCM	Zurich	Zurich	HT B
Specimen	3553	M371	ZVI35	M170	M455	11037	PAL 112	1767
Sex	Male	Female	Male	Male	Male	Female	Female	?
Age	7.5	7.5	7.5	7.5	7.5	7.5	7.5	9.0
Age Group	3	3	3	3	3	3	3	4
Calc1	50.9	40.3	46.3	41.0	44.5	51.2	47.5	51.1
Calc2	35.4	26.6	32.3	26.7	33.8	37.7	35.5	38.8
Calc3	34.8	28.9	31.0	28.8	31.2	33.6	32.4	35.0
Calc4	18.3	14.3	16.8	15.6	21.0	19.3	19.5	19.6
Calc5			19.3		21.9	22.7	22.9	
Calc6			15.8		17.5	17.9	19.8	
Calc7			27.4		28.2	27.8	32.6	
Calc8			15.6		14.4	16.3	18.5	
Talus1		36.1	38.9	35.5	42.2	40.7	42.8	
Talus2	42.6	36.1	40.3	35.6	43.3	44.1	45.5	42.6
Talus5			21.9		23.0	26.5	24.5	
Talus6	22.5	19.7	21.6	19.4	21.7	22.0	24.1	23.9
Nav1	29.7	19.9	25.4	21.7	22.3	32.8	36.5	
Nav2	9.1	6.3	7.7	7.1	6.3	11.9	12.5	
MCun1	15.9	15.9	14.5	14.2	16.3	17.1	18.2	14.6
ICun1	9.4	8.9	8.0	6.5	8.7	10.7	11.0	10.5
ICun2	8.1	6.7	6.5	6.3	8.7	9.8	10.6	10.2
ICun3	9.3	9.1	9.3	10.0	9.9	10.9	10.9	11.6
ICun4	9.3		8.2		9.1	9.9	10.4	10.9
LCun1	9.8	11.5	12.1	8.9	12.3	13.8	13.8	12.3
LCun2	14.1	11.9	13.1	11.0	15.1	15.9	16.4	14.3
LCun3	13.4	10.1	11.3	9.8	12.6	12.1	13.0	13.5
LCun4	9.4		13.1		9.7	10.0	10.4	11.0
Cub1	19.1	15.7	16.9	14.8	17.1	19.9	22.5	17.4
Cub2	5.6	5.4	4.2	5.7	8.0	10.8	10.1	11.0
Cub3					18.8	19.6	21.1	
Cub4	20.7	16.2	17.7	14.0	18.1	22.4	22.2	22.3
MT5	58.8	51.4	56.0	51.0	56.2	63.0	63.6	64.4
MT5D		45.1	49.9		48.5		56.7	52.2
MT4	59.0	54.0	55.0	51.3	57.3	64.1	65.7	66.1
MT4D		45.8	47.9		48.7		55.7	57.6
MT3	62.0	55.5	55.9	52.0	60.5	68.5	64.8	69.6
MT3D		47.2	47.7		50.9		55.4	60.5
MT2	66.3	58.9		55.5	65.8	72.3	69.6	75.8
MT2D		50.8	53.3		56.3		60.3	66.7

MT1	48.9	43.8	43.0	40.6	50.1	57.6	53.6	56.1
MT1D			41.2		47.3		50.8	51.9
PH1	26.5	23.2	26.4	22.4	26.1	29.8	30.2	
PH2	36.5	29.7	30.7	30.9	30.7	36.8	34.7	
PH3		32.7	36.2	32.3	37.9	42.3	40.3	
PH4	35.9	32.5	34.4	28.1	35.8	40.6	36.9	
PH5	27.7	25.3	26.9	24.3	25.5	32.5	30.1	
FemurL	264	213	230	225	242	266	276	280
FemurLD								
FHB	29.3	26.1	27.8	26.0	30.6	32.2	29.2	33.5
TibL	220	179	195	190	203	228	232	244
TibLa	209	171	185	181	216	218	222	232
TibLD								214
FibL	200	168			184	206	209	217
FibLD	180		155	160	172			196

Taxon	***Pan troglodytes troglodytes***							
Location	HT B	Zurich	Zurich	Zurich	Zurich	HT B	PCM	PCM
Specimen	1800	AS 1568	AS 1680	PAL 215	PAL 223	346	M52	M707
Sex	Female	Female	Female	Female	Female	?	Male	Male
Age	8.5	10.5	8.5	9.0	8.0	8.0	8.0	8.0
Age Group	4	4	4	4	4	4	4	4
Calc1	45.0	47.0	50.7	52.7	49.1	52.5	47.6	50.8
Calc2	32.0	35.5	38.1	38.2	36.3	36.9	33.0	36.9
Calc3	34.0	31.2	33.3	35.0	33.2	36.0	33.8	33.6
Calc4	19.4	19.5	19.2	20.0	20.6	21.4	17.6	19.1
Calc5		21.9	22.3	23.2	22.7			21.9
Calc6		16.5	17.1	17.3	16.5			18.9
Calc7		31.6	30.8	31.2	30.5			34.7
Calc8		18.5	18.2	20.2	18.4			18.1
Talus1		38.1	40.9	43.0	39.6		41.5	41.7
Talus2	37.2	44.0	45.9	46.9	42.4	42.6	41.5	45.1
Talus5		23.9	23.1	26.0	23.6			26.0
Talus6	20.4	20.6	21.4	22.6	19.7	21.7	21.1	23.6
Nav1	29.6	32.6	34.7	36.9	32.5	34.6	31.0	35.3
Nav2	10.1	10.8	11.9	12.8	10.4	9.0	8.5	12.2
MCun1	14.8	16.7	17.7	18.0	17.5	18.7	16.6	17.5
ICun1	9.7	10.0	9.3	9.5	9.4	9.3	11.0	12.2
ICun2	7.2	9.0	9.1	9.1	8.6	9.4	7.8	9.1
ICun3	9.8	10.6	11.7	10.4	9.7	9.2	10.5	12.2
ICun4	9.8	10.2	10.8	9.7	9.1			11.9
LCun1	10.9	11.2	13.4	12.9	13.1	14.2	11.9	12.0
LCun2	11.7	14.5	16.7	14.2	15.5	16.1	13.9	15.1
LCun3	9.5	14.6	14.5	12.7	13.1	12.9	13.0	14.4
LCun4	8.4	10.1	10.4	10.5	9.8			10.5
Cub1	16.7	18.7	19.6	19.9	18.9	20.0	15.9	19.5

Cub2	5.3	9.7	10.4	8.9	7.9	10.4	6.6	9.5
Cub3		18.1	20.3	19.1	18.5			23.0
Cub4	19.7	18.4	21.1	21.1	19.1	21.3	16.2	22.2
MT5	55.5	64.1	66.7	72.4		60.6	51.3	66.4
MT5D	46.6				57.8	55.2		58.9
MT4	58.6	62.9	65.7	73.3	63.4	63.0	57.4	63.8
MT4D	51.8				65.1	53.8		55.1
MT3	55.5	65.0	66.7	75.1	65.0	65.3	59.8	66.3
MT3D	52.2					56.9		55.6
MT2	62.5	69.8	71.8	79.6	70.4	69.0	67.2	72.4
MT2D	55.6					59.3		62.6
MT1	48.5	51.3	57.2	59.7	56.0	50.8	47.7	53.2
MT1D	45.3					49.2		51.0
PH1	26.1	29.1	32.4	31.7	30.1	29.5	26.1	28.2
PH2	32.2	35.3	36.4	36.8	36.3	34.3	31.1	35.5
PH3	37.2	40.0	42.9	41.2	41.8	37.7	36.1	40.4
PH4	36.1	38.1	41.1	39.4	39.2	35.2	34.2	35.4
PH5	27.6	29.8	31.4	31.0	29.8	27.3	26.3	27.9
FemurL	257	272	294	262	279	272	250	270
FemurLD						245		
FHB	27.0	28.4	31.9	31.5	28.8	29.9	30.1	33.3
TibL	225	220	250	263	235		214	233
TibLa	215	211	238	251	224	220	204	222
TibLD						210		
FibL	202	201	228	236	212		193	213
FibLD						196		

Taxon	***Pan troglodytes troglodytes***							
Location	PCM	PCM	HT B	HT B	HT B	HT B	HT B	HT B
Specimen	C370	M719	1056	1426	1434	1708	1713	1719
Sex	Female	Male	Male	Female	Female	Male	Female	Female
Age	9.0	11.0	Adult	Adult	Adult	Adult	Adult	Adult
Age Group	4	4	5	5	5	5	5	5
Calc1	43.8	53.4	60.0	53.4	55.0	57.5	53.0	48.0
Calc2	31.5	37.9	43.0	38.8	40.2	44.3	38.0	33.3
Calc3	29.3	34.9	41.7	36.8	37.6	39.0	35.8	33.4
Calc4	16.4	21.5	21.3	22.2	24.4	25.6	22.3	20.1
Calc5		23.3						
Calc6		16.2						
Calc7		30.6						
Calc8		20.7						
Talus1	37.9	44.8						
Talus2	36.8	48.6	48.0	42.0	44.0	43.9	43.8	44.8
Talus5		28.5						
Talus6	18.9	20.7	29.1	22.8	22.3	24.7	23.8	23.5
Nav1	27.8	33.6	42.3	33.9	34.6	39.2	36.7	35.2

Nav2	8.5	11.2	13.5	12.5	11.7	13.3	10.8	11.4
MCun1	15.6	18.2	22.2	18.4	16.7	19.1	20.5	18.3
ICun1	10.0	10.6	14.0		10.2	12.7	12.7	9.1
ICun2	7.3	9.2	11.3		9.6	11.3	9.6	12.0
ICun3	9.3	11.0	11.5		11.8	11.7	9.9	9.4
ICun4		10.9			10.3	11.0		
LCun1	11.3	13.5	13.8	12.0	12.7	14.7	14.7	12.2
LCun2	12.9	15.8	18.0	15.1	15.1	14.2	16.6	14.7
LCun3	10.9	13.9	15.3	14.1	11.6	11.6	14.2	12.2
LCun4		10.7			8.5	10.8		
Cub1	16.9	17.9	23.9	19.9	19.3	19.6	21.2	19.7
Cub2	9.7	9.3	8.7	8.7	12.1	10.6	9.5	9.4
Cub3		20.5						
Cub4	19.1	20.0	24.8	20.9	20.0	22.4	22.2	20.8
MT5	51.6	69.3	78.7		66.4	72.3	69.1	62.9
MT5D	45.1				60.0			
MT4	51.4	67.4	74.6	66.5	67.0	68.6	69.9	63.1
MT4D								
MT3	52.2	67.9	77.9	71.0	72.5	69.1	71.0	65.0
MT3D								
MT2	56.0	72.0	82.7	74.7	73.5	75.4	76.1	68.2
MT2D								
MT1	39.5	54.6	57.5	52.7	58.4	58.1	57.9	51.8
MT1D								
PH1	24.7	30.5	32.4	33.8	33.1	33.5	29.6	27.7
PH2	28.8	33.9	39.1		41.6	40.2	36.5	35.5
PH3	32.4	38.8	46.2	41.9	47.5	47.0	43.2	40.5
PH4	30.5	38.6	43.5		44.7	45.1	41.1	38.7
PH5	22.8	30.4	34.4		31.5	35.9	31.2	30.4
FemurL	235	277	325	289	321	280	291	293
FemurLD								
FHB	28.3	31.2		31.7	35.6	35.4		
TibL	190	248	273		265	246	245	252
TibLa	183	234	263		255	231	233	241
TibLD								
FibL	175	222	253		241	226	222	233
FibLD								

Taxon	***Pan troglodytes troglodytes***							
Location	HT B	HT B	HT B	HT B	HT B	HT B	HT B	HT B
Specimen	1720	1721	1722	1723	1735	1739	1744	1745
Sex	Female	Female	Male	Female	Female	Male	Female	Male
Age	Adult	Adult	Adult	Adult	Adult	Adult	Adult	Adult
Age Group	5	5	5	5	5	5	5	5
Calc1	52.3	49.6	57.8	54.2	56.2	57.6	51.0	53.8
Calc2	36.4	35.7	41.6	38.5	39.1	39.2	37.6	38.2
Calc3	35.7	37.8	37.8	37.3	36.1	40.5	32.7	38.2
Calc4	21.3	22.2	22.8	22.9	18.6	21.3	20.2	23.6

Calc5								
Calc6								
Calc7								
Calc8								
Talus1								
Talus2	41.7	41.4	45.0	43.8	39.7	45.2	39.1	41.4
Talus5								
Talus6	21.9	21.1	23.7	27.2	23.2	25.4	20.8	24.5
Nav1	33.6	32.9	40.2	36.7	35.1	41.1	33.8	
Nav2	9.4	11.4	10.0	11.6	10.1	10.9	9.8	11.2
MCun1	16.9	15.9	19.4	16.3	16.7	20.3	16.5	19.3
ICun1	8.7	10.4	12.6	10.7	11.8	11.8	9.9	12.6
ICun2	7.4	8.6	10.2	10.0	10.2	10.9	9.3	8.1
ICun3	10.3	10.4	12.4	10.9	10.2	10.7	9.8	11.1
ICun4	9.2	9.9	12.6	10.1	10.2	11.2	9.7	10.3
LCun1	10.5	11.8	13.2	11.7	11.9	13.6	12.1	11.4
LCun2	12.9	14.2	13.9	16.2	15.3	15.7	14.9	14.6
LCun3	12.6	11.6	13.8	14.3	12.2	15.1	13.4	14.2
LCun4	9.4	9.2	10.4	11.5	10.0	10.9	9.5	10.7
Cub1	16.9	18.3	20.2	19.3	18.2	20.0	18.9	20.2
Cub2	7.8	8.4	8.7	9.6	8.5	11.3	8.8	7.2
Cub3								
Cub4	19.2	19.2	21.5	21.7	21.3	21.8	21.3	20.8
MT5	68.2	65.1	70.7	64.4	66.7	66.9	64.5	68.3
MT5D	60.5		56.6			60.5		
MT4	63.6	63.6	72.6	68.3	64.7	65.6	65.1	65.2
MT4D								
MT3	66.2	66.3	74.1	72.4	67.6	67.8	68.1	67.4
MT3D								
MT2	71.0	71.0	80.9	76.7	72.4	72.5	72.9	70.9
MT2D								
MT1	53.0	54.4	59.5	56.2	54.6	54.4	55.8	52.1
MT1D								
PH1		28.8	29.7	32.7	30.6	31.1	28.4	29.8
PH2	37.5		39.3	37.7	35.6	38.1	35.7	35.3
PH3	43.1		44.2	43.1	41.2	43.7	40.3	40.4
PH4	39.8		41.9	41.9	39.4	41.4	39.2	38.6
PH5	30.5		32.0	32.3	30.6	31.3	30.3	29.3
FemurL	296	275	308	290	302	299	296	301
FemurLD								
FHB	30.0	31.5	36.9	35.9	33.5	34.4	32.1	34.7
TibL	245	239	269	240	264	248	239	249
TibLa	234	227	256	227	254	235	229	237
TibLD								
FibL	223	216	243	219	238	228	219	226
FibLD								

Taxon	***Pan troglodytes troglodytes***							
Location	HT B	HT B	HT B	HT B	HT B	HT B	HT B	HT B

Specimen	1748	1755	1758	1768	1769	1770	1775	1777
Sex	Female	Female	Male	Male	Female	Female	Female	Male
Age	Adult	Adult	Adult	Adult	Adult	Adult	Adult	Adult
Age Group	5	5	5	5	5	5	5	5
Calc1	48.3	53.4	58.4	54.4	50.9	50.9	57.4	49.0
Calc2	33.4	37.6	41.1	38.0	39.3	34.6	39.8	36.2
Calc3	36.6	35.5	42.0	37.5	33.2	35.2	43.6	35.8
Calc4	20.1	19.0	25.2	20.4	19.7	19.2	24.7	20.6
Calc5								
Calc6								
Calc7								
Calc8								
Talus1								
Talus2	41.1	41.9	45.9	41.8	38.7	40.1	47.9	43.2
Talus5								
Talus6	22.3	23.2	23.7	22.4		21.9	24.5	20.5
Nav1	34.1	34.1	38.4	36.0	36.8	34.1	38.2	34.7
Nav2	10.5	11.4	11.1	11.1	11.9	11.6	12.0	10.7
MCun1	16.3	16.4	18.0	16.7	16.2	19.0	19.4	17.4
ICun1	11.1	11.3	9.2	10.1	10.1	10.2	11.2	9.9
ICun2	8.7	9.7	10.2	9.1	9.1	8.9	9.8	8.1
ICun3	10.3	9.6	11.3	11.8	11.4	11.6	11.5	9.8
ICun4	10.3	9.3	11.3	10.7	10.7	10.2	13.5	9.7
LCun1	12.8	12.2	13.5	11.4	11.0	10.6	13.5	12.1
LCun2	14.7	15.4	14.2	14.5	13.9	12.3	17.3	13.8
LCun3	12.4	12.8	12.4	12.7	13.7	11.5	16.3	14.4
LCun4	9.8	9.7	9.5	9.3	9.9	8.8	11.6	9.2
Cub1	18.3	20.1	19.6	18.5	18.3	16.2	21.3	19.6
Cub2	8.5	9.0	8.4	10.0	7.8	7.3	12.2	6.9
Cub3								
Cub4	22.3	20.8	22.3	19.6	19.9	18.9	21.4	20.8
MT5	59.0	71.1	70.6	65.7	67.8	61.5	67.1	
MT5D		60.5					59.6	47.1
MT4	55.1	69.1	70.5	67.0	68.5	63.1	67.6	
MT4D							67.5	51.8
MT3	57.0	69.9	73.8	69.2	70.7	66.1	70.2	62.0
MT3D								52.4
MT2	62.0	73.4	78.9	73.1	75.5	69.0	75.8	
MT2D								57.1
MT1	47.0	55.0	55.7	55.8	58.1	52.3	59.6	
MT1D								50.1
PH1	27.1	32.3	30.5	30.5	32.4	30.8	30.5	28.9
PH2	32.6	39.2	38.5	39.4	41.2	36.0	37.4	34.4
PH3	36.2	44.3	43.1	42.8	46.8	40.1	44.1	37.9
PH4	36.0	43.0	40.9	40.2	41.6	38.0	42.7	36.1
PH5	28.2	34.0	32.1	32.3	32.9	29.6	32.4	30.5
FemurL	268	304	315	306	288	265	308	268

FemurLD								243
FHB	31.3	31.0	36.8	32.4	30.9	30.3	34.6	32.1
TibL	216	260	264	259	245	221	258	232
TibLa	206	252	251	247	231	211	246	221
TibLD								205
FibL	200	238	245	236	222	198	238	209
FibLD								185

Taxon	***Pan troglodytes troglodytes***							
Location	HT B	HT B	HT B	HT B	HT B	HT B	HT B	HT B
Specimen	1843	1853	1880	1882	2027	2746	2771	3537
Sex	Female	Female	Female	Male	Male	Male	Female	Male
Age	Adult	Adult	Adult	Adult	Adult	Adult	Adult	Adult
Age Group	5	5	5	5	5	5	5	5
Calc1	56.1	54.3	59.6	53.6	56.6	50.4	49.6	57.3
Calc2	40.0	38.3	42.0	36.7	41.5	34.2	35.8	39.9
Calc3	37.4	40.1	40.2	36.0	39.1	35.0	34.9	41.6
Calc4	20.9	23.9	21.2	19.4	22.7	18.1	19.7	21.9
Calc5								
Calc6								
Calc7								
Calc8								
Talus1								
Talus2	43.3	43.1	46.7	43.4	44.6	43.7	38.2	48.1
Talus5								
Talus6	23.9	24.0	25.5	24.7	24.3	23.9	21.1	24.7
Nav1	39.0	37.1	35.5	37.7	37.5	34.8	32.7	36.3
Nav2	11.4	11.3	13.7	12.8	11.2	10.5	8.2	12.7
MCun1	17.0	18.5	19.3	19.4	18.2	17.2	16.6	19.8
ICun1	12.2	12.8	13.7	12.9	11.7	11.4	11.7	11.3
ICun2	9.8	9.1	10.3	9.0	9.8	9.7	10.0	7.9
ICun3	10.4	9.9	12.1	11.1	10.9	12.2	10.0	10.5
ICun4	10.2	10.2	11.3	13.2	10.9	10.5	9.6	12.2
LCun1	13.4	13.0	12.9	10.5	13.0	13.7	12.7	12.4
LCun2	15.4	15.2	15.5	14.0	15.5	16.1	13.6	15.3
LCun3	15.0	13.6	12.9	12.7	15.1	13.0	11.1	13.6
LCun4	11.2	11.2	11.2	10.4	10.0	10.2	8.8	11.4
Cub1	20.8	17.1	21.0	20.4	20.1	18.0	16.5	19.7
Cub2	10.0	9.5	11.4	10.7	8.8	6.5	6.8	9.5
Cub3								
Cub4	20.9	21.4	21.8	20.5	22.4	24.0	18.3	23.9
MT5	69.1	69.3	71.1	63.9	66.6	62.6	60.8	66.1
MT5D	62.0		65.4	59.8				
MT4	67.7	71.7	73.7	67.7	64.3	63.8	61.3	66.4
MT4D								
MT3	70.7	71.6	75.8	69.6	63.7	65.8	62.7	69.3
MT3D								

MT2	74.2	77.0	78.0	72.0	68.2	68.8	68.0	72.8
MT2D								
MT1	55.6	59.1	57.5	58.5	51.7	47.6	50.9	55.1
MT1D								
PH1	29.4		32.6	31.9	30.0	28.6	29.0	29.1
PH2	38.9	38.3	40.6	38.2	37.0	37.6	37.4	
PH3	45.3	44.6	45.8	44.7	42.6	42.1	41.6	
PH4	43.5	42.3	43.2	42.0	39.9	40.8	40.3	
PH5	34.5	34.2	34.3	32.6	31.6	31.7	29.1	30.9
FemurL	300	302	307	312	296	285	299	304
FemurLD								
FHB	34.0	34.2	37.2	32.6	34.0	33.1	29.9	36.9
TibL	257	264	264	265	250	236	247	257
TibLa	244	255	253	253	238	225	235	244
TibLD								
FibL	236	237	240	234	222	216	228	232
FibLD								

Taxon	***Pan troglodytes troglodytes***							
Location	HT B	Zurich	HT B	HT B	HT B	HT B	HT B	HT B
Specimen	3552	AS 1695	1749	1741	2823	1195	1706	1738
Sex	Male	Male	Female	Female	Female	Male	Male	Male
Age	Adult	Adult	Adult	Adult	Adult	Adult	Adult	Adult
Age Group	5	5	5	5	5	5	5	5
Calc1	57.7	55.1	54.2	54.5	48.7	55.1	50.0	58.8
Calc2	41.3	40.9	39.3	37.6	36.4	39.6	36.7	40.8
Calc3	39.3	35.2	37.4	38.8	34.0	41.1	37.0	42.5
Calc4	25.5	20.3	23.0	22.7	18.1	23.8	20.8	24.3
Calc5		23.7						
Calc6		20.2						
Calc7		32.6						
Calc8		18.1						
Talus1		41.7						
Talus2	45.2	49.0	39.0	40.1	39.5	41.6	43.1	42.8
Talus5		23.4						
Talus6	25.0	22.1	24.9	21.7	22.7	24.2	22.6	24.6
Nav1	38.5	36.0	35.8	33.5	36.2	34.7	35.8	36.2
Nav2	11.8	11.7	12.6	11.2	9.4	11.0	11.3	10.7
MCun1	18.6	18.8	17.2	16.5	15.1	22.0	17.4	18.3
ICun1	12.7	11.2	10.2	10.8	11.0	11.5	12.2	11.3
ICun2	8.9	9.4	9.5	9.5	8.8	9.6	8.5	10.8
ICun3	12.5	12.7	9.8	9.2	8.9	10.6	10.3	10.8
ICun4	11.2	11.7	9.8	9.2	8.9			10.8
LCun1	12.9	13.4	11.1	12.5	12.9	13.5	11.3	12.5
LCun2	15.6	16.6	14.6	13.5	13.3	17.1	14.1	14.9
LCun3	15.3	15.1	14.9	12.4	13.3	14.6	14.2	14.2

LCun4	11.7	8.9	10.0	8.4	9.3			8.9
Cub1	19.2	20.9	16.9	18.7	18.6	22.8	19.3	18.2
Cub2	9.7	8.8	7.4	8.7	8.1	10.6	10.7	8.1
Cub3		20.5						
Cub4	23.3	22.8	19.8	20.6	19.4	21.3	21.3	20.9
MT5	71.5	66.5	66.2	59.4	63.2	62.7	59.9	73.9
MT5D				50.1				65.2
MT4	70.3	67.9	64.7	59.5	61.9	60.4	62.0	68.0
MT4D		67.9						
MT3	73.9	67.8	66.5	63.3	63.5	64.2	66.4	69.0
MT3D								
MT2	78.0	73.9	70.8	67.8	66.4		67.7	73.6
MT2D								
MT1	59.1	57.2	56.9	48.9	52.0	53.9	56.3	56.2
MT1D								
PH1	31.6	31.3	29.3	27.7	31.0	28.6	29.8	33.2
PH2		37.2	35.2	34.6	36.8	33.1	36.1	38.5
PH3	46.9	41.3	39.6	37.5	41.2	39.3	41.5	43.5
PH4	44.1	38.9	39.3	35.7	40.2	37.7	39.9	41.5
PH5		31.1	31.9	28.7	32.9	28.9	30.2	34.8
FemurL	292	285	319	270	274	296	295	305
FemurLD								
FHB	35.1	31.3	34.2	31.2	32.8			34.8
TibL	250	242	271	219	230	237	246	260
TibLa	238	231	260	210	221	227	237	246
TibLD								
FibL	228	219	240	201	213	218	229	238
FibLD								

Taxon	***Pan troglodytes troglodytes***							
Location	HT B	PCM	PCM	PCM	PCM	PCM	PCM	PCM
Specimen	2026	CAMI1 47	CAMI2 03	CAMI2 04	CAMI2 07	CAMI2 16	CAMII3 01	ZVIII10
Sex	Male	Female	Female	Female	Female	Female	Female	Female
Age	Adult	Adult	Adult	Adult	Adult	Adult	Adult	Adult
Age Group	5	5	5	5	5	5	5	5
Calc1	57.8	49.9	55.2	53.4	54.7	50.9	51.4	56.4
Calc2	42.0	36.3	38.4	39.1	39.9	36.6	36.8	40.2
Calc3	41.1	35.2	36.7	33.9	36.5	33.8	35.0	37.6
Calc4	25.9	19.7	21.4	18.1	21.0	18.0	20.2	22.3
Calc5						20.7	23.2	25.3
Calc6						20.9	18.0	19.5
Calc7						33.9	32.0	33.3
Calc8						17.5	16.8	18.4
Talus1		42.1	42.7	39.6	45.2	43.1	42.7	44.6
Talus2	45.5	45.1	48.0	42.9	45.2	44.8	46.3	49.3
Talus5						23.9	25.1	27.3

Talus6	26.2	22.6	23.5	23.2	23.3	24.5	23.8	23.7
Nav1	41.4	34.2	34.1	30.8	38.0	36.0	35.4	36.6
Nav2	14.3	11.0	9.9	9.1	10.1	9.6	9.8	11.2
MCun1	19.8	18.0	18.4	18.3	18.4	18.2	16.5	18.7
ICun1	12.6	11.7	10.9	11.6	9.7	10.6	10.4	12.1
ICun2	9.9	9.3	10.3	11.4	8.6	9.9	7.8	10.3
ICun3	12.3	11.3	11.6	10.6	10.2	11.3	11.8	10.3
ICun4	13.4					10.7	11.1	11.2
LCun1	11.6	13.1	13.5	14.3	13.5	12.8	10.8	14.1
LCun2	13.9	15.0	16.2	14.6	15.3	14.7	14.3	15.6
LCun3	12.8	12.5	14.1	12.8	14.4	12.8	13.3	14.5
LCun4	10.6					9.2	9.7	11.4
Cub1	20.8	19.0	18.8	18.0	20.8	18.3	18.0	21.8
Cub2	9.9	8.4	9.9	10.0	9.8	8.8	7.8	8.1
Cub3								
Cub4	23.3	20.1	21.2	20.7	21.4	21.5	18.9	21.3
MT5	69.5	61.5	67.7	70.1	68.7	64.7	62.0	69.7
MT5D								
MT4	72.4	59.5	66.7	68.8	66.0	66.1	63.0	69.8
MT4D								
MT3	75.5	61.4	67.7	70.0	69.0	69.4	64.7	71.4
MT3D								
MT2	79.8	65.6	74.0	77.1	74.4	72.4	74.1	75.5
MT2D								
MT1	58.8	51.0	55.8	56.3	56.0	53.3	54.8	57.0
MT1D								
PH1	31.1	29.7	33.8	29.3	30.8	27.7	29.5	31.6
PH2	37.8	35.4	38.8	37.4	37.9	36.1	35.0	35.8
PH3	43.8	39.2	44.4	42.3	43.1	40.5	39.6	44.9
PH4	40.6	38.8	42.4	41.8	42.0	39.9	38.6	39.6
PH5	30.6	31.2	33.2	32.3	32.9	30.7	29.5	31.1
FemurL	303	261	290	293	281	295	294	297
FemurLD								
FHB	35.6	31.0	29.7	34.3	35.6	31.7	33.2	33.0
TibL	261	224	248	245	243	261	243	255
TibLa	247	213	240	234	231	250	232	244
TibLD								
FibL	236	203	230	222	219	236	220	230
FibLD								

Taxon	***Pan troglodytes troglodytes***							
Location	PCM	PCM	PCM	PCM	PCM	PCM	PCM	PCM
Specimen	ZVII23	ZVII26	ZIX51	ZIX52	ZV83	M78	M105	M148
Sex	Female	Female	Female	Female	Female	Female	Female	Female
Age	Adult	Adult	Adult	Adult	Adult	Adult	Adult	Adult
Age Group	5	5	5	5	5	5	5	5
Calc1	50.8	50.6	55.6	52.2	52.4	49.5	55.1	51.3

Calc2	37.5	35.6	39.5	39.1	38.0	36.4	38.9	38.1
Calc3	31.3	33.4	36.9	32.6	33.2	32.6	39.0	33.0
Calc4	18.3	16.6	20.0	18.4	19.5	18.9	22.6	19.5
Calc5	20.5	21.4	22.1	21.0	21.9	20.6	25.3	21.6
Calc6	19.2	17.2	18.1	17.4	15.9	19.8	21.2	17.3
Calc7	31.2	32.0	30.6	31.2	29.6	30.7	33.7	31.6
Calc8	20.1	16.9	19.3	19.8	17.2	18.8	21.0	17.7
Talus1	42.8	40.5	45.4	43.0	40.6	43.1	47.6	42.7
Talus2	44.4	43.9	49.0	45.2	44.7	44.0	51.1	46.0
Talus5	25.2	22.9	26.9	25.8	26.4	28.0	28.8	27.9
Talus6	22.1	20.4	21.0	23.0	21.3	24.6	25.4	24.4
Nav1	36.4	34.2	33.8	34.9	32.8	35.4	39.3	35.3
Nav2	9.6	10.6	11.0	9.3	11.2	10.0	10.7	10.5
MCun1	16.4	16.4	17.7	18.2	15.3	17.6	19.1	17.9
ICun1	11.4	11.0	10.1	12.3	11.4	10.6	10.3	11.9
ICun2	8.8	8.8	10.0	9.0	9.5	8.6	9.0	9.4
ICun3	12.9	10.4	11.8	10.7	9.3	10.1	12.9	10.6
ICun4	10.7	9.5	10.9	10.6	9.8	10.3	11.3	10.8
LCun1	14.3	12.1	14.4	13.1	12.8	11.4	13.3	13.1
LCun2	15.5	13.1	17.1	15.8	13.6	13.3	16.1	15.3
LCun3	14.1	13.1	13.7	13.3	12.6	13.8	14.5	13.9
LCun4	10.2	10.0	9.2	10.2	9.2	10.9	10.7	11.2
Cub1	18.7	16.9	19.9	18.8	19.1	17.7	18.9	20.0
Cub2	9.5	7.7	11.6	9.3	7.2	6.7	7.4	6.2
Cub3						20.4	22.4	21.7
Cub4	21.9	17.2	21.5	21.4	20.6	21.9	22.7	22.8
MT5	62.7	67.5	66.3	66.2	70.1	61.1	68.7	67.1
MT5D								61.2
MT4	64.0	68.7	67.7	64.3	69.1	63.3	66.2	64.3
MT4D								
MT3	65.8	72.3	68.7	66.6	73.2	65.0	70.0	70.7
MT3D								
MT2	69.9	75.6	74.7	71.8	76.4	69.1	76.9	76.1
MT2D								
MT1	53.9	56.6	54.2	52.7	57.2	53.5	57.2	55.5
MT1D								
PH1	30.0	32.4	32.3	28.6	30.1	28.8	31.4	30.9
PH2	40.5	38.2	38.0	35.8	38.3	35.5	39.1	38.8
PH3	41.2	43.4	41.3	41.0	44.9	41.1	43.3	43.4
PH4	40.1	42.1	40.1	38.6	43.2	39.9	41.9	42.3
PH5	26.8	34.2	32.4	29.5	32.5	31.0	33.0	33.0
FemurL	283	280	285	280	292	290	315	295
FemurLD								
FHB	32.5	30.7	34.5	32.3	30.8	32.4	35.4	35.3
TibL	240	241	239	234	247	228	269	250
TibLa	229	231	228	224	238	217	257	238
TibLD								
FibL	218	220	221	216	229	206	247	228

FibLD								

Taxon	***Pan troglodytes troglodytes***							
Location	PCM	PCM	PCM	PCM	PCM	PCM	PCM	PCM
Specimen	M155	M158	M169	M171 S3	M172	M184	M254 S2	M277
Sex	Female	Female	Female	Female	Female	Female	Female	Female
Age	Adult	Adult	Adult	Adult	Adult	Adult	Adult	Adult
Age Group	5	5	5	5	5	5	5	5
Calc1	49.0	48.4	47.9	50.6	51.1	47.4	52.4	51.9
Calc2	34.8	36.0	35.1	39.0	38.9	33.8	39.2	37.9
Calc3	31.8	31.5	31.7	32.5	32.2	29.2	32.3	33.6
Calc4	17.3	19.8	18.6	19.7	18.4	17.0	18.7	20.2
Calc5	19.6	22.4	20.6	21.8	21.9	19.8	21.0	22.1
Calc6	16.5	17.9	16.1	17.5	20.4	17.5	18.5	18.4
Calc7	31.4	33.5	27.9	31.5	32.9	31.0	33.6	32.9
Calc8	16.9	18.6	16.8	18.5	17.1	17.2	19.0	16.8
Talus1	41.4	44.5	40.2	40.3	41.6	39.3	42.2	42.7
Talus2	44.9	45.2	42.5	47.4	45.9	41.3	47.5	46.0
Talus5	25.4	27.8	24.4	25.7	24.2	24.2	25.4	25.4
Talus6	23.1	21.0	21.1	23.5	23.5	21.7	21.4	22.5
Nav1	34.2	33.7	31.9	37.2	36.3	31.6	34.9	33.7
Nav2	10.0	10.9	8.4	11.7	10.2	9.7	12.6	11.0
MCun1	16.1	19.0	18.2	17.2	15.9	15.3	17.3	16.5
ICun1	11.0	10.6	10.1	10.6	10.5	9.7	12.2	11.2
ICun2	7.6	10.3	8.1	10.7	9.8	7.9	7.9	8.9
ICun3	11.1	11.9	10.3	13.1	10.7	9.4	12.1	11.2
ICun4	11.7	10.4	10.8	11.2	9.2	8.7	10.6	11.1
LCun1	11.6	14.4	11.7	13.6	13.4	11.5	13.2	11.7
LCun2	13.4	15.6	13.9	15.9	15.4	13.6	15.9	13.7
LCun3	11.8	13.3	13.3	13.9	15.3	11.7	15.2	12.1
LCun4	9.1	8.7	9.5	10.9	11.2	9.3	9.8	9.8
Cub1	17.1	20.4	18.1	19.0	19.7	17.1	20.8	19.1
Cub2	7.6	11.1	7.6	8.5	9.8	6.0	9.7	7.8
Cub3	19.4	19.2	18.2	20.5	21.2	19.3	20.8	20.6
Cub4	20.1	21.0	19.5	21.0	20.6	19.7	21.6	20.0
MT5	65.8	66.1	61.9	71.3	65.5	61.8	71.0	64.4
MT5D								
MT4	65.5	66.3	64.7	72.4	65.1	59.9	70.3	63.1
MT4D								
MT3	68.2	67.0	66.1	70.5	67.6	61.1	71.9	64.5
MT3D								
MT2	73.2	70.6	69.7	78.1	72.3	63.3	77.3	69.8
MT2D								
MT1	53.8	53.1	53.7	57.3	55.6	50.3	58.2	53.5
MT1D								
PH1	30.4	31.1	30.5	29.8	30.7	27.9	32.6	30.0

PH2	35.7	36.3	39.8	37.6	36.9	35.2	39.9	40.0
PH3	41.9	40.1	43.3	42.6	41.1	40.5	43.6	43.1
PH4	41.0	39.4	42.1	41.8	39.2	38.7	43.1	41.1
PH5	32.2	30.7	27.0		30.6	29.3	34.8	38.6
FemurL	282	271	280	293	295	269	312	283
FemurLD								
FHB	30.1	31.7	29.9	35.6	31.8	29.2	34.0	32.3
TibL	248	227	233	255	243	225	262	242
TibLa	237	216	223	245	233	215	251	232
TibLD								
FibL	230	208	215	235	224	204	243	222
FibLD								

Taxon	***Pan troglodytes troglodytes***							
Location	PCM	PCM	PCM	PCM	PCM	PCM	PCM	PCM
Specimen	M279	M299	M348	M424	M425	M450	M475	M501
Sex	Female	Female	Female	Female	Female	Female	Female	Female
Age	Adult	Adult	Adult	Adult	Adult	Adult	Adult	Adult
Age Group	5	5	5	5	5	5	5	5
Calc1	55.5	47.5	50.4	52.3	56.6	51.4	47.9	52.7
Calc2	40.8	32.7	35.5	39.6	40.8	35.7	35.8	38.8
Calc3	33.3	34.7	34.4	32.6	34.7	35.8	32.3	34.7
Calc4	19.4	17.8	19.6	20.7	21.1	20.0	20.1	21.2
Calc5	22.0	22.0	22.0	24.5	22.9	23.2	22.6	23.2
Calc6	18.1	18.7	16.8	19.9	21.1	19.8	18.0	16.8
Calc7	32.1	31.6	27.6	33.2	33.2	33.8	33.6	31.8
Calc8	19.9	18.9	17.1	18.2	21.0	20.6	19.6	17.9
Talus1	45.6	43.9	40.3	42.1	46.0	46.4	43.0	42.2
Talus2	47.2	47.5	43.6	47.0	50.7	48.1	47.4	46.0
Talus5	28.6	26.1	24.2	27.5	27.6	28.2	26.7	26.3
Talus6	25.1	24.3	22.6	21.7	24.3	24.0	22.4	22.0
Nav1	38.0	36.0	34.7	36.2	38.0	37.6	34.5	32.1
Nav2	12.3	9.3	12.3	11.4	10.7	11.2	11.1	10.4
MCun1	18.2	17.3	16.9	18.6	17.7	17.3	16.4	16.2
ICun1	12.8	11.1	11.9	9.8	10.7	12.1	12.1	11.2
ICun2	9.6	9.2	8.3	8.8	9.2	9.5	10.3	9.9
ICun3	11.9	11.8	11.7	13.3	11.0	12.4	12.7	12.2
ICun4	11.6	11.1	10.6	12.5	10.8	13.2	10.7	12.1
LCun1	14.3	12.7	12.1	12.1	11.6	13.3	13.7	12.5
LCun2	16.0	14.1	13.6	15.7	15.4	16.4	15.0	15.3
LCun3	15.1	14.3	12.6	13.7	15.0	13.8	13.6	12.3
LCun4	10.2	10.7	9.6	10.7	10.4	10.1	9.4	10.1
Cub1	20.0	18.9	17.5	19.9	20.2	20.7	16.4	18.6
Cub2	6.3	8.5	9.4	7.6	9.8	9.1	8.1	8.3
Cub3	25.4	21.7	19.4	22.3	20.5	19.3	20.3	19.9
Cub4	22.1	21.7	19.5	21.9	21.9	22.3	21.2	20.2
MT5	69.3	65.1	61.4	65.4	75.7	62.5	64.9	68.7

MT5D								
MT4	67.9	61.6	60.3	64.6	71.7	63.2	65.1	69.2
MT4D								
MT3	68.9	64.9	63.2	67.3	72.5	65.6	67.4	69.2
MT3D								
MT2	74.1	70.5	67.1	73.1	81.1	72.6	73.4	74.0
MT2D								
MT1	57.8	51.9	52.1	56.4	60.3	54.7	55.4	52.9
MT1D								
PH1	28.8	27.8	31.6	31.5	29.1	32.1	30.3	29.4
PH2	38.0	37.2	36.1	39.7	42.3	36.5	36.0	35.1
PH3	42.2	41.2	41.7	43.2	46.1	41.8	40.7	40.9
PH4	40.3	40.0	41.6	39.7	46.9	35.2	39.5	40.7
PH5	31.3	32.8	31.9	32.3	37.3	31.4	30.5	31.9
FemurL	285	295	282	285	301	283	290	284
FemurLD								
FHB	31.8	32.6	29.4	33.0	34.6	33.4	33.4	32.0
TibL	250	242	233	238	250	241	246	236
TibLa	240	231	225	227	241	231	236	226
TibLD								
FibL	224	217	218	221	227	224	226	216
FibLD								

Taxon	***Pan troglodytes troglodytes***							
Location	PCM	PCM	PCM	PCM	PCM	PCM	PCM	PCM
Specimen	M506 S3	M576	M650	M655	M664	M670	M676	M677
Sex	Female	Female	Female	Female	Female	Female	Female	Female
Age	Adult	Adult	Adult	Adult	Adult	Adult	Adult	Adult
Age Group	5	5	5	5	5	5	5	5
Calc1	50.3	50.2	52.8	55.6	47.6	45.8	47.1	53.3
Calc2	37.8	36.8	40.7	40.3	33.8	33.1	34.1	38.5
Calc3	31.5	30.2	29.7	37.3	31.5	30.5	31.2	33.1
Calc4	18.3	17.2	17.1	21.9	17.7	16.6	18.8	18.8
Calc5	21.9	20.6	19.7	24.9	19.9	19.1	21.4	22.0
Calc6	16.9	15.9	19.7	18.2	17.6	17.7	16.9	18.2
Calc7	28.4	32.4	28.2	34.2	31.0	30.0	31.3	34.1
Calc8	17.4	18.0	18.6	19.3	17.0	17.0	18.3	18.5
Talus1	41.5	40.7	41.3	44.1	39.8	38.8	39.4	41.2
Talus2	44.2	42.9	42.9	50.0	45.5	41.0	41.2	44.8
Talus5	25.3	25.5	24.5	26.4	24.9	24.8	24.5	24.7
Talus6	23.2	20.1	22.1	24.5	20.4	19.3	19.5	22.7
Nav1	32.6	32.8	34.8	36.9	32.2	32.4	31.2	34.1
Nav2	9.6	10.7	10.2	12.5	9.4	9.4	8.7	9.1
MCun1	17.3	15.7	16.7	17.9	16.6	14.9	17.6	17.6
ICun1	11.4	9.1	11.3	11.9	11.2	8.7	11.4	11.5
ICun2	7.8	8.1	8.1	10.2	9.3	7.4	9.5	8.6

ICun3	11.2	9.4	10.0	10.8	11.6	9.7	10.3	12.9
ICun4	11.2	10.7	10.0	12.3	10.3	8.8	10.6	11.9
LCun1	12.7	10.1	12.3	12.8	13.0	10.9	13.9	12.5
LCun2	14.9	13.6	13.6	14.1	15.5	11.2	14.9	14.2
LCun3	12.9	13.1	13.3	15.2	13.4	12.4	12.3	14.7
LCun4	11.3	9.2	9.0	10.5	10.0	9.9	9.1	11.9
Cub1	18.0	16.8	18.1	20.6	17.8	16.9	18.5	19.5
Cub2	10.5	7.0	6.9	9.3	8.5	3.3	9.2	8.5
Cub3	22.1	19.7	20.0	22.3	19.8	17.4	18.9	20.9
Cub4	21.3	20.4	19.2	20.5	20.4	19.5	20.6	19.0
MT5	63.7	69.5	63.5	67.8	66.6	58.1	57.2	68.3
MT5D	58.2							
MT4	65.3	65.7	64.2	70.9	68.8	53.7	57.7	69.8
MT4D	56.2							
MT3	65.7	67.4	66.9	73.4	71.0	55.4	61.3	72.7
MT3D	56.4	67.4	66.9	73.4	71.0	55.4	61.3	72.7
MT2	70.1	71.0	71.3	78.5	74.1	64.0	64.0	77.5
MT2D	62.2							
MT1	51.6	53.2	53.3	58.6	54.3	47.5	51.5	56.8
MT1D	47.0							
PH1	30.2	30.5	31.0	33.7	23.2	26.5	26.7	32.5
PH2	37.5	36.4	37.0	40.0	38.2	31.8	34.0	34.0
PH3	40.5	43.4	43.2	46.3	44.6	36.5	37.9	47.3
PH4	39.7	42.1	41.4	44.1	42.5	33.8	35.5	45.0
PH5	30.8	33.1	31.5	35.3	32.4	27.1	27.1	32.2
FemurL	275	268	290	306	298	257	275	315
FemurLD								
FHB	31.7	31.9	31.8	31.1	30.2	28.7	30.9	35.4
TibL	233	235	252	263	250	219	227	259
TibLa	228	225	243	250	239	208	217	251
TibLD								
FibL	216	215	234	233	228	201	206	241
FibLD								

Taxon	***Pan troglodytes troglodytes***							
Location	PCM	PCM	PCM	PCM	PCM	PCM	PCM	PCM
Specimen	M702	M706	M720	M742	M743	M800	M873	M967
Sex	Female	Female	Female	Female	Female	Female	Female	Female
Age	Adult	Adult	Adult	Adult	Adult	Adult	Adult	Adult
Age Group	5	5	5	5	5	5	5	5
Calc1	50.7	57.1	51.7	50.2	53.3	46.4	45.2	54.0
Calc2	37.5	42.7	36.6	38.6	43.2	33.7	32.9	39.6
Calc3	30.2	34.9	35.0	32.3	34.5	33.0	29.5	36.4
Calc4	19.2	21.2	20.8	19.7	22.4	20.3	17.9	21.0
Calc5	21.4	23.5	23.3	22.0	24.9	22.1	20.8	22.9
Calc6	16.3	18.4	17.5	19.2	19.9	17.3	16.2	21.3
Calc7	29.9	34.3	34.4	31.3	30.1	31.5	27.4	34.9

Calc8	19.4	19.4	18.1	19.2	18.7	18.0	17.4	18.5
Talus1	40.8	41.8	45.8	40.4	43.0	42.8	41.3	45.3
Talus2	48.0	46.0	48.6	42.7	46.1	47.1	44.1	47.6
Talus5	25.3	24.5	28.7	25.4	26.2	25.0	25.3	27.9
Talus6	24.5	24.0	23.7	21.9	23.2	23.1	21.9	24.2
Nav1	34.6	34.7	36.0	35.0	37.2	33.0	34.7	37.0
Nav2	10.9	12.0	11.8	9.8	11.4	9.1	9.8	9.7
MCun1	17.2	19.5	16.4	16.6	19.7	16.2	16.2	17.9
ICun1	10.7	11.6	8.5	9.9	12.4	9.5	10.6	10.9
ICun2	8.7	9.8	8.3	10.3	9.7	9.1	9.8	9.1
ICun3	12.3	11.6	10.8	10.8	12.8	10.9	12.5	11.5
ICun4	10.8	12.2	10.8	9.1	13.7	10.0	11.7	9.8
LCun1	11.2	12.5	11.6	13.1	13.0	12.2	12.8	14.5
LCun2	14.5	14.8	15.3	16.4	15.5	13.1	14.5	15.3
LCun3	13.9	13.4	14.1	14.1	13.0	13.0	13.3	13.5
LCun4	11.9	8.9	10.1	9.9	9.5	9.5	9.2	11.3
Cub1	17.5	20.0	19.7	19.5	18.7	18.1	17.3	20.6
Cub2	9.0	8.2	8.7	9.3	10.9	8.4	9.4	9.6
Cub3	21.3	21.0	20.6	19.9	21.8			
Cub4	20.6	22.1	20.2	21.2	22.3	20.7	19.9	21.6
MT5	69.7	67.1	64.5	73.2	70.4	58.0	58.1	65.0
MT5D	61.3							
MT4	71.8	67.8	66.2	74.6	73.5	59.5	62.4	66.9
MT4D	61.7							
MT3	73.1	70.9	70.2	77.6	74.8	61.3	66.0	69.0
MT3D	62.5							
MT2	76.4	76.5	75.2	82.0	79.2	67.3	71.6	71.4
MT2D	66.1							
MT1	55.1	56.7	54.7	61.8	60.0	49.8	55.2	54.1
MT1D	51.3							
PH1	30.3	32.3	29.0	33.8	33.5	28.2	31.7	29.0
PH2	36.9	41.3	38.2	37.4	40.3	33.6	37.9	35.8
PH3	44.6	44.2	39.9	47.2	45.8	38.7	42.1	42.0
PH4	42.6	44.1	40.7	45.4	43.4	37.2	39.1	40.4
PH5	32.7	32.6	30.3	35.8	34.8	27.8	30.9	30.8
FemurL	304	299	298	304	303	263	285	275
FemurLD								
FHB	30.8	33.3	32.2	34.2	31.7	29.2	30.9	34.0
TibL	271	251	255	252	267	216	244	225
TibLa	260	242	246	242	257	206	234	215
TibLD								
FibL	246	232	235	234	248	199	218	210
FibLD								

Taxon	***Pan troglodytes troglodytes***							
Location	PCM	PCM	PCM	PCM	PCM	PCM	PCM	PCM
Specimen	M986	CAMI206	CAMI219	CAMI228	C372	ZVII25	ZVI34	ZIX49
Sex	Female	Male	Male	Male	Male	Male	Male	Male

Age	Adult	Adult	Adult	Adult	Adult	Adult	Adult	Adult
Age Group	5	5	5	5	5	5	5	5
Calc1	47.1	53.1	57.0	55.4	48.2	58.4	50.8	51.9
Calc2	35.2	40.5	43.0	41.4	35.2	42.4	38.0	37.2
Calc3	31.2	33.5	40.5	36.9	29.6	40.5	32.9	34.2
Calc4	18.7	18.6	24.0	22.0	17.6	22.9	20.2	18.2
Calc5	20.9		27.0	24.0	19.9	26.0	23.7	22.6
Calc6	16.5		22.2	19.3	16.0	22.5	18.2	17.6
Calc7	34.2		33.9	37.0	27.2	36.5	31.7	33.4
Calc8	19.6		21.9	21.9	18.5	21.0	19.0	18.7
Talus1	39.7	46.8	46.6	45.5	42.8	48.5	44.1	41.6
Talus2	44.1	48.4	51.6	50.1	46.6	53.8	48.0	44.0
Talus5	26.3		30.1	25.8	23.5	30.3	25.3	25.1
Talus6	21.4	23.4	27.2	23.7	19.8	26.4	23.1	23.2
Nav1	34.6	37.9	38.2	38.3	31.4	41.3	35.6	37.9
Nav2	10.0	11.7	12.3	12.5	10.7	12.1	11.9	12.1
MCun1	17.7	18.2	17.0	19.2	18.6	19.9	18.6	18.5
ICun1	9.2	11.3	10.9	12.4	12.5	12.5	10.2	12.0
ICun2	9.5	10.1	8.8	10.5	9.3	10.0	8.8	10.2
ICun3	10.8	13.1	12.0	11.7	11.5	12.1	11.6	12.0
ICun4	9.9		11.3	12.2	11.3	11.0	12.3	12.6
LCun1	13.2	11.8	10.4	14.5	12.6	14.3	12.5	13.2
LCun2	14.0	14.4	14.8	16.4	13.8	16.0	15.8	15.7
LCun3	12.8	14.4	15.4	13.9	11.7	15.0	13.0	15.0
LCun4	8.4		11.0	11.1	9.4	11.2	10.2	10.4
Cub1	19.4	19.0	20.1	20.9	19.2	23.1	17.7	20.8
Cub2	8.1	8.2	9.0	10.4	8.0	12.3	9.9	9.8
Cub3	20.7							
Cub4	20.3	21.6	22.1	23.0	19.6	24.7	21.2	20.6
MT5	61.8	73.5	75.1	77.8	61.6	75.3	67.6	67.0
MT5D								
MT4	61.7	70.1	76.1	72.4	58.1	71.2	70.1	69.0
MT4D								
MT3	63.1	71.6	76.9	76.5	59.5	74.0	71.9	71.6
MT3D								
MT2	68.0	77.4	82.6	81.4	65.8	77.6	75.0	77.1
MT2D								
MT1	54.3	55.9	59.0	59.5	46.8	61.7	51.3	56.8
MT1D								
PH1	30.1	29.6	33.8	33.8	28.6	35.5	29.1	32.3
PH2	35.3	36.9	41.1	42.1	33.7	40.2	36.0	38.2
PH3	40.4	41.6	48.3	47.3	36.1	45.8	42.0	42.8
PH4	40.2	39.5	46.7	44.8	36.3	45.5	37.0	41.5
PH5	29.9	31.0	37.8	34.6		35.4	28.2	32.6
FemurL	295	297	312	284	260	310	285	283
FemurLD								
FHB	31.8	33.2	37.2	35.3	30.5	39.1	32.1	34.1

TibL	233	255	271	253	216	269	251	245
TibLa	221	245	259	241	206	256	238	235
TibLD								
FibL	213	235	249	231	197	246	229	222
FibLD								

Taxon	***Pan troglodytes troglodytes***							
Location	PCM	PCM	PCM	PCM	PCM	PCM	PCM	PCM
Specimen	M144	M278	M347	M401	M440	M712	M724	M984
Sex	Male	Male	Male	Male	Male	Male	Male	Male
Age	Adult	Adult	Adult	Adult	Adult	Adult	Adult	Adult
Age Group	5	5	5	5	5	5	5	5
Calc1	53.0	49.4	50.4	53.2	52.8	56.1	54.2	56.9
Calc2	39.8	36.1	34.9	38.3	39.6	41.0	38.7	41.5
Calc3	34.3	27.8	37.5	36.3	34.0	34.6	37.1	36.4
Calc4	19.8	14.9	21.1	20.9	21.1	19.2	21.2	20.9
Calc5	22.3	19.3	23.6	25.2	22.6	24.3	24.2	24.2
Calc6	18.9	16.7	15.7	22.4	19.5	19.7	20.3	20.5
Calc7	33.8	29.3	29.2	34.6	31.6	44.3	34.1	32.9
Calc8	18.8	17.5	18.5	18.3	18.6	17.7	21.1	18.6
Talus1	45.5	42.4	45.0	46.8	42.7		48.5	48.1
Talus2	50.5	47.2	48.2	51.0	43.9		52.0	52.5
Talus5	26.1	24.2	24.7	29.2	26.0	33.4	29.2	28.5
Talus6	23.2	21.5	21.8	24.6	22.9	39.7	26.0	24.8
Nav1	36.6	32.6	32.8	35.6	36.9	18.2	39.8	38.6
Nav2	10.7	9.8	9.2	10.8	12.2	5.3	12.3	11.2
MCun1	20.0	16.8	17.1	19.4	17.9	10.4	18.3	18.9
ICun1	13.6	11.4	11.2	12.0	13.8	12.7	11.4	13.5
ICun2	10.5	7.9	9.1	8.9	8.8	10.1	9.8	9.7
ICun3	12.1	10.3	10.2	12.0	12.9	11.3	12.0	12.5
ICun4	11.2	10.3	11.3	12.2	13.3	11.7	11.9	11.1
LCun1	14.2	12.9	12.7	13.0	13.8	13.2	13.9	13.5
LCun2	15.2	14.1	13.2	15.3	15.4	14.7	16.9	16.7
LCun3	13.2	12.7	11.9	13.9	14.2	11.9	14.0	15.4
LCun4	10.7	9.2	8.5	9.7	9.7	10.2	9.9	11.6
Cub1	19.7	17.5	17.4	19.8	20.4	21.8	21.8	19.9
Cub2	7.7	6.4	7.2	9.2	10.9	9.9	11.9	8.8
Cub3	22.4	19.4	19.3	23.4	21.9	23.1	21.0	23.4
Cub4	22.9	20.7	19.5	23.8	22.4	24.3	23.1	22.8
MT5	59.1	63.2	60.9	66.7	66.4	66.6	70.8	65.3
MT5D		54.8						
MT4	62.2	62.4	60.1	70.7	66.9	64.3	71.0	65.9
MT4D		54.6						
MT3	66.3	63.2	61.8	72.4	68.3	64.9	71.9	66.5
MT3D		53.1						
MT2	69.6	69.1	65.6	79.2	75.0	71.5	77.5	72.9
MT2D		60.4						

MT1	56.1	55.0	50.4	54.6	51.7	53.8	58.8	55.4
MT1D		50.6						
PH1	29.4	29.3	28.2	29.1	27.7	32.3	33.2	30.0
PH2	36.6	30.3	38.3	35.9	34.6	37.1	40.1	37.7
PH3	42.3	41.2	40.9	42.9	39.3	41.7	46.0	40.9
PH4	37.7	39.4	38.8	41.4	38.0	40.5	45.1	39.0
PH5	27.3	31.9	31.7	33.3	30.2	33.9	33.4	29.3
FemurL	296	265	286	304	280	294	292	290
FemurLD								
FHB	34.8	28.6	29.8	33.4	31.7	35.4	36.0	34.2
TibL	241	230	235	260	238	234	255	249
TibLa	231	219	234	250	228	231	243	238
TibLD								
FibL	223	207	119	240	214	217	234	226
FibLD			193					

Taxon	***Pan troglodytes troglodytes***				
Location	PCM	Zurich	Zurich	Zurich	Zurich
Specimen	M988	10280	AS 1763	PAL 219	PAL 220
Sex	Male	Female	Female	Female	Male
Age	Adult	Adult	Adult	Adult	Adult
Age Group	5	5	5	5	5
Calc1	55.8	51.7	50.6	47.8	56.3
Calc2	40.5	40.1	37.1	36.9	42.5
Calc3	36.7	40.5	33.9	29.6	35.4
Calc4	21.0		20.7	16.6	20.7
Calc5	22.9		22.5	20.0	23.7
Calc6	19.2		19.3	16.2	17.7
Calc7	35.9	32.6	30.0	29.4	35.0
Calc8	20.5	19.5	20.8	17.4	22.9
Talus1	45.0	41.8	41.7	38.5	44.8
Talus2	48.9	44.7	44.7	45.4	46.0
Talus5	28.5	28.2	27.3	24.5	21.5
Talus6	25.4	24.6	21.0	20.1	35.9
Nav1	40.7	38.5	33.5	32.2	12.2
Nav2	11.9	12.5	12.0	10.1	19.8
MCun1	20.5	19.3	18.9	16.9	18.4
ICun1	13.7	10.6	10.8	10.9	10.8
ICun2	10.2	9.7	9.5	9.0	10.7
ICun3	13.1	10.3	9.5	10.1	12.3
ICun4	13.9	10.3	9.5	10.1	11.2
LCun1	12.0	13.4	13.2	12.0	13.9
LCun2	16.3	16.1	16.4	14.7	17.0
LCun3	15.2	14.0	13.0	12.7	13.7
LCun4	11.9	9.2	9.7	9.7	10.3
Cub1	21.6	22.8	21.5	18.7	23.3
Cub2	9.4	6.1	9.0	7.4	8.7

Cub3	22.5	21.2	20.1	17.7	20.8
Cub4	23.8	23.5	20.7	18.4	23.3
MT5	65.8	62.9	61.8	54.7	68.3
MT5D					
MT4	66.5	66.7	62.4	58.0	67.5
MT4D					
MT3	70.0	69.5	64.2	60.1	68.8
MT3D					
MT2	73.6	74.2	68.9	67.2	72.7
MT2D					
MT1	54.0	58.1	53.8	52.8	56.8
MT1D					
PH1	30.7	29.9	31.1	28.6	30.7
PH2	38.6	37.1	35.9	33.5	37.3
PH3	43.7	40.5	39.4	37.0	42.4
PH4	41.7	39.6	38.1	35.1	40.1
PH5	32.7	31.2	29.5	26.4	31.7
FemurL	300	296	268	273	284
FemurLD					
FHB	34.4	35.0	30.4	28.6	30.6
TibL	252	253	230	224	241
TibLa	240	243	221		229
TibLD					
FibL	224	227	213	202	222
FibLD					

CURRICULUM VITAE

Holly M. Dunsworth

November 20, 2006

Ph.D. Anthropology, Pennsylvania State University, defended September 12, 2006
M.A. Anthropology (Distinction), Penn State University, May 2001
B.A. Anthropology (High Honors), University of Florida, May 1999

Current Position

Postdoctoral Scholar, Department of Biochemistry & Molecular Biology, Penn State

Selected Publications

2005 Dunsworth HM. Ontogeny and proportions of new *Proconsul heseloni* tarsals and metatarsals from the Kaswanga Primate Site, Rusinga Island, Kenya. (Abstract) PaleoAnthropology.

2005 Walker A, Dunsworth HM, Kozakowski S, Krovitz GE, Orkin JD, Welker KL. Thinking outside the book: Escaping traditional representations of hominin evolution through computer animation. (Abstract) PaleoAnthropology.

2004 Dunsworth HM, Challis JH. Throwing ability in fossil hominins. AJPA Supplement 38: 90.

2003 Dunsworth HM, Challis JH, Walker A. Throwing and Bipedalism: A new look at an old idea. In Franzen JL, Dohler M, Moya-Sola S (eds). Upright Walking. Senckenberg Institute, Frankfurt, pp. 105-110.

2002 Dunsworth HM, Walker A. Early Genus *Homo*. In Hartwig W (ed) The Primate Fossil Record. Cambridge: Cambridge University Press, pp. 419-426.

2002 Dunsworth HM, Walker A. Early *Homo*. In Pagel M (ed) The Oxford Encyclopedia of Evolution. Oxford: Oxford University Press, pp. 485-489.

Selected Grants

2004 The Leakey Foundation. $11,200. “Ontogeny and Functional Morphology of the *Proconsul* Foot”

Selected Honors

2005 Alumni Association Dissertation Award, Penn State
2004 Matson-Benson Museum Award, Penn State
2004 Hill Foundation Fellowship, Anthropology Department, Penn State
2000-2003 National Science Foundation Graduate Research Fellowship
1999 Phi Beta Kappa

Selected Fieldwork

2006 Co-leader. Survey and excavation at Miocene and Pleistocene fossil sites on Rusinga and Mfangano Islands, Kenya.

2002 & 2003 Team member. Excavation at Dmanisi, Georgia, a Lower Pleistocene *Homo erectus* site.